University of Strathclyde

Glasgow

Department of Pharmaceutical Sciences

Formulation Strategies In Developing An Oil-Filled Capsule For Time-Delayed Release

Lee Ann Hodges

MPharm (Hons)

Ph.D Thesis

May 2005

DECLARATION

The copyright of this thesis belongs to the author under the terms of the United Kingdom Copyright Acts as qualified by University of Strathclyde Regulation 3.49. Due acknowledgement must always be made of the use of any material contained in, or derived from, this thesis.

This PhD thesis is dedicated to my Mum and Dad,

who allowed me to spread my wings and experience new pastures;

for all their prayers, love and support throughout my life.

ACKNOWLEDGEMENTS

All glory and honour to God, who was and who is and who is to come. My Rock and my Redeemer, the pillar of my salvation and my eternal strength.

Love and thanks to my parents, John and Poh Sim Hodges, who encouraged me to reach for the stars, and never ceased to help me get there.

My heartfelt thanks and deep appreciation to

Professor Howard Stevens and Dr Alex Mullen who were not merely academic supervisors but good, dependable friends as well.

Pastor Winston and Sister Eunice Lee, my spiritual parents throughout my time in Glasgow, for their guidance, love and care.

Pui Ee Wong, Chin Thye Lee, Yvonne Hu, Ashley Liew, David Foo, Patrick Shi, Joseph Chew, Donna Shek, Su Yin Lim, Chris and Eileen Lim, Gideon and Annie Ho, Willy and Lynn Tee, my spiritual brothers and sisters here in Glasgow, who were always there when I needed them.

Jaclyn Lee, Michelle Tan, Terri Kong and Su Leen Ho, my best friends in Malaysia whose love and support have always traversed the miles.

Linda Wong, my kindred spirit.

Alistair Ross, Fiona McInnes, Jobina Lee, Sigrunn Osmundsen, Joshua Boateng, Maria Cristina Coelho, Hardik Shah, Doungkamol Leaokittikul, Leigh Dixon, Bee Koen Low, Jason McConville, Raymond Ng, Vu Dang Hoang and Shiow Fern Ng, for making SIBS 218 a great place to work.

Anne Goudie, Steve Steer, Peter Constable, Tommy McGrory, Ian Simpson, John Nevin and Richard Pratt for excellent technical help.

Liz Carruthers and Allison Reid, for help in printing out this thesis and especially for all the encouragement over the years.

Laurence Tetley, Margaret Mullen and Eoin Robertson at the Institute of Biological Life Sciences, University of Glasgow, for help with SEM.

ABSTRACT

A rational approach was adopted in the design of a novel controlled release system aimed at delivering hydrophobic drugs in a wholly time-dependent manner. A swellable, rupturable system in which hydrophobic drugs were solubilised in vegetable oils was proposed. Two main components of the system, the swelling agent low-substituted hydroxypropylcellulose (grade LH-21) and brittle outer coating of ethylcellulose (EC) were individually characterised. Upon contact with water, LH-21 swelled rapidly and to a great extent, exemplified by using simple apparatus to measure water uptake and swelling force. Mixing it with other excipients such as vegetable oils, surfactants and drugs tended to decrease LH-21 water uptake rate and subsequent force generation rate. Solution-cast EC films enabled thorough investigations into the mechanical integrity and physicochemical properties of the proposed outer coating of the capsule. Plasticisation decreased the strength while increasing the malleability of the film while increasing polymer content toughened the film and increased its elastic modulus. These findings were extrapolated to the construction of the dosage form in its two configurations. The first involved filling a hard gelatin capsule with a dispersion of LH-21 in corn oil and coating it with EC. In the second, a gelatin-based tablet separated LH-21 and corn oil. Burst release following a lag time was obtained with both configurations. In general, decreasing the LH-21 concentration and increasing the EC coating level prolonged the lag time. A limit of LH-21 concentration was identified below which more sustained release was observed indicating sufficient LH-21 was required to efficiently expel the capsule fill. Problems with leakage of the oil component were addressed in the hope of manufacturing reproducible dosage forms. Improvements to the construction process are essential if successful drug delivery is to be achieved.

PUBLICATIONS

Hodges, L.A., Stevens, H.N.E., Mullen, A.B. (2002) Preliminary investigations into a novel controlled release mechanism – the influence of water uptake rates. *J. Pharm. Pharmacol.* 54:S-46.

Hodges, L.A., Stevens, H.N.E., Mullen, A.B. (2002) Water uptake by a swellable polymer dispersed in oil. *AAPS PharmSci.* 4(S1). Abstract W4139.

Hodges, L.A., Stevens, H.N.E., Mullen, A.B. (2003) From concept to construction – processing variability of a time-delayed oil-filled capsule. *Proceed. Intern. Symp. Control. Rel. Bioact. Mater.* 748.

Hodges, L.A., Stevens, H.N.E., Mullen, A.B. (2003) Ethylcellulose dipcoating to incorporate time-delay in an oil-filled capsule. *J. Pharm. Pharmacol.* 55:S-130.

Hodges, L.A., Stevens, H.N.E., Mullen, A.B. (2003) Time-delayed release from an oil-filled capsule coated with ethylcellulose. *AAPS PharmSci.* 5(S1). Abstract T3030.

Hodges, L.A., Stevens, H.N.E., Mullen, A.B. (2004) Tensile properties of ethylcellulose coatings of a time-delayed oil-filled capsule. *Proceed. Intern. Symp. Control. Rel. Bioact. Mater.* 442.

Hodges, L.A., Stevens, H.N.E., Mullen, A.B. (2004) Mechanical integrity of polymer films used in time-delayed release capsules. *J. Pharm. Pharmacol.* 56:S-82.

Hodges, L.A., Stevens, H.N.E., Mullen, A.B. (2004) Puncture test to simulate rupturing of ethylcellulose coat of a time-controlled delivery system. *AAPS PharmSci.* 6(S1). Abstract T3272.

Hodges, L.A., Stevens, H.N.E., Mullen, A.B. (2004) Solution-cast films as a predictive tool in formulating rupturable coat of time-delayed capsules. *AAPS PharmSci.* 6(S1). Abstract T3273.

CONTENTS

CHAPTER 7. FORMULATION, MANUFACTURE AND TESTING OF THE COMPARTMENTALISED CAPSULE

CHAPTER 8. GENERAL DISCUSSION AND FUTURE WORK

REFERENCES

CHAPTER 1

INTRODUCTION

The efficacy of controlled release drug delivery systems hinges on their ability to accurately reproduce the desired drug release profile. This property is especially imperative in the chronopharmaceutical arm of drug delivery, where literally, 'timing is everything'.

The following review considers the current trends in controlled release in general, while placing emphasis on chronopharmaceutics. It also details the utilisation of various GRAS excipients in other controlled release dosage forms and infers the possibilities of incorporating them into our drug delivery system. A comprehensive discussion on certain excipients and processing equipment selected for our system concludes the chapter.

1.1 Oral controlled release drug delivery systems

The need for controlled release (CR) technology in the field of drug delivery today is undeniable. While CR systems with high in-built technology still do not command a great proportion of market share, all the signs point to this fact being rapidly reversed.

The limitations of conventional drug delivery systems are becoming all the more apparent. For instance, the fluctuating and sub-optimal drug levels from these systems result in reduced therapeutic efficacy possibly leading to excessive use of drug (Vergnaud, 1993). Their efficiency is also restricted by the reliability of the patient in complying with the recommended dosing regimen. Improper formulation techniques may also compromise the potency of certain drugs.

Hence the trend now is to look towards specialised delivery systems that offer the advantage of lowering the amount of drug required by improving bioavailability through programmed drug release, for example. With less drug ingested, the possibility of side effects occurring simultaneously decreases. Devices with timed-

release characteristics enable reduced frequency of administration thereby allowing for improvement of patient compliance. Nevertheless, CR systems need to release the total amount of drug within the timeframe afforded by the gastrointestinal transit time which may range from 2 to 12 hours.

With the advent of novel polymers and devices, the popularity of oral CR systems, specifically, is on the rise (Fassihi and Ritschel, 1993). Another impetus for the development of oral CR systems is the improved understanding of formulation and physiological limitations as applicable to oral drug delivery. Barriers to optimal formulation include the physico-chemical properties of the drug such as solubility, polymorphism, compressibility and its crystalline/amorphous nature. Physiological constraints mainly relate to the inherent nature of the gastrointestinal tract with regards to permeability, transit time, pH and effects of the fed and fasted state.

Economic considerations come into play with the expiration of existing patents as well as the prohibitively high cost of developing new chemical entities. The rationale is to formulate CR dosage forms of approved drugs in order to improve therapeutic efficacy rather than develop new drugs which will have to undergo years of testing before being approved by the relevant authorities.

CR systems generally produce two types of plasma drug level – time profiles: the rate-controlled type and the time-controlled (delayed release) type (Hirayama and Uekama, 1999). The rate-controlled profiles can be further subdivided into immediate-release, prolonged-release and modified-release. These profiles are illustrated in Figure 1.1 (a-d).

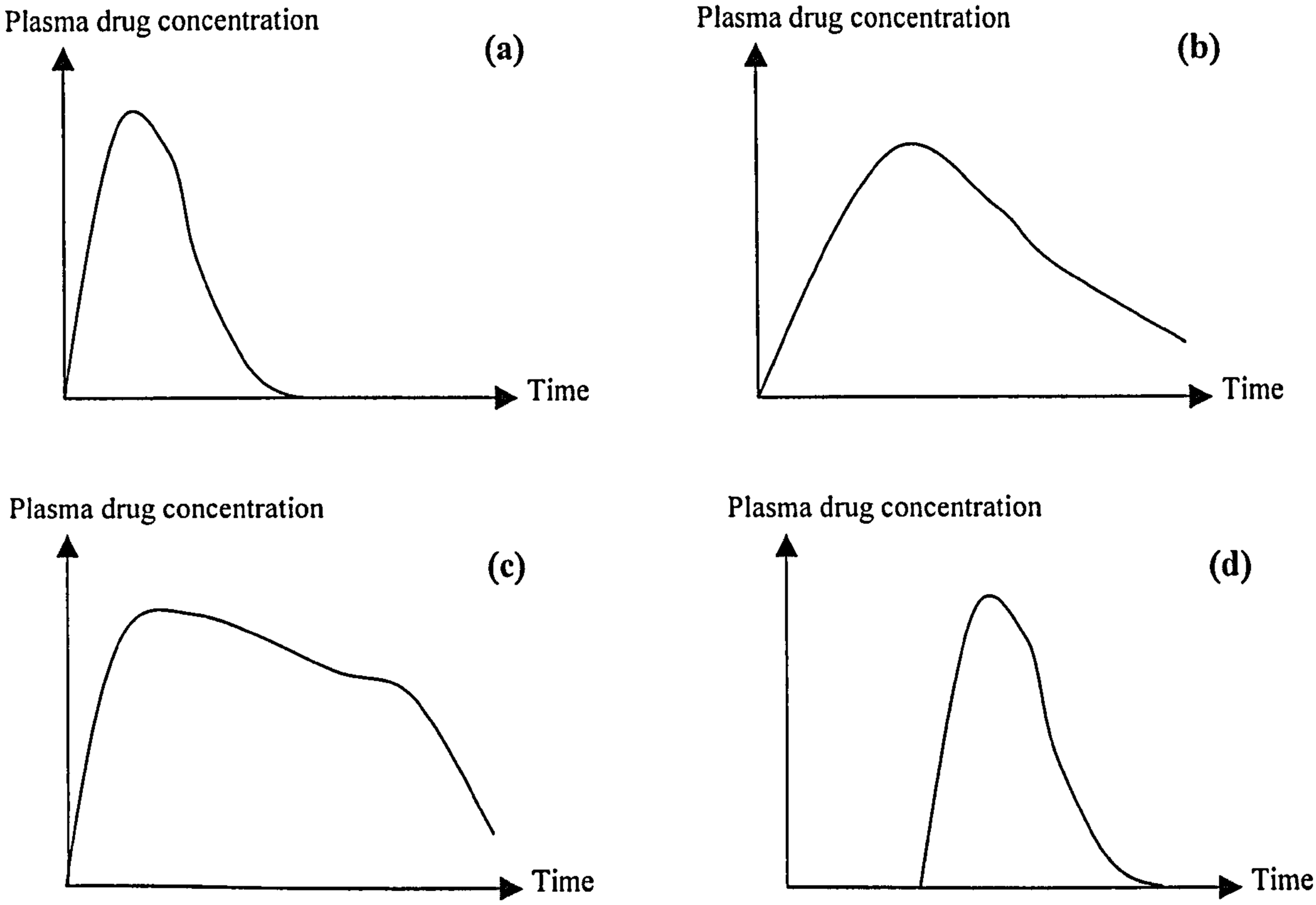

Figure 1.1: Typical drug release profiles following drug administration from dosage forms with (a) immediate release, (b) prolonged / sustained release, (c) modified release and (d) delayed release characteristics.

In order to give a brief overview of CR systems they are classified here in terms of their mechanism of drug release. Langer (1980) puts them into four categories, some with further subcategories, shown in Figure 1.2. It must be noted however, that not all systems can be clearly defined in one category as some may depend on more than one mechanism for drug release.

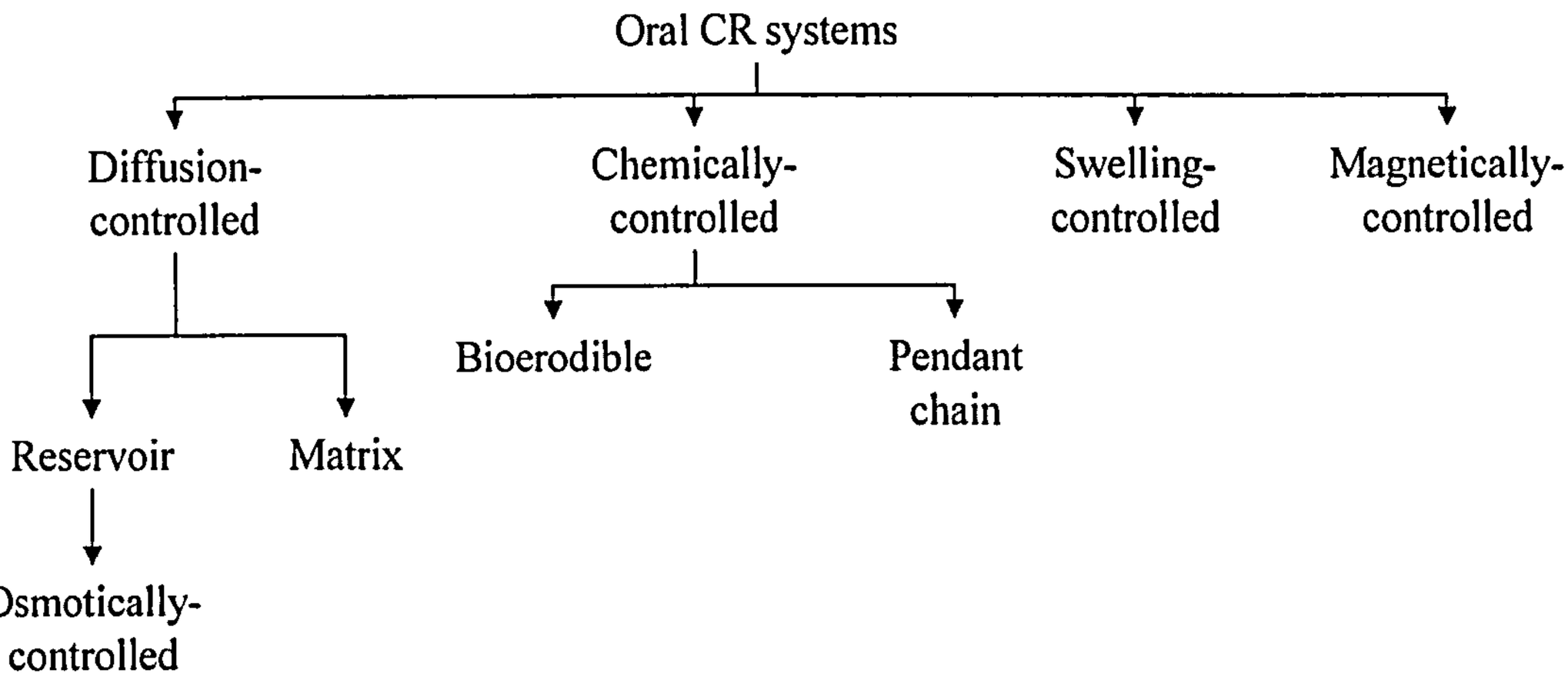

Figure 1.2: Classification of oral CR systems based on drug release mechanisms.

1.1.1 Diffusion-controlled systems

The rate-limiting step in this type of CR system, as evident from the name itself, is the diffusion of drug through polymer. Two subdivisions exist: one in which the drug is separate from the polymer and another where the drug is dispersed in the polymer. By definition, diffusion is the transfer of matter from one region to another, usually from an area of high concentration to one of lower concentration, as a result of random molecular motion. To achieve a constant release rate, three parameters need to, theoretically, be kept constant: diffusional pathlength, area for diffusion and drug concentration (Lee and Robinson, 1978).

Drug release from these systems generally abides by Fick's first law (Equation 1.1), which describes the diffusion process at steady state i.e. the concentration gradient does not change with time. It can be rewritten as Equation 1.2 when the diffusion coefficient and membrane thickness are assumed to be constant.

$$J = -D\frac{dC_m}{dx} \quad \textbf{(Equation 1.1)}$$

$$J = D\frac{\Delta C_m}{l} \quad \textbf{(Equation 1.2)}$$

Where J = flux (mol m^{-2} s^{-1}), C_m = drug concentration in membrane (mol m^{-3}), dC_m/dx = concentration gradient where x is in m, D = drug diffusion coefficient in the membrane (m^2 s^{-1}) and l = membrane thickness (m).

D is a measure of the rate at which molecules move within the polymer. The value of D increases with increments in the environmental temperature and reduction in the molecular weight of the dissolving particle (solute). The concentration gradient reflects the total number of molecules undergoing transport at a given time. It must also be noted that the thickness of the membrane film is really the distance from the edge of the polymer sheet to a point in the matrix where undissolved drug particles exist (Thombre and Cardinal, 1990). This point gradually moves inward as the device is depleted of drug.

1.1.1.1 Reservoir systems

The basic structure of these systems is that of a drug core surrounded by a polymer (Figure 1.3a, b).

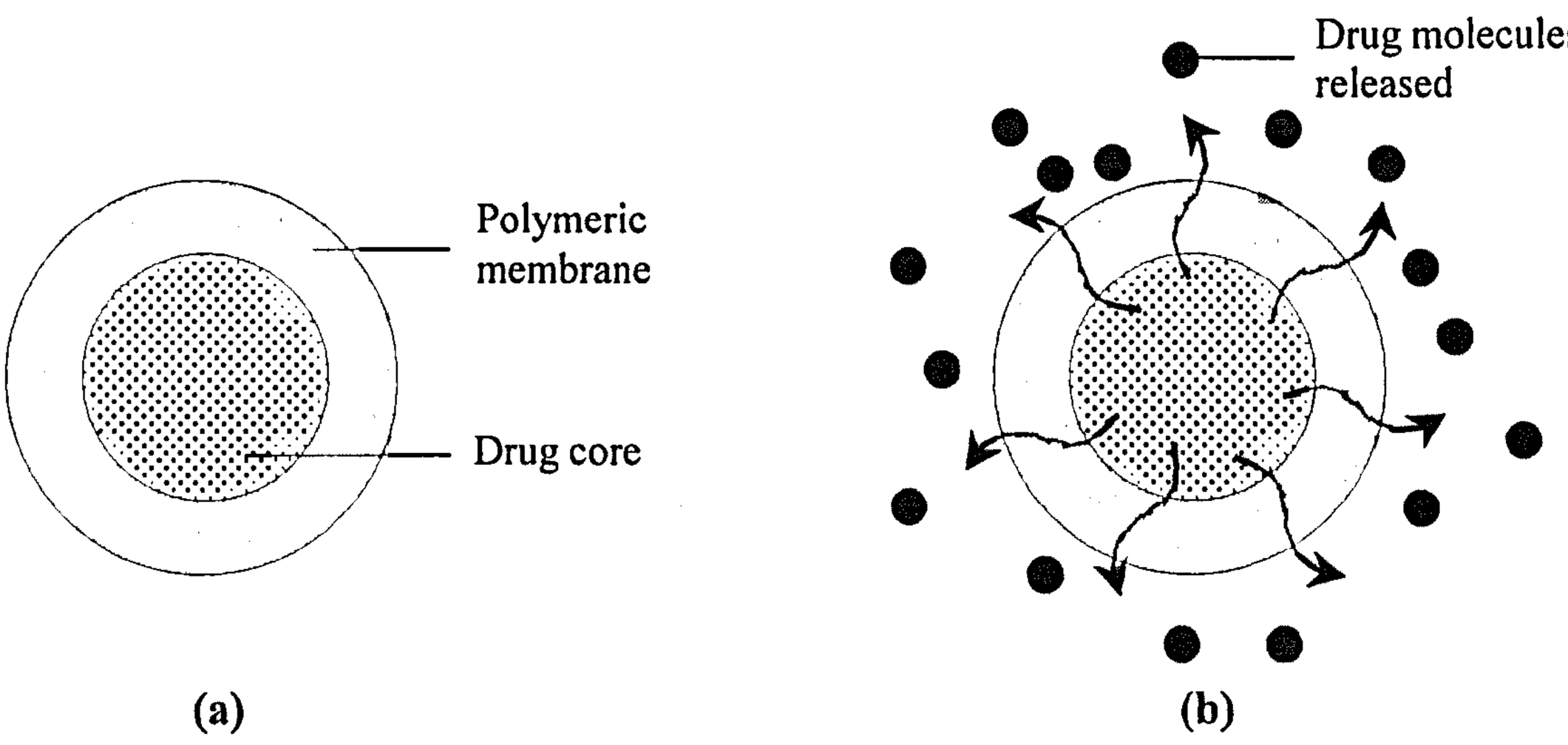

Figure 1.3: (a) Typical membrane-enclosed reservoir system; and (b) Diffusion of drug from core through polymeric membrane once in solution.

When considering permeation through membranes, the basic preposition is that, in thermodynamic terms, pressure, temperature, concentration and electromotive force are intercalated and the chemical potential gradient is the main driving force for movement of the permeant (Wijmans and Baker, 1995). A solution-diffusion or

partition mechanism governs drug release whereby solute dissolves in the membrane, then diffuses along and between polymer segments.

Derived from Fick's first law, Equation 1.3 describes the release rate from a typical reservoir device (Thombre and Cardinal, 1990).

$$M_t = \frac{ADK_dC_at}{H} \qquad \textbf{(Equation 1.3)}$$

M_t = amount released at time, t (mol)

A = surface area (m^2)

D = drug diffusion coefficient ($m^2\ s^{-1}$)

K_d = partition coefficient of drug between polymer and reservoir (unitless)

C_a = saturation solubility of drug in reservoir compartment (mol m^{-3})

H = thickness of diffusing layer (m)

t = time (s)

This equation is based on the assumptions that steady state and sink conditions exist and that the polymer coat is homogeneous and non-porous. In this type of system, transport is assumed to occur only within the polymer, not through solvent-filled channels within the film. If the drug loading in the polymer film is high or if porosigens (materials that dissolve and diffuse over time) are added to the system, molecules are able to diffuse out through these channels which develop when the porosigens create void spaces that eventually fill with solvent.

The assumption that the rate of drug diffusion through the membrane is the sole determinant of drug release does not hold true in practice. There exists a boundary diffusional layer on the outer surface of the membrane adjacent to the surrounding solvent which effectively constitutes a "dead zone" and hinders molecular transport. The thickness of this zone depends on the rate of stirring or agitation of the surrounding medium for dissolution.

While this type of system can be quite easily designed for near-zero order release, at least two scenarios may arise, resulting in the achievement of zero order release only

in the steady state. Firstly, if the device is prepared and used immediately, the membrane has yet to be saturated with drug and concentration of drug in the membrane is therefore far below the saturation solubility of the drug in the membrane. A time lag prior to initial drug release is then observed, dependent on the rate at which equilibration of drug concentration between the core and the polymeric membrane occurs, establishing a concentration gradient to drive diffusion.

If however, the device is stored for a period of time before administration, an initial burst release is to be expected as the membrane has been gradually saturated with drug. The molecules on the outer surface of the membrane dissolve in the solvent and quickly diffuse out.

While reservoir systems are able to produce near-zero order release rates at steady state, their main disadvantage is that "dose-dumping" is a serious threat to the patient's well being if a leakage arises from poor membrane integrity and the entire dose is released at once.

Drug delivery by diffusion-controlled membrane-enclosed reservoir systems is undoubtedly flexible and dependable but the rate of delivery is limited in magnitude, with an upper limit of about $0.2\mu gcm^{-1}hr^{-1}$ (Theeuwes, 1975). This, and other constraints as described above, led to the advent of a spin-off: the osmotically-controlled device. A core of drug and osmotically-active solid agent is encapsulated by a rate-controlling, semi-permeable membrane in which a single, minute orifice is (usually) laser-drilled.

The mechanism of drug release is as follows: the osmotic pressure gradient due to the high osmotic force within the system results in water ingress, which dissolves the drug. Consequently, the drug solution is pumped out through the orifice in amounts volumetrically equal to the volume of solvent uptake, provided the internal volume is constant. Hence the rate of drug delivery is most affected by the osmotic pressure of the internal environment of the system, the membrane permeability and the size of the orifice.

Bearing in mind that controlling water uptake effectively controls the rate of drug delivery, a greater osmotic pressure generated by the use of more osmotically-active core excipients increases the rate of pumping out drug solution. The hydrostatic pressure difference is affected by the size of the orifice, whereby dimensions that are too small result in the build up of hydrostatic pressure internally, impeding the achievement of a zero order release rate in two ways. Firstly, excessive internal hydrostatic pressure decreases the net osmotic influx, and secondly, it increases the volume of the system (Theeuwes, 1975). During the time period of volume increment, the outflow is less than the inflow, therefore depressing the release rate. However, while the orifice size must be sufficiently large, it must also not exceed an upper limit in order to minimise the possibility that the drug simply diffuses out rather than being pumped out at a controlled rate. The membrane permeability determines the rate of solvent influx and a higher permeability contributes to increased delivery rates.

Two versions of the basic osmotic device exist: the miniosmotic pump and the elementary osmotic pump (Figures 1.4a and b).

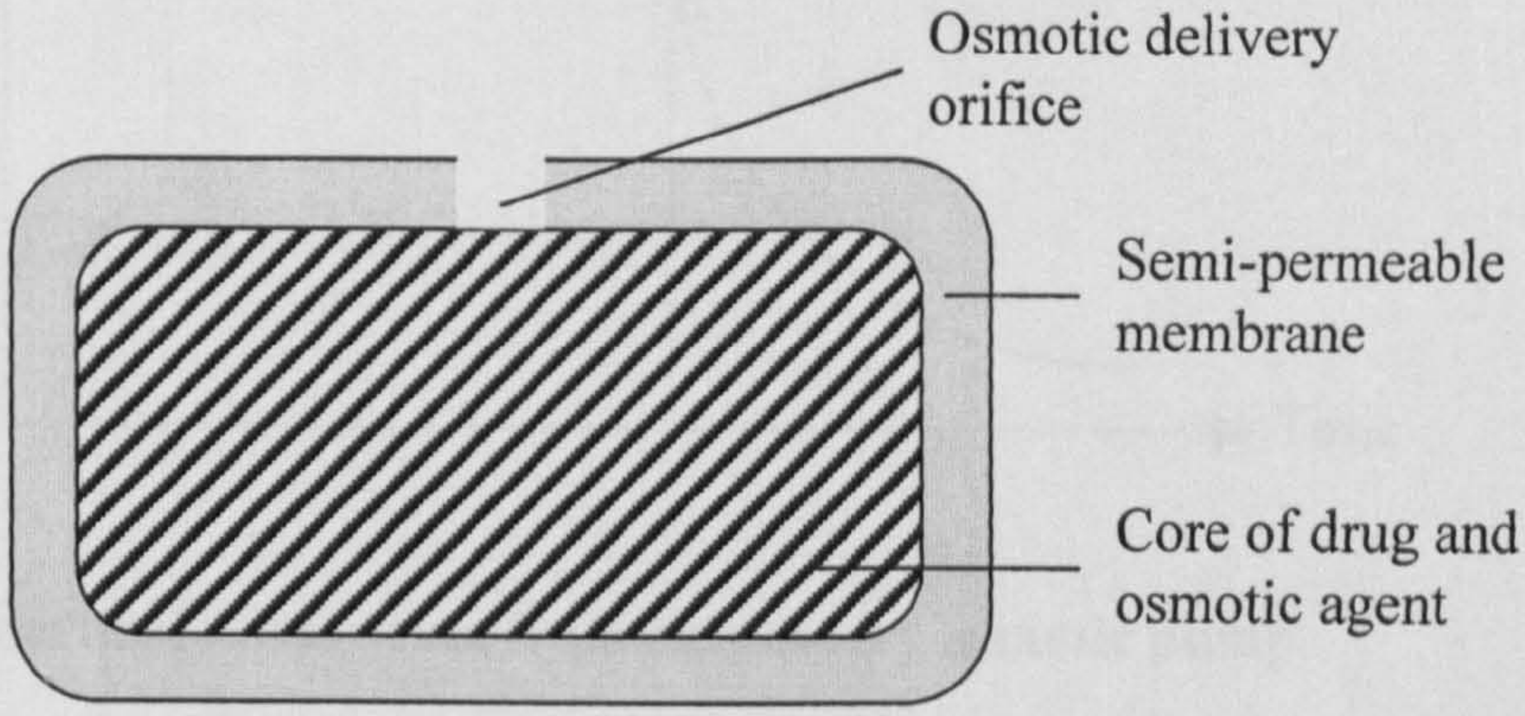

Figure 1.4(a): Cross-section of elementary osmotic pump.

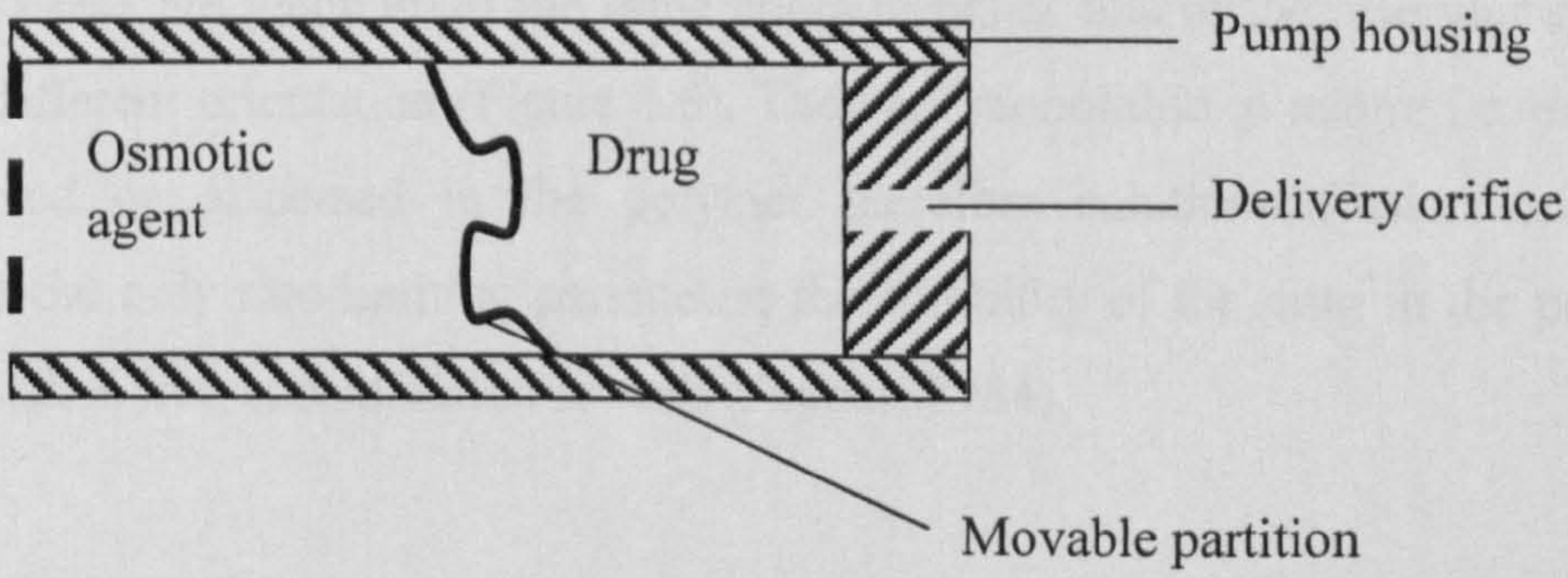

Figure 1.4(b): Miniosmotic pump.

The miniosmotic pump separates the drug and the osmotic agent with a movable partition, while in the elementary osmotic pump, the drug and the osmotic agent are mixed together to form the core.

Delivery rate is relatively easily and accurately predicted while considering influences from other factors. It is important to appreciate that the delivery rate is independent of stirring rate, pH and delivery port sizes, within predictable limits (Theeuwes, 1975). Excellent *in vivo – in vitro* correlations are obtained from these systems.

Zero-order release is possible as long as the drug concentration in the osmotic core is less than saturation solubility; once it dips below this value, the release rate declines exponentially, as shown in Figure 1.5.

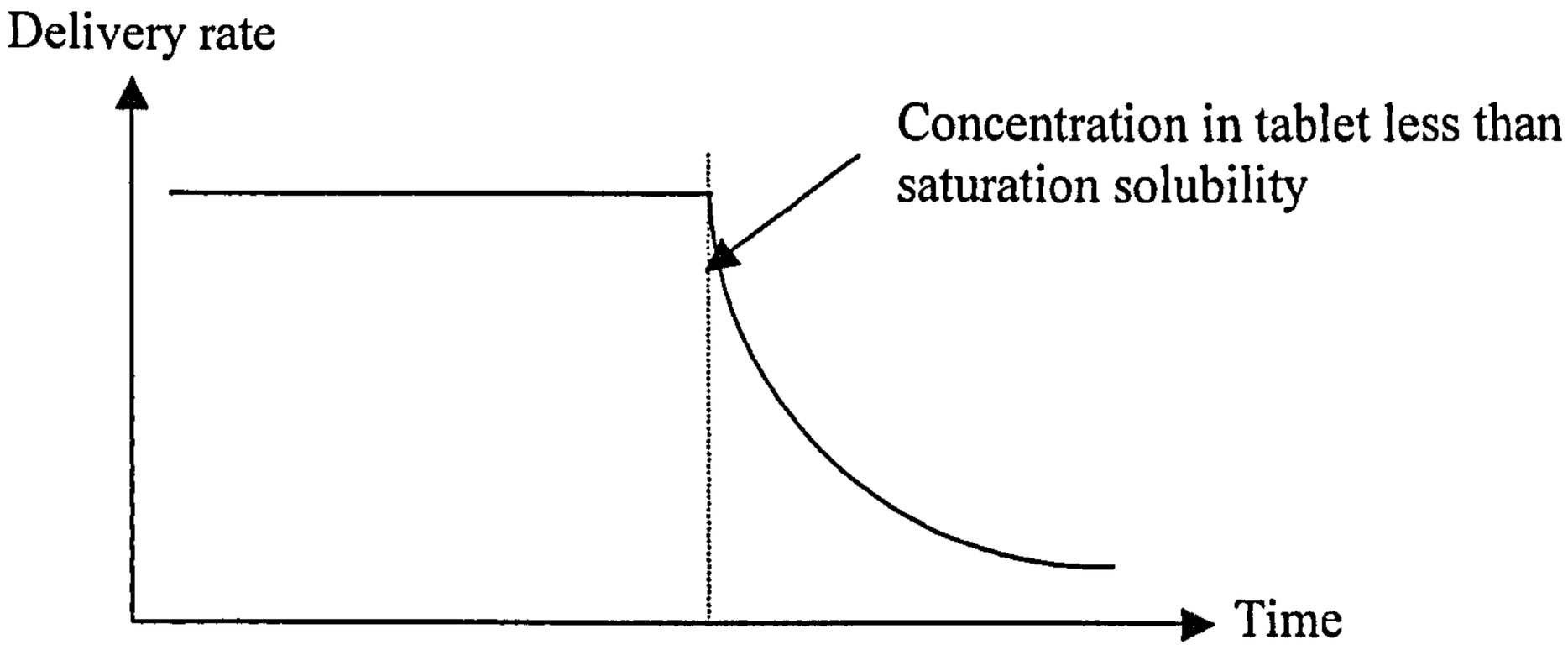

Figure 1.5: Theoretical release rate from elementary osmotic pump.

1.1.1.2 Matrix systems

Matrix systems are made up of the same components as that of the reservoir systems but in a different orientation (Figure 1.6). They are monolithic in nature i.e. the drug is dissolved or dispersed in the polymer therefore solution-diffusion does not constitute the only rate-limiting parameter; the solubility of the drug in the polymer has to be taken into consideration as well (Peppas, 1984).

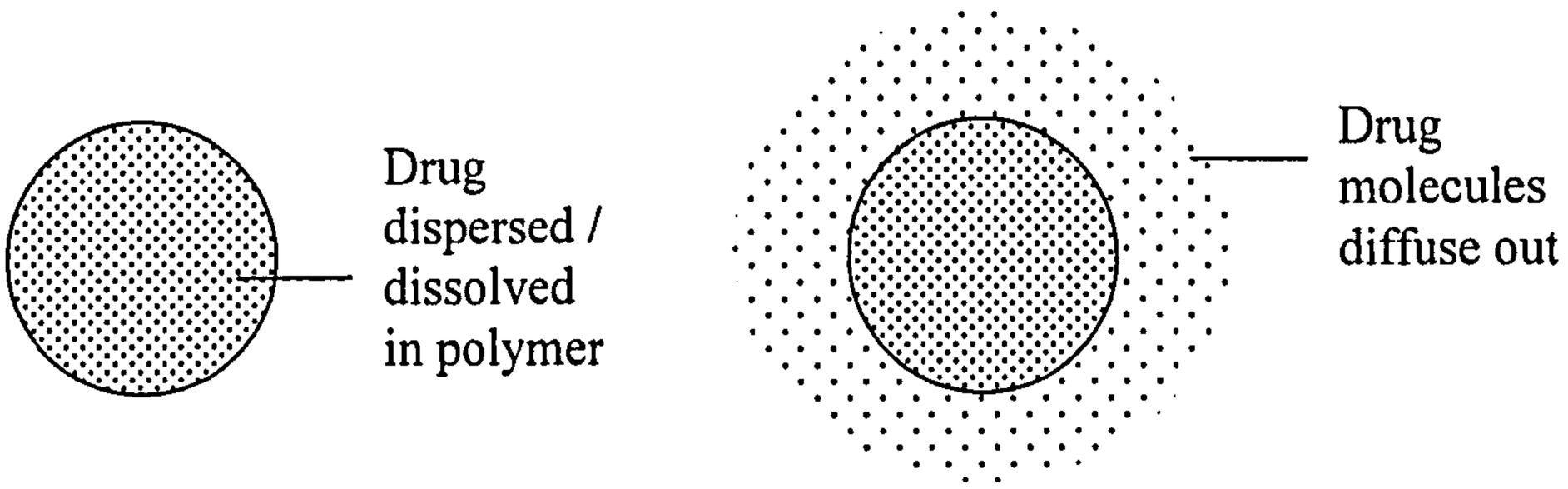

Figure 1.6: Idealised diagram of cross-section of spherical / cylindrical matrix system in the (a) dry state and (b) when immersed in water (Langer, 1980).

Different mathematical models are applied to the system depending on whether the drug is dissolved or dispersed in the polymer, and when it is dispersed, whether the drug is loaded above or below its saturation solubility in the polymer. Nevertheless, the basic diffusion mechanism still applies. As the dosage form comes into contact with a liquid, the liquid enters the polymer and dissolves the drug allowing the drug to diffuse out through the liquid in the dosage form.

When the matrix-type system is placed in an aqueous environment, hydration of the polymer occurs from the outside in and results in the formation of two states of polymer within the same system. At the outermost region, the polymer is hydrated and is hence in a rubbery state, whereas moving inwards towards the core, the polymer remains in the dry, glassy state (Figure 1.7).

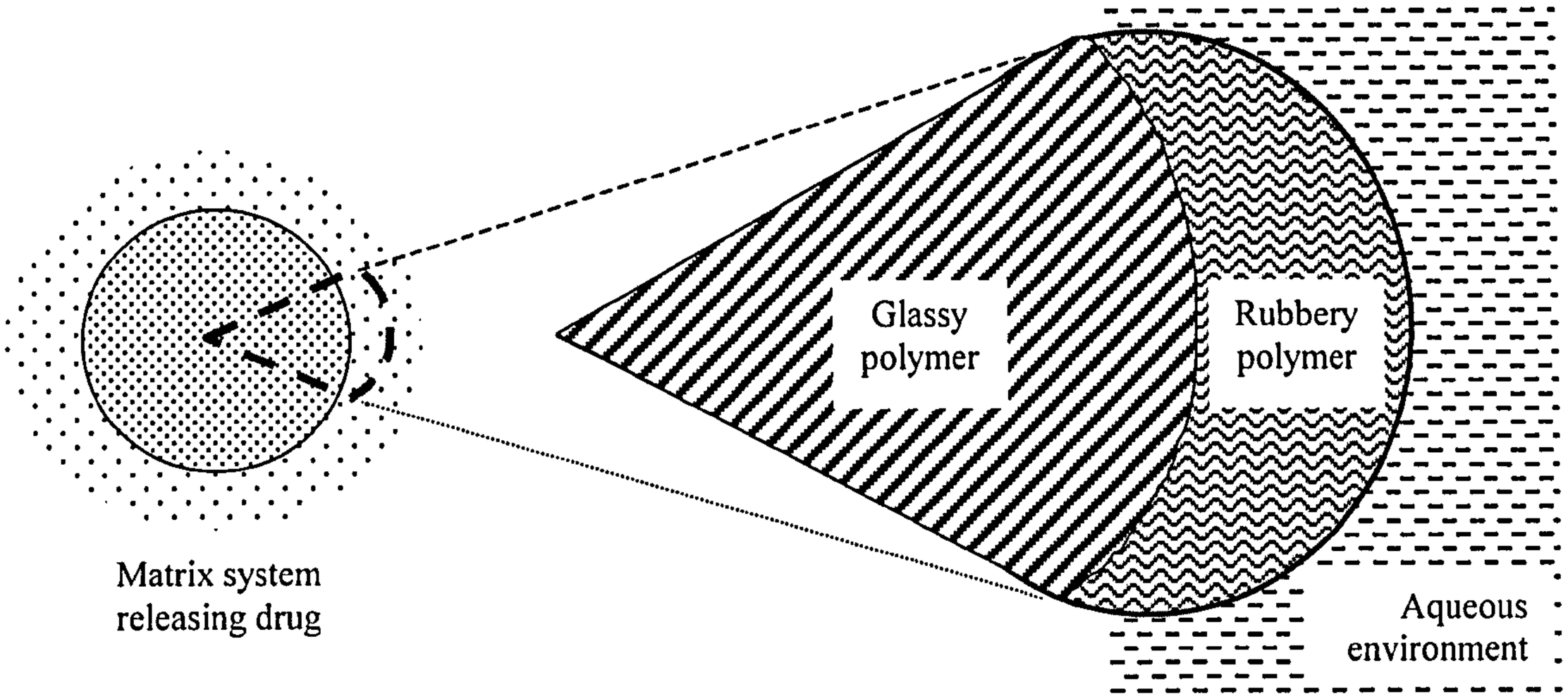

Figure 1.7: Diagram of glassy and rubbery regions within a matrix-type dosage form.

Drug molecules in the different states of polymer tend to follow slightly different mechanisms of diffusion mainly due to the physical properties of the two polymer states. When rubbery, it responds rapidly to changes in its condition i.e. the polymer chains are able to adjust very rapidly to the presence of liquid molecules (Vergnaud, 1993). Here the diffusion rate is far lower than the rate of relaxation of polymer chains and the diffusion is Fickian in nature. Under these conditions, the diffusion is of the Case I type. At time, *t*, the amount of diffusing substance absorbed or desorbed, M_t, can be determined from Equation 1.4:

$$M_t = k\sqrt{t} \qquad \textbf{(Equation 1.4)}$$

where *k* is a constant dependent on total drug loading, polymer shape and diffusivity. This only holds true when M_t is significantly lower than the total drug loading.

Case II diffusion occurs mainly when the polymer is in the glassy state whereby the rigidity of the polymer chains in space restricts the decay of the stress generated from stretching the polymer. Therefore, the rate of relaxation of the polymer is far lower than the rate of diffusion of solute molecules. The amount of liquid absorbed at time, *t* (M_t), is given by Equation 1.5.

$M_t = kt$ **(Equation 1.5)**

While Case II diffusion is still of the Fickian type, Case III is regarded as non-Fickian or anomalous. This occurs when the relaxation rate is equal to the diffusion rate. M_t is now directly proportional to t^n (where $\frac{1}{2} < n < 1$) in the relationship shown in Equation 1.6.

$M_t = kt^n$ **(Equation 1.6)**

Reservoir-dispersed and porous matrix systems are described by Cardinal (1984). The former is simply a combination of both the reservoir and matrix characteristics whereby the drug is dispersed in the polymer and encased by a polymer of lower permeability than the inner-core matrix, acting as a further rate-limiting barrier to water ingress. Porous matrix devices are so named because of the continuous macroscopic channels or pores that develop in the polymer matrix once the dissolved drug leaches out of the system. Therefore, release rates are dependent on transport via these solvent-filled channels as well as diffusion through the polymer.

By comparison, matrix-type systems are generally easier to manufacture with a lower degree of quality control required than reservoir systems due to the decreased risk of dose-dumping (Huang and Brazel, 2001).

1.1.2 Chemically-controlled systems

In the previous section, the mechanism of drug release relied mainly on controlling physical parameters. There exist drug delivery systems that are dependent on the making and/or breaking of chemical bonds for drug release. Currently there are two types of chemically-controlled systems: the bioerodible and the pendant-chain.

1.1.2.1 Bioerodible systems

Bioerodible systems are similar to matrix systems in that the drug is dispersed uniformly within the polymer, but unlike their matrix-type counterparts, bioerodible

systems behave exactly as their name implies: they erode and disappear over time. Figure 1.8 illustrates how this process occurs.

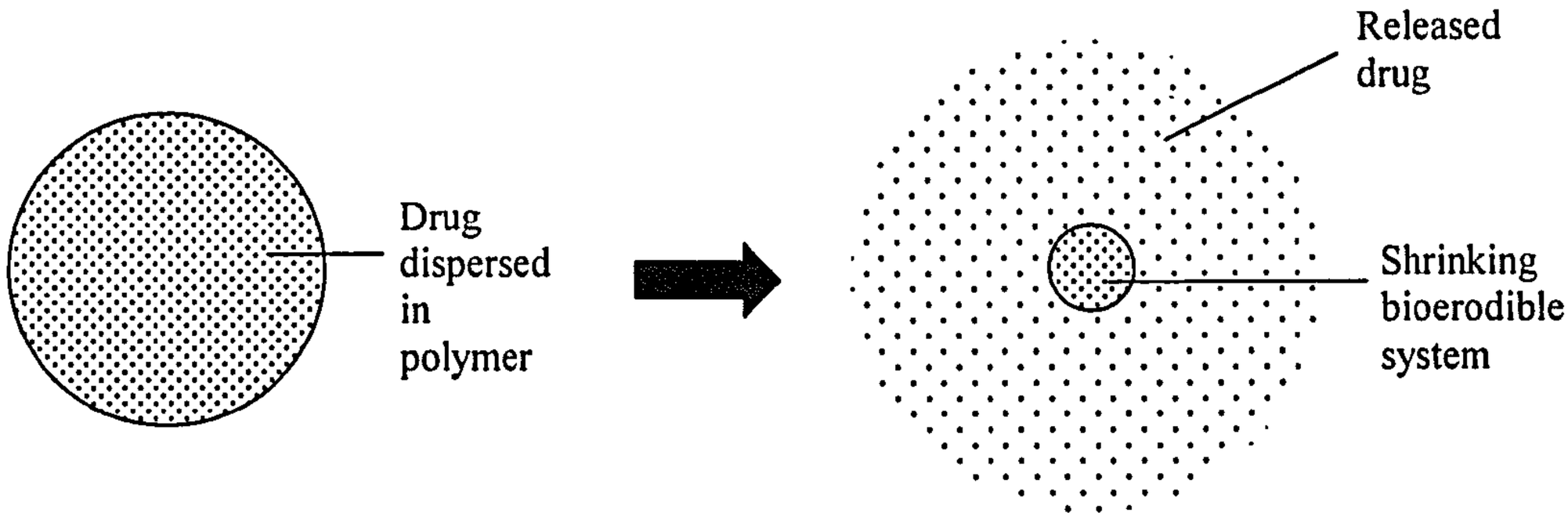

Figure 1.8: Idealised diagram of drug release from a bioerodible system when immersed in water.

These polymeric systems offer the advantage over conventional nonbiodegradable matrix systems in that they are eventually absorbed by the body. This necessitates the prerequisite that the degradation products must be non-toxic, non-immunogenic and non-carcinogenic.

In an ideal situation, drug release from this type of system should be solely dependent on erosion of the polymer, allowing drug molecules to dissolve and diffuse into the surrounding medium only as they become exposed to the aqueous environment. However, in practice, this does not occur as simple dissolution-diffusion of the drug may also contribute to drug release.

In order to achieve near-zero order release, the effect of drug dissolution on drug release rate must be minimised. This can be achieved by choosing a drug that is suitable for this type of system i.e. one that has limited permeability and solubility within the polymer matrix (Thombre and Cardinal, 1990). Furthermore, the level of drug loading should also be low. A highly crystalline polymer (c.f. in Type II diffusion in glassy polymers) will also limit the effect of drug dissolution and diffusion on drug release.

Classifying bioerodible systems by virtue of the mechanism of polymer erosion seems to be a convenient way of describing these systems in detail. Heller (1984) names them Type 1, 2 and 3, which in fact are not segregated *per se* in practice but most bioerodible systems release drug via a combination of these three mechanisms.

Type 1 erosion is displayed by water-soluble polymers which have been made non-soluble by cross-linking them with chains that are susceptible to hydrolysis. When initially placed in an aqueous environment, the polymer chains are mobile, causing swelling of the network but only to a limit permissible by the cross-links present. Hydrolysis of the cross-links results in decreasing cross-link density and the matrix swells until it eventually dissolves once the majority of the cross-links are cleaved (Figure 1.9).

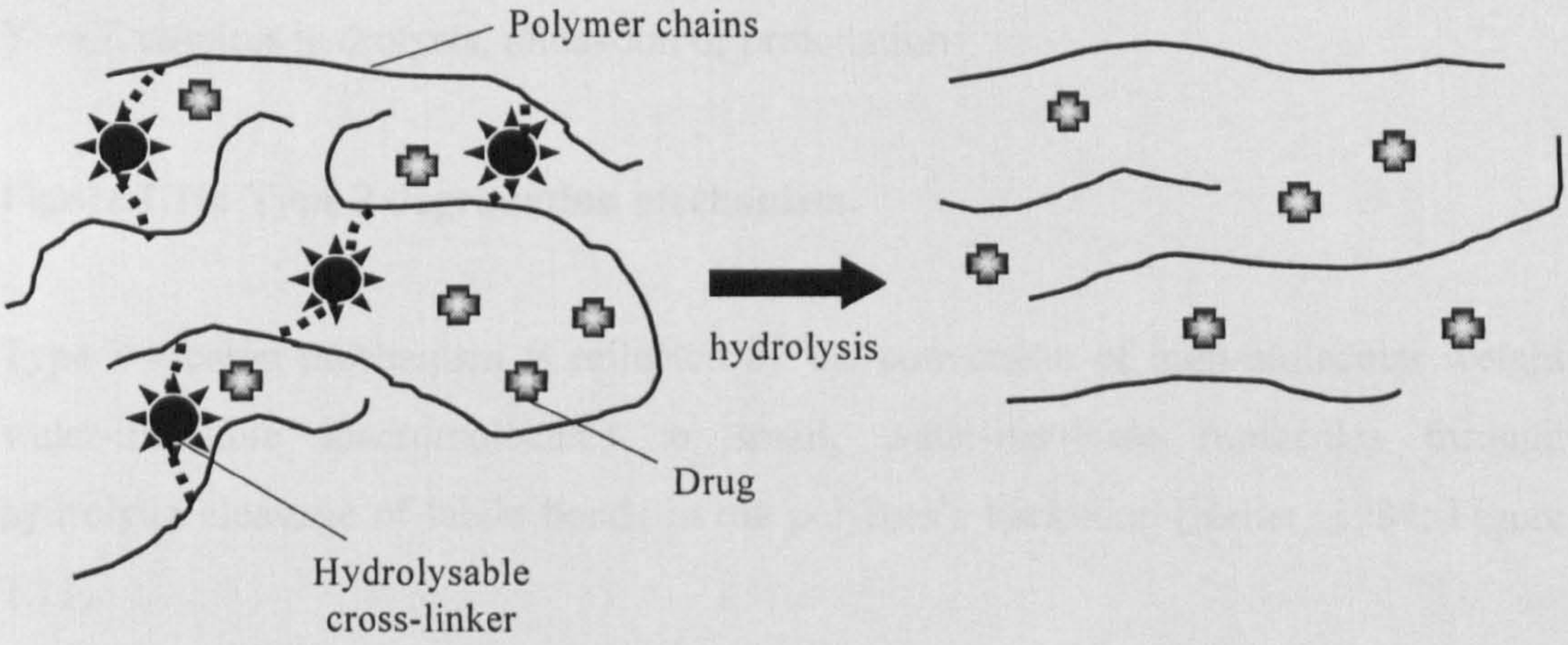

Figure 1.9: Type 1 degradation mechanism.

A system predominantly reliant on this mechanism has at least two possible failings. One, initial matrix swelling may not be tolerated in certain cases because of the increase in actual physical dimensions. Secondly, since the polymer is itself water-soluble (minus the cross-links), the swollen system is in fact a hydrogel hence is completely permeated by water. Therefore, drugs of low molecular weight and of appreciable hydrophilicity are poor candidates for this system.

Nevertheless, applications have been found whereby the drug to be delivered is of low solubility and/or is a macromolecule that becomes physically entangled with the

cross-linked hydrogel matrix thereby restricting its outward diffusion despite its inherent water solubility.

Type 2 erosion proceeds through conversion of a water-insoluble polymer to a water-soluble one by hydrolysing, ionising or protonating a pendant group (Figure 1.10). No significant dimensional changes are observed because backbone cleavage does not happen.

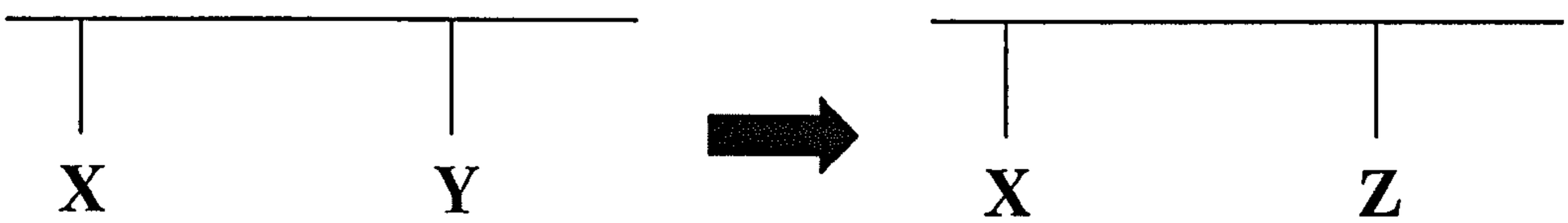

X = hydrophobic substituent

Y → Z requires hydrolysis, ionisation or protonation

Figure 1.10: Type 2 degradation mechanism.

Type 3 erosion mechanism is reflected by the conversion of high-molecular weight water-insoluble macromolecules to small, water-insoluble molecules through hydrolytic cleavage of labile bonds in the polymer's backbone (Heller, 1984; Figure 1.11).

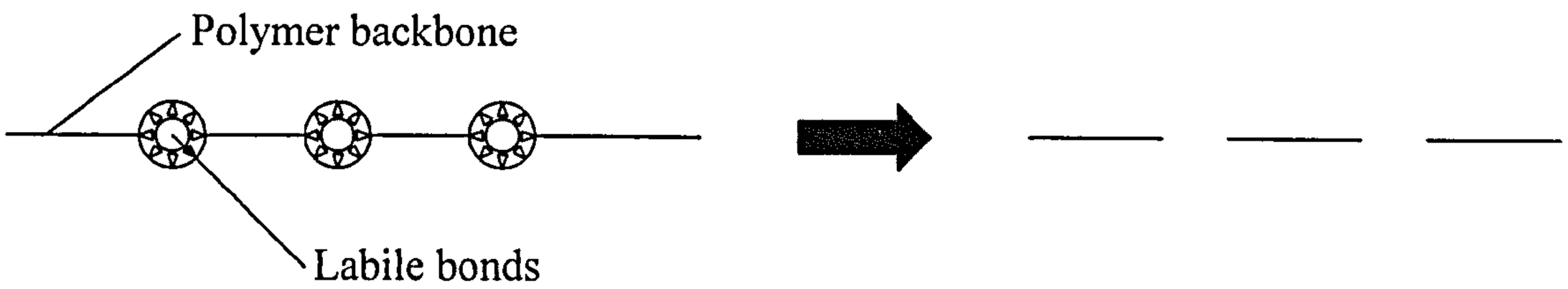

Figure 1.11: Type 3 degradation mechanism.

This type of erosion mechanism has been applied in (a) diffusional systems which are encapsulated by an eroding rate-limiting barrier, (b) bioerodible microcapsules, (c) monolithic devices in which the drug is dispersed or dissolved and (d) bioerodible polymers with active groups chemically bonded to the polymer backbone. The most widely used polymer in these systems is polylactide-co-glycolide.

After considering these three types of erosion mechanisms separately and appreciating that in practice, they do not operate independently of each other within a system, it is also necessary to examine the actual mechanism of drug release from specific bioerodible systems. If the bioerodible polymer component of the system is present as a rate-limiting barrier membrane surrounding the drug core, it is foreseeable that membrane thickness is one of the main controllers of drug release rate.

Monolithic devices with drug dispersed in the bioerodible polymer network are usually diffusion and/or erosion-dependent. If diffusion predominates, the Higuchi model explains the release kinetics well, i.e. the drug at the outermost surface diffuses out rapidly leaving behind a drug-depleted layer increasing gradually in thickness. This layer provides resistance to further drug diffusion hence the release rate declines continuously.

In cases where the drug is well immobilised in the solid matrix so that diffusion is limited and erosion is relatively fast, erosion thus becomes the major mechanism for drug release. However, two types of erosion exist: homogeneous and heterogeneous (or more commonly known as surface erosion). While at first glance, homogeneous erosion i.e. hydrolysis occurring at a similar pace throughout the matrix may seem desirable, close inspection reveals that this is not the case. As a result of overall matrix changes throughout the process, permeability of drug in polymer may increase with time. Therefore, initially decreased release rates as predicted by Higuchi's relationship will be superseded by increased drug release when polymer permeability offsets this decline. In extreme cases, if the matrix completely disintegrates before the drug reservoir is exhausted, a burst release will be observed. Clearly it will be more difficult to control drug release in the case of homogeneous erosion.

A heterogeneous, or surface, erosion process limits the erosion to the outermost surface allowing for more predictable near-zero order release rates provided the erosion is uniform, although as erosion continues, the surface area of the system becomes significantly lower and release rate decreases.

1.1.2.2 Pendant-chain systems

These systems are chemically constructed to comprise a polymer backbone to which drug molecules are attached. Drug release proceeds by way of hydrolytic or enzymatic cleavage, thereby liberating the drug from the polymer for consequent absorption (Figure 1.12).

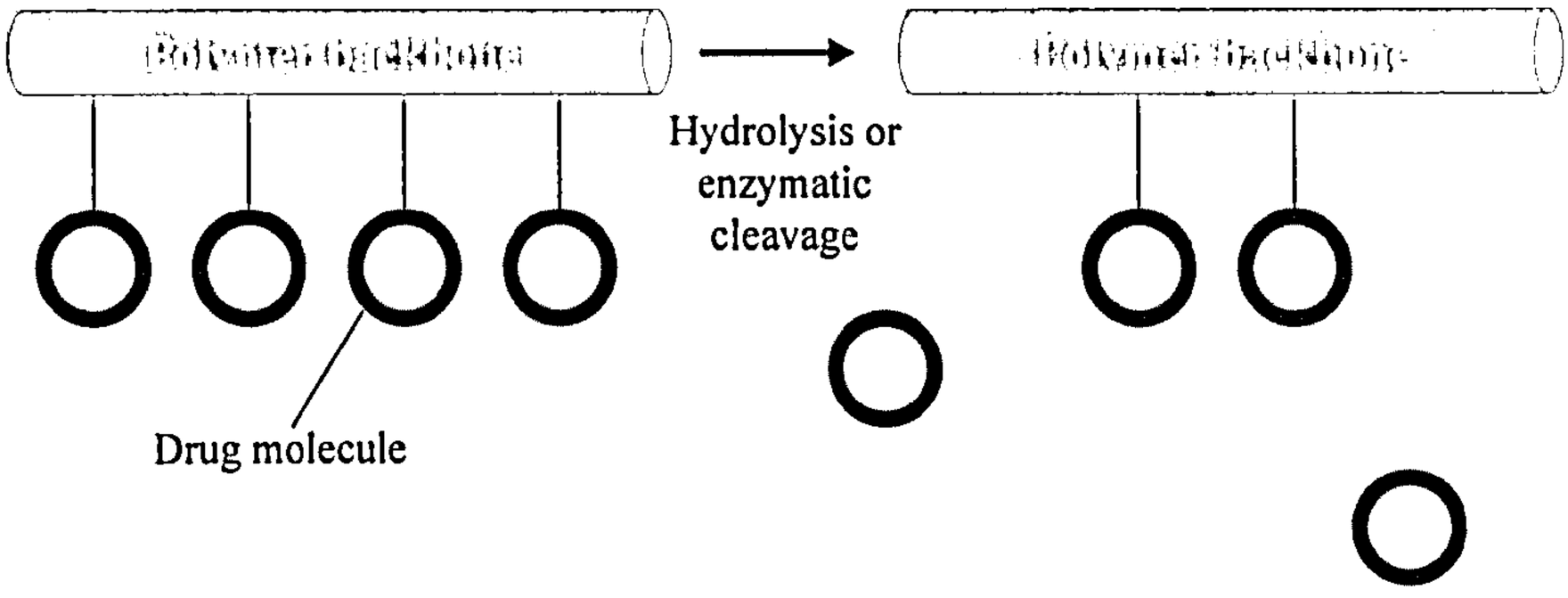

Figure 1.12: Drug release from pendant-chain systems.

Both short and long term therapeutic applications are possible with these systems; the time span being fundamentally dependent on (a) the susceptibility of the binding group to cleavage and (b) the solubility of the polymer backbone in the media within which it is contained.

1.1.3 Swelling-controlled systems

Swelling upon hydration has been the mainstay in many controlled release systems as a means of regulating e.g. tablet disintegration and capsule rupture, and therefore, drug release rate. The most attractive facet of swelling-controlled release systems is the relative ease of delivering drugs at constant rates over an extended period of time.

Drug delivery rate is determined by the net effect of three main driving forces for transport within these systems i.e. penetrant/solvent concentration gradient, polymer stress-relaxation gradient and osmotic forces (which are due to the high concentration of drug; Brazel and Peppas, 1999). These systems are also capable of delivering drugs

according to zero-order kinetics through the manipulation of the transport properties of the device and the synthesis of novel, specific polymer carriers.

The swelling of several cellulose derivatives such as hydroxypropylmethylcellulose, methylcellulose and hydroxypropylcellulose has been studied in order to ascertain its mechanistic and molecular aspects. This is of particular interest as it has been identified that rate and mechanism of drug release from these polymers are highly dependent on the rate and extent of swelling, subsequent drug diffusion through the outer layer and the change in matrix area exposed to water (Kojima *et al.*, 1998).

The swelling process (Figure 1.13) has been investigated by many workers and many valuable contributions have been made in this area.

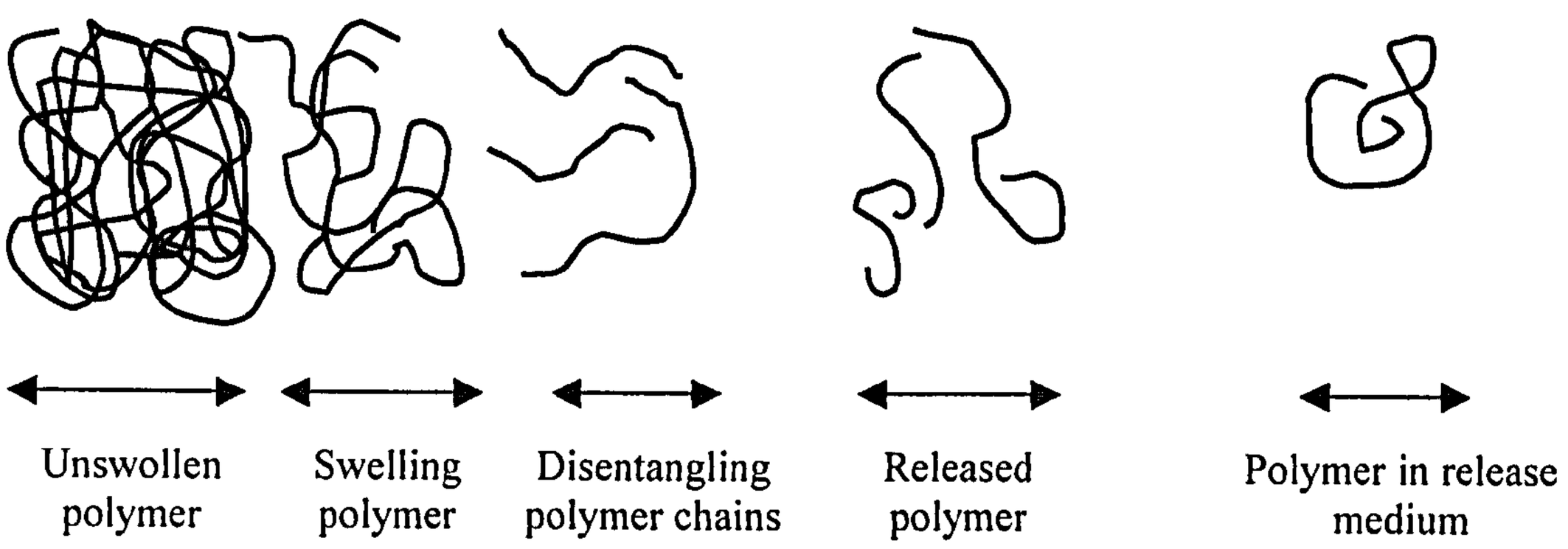

Figure 1.13: The swelling process.

The basic mechanism of drug release for most swellable and gel-forming matrices is the fast hydration upon contact with water resulting in the formation of a diffusion-limiting pseudogel layer at the polymer-water interface which then retards drug release and impedes further water penetration. Design and selection of a polymer with optimal properties for a controlled release system necessitates in-depth understanding of factors relating to the structure and morphology of the polymer and its properties related to its interaction with the aqueous environment (Panomsuk *et al.*, 1996).

The first step of the mechanism, water uptake, is possibly rate-limiting and can be analysed mathematically by the Washburn equation which describes the penetration of liquid into a tablet (Equation 1.7).

$$\frac{dL}{dt} = \frac{r\gamma\cos\theta}{4\eta} \qquad \textbf{(Equation 1.7)}$$

Where L is the penetration length of the capillary (m), t the time over which the penetration was measured (s), r the radius of the capillary (m), η the viscosity of the liquid (Nsm^{-1}), θ the angle of contact (°) and γ the surface tension of the liquid (Nm^{-1}).

Examples of swelling-controlled systems will be discussed in Section 6.1.

1.1.4 Magnetically-controlled systems

In these systems, drug and small magnetic beads are contained within a polymer matrix. Application of an external oscillating magnetic field greatly increases the rate of drug release over and above the basal rate which is mostly dependent on simple diffusion of drug particles out of the matrix (Langer, 1980). The actual mechanism of drug release for this type of system has yet to be ascertained. However, it is possible that the external magnetic field causes the beads to alternately compress and expand channels within the polymer matrix and decrease the structural integrity of the matrix thereby facilitating drug diffusion. However, none of these systems are currently being marketed.

The Enterion™ capsule was developed by Phaeton Research, Nottingham, UK, to enable targeting of drug delivery to specific regions of the gastrointestinal tract, mainly for absorption studies. The capsule itself is 32mm in length and is round at one end, containing a drug reservoir with a volumetric capacity of 1mL. Solid or liquid formulations can be filled into the capsule and subsequently sealed by a push-on cap fitted with a silicone O-ring.

Gamma scintigraphy is used to track the capsule *in vivo*, following the path of an embedded radioactive marker. Once it has travelled to the desired site, an oscillating magnetic field (in the low MHz region) is applied. The strength of this field is low enough to prevent absorption by human tissue but is sufficient to induce usable power in a tuned coil antenna located in the capsule wall. This power is conducted to a tiny

heater resistor which is in direct contact with a restraining filament composed of high tensile strength polymer. The heat generated softens and breaks the filament which is connected to a spring and the ejection piston. Hence the sudden increase in internal pressure forces off the O-ring sealed cap and quickly releases the drug. Movement of the piston operates a switch which diverts some of the electrical energy away from the heater and induces a weak radio signal of a specific frequency. The detection of the signal confirms that the capsule has opened successfully.

Oo *et al.* (2003) have used the Enterion^{TM} capsule to determine the pharmacokinetic variability of oseltamivir, used in the treatment of influenza A and B, when delivered to specific sites of the small intestine and colon. Once the capsule reached the desired target site, it was triggered to release the drug in the human volunteers and venous blood samples were collected at specific time points after that. They concluded that absorption from any region in the small intestine was comparable but absorption from the colon was significantly reduced. However, they proposed that the colonic absorption was sufficiently substantial to supplement small intestine absorption.

Fujimori *et al.* (1995) employed magnetism in an alternative manner. They developed a magnetic tablet which could be retained in the stomach by an externally applied magnetic field. Here, the aim was to control gastric emptying time in order to achieve more predictable or improved drug bioavailability. Bilayered magnetic tablets were made by separate direct compression i.e. the drug layer and the magnetic layer were prepared separately and then combined using a cyanoacrylate-type adhesive. They conducted their studies in beagle dogs and came to the conclusion that delaying gastric emptying time by magnetically retaining the formulation in the stomach improved bioavailability of the model drugs, acetaminophen and theophylline, and increased mean residence time.

These systems described here however are mainly used for investigational purposes e.g. absorption studies rather than as pharmacotherapy. The feasibility of magnetically-controlled systems is limited by the fact that an essential component is an external generator of a magnetic field.

1.2 Biopolymers used in oral drug delivery systems

Characterising polymers for use in oral drug delivery systems by virtue of their biodegradability and non-biodegradability is a convenient method as it alludes to the function of the individual polymers as well. Biodegradable polymers slowly degrade, erode and dissolve and these polymers are often used in dissolution-controlled and erosion-controlled systems. On the other hand, polymers that do not degrade are utilised to limit the diffusion and/or dissolution of the drug. Drug can be dispersed in the polymer or encapsulated by a film of the non-biodegradable polymer. Thombre and Cardinal (1990) further subdivided the polymers into the following classes.

1.2.1 Non-biodegradable hydrophobic polymers

These polymers are generally inert at the site of administration, exerting their effects mainly through the creation of a physical barrier to solvent ingress and solute dissolution and diffusion. Their insolubility and resistance to degradation result in their being eliminated intact upon passing through the gastrointestinal tract. Examples of these polymers include polyethylene vinyl acetate, polydimethyl siloxane, polyether urethane, ethylcellulose, cellulose acetate, polyethylene and polyvinyl chloride.

Schultz and Kleinbudde (1997) reported the design of a multiparticulate delayed release system consisting of a water-soluble core film-coated with cellulose acetate. Upon water ingress, internal volume increases and the pressure generated results in the formation of pores through which the dissolved drug diffuses out.

Khan *et al.* (2000) devised a gastrointestinal therapeutic system (GITS) in the form of an osmotically-controlled coated tablet for the delivery of captopril. Cellulose acetate (CA), applied as a pseudolatex (definition in Section 1.8.2.2), was used as a film coat while the core of the tablet was a bilayer, containing a drug and an osmotic layer (Figure 1.14). An orifice was pierced through the CA layer to allow for controlled pumping out of drug solution.

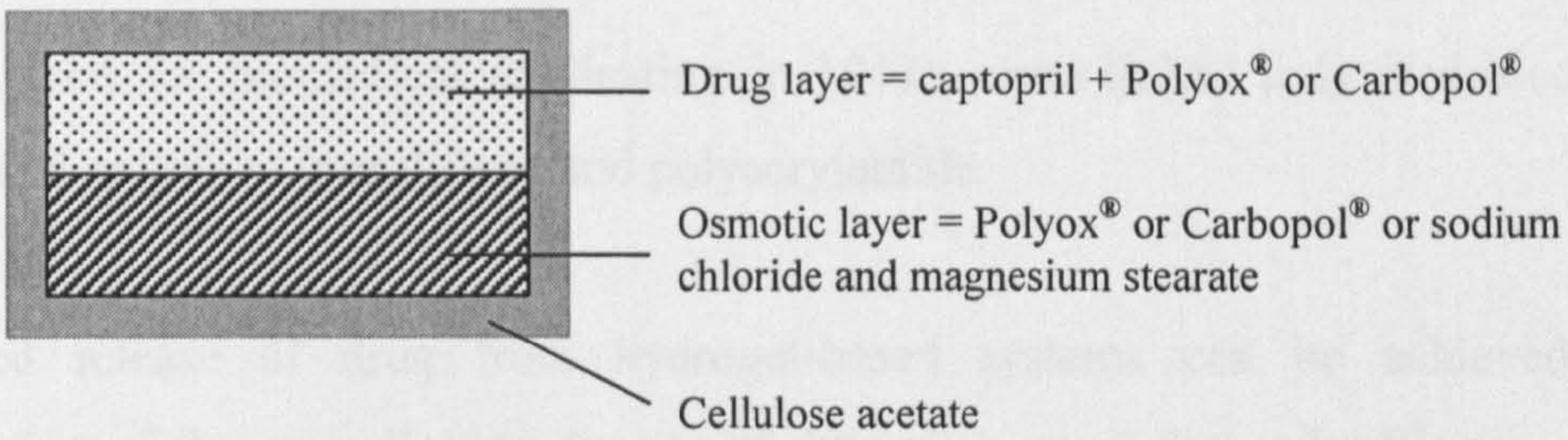

Figure 1.14: GITS of Khan *et al.* (2000).

1.2.2 Hydrogels

A polymer is defined as a hydrogel if it swells but does not dissolve in contact with water. It should not, however, be misconstrued as being the same as a gel. They are both polymeric networks that are chemically similar but their main differences lie in their physical properties. Definition-wise, gels are semi-solid systems made up of small quantities of solid, dispersed in relatively large amounts of liquid but retaining more solid-like rather than liquid-like properties (Gupta *et al.*, 2002).

The simplest means of differentiating 'gel' and 'hydrogel' is that hydrogels are capable of absorbing large amounts of water and consequently swell yet maintaining their three-dimensional structure. Conversely, gels have already been swollen to equilibrium and further addition of fluids only causes dilution of the polymeric network.

Hydrogel networks are either homopolymers or copolymers, dependent on the method of preparation, and are insoluble as a result of the presence of chemical cross-links (tie-points, junctions) or physical cross-links (entanglements, crystallites; Peppas *et al.*, 2000). The physical cross-links impart network structure and physical integrity. Their elasticity arises from the inherent memorised reference configuration to which they return despite long-term deformation (Gupta *et al.*, 2002).

Hydrogels can be considered the most similar to living tissue as compared to other synthetic biomaterials due to their high water content and soft consistency. These polymers may be used for the delivery of drugs, peptides and proteins, as targeting agents for site-specific delivery or as components in the preparation of protein or enzyme conjugates. Examples include poly(hydroxyethyl methacrylate) (the first

hydrogel used for biomedical application in 1961), cross-linked polyvinyl alcohol, cross-linked polyvinyl pyrrolidone and polyacrylamide.

Controlled release of drug from hydrogel-based systems can be achieved by manipulation of the cross-linking density of the polymers as shown by Blanco *et al.* (1997). Release rates of cytarabine from poly(2-hydroxyethyl methacrylate-co-N-vinyl-2-pyrrolidone) hydrogels cross-linked with ethylene glycol dimethacrylate were dependent on the ratio of cross-linking agent to polymer. Increasing this ratio resulted in prolonged sustained release.

Drug release from hydrogels occurs primarily via diffusion through space available between macromolecular chains, often termed 'pores'. Hence, hydrogels can be classified as macro-porous, micro-porous or non-porous, wholly dependent on the average size of the pore (Peppas *et al.*, 2000). The rate of diffusion is generally controlled by the resistance of the polymer to an increase in volume and change in shape (Gupta *et al.*, 2002). Microscopically, solvent penetration into a glassy polymer occurs in the free spaces between the macromolecular chains. Upon accumulation of a sufficient amount of water within the matrix, the glass transition temperature of the polymer drops to the temperature at which the process is being conducted. Stresses which develop from the presence of solvent in the glassy polymer are accommodated by an increase in the radius of gyration and end-to-end distance of polymer molecules, i.e. the polymer swells.

Some hydrogels exhibit varying responsiveness dependent on the external environment and these are termed physiologically-sensitive hydrogels. These 'smart' or 'intelligent' hydrogels are capable of changing their gel structure in response to environmental stimuli in order to control drug release (Qiu and Park, 2001). This is effected through reversible volume phase transitions or gel-sol phase transitions upon minute changes in terms of temperature, electric fields, solvent composition, light, pressure, sound, magnetic fields, pH, ions or specific molecular recognition events. Examples of polymers which are sensitive to these physical and chemical stimuli are detailed in Table 1.1.

Table 1.1: Polymers used in synthesis of environmentally-sensitive hydrogels.

Environmental stimuli	Polymer for 'smart' hydrogel
Temperature	Poly(N-isopropylacrylamide)
	Poly(N,N'-diethylacrylamide)
pH	Poly(acrylic acid)
	Poly(N,N'-diethylaminoethyl methacrylate)
Glucose	Poly[3-(acrylamido) phenylboronic acid]
Electrical signal	Poly(2-acrylamido-2-methylpropane sulfonic acid-co-n-butylmethacrylate)

1.2.3 Soluble polymers

Polymers in this class are generally of a moderate molecular weight i.e. <75000 daltons. Since they do not possess cross-links, their water solubility is appreciable. These polymers are either used alone or in conjunction with other, more hydrophobic, polymers in order to control drug release by slow erosion. Examples include polyethylene glycol, uncross-linked poly(vinyl pyrrolidone) or polyvinyl chloride and hydroxypropylmethylcellulose (HPMC).

HPMC is one of the most widely utilised and hence, one of the most important hydrophilic carrier materials for the development of oral controlled release systems (Siepmann and Peppas, 2001). It is a propylene glycol ether of methylcellulose and its physicochemical properties are strongly governed by the methoxy group content, the hydroxypropoxy group content and the molecular weight. HPMC is subclassified by the USP into four groups: HPMC 1828, HPMC 2208, HPMC 2906 and HPMC 2910. The first two numbers reflect the percentage of methoxy groups while the last two numbers, the percentage of hydroxypropoxy groups, determined after drying at 105°C for 2 hours.

The high swellability of HPMC impacts greatly on the release kinetics of the incorporated drug. Although no universal drug release mechanism exists for HPMC-based systems, a general mechanism involves several common phenomena. Initially, steep water concentration gradients are formed at the polymer/water interface and as a

result, water ingress occurs. Water functions as a plasticiser, lowering the glass transition temperature (T_g) of the polymer. When the T_g reaches the temperature of the overall system, the polymer converts from the glassy to the rubbery state. The HPMC swells and this changes the polymer and drug concentrations to a great extent and causes macroscopic dimensional increments. Drug diffuses out after dissolving in the water that has penetrated the device. As water content of the matrix increases, the drug diffusion coefficient increases accordingly. If the initial drug loading is high, diffusion of drug consequently leaves behind large channels or pores which compromise the integrity of the matrix and less restriction to drug diffusion is observed. Most devices that contain HPMC as the main rate-controlling excipient rely on polymer swelling, drug dissolution, drug diffusion or combinations of these as a mechanism for controlling drug release.

An example of HPMC utilised in time-delayed release is the Chronotopic® system which targets release specifically to the colon. Here, a drug-loaded core is coated with a swellable hydrophilic polymer (HPMC) and over that is applied a gastroresistant film (Sangalli *et al.*, 2001). In an aqueous environment, HPMC changes from glassy to rubbery and in the latter state, becomes more permeable, dissolves and/or erodes. Dependent on the physicochemical properties and the thickness of the HPMC layer, it is this transition from glassy to rubbery that impedes water ingress and incorporates the lag phase prior to drug release. The presence of the gastroresistant layer obviates the variations in gastric emptying time and colon-specific time-delayed release is possible due to the relative consistency in small intestinal transit time. Good *in vivo in vitro* correlation was obtained from both scintigraphic studies and pharmacokinetic studies of salivary concentrations of the model drug, antipyrine.

1.2.4 Biodegradable polymers

These polymers, as their name suggests, slowly disappear from the site of administration through degradation mechanisms such as hydrolysis which form biocompatible, non-toxic degradation products. The average molecular weight of these polymers decrease over time through surface erosion and it is this that controls drug release. Polylactide, polyglycolide and poly(caprolactone) are some of the more common examples of biodegradable polymers.

The lactide and glycolide polymers and copolymers can be considered the most utilised of the biodegradable polymers. These are aliphatic polyesters, which degrade slowly, hydrolytically, to lactic and glycolic acid which are natural body metabolites. Their biocompatibility is exemplified by the little or no systemic toxicity reported on human administration.

Strictly speaking, the correct terminology for the high molecular weight polymers are polylactide (PL), polyglycolide (PG) and poly(lactide-co-glycolide) (PLG) simply because they are derived from the dimers lactide and glycolide rather than directly from lactic acid and glycolic acid.

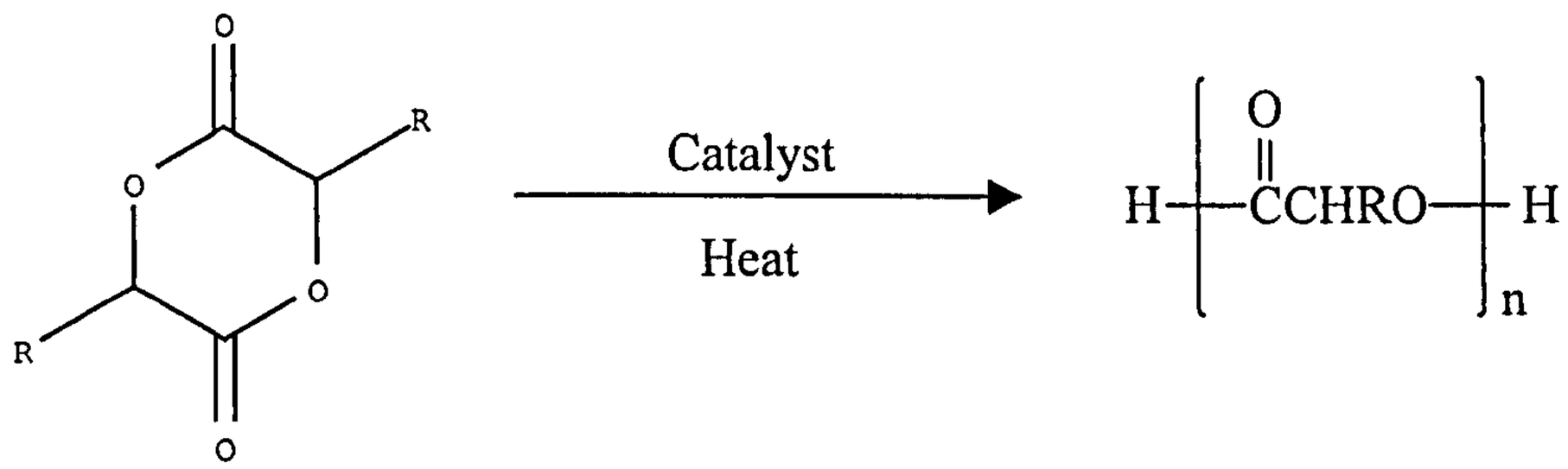

R=H → glycolide; R=CH_3 → lactide

Figure 1.15: Basic polymerisation reaction for polymers of lactide and glycolide.

The essential polymerisation reaction is shown in Figure 1.15 and this occurs in both homo- and copolymerisation of the two dimers. The presence of a methyl group in PL renders the carbonyl of the ester linkage less susceptible to hydrolytic attack. Therefore, PL is more hydrolytically stable in comparison to PG. Nevertheless, the copolymers (PLG) tend to exhibit a higher rate of degradation in comparison to the homopolymers as copolymerisation reduces overall crystallinity resulting in a more open structure for moisture penetration.

Perrin and English (1997) describe five fundamental steps in the degradation of PG, PL and PLG in drug delivery devices implanted in the body. The first stage, hydration, proceeds by way of the device absorbing water and diffusion occurs dependent on the mass and surface area. Depolymerisation ensues: chemical cleavage of the polymer backbone causes a decrease in mechanical strength. Mass integrity

decreases substantially resulting in a loss of cohesive strength and the polymer fragments into pieces of low molecular weight polymer. Further hydrolysis forms fragments which are absorbed, either assimilated by phagocytes or by dissolution of soluble monomeric (lactate or glycolate) anions into intercellular fluids. Elimination of L-lactate and glycolate occurs. The former is converted to carbon dioxide (exhaled during respiration) and pyruvate (enters the Krebs cycle through acetylation of CoA). Glycolate is partially eliminated through the urine and the rest is oxidised to glyoxylate which is then converted to glycine, serine and pyruvate. It is therefore possible to incorporate drug into this slowly degrading matrix to allow for sustained release, dependent also on the physicochemical properties of the drug itself.

1.3 Principles of time-delayed drug delivery

After considering the field of controlled release in general, the focus is now diverted to time-delayed drug delivery, chronotherapeutics. The recent emergence of drug delivery systems with "built-in timers" can be attributed to the realisation and greater understanding of circadian rhythm, postulated to be controlled by a negative feedback loop in clock genes (Miyazaki *et al.*, 2001).

1.3.1 Circadian rhythm

Rhythmicity is ubiquitous in the daily lives of all eukaryotes and even some prokaryotes (Hastings, 1997). In man, the main and most obvious temporal cycle is that of sleep and wakefulness but it must be appreciated that the internal environment is also in a constant state of flux.

For example, just before falling asleep, the secretion of melatonin from the pineal gland increases and the core body temperature decreases irrespective of the current locomotor activity. As one prepares to awaken, the adrenal glands secrete higher levels of corticosteroids in anticipation of the new day.

This example of a cyclical variation in hormonal secretions is just one of many that conform to the phenomenon of circadian rhythm. *Circa* which means "about" and

dies, referring to "daily", reflect the almost exactly 24-hourly patterns by which metabolic, behavioural and physiological responses adhere.

Lemmer (1996) proposed that the endogenous clock in humans naturally runs slower than 24 hours, about 25 hours in fact. This occurs only in free-running conditions, i.e. when the body is not exposed to any environmental cues known as 'zeitgebers'. The function of zeitgebers (e.g. light, temperature) is to precisely entrain the circadian rhythm to 24 hours.

This exact synchronisation is reliant on small daily adjustments to the endogenous clock (Hastings, 1997). Consequently, rhythms are set in a particular temporal order or phase relationship whereby the circadian cycle is divided into subjective day and subjective night during which typical diurnal and nocturnal activities respectively, are performed. The most potent entrainment cue is the light-dark cycle arising from the regular spin of the earth on its axis.

After discussing the various cues for synchronisation of circadian rhythm, it is apt now to define the criteria of endogenous circadian "clocks" that inherently regulate rhythmicity in the body.

Hastings (1997) sets down four:

i. Removal of the structure compromises free-running circadian rhythms.
ii. In isolation from the animal, the structure exhibits circadian rhythmicity *in vivo* and *in vitro*.
iii. The structure reinstates free-running circadian rhythms when transplanted into lesioned animals.
iv. The structure responds to cues known to affect entrainment.

Some structures in the vertebrate can be considered possible circadian oscillators by virtue of fulfilling some or all of these conditions and they include the retina, the pineal gland and the suprachiasmatic nuclei.

1.3.2 Influence of circadian rhythm on drug delivery

Derivation of scientific terms with the prefix chrono- has been occurring since the 1970s. The term chronopharmacology refers to the study of how the effects of drugs vary with biological timing and endogenous periodicities (Reinberg, 1992). The main aim of this field is to improve understanding of the mechanistic aspect of circadian-type variations in both desired and undesired effects of medications.

Spin-off terms from chronopharmacology which impact greatly on drug delivery include chronokinetics, chronesthesy, chronergy and eventually, chronotherapy.

1.3.2.1 Chronokinetics

Chronokinetics details how measurements of pharmacokinetic parameters e.g. maximum concentration (C_{max}), time to reach C_{max} (t_{max}), area under the concentration-time curve (AUC) and half-life ($t_{1/2}$) are dependent on the time of dosing. These time-dependent variations which may be age-, sex- or phenotype-related, are likely to be a consequence of circadian rhythm exhibited by body systems associated with absorption, distribution, metabolism and excretion of exogenously-applied drug.

For example, it has been shown that liver enzymes, specifically the monooxygenases, display functional rhythmicity therefore the metabolism of drugs such as imipramine and hexobarbital through oxidative reactions catalysed by this system is consequently dependent on the time of day (Reinberg, 1992).

1.3.2.2 Chronesthesy

Initially chronesthesy was defined as the rhythmic changes in susceptibility of a target system to a drug, not covered by the chronokinetic theory. However, now it is taken to be the chronopharmacologic counterpart of pharmacodynamics (Reinberg, 1992). Developments in this field, along with those in chronokinetics have effectively nullified "the flatter the better" theory as relating to plasma drug concentration-time profiles. Not only does constant rate infusion of drug not result in constant plasma levels, constant plasma levels do not equate to constant drug effects.

Furthermore chronesthesy highlights the importance of dosing time, deeming it as important as the quantity of the dose itself.

1.3.2.3 Chronergy

Chronergy is a more empirical term, describing the temporal variations of both the desired (therapeutic) and undesired (toxic, tolerance) effects of drugs on the organism as a whole. It encompasses both the chronokinetic and chronesthetic aspects.

1.3.2.4 Chronotherapy

Practical application of all these "chrono" aspects of drug delivery culminates in the use of chronotherapy: the design of a dosing regimen or dosage form that best exploits chronokinetics and chronesthesy. While it is of the essence to deliver the drug at a time of optimal absorption and maximal effect, it is also imperative that the issue of toxicity and avoidance of tolerance not be neglected.

1.3.3 Chronotherapeutic applications in disease states

The exacerbation of some diseases has been shown to be circadian rhythm-dependent and can be referred to as chronopathology. The frequency and onset of symptoms can be localised to certain times of the day. It is interesting to note that not only is the disease circadian-dependent, the mainline drug therapy can also be circadian-dependent resulting in the need for innovative design of dosing regimens and/or dosage forms.

1.3.3.1 Chronotherapy of asthma

The nocturnal nature of asthma attacks is well documented and has been reported as early as 1698 by John Floyer (Lemmer, 1996). The lungs are more sensitive to the allergenic potential of e.g. house mite dust and grass pollen as well as the bronchoconstrictory effects of e.g. acetylcholine and histamine during the night. Patients with chronic obstructive pulmonary disease are at higher risk of exacerbations at night due to the reduction in ciliary beating frequency.

Common anti-asthmatic drugs have been studied in terms of their chronokinetic and chronesthetic effects. Theophylline, a bronchodilator which possesses significant anti-inflammatory activity, tended to exhibit a shorter t_{max} and greater C_{max} when taken in the morning as compared to just before bedtime (Smolensky and D'Alonzo, 1997).

Since equal amounts of theophylline taken at equal intervals throughout the day have not been shown to provide adequate prophylaxis, dosage regimens advocate increased doses at night when the risk of dsypnoea is elevated and lower amounts during the day when the risk is significantly lower.

Current asthma therapy for patients whose attacks are predominantly nocturnal involves taking medication prior to bedtime; the beneficial effects of which are obvious through chronopharmacological evidence presented.

1.3.3.2 Chronotherapy of peptic ulcer disease

One of the targets of peptic ulcer disease therapy is the reduction of gastric acid secretion for which the first-line therapy is histamine H_2-blockers e.g. ranitidine and cimetidine. Reports of the circadian rhythm exhibited in gastric acid secretion have led to the timed delivery of these drugs; concentrating the doses to late afternoon or early night when acid secretion is increasing (Lemmer, 1996).

However it has also been shown that the ability of H_2-blockers to effectively reduce gastric acid secretion is compromised at night; a phenomenon described as 'partial nocturnal resistance'. It may then be of use to add a separate drug with a different mechanism of action e.g. a proton-pump inhibitor to the regimen in order to provide adequate cover for the loss of H_2-receptor antagonism.

1.3.3.3 Chronotherapy of hypertension

24-hour blood pressure (BP) profiles are easily obtained with ambulatory BP-monitoring devices and the circadian rhythmicity of BP in both normotensive and hypertensive patients is evident. In normotension and primary hypertension, BP is generally lower at night but for secondary hypertension due to e.g. renal disease and

gestation, highest values for BP are noted at night in about 70% of the cases (Lemmer, 1996).

The conventional antihypertensives also exhibit circadian dependency. Immediate-release nifedipine given to healthy volunteers showed increased bioavailability, higher C_{max} and shorter t_{max} after morning dosing in comparison to evening dosing. However, a sustained release formulation of nifedipine administered to primary hypertensives was not circadian-dependent in its effects.

Other antihypertensives including enalapril, verapamil and β-blockers also show circadian-dependent pharmacokinetics. In general, β-blockers are more effective at lowering BP in the daytime rather than at night (Lemmer, 1996).

Evidence-based medicine suggests that antihypertensives should be given to primary hypertensives in the morning whereas the evening seems to be the optimal dosing time for secondary hypertensives, be it an additional dose complementary to one in the morning or a single evening dose.

1.3.4 Advantages of timing drug delivery

As is evident from the discussion on chronopharmacology and its repercussions, the ability to time delivery of drugs is essential in designing new dosage forms in order to achieve maximum therapeutic benefit while minimising toxic effects. The mantra of time-delayed release of drugs is to deliver the right drug, in the right amount, at the right time, to the right target.

There are various benefits in timing drug delivery, one of which is the avoidance of tolerance whereby responsiveness to a drug gradually decreases over a period of perhaps days or weeks upon continuous or repeated administration of the drug. Many conventional drug delivery systems subject the body (specifically receptors) to consistent levels of drug, for example transdermal patches of glyceryl trinitrate; the incidence of nitrate tolerance is hardly uncommon. Timing doses as and when needed, will theoretically minimise the occurrence of tolerance.

Another advantage of time-delayed drug delivery is the ability to mimic the body's endocrine systems in which, for instance, insulin is released into the bloodstream when higher-than-normal glucose levels are detected. Especially in the area of delivering hormonal treatment such as luteinising hormone releasing hormone antagonists (goserelin, buserelin), the importance of following the normal physiological release of the hormone as closely as possible cannot be undermined.

1.4 Conceptualisation of a novel drug delivery system

With all these materials available for use, designing a delivery system suited to a particular type of drug release profile seems to be a mix-and-match affair which needs to consider the compatibility and suitability of all the components involved. Another important key lies in the simplicity of the device. All components have to play an indispensable role thereby keeping the concept behind the device as basic as possible, yet effective.

We propose a prototype of a two-piece hard gelatin capsule coated with a water-insoluble, rupturable layer. Two variations of the capsule fill are suggested:

(a) dispersion of swelling agent and drug in a vegetable oil; and

(b) compartments of (i) swelling agent, and (ii) drug in vegetable oil, separated by a compressed tablet.

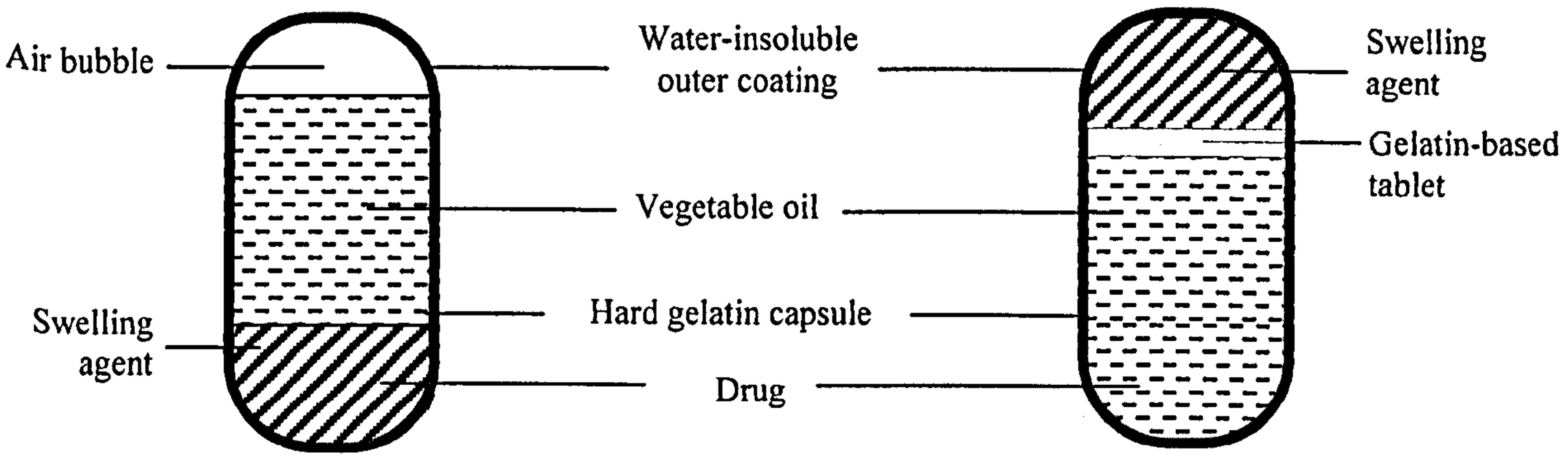

Figure 1.16: The two proposed time-delayed drug delivery devices.

In the first, water ingress through the outer coat will cause the expansion of the swelling agent, increasing the internal hydrostatic pressure of the capsule until the limits of free space and elastic tolerance of the brittle outer coating are reached and rupture of the outer coating is achieved. Release of the drug then occurs through the crack in the coating.

The second configuration eliminates the air space that is present in the first device. Water ingress causes expansion of the swelling agent, generating a force sufficient to rupture the brittle outer coat over the capsule cap. Dislodgement of the swelling agent then allows access of water to dissolve and disintegrate the tablet. This results in the release of oil and drug.

Factors which will probably affect the programmed capsule rupture include the concentration of swelling agent filled into the capsule, the type and thickness of the outer coating, the composition of the tablet and the incorporation of other excipients which may retard or accelerate LH-21 swelling.

Here the focus of the review shifts to discuss the various components of our novel dosage form. Components which are not examined here will be discussed in later chapters.

1.5 Capsule-based dosage forms

The European Pharmacopoeia defines capsules as being "*...solid preparations with hard or soft shells of various shapes and capacities, usually containing a single dose of medicament. They are normally intended to be taken by mouth.*" They have gained ubiquitous use over the years due to the various advantages they possess, for example, their simplistic elegance, ease of use and portability (Hostetler, 1986). Encapsulating drugs also allows masking of unpleasant tastes and odours. From an economical viewpoint, capsule production in large quantities and a wide variety of colours is financially viable. Furthermore, as there are minimal excipients added and little pressure is necessary to compact the materials (as compared with tabletting), the encapsulated drug is readily available for release and subsequent absorption.

However, certain materials should be avoided for use in capsules e.g. potassium bromide and ammonium chloride as their sudden release in the stomach may result in irritating concentrations. Highly efflorescent and highly deliquescent materials tend to cause softening and excessive brittleness of the capsules, respectively.

The main raw material used is gelatin which is prepared from collagen, a fibrillary protein forming connective and supportive tissues of the mammalian body. The collagen of bones and hides is subjected to maceration and purification with alkalis and acids respectively that hydrolyse it to an almost unbranched amino acid chain of variable length i.e. gelatin. Specifically, type A gelatin is produced from acid pre-treatment and has an iso-electric point of between 7.0 and 9.0 whereas pre-treatment in an alkaline medium followed by hot water extraction yields Type B gelatin with an iso-electric point of approximately 5.0.

Gelatin is deemed acceptable as a pharmaceutical excipient due to its non-toxic nature and is readily soluble in biological fluids at body temperature.

Excipients are added to the gelatin in order to modify its properties to suit particular requirements. Plasticisers, in essence, change the nature of materials from glassy to rubbery. Glycerol is the most popular example. Others include sorbitol, propylene glycol, sucrose and acacia. They are only found in soft gelatin capsules.

Bloom strength, a measure of gel rigidity, quantifies the hardness (or softness) of a gelatin capsule. It is defined as the load, in grams, required to push a standard plunger a set distance into a prepared gelatin gel (6.66% solution at 10°C). A high bloom indicates a 'hard' gelatin capsule while conversely, a low bloom, a 'soft' gelatin capsule.

For ease of identification and disguising the fill of the capsule, both soluble and insoluble colourants are employed. The soluble dyes are synthetic and are prepared using mixtures of the three basic colours giving an array that covers the entire colour spectrum. Only two types of insoluble pigments are used, i.e. titanium oxide which is white and is generally employed as an opacifying agent, as well as the red, black and

yellow of the iron oxides. Aluminium lakes are used when preparing bicoloured soft gelatin capsules as they minimise colour transfer.

Preservatives are added in-process to prevent microbiological contamination during manufacture rather than on storage. This is simply because the finished capsules have a relatively low moisture content which does not provide a platform for bacterial growth. In soft gelatin capsules however, antifungal preservatives are sometimes added.

1.5.1 Hard gelatin capsules

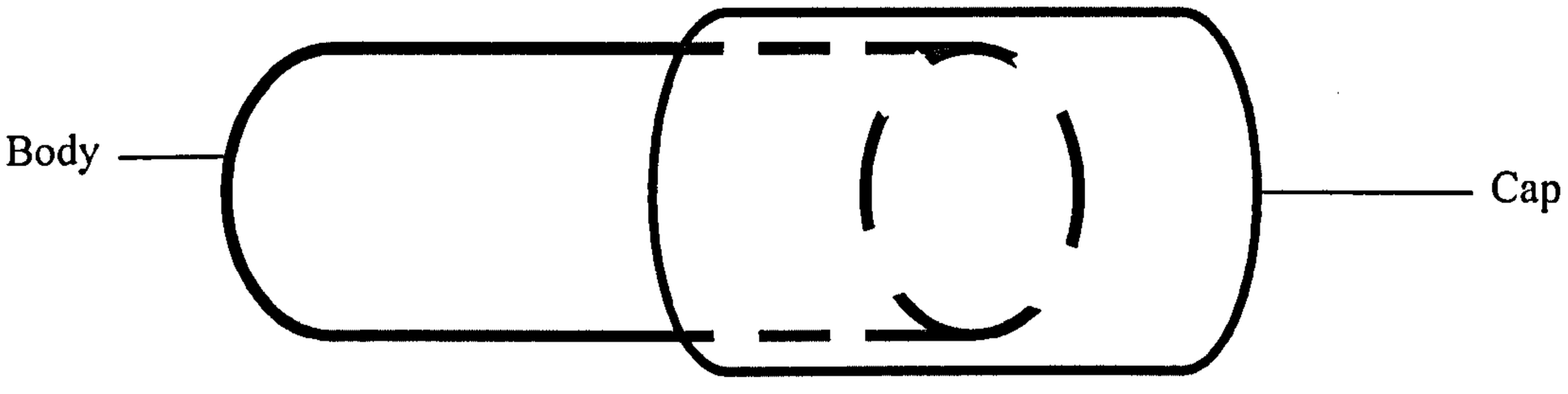

Figure 1.17: A hard gelatin capsule

Hard gelatin capsules (HGCs), as the adjective suggests, are firm and rigid in nature as compared to the more pliable soft gelatin capsules. HGCs consist of two separate parts, each of which is shaped like a semi-closed cylinder (Ridgway, 1987). The 'cap' is of a slightly larger diameter than the 'body' which is in turn, longer than the 'cap' (Figure 1.17). Once filled, the 'cap' fits snugly over the body to form a sealed unit.

HGCs usually contain 13-16% water which acts as a plasticiser for gelatin. Values lower than this cause the capsules to be too brittle and dry whereas with excessive water content, deformation of the capsule shape and stickiness of gelatin occur. On average, an HGC takes 2.5–10 minutes to disintegrate and dissolve. Initially the capsule breaks down at the weakest pressure points i.e. the shoulders and following that, the gelatin cylinder completely dissolves.

More often than not, HGCs are filled with powders of which the prerequisite is that they do not react with gelatin or in any other way compromise the integrity of the shell. They must be able to be dosed accurately and precisely into the capsule shell and to release the active contents in a form available to the patient. The formulation to be filled usually consists of the active ingredient and adjuvants which may be, for instance, glidants, lubricants, diluents and surfactants.

It is also possible to fill HGCs with semisolids e.g. thermosoftening mixtures, thixotropic mixtures and pastes. These possess the unique property of being 'liquid' during the filling process and turning 'solid' when filled. For this purpose, the filling machines have heated hoppers with stirrers to keep the fill in liquid form and evenly mixed. Semisolid filling significantly decreases the problem of cross-contamination as faced with the dust clouds forming when filling with powders. High uniformity of fill weight and content is achievable with the usage of solutions and volumetric dosing pumps.

1.5.1.1 Liquid-filled hard gelatin capsules

Recent advances in capsule technology have allowed the filling of liquids into hard gelatin capsules instead of just soft ones. The main obstacle to filling liquids into HGCs previously was leakage, but a new product claims to have overcome this problem.

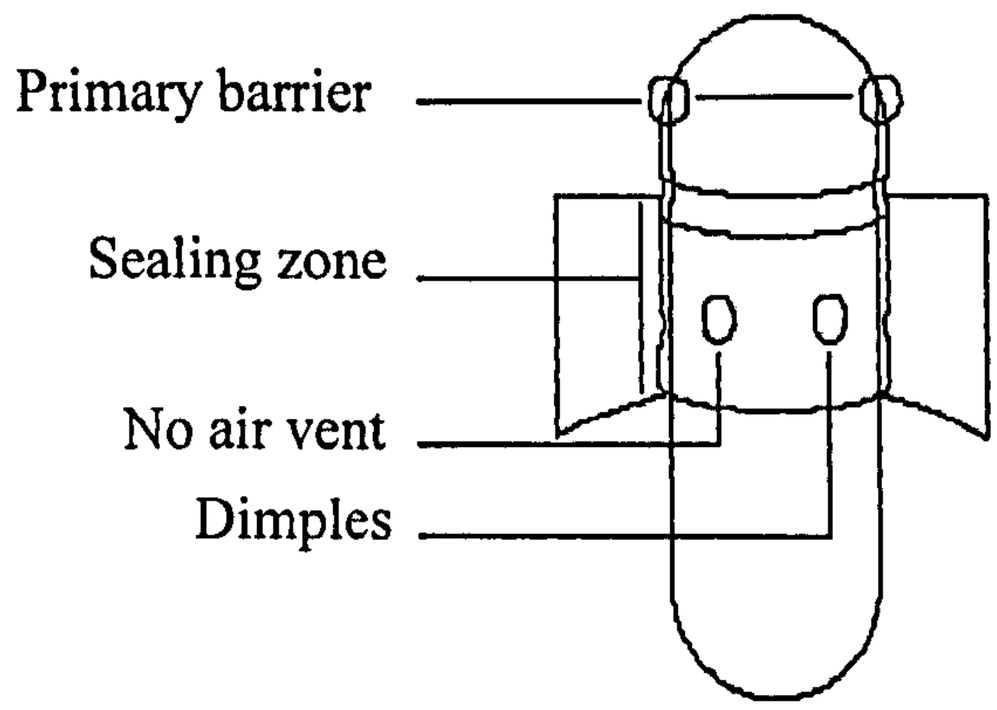

Figure 1.18: Licaps® capsule (Licaps® brochure)

Licaps®, manufactured by Capsugel, has several modified features in comparison to their conventional Coni-snap® HGC used mainly for powder fill. While the composition of the shell is essentially the same and comprises gelatin, water and colouring and opacifying agents, the design of the new capsule has eliminated air vents to prevent leakage prior to sealing and has a six-dimple configuration on the body and cap to maximise the area of sealing (Figure 1.18).

HGCs hold the upper hand in filling of liquids over their soft counterparts in that in-house development and manufacture and the ability to manufacture small batches and consequent scale-up are both feasible and economical. Hot melts of up to 70°C are tolerated by the HGC while 35°C is the maximum for the SGC. With the presence of plasticiser in SGCs, risk of drug migration is high for drugs soluble in the plasticiser. Oxygen permeability is also increased in addition to the added sensitivity to heat and humidity; both phenomena being due to the presence of plasticiser in SGCs.

Traditional banding technology for the sealing of capsules which involves applying a thin band of liquid gelatin at the junction of the body and cap and subsequent drying looks to be superseded by a new technology introduced by Capsugel. LEMS®, short for Liquid Encapsulated by Microspray Sealing adopts a process whereby each capsule is sprayed with a minute (microlitre quantity) amount of hydroalcoholic solution (usually 50:50 water/ethanol) at the body and cap junction. This solution is drawn up into the gap by capillary action and hence lowers the melting point of gelatin at the sealing area of the capsule. In order to complete the melting and fusion process, air at 40-60°C is gently blown across the capsule. The capsules are then dried by gently tumbling in a rotating drum followed by airing in open trays.

1.5.2 Soft gelatin capsules

As described earlier, soft gelatin capsules (SGCs) differ from HGCs mainly in their content of plasticiser rendering them more flexible and turgid. They are a one-piece container with variable shape (round, oblong, oval or tubular) and are either seamed along the axis or seamless (Ridgway, 1987).

Unlike HGCs, SGCs are made simultaneously as the formulation is filled into them using an encapsulation machine and a rotary die process. Two tanks, one containing the molten gelatin and the other the medicinal liquid fill material, feed into the encapsulation machine. The molten gelatin is formed into two flat solid ribbons then the medicinal fill is injected through the gap between the ribbons and finally the capsule is sealed via application of heat and pressure.

SGCs are advantageous in that they do not require a compression stage in the manufacturing process and are useful for poorly compressible drugs and excipients which would not be suitable for tabletting (Jones *et al.*, 1996). Accurate dosing is possible through volumetric dispensation of the liquid fill containing dissolved or uniformly dispersed drug. For drugs susceptible to oxidation or hydrolysis on long term storage, dissolution or dispersion in oil and encapsulation by gelatin prevents detrimental effects of the environment as these formulations are resistant to gaseous diffusion and their labile water content is low. Furthermore, drugs dissolved or dispersed in a water-miscible or oily liquid are released when the capsule ruptures and then dissolve into the gastric medium or are emulsified to give a drug dispersion with high surface area and consequently high bioavailability.

1.6 Swelling agent

The function of the swelling agent in our novel delivery system is to swell at a controlled rate as the water diffuses in. Consequent increase in the internal hydrostatic pressure is expected to rupture the brittle outer coating in a wholly time-dependent manner thereby initiating drug release. Various cellulose derivatives are available for selection as a swelling agent and it is apt here to detail the many types on the market.

A detailed description of the cellulose derivative selected for further study, low-substituted hydroxypropylcellulose, is given in Section 3.1.

1.6.1 Cellulose derivatives

Anselme Rayen, in 1838, put forward the hypothesis that the cell walls of most plants were made up of the same substance, which he named cellulose (Nevell and Zeronian,

1985). It commonly accepted today that the structural building block of higher plants is a polymer of D-glucose with a characteristic X-ray diagram. More specifically, it is a linear condensation polymer of D-anhydroglucopyranose units joined together by β-1,4-glycosidic bonds.

It is as a result of the molecule's stereochemistry that the majority of the hydroxyl groups form intra- or inter-chain hydrogen bonds with adjoining molecules. Therefore, cellulose is partly crystalline, the degree of crystallinity being dependent upon the source of the cellulose. Cellulose's insolubility in water is attributed to its high cohesive energy density.

In order to improve the processability and the performance of cellulose, and also to obtain derivatives that are soluble in water and organic solvents, several chemical transformations have been undertaken. These transformations involve partial or total esterification or etherification of the three hydroxy groups on the anhydroglucopyranose unit (Doelker, 1993). Classification of cellulose derivatives is possible by identifying them through the type of chemical reaction taking place on the hydroxyl groups. They are detailed as follows:

i) Substitution of H atom in –OH, which is basically esterification and etherification
ii) Substitution of the hydroxy group, either intramolecular or intermolecular
iii) Selective and controlled concentration of hydroxyl groups
iv) Radical addition
v) Electrophilic substitution
vi) Interaction of cellulose with organometallic compounds
vii) Synthesis of block or graft copolymers of cellulose

Cellulose derivatives are also differentiated in terms of degree of substitution (DS) i.e. the average number of substituted groups of which the maximum is three. For ethers or esters with hydroxypropyl groups attached, the degree of reaction or molar substitution (MS) reflects the average number of molecules of alkylene oxide reacted with each anhydroglucose unit. The ratio MS:DS gives the average length of a cellulose pendant chain.

Various parameters affect the properties of the synthesised cellulose derivatives, the first of which is the nature of the substituent, especially its polarity. Non-ionic ethers with DS of about 1 are generally water-soluble but if hydrophobic ethers predominate, water-solubility usually disappears when the DS is greater than 2. The presence of polar groups will impart increased hydrophilicity to the derivative.

Another aspect is the proportion of hydroxyl groups which has been substituted. Again the stereochemical structure plays an important role. The restricted access to some parts of the macromolecule arising from extensive inter- and intra-molecular hydrogen bonding renders the primary hydroxyl group less reactive than expected. It is the secondary hydroxyl group that often shows higher reactivity. Nevertheless, the relative reaction rates are dependent on the reactant and the starting material. For example, etherification of alkylene oxide occurs preferentially on the hydroxyl of the C-6. Therefore, non-uniformity of distribution occurs within the anhydroglucose unit as well as throughout the polymer chain resulting in fully substituted, irregularly substituted and even unsubstituted cellulose molecules. Lastly, the average chain length and molecular mass distribution have an impact on the viscosity of the synthesised derivative.

While cellulose esters are generally not widely used as excipients in drug delivery systems, the opposite is true of their ether counterparts. The most common synthetic route is that of nucleophilic substitution which is irreversible and gives a rate-controlled distribution of substituents (Nicholson and Merritt, 1985). Ethylcellulose and carboxymethylcellulose are prepared by methylation of alkali cellulose with a methyl halide (CH_3X). Ring opening of the reagent before forming the ethylcellulose ether is used to form hydroxyethylcellulose, with ethylene oxide, and hydroxypropylcellulose, with propylene oxide.

Michael addition, the other type of etherification reaction, is reversible and involves the alkali-catalysed addition of an activated vinyl group to the cellulose. The reaction of acrylonitrile with alkali cellulose i.e. cyanoethylation produces derivatives such as cyanoethylcellulose. Common cellulose ethers and their uses are listed in Table 1.2.

Table 1.2: Common cellulose ethers and their uses.

Cellulose ether	Uses and applications
Carboxymethylcellulose	Thickener for aqueous solutions, food additive, additive in paint, printing-ink, cosmetics
Hydroxyethylcellulose	Coatings, cements and plasters, thickeners, emulsifying agents, pharmaceuticals, anti-fogging agents, oil-well fracturing and drilling fluids, wetting solutions, binding and dispersing agents, films, inks, corrosion and scale inhibitors, cosmetics, mould casting, thermal recording papers, lubricants, sealants, gels, waterproofing, adhesives, culture media for bacterial growth
Hydroxypropylcellulose	Manufacturing of injection-mould articles, pharmaceutical and personal hygiene preparations, tablet coatings with extended release characteristics, films, textiles, flocculants, wetting agents, thickeners, binders, absorbents, water-activated cementing tapes, antistatic coatings, gel formulations
Hydroxypropylmethylcellulose	Food and cosmetic applications, tablet binder, film coating, extended release tablet matrix, suspending and thickening agent in ophthalmic preparations, emulsifier and stabiliser in topical gels and ointments, manufacture of capsules, adhesives in plastic bandages, wetting agent for contact lenses

1.7 Hydrophobic phase

One of the initial aims of developing this system was to deliver hydrophobic drugs which tend to display significant problems with dissolution into gastric media. This is of graver consequence when the dissolution of the drug is the rate-limiting step to absorption, limiting bioavailability of the more hydrophobic drugs. The use of a hydrophobic carrier phase is hoped to allow avoidance of the dissolution step,

presenting the drug in solubilised form for absorption. Two such carriers are described here: vegetable oils and self-emulsifying drug delivery systems.

1.7.1 Vegetable oils

Vegetable oils are synonymous with cooking but have also gained widespread use in many industries; ranging from the pharmaceutical e.g. as excipients in drug delivery systems to the automotive as a prospective alternative to fossil fuels.

Seed oils derived from corn, coconut and soybean are only a few of the many available for incorporating into delivery systems due to their usually inert character, low toxicity and GRAS status.

At times the oils themselves are the active ingredient, for example fish oils which contain e.g. omega-3 fatty acids, purportedly useful for alleviating the painful symptoms of rheumatoid arthritis.

Peppermint and caraway oil received a positive risk-benefit analysis from the German authorities as to their pharmacological effects on improving the digestion process and gastrointestinal motility (Mascher *et al.*, 2001). An enteric-coated formulation is available for the delivery of these two oils.

Another formulation that incorporates a vegetable oil is a pH-sensitive drug delivery system that is prepared from an oil-in-water emulsion (Yuk *et al.*, 1995). The core comprises drug-in-oil dispersion (hydrocortisone in coconut oil) and the capsule is made up of semi-interpenetrating networks (semi-IPNs). This is a polymeric network consisting of two chemically-independent polymers, the proportions and properties of which can be varied exclusively of each other. The first polymer is sodium alginate which disintegrates in intestinal fluid while the second, polyacrylic acid, lends its pH-sensitive swelling capacity to the entire capsule network. The final delivery system is prepared as shown in Figure 1.19.

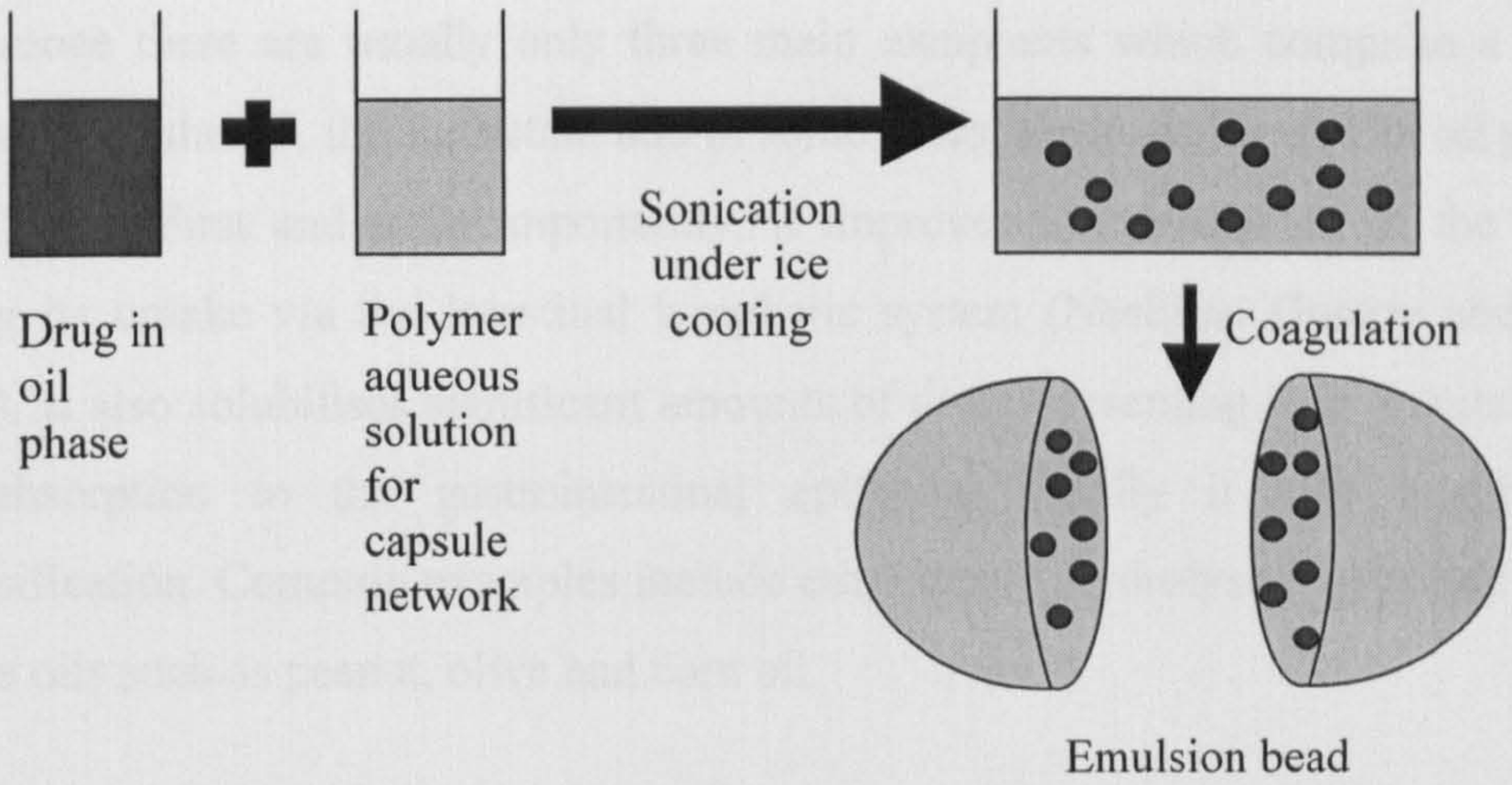

Figure 1.19: Preparation of emulsion bead from oil-in-water emulsion (Yuk *et al.*, 1995).

The major factor for controlling the release pattern of this formulation is the swelling behaviour of the capsule network which is in turn, dependent on the surrounding pH. In acidic environments, the carboxylate groups are protonated causing the capsule network to shrink. As the pH increases, the concentration of negatively charged carboxylic groups (COO^-) also rises accompanied by a dramatic increase in swelling. The extent of swelling therefore increases with the increase of polyacrylic acid content. This system may be a suitable carrier for oral delivery of lipophilic drugs such as steroids and vitamins.

1.7.2 Self-emulsifying drug delivery systems

Aside from just being solubilisers of lipophilic drugs, vegetable oils have been utilised in a very promising field of drug delivery i.e. self-emulsifying drug delivery systems (SEDDS). Self-emulsifying systems in general are defined as isotropic mixtures of oil and surfactant which form fine oil-in-water emulsions when gently agitated in an aqueous environment (Charman *et al.*, 1992). Previously, their use was confined to the chemical industry for the transport of concentrated herbicides and pesticides but when formulated using medium-chain triglyceride oils and ionic / non-ionic surfactants deemed safe for oral administration, SEDDS were developed. Filled in soft gelatin capsules, they offered formulation scientists another option for precise and convenient unit dosing.

In essence there are usually only three main excipients which comprise a SEDDS formulation: the oil, the surfactant and in some cases, the co-solvent. The oil performs three roles. First and most importantly, it improves the absorption of the drug by aiding its uptake via the intestinal lymphatic system (Neslihan Gursoy and Benita, 2004). It also solubilises significant amounts of drug; presenting it in a suitable form for absorption to the gastrointestinal epithelia. Finally it also enables self-emulsification. Common examples include ethyl oleate, hydrolysed vegetable oils and edible oils such as peanut, olive and corn oil.

Once in the gastric environment, the gelatin capsules dissolve and disintegrate releasing the capsules' contents. Agitation of the mixture afforded by inherent gastrointestinal motility results in the formation of the fine oil droplets, usually possessing dimensions of between 100 and 300nm (Neslihan Gursoy and Benita, 2004). This not only favourably influences the dissolution of lipophilic drugs by increasing interfacial area for partitioning of the drug between oil and water, but also avoids possible irritant effects of the sudden high concentrations of certain drugs (Halbaut *et al.*, 1996). In comparison to simple oily solutions, the fine oil droplets of SEDDS empty rapidly from the stomach thereby promoting wide distribution of drug throughout the gastrointestinal tract.

For drugs which are prone to dissolution rate-limited absorption, SEDDS have been shown to increase the rate and extent of absorption and reproducibility of plasma concentration profiles. Improvements in terms of bioavailability of hydrophobic drugs are attributed to the digestion of the incorporated triglycerides to free fatty acids and 2-monoglycerides. The hydrophobic drug is co-solubilised with these lipolysis degradation products to produce colloidal dispersions within mixed micelles of bile salts and lecithin, effectively creating a reservoir of drug for consequent passive absorption (Pouton, 2000).

However, the use of SEDDS in pharmaceutics is not widespread, the possible causes being two-fold: custom and habit of the industry players and genuine physicochemical constraints (Pouton, 1997). Most pharmaceutical companies tend to rely on technologies which they are familiar with and have the equipment for. Generally, once formulation of a new chemical entity goes down the path of e.g. tabletting, it

becomes difficult to revert to an alternative method of formulation such as SEDDS unless explicitly necessary. Another important aspect not to be ignored is the limited solvent capacity of oily formulations hence the incorporated drug has to be very potent in small doses. It is a possibility that the solubilised drug is chemically unstable in oily formulations but in terms of SEDDS, there is inadequate stability data available to accurately confirm this. Furthermore, there is a concern that the high usage of surfactants poses a toxicological hazard.

The gastric emptying rate of SEDDS is comparable to that of solutions and this is advantageous when rapid onset of drug action is required. However, if the therapeutic window of the drug is narrow, the sudden high dose and subsequent high C_{max} may cause severe side-effects.

1.8 Film coating

Tablet coating can be considered one of the oldest pharmaceutical arts still in current practice as reports of its implementation date back to *circa* 850 A.D. (Campbell and Sackett, 1999). However, modern processes have their origins in the 1950s, exacerbated by the boom in synthesis of many new polymeric materials. The main benefits of film coating are detailed in Table 1.3.

Table 1.3: Benefits of film coating (Campbell and Sackett, 1999).

Mask unpleasant odours
Improve ease of ingestion
Improve product appearance
Protect product from surrounding environment
Control rate of release
Separate incompatible materials
Improve product identification
Facilitate handling
Prevent contaminants from reacting with product
Apply active coating to substrate (i.e. apply active as a solution / slurry)

The process of coating basically involves three steps: atomisation of the polymer solution, coalescence of the spray droplets on the dosage form and finally drying of the coated dosage form. The most challenging aspect of film coating is to ensure both the uniform application of the droplets and the subsequent drying occurring at a proper evaporative rate. Theoretically, this is possible if the spray droplets possess a desired level of liquid upon impacting the dosage form surface. If there is excessive liquid, overwetting occurs but if there are inadequate amounts, spreading out and coalescence to form a smooth film is hindered.

1.8.1 Raw Materials

The three basic components of a film coating solution are the film-forming polymer, the plasticiser and the solvent. Most industrial applications include the use of colourants but these will not be discussed in detail here.

To be considered film formers, polymers have to possess certain characteristics of which the first is the ability to form a continuous film. Compatibility with the product substrate is also essential. From a manufacturing standpoint, the polymer should be able to form a solution of low viscosity in order to atomise adequately and this solution should be in a solvent of minimal toxicity.

Sakellariou and Rowe (1995a) outline four main criteria that must be fulfilled in the preparation of film coatings.

i) The films must be of uniform thickness especially if the dosage form relies on the films to control drug release by diffusion and osmosis.
ii) The films must be coherent and free from flaws and cracks in order to prevent premature drug release.
iii) The films must display adequate adherence to the substrate.
iv) The films must be stable on storage and handling so that drug release kinetics do not change over time.

In general the water-soluble polymers such as hydroxypropylmethylcellulose (HPMC), methylcellulose (MC), hydroxypropylcellulose (HPC) and poly(vinyl

pyrrolidone) (PVP) dissolve independently of pH. They are also, as their designation implies, readily soluble in water and a variety of organic solvents. HPMC is regarded the most common polymer used in immediate release dosage forms. In comparison, MC forms films with a higher gel strength but lower gelling temperature than HPMC while films of HPC are slightly tackier than HPMC films.

Of the sustained-release polymers, ethylcellulose is the most widely used. It can be used alone or in combination with a water-soluble ingredient in order to manipulate the release rate of the incorporated drug by functioning as a rate-controlling membrane. This particular polymer will be discussed in greater detail in Section 5.1.

Polymers that are soluble above a certain pH are termed enteric-release polymers and are frequently used to protect gastrolabile drugs and to delay release of drug until after gastric emptying. These include hydroxypropylmethylcellulose phthalate, cellulose acetate phthalate and the methacrylic acid copolymers (e.g. Eudragit® L and S) which can be used either as organic solutions or aqueous dispersions.

The second essential component of a film coating solution is the plasticising agent which functions mainly to lower the glass transition temperature (T_g) of the polymer which usually is higher than 100°C, unsuitable for scale-up ventures. Adequate plasticisation also ensures a reduction in brittleness, an increase in tensile strength and an improved resistance to tear and impact. Properties of the plasticiser i.e. its chemical structure, molecular weight and concentration influence its ability to depress the T_g. The plasticiser interacts with the polymer through equal distribution throughout the polymer chain, creating additional free volume.

Permanence of the plasticiser within the film coat is very important as leaching resulting in a reduction in the plasticiser concentration impacts greatly on the properties of the film coat. The ability of the plasticiser to remain within the film coat is dependent on its volatility, its solubility and its interaction with the polymer. Efficacy of the plasticiser lies in choosing the right one to complement the film-forming polymer whereby the closer the structural resemblance between the two, the more efficacious the plasticisation. In fact, water-solubility is generally a good

indicator where water-soluble polymers work best with water-soluble plasticisers and the same goes for their water-insoluble counterparts.

Polyethylene glycol (PEG) is one of the most commonly used water-soluble plasticisers and is available in molecular weights ranging from 300 to 20,000. The lower molecular weight PEGs which are liquid at room temperature are used for the coating of small particles whereas PEGs above 3350 molecular weight are employed in tablet coating. Plasticisation with propylene glycol tends to form softer, more flexible films than high molecular weight PEGs and it can be applied to both small particle and tablet coating. Triacetin, triethyl citrate and glycerin are other examples of water-soluble plasticisers.

The more common water-insoluble plasticisers are tributyl citrate, acetylated monoglyceride, castor oil, dibutyl sebacate, acetyl triethyl citrate and acetyl tributyl citrate. These are frequently used to plasticise films of the less polar cellulose ethers e.g. cellulose acetate phthalate and hydroxypropylmethylcellulose phthalate.

Organic solvents have, of late, been gradually phased out of the coating process, due to environmental and safety concerns. Nevertheless, their efficacy in producing good quality films cannot be undermined and the common solvent/solvent combinations are as follows: ethanol / water, acetone / water, methanol, methylene chloride / methanol, methylene chloride / ethanol, acetone / methylene chloride, acetone / ethanol / isopropanol and acetone / ethanol / methylene chloride (Campbell and Sackett, 1999).

1.8.2 Aqueous-based coating

The term aqueous here does not imply absolute desertion of the use of organic solvents but rather the overall decrease in their use, and the advocated use of the more pharmaceutically acceptable ones e.g. ethyl acetate and butanone in water-based systems. There are two main branches in aqueous-based coating which denote the type of film or membrane formed i.e. latex or pseudolatex.

1.8.2.1 Latexes

The main method of forming latexes is by emulsion-polymerisation which synthesises the polymers used for coating directly from the monomers. However, this process can only be used for liquid precursor monomers that polymerise in an aqueous medium, activated by free radical initiators (Quintanar-Guerrero *et al.*, 1999). Furthermore, residual monomers or oligomers and traces of initiator constitute potentially toxic by-products.

1.8.2.2 Pseudolatexes

It was the limitations of latex preparations that led to the advent of pseudo- or artificial latexes; the terminology derived from the fact that they are not obtained directly from monomers. Conversely, they are formed by emulsifying organic polymer solutions in water (hence the aqueous base) then removing the organic solvent in vacuum.

The original method was devised by Vanderhoff *et al.* (1993) and involved firstly, emulsifying the polymer solution in water-immiscible organic solvents in an aqueous phase containing emulsifiers. Emulsifiers (or stabilisers) such as polyvinyl alcohol and poloxamer 407 facilitated the formation of the emulsion and prevented the agglomeration and coalescence of the dispersed polymer particles during storage. However, a balance had to be struck in that once the solvent was displaced, coalescence of the polymeric particles had to occur in order for the film to form. The second step in Vanderhoff's method is to submit the polymer solution to a high energy source such as ultrasound radiation, homogenisers, high pressure dispensers or colloid mills to reduce the size of the polymer emulsion droplets to less than 0.5μm. Following removal of the solvent by vacuum steam distillation, a fine aqueous dispersion of polymeric particles is obtained.

Quintanar-Guerrero *et al.* (1999) suggest an alternative method, emulsion-diffusion, which eliminates the need for a high energy source. They replace that step of Vanderhoff's process with one in which water is added to the system and the water-

miscible solvent diffuses into the external phase, leaving aggregates of polymer in nanoparticulate dimensions. The method claims to be highly efficient, reproducible, amenable to scale up and adaptable to several coating polymers. In the final step, solvent and water are removed, resulting in a final dispersion of highly concentrated polymer.

Instead of preparing the aqueous polymeric dispersion from scratch, there are at least two commercially available products i.e. Aquacoat® and Surelease®. All the user has to do is to add water and/or plasticiser to the prepared dispersion of ethylcellulose which already contains stabilisers.

Aquacoat® contains 30%(w/v) solid dispersion of particles with an average diameter of 0.2μm of which the solid portion is made up of 90% ethylcellulose, sodium lauryl sulphate (surfactant) and cetyl alcohol (stabiliser) (Sun *et al.*, 1999). A recommended plasticiser is dibutyl sebacate which can be added in varied quantities, according to the process requirements.

Most applications of film coating are performed in a fluidised bed coater. The aqueous polymeric dispersions are sprayed onto the surfaces to be coated and the water evaporates. As the particles or droplets encounter the surface, they coalesce, possibly driven by polymer-water interfacial tension or capillary forces or a combination of both (Quintanar-Guerrero *et al.*, 1999). A phenomenon termed further gradual coalescence (FGC) in which the film becomes more homogeneous upon aging occurs and the impact of this is the inability to guarantee consistency of the films' performance over periods of storage. An extra thermal treatment step is carried out to enhance the coalescence of the particles in an effort to reduce the effects of FGC.

This heating step claims also to decrease or eliminate the pH-dependent drug release seen with formulations coated with Aquacoat®. Residual carboxyl groups in ethylcellulose and/or the presence of sodium lauryl sulphate may contribute to the increase in drug release rates in a higher pH environment.

1.8.3 Organic coating

Curing (thermal treatment) and the type of dissolution media in which the coated formulations are tested do not seem to affect the films formed by coating with organic solvent-based systems (Wesseling and Bodmeier, 1999). A typical organic ethylcellulose (EC) solution consists of 50:50%(v/v) acetone and isopropyl alcohol, 3%(w/v) of EC and 5%(w/w) of triacetin (based on weight of EC). This solution is sprayed onto the surface to be coated, the solvent thus evaporates, initiating an increase in polymer concentration. An intermediate gel-like stage precedes the formation of a solvent-free polymeric film once sufficiently dry. Organic polymer solutions also do not require addition of surfactants such as sodium lauryl sulphate.

1.8.4 Dry powder coating

The transition from organic to aqueous coating was due to the environmental, safety and economic benefits offered by the latter. Currently, an alternative to aqueous coatings, dry coating, is being actively developed and improved. This method overcomes the limitation imposed by aqueous coating in terms of a minimum coating time required as a result of maximum concentration of coating solution permitted before the solution becomes too concentrated and nozzle blocking occurs. Furthermore, the minimal amount of water involved renders this method suitable for the coating of dosage forms containing water-sensitive active ingredients. The costs involved in this method are comparatively lower than the conventional organic and aqueous coatings as the process time is greatly reduced and the need for the preparation of a coating solution is negated.

The principle is to introduce the polymer and the plasticiser, dry, under heated air. Synchronisation of the delivery rates of both components is necessary to allow the two processes to begin and end at the same time. Similar to aqueous coating, the coated product has to undergo a curing process in order that coalescence is enhanced to encourage the formation of a smooth, uniform coat. This curing step involves the spraying of water or a solution of HPMC and consequent drying of the product. It is speculated that the evaporation of water provides a driving force to fuse the polymeric particles together, akin to the mechanism observed in aqueous latex systems (Obara *et*

al., 1999). Hence, dry coating is not strictly free from the use of water but rather, incorporates it in a relatively small quantity.

Obara *et al.* (1999) developed methods to dry coat using a centrifugal granulator (CF-granulator), a fluidised bed coater and a pan coater. The original piece of equipment was modified by adding attachments for powder feeding of the polymer and liquid spraying of the plasticiser. Figures 1.20a-c illustrate the coating process in each of these three machines.

It was concluded that although the dry coating technique required the application of a higher level of polymer coating in order to achieve the same depression of drug release rate as conventional aqueous coating, this method was effective in reducing overall cost. The plus-points of reduction in processing time and the ability to use already available equipment with just minor modifications are encouraging greater use of this method in industry.

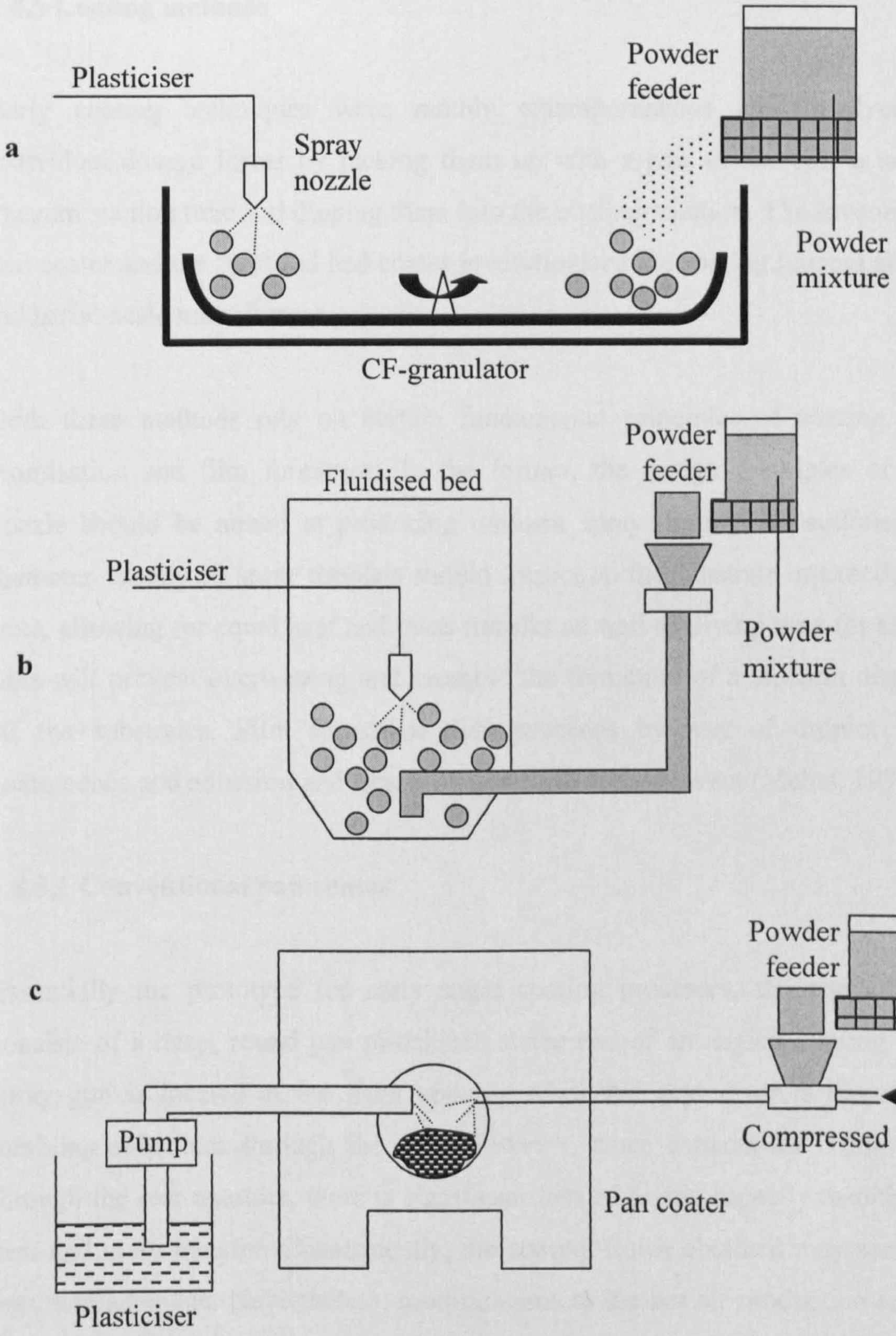

Figure 1.20: Dry coating with (a) CF-granulator, (b) fluidised bed coater and (c) pan coater (Obara *et al.*, 1999).

1.8.5 Coating methods

Early coating techniques were mainly extemporaneous and involved coating individual dosage forms by picking them up with a pair of forceps, a needle or a vacuum suction tube and dipping them into the coating solution. The inventions of the pan coater and the fluidised bed coater revolutionised the coating process and enabled industrial-scale manufacture.

Both these methods rely on certain fundamental principles of coating, primarily atomisation and film formation. In the former, the design principles of the spray nozzle should be aimed at producing uniform spray droplets of sufficiently small diameter. Ideally all spray droplets should impact on the substrate in exactly the same state, allowing for equal heat and mass transfer as well as drying time for all droplets. This will prevent overwetting and promote the formation of a uniform dispersion on all the substrates. Film formation then proceeds by way of droplet spreading, coalescence and adhesion and finally evaporation of the solvent (Mehta, 1997).

1.8.5.1 Conventional pan coater

Essentially the prototype for early sugar coating processes, the conventional pan consists of a deep, round pan positioned at the end of an angled rotating shaft. The spray gun is located at the front opening while hot drying air is blown onto the tumbling substrates through the rear. However, since exhaust air is also extracted through the rear aperture, there is significant loss of drying capacity resulting in poor heat and mass transfer. Consequently, the coating finish obtained may sometimes be less than adequate. Nevertheless, modifications to the hot air production and exhaust equipment improved the method sufficiently for use with organic solvent systems.

1.8.5.2 Perforated pan coater

The gradual shift from organic to water-based coating solutions necessitated the simultaneous adaptation of the pan coater for ultra-efficient removal of solvent. The latent heat of evaporation of water is almost three times that of conventional organic solvents such as ethanol and must be taken into consideration when deliberating

appropriate coating parameters such as drying time, pan speed and air flow rate. Overwetting is detrimental not only in that it increases the likelihood of tackiness and 'clumping' of the substrate, but it also may degrade any hygroscopic, water-sensitive active ingredient or excipient.

The perforated pan draws hot drying air through the substrate bed as compared to the conventional pan which only directs air onto the bed surface. This approach, which markedly improves drying efficiency, is implemented in various ways which basically involve different positioning of the supply and exhaust ducts and vents.

The main advantage of the perforated pan is its ability to achieve a processing speed such as that of the fluidised bed coater while retaining the gentle tumbling motion of the pan coater. This is especially important with fragile substrates such as friable tablets and liquid-filled hard gelatin capsules.

1.8.5.3 Fluidised bed coater

Fluidisation, a process where a bed of small solid particles is suspended and agitated by a rising stream of gas enabling a thorough gas-solid contact throughout the bed, has been employed in various pharmaceutical operations e.g. drying, granulation, pelletisation and coating (Yang *et al.*, 1992). They are usually performed in a fluidised bed coater, developed by Wurster in 1960, which comes in three basic spray mode configurations.

The top spray mode which can be used for granulation and coating, employs similar geometries for both processes i.e. both have a product container and an expansion chamber. However, for coating procedures, the expansion chamber is longer to permit higher fluidisation and has a conical shape (a granulator has a cylindrical one) to reduce the velocity of the particles as they near the filter section. The spray nozzle located in the expansion chamber sprays droplets of the coating suspension or solution which travel countercurrently to the fluidised air current.

For the bottom spray mode, the nozzle is located at the centre of the gas distributor plate. Unlike the top spray, the liquid is sprayed concurrently with the fluidisation air.

The processing chamber goes from a narrow diameter in the product-containing area to a larger diameter in the upper regions. Well-organised particle motion and hence reproducible coating results are obtained in the lower area but the higher, larger area causes particle motion to lose its regular and circulatory pattern and become disorganised. Hence a Wurster chamber, a cylindrical partition mounted in the centre, slightly above the gas distributor plate is often attached to produce a more organised flow of particles.

The tangential spray mode has the spray gun located at the side of the product chamber and liquid is therefore sprayed tangentially to a rotating bed of particles. The effects of a rotating disk in the product chamber and the fluidisation air combine to generate gravitational, centrifugal and vertical forces which maximise the machine's efficacy.

The top and bottom spray modes are graphically illustrated in Figure 1.21.

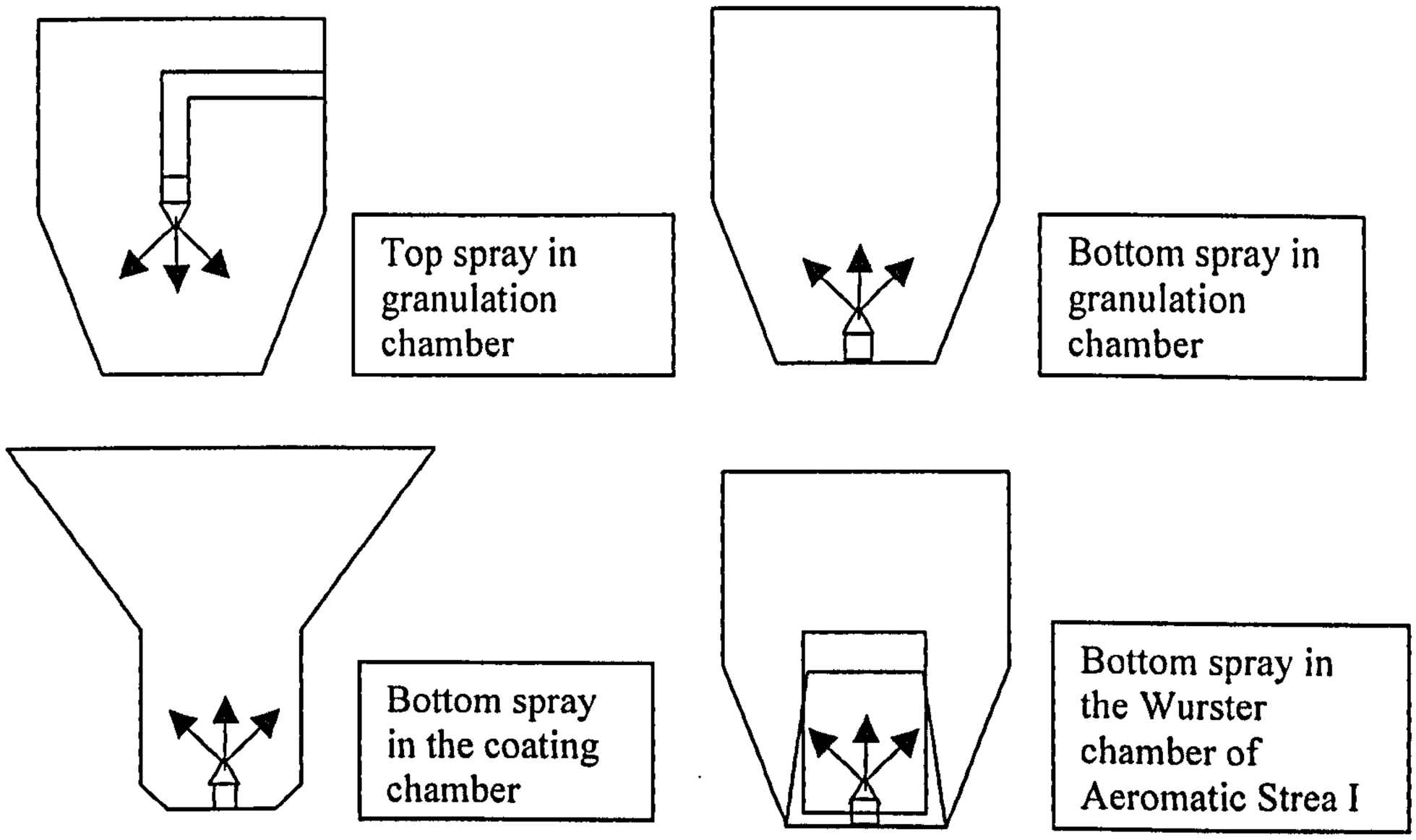

Figure 1.21: Modes of the fluidised bed coater (Yang *et al.*, 1992)

Bertelson *et al.* (1994) studied the effects of spray modes on the film coats prepared by top and bottom spray coaters. They found that potassium chloride crystals coated by bottom spray equipment had significantly slower dissolution rates as compared to those prepared by the top spray. In the top spray mode, it is believed that drying of the

spray droplets occurs before impacting the substrate causing a loss of coating material hence the film formation is less than optimal.

1.9 Aims and objectives

It was the aim of this piece of research to comprehensively design a novel time-delayed drug delivery system which would depend solely on its inherent physical properties to produce a release profile that would consist of a pre-programmed lag time followed by a pulsed release of drug.

Rational approaches to achieving this involve the characterisation of the major components of the system i.e. the swelling agent and the outer coating as well as *in vitro* testing of the complete dosage form.

CHAPTER 2

MATERIALS AND METHODS

This chapter details the various materials and pieces of equipment utilised in the course of this research. It also contains comprehensive descriptions of all methods employed in formulation and subsequent analysis.

2.1 Materials

The chemicals and reagents used are listed below (Section 2.1.1 – 2.1.5) together with their respective suppliers.

2.1.1 Formulation excipients

Corn oil	Fluka, Buchs, Switzerland
Dibasic calcium phosphate (Emcompress®)	Supplied by Pfizer Ltd., Sandwich, Kent, UK
Dibutyl phthalate	Sigma Chemical Company, St Louis, Missouri, USA
D-tartaric acid	May & Baker Ltd., Dagenham, UK
Ethylcellulose, Ethocel Standard 10	Dow Chemical Company, Midland, Michigan, USA
Ethylcellulose, Ethocel Standard 20	Dow Chemical Company, Midland, Michigan, USA
Fast-Flo lactose (Ph.Eur / NF)	Formost Farms, Baraboo, WI, USA; supplied by Pfizer Ltd., Sandwich, Kent, UK
Gelatin Type B, approx. 75 bloom	Sigma Chemical Company, St Louis, Missouri, USA
Gelatin Type B, approx. 225 bloom	Sigma Chemical Company, St Louis, Missouri, USA
Hydroxypropylcellulose (Klucel EF)	Hercules GmbH, Aqualon Division, Düsseldorf Germany
Low-substituted hydroxypropylcellulose (LH-21)	Shin-Etsu Chemical Company, Japan

Microcrystalline cellulose (Avicel PH101)	FMC Europe N.V. Brussels, Belgium
Pemulen TR1 NF	BF Goodrich, Cleveland, Ohio, USA
Polyethylene glycol, average MW 400	Sigma Chemical Company, St Louis, Missouri, USA
Polyvinylpyrrolidone, MW approx 40 000	BDH Chemicals Ltd., Poole, UK
Sodium chloride	BDH Laboratory Supplies, Poole, UK
Sodium dodecyl sulphate	BDH Laboratory Supplies, Poole, UK
Sodium hydrogen carbonate	BDH Laboratory Supplies, Poole, UK
Sorbitan monooleate (Span 80)	Sigma Chemical Company, St Louis, Missouri, USA
Soybean oil	Sigma Chemical Company, St Louis, Missouri, USA
Surelease®	Colorcon Ltd., Dartford, Kent, UK
Triacetin (Glyceryl triacetate)	Multisol Ltd., Nantwich, Cheshire, UK

2.1.2 Model drugs

Griseofulvin	Sigma Chemical Company, St Louis, Missouri, USA
Paracetamol	Sigma Chemical Company, St Louis, Missouri, USA

2.1.3 Solvents

Acetone	Bamford Laboratories, Nordon, Rochdale, UK
Ethanol	Bamford Laboratories, Nordon, Rochdale, UK
Propan-2-ol	BDH Laboratory Supplies, Poole, UK

2.1.4 Gases

Gaseous nitrogen (oxygen free)	BOC Gases Ltd., Guildford, Surrey, UK
Liquid nitrogen	BOC Gases Ltd., Guildford, Surrey, UK
Helium	BOC Gases Ltd., Guildford, Surrey, UK

2.1.5 Consumables

Aluminium foil	Bacofoil Consumer Services, Amersham, Bucks, UK
Aluminium crucibles with lids, 40µl	Mettler-Toledo Ltd., Leicester, UK
BD Plastipak disposable plastic syringes, 5mL and 60mL	Supplied by VWR International Ltd., Poole, UK
Beem® plastic capsules, Size 00	Emitech Limited, Ashford, Kent, UK
Cling film, Clingorap	Terinex Ltd., Bedford, UK
Cover glass, 22X50mm, borosilicate glass	BDH Laboratory Supplies, Poole, UK
Dissolution filters	Copley Scientific Ltd., Nottingham, UK
Disposable Pasteur pipettes	Fisher Scientific, Loughborough, UK
Dissolution tubings	Copley Scientific Ltd., Nottingham, UK
Filter paper, Qualitative 1 grade, Ø 11.0cm	Whatman plc, Brentford, Middlesex, UK
Hard gelatin capsules, Coni-snap® and Licaps®, Size 1 and 00	Capsugel, Bornem, Belgium
Micropipette, 1mL	Gilson, Middleton, WI, USA
Microscope slides, Super Premium, 0.8-1.0mm thick/plain	BDH Laboratory Supplies, Poole, UK
Silicone tubing, platinum cured, ID 3.2mm, thickness 1.6mm	Watson-Marlow Bredel Pumps Ltd., supplied by VWR International Ltd., Poole, UK
Tygon flexible plastic tubing, ID $^{1}/_{8}$", OD $^{3}/_{16}$", wall $^{1}/_{32}$"	Saint-Gobain Performance Plastics, Charny, France

2.2 Equipment

2.2.1 Formulation and manufacture

Balances :	
a) Sartorius	Sartorius AG, Goettingen, Germany
b) AG 135	Mettler-Toledo Ltd., Leicester, UK
c) AG 204	Mettler-Toledo Ltd., Leicester, UK

Fluidised bed coater, Aeromatic Strea-1, connected to	Aeromatic AG, Bubendorf, Switzerland
Watson-Marlow 313S peristaltic pump	Watson-Marlow Bredel Pumps Ltd., Falmouth, Cornwall, UK
Hotplate stirrer, Bibby	Supplied by VWR International Ltd., Poole, UK
Manesty SP single tablet hand press	Manesty, Knowsley, Merseyside, UK
Mini coater / drier	Caleva Process Solutions Ltd., Dorset, UK
Oven, forced-air	Mitchell Dryers Ltd., Carlisle, Cumbria, UK
Sieve, brass, 150μm	Endecotts Ltd., London, UK

2.2.2 Analytical

Aluminium crucible lid sealer	Mettler-Toledo Ltd., Leicester, UK
Automated dissolution apparatus	
a) Caleva dissolution bath connected to:	G.B. Caleva Ltd., Dorset, UK
Unicam UV2 spectrometer;	Unicam UV-Visible Spectrometry, Cambridge, UK
Watson-Marlow 205U multichannel peristaltic pump	Watson-Marlow Bredel Pumps Ltd., Falmouth, Cornwall, UK
b) Copley ST7 dissolution bath connected to:	Copley Scientific Ltd., Nottingham, UK
Cecil 3021 UV spectrophotometer;	Cecil Instruments Ltd., Cambridge, UK
IPC multichannel dispenser; controlled by Copley Dissobox	Ismatec, Glattbrugg-Zurich, Switzerland Copley Scientific Ltd., Nottingham, UK
Differential scanning calorimeter connected to measuring cell DSC 30 Module controlled by TA controller TC15	Mettler-Toledo Ltd., Leicester, UK
Dynamic vapour sorption apparatus, DVS 1/1000	Surface Measurement Systems, London, UK
Polarised light microscope, Polyvar	Reichert-Jung, Arnsberg, Germany
Scanning electron microscope, Jeol JSM 6400	JEOL USA, Inc. Peabody, MA, USA
Sputter coater, Polaron SC515	Enutech Ltd., Ashford, Kent, UK

Tablet hardness tester, Schleuniger	Schleuniger AG, Thun, Switzerland
Texture Analyser, TA-XT2	Stable Micro Systems, Surrey, UK
Thermogravimetric analysis (TG 50) connected to MTS Cahn balance controlled by TA controller TA15	Mettler-Toledo Ltd., Leicester, UK

2.3 PC software

Dissolution software	
a) Caleva apparatus	Conat Instruments Ltd., UK
b) Copley apparatus	Copley Scientific Ltd., Nottingham, UK
Differential scanning calorimetry software, Star^{e} system	Mettler-Toledo Ltd., Leicester, UK
Dynamic vapour sorption software, DVS Win v2.16	Surface Measurement Systems, London, UK
Statistical software, Minitab v.13	Minitab Ltd., Coventry, UK
Texture Analyser software, Texture Expert v1.22	Stable Micro Systems, Surrey, UK
SEM software, ImageSlave	Meeco-Dindema, Sydney, Australia

2.4 Preformulation testing

2.4.1 Partitioning of LH-21 in oil and water

In Method I, a 10mL measuring cylinder was filled with 4mL of distilled water. Separately in another vessel, 4mL of soybean oil was mixed with a specified amount of LH-21 and added to the cylinder. The mixture was agitated. The settling of a swollen layer of LH-21 (visibly noticeable) was quantified by recording the height of the increasing white mass at the base of the cylinder.

Alternatively, Method II was employed whereby a specified amount of LH-21 was weighed into a measuring cylinder, carefully avoiding the internal walls of the vessel. The initial height of the dry powder was recorded. 4mL each of soybean oil and distilled water were added; agitation of the mixture performed after each addition. The height of the swollen mass was recorded over time.

Methods I and II were repeated with varying amounts of LH-21 and are depicted in Figures 2.1a and b.

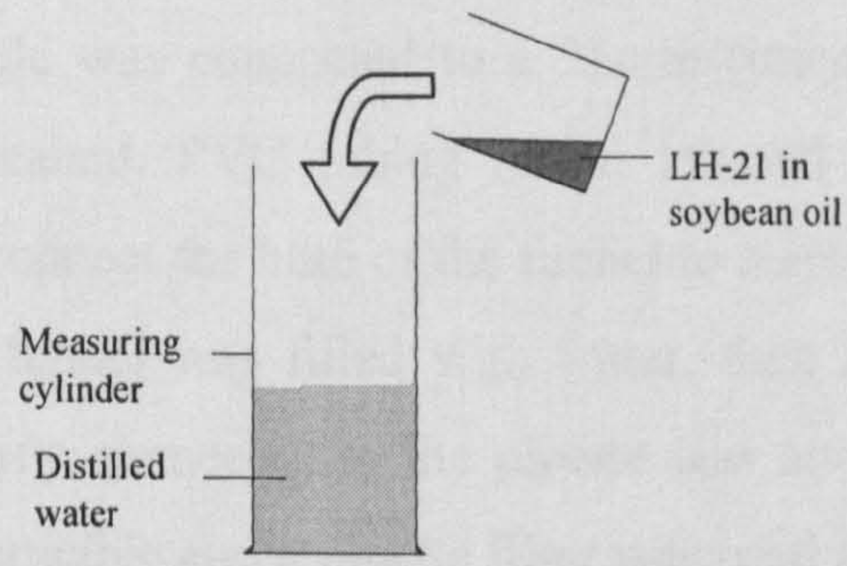

Figure 2.1a: Method I of LH-21 partitioning study: oil added to water.

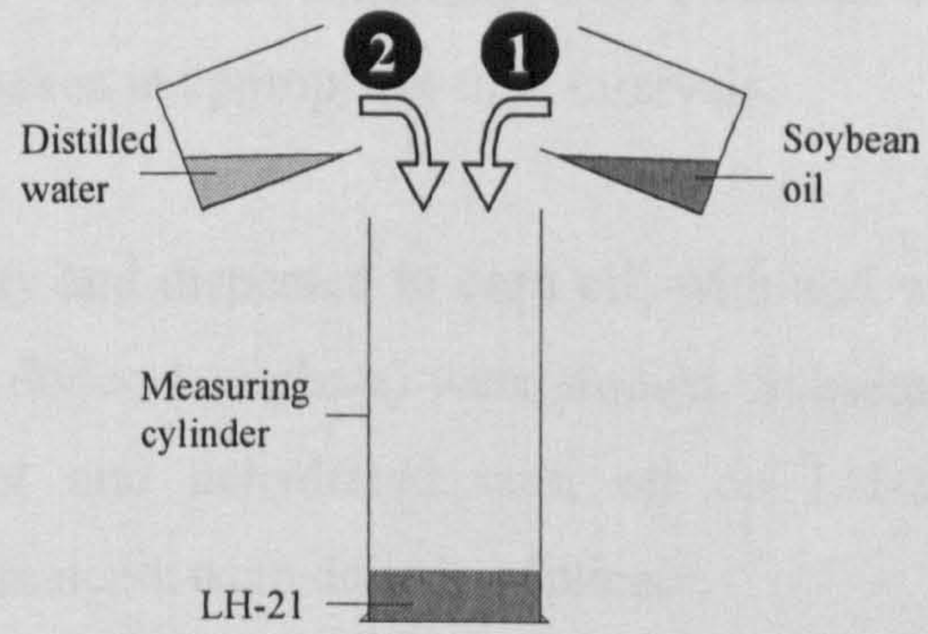

Figure 2.1b: Method II of LH-21 partitioning study: water added to oil.

2.4.2 Water uptake studies

A simple apparatus, modified from Kawashima *et al.* (1993a) was designed to investigate the water absorption characteristics of LH-21 (Figure 2.2).

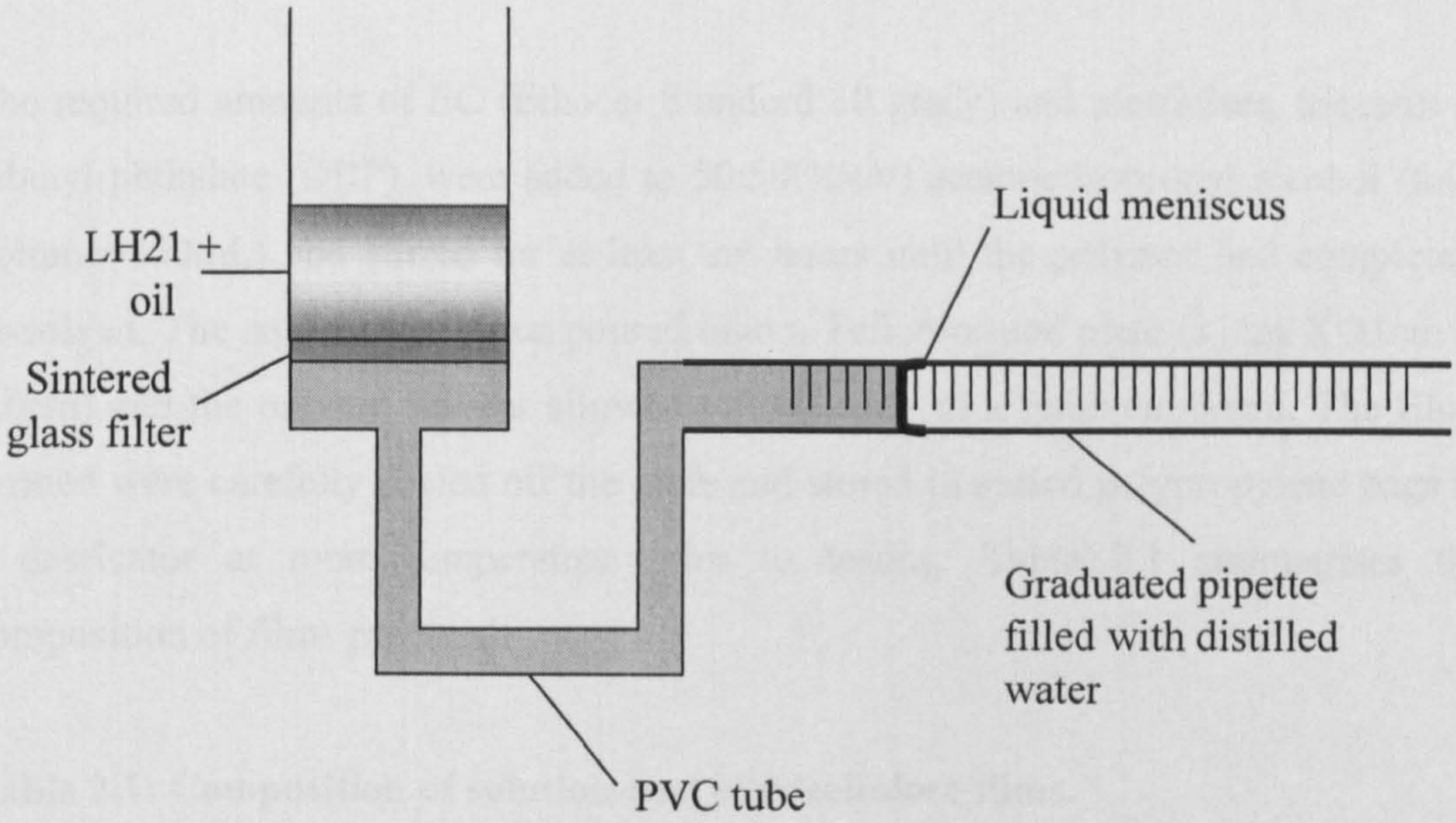

Figure 2.2: Water uptake apparatus.

A sintered glass crucible was connected to a 25mm (internal diameter) glass filter funnel with silicone sealant. PVC tubing (6mm internal diameter, 9mm external diameter) was used to connect the base of the funnel to a graduated pipette. To fill the apparatus, the conical funnel was filled with water, then inverted and the silicone tubing which was already connected to the pipette was attached. Water was poured into the sintered glass crucible and a pipette filler was used to draw water through the apparatus, avoiding air bubbles. The sample was then placed into the sintered glass crucible and the timer was started simultaneously. Readings of the water meniscus in the pipette were then taken at appropriate time intervals.

Samples of LH-21, dry and dispersed in corn oil, with and without added surfactant (Span 80 and sodium dodecyl sulphate) were studied. Subsequent experiments on the effect of paracetamol and dehydrated corn oil on LH-21 swelling were also conducted. All measurements were done in triplicate.

2.4.3 Preparation of solution-cast ethylcellulose films

These cast films were prepared to investigate the mechanical properties of ethylcellulose (EC), independently of the final dosage form, in order to postulate general effects of excipients on the rupturable film.

The required amounts of EC (Ethocel Standard 10 grade) and plasticiser, triacetin or dibutyl phthalate (DBP), were added to 50:50(%v/v) acetone:isopropyl alcohol (total volume=150mL) and stirred for at least six hours until the polymer had completely dissolved. The solution was then poured onto a Teflon-coated plate (31cm X 31cm X 0.6cm) and the organic solvent allowed to evaporate in a fume cupboard. The films formed were carefully peeled off the plate and stored in sealed polypropylene bags in a dessicator at room temperature prior to testing. Table 2.1 summarises the composition of films prepared.

Table 2.1: Composition of solution-cast ethylcellulose films.

EC (%w/v)	Triacetin (%w/w of EC)	DBP (%w/w of EC)
2	10-60	20-60
3	20-60	20-60
4-6	20	-

EC (%w/v)	Triacetin (g)	DBP (g)
2-6	1.8	1.8

2.4.4 Swelling force studies

These studies, as well as those described in Sections 2.4.5.1 and 2.4.5.2, were performed using the Texture Analyser TA-XT2 (Stable Micro Systems, Surrey, UK) hence it is appropriate to describe this particular piece of instrumentation before proceeding.

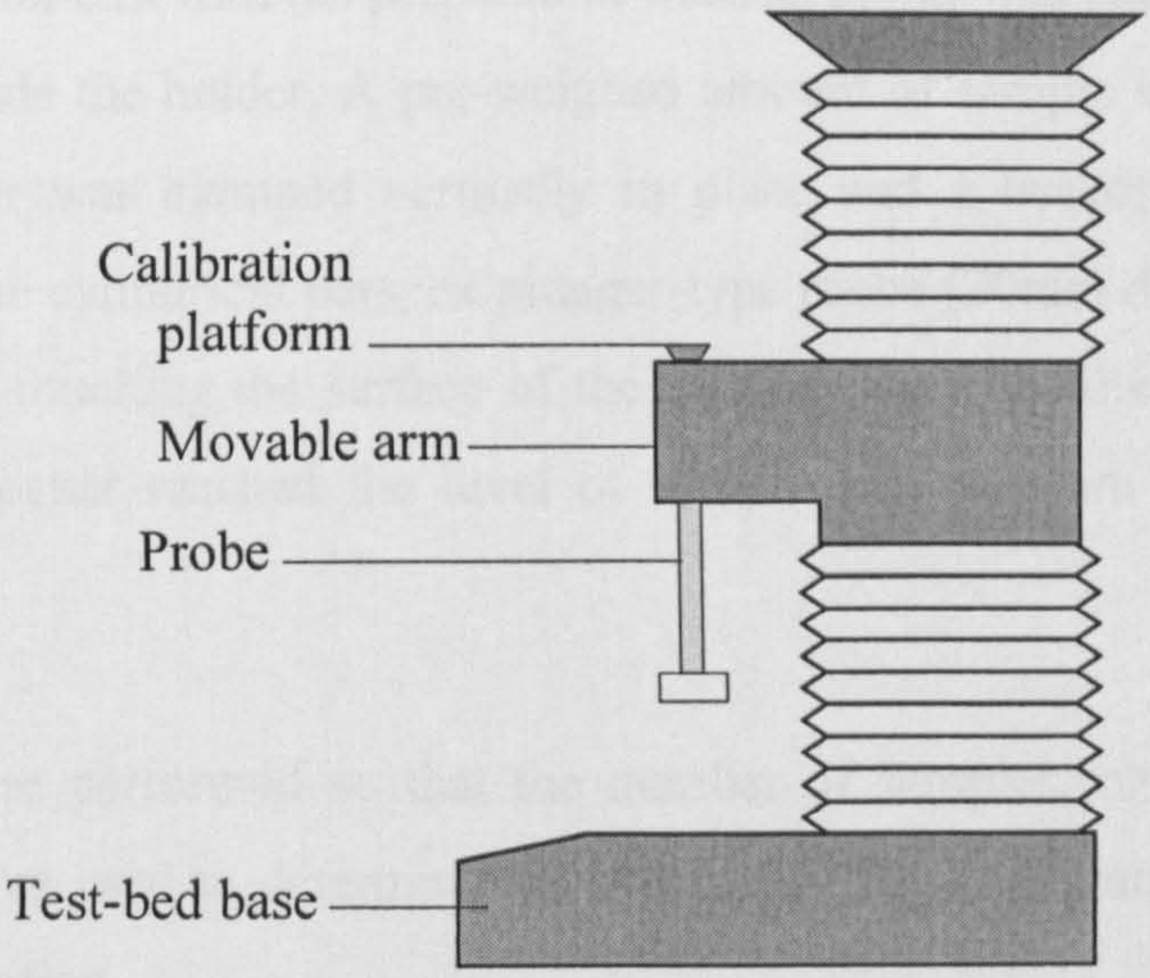

Figure 2.3: Basic setup of Texture Analyser TA-XT2.

The Texture Analyser was first designed for use in the food industry, tackling problems such as the determinations of resistance of ice cream, the firmness or stickiness of pasta and the fracturability of crisps. Gradually it was incorporated into the pharmaceutical industry as it was capable of characterising physical properties such as mucoadhesion, tablet coating adhesion and swelling force.

In essence, the apparatus consists of a flat base upon which the sample rests, a probe for detecting the parameter being measured and a moving arm. A keyboard panel is attached to the unit and functions as a control box, complementing the Texture Expert v1.22 software that receives and transmits the operating instructions. The software also possesses features for data analysis, providing information such as maximum force generated, gradient of force-distance curves and area under the curve.

Swelling force studies were undertaken in order to quantify the amount of force generated per gram of LH-21 when in contact with water and to determine the effect of changing concentrations of LH-21, corn oil and other excipients on the force generated.

For the swelling force studies, a sample holder was prepared using a perspex tube with one end covered with a wire mesh. A circle of filter paper (Whatman Qualitative

1) or disc of solution-cast film (as prepared in Section 2.4.3) was placed on the top of the wire mesh inside the holder. A pre-weighed amount of sample was placed in the holder. The holder was clamped vertically in place and a beaker placed under it (Figure 2.4) and the cylindrical perspex plunger-type probe (20mm diameter) lowered into place directly touching the surface of the sample. Once distilled water that was poured into the beaker reached the level of sample, the program (Table 2.2) was started.

Measurements were performed so that the number of samples, n≥10. The Texture Expert software was used to determine the maximum force generated and the initial rate of force generation.

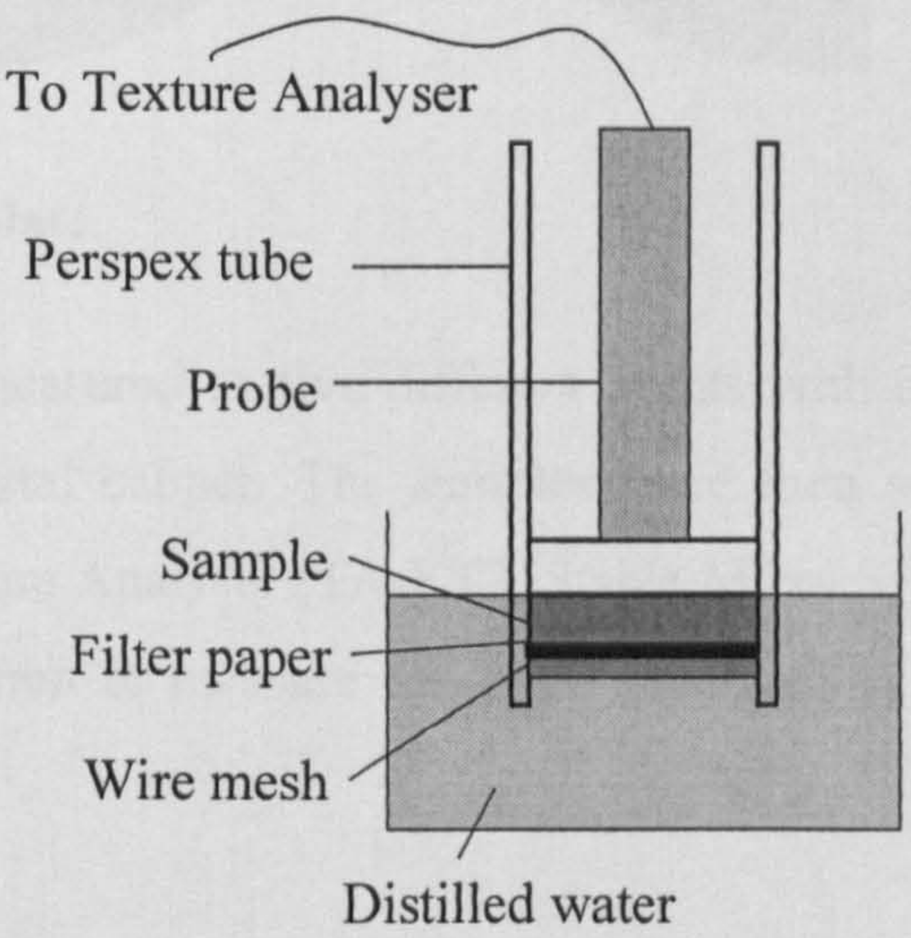

Figure 2.4: Apparatus for force measurement.

Table 2.2: Texture Expert v1.22 program for force measurement.

Force Relaxation (HLDD)	
Pre-Speed	2.0mm/s
Test Speed	1.0mm/s
Post-Speed	10.0mm/s
Trigger force	20g
Time	1800s
Load cell	5kg

2.4.5 Characterisation of mechanical properties of ethylcellulose films

Films used in these studies were prepared according to the method described in Section 2.4.3.

2.4.5.1 Tensile properties

Films were cut into dumbbell-shaped samples using a sharp scalpel and an American Society for Testing and Materials (ASTM) metal template (Figure 2.5).

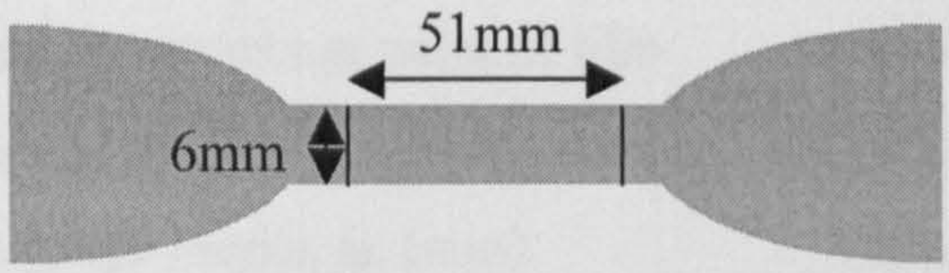

Figure 2.5: ASTM template.

Sample thickness was measured at five different points with a Mitutoyo Absolute Digimatic CD-15CP digital caliper. The samples were then secured between two tensile grips on the Texture Analyser (TA-XT2, Stable Micro Systems, Surrey, U.K.) and subjected to a program to measure the force generated in stretching the films (Table 2.3).

Table 2.3: Texture Expert v1.22 program for stretching of films.

Measure Force in Tension	
Return to Start	
Pre-Speed	0.1mm/s
Test Speed	0.1mm/s
Post-Speed	0.1mm/s
Distance	10.0mm
Trigger Force	0.001N
Load cell	5kg

The data obtained were analysed to determine the following parameters summarised in Table 2.4.

Table 2.4: Tensile properties of EC films determined by stretching of films.

Tensile property	Definition	Raw data required
Tensile stress at break of film, σ_b	Tensile force subjected to film at break, per unit area of initial cross-sectional area of specimen within gauge length, A (mm^2). $\sigma_b = \frac{F_b}{A}$ (N/mm^2 or MPa)	Maximum force at break of film, F_b (N)
Tensile strain at break of film, ε_b	Ratio of increase in length of sample between gauge marks at point of film break ($l_b - l_0$) to initial length of sample between gauge marks, l_0, (mm). $\varepsilon_b = \frac{l_b - l_o}{l_o}$	Maximum distance travelled by upper tensile grip before film break, l_b (mm)
Work done to break film, W	Work expended in straining the sample to failure. W = **AUC** (Nm)	Area under the curve, **AUC**
Elastic modulus of film, E	Slope of regression of stress, σ, (MPa) on strain, ε, in region of linear elastic deformation. $E = \frac{\Delta\sigma}{\Delta\varepsilon}$ (N/mm^2)	Gradient of curve in linear region, $m = \frac{\Delta F}{\Delta l}$ where ΔF (N) and Δl (mm) are the change in force and distance over time respectively

2.4.5.2 Puncture properties

Solution-cast films (Section 2.4.3) were cut into 25mm diameter discs for testing. The discs were immersed in a 37°C water bath. At 30-minute intervals, from 0 to 150 min, samples were removed, dried between two sheets of filter paper and stored in a 37°C hot cupboard.

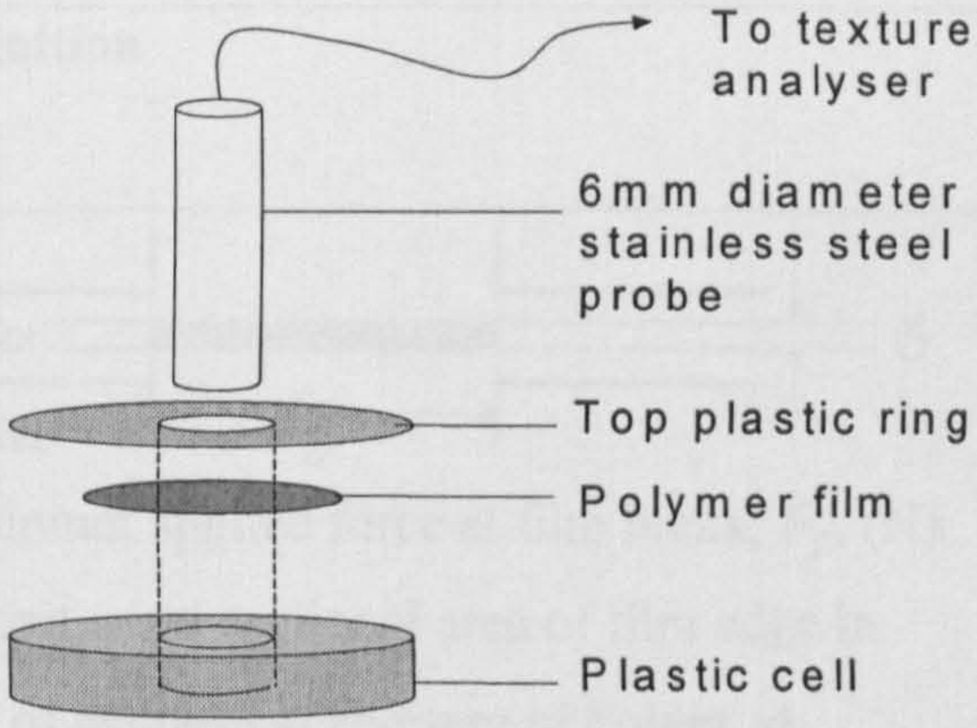

Figure 2.6: Setup for puncture test.

Table 2.5: Texture Expert v1.22 program for film rupture test.

Measure Force In Compression	
Pre-test Speed	0.2mm/s
Test Speed	0.1mm/s
Post-test Speed	0.2mm/s
Distance	8.0mm
Trigger type	Auto
Trigger force	0.001N
Acquisition rate	25pps

The discs were secured between two cylindrical Perspex blocks with an 8mm diameter aperture (adapted from Bussemer *et al.*, 2003) as shown in Figure 2.6. A 6mm diameter stainless steel probe attached to a Texture Analyser TA-XT2 (5kg load cell) was driven through the film controlled by the Texture Expert v1.22 program in Table 2.5. The data obtained ($10 \leq n \leq 15$) was analysed for statistical significance at 5% level using ANOVA in Minitab v.13. Remaining films were stored in sealed polypropylene bags in dessicators at room temperature for three months prior to testing.

The puncture properties analysed and calculated from the raw data are summarised in Table 2.6.

Table 2.6: Puncture properties of EC films determined by rupturing of films.

Puncture property	Definition	Raw data required
Puncture strength, σ_p	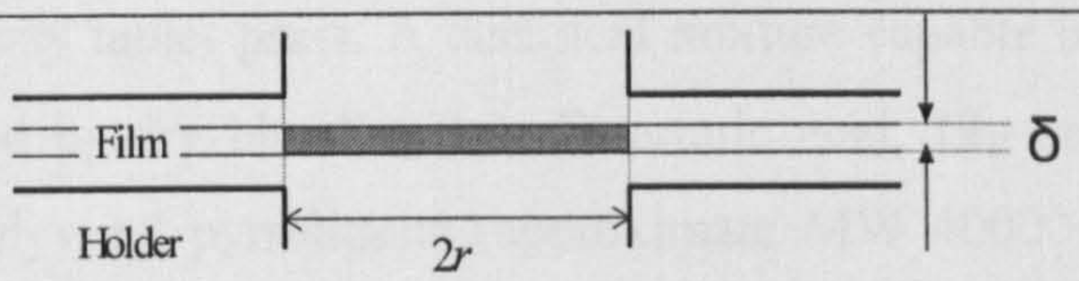 Maximum applied force at film break, F_p, (N) per unit cross-sectional area of film edge in path of cylindrical aperture of holder, A, (mm^2) where A is approximately equal to the product of the diameter of the film exposed ($2r$) and its mean thickness, δ. $$\sigma_p = \frac{F_p}{A} (N/mm^2)$$	Maximum force at film puncture, F_p (N)
Strain at film puncture, ε_p	The ratio of the linear expansion of the film (Δl) to the radius of the film exposed, r, (mm). 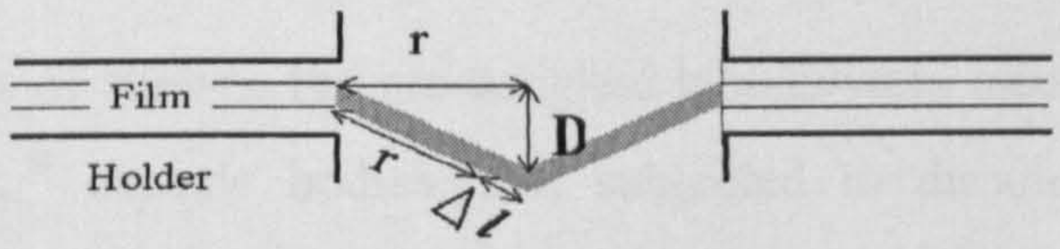 $$\varepsilon_p = \frac{\Delta l}{r} = \frac{\sqrt{(r^2 + D^2)} - r}{r}$$	Maximum distance travelled by punch prior to film rupture, D (mm)
Work done to puncture film, **W**	Energy expended in puncturing film. **W = AUC** (Nm)	Area under the curve, **AUC**
Modulus, **E**	Slope of stress-strain curve before film break (N/mm^2).	Gradient of curve at linear region, $m = \frac{\Delta F}{\Delta l}$ where ΔF (N) and Δl (mm) are the change in force and distance over time respectively

2.4.6 Tablet erosion study

Gelatin-based tablets (convex, 8mm diameter) were manufactured using a single punch Manesty tablet press. A chemical mixture capable of producing effervescence was prepared by dry blending 10g D-tartaric acid, 12g sodium hydrogen carbonate and 1.1g polyvinyl pyrrolidone (approximate MW 40000) prior to wet granulation with 6-7mL ethanol. The slurry was then dried in a 60°C fan oven; the resultant brittle mass was crushed using a mortar and pestle and passed through a 150μm sieve. (From here on, this mixture will be referred to as effervescent material.) The compositions of the tablets were as follows: 120mg 75b gelatin with 0mg, 12mg, 24mg, 36mg, 48mg and 60mg effervescent material.

Separately, 120mg, 75b gelatin tablets were made of varying degrees of hardness: 2-2.9kp, 3-3.9kp, 4-4.9kp, 5-5.9kp and 6-6.9kp. The hardness was determined by sampling 9-10 tablets in a Schleuniger tablet hardness tester, and the mean and standard deviation calculated.

For both sets of studies, the pre-weighed tablets were inserted at the neck of Size 00 plastic Beem® capsule bodies, and subjected to dissolution in 1000mL distilled deaerated water at 37°C, 50rpm paddle speed (complete description of dissolution system in Section 2.6.6).

A Beem®-tablet assembly was removed at intervals of 10 or 15 min and each timepoint was represented by readings of 6 tablets. Once removed, the assembly was wiped dry with tissue and stored in a 37°C hot cupboard for at least 24 hours. The final weight of the assembly was recorded.

2.5 General analytical techniques

2.5.1 Microscopic techniques

2.5.1.1 Light microscopy

A Polyvar microscope connected to a Reichert-Jung control box was used to observe the structural morphology of LH-21 at low magnification. Figure 2.7 shows the various functional parts of this microscope. Although this research microscope possessed features for dark-field, fluorescence, phase contrast and interference contrast microscopy, bright-field (Köhler) and polarised light microscopy were sufficient to provide the detail required.

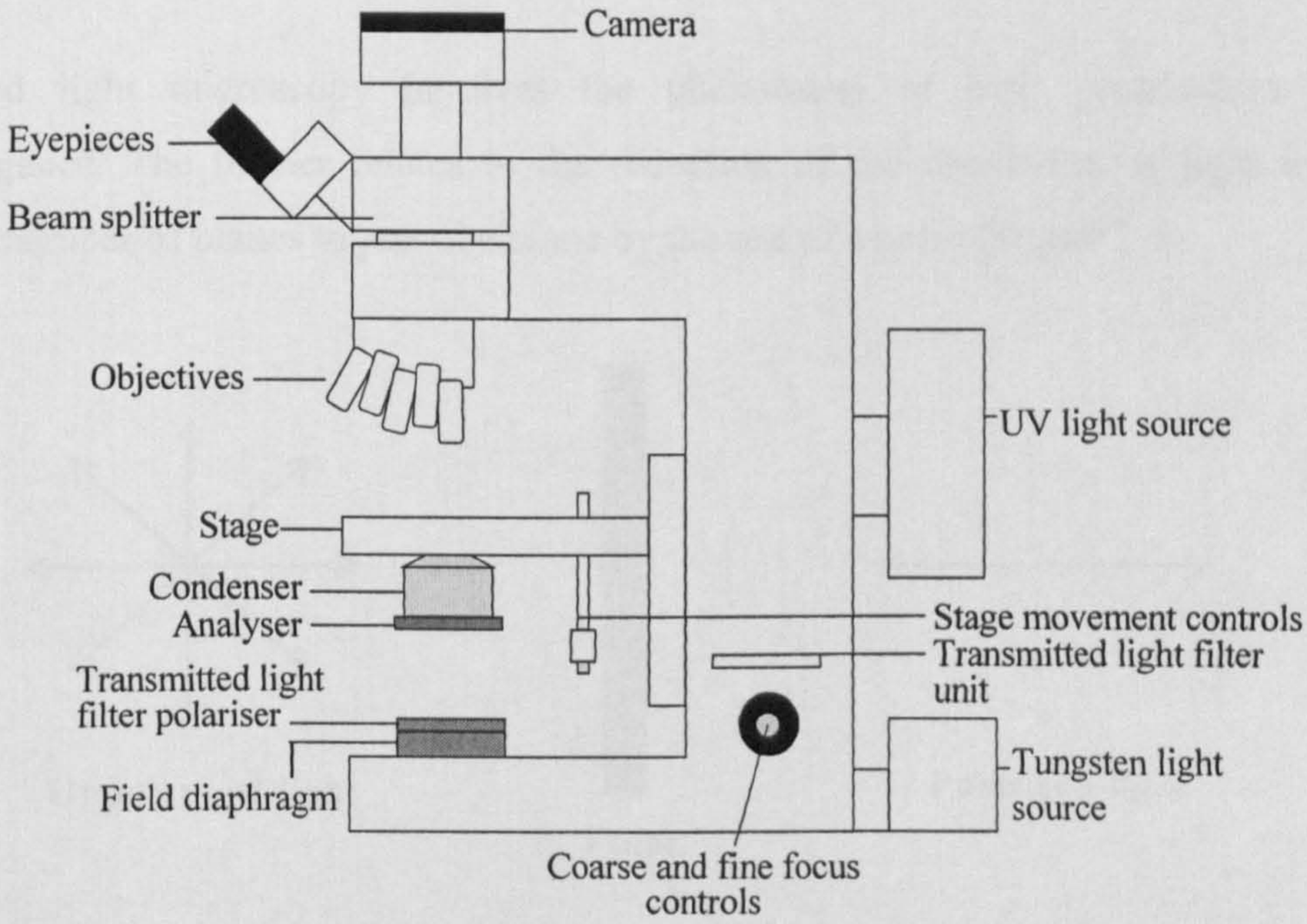

Figure 2.7: Components of the Polyvar microscope.

Samples were mounted on 0.8-1.0mm thick plain glass slides and 0.17mm glass cover slips were gently laid over them. The beam splitter was adjusted to divert the light from the specimen to the camera, which was loaded with colour 35mm film (ISO 200). Initially, the transmitted light filter polariser was set to illuminate the specimen in unpolarised light. Once in focus, the image was captured on film then the polariser manipulated to polarise the light transmitted. Hence the same area of the specimen

was imaged in both polarised and unpolarised light. The objectives used varied in magnification i.e. X10, X25 and X40. Therefore upon taking into consideration the eyepiece magnification being X10, the total magnification values were X100, X250 and X400 respectively.

It is useful here to discuss the general theory behind light microscopy, focusing on the two methods employed in our studies. Bright field or Köhler illumination, so named after August Köhler who first described it at the turn of the 20th century, depends on the inherent colour or contrast of the specimen to produce a satisfactory image. While it is the method which introduces the least number of unwanted artefacts to the resultant image, absence of colour or contrast of the specimen severely hampers the ability to obtain an image of sufficient detail. It is obviously first choice for the imaging of coloured or stained specimens.

Polarised light microscopy involves the phenomena of both polarisation and birefringence. The former relates to the reduction of the oscillation of light in an infinite number of planes to just one plane by the use of a polar (Figure 2.8).

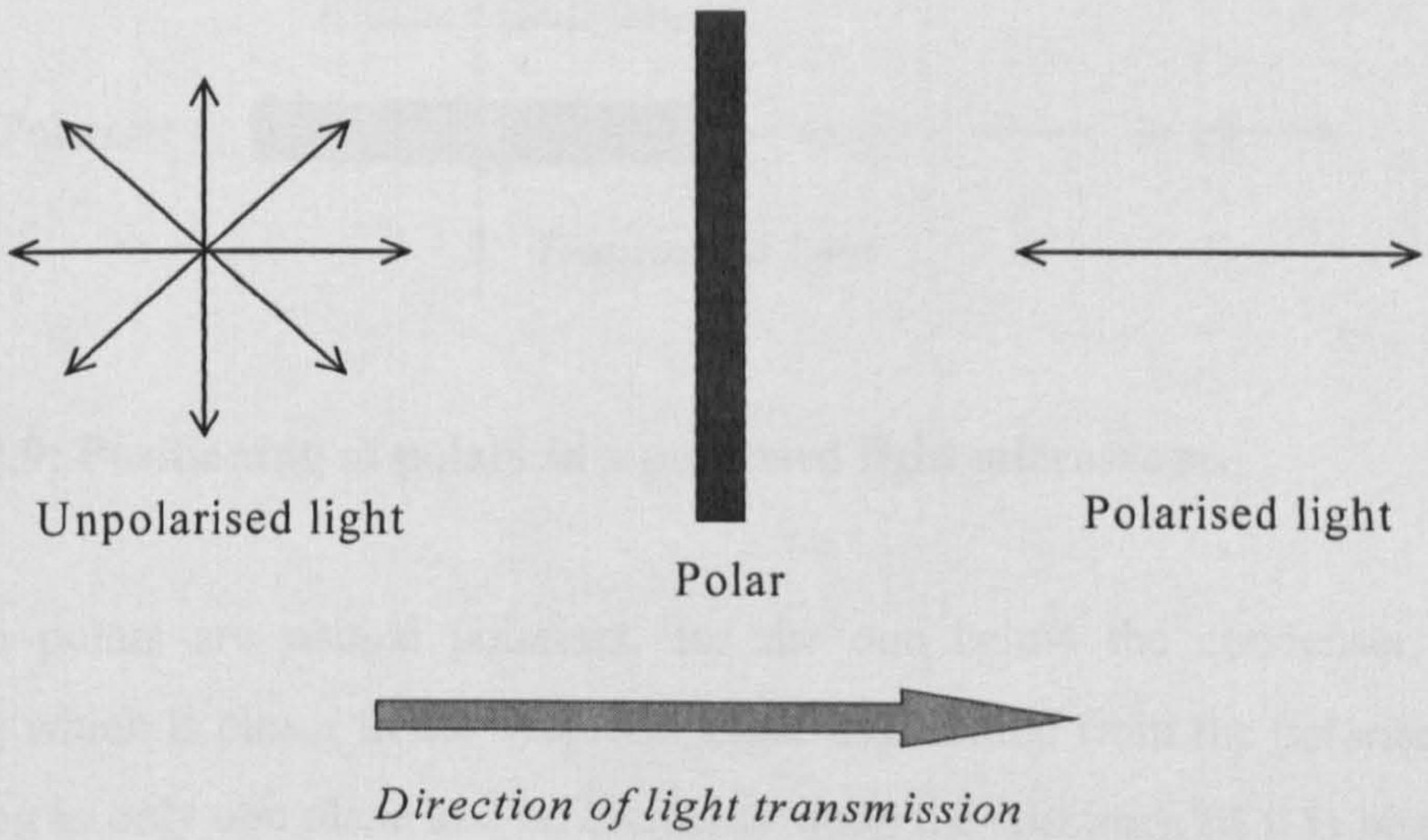

Figure 2.8: Polarisation of light.

In optical terms, materials can generally be categorised as isotropic or anisotropic. Isotropism indicates that the light incident on that particular substance has the same velocity / refractive index in all directions. Anisotropic materials however, exhibit

birefringence: all incident light rays are split into two part-rays, oscillating at perpendicular angles to each other, neither of which are of the same intensity as the original ray. Birefringence (Δn) can be numerically described as the difference between the refractive indices of the two split beams.

A polarised light microscope has two polars positioned so as to sandwich the specimen, as shown in Figure 2.9.

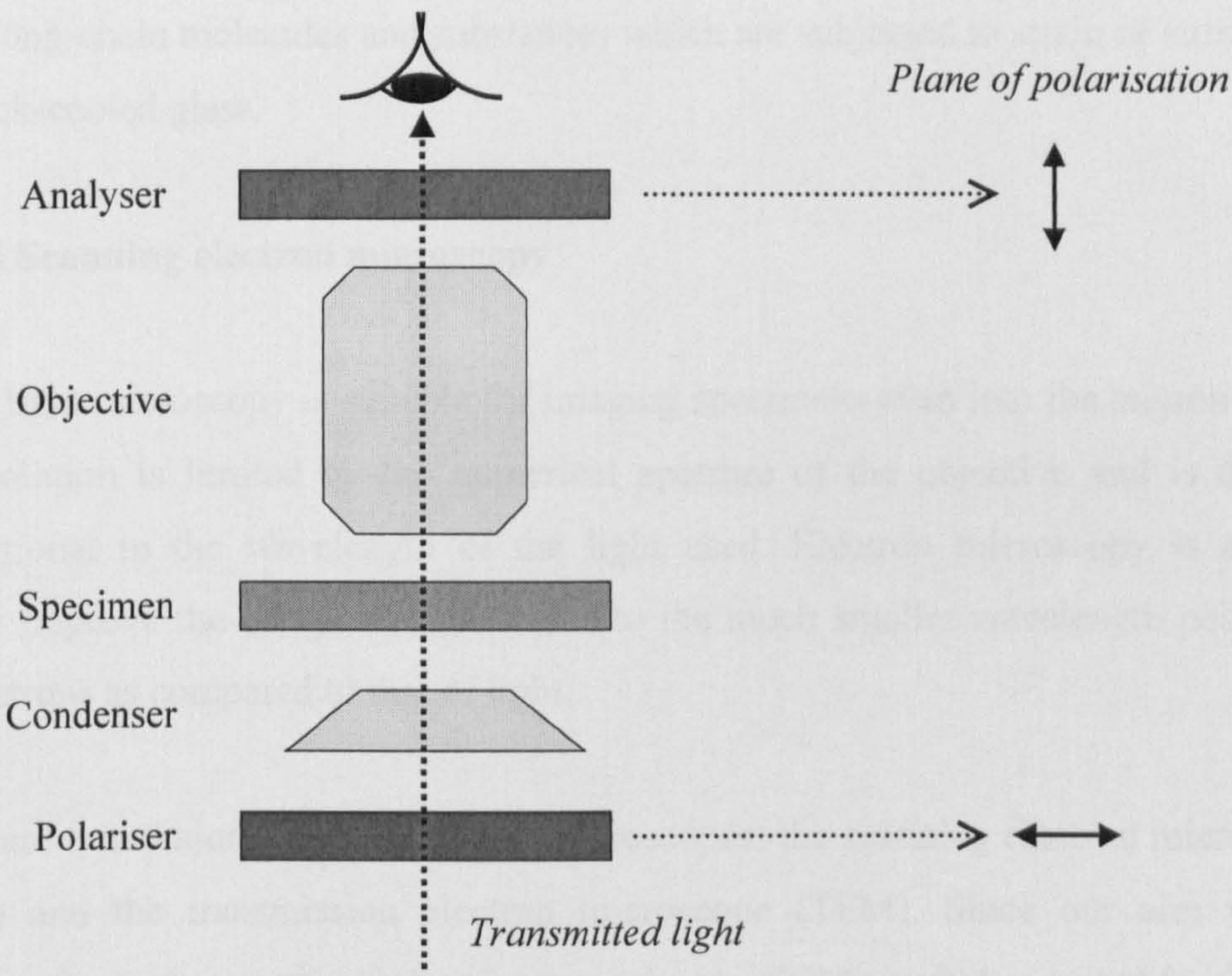

Figure 2.9: Positioning of polars in a polarised light microscope.

The two polars are named polariser, for the one below the condenser, and the analyser, which is closer to the eyepiece. Light transmitted from the polariser will be oscillating in only one plane and on incidence upon the specimen (if it is birefringent) splits into two beams oscillating at right angles to each other. The analyser is set to polarise light in a direction perpendicular to the polariser; the polars are said to be crossed. This orientation will result in the production of one of two types of images:

a) total darkness due to the specimen being isotropic; or
b) coloured image of the birefringent specimen due to the splitting of the incident beam.

Simply obtaining a coloured image of the specimen indicates that it exhibits birefringence but to relate this information to its molecular structure, requires the calculation of its birefringence by comparing it to a specimen of known birefringence, a compensator. Rotation of the specimens, one with respect to the other, and determining the relative angles between the two at positions which result in maximal brightness and darkness can be used to calculate Δn of the unknown specimen.

Birefringence is exhibited by crystals, liquid crystals, certain biological specimens, some long-chain molecules and substances which are subjected to strain or stress such as shock-cooled glass.

2.5.1.2 Scanning electron microscopy

While light microscopy is suitable for imaging specimens even into the micron range, its resolution is limited by the numerical aperture of the objective and is directly proportional to the wavelength of the light used. Electron microscopy is able to greatly improve the image resolution due to the much smaller wavelength possessed by electrons as compared to that of light.

There are two major types of electron microscopes: the scanning electron microscope (SEM) and the transmission electron microscope (TEM). Since our aim was to visualise the surface morphology of our specimens, SEM was better suited for the task rather than TEM which is more adept at exploring internal structure.

Figure 2.10 illustrates very simply the workings of the SEM.

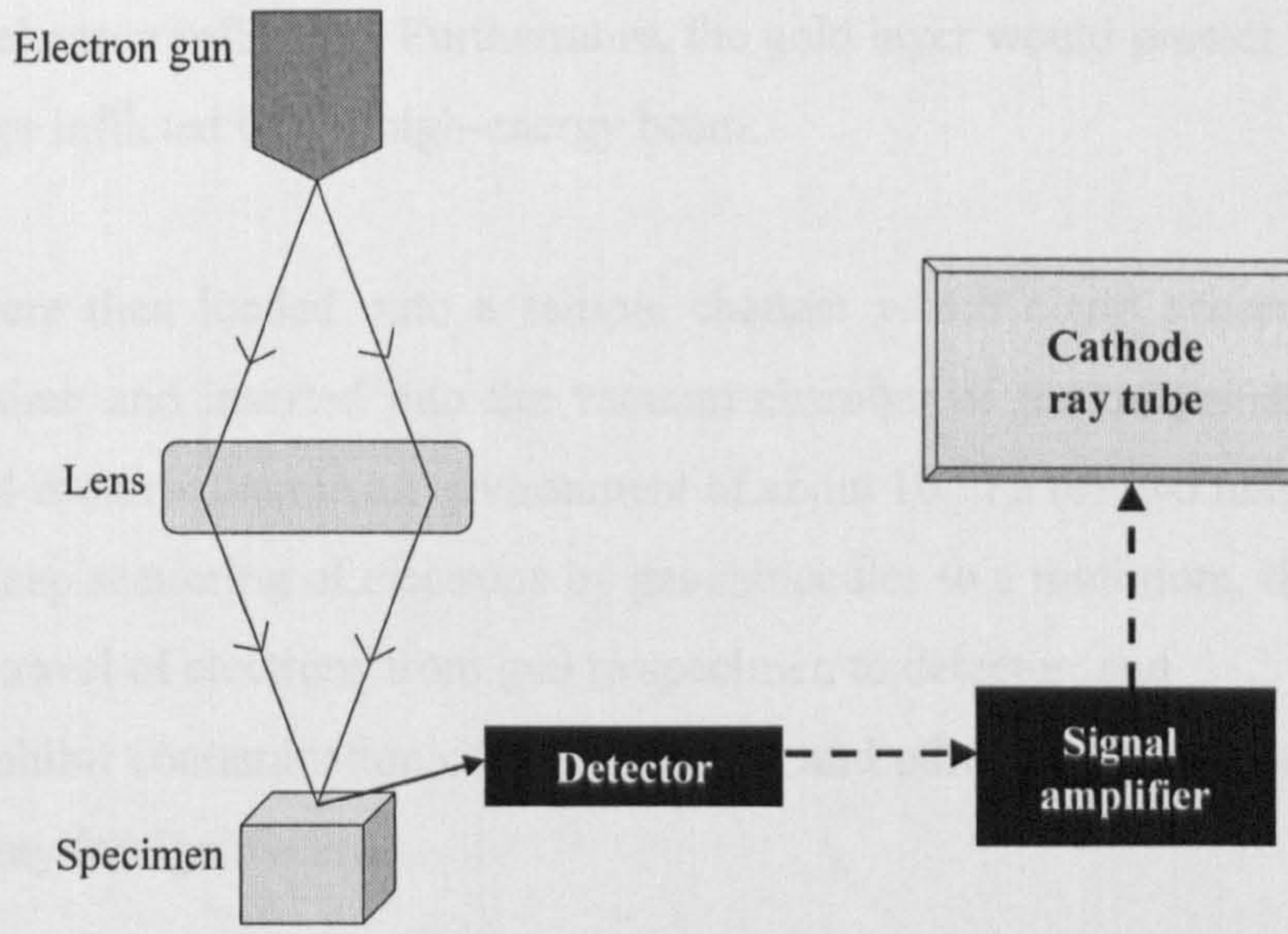

Figure 2.10: Simple schematic of SEM.

A fine beam of electrons generated by an electron gun is scanned across the surface of the specimen resulting in the emission of a secondary signal e.g. secondary electrons, back-scattered electrons or X-rays. The intensity of the signal varies according to the surface structure of the specimen be it peaks or valleys and the detector then relays the signal to an amplifier which improves on the signal quality. Through a series of electronics, the signal is converted into an image, comprehensible to the human eye, and displayed on a TV screen.

Preparation of the sample involved firstly mounting the specimen on 10mm aluminium stubs with double-sided carbon or copper tape. Two types of sample were used in our studies: powder and film. Any excess powder was gently tapped away as too thick a layer would hinder optimal focusing. The film samples were cut into squares of about 5mm x 5mm and carefully pressed down onto the tape using forceps at the edges of the film, avoiding the central part which should remain free from indentations.

The mounted samples were then sputter coated with a thin (about 10nm) layer of gold in a Polaron SC515 SEM coating system. This layer of metal would improve image contrast by providing a consistent source of secondary electrons while simultaneously

promoting electron reflection. Furthermore, the gold layer would protect the specimen from damage inflicted by the high-energy beam.

Samples were then loaded onto a sample changer which could accommodate four stubs at a time and inserted into the vacuum chamber of the instrument (Jeol JSM 6400). SEM is carried out in an environment of about 10^{-2} Pa for two reasons:

a) to keep scattering of electrons by gas molecules to a minimum, thereby easing the travel of electrons from gun to specimen to detector; and
b) to inhibit contamination of the specimen, and other components of the system by any foreign material.

Magnification was initially increased to a level greater than required in order to better focus the image using both coarse and fine controls. Spot size i.e. the diameter (and hence intensity) of the electron beam was then adjusted. While decreasing the spot size improves the resolution of the image, there is potential risk of lowering the number of secondary electrons emitted to such an extent that the image will be 'noisy'. Hence the spot size was gradually decreased to the optimal level for the magnification used. Stigmators were also used to improve the resolution of the image produced. The magnification was then lowered to the level required and final adjustments to focus were performed prior to capturing the image on the PC using the ImageSlave software.

All samples were imaged at two or three levels of magnification. The accelerating voltage of the electron gun was maintained at 6kV.

2.5.2 Thermal analysis techniques

Two such techniques i.e. thermogravimetric analysis (TGA) and differential scanning calorimetry (DSC) were used in the course of this research and are described in the following sections. In our laboratory, both these instruments are linked to the same control unit, a Mettler-Toledo TA Controller TC15.

2.5.2.1 Thermogravimetric analysis (TGA)

In essence, TGA determines the weight change of a sample subjected to a heating / cooling cycle. The essential component for operation is a thermobalance which itself comprises of an electronic microbalance, a furnace, a temperature programmer as well as instrumentation for recording the weight change and temperature ramp. General setup of a TGA is represented in Figure 2.11.

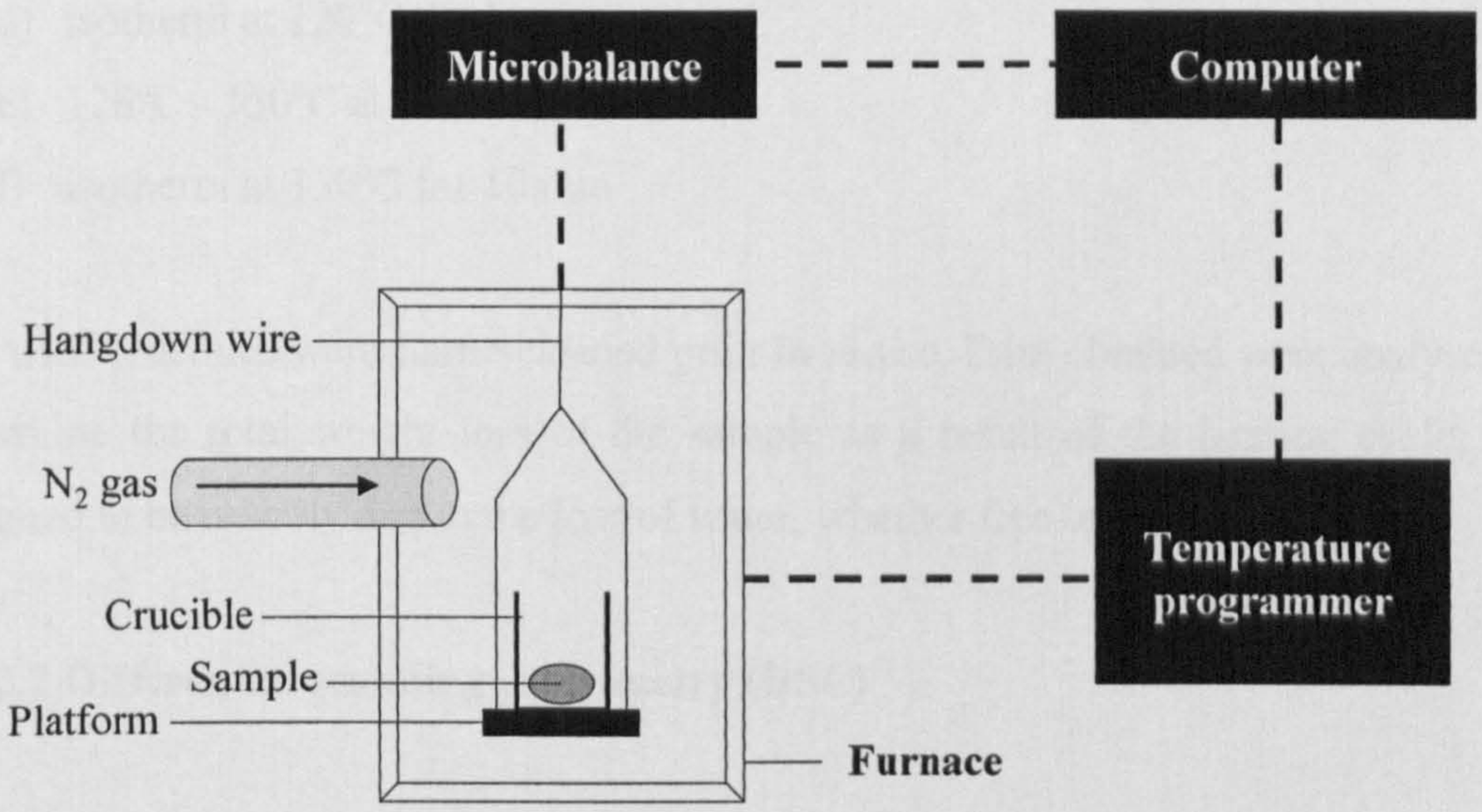

Figure 2.11: Schematic of TGA setup.

The thermobalance, being inherently a very sensitive instrument capable of detecting weight changes in the micron range, has to be situated in isolation from mechanical vibrations (an anti-vibration bench, in our laboratory) which could trigger false readings. Within the furnace, constant nitrogen gas flow, at a rate of about 30-40mL/min is employed in order to

a) purge air from the chamber as its composition is quite complex and also contains relatively high amounts of water vapour which could interact with the sample; and
b) remove gaseous products from the heating of the sample.

For our studies, corn oil was dehydrated by shaking with excess amounts of anhydrous sodium sulphate and stored overnight in a well-sealed, amber glass bottle. Water (10, 25, 50 and 80%v/v) was added to the dehydrated oil by shaking in

separating funnels; the water drained off from the bottom layer leaving behind the partially saturated corn oil.

15-20mg of the samples were loaded into 70μL alumina crucibles (uncovered) and subjected to the following heating cycle:

a) 25°C - 95°C at 5°C/min
b) isotherm at 95°C for 5 min
c) 95°C - 120°C at 5°C/min
d) isotherm at 120°C for 10 min
e) 120°C - 150°C at 5°C/min
f) isotherm at 150°C for 10 min

The used crucibles were flame-cleaned prior to re-use. Data obtained were analysed to determine the total weight loss of the sample as a result of the heating cycle, and assumed to be entirely due to the loss of water, whether free or bound.

2.5.2.2 Differential scanning calorimetry (DSC)

There are in general two types of DSC: the heat-flux and the power compensation. Various modifications to the basic systems have been incorporated to produce, for example, high-sensitivity DSC and temperature-modulated DSC. The Mettler DSC 30 in our laboratory is of the heat-flux genre, possessing a unique five-junction thermocouple, vapour-deposited on a ceramic die to detect differential temperature and operates in the range –170 to 600°C (Mettler, 1986).

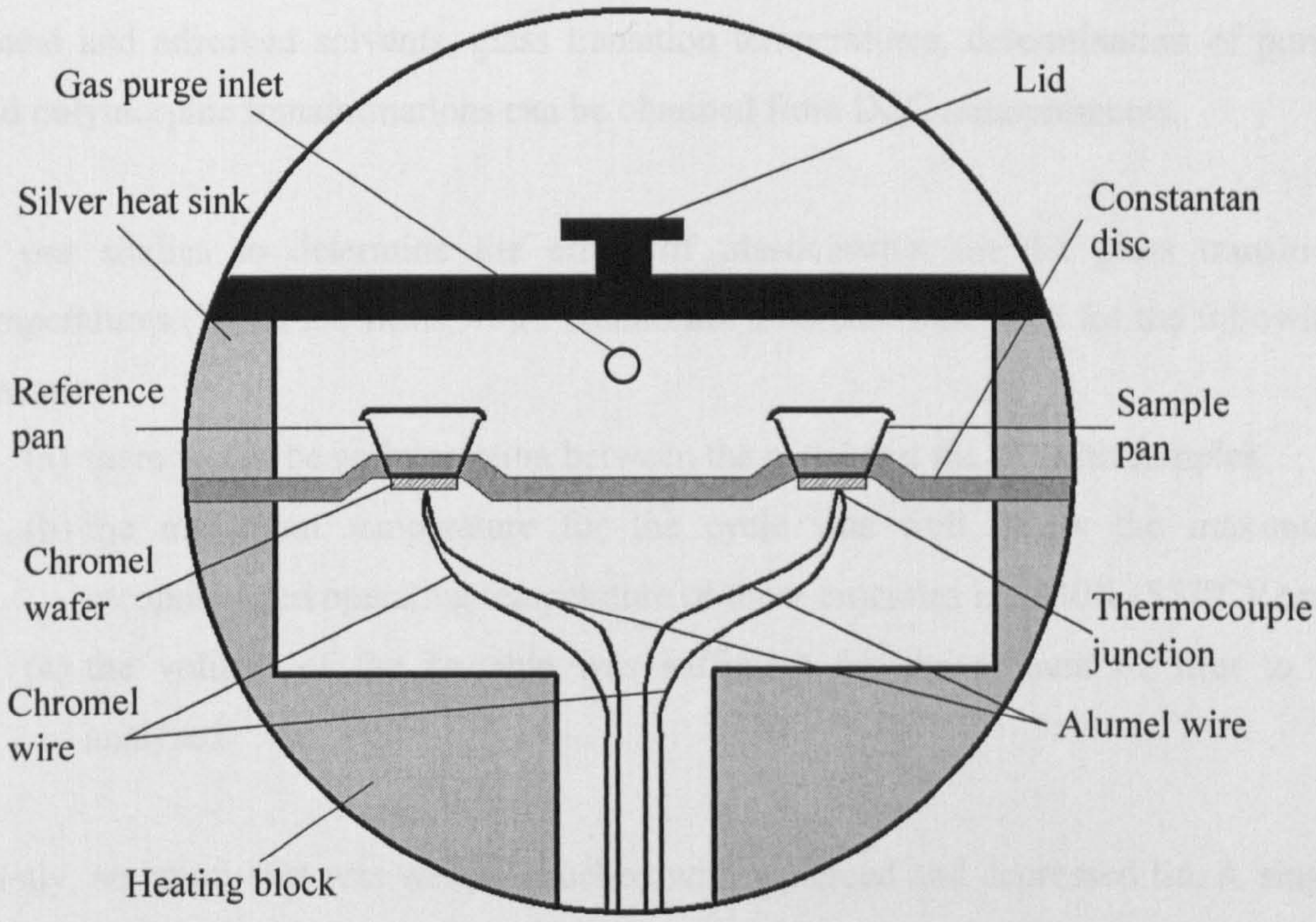

Figure 2.12: Cross-section of heat-flux DSC system.

The operating principle of the DSC is based on detection of temperature differences between the sample and reference pans when subjected to a controlled temperature cycle. There are two sets of thermocouples within the system:

(a) the junction of the chromel wafer and the heat-sensitive constantan disc measures the temperature of the furnace and the heat flux through the constantan disc

(b) chromel-alumel thermocouples located on the underside of the pans monitor the temperatures of the sample and the reference.

A phase change results in absorption or emission of heat from the sample which is detected as an alteration in heat flux through the thermosensitive constantan disc. This measurement is correlated to the pre-calibrated heat capacity of the constantan as a function of temperature, thereby calculating the heat of transition of the sample.

Much useful information such as melting points, desolvation temperatures of both bound and adsorbed solvents, glass transition temperatures, determination of purity and polymorphic transformations can be obtained from DSC measurements.

In our studies to determine the effect of plasticisation on the glass transition temperatures (T_g) of EC films, 40μL aluminium crucibles were used for the following reasons:

(a) there would be no interaction between the metal and the EC film samples;
(b) the maximum temperature for the cycle was well below the maximum recommended operating temperature of these crucibles i.e. 830K (557°C); and
(c) the volume of the crucible was sufficient for the amount of film to be analysed.

Firstly, an empty pan was weight-matched with a pierced and depressed lid. A single square of solution-cast EC film (method of preparation described in Section 2.4.3) of about 4mmX4mm was cut with a sharp scalpel and placed into the crucible, its weight obtained by difference from the weights of the empty and the filled pan/lid set. The crucibles were hermetically sealed by cold welding with a crucible sealing press.

A weight-matched reference pan, constructed in the same way but which did not contain any sample, was used throughout the study.

The following method was employed for all the samples:

Segment 1: 25°C - 170°C at 10°C/min
Segment 2: shock cooling from 170°C - 25°C at 50°C/min
Segment 3: 25°C - 170°C at 10°C/min

Two cycles were used to confirm the T_g, as residual solvent may have been present in the film and its evaporation detected in the first cycle. The data was analysed using the StarE system software to obtain the onset temperatures of any heat of transition.

2.5.3 Spectroscopic techniques

2.5.3.1 Fourier-Transform infrared spectroscopy

Infrared (IR) spectroscopy exploits the facts that (a) the energy of almost all molecular vibrations fall within the IR region of the electromagnetic spectrum; and (b) functional groups have characteristic bandwidths of IR absorption, to classify a chemical compound simply and quickly.

The original IR spectrometer splits a beam of IR light into two: one passes through the sample and the other does not. Absorption of energy corresponding to the frequency of vibration of a molecule in the sample occurs and the final spectrum is derived from the comparison of final intensities of the two beams.

With Fourier-transform technology, splitting of the IR beam also occurs but the beamlets are then caused to traverse varying distances; one or both passing through the sample. Recombination of the beamlets which have undergone methodical variations of path differences produces an interferogram which is then Fourier-transformed into an absorption-wavenumber plot, identical to that obtained from conventional IR methods. This allows for improvements in, among others, the resolution of and the speed at which data is acquired.

It is possible to analyse samples which are in the vapour phase, as liquids, in solution and in the solid state, which affects the method of preparation of sample discs, summarised in Table 2.7.

Table 2.7: Methods of preparation of samples for IR analysis (Williams and Fleming, 1989).

Vapour phase	Vapour is introduced into a cell of about 10cm in length which has end walls made of sodium chloride.
Liquid phase	Drop of liquid squeezed between flat plates of sodium chloride.
Solution	1-5%(w/v) solution is prepared in carbon tetrachloride or alcohol-free chloroform and placed in sodium chloride cell, about 0.1-1mm thick. Reference cell containing pure solvent is also used.
Solid state	Solid is ground with about 10-100 times its bulk of potassium bromide in an agate mortar and compressed into a clear disc using a hydraulic press.

The method for preparing samples in liquid form was used in our studies of corn oil, saturated with various levels of water. Solid sample preparation was employed for analysis of LH-21 and other cellulose derivatives.

2.5.3.2 Ultraviolet spectroscopy

Whenever ultraviolet (UV) or visible light traverses a chemical compound, the energy associated with it may be used to excite electrons within the molecules to higher energy levels. These excitations can be measured in a UV/visible spectrophotometer and analysed to produce characteristic absorption-wavelength spectra.

It is common to use these spectrophotometers to determine concentrations of chemical solutions, corresponding to the two empirical absorption laws, Lambert's and Beer's. The former states that the amount of incident light absorbed by a sample is independent of the intensity of the source while the latter dictates that the absorption of light is directly proportional to the number of absorbing molecules which is in turn proportional to the concentration of the solution.

When considered in combination, the Beer-Lambert law is described as follows:

$$\log_{10}\left[\frac{I_0}{I}\right] = \varepsilon.\ell.c$$

where I_0 and I are the intensities of the incident and transmitted light respectively, ε is the molar extinction coefficient, l is the pathlength of the absorbing solution in cm, and c is the concentration of the absorbing solution in mol/L. The logarithm of the ratio I_0:I is then referred to as absorbance or optical density, A, which by convention, does not have any units.

If ε and l are constants, the following relationship holds true:

$$\frac{A_1}{A_2} = \frac{C_1}{C_2}$$

where $A_{1,2}$ and $C_{1,2}$ are the absorbance and concentration of solutions 1 and 2 respectively. This is the basis of determining concentration of a solution as a function of its UV/visible absorbance, used here to plot calibration curves of model drugs and to obtain the dissolution profiles of dosage forms.

In the first instance, calibration curves of both model drugs, griseofulvin and paracetamol, were plotted from the absorbances of serially diluted solutions of the pure drug in order to input the appropriate E_{max} value (the absorbance at maximum drug dissolution) into the dissolution software. A double beam spectrophotometer was used in this case, one beam was continuously directed through a reference solution while the other beam traversed the sample solutions of varying concentrations.

A multi-cuvette UV/visible spectrophotometer was an integral part of the dissolution apparatus (described in Section 2.6.6) and was utilised to detect the UV/visible absorbance of the dissolution fluid during the process, which was then converted to percentage drug dissolved. Two different dissolution apparatus were used; the configuration of the UV/visible absorbance measuring systems also differed slightly. In the Caleva dissolution apparatus connected to a Unicam UVII spectrophotometer, the reference was dynamically measured throughout the process from a dissolution vessel in the dissolution bath containing reference solution. The Copley dissolution apparatus however was attached to a Cecil CE3021 spectrophotometer which had a separate quartz cell containing reference solution, not linked to the vessels in the dissolution bath.

2.5.4 Dynamic vapour sorption

The water sorption capacity of our excipients was of interest, therefore a dynamic vapour sorption (DVS) system, DVS1/1000, Surface Measurement Systems, London, was utilised to accurately determine the latent content of water as well as the excipients' ability to sorb water.

Two matched glass pans are housed in a temperature-controlled incubator; one containing the sample, the other an empty reference pan. The regulated mixing of humidified and dry nitrogen gas according to the specifications set enables changes in humidity within the chamber. A highly sensitive microbalance, capable of detecting mass changes to the 0.0000001g, is connected to both the pans for measurements of mass per unit time. Figure 2.13 shows the main components of the DVS system.

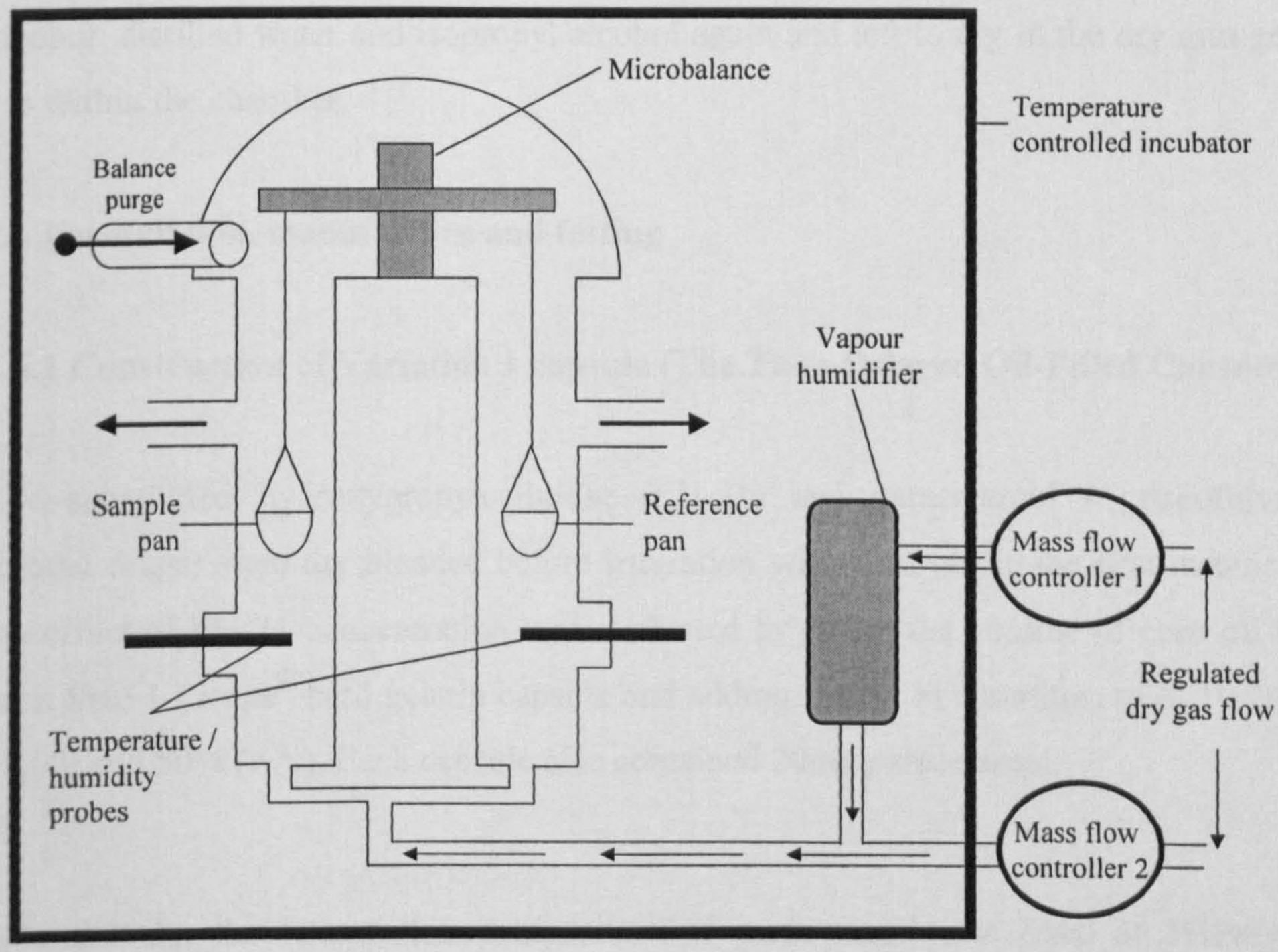

Figure 2.13: DVS 1/1000 system.

The entire system is remotely controlled by a PC, which receives inputs from a balance control unit as well as a National Instruments analogue/digital data

acquisition card that provides information on the DVS electronics. A software package, DVSWin v2.16, provides a simple user interface to program the humidity cycles and monitor the conditions of the instrument while DVS Analysis Suite v3.3 is a macro that embeds itself in Microsoft Excel for plotting and analysis of the data obtained.

Samples of corn oil, LH-21 and EC films were analysed in the DVS; each run lasting from 2-5 days. For the corn oil samples, a drying cycle was implemented by programming the instrument to purge the chamber with dry nitrogen gas i.e. relative humidity, RH = 0%. The EC films however, were subjected to a double cycle of increasing the RH from 0 to 95% in steps of 10%. The criterion for the progression from one RH step to another was the change in mass, expressed as *%dm/dt* falling below 0.002% or the cycle time exceeding 99 hours, whichever occurred first. Between each run, the pans were cleaned by successive rinsing with isopropyl alcohol, distilled water and isopropyl alcohol again and left to dry in the dry nitrogen gas within the chamber.

2.6 Formulation, manufacture and testing

2.6.1 Construction of Variation 1 capsule (The Time-Delayed Oil-Filled Capsule)

Low-substituted hydroxypropylcellulose (LH-21) and paracetamol / griseofulvin (model drugs) were dry blended before trituration with corn oil. In the first instance, the effect of LH-21 concentration was evaluated by fixing the volume of corn oil in each Size 1 Licaps® hard gelatin capsule and adding LH-21 in quantities of 5, 10, 20, 30, 40 and 50% (w/v). Each capsule also contained 20mg paracetamol.

Alternatively, the formulation composition of paracetamol was fixed at 5%(w/w) whilst the quantities of LH-21 and corn oil were varied by weight as shown Table 2.8.

Table 2.8: LH-21:corn oil weight ratios.

LH-21 (%w/w)	Corn oil (%w/w)
70	25
65	30
60	35
55	40
50	45

Increasing the amount of corn oil added changed the consistency of the capsule fill from that of a paste to that of a suspension. The mixtures classed as suspensions were filled into the Size 1 Licaps® by volume using a micropipette from a stock suspension which was constantly stirred. The paste-like mixtures were filled into the capsules using the brass filling device as shown in Figure 2.14. The capsules were filled with 400mg of the mixture and compressed using the 200g weight.

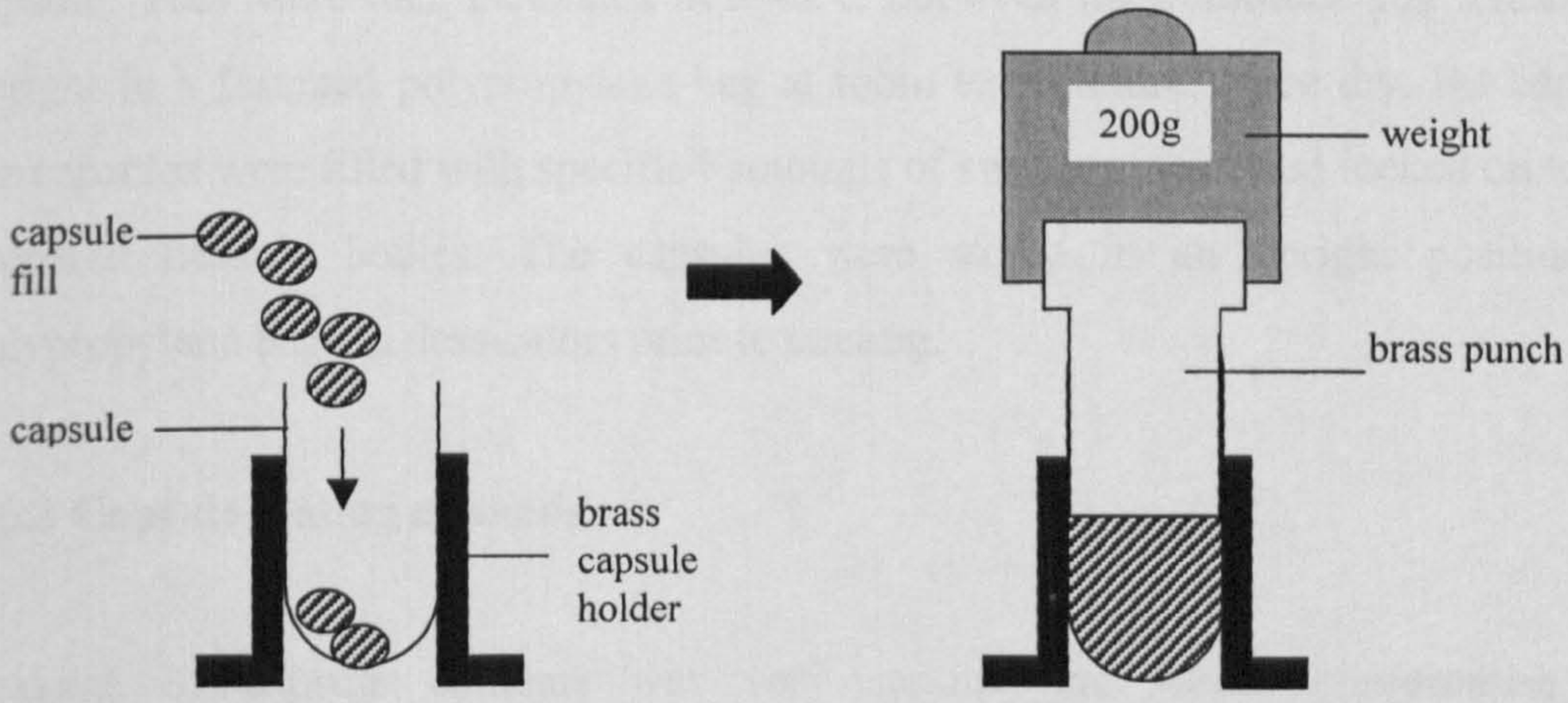

Figure 2.14: Brass capsule filling device.

The prepared capsules were stored upright in dessicators at room temperature prior to coating.

2.6.2 Construction of Variation 2 capsule (The Compartmentalised Capsule)

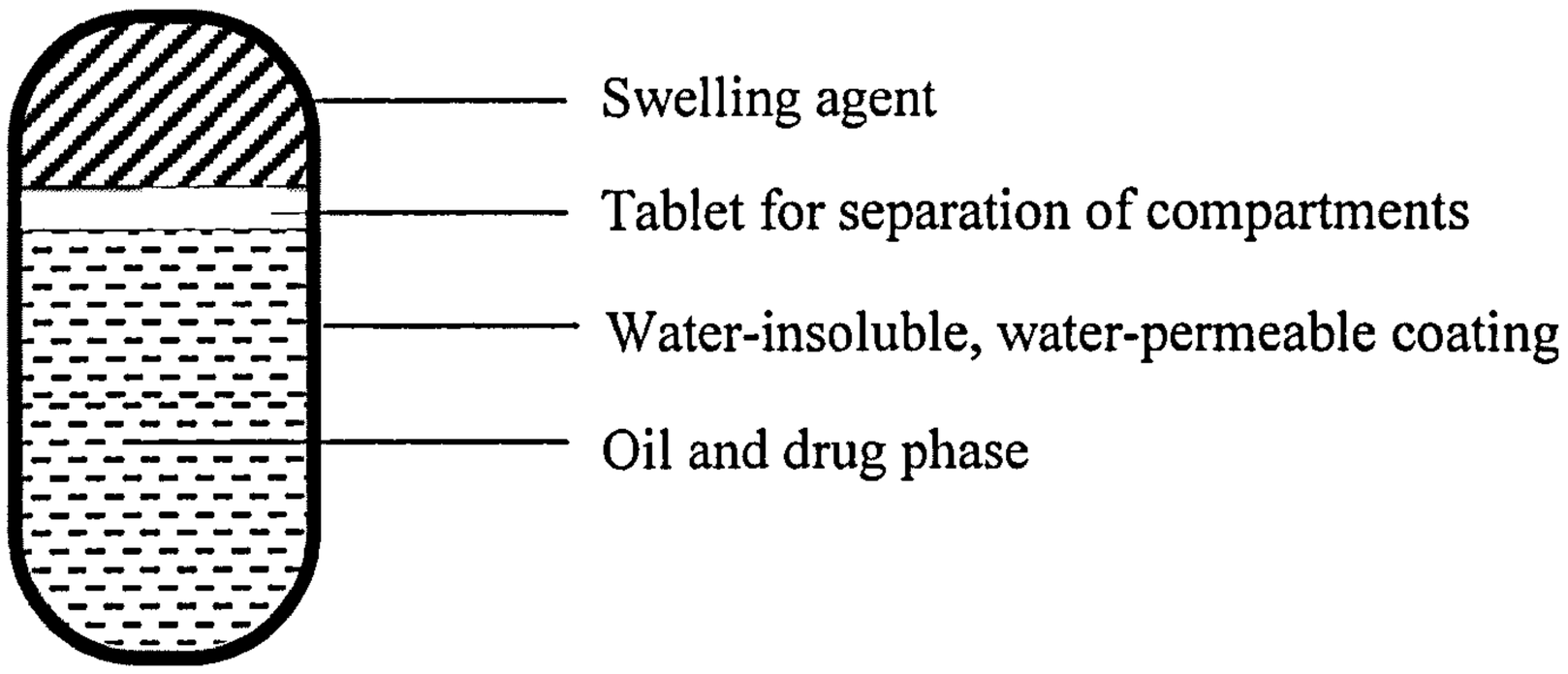

Figure 2.15: Basic construction of compartmentalised capsule.

The bodies of size 00 Coni-snap® hard gelatin capsules were filled with 0.75mL of a 20mg/mL suspension of paracetamol in corn oil with a micropipette. Gelatin-based tablets were prepared using a Manesty SP single punch tablet machine. These tablets were pre-wetted on the sides with warm water, then inserted at the neck of the capsule. They were then incubated in a 45°C fan oven for 2 minutes and left to dry upright in a fastened polypropylene bag at room temperature. Once dry, the caps of the capsules were filled with specified amounts of swelling agent and locked on to the prepared capsule bodies. The capsules were stored in an upright position in polypropylene bags in dessicators prior to coating.

2.6.3 Capsule sealing methods

Leakage of capsule contents was very serious and would compromise the performance of the device. Hence the following approaches were implemented in the hope of eradicating this problem.

2.6.3.1 Gelatin banding with brush

A solution of 25%(w/v) 225 bloom gelatin was prepared by dissolving the pre-weighed dry gelatin powder in 60°C distilled water on a hotplate stirrer. The solution was carefully applied in a single layer to the junction of the cap and body of the

capsule using a thin paint brush. The capsules were then air-dried upright and stored in dessicators at room temperature.

2.6.3.2 Gelatin banding with bench-scale capsule banding machine

A Qualiseal bench-scale capsule banding machine, courtesy of Encap Drug Delivery, Livingstone, Scotland, was used. Each capsule was placed on a sealing tray, horizontally, and rolled over a wheel with a thin gelatin layer on it. Figure 2.16 shows the schematic of the banding process. The sealed capsules were allowed to dry upright, overnight, at room temperature.

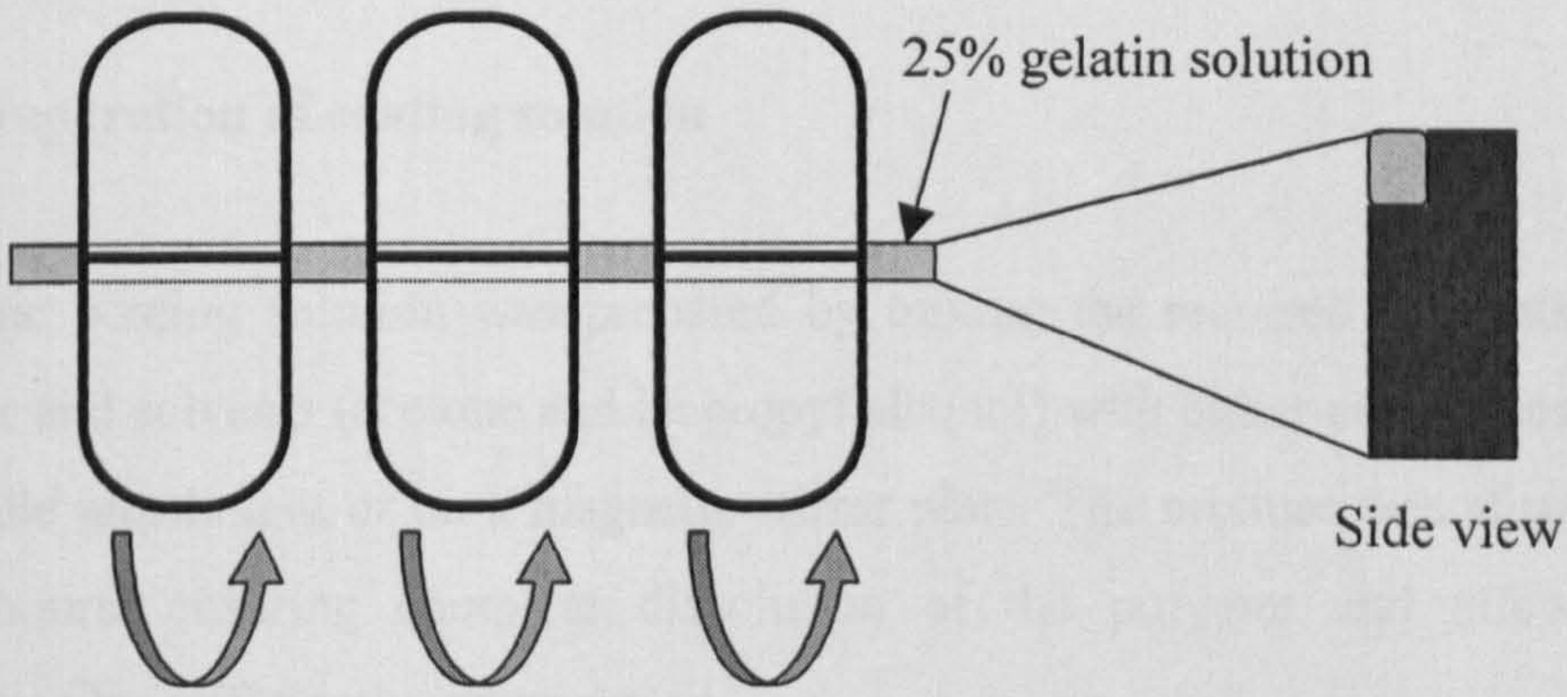

Figure 2.16: Graphical depiction of capsule banding process.

2.6.3.3 Adaptation of LEMS® technique

LEMS®, short for Liquid Encapsulated by Microspray Sealing, is a process whereby each capsule is sprayed with a minute (microlitre quantity) amount of hydroalcoholic solution (usually 50:50 water/ethanol) at the body and cap junction. This solution is drawn up into the gap by capillary action and hence lowers the melting point of gelatin at the sealing area of the capsule. In order to complete the melting and fusion process, air at 40-60°C is gently blown across the capsule. The capsules are then dried by gently tumbling in a rotating drum followed by airing in open trays.

In modifying this technique, a 50:50(%v/v) solution of water:ethanol was brushed onto the edge of the filled capsule body prior to capping. Once the cap was firmly put into place, a hair dryer was used to apply a stream of hot air to slightly melt the gelatin at the cap and body junction then the capsule was left to dry upright, for fusion of the gelatin to occur.

2.6.4 Capsule coating methods

Application of an even coating was imperative for the optimum performance of both variations of capsules. Three methods were employed over the course of our studies, all using the same coating solutions prepared as described below.

2.6.4.1 Preparation of coating solution

An organic coating solution was prepared by mixing the required amounts of EC, plasticiser and solvents (acetone and isopropyl alcohol) with either an overhead stirrer with paddle attachment or on a magnetic stirrer plate. The mixture was stirred for at least 6 hours, ensuring complete dissolution of the polymer and allowing the plasticiser to be sufficiently incorporated.

Alternatively, preparation of an aqueous-based coating solution involved the mixing of 60%(w/w) of Surelease (containing ethylcellulose 20cP, ammonium hydroxide 28%, medium chain triglycerides and oleic acid) with 40%(w/w) of distilled water. Colouring (methylene blue and cochineal food colouring) was added to the mixture during stirring using a magnetic stirrer.

2.6.4.2 Spray coating with Aeromatic Strea fluidised bed coater

An Aeromatic Strea-1 fluidised bed coater (bottom spray mode) was used to apply varying levels of coating on the filled capsules. The capsules to be coated were pre-heated (60°C) within the coating chamber to ensure a suitable temperature for rapid solvent evaporation upon impact of the coating solution onto the capsule surface.

The capsules (and dummy capsules) to be coated were weighed and the volume of coating solution required for the desired level of coating (%w/w) was calculated. This volume and about 10mL extra was delivered using a Watson-Marlow 313S peristaltic pump as shown in Figure 2.17. Compressed air was used to aerosolise the coating solution for even distribution onto the surface of the capsules. Fan speed was adjusted to compensate for the increasing weight of the capsules as the coating process progressed in order to maintain a well-dispersed flow pattern.

The capsules were coated according to the following parameters:

Flow rate of solution	= 5mL/min
Outlet temperature	= 50±5°C
Drying temperature	= 60±2°C
Pressure	= 1 bar
Drying time	= 99 min

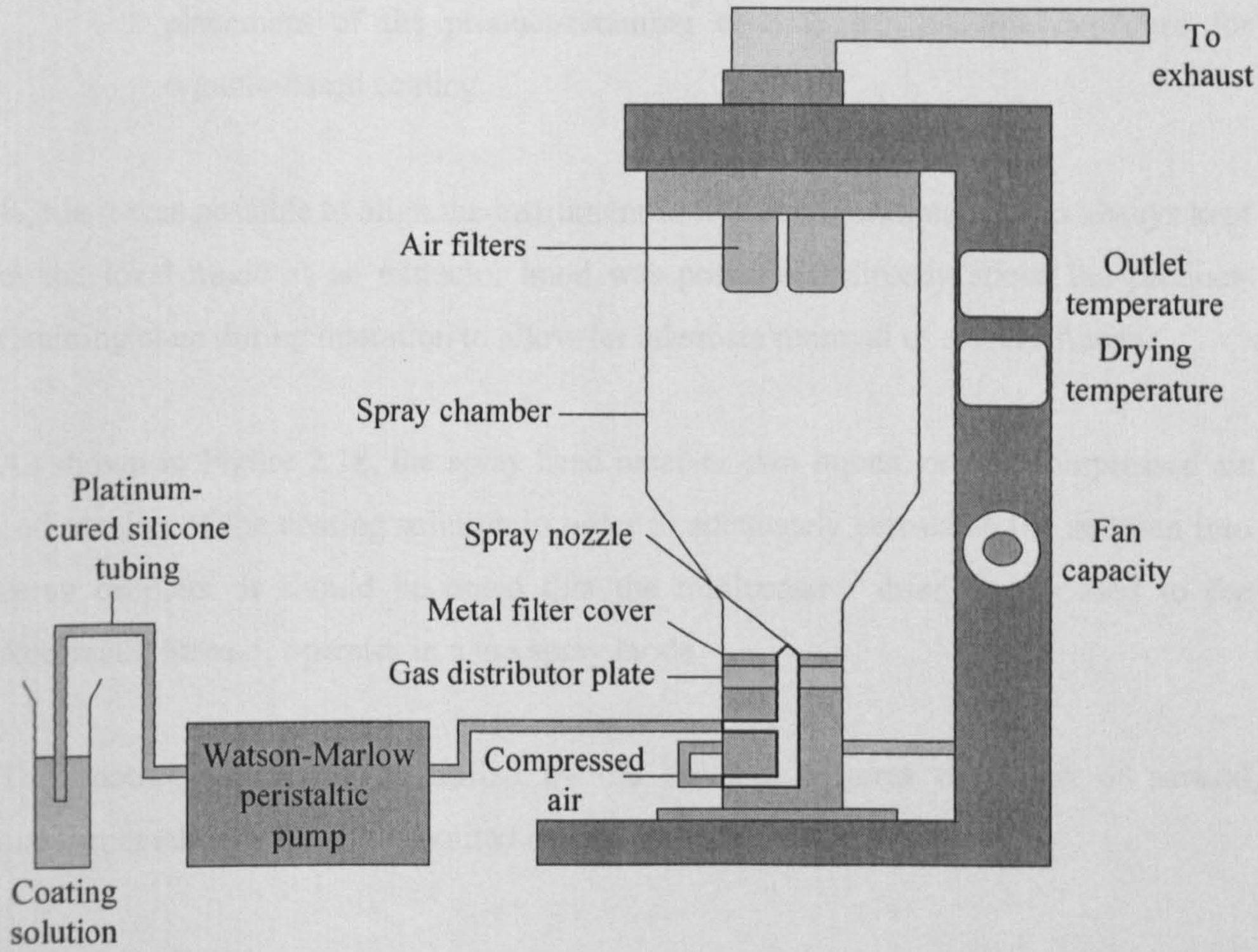

Figure 2.17: Schematic of Aeromatic Strea-1 fluidised bed coater.

2.6.4.3 Spray coating with minicoater / drier

Coating with the Aeromatic Strea-1 required large numbers of capsules to be prepared in order to produce a suitable flow pattern. The minicoater / drier (Caleva Process Solutions, Dorset, UK) offered a convenient means of coating small quantities of capsules. It comprises a base module and a remote module connected to a PC which provides instrument control and allows storage of experimental procedures. The base module houses the hot air generator while within the remote module is situated a vibrating membrane that generates the motion of the product retaining cone during coating.

The instrument may be operated in one of two configurations:

i) 'local'; the base and remote modules are connected via a rigid plastic tube in close proximity (as shown in Figure 2.18) and,

ii) 'remote'; the two modules are connected via a flexible hose to allow for placement of the product-retaining cone in e.g. a fume cupboard for organic-based coating.

While it was possible to align the instrument in two configurations, it was always kept in the local mode as an extractor hood was positioned directly above the product-retaining cone during operation to allow for adequate removal of solvent fumes.

As shown in Figure 2.18, the spray head receives two inputs, one of compressed air and another of the coating solution in order to adequately aerosolise the solution into spray droplets. It should be noted that the minicoater / drier, as opposed to the Aeromatic Strea-1, operates in a top spray mode.

The coating process is controlled by the PC and requires the input of several experimental parameters as detailed in Table 2.9.

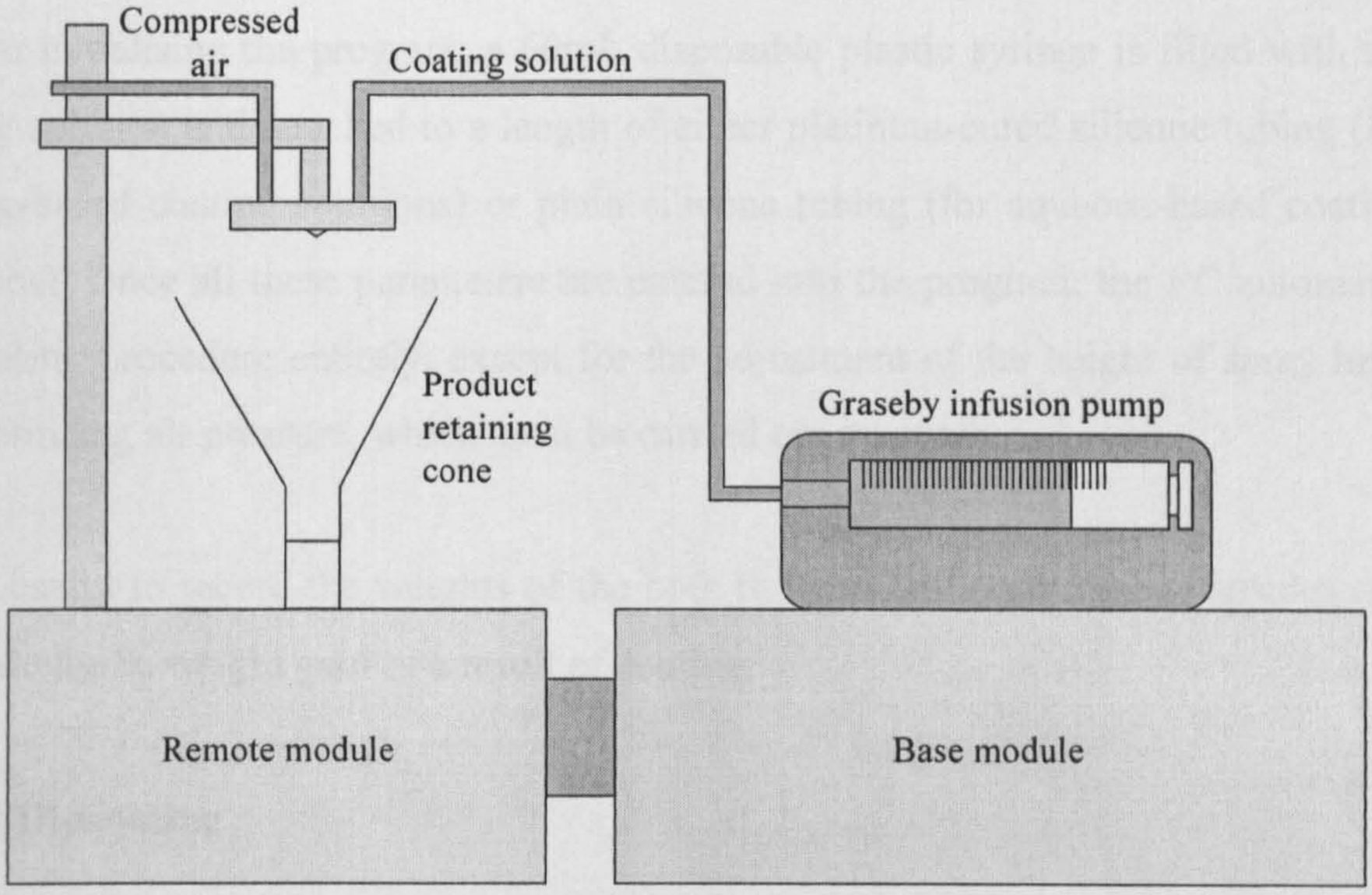

Figure 2.18: Schematic of minicoater / drier

Table 2.9: Experimental parameters for minicoater / drier.

Parameter (unit)	Description	Limits
Vibration frequency (Hz)	Vibration frequency of product-retaining cone	10-30
Vibration amplitude (mm peak-peak)	Total vibration amplitude of product-retaining cone	0-8
Airflow temperature (°C)	Temperature	20-70
Inlet airflow (m/s)	Drying airflow speed at inlet	2-7
Coating solution flowrate (mL/h)	Flowrate of coating solution infused by Graseby syringe pump	10-150
Atomising air pressure (bar)	Pressure of atomising air to spray head	0-1
Height of spray head (mm)	Height of spray head above product support mesh	140-220
Spray period	Length of time during which coating solution is applied to samples	N/A
Drying period	Length of time during which all operating parameters are maintained after conclusion of spray period	N/A
Manual drying	Alternative to 'Drying period' whereby only operator intervention halts the drying step	N/A

Prior to initialising the program, a 60mL disposable plastic syringe is filled with the coating solution and attached to a length of either platinum-cured silicone tubing (for organic-based coating solutions) or plain silicone tubing (for aqueous-based coating solutions). Once all these parameters are entered into the program, the PC automates the coating procedure entirely, except for the adjustment of the height of spray head and atomising air pressure, which must be carried out manually.

It was useful to record the weights of the both the pre- and post-coated capsules and calculate the % weight gain as a result of coating.

2.6.4.4 Dipcoating

Dipcoating capsules avoided the rough tumbling motion of the spray coater and allowed for a simpler, less time-consuming method of coating. A six-armed wire frame was prepared and secured by soldering. A drop of cyanoacrylate-based adhesive was placed on the head of the pre-weighed individual capsules and a strand of thread attached (Figure 2.19). Six of the capsules were prepared in this way and hung on the wire frame. The capsules on the frame were lowered simultaneously into coating solution and removed after 10 seconds. The capsules were allowed to dry for at least one hour in a fume cupboard. Once dry, the capsules were weighed to calculate the % weight gain. Coating was repeated until the desired coating level was achieved. At each coating stage, the weight of pre- and post-dipcoated capsules were recorded to determine the efficacy of the process.

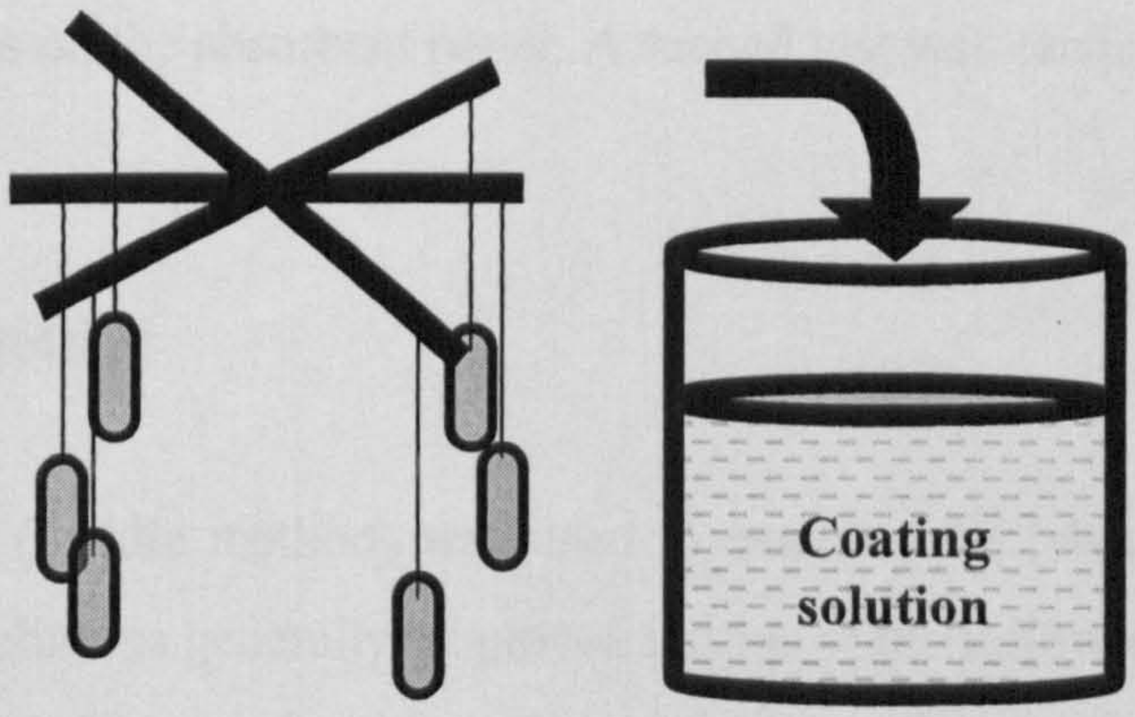

Figure 2.19: Dipcoating capsules.

2.6.5 Capsule leak test

A vacuum test was developed to evaluate the integrity of the gelatin banding and to compare the banded capsules with the unbanded ones. The capsules to be tested were placed on a holder made of a cardboard base covered with absorbent paper and compartments derived from aluminium slats (n=49) (Figure 2.20).

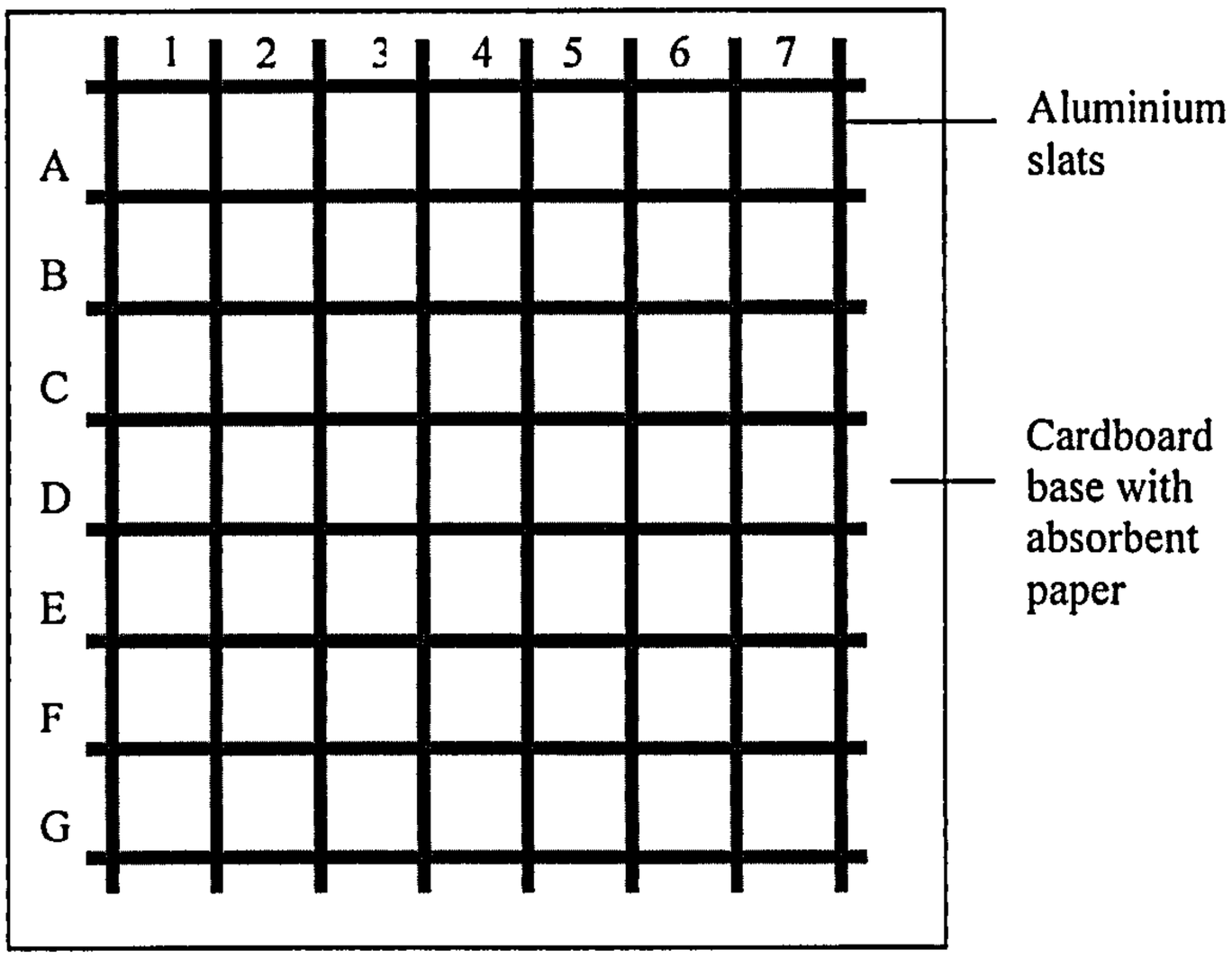

Figure 2.20: Holder for capsule leak test

This assembly was placed into a portable pressure vessel and the vessel securely fastened. The vacuum pump was turned on and the pressure allowed to drop to –0.5 bar. Both banded and unbanded capsules were incubated at this pressure for 15 min. After this time, the vacuum was released and the capsules checked for any leakage, evidenced by stains on the absorbent paper. A second test was carried out at –0.75 bar for 30 min.

2.6.6 Dissolution testing

USP Apparatus II (paddle method) was used to evaluate the release profiles of the capsules. The dissolutions generally employed the use of the following parameters:

a) Paddle speed: 50rpm
b) Dissolution media: 1000mL distilled, deaerated water
c) Temperature: 37°C

The dissolution apparatus comprised of a dissolution bath containing six separate dissolution vessels, a UV / visible range spectrophotometer set to the appropriate wavelength for detection and a peristaltic pump connecting the tubings between the vessels and the individual quartz cells within the spectrophotometer. A dissolution software program controlled the procedure which was generally carried out for between 8 to 16 hours. The data obtained of the release of drug over time was analysed in terms of mean lag time and mean time to 50% drug release ($T_{50\%}$). The means and standard deviations were then analysed for statistical significance at 5% level using ANOVA and Tukey's pairwise comparisons in Minitab v.13.

CHAPTER 3

CHARACTERISATION OF SWELLING AGENT, LH-21

3.1 Introduction

The main function of a swelling agent in our proposed drug delivery device is to expand upon exposure to water, generating sufficient force to rupture the brittle outer film coating of the capsule. Water uptake and consequent swelling of this excipient should be at a controlled rate, regardless of the pH of the media. Low-substituted hydroxypropylcellulose (L-HPC, grade LH-21) has been extensively used in many swelling-controlled release systems. Its highly hydrophilic nature and considerable swelling capacity made it an attractive choice. The following introductory review discusses the physicochemical properties of L-HPC, compares it with the more commonly utilised hydroxypropylcellulose (HPC) and concludes with L-HPC's utilisation in several current time-delayed delivery technologies.

3.1.1 Physicochemical properties of L-HPCs

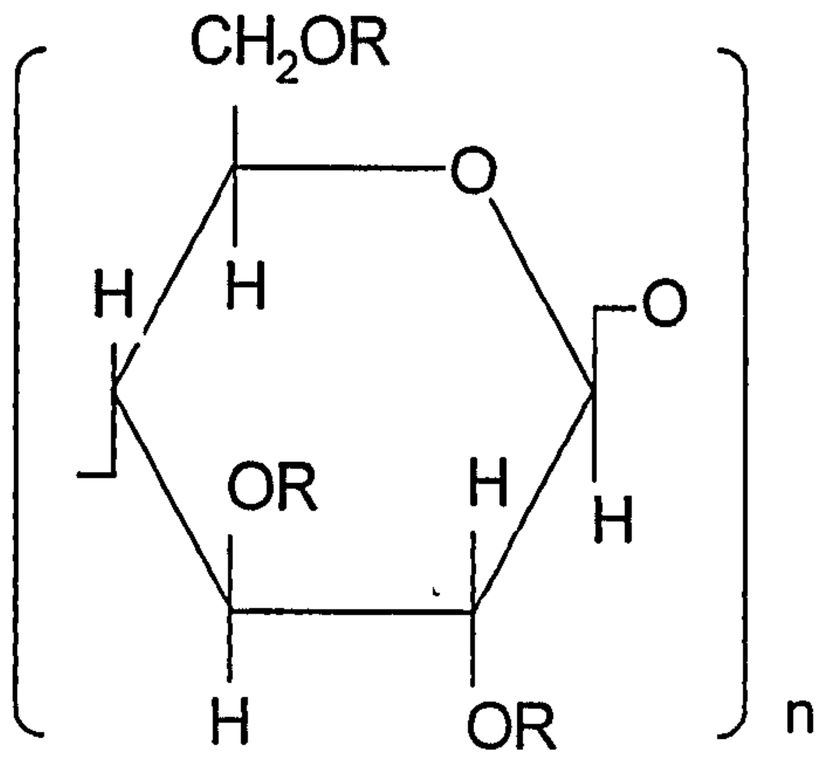

R = -H, -CH_2 – CH(OH) – CH_3

Figure 3.1: Chemical structure of hydroxypropylcellulose.

The degree of substitution of hydroxypropylcellulose (Figure 3.1) is one of the main determinants of the specific utility of the various commercially available types (Alvarez-Lorenzo *et al.*, 2000a). Table 3.1 highlights the differences between low-substituted hydroxypropylcelluloses (L-HPCs) and hydroxypropylcellulose (HPCs).

Table 3.1: Properties of L-HPC and HPC.

Property	L-HPC	HPC	Reference
Hydroxypropoxyl content (%w/w)	5 – 16	53 – 78	Shin-Etsu, 1992
Molar substitution per glucose unit	0.1 – 0.4	2.0 – 4.2	Shin-Etsu, 1992
Position of substitution	Mainly glucopyranose carbon 6	Glucopyranose carbon 2, 3, 6	Alvarez-Lorenzo *et al.*, 2000b
Enthalpy of hydration / dissolution (Jg^{-1})	-62.9 to -71.4	-83.0 to -100.0	Alvarez-Lorenzo *et al.*, 2000b
Crystallinity indices	0.43 - 0.69	0.38 – 0.44	Alvarez-Lorenzo *et al.*, 2000b
Use	Disintegrant and binder in tablet and pellet formulations	Thickeners in aqueous solutions or suspensions, matrix tablet excipient	Shin-Etsu, 1992, Alvarez-Lorenzo *et al.*, 2000a

The soluble hydroxypropoxyl component, being present in a lower degree in L-HPCs compared to HPCs, impacts greatly on its lack of solubility in water. Both L-HPCs and HPCs exhibit exothermic reactions in contact with water, the magnitude of enthalpy being greater in HPCs. This can be attributed to the aforementioned poor water solubility of L-HPCs, resulting in the enthalpy of interaction with water being almost entirely a consequence of hydration only. HPCs on the other hand, hydrate and dissolve through breaking of intermolecular bonds, coupling of the polymer

molecules with water and conformational changes; the net result giving rise to a higher total enthalpy. However, L-HPCs seem to be more crystalline than HPCs, as determined by Alvarez-Lorenzo *et al.* (2000b), using the method described by Nelson and O'Connor (1964), which will be elaborated upon in Section 3.4.2. The lower degree of substitution of hydroxyl groups by ether groups allows for more ordered packing within the structure. Alvarez-Lorenzo *et al.* (2000a) concluded that L-HPCs have intermediate crystallinity, between the almost entirely amorphous HPCs and the more crystalline microcrystalline celluloses. This relatively high crystallinity contributes to the poor solubility of L-HPC because of the greater amount of energy required to break bonds within the more ordered crystalline structure.

Hence L-HPCs have been propagated for use as disintegrants and binders in conventional tablet and pellet formulations. In the former function, upon exposure to the aqueous environment, polymer-water interactions are preferred to polymer-polymer interactions (Wan *et al.*, 1991). Incorporation of water molecules within the polymer network causes hydration and consequent swelling of the polymer, increasing the hydrodynamic volume, aiding disintegration of the matrix. Swelling of L-HPCs is not compromised by the chemical composition of the hydrating fluid be it water, Japanese Pharmacopoeia (JP) 1st fluid (pH1.2) or JP 2nd fluid (pH6.8) (Shin-Etsu, 1992). Their binding capability arises from the retention of the general properties of the original cellulose i.e. plastic deformability and good compressability thereby increasing tablet strength.

In general, the L-HPCs are white to yellowish-white powders or granules, tasteless and are either odourless or have a slight characteristic odour. The grades of L-HPC available include LH-11, LH-21, LH-31, LH-41, LH-20, LH-30, LH-22 and LH-32 which differ in two ways: average particle size and degree of hydroxypropoxyl substitution (Shin-Etsu, 1992). These data are summarised in Tables 3.2a and 3.2b.

Table 3.2a: Properties of L-HPC grades LH-11 – LH-41.

Type	LH-11	LH-21	LH-31	LH-41
Mean particle size (μm)*	50	40	25	10

***By sieving method**

Table 3.2b: Properties of L-HPC grades LH-20, LH-21, LH-22, LH-30, LH-31 and LH-32.

Type	LH-20	LH-21	LH-22	LH-30	LH-31	LH-32
Hydroxypropoxyl content (%)	13.7	11.2	8.1	13.5	10.9	7.5

Table 3.2a shows that as the first digit of the grade description increases, the mean particle size decreases but the degree of hydroxypropoxyl substitution remained between 10-12.9%(w/w). Table 3.2b on the other hand shows the meaning of the second digit. The higher the numerical value, the lower the hydroxypropoxyl content, as seen with both LH-2x and LH-3x series. Inter-batch variation of these parameters is controlled during manufacture and can be determined from the Certificate of Analysis.

The differing particle sizes and degrees of substitution make an impact on the extent and rate of swelling. Grades with lower particle sizes and hydroxypropoxyl content tend to exhibit a lower degree and slower rate of swelling respectively.

Scientists at Shin-Etsu have also found a correlation between content of water-soluble material and saturation time i.e. time to achieve maximum swelling. L-HPC grades with smaller particle size and higher degrees of substitution contain more water-soluble material (Shin-Etsu, 1992). The higher the content of water-soluble material, the longer it takes the L-HPC to achieve maximum swelling i.e. it decreases its swelling rate.

Through this brief overview of the properties of various grades of L-HPCs, it is evident that manipulation of the basic chemical structure i.e. degree of

hydroxypropoxyl substitution and the physical property of particle size allows for tailoring of the L-HPC grade to specific purposes, as described in the following section.

3.1.2 Uses and applications of L-HPCs in drug delivery systems

While L-HPCs have been less utilised in drug delivery in comparison to other cellulose derivatives such as hydroxypropylcellulose (HPC), hydroxypropylmethylcellulose (HPMC) and hydroxyethylcellulose (HEC), its unique property of swelling but not dissolving in aqueous systems has caught the attention of certain workers in the field.

3.1.2.1 Disintegrant

The L-HPCs have been described as super-disintegrants, referring to their ability for rapid water uptake resulting in simultaneously rapid expansion of the polymer chains and hence destruction of the matrix structure within which they are contained.

Bi *et al.* (1996) recognised the need to develop a rapidly disintegrating dosage form for the elderly and others who have difficulty swallowing. They identified the prerequisites for excipients that could be incorporated into such a system: good compactibility, excellent disintegration capacity and pleasant taste. The two major components of their tablet dose form were MCC and L-HPC, the grades used being Avicel PH102 and LH-11, respectively.

As discussed previously in Section 3.1.1, the crystallinity of MCC is higher than that of L-HPC, impacting on their water uptake rates. The amorphous regions of L-HPC are much more amenable to water ingress, consequent swelling and matrix disintegration as compared to MCC which reaches equilibrium rapidly. MCC however imparts excellent tensile strength through its ease of compressibility resulting in increased contact points between powder particles and improved interparticular bonding forces e.g. surface molecular interaction and mechanical interlocking. Furthermore the larger number of free hydroxyl groups in MCC provides greater opportunity for hydrogen bonding between hydroxyl groups to occur. This is

generally considered stronger than that between hydroxypropoxyl groups of L-HPC. Hence the workers had to strike a balance between the improved tensile strength afforded by higher concentrations of MCC while retaining sufficient disintegrant power of L-HPC.

Through disintegration, crushing and *in vivo* testing in the oral cavity, it was determined that a formulation consisting of 60mg MCC, 15mg L-HPC, 75mg Tabletosse (lactose-based glidant) and 2mg magnesium stearate (lubricant) formed the ideal composition for a rapidly disintegrating tablet.

Instead of the compressed tablet approach, Takeuchi *et al.* (1987) employed spray drying as a means of improving the dissolution rate of a poorly water-soluble drug. They prepared spray-dried particles from a solution of tolbutamide in 2%(w/v) aqueous ammonia mixed with the disintegrant (partly pre-gelatinised corn starch, PCS, or L-HPC, grade not specified). From photomicrographs, the surface topographies of spray-dried particles derived from the two disintegrants were clearly different. L-HPC-based particles had drug situated both on and within the agglomerates of disintegrant. The PCS particles however had an inner core of disintegrant and a clear outer layer of drug.

It was shown that spray-dried particles of drug with disintegrant had improved dissolution rates over those of spray-dried drug alone. However, PCS particles had higher dissolution rates than the L-HPC particles, possibly due to the internalisation of the drug within the particles of the latter disintegrant, impeding drug release.

Maintaining the approach with spray drying, Takeuchi *et al.* (1991) incorporated L-HPC (grades LH-21 and LH-31 in separate formulations) into designing a powder dosage form of an oily drug having good water dispersibility and drug-releasing property by using a spray-drying technique. They prepared DL-α-tocopherol acetate (VEA)-containing powders by spray-drying emulsified VEA with various excipients. The role of the L-HPC here was to act as a disintegrant, causing significant water uptake and bulking, producing small VEA droplets, presenting the drug in a solubilised form, available for absorption. *In vitro*, the spray-dried particles with L-

HPC formed a stable emulsion in water when gently agitated. Drug release studies on this system, performed by testing aliquots of the dissolution media using HPLC, showed that L-HPC effectively released VEA droplets in a concentration-dependent manner. This was a promising system, affording potentially improved delivery of an oily drug or an oily solution of a poorly water-soluble drug.

3.1.2.2 Sustained-release matrix

Although L-HPCs have been propagated for use as super-disintegrants promoting rapid drug release, Kawashima *et al.* (1993a) discovered that micronised L-HPCs can be used as excipients in sustained-release matrices. Here, gradual release of drug entrapped in the matrix is obtained as the rate of swelling of L-HPC is suppressed.

However, poor flowability and packability of the L-HPC powder led Kawashima and his co-workers to produce granules via wet granulation for tablet compression (Kawashima *et al.*, 1993b). They used the micronised forms of both the L-HPC (grade LH-41; mean particle size = 4.4μm) and model drug (paracetamol = 30μm) to prepare granules with either water or ethanol as granulating fluid. L-HPC was obtained micronised from manufacturer while the drug was firstly sieved, retaining the fraction between 177μm and 500μm for further pulverising. Three methods of granulation were employed: high-speed agitation, centrifugal-fluidised granulation and spray drying.

The most significant finding was that water proved an unsuitable choice as a granulating fluid; the tablets lost their sustained-release characteristic, reverting instead to the rapidly disintegrating property of the original, unmicronised L-HPC. Granulation with ethanol allowed the sustained-release property to be retained, the combination of ethanol-granulated micronised LH-41 and micronised paracetamol giving the greatest degree of prolonged release; up to 15 hours with 5%(w/w) drug loading.

In an effort to prepare granules by dry granulation, avoiding the need for granulating fluid completely, Kawashima *et al.* (1993c) engaged two means: slugging and roller compaction. The former method necessitated slug formation using a hydraulic press

then crushing them with a roller mill. Granules sized between 177μm and 710μm were tabletted. The other method involved flaking the mixture of micronised LH-41 and micronised paracetamol with a roller compactor then grinding with a roller-rotator. Dry granules over and above the size of 177μm were retained for tabletting.

The composition of the tablets prepared were as follows:

(a) micronised paracetamol physically mixed with LH-41 dry granules

(b) dry granules of micronised LH-41 and micronised paracetamol

Increasing the loading of LH-41 decreased the rate of drug release. It was suggested that a higher concentration of LH-41 promoted a more cohesive envelopment of the drug in the tablet, thereby enhancing sustained release. Slugging and compaction pressures were found to be the main determinants of drug release, although not the only ones. Tensile strength and mean pore size of the internal structure of the tablets also contributed. For formulations (a) and (b), there was a maximum pressure of slugging or compaction beyond which the sustained-release nature of the tablet gradually diminished. An explanation proffered by the authors was that the internal structure, quantified through pore size and swelling force measurements, was a critical factor in determining initial water uptake rates. The granules formed at the lowest slugging pressure (5MPa) had the most similar internal structure to that of the control ungranulated micronised LH-41 and drug mixture.

3.1.2.3 Swelling agent in rupturable systems

One of the simplest, yet most effective, controlled release systems available today was developed by a Japanese group led by Satoshi Ueda, in which the swellability of L-HPC is exploited. The Time-Controlled Explosion System (TES) does exactly what its name implies: it ruptures and releases drug after a controlled lag time. The concept is simple: an inert core (Non-Pareil® bead) on which a drug layer is compressed is then covered with a layer of swelling agent and subsequently the system is coated with an ethylcellulose layer which is water-insoluble and brittle but semi-permeable (Figure 3.2). Water ingress causes the swelling agent to expand, which in turn cracks the outer coat and the drug is released.

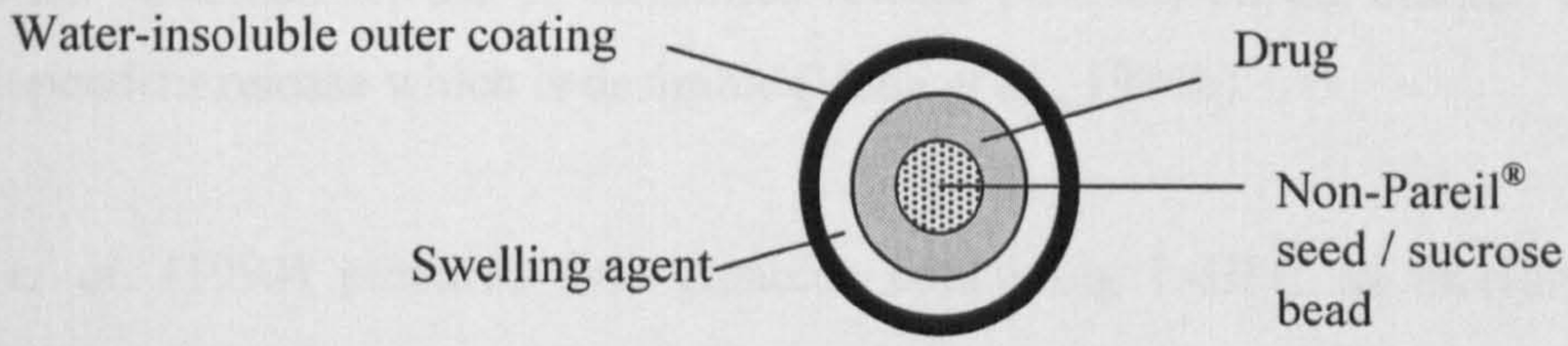

Figure 3.2: Time-Controlled Explosion System (TES)

The swelling agent selected was L-HPC grade LH-31 as it possessed a relatively high swelling equilibrium and pH-independency due to its non-ionic nature, as compared to carboxymethylcellulose sodium and sodium starch glycolate (Ueda *et al.*, 1994a). It was the inclusion of the layer of swelling agent that gave TES the distinction of not being merely a membrane-controlled system. In fact it was neither merely diffusion- nor dissolution-controlled but rather, it relied on the swelling of LH-31 (or any other swelling agent as specified in the patent - Ueda *et al.*, 1989) to rupture the water-insoluble, brittle outer coating of ethylcellulose (EC).

It then follows that the diversity of applications of the TES is quite extensive as manipulation of the type and amount of swelling agent as well as the thickness and characteristics of the coating used offers various release profiles. Multiple layering of drug and swelling agent is also possible albeit requiring quite a complex, multi-step manufacturing process with sequential drying times between applications of the different coats.

Specifically, increasing the membrane thickness both prolonged the lag time and retarded the drug release rate, mainly due to the wider variation of initiation of membrane destruction (Ueda *et al.*, 1994a). The workers also realised the importance of having a sufficiently thick layer of swelling agent as TES with a swelling agent layer only 120μm thick exhibited typical diffusion-controlled dissolution (Ueda *et al.*, 1994b). They believed that water is able to penetrate through the (thinner) layer of swelling agent to the drug layer, allowing the drug to leach out through these channels before complete destruction of the outer membrane. Further studies showed that water absorption, the key determinant of lag time length, was dependent not only on

the L-HPC layer but also on membrane thickness (Ueda *et al*., 1994c). TES, unlike some other sustained release or controlled release products on the market, exhibited pH-independent release which is desirable (Ueda *et al*., 1994b).

Shirai *et al*. (1994) prepared fine granules containing L-HPC as swelling agent, utilised in order to rupture a brittle outer coating. While the TES configuration separated the swelling component from the drug, this system had a core of drug (sparfloxacin), L-HPC (grade LH-31), lactose and HPC (as binder) and was layered with a coating consisting of EC, HPC, titanium oxide and sucrose fatty acid ester (Figure 3.3).

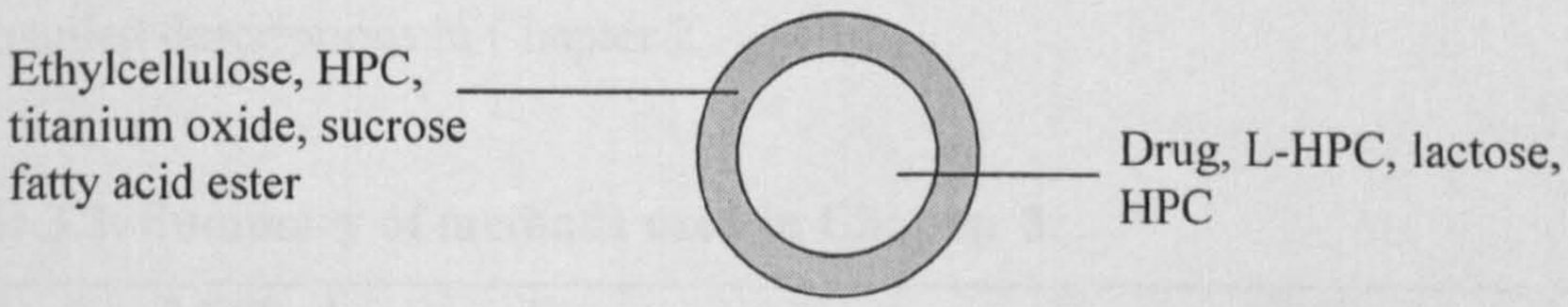

Figure 3.3: Swellable fine granules of Shirai *et al*. (1994).

The function of the coating was two-fold: firstly to form a water-insoluble, rupturable coating and secondly, to mask the taste of the bitter encapsulated drug. Increasing the concentration of LH-31 increased the rate of drug release *in vitro*. The workers determined that 52%(w/w) of LH-21 in the core was the minimum amount required for complete bursting of the granule, allowing total drug release. Any concentration below 40%(w/w) resulted in time to complete drug release (T_{max}) to be unpredictable. While they had success *in vitro*, the *in vivo* studies in rat and dog were not as optimistic because of poor drug bioavailability arising from transformation of sparfloxacin to the trihydrate which was of lower solubility. Nevertheless, as the coated granules had similar bioavailability to the uncoated granules as well as a control oral aqueous suspension of sparfloxacin, they postulated that bursting of the granules was almost perfect and the low pharmacokinetic parameter levels were caused by physiological factors such as gastrointestinal motility, pH of the gastrointestinal fluid and the gastrointestinal transit time. This formulation was promising in that it enabled taste masking as well as promoted rapid drug release.

3.2 Aims and objectives

In order to determine its potential as a swelling agent in our time-delayed capsule, LH-21 characterisation studies were carried out. This was timely, as few workers had embarked on this field of study. This chapter focuses on determining some of the inherent physical properties of LH-21 itself, which would impact on the rational design of our dosage form.

3.3 Methods

The methods used are summarised in Table 3.3 and referenced, where appropriate, to the detailed descriptions in Chapter 2.

Table 3.3: Summary of methods used in Chapter 3.

Section	Method	Methods section
3.5.1	**Morphology of LH-21**	
	Scanning electron microscopy	2.5.1.2
	Light microscopy	2.5.1.1
3.5.2	**Crystallinity of LH-21**	
	Fourier-transform infrared spectroscopy	2.5.3.1
3.5.3	**Moisture content and sorption of LH-21**	
	Dynamic vapour sorption	2.5.4
	Thermogravimetric analysis	2.5.2.1
3.5.4	**Water uptake and force generation of LH-21**	
	Light microscopy	2.5.1.1
	Water uptake apparatus	2.4.2
	Force measurement apparatus	2.4.4

3.4 Results and discussion

3.4.1 Morphology of LH-21

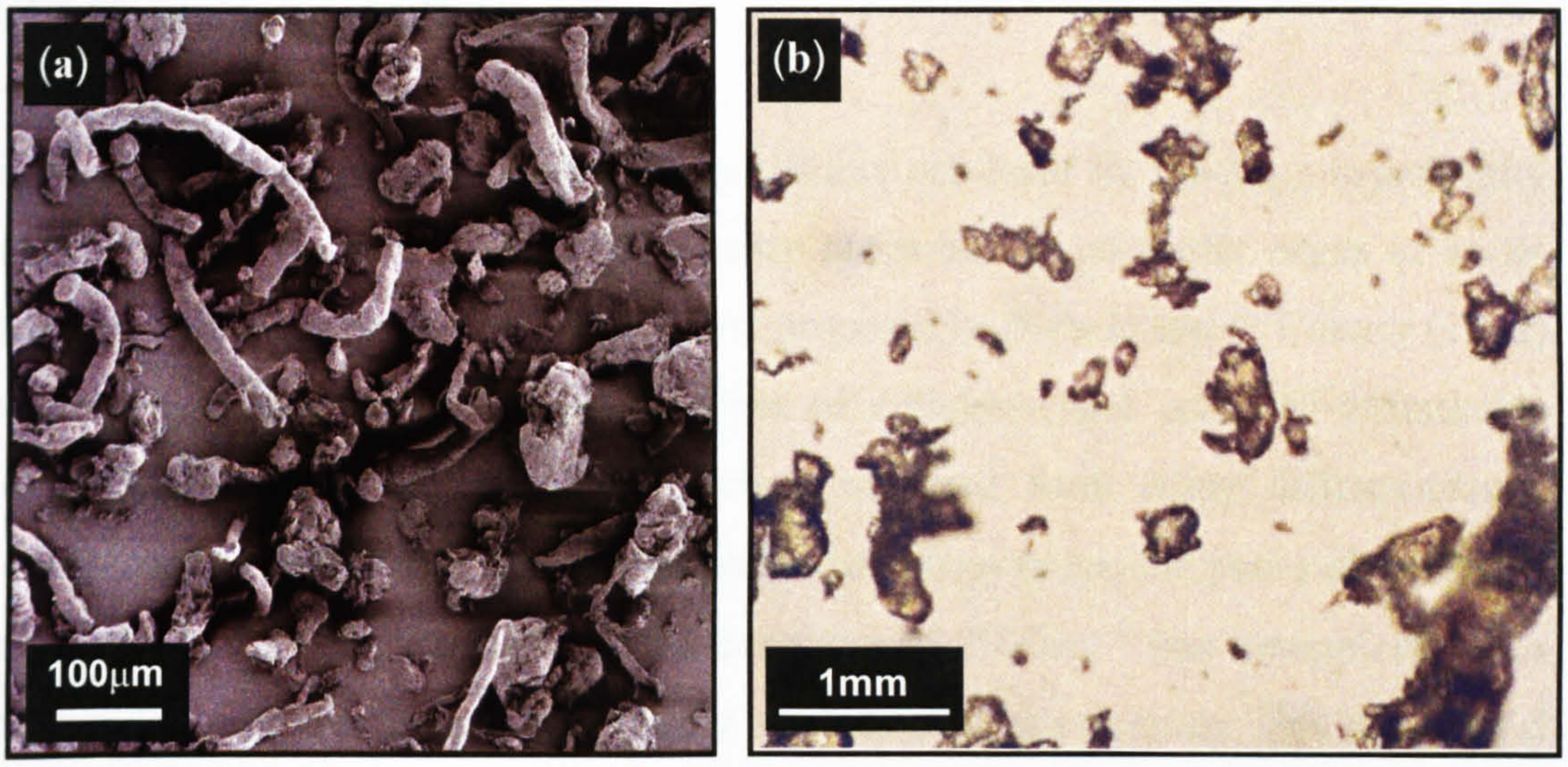

Figure 3.4: LH-21; (a) electron micrograph, X150, (b) light micrograph, X100.

LH-21 was found to consist of both irregularly-shaped particles ranging from 30μm to 130μm in size, as well as long, fibrous particles, as shown in Figure 3.4.

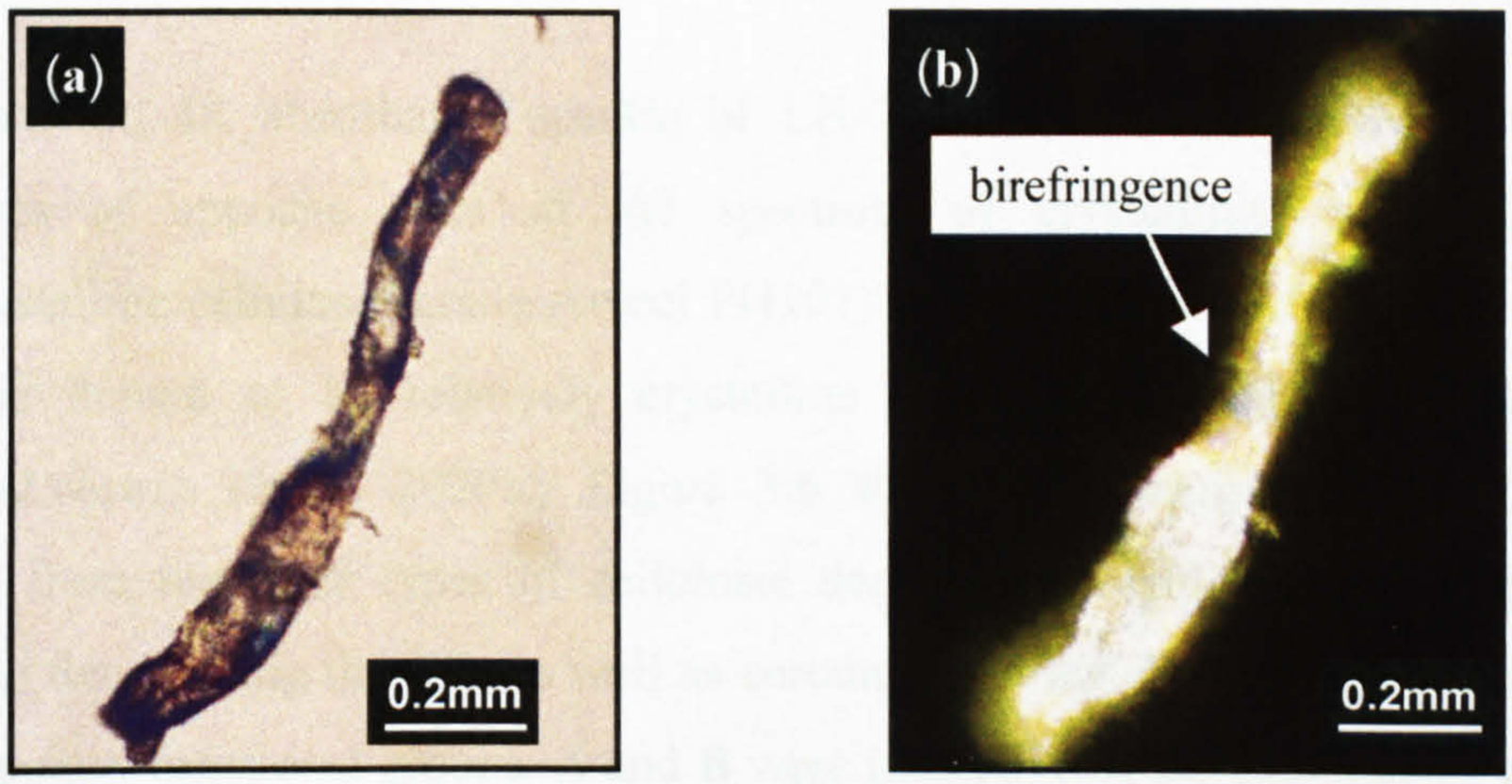

Figure 3.5: Fibrous LH-21 particle X400; imaged under (a) unpolarised light, (b) polarised light.

The fibrous particle is shown in Figure 3.5, both in unpolarised and polarised light. A small area of colour was seen in the polarised image, indicating birefringence and a certain degree of crystallinity. This was not totally unexpected, as LH-21 should have

retained some characteristics of the original cellulose, crystallinity being one of them (Alvarez-Lorenzo *et al.*, 2000b).

3.4.2 Crystallinity of LH-21

In an effort to ascertain the extent of crystallinity exhibited by LH-21, a crystallinity ratio (CR) was derived from the absorbance ratios of two particular peaks of an IR spectrum of the material. The CR was first proposed by Nelson and O'Connor (1964) who applied this method to various types of celluloses and achieved remarkable comparability with the crystallinity values obtained from x-ray diffractograms, density measurements and moisture sorption data. They chose the peaks at 1372cm^{-1} and 2800cm^{-1} as the absorbance of the band around 2900cm^{-1} was determined to be independent of the cellulosic crystallinity and was used as reference. This band could be attributed to the ether group of the original cellulose (Smith, 1999). Nelson and O'Connor (1964) also believed that the band around 1500-1200cm^{-1} was extremely influenced by crystallinity but almost unaffected by water absorbed into the polymer. It was possible that this band corresponded to the O-H bend of the substituent hydroxypropoxyl groups (Smith, 1999).

In our studies, IR absorbance spectra of LH-21 as well as two other cellulosic derivatives at opposite ends of the spectrum of crystallinity were obtained. Microcrystalline cellulose (grade Avicel PH101) and hydroxypropylcellulose (Klucel EF) were known to be relatively crystalline and near amorphous, respectively (Alvarez-Lorenzo *et al.*, 2000b). Figure 3.6 showed the sample infrared spectra obtained from the three types of cellulosic derivatives, highlighting the bands of interest in determining the CR, as well as certain peaks which were representative of some common functional groups. **A** and **B** were indicative of the presence of water in the sample; the O-H stretch (3500-3200cm^{-1}) and the O-H bend (1630cm^{-1}). The asymmetric C-C-O stretch (**C**) was observed between 1150-1075cm^{-1} while **D** was due to the O-H bend of alcohol groups (700-600cm^{-1}; Smith, 1999).

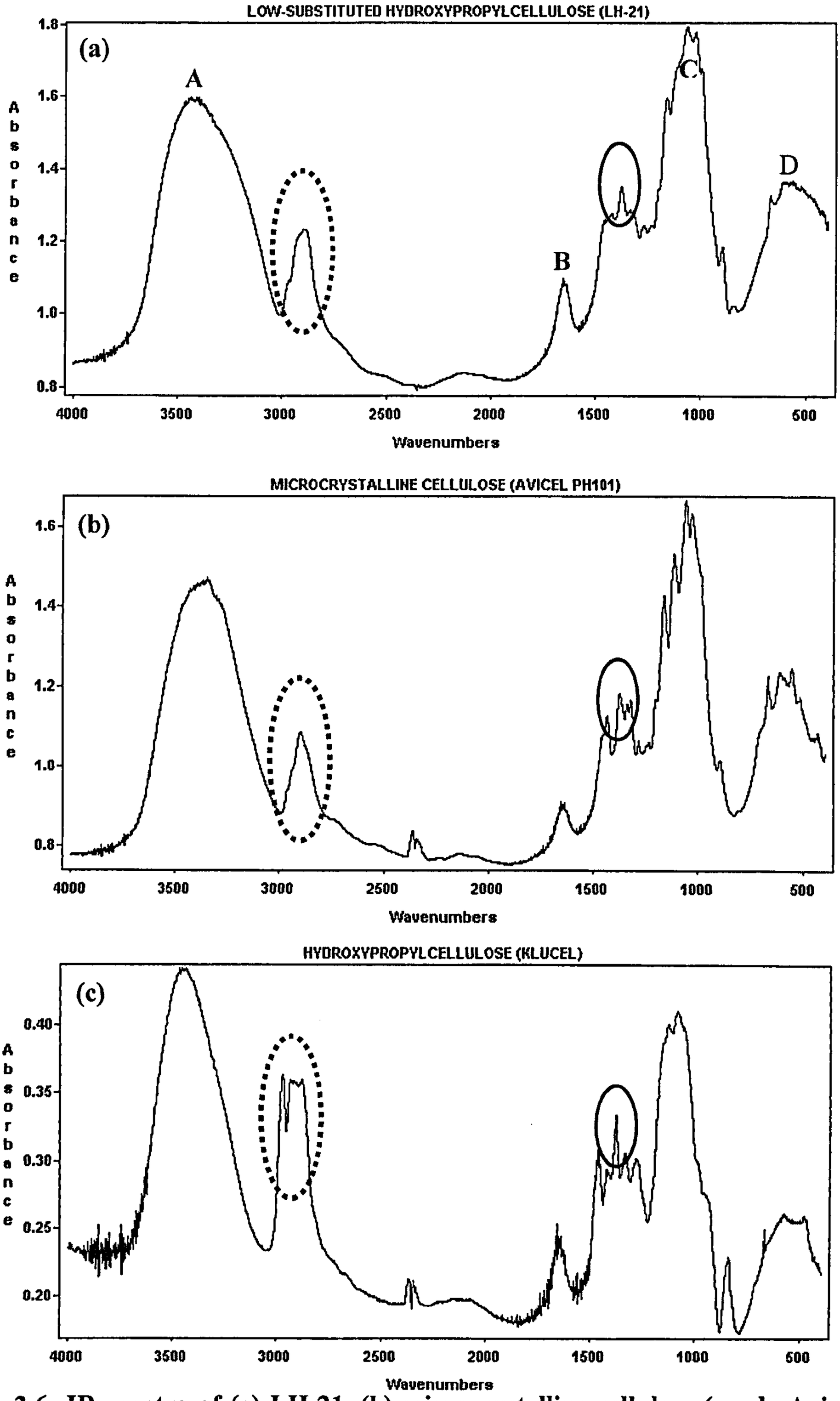

Figure 3.6: IR spectra of (a) LH-21, (b) microcrystalline cellulose (grade Avicel PH101) and (c) hydroxypropylcellulose (grade Klucel EF). The circles represent the bands chosen for the crystallinity ratio. Spectral regions A-D are described in the text.

Applying the method of Nelson and O'Connor to three cellulose derivatives, namely LH-21 and grades of microcrystalline cellulose (Avicel PH101) and hydroxypropylcellulose (Klucel EF), it was determined that the bands to be analysed were as follows:

Table 3.4: Bands of interest in IR spectra of cellulose derivatives.

LH-21	2890cm^{-1} and 1375cm^{-1}
Avicel PH101	2900cm^{-1} and 1375cm^{-1}
Klucel EF	2972cm^{-1} and 1375 cm^{-1}

Hence the CR was defined as the ratio of the absorbance at the wavenumber 1375cm^{-1} to the absorbance of the band around 2900cm^{-1}. Six IR spectra of the same polymer batch were obtained and the means and standard deviations were calculated and presented in Table 3.5. All polymers, stored at room temperature, were analysed without prior treatment.

Table 3.5: CRs of cellulose derivatives (n=6).

Cellulose derivative	**Mean CR (± S.D.)**
LH-21	1.11 (0.05)
Avicel PH101	1.16 (0.07)
Klucel EF	0.94 (0.03)

However, the values obtained were not comparable to those found in the literature. Alvarez-Lorenzo *et al.* (2000a) reported a value of 0.60 for LH-21, while Landin *et al.* (1993), determined the CRs of microcrystalline celluloses from four different manufacturers to be between 0.506 – 0.583. Although Klucel EF was not among the polymers studied by Alvarez-Lorenzo *et al.* (2000b), the CRs of two other grades of Klucel, GF and MF, were both 0.44. The disparity between the numerical values cannot be explained, as the Genesis FT-IR spectrometer used in our laboratory met the minimum requirements of British Pharmacopoeia 2000 comfortably at a resolution of 2cm^{-1}. The instrument was deemed to be well within the BP requirements in every respect. Furthermore, neither Nelson and O'Connor (1964) nor Alvarez-Lorenzo *et al.*

(2000a) specified the resolution at which they conducted their experiments. Hence exact replication of their methodology was not possible.

Nevertheless, the data obtained qualitatively suggested that the crystallinity of LH-21 lay between those of Avicel PH101 at the upper end and Klucel EF at the lower. This was in correlation with the assertion that increasing hydroxypropoxyl substitution decreased the crystallinity of the cellulose derivative due to the inability to pack the polymer chains uniformly due to the bulky side chains.

3.4.3 Moisture content and sorption of LH-21

Quantifying the residual moisture content of LH-21 was performed using both thermogravimetric analysis (TGA) and dynamic vapour sorption (DVS). In the former technique, the sample of about 10mg was heated from 25°C to 105°C at 2°C/min. This method was implemented on LH-21 samples that (a) had been transferred from the manufacturer's packaging into an amber glass jar, closed tightly with a lid, and left on a laboratory bench for about 3 months, and (b) were obtained fresh from the manufacturer's packaging. Sample (a) recorded a weight loss of 7.9% while sample (b) lost 6.4%. This showed that the polymer was indeed capable of absorbing moisture from the atmosphere. Over-exposure to the environment may pre-hydrate the polymer to a significant extent that would prove detrimental to its swelling capacity.

The DVS protocol subjected around 30mg of sample (a) to two consecutive cycles of increasing the relative humidity (R.H.) from 0 to 95% in steps of 10% then decreasing it back to 0 at 25°C. However, prior to beginning the cycle at 0%R.H., the sample was dried from its initial state to 0%R.H., and the weight loss from this preliminary step was 4.4%. This was lower than that determined by TGA, demonstrating that energy input from heating was required to remove the remaining water, possibly more tightly interacting with the polymer, from the sample.

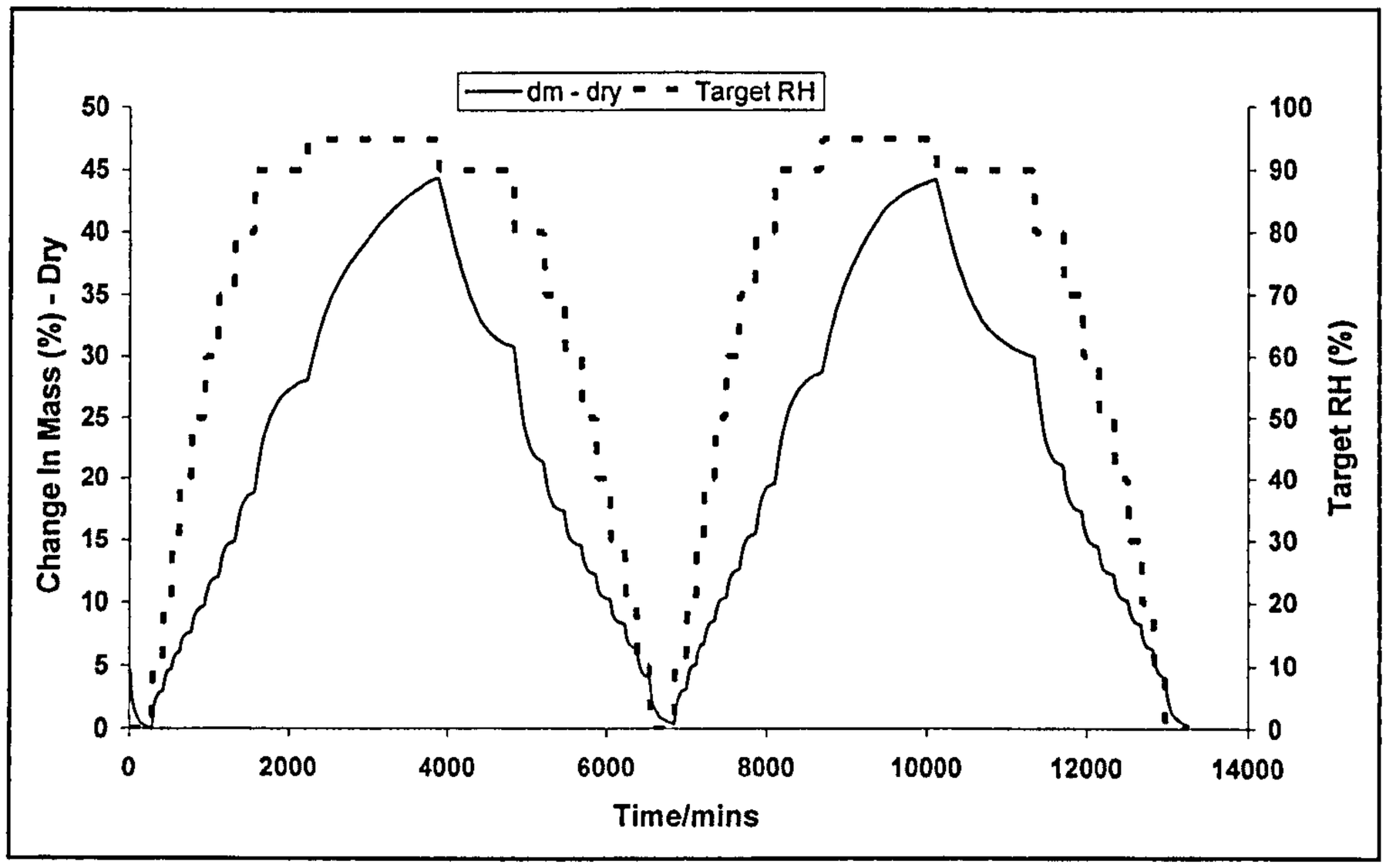

Figure 3.7: DVS plot of sorption and desorption of LH-21.

Figure 3.7 showed the sorption and desorption plot of LH-21. Both the first and second cycles resulted in similar shapes and heights of curves, indicating that the LH-21 did not undergo any permanent chemical change from hydration. The mean maximum water absorbed at 95%R.H. was 44.3%(w/w of sample). This further reiterated the hydrophilicity of LH-21, being capable of absorbing nearly half its own weight in water when exposed to a maximum of 95%R.H.

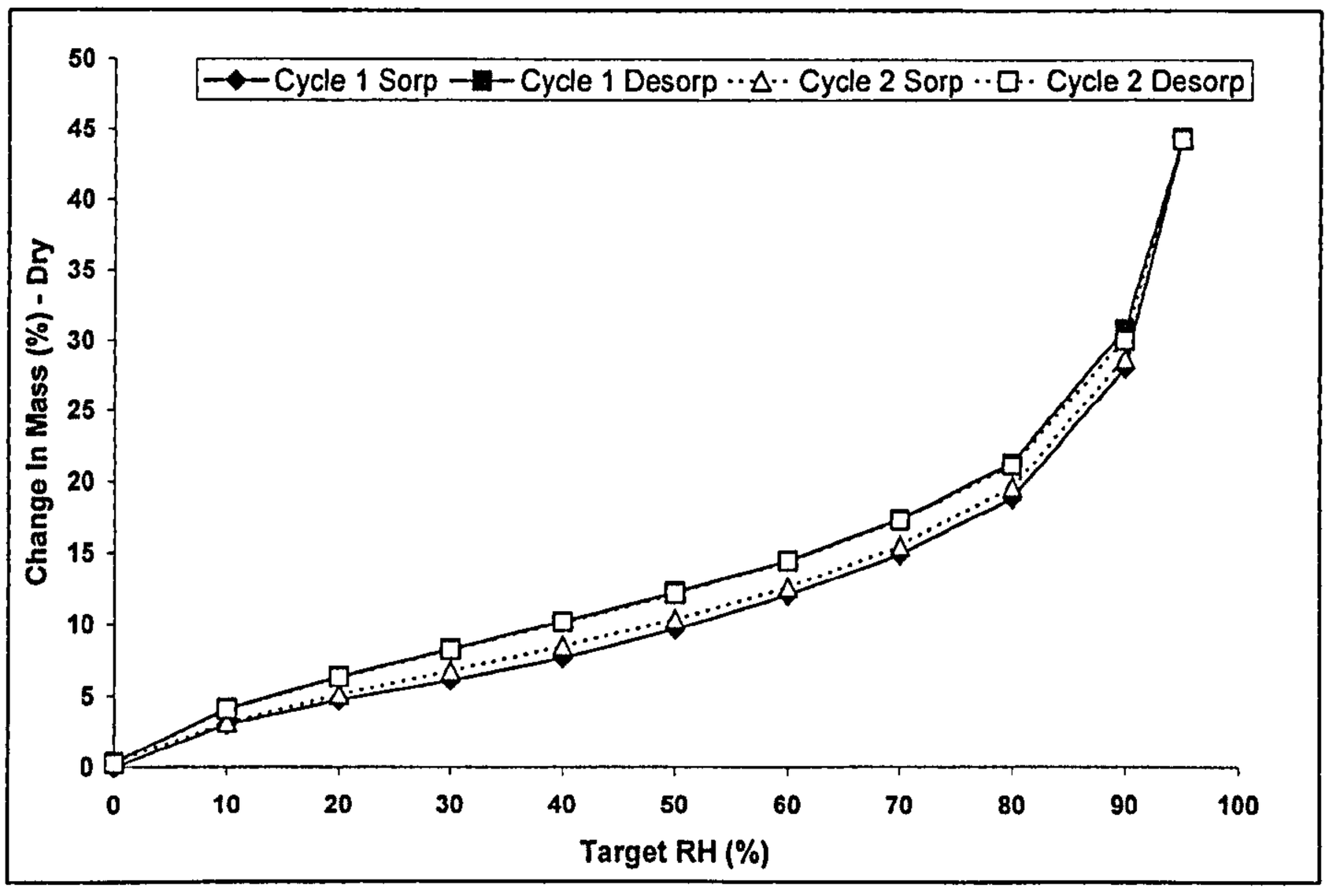

Figure 3.8: Isotherm plot showing % change in mass per step of R.H.

An interesting observation from Figure 3.8 was that the sorption and desorption curves of individual cycles did not overlap. Rather, the desorption curve was quantitatively higher that the sorption curve for both cycles, indicating that the amount of water lost from the sample was more than the amount of water taken up. Although a drying step preceded the cycles, there may yet be water contained within the sample, more strongly attached to the polymer particles.

3.4.4 Interaction of LH-21 with water

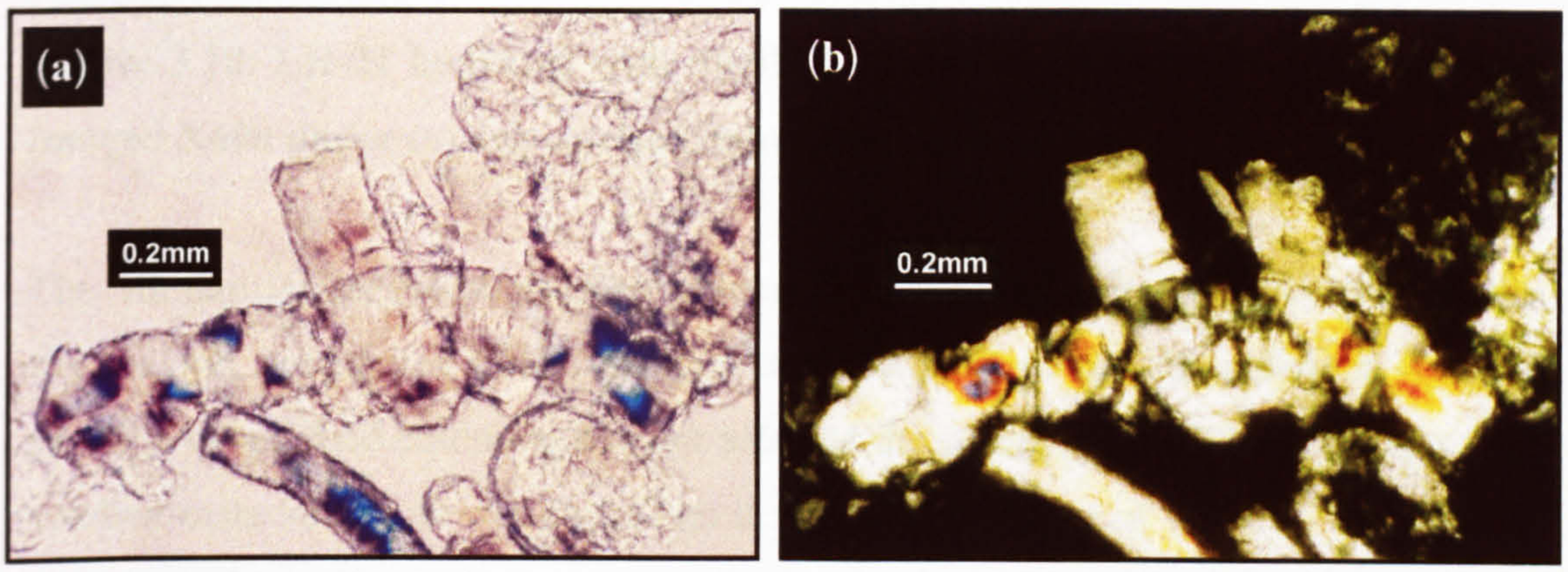

Figure 3.9: Hydrated LH-21, X400; imaged under (a) unpolarised light, (b) polarised light.

Distilled water was applied to the edge of the sample on the microscope slide with a plastic pipette, allowing water movement by capillary action. Figure 3.9a highlighted the fact that the LH-21 was not fully hydrated, as evidenced by the retention of the familiar fibrous shape. However, particles that were hydrated assumed transparent mass-like shapes. Under polarised light, hydrated LH-21 (Figure 3.9b) could not be seen while those yet to be hydrated were visible. A coloured segment was observed on one of the fibres, further reiterating the partially crystalline nature of the polymer.

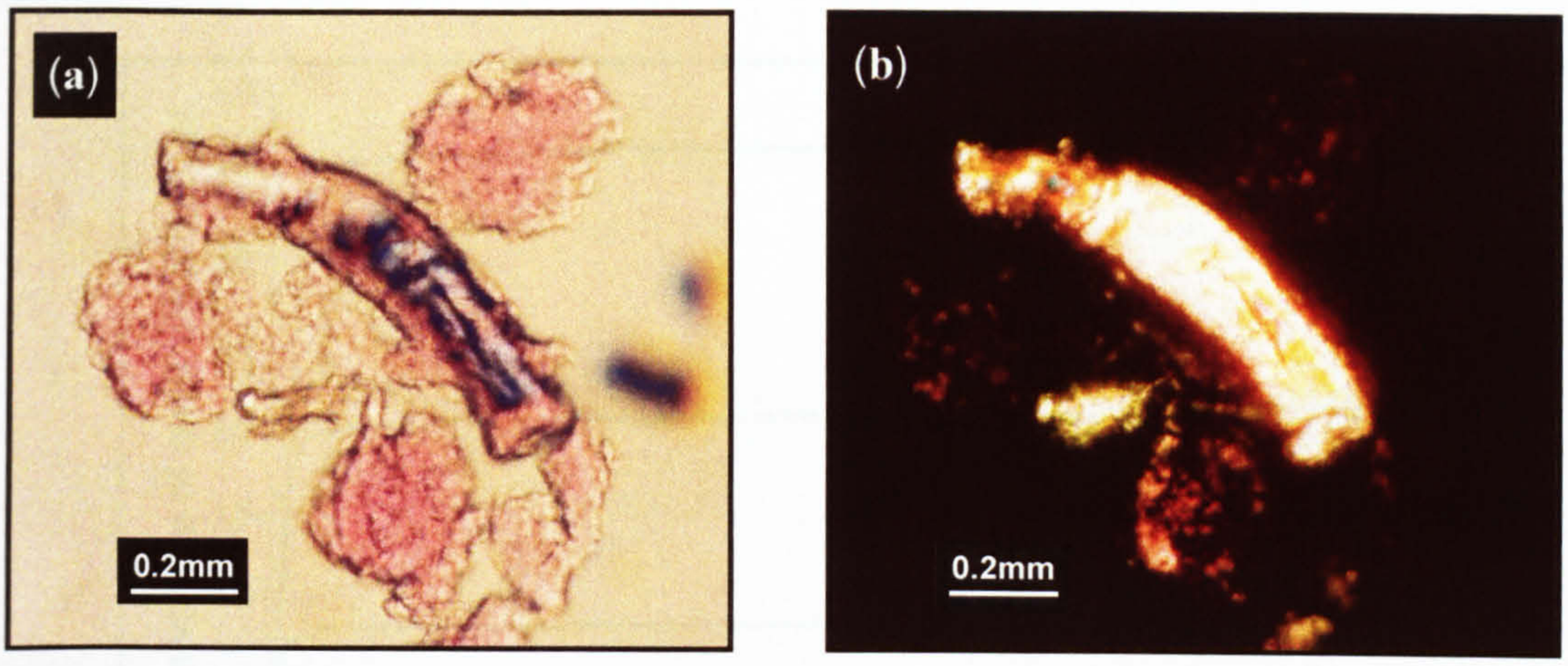

Figure 3.10: LH-21 hydrated with distilled water dyed with red food colouring; imaged X400 under (a) unpolarised light, (b) polarised light.

The similarities in morphological structure between Figures 3.9 and 3.10 i.e. the fibrous, yet unhydrated LH-21 particle and the swollen masses indicated that the addition of red food colouring had not affected the swelling of LH-21. Dyeing of the swollen mass structures confirmed that it was indeed uptake of water by the polymer that caused swelling. Furthermore, the integration of water within the swollen polymer network was clearly visualised by the localisation of red dye in Figure 3.10a. In polarised light (Figure 3.10b), the swollen particles could not be clearly seen, and an area of colour was observed within the unswollen fibre, again indicating crystallinity.

Quantification of the volume of water absorbed by the polymer was undertaken using the water uptake apparatus described in Section 2.4.2. The LH-21 powder was not compressed at all for this study, only poured into the sample holder from a weighing boat. Hence, any effects of compression were not studied, as it did not seem necessary since the powder would not be in a compressed form when mixed with corn oil and other excipients in our dosage form.

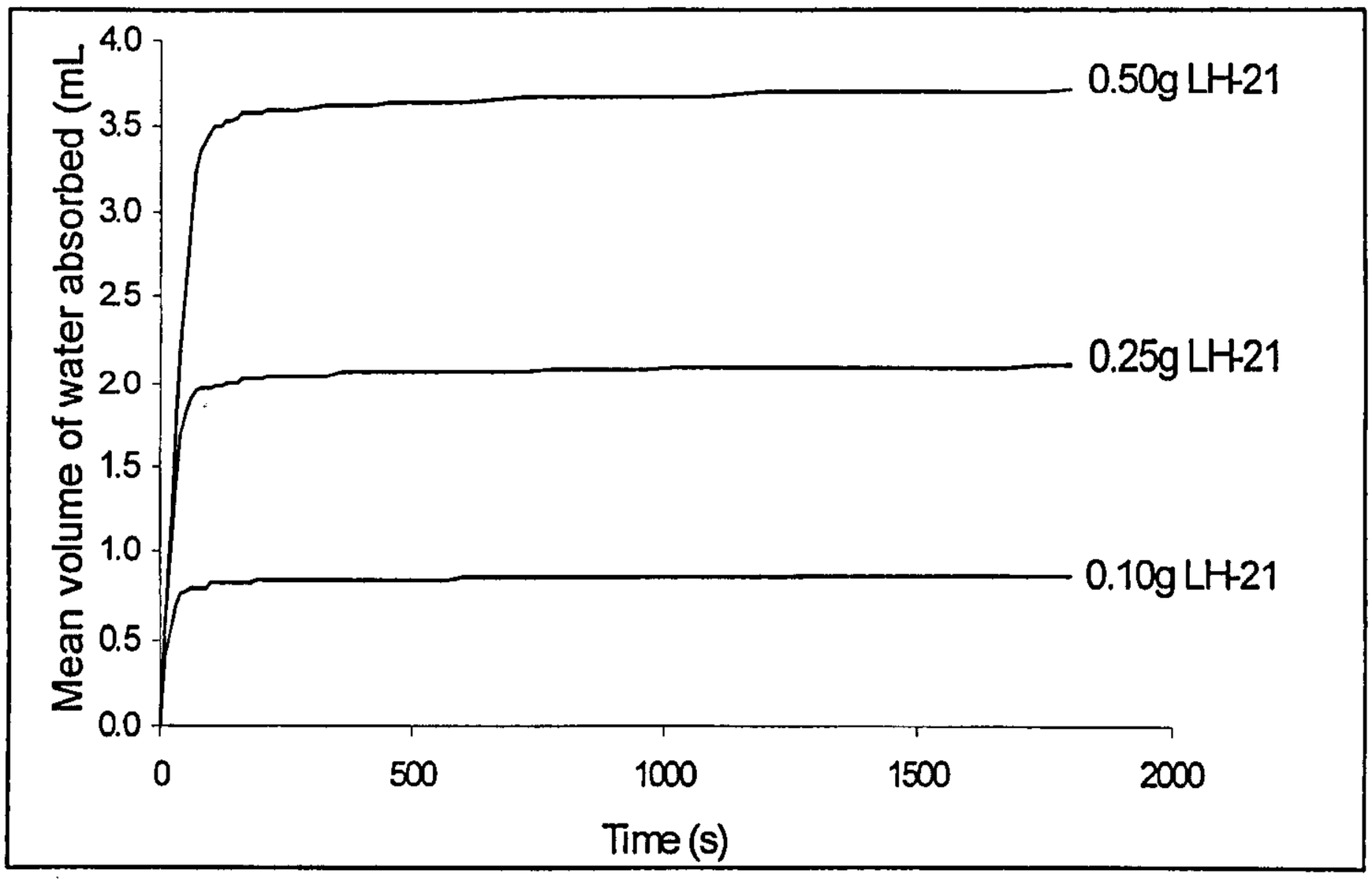

Figure 3.11: Mean water uptake curves of varying amounts of LH-21 (n=3).

Figure 3.11 highlighted that the water uptake by LH-21 was very rapid, achieving saturation levels within 4 to 5 minutes.

Table 3.6: Initial water uptake rates of dry, uncompressed LH-21. (n=3, ±S.D.)

LH-21 (g)	Initial water uptake rate (mL/min) *
0.10	0.24 (0.02)
0.25	0.35 (0.02)
0.50	0.34 (0.03)

***Measured over initial 10 seconds, where gradient of curve was greatest.**

While the initial water uptake of 0.25g LH-21 was higher than that of 0.10g, it was almost the same as that of 0.50g (Table 3.6). Wan *et al.* (1991) proposed that the rate of water uptake by a hydrophilic polymer is governed by the net effect of driving force promoting liquid uptake and the viscous force opposing it, that develops once dissolution and / or swelling of the polymer occurs. In this instance, the increase of water uptake rate as LH-21 increased from 0.10g to 0.25g could have been due to the increasing driving forces such as capillary action and diffusion exerted by the greater amount of polymer. However, at 0.5g, the contributory effect of the growing viscous layer may have been impeding water uptake to a greater extent than observed with the lower amounts of LH-21.

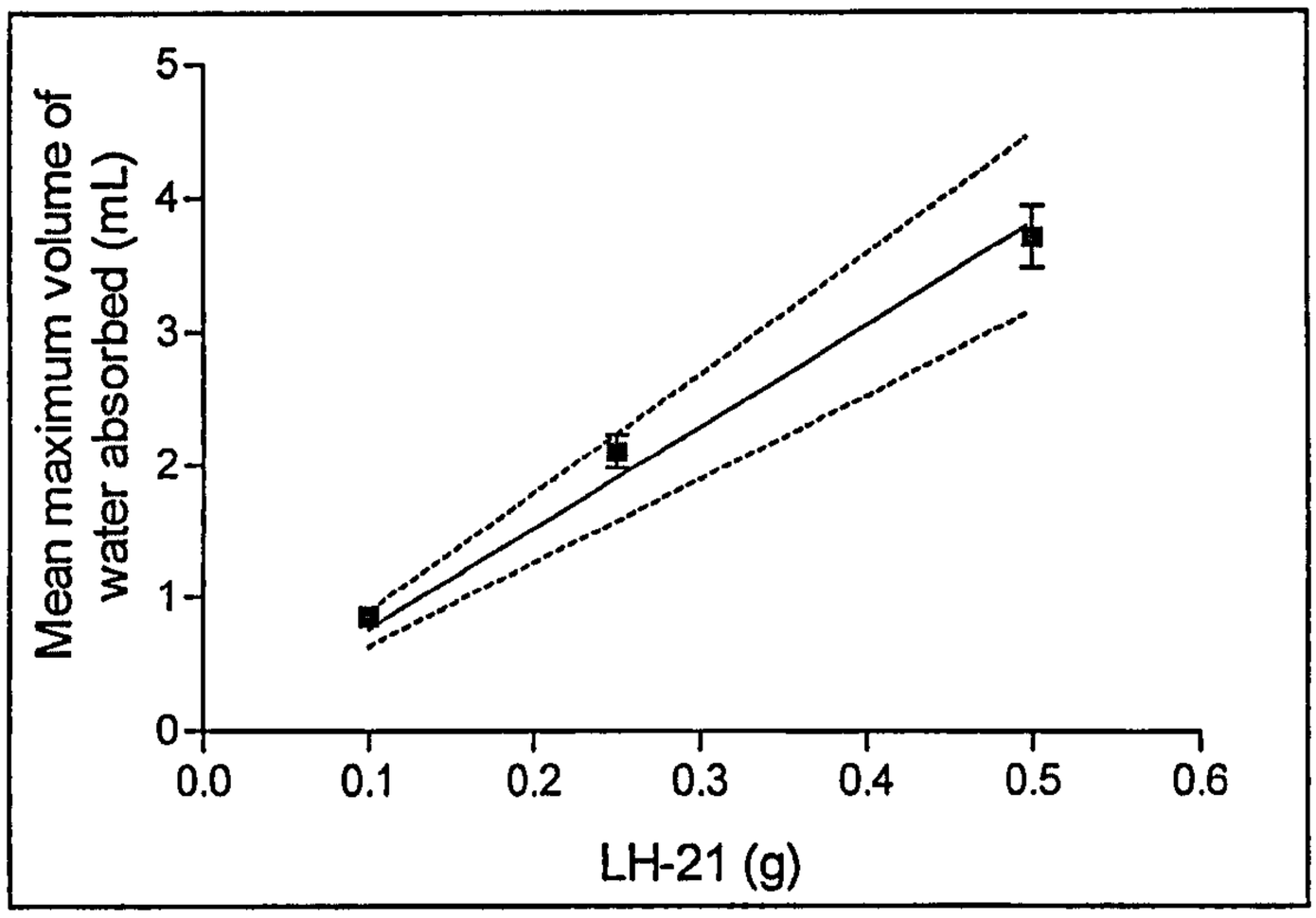

Figure 3.12: Mean maximum volume of water absorbed by LH-21 (n=3, ±S.D.).

The mean volume of water absorbed by increasing amounts of LH-21 increased linearly, the equation of the curve obtained by linear regression being

$$W = 7.6L \qquad \textbf{(Equation 3.1)}$$

where W and L are mean volume of water (mL) absorbed by LH-21 and amount of LH-21 (g) respectively. The R^2 value for the line was 0.985 and the 95% confidence interval of the slope was (6.331, 8.967), represented by the dotted lines in Figure 3.12. One-way ANOVA showed that increasing LH-21 significantly increased the mean volume of water absorbed ($p<0.0005$) and it followed that from Tukey's pairwise comparisons that each mean was significantly different from the others.

This meant that dry LH-21 was capable of absorbing almost eight times its own weight in water, contributing to its ability to generate adequate volumes of swollen mass to further strengthen its role in rupturing the brittle outer coating of our capsule (Variation 2). Note the difference of this value to that obtained by DVS (Section 2.5.4). The DVS program only subjected the polymer to 95%R.H., while in the water uptake study (and in the following force measurement study) the polymer is in contact with an entirely liquid aqueous phase.

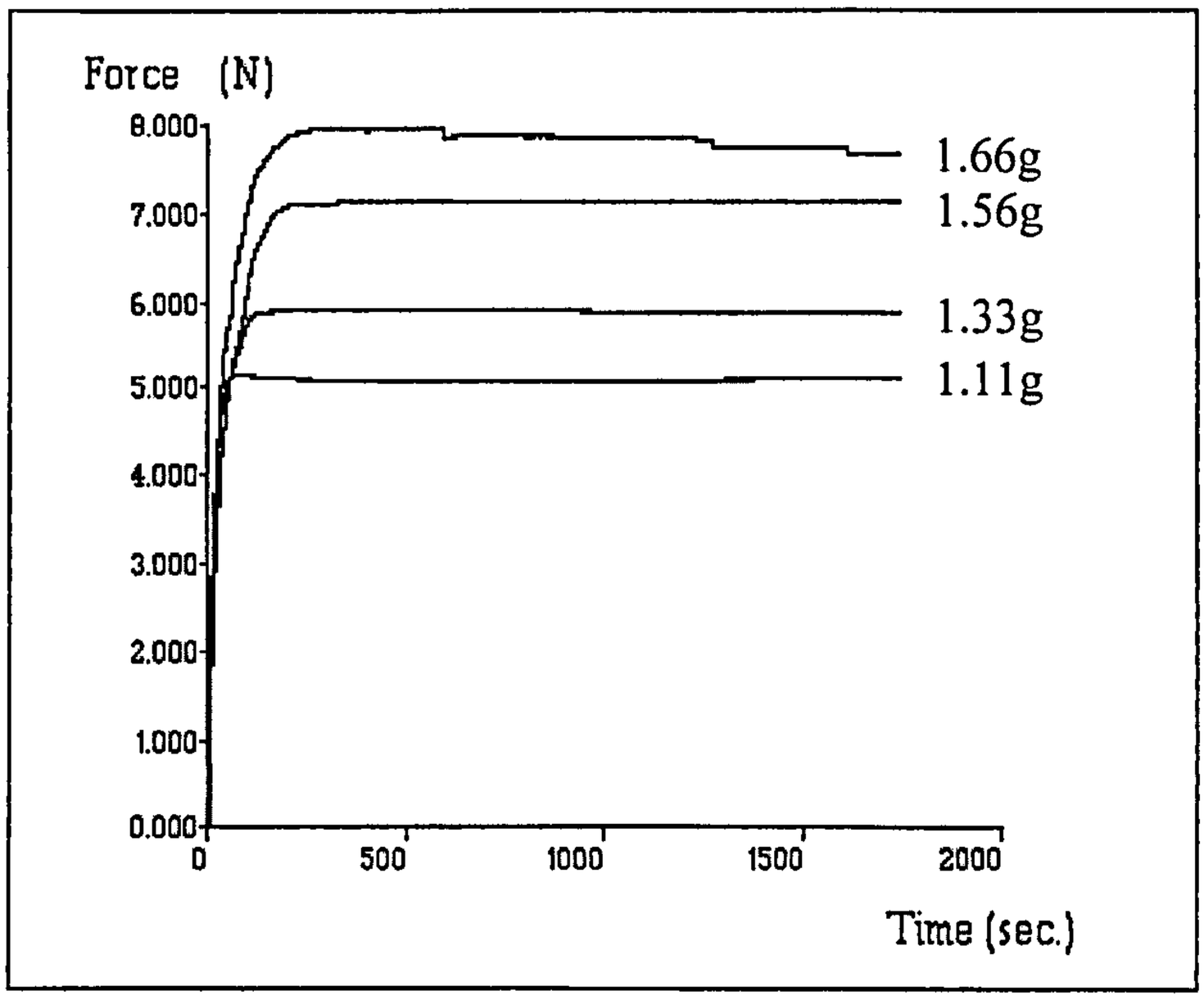

Figure 3.13: Mean force curves generated from swelling of LH-21 (n=3).

In order to determine the swelling force generated by LH-21, force measurement studies (Section 2.4.4) were implemented. Figure 3.13 showed the mean force curves (n=3) derived from the swelling of varying amounts of LH-21. Swelling of LH-21 produced a force curve consisting of three distinct phases. The swelling phases were divided into two portions of linearity, the initial rapid generation of force was superseded by a more gradual slope prior to achieving the plateau of maximum force (Figure 3.14). This was due to the formation of a viscous hydrogel layer at the base of the sample holder, at the boundary of swelling polymer and water, impeding water uptake by capillary action. The effect was probably more prominent at the higher levels of LH-21 concentration because of the packing of the dry powder, being thicker as the amount of LH-21 increased. Water for swelling would have been more accessible to thinner layers of LH-21. This effect is diagrammatically represented in Figure 3.15.

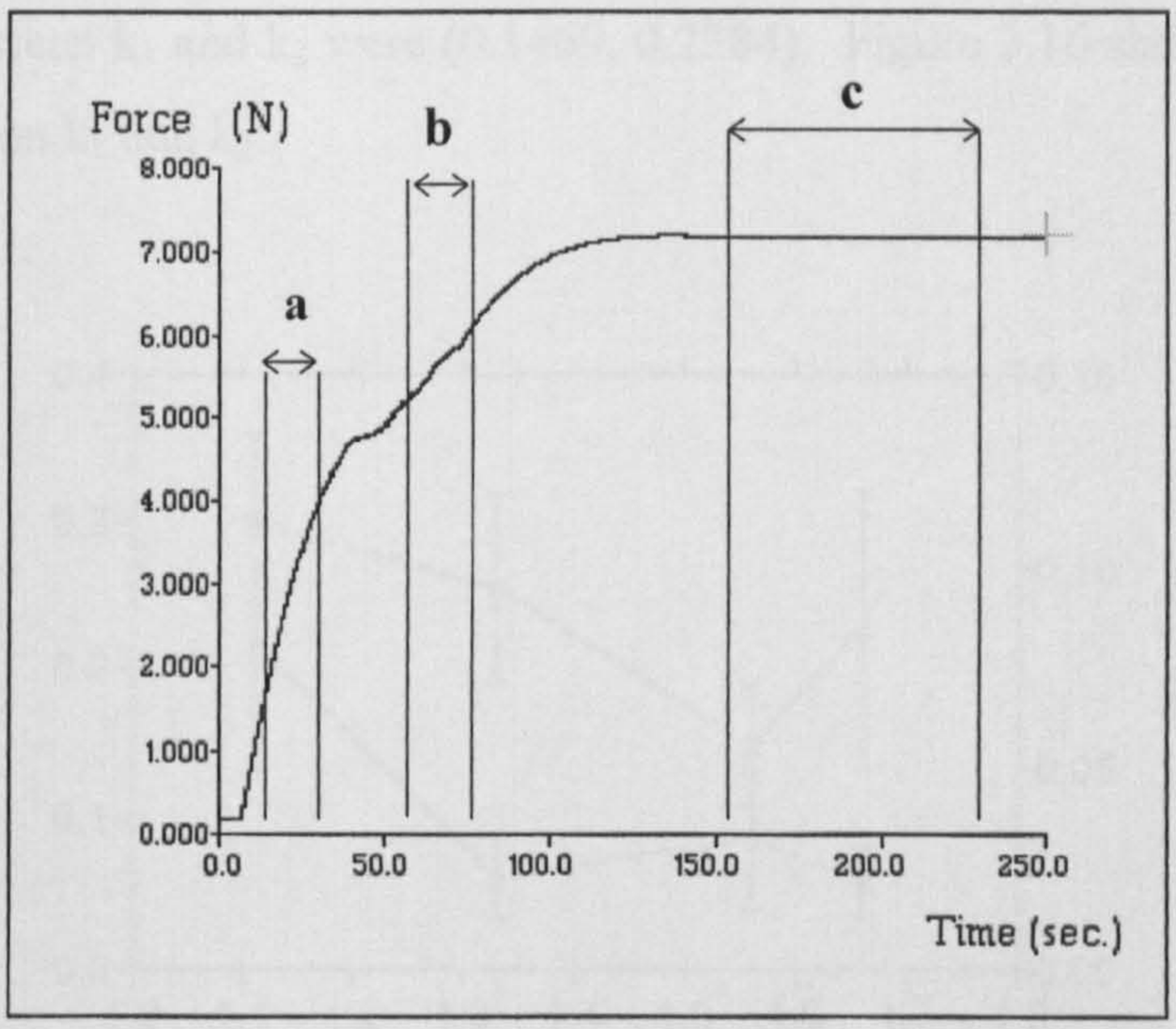

Figure 3.14: Typical force curve: (a) initial high rate of force generation, (b) slower rate of force generation, (c) maximum force generated.

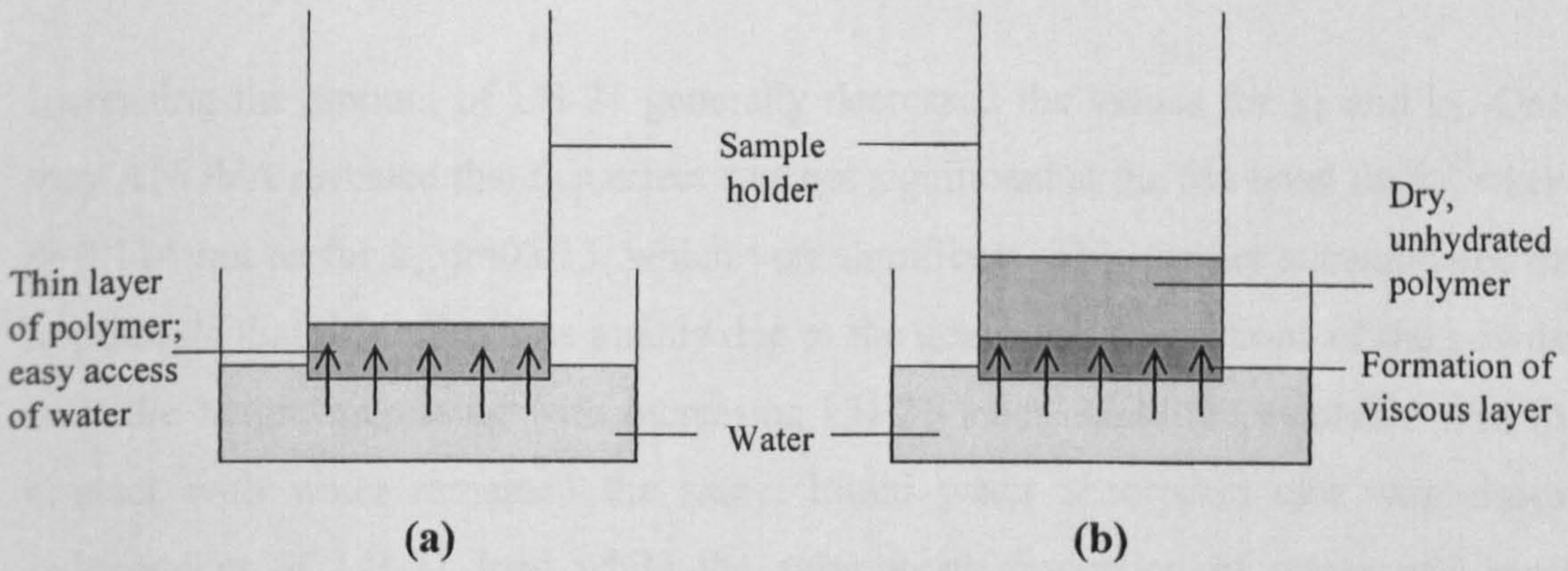

Figure 3.15: Water uptake by (a) thin layer of polymer; and (b) thicker layer of polymer, showing viscous layer opposing capillary-driven ingress of water.

Hence there existed two separate rates of force generation, here named k_1 and k_2. Both were the net results of the capillary forces that drive water uptake and consequent swelling and the viscosity of the growing hydrogel layer that impedes the two processes. The effect of the viscous layer was seen to be greater as the swelling progressed, hence k_1 was always significantly larger in value than k_2. Paired t-test at 5% significance level resulted in $p<0.0005$ and 95% confidence intervals of the mean

differences between k_1 and k_2 were (0.1469, 0.2384). Figure 3.16 shows the effect of LH-21 amount on k_1 and k_2.

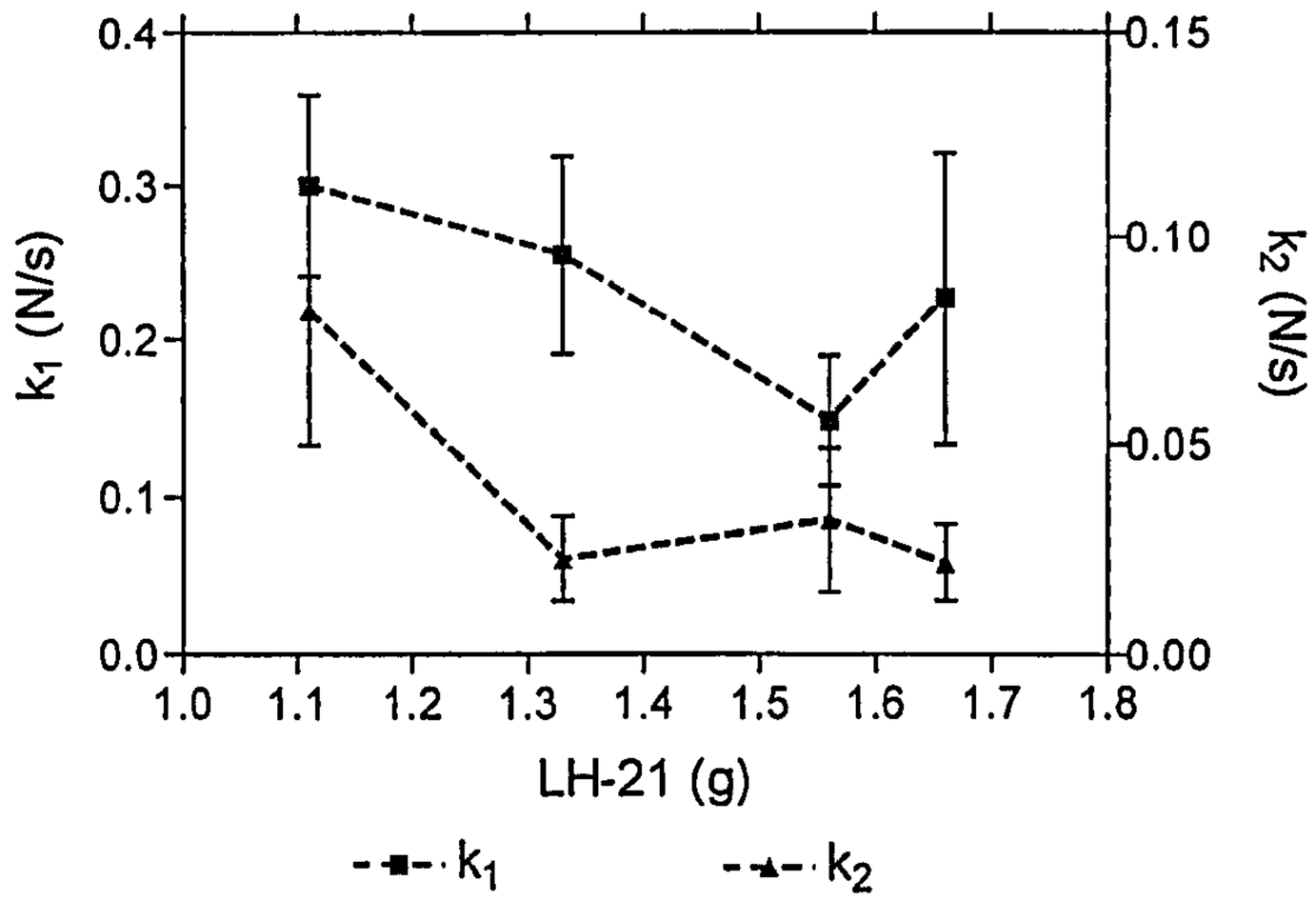

Figure 3.16: Rates of force generation, k_1 and k_2 (n=3, ± S.D.)

Increasing the amount of LH-21 generally decreased the values for k_1 and k_2. One-way ANOVA revealed that this effect was not significant at the 5% level for k_1, where p=0.114 but as for k_2, p=0.015, which was significant. This further substantiates the hypothesis that this effect was mainly due to the geometric proportions of the powder bed: the height increasing with increasing LH-21 loads while the available area for contact with water remained the same. Initial water absorption rate was almost independent of LH-21 load while the subsequent absorption of water was more influenced by the amount of LH-21 present.

It was possible that the increase seen in k_1 for 1.66g LH-21 was due to the extra water absorbing potential of the increased amount of polymer overriding the viscosity of the hydrogel layer. As for k_2, it remained low despite the higher amounts of LH-21 as the initial thickness of the hydrogel layer would have been independent of the total amount of LH-21. However, the load of 1.11g formed a sufficiently thin layer of polymer for capillary-driven water uptake to dominate the force generation rate.

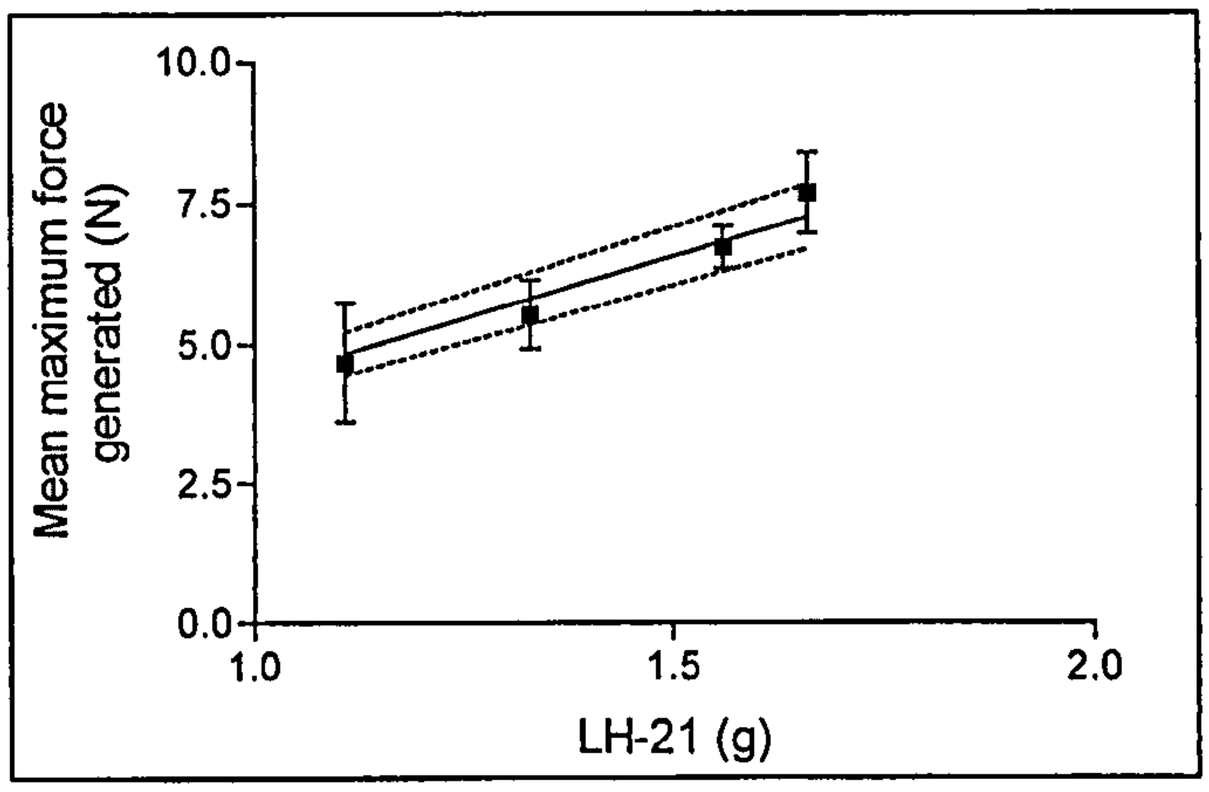

Figure 3.17: Mean maximum force generated by LH-21 (n=3, ± S.D.)

The mean maximum force generated was found to increase linearly with the increasing amounts of LH-21 (Figure 3.17), the equation derived from linear regression of the points being:

$$F = 4.4L \qquad \textbf{(Equation 3.2)}$$

where F is the mean maximum force generated (N) and L is the amount of LH-21 (g). The dotted lines on Figure 3.17 represent the 95% confidence interval of the slope, which was (4.020, 4.709).

Combining the equation above with Equation 3.1, gave the relationship between volume of water uptake and the consequent swelling force generated i.e.

$$W = 1.7F \qquad \textbf{(Equation 3.3)}$$

This meant that the absorption of 1mL of water would result in the generation of 0.6N of swelling force. For example, if our capsule were filled with 0.5g LH-21, in theory, 2.2N of force would be generated from the absorption of 3.8mL of water.

3.5 Conclusions

- These initial characterisation studies with LH-21 provided an insight into the effect that certain physicochemical features had on the swelling properties of the polymer.

- Images from polarised light microscopy indicated the possession of some crystalline structure by LH-21.

- A crystallinity ratio, derived from the absorbances of two particular peaks in the infrared spectrum confirmed the intermediate crystallinity of LH-21 between those of hydroxypropylcellulose and microcrystalline cellulose.

- Simple models to determine water uptake and force generation parameters of the polymer proved useful in predicting the mechanisms of water uptake and consequent swelling of polymer.

- The numerical equations of water uptake and force could then be used to extrapolate the effects of filling varying amounts of LH-21 into our dosage form.

CHAPTER 4

COMPATIBILITY OF LH-21 WITH FORMULATION EXCIPIENTS

4.1 Introduction

The initial premise of our novel drug delivery system was to combine the swelling power of LH-21 with the solubilising capacity of a vegetable oil in order to time the delivery of a hydrophobic drug. Hence in both Variations 1 and 2 of our delivery device (Section 1.4 and Chapters 6 and 7), it was imperative to first evaluate the effect formulation excipients we proposed to combine with LH-21 would have on the inherent swellability of the cellulose derivative.

Several dosage forms have been developed that contain L-HPCs in combination with other formulation excipients. Some were described in Section 3.1.2. The examples that follow here specifically discuss the effects addition of L-HPC had on certain physical and chemical properties of the formulation mixtures.

Ho *et al.* (2002) identified a means of improving the flowability of microcrystalline cellulose (MCC) by co-drying it with L-HPCs. A slurry of MCC, with a degree of polymerisation of about 230 obtained by acid-hydrolysing wood pulp, was then wet granulated in water either (a) on its own, or (b) blended with 10%(w/w) LH-11, LH-21, LH-31, LH-20 or LH-30. After sieving, drying and milling, the granules that were obtained via method (b) constituted the co-dried variety, while the granules from method (a) were dry-blended with pulverised L-HPC to form the physical mixtures which were then investigated in comparison to the co-dried granules. As a control, the MCC granules from method (a) were also used in the study.

The improved flowability of the co-dried granules was attributed to the rounder, smoother shape of the individual granules, confirmed through scanning electron microscopy, instead of the irregular, chipped edges of the granules that were only physically mixed together or of MCC only.

The granules of the three varieties were also compressed into flat-faced tablets which were then subjected to various tests. Although the water uptake rates of the tablets containing L-HPC (co-dried or physically mixed) were lower than that of the MCC-only tablets, the disintegration times of the L-HPC-containing tablets were much shorter than those without L-HPC. This was a consequence of the ability of L-HPC to swell and hence disrupt the integrity of the tablet matrix.

L-HPC-free tablets exhibited a greater stiffness, as reflected by the Young's Modulus, compared to those that contained co-dried L-HPC. L-HPC physically mixed also decreased the Young's Modulus but not to such a great extent as the co-dried granules. The authors showed that the Young's Modulus linearly decreased with increasing porosity of the tablets, which correlates with the preposition that intragranular entanglement of L-HPC and MCC fibres would contribute to greater porosity in addition to the intergranular arrangement.

The presence of L-HPC physically mixed in the granules also decreased the brittleness of the prepared tablets whereas the opposite was true when the co-dried variety of the same grade of L-HPC was considered. This implied that co-drying reduced the intergranular forces, taking into consideration that the rounder, smoother granules would exert less cohesive force than the rough edges of the physically mixed granules.

Although the improvement in powder flowability was observed, this study showed that addition of L-HPC, whether co-dried or simply physically mixed, exerted effects on the physical parameters of the tablets formed. While this study did not investigate the effects on tablet dissolution and drug release, it is likely that these parameters would also be affected by incorporation of L-HPC.

In a separate study, Kleinbudde (1994a and b) investigated the effect L-HPCs had on the shrinking and swelling properties of conventional MCC pellets prepared by extrusion-spheronisation. Control pellets contained 30% drug, 69.5% MCC (Avicel PH101) and 0.5% Aerosil 200 whereas the test pellets contained 20% L-HPC (grades LH-20 or LH-30) and 49.5% MCC but maintained the same content of drug and Aerosil 200 as the control.

Inclusion of L-HPC affected the dimensions of the pellets both before and after drying, regardless of method, whether oven drying, fluid bed drying or freeze drying, though the effects were least with lyophilisation (Kleinbudde, 1994a). Image analysis conducted on the pellets revealed that:

a) L-HPC did not affect the width distribution of wet pellets as that was governed wholly by the die diameter
b) L-HPC shifted the width distribution of the dried pellets to the lower values to a greater extent compared to the L-HPC-free pellets. This was most likely to be a result of the higher water content of pellets containing the hydrophilic L-HPC.
c) Wet pellets containing L-HPC had larger length distributions than those pellets that did not. It was possible that L-HPC increased the elasticity of the extrudate to a degree that it was insufficiently brittle to break apart during spheronisation for production of particles with similar length.
d) Once dried, both pellets with and without L-HPC possessed similar length distributions.

In the same study, it was also shown that fluid bed-dried pellets containing L-HPC had greater porosity (17-23%) than those without L-HPC (3-7%). This could have been a consequence of greater water absorption by L-HPC resulting in the formation of pores post-evaporation of water.

Image analysis was also performed for swelling studies, in which water was added to the glass petri dish containing a certain number of pellets (Kleinbudde, 1994b). A constant frame containing about 15-70 pellets was analysed over a 20-minute period. Pellets with L-HPC dried in the fluid bed swelled to a greater extent compared to L-HPC-free pellets, as expected.

Dissolution studies showed that the increase in dissolution rate of the model drugs (acetaminophen, caffeine and propyphenazone) was attributable to the inclusion of L-HPC. Although L-HPC affected the dimensions of the pellets produced, careful manipulation of drying procedures should be sufficient to overcome this problem, as improved dissolution rates should be capitalised on.

4.2 Aims and objectives

Most of the publications to date with regards to L-HPC deal with its incorporation into formulations to exploit its excellent swelling capacity, disintegrating power and sustained-release matrix capability. However, not much has been discussed about the effects other formulation excipients may have on the inherent properties of this hydrophilic polymer.

Compatibility studies were carried out with the aim of determining the suitability of proposed excipients to be included in the construction of our novel time-delayed drug delivery device. Unique models for water uptake and force generation were designed and modified to assess the effects of certain excipients on these parameters, while conventional methods such as microscopy and thermal analysis were also employed.

4.3 Methods

The methods used are summarised in Table 4.1 below and referenced, where appropriate, to the detailed descriptions in Chapter 2.

Table 4.1: Summary of methods used in Chapter 4.

Section	Method	Methods section
4.4.1	**Dispersion of LH-21 in vegetable oils**	
	Partitioning of LH-21 in oil and water	2.4.1
	Water uptake studies	2.4.2
	Swelling force studies	2.4.4
	Light microscopy	2.5.1.1
	Dynamic vapour sorption	2.5.4
	Thermogravimetric analysis	2.5.2.1
4.4.2	**LH-21 dispersed in corn oil with surfactants**	
	Water uptake studies	2.4.2
4.4.3	**LH-21 and paracetamol dispersed in corn oil**	
	Light microscopy	2.5.1.1
	Water uptake studies	2.4.2
4.4.4	**Mixture of LH-21 with effervescent material**	
	Preparation of effervescent material	2.4.6
	Swelling force studies	2.4.4

4.4 Results and discussion

4.4.1 Dispersion of LH-21 in vegetable oils

Vegetable oils, described in detail in Section 1.7.1, were chosen as potential solubilisers for improving delivery of hydrophobic drugs in conjunction with our system, so their compatibility with LH-21 was investigated.

4.4.1.1 Partitioning of LH-21 in oil and water

Mixing 0.1g LH-21 in 2mL soybean oil in a 10mL measuring cylinder resulted in a pale cream-coloured dispersion which had a visibly higher viscosity than that of pure oil. When 1mL distilled water was added, the denser water layer flowed slowly to the bottom. Particles of LH-21 were seen to partition out of the oil into the water.

Another 1mL distilled water was added when the water layer seemed to be saturated with LH-21. More partitioning of solid into the aqueous phase was observed and the mixture was left, covered, overnight at room temperature.

Upon inspection the next day, there were two clear aqueous and oil phases present. Almost all the LH-21 had migrated into the water and a layer of swollen LH-21 was formed at the bottom of the measuring cylinder. These preliminary studies indicated the preference of LH-21 for the aqueous phase which would be advantageous in our system for the rapid hydration and swelling effect.

Methods I and II (Section 2.4.1) were then used to quantify the swelling of 0.1g, 0.2g and 0.3g LH-21 in terms of swollen LH-21 volume over time. Varying the sequence of addition i.e. whether LH-21/oil dispersion was added to water (I) or water was added to LH-21/oil dispersion (II) was employed to investigate the effect of gravity on the results.

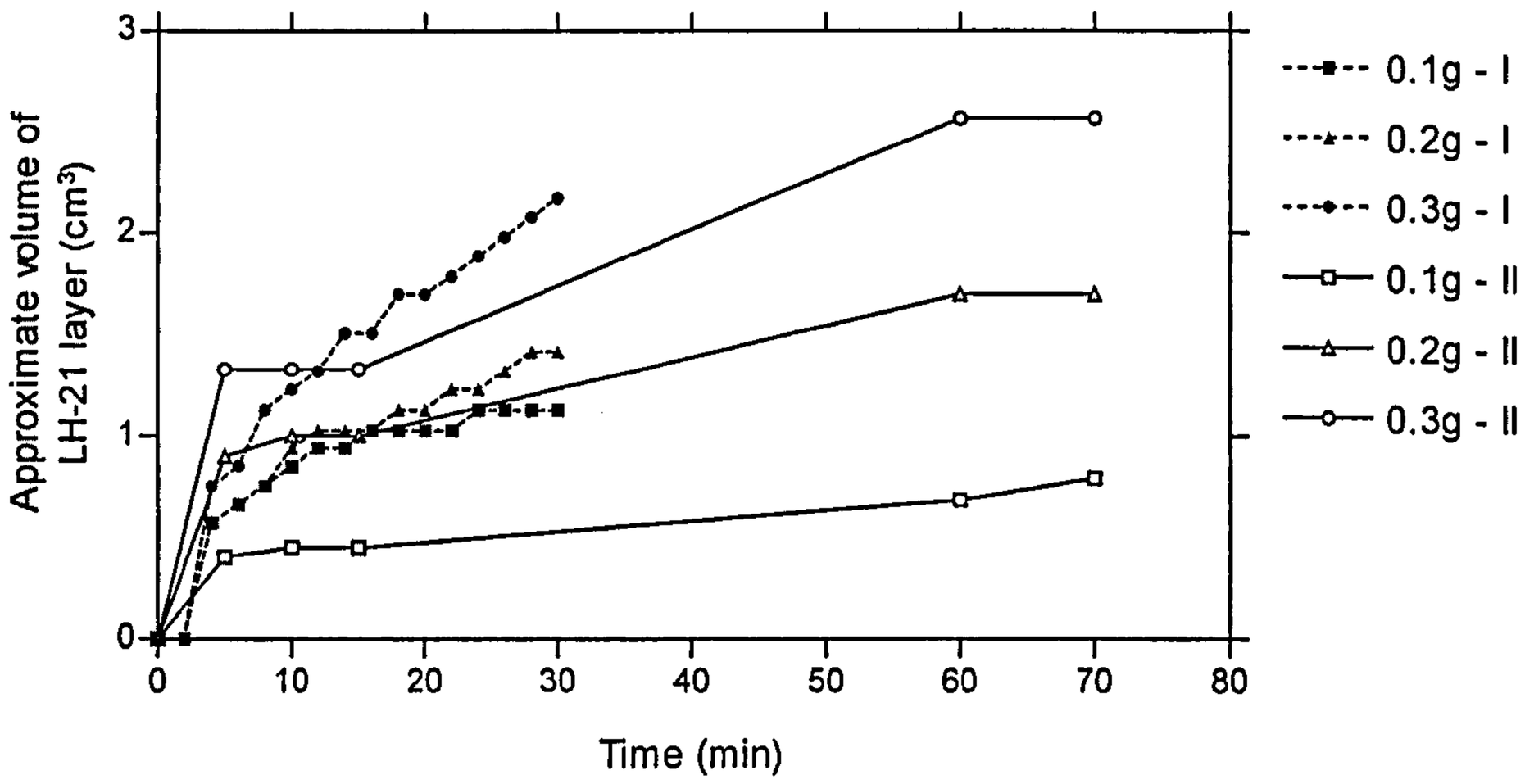

Figure 4.1: Effect of alternate sequences of addition on rate of swelling of LH-21.

Figure 4.1 illustrated the quantitative difference between the results obtained for the different methods of addition. The heights of the swollen mass were converted to volumes, assuming the internal space of the vessel was a perfect cylinder. There did not seem to be much effect exerted by the two methods, only the lowest concentration of LH-21 had a higher rate of swelling when the LH-21 / oil dispersion was added to water. This could be an effect of gravity, which was not as evident when larger amounts of LH-21 were used.

Nevertheless, these initial investigations highlighted the fact that although LH-21 was dispersed in oil, it could still migrate from the oil to the aqueous phase and swell to an appreciable extent.

4.4.1.2 Water uptake of LH-21 dispersed in corn oil

The water uptake apparatus, described in Section 2.4.2, proved to be a reliable and simple means of determining the water uptake rates of LH-21, dry or dispersed in corn oil.

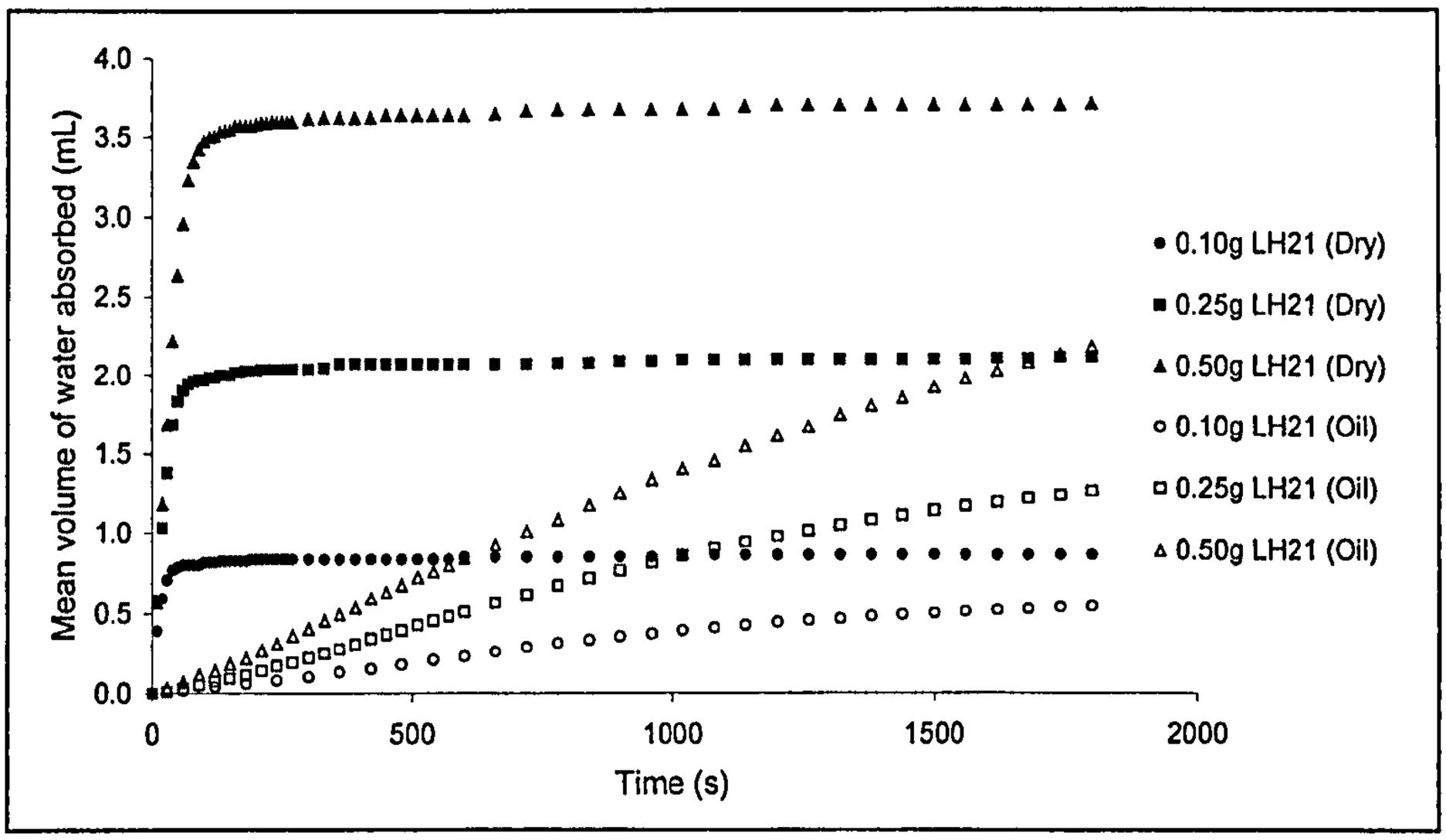

Figure 4.2: Effect of corn oil on water uptake profile of LH-21 (n=3).

Overlaying the water uptake profiles of LH-21, dry and dispersed in corn oil, clearly showed the disparity between the shapes of the curves (Figure 4.2). While dry LH-21 displayed very rapid initial water uptake rates, achieving the maximum water absorbing capacity within minutes, addition of just 5mL of corn oil drastically depressed the water uptake rate. Even after 35 minutes, all the concentrations of LH-21 had yet to be fully saturated with water.

Figure 4.3 showed that the addition of 5mL corn oil significantly decreased the mean volume of water absorbed by the varying amounts of LH-21 at 30 minutes. Although the studies on LH-21 dispersed in corn oil were not carried out to saturation, it could be postulated that corn oil also suppressed the total water uptake capacity of LH-21, especially at higher concentrations of polymer.

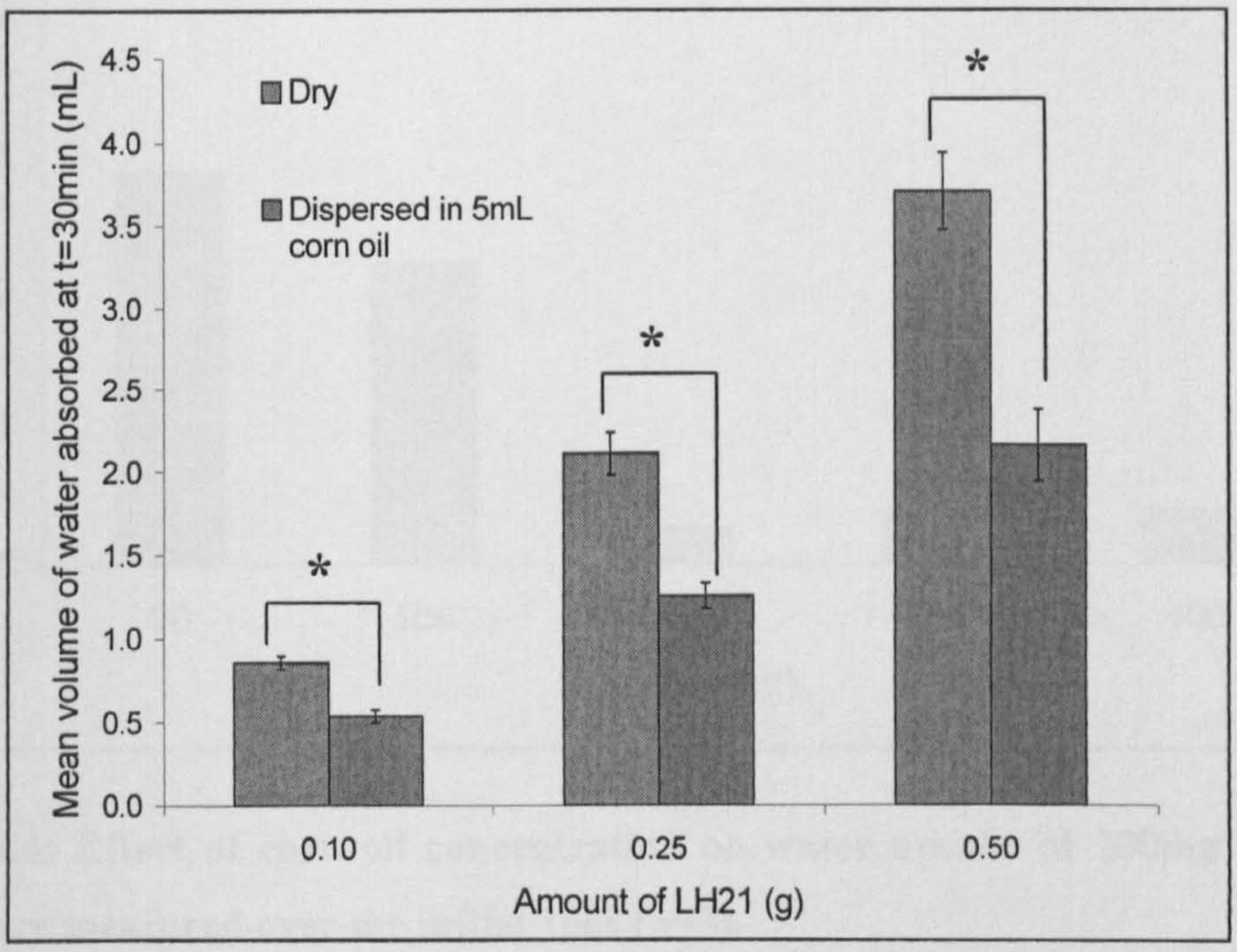

Figure 4.3: Effect of corn oil on water uptake by LH-21 at t=30min, n=3, ±S.D.

*** denotes significant difference at 5% significance level, determined from two-sample T-test.**

Figure 4.4 confirmed the concentration-dependent effect of corn oil in suppressing the rates of water uptake by LH-21. Varying amounts of corn oil was added to 200mg of LH-21 in this set of experiments. As the weight ratio of LH-21 to corn oil increased from 1:4 to 1:2, the corresponding decrease in initial water uptake rate was about 23%. A drastic drop in water uptake rate was observed as the LH-21:corn oil weight ratio was equivalent to or exceeded 1:1. The rates remained roughly the same despite increasing weight ratios, indicating that there was possibly a saturation point to which corn oil could impede water uptake of LH-21.

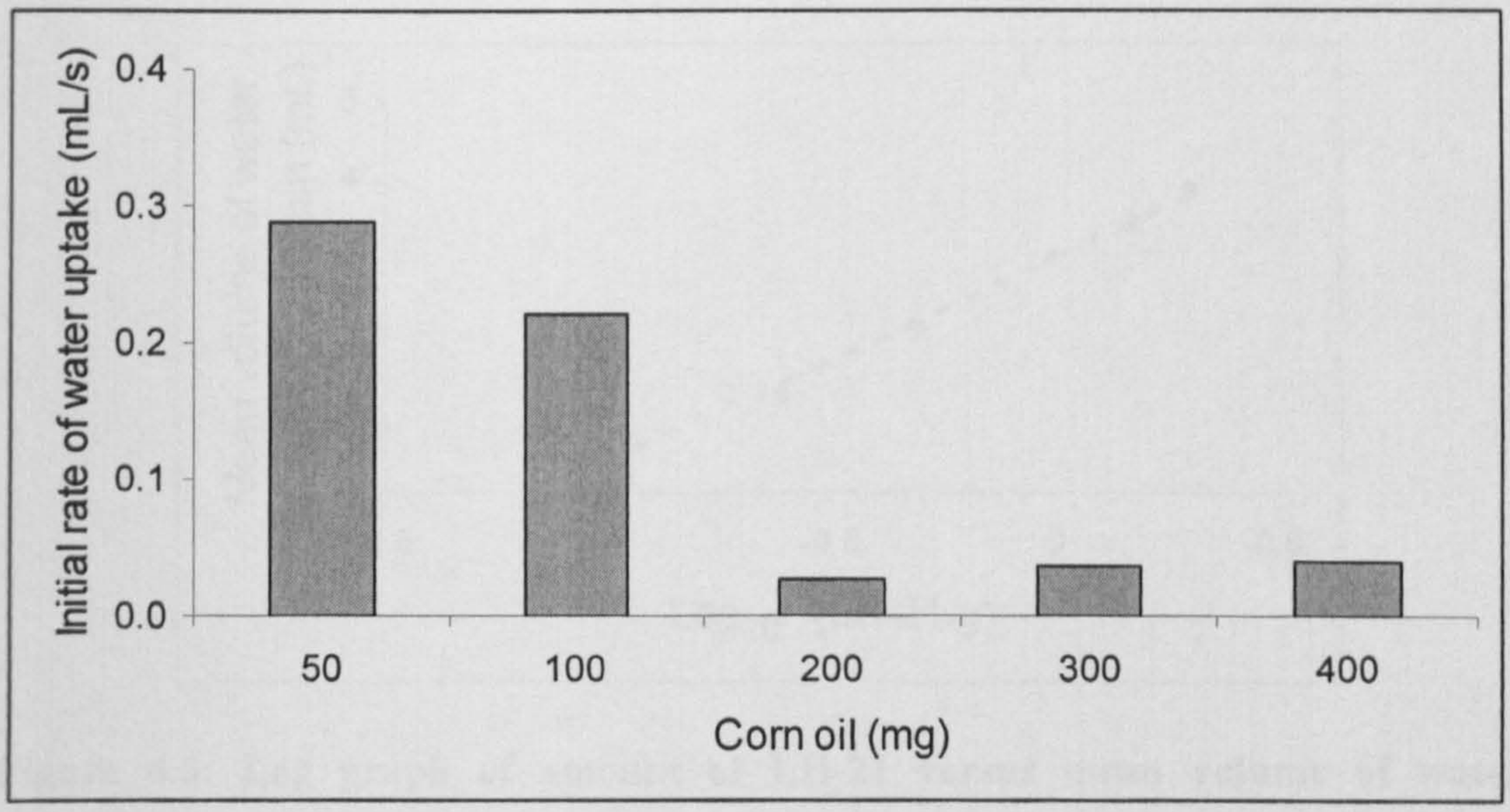

Figure 4.4: Effect of corn oil concentration on water uptake of 200mg LH-21. Rates were measured over the initial 100s (n=3).

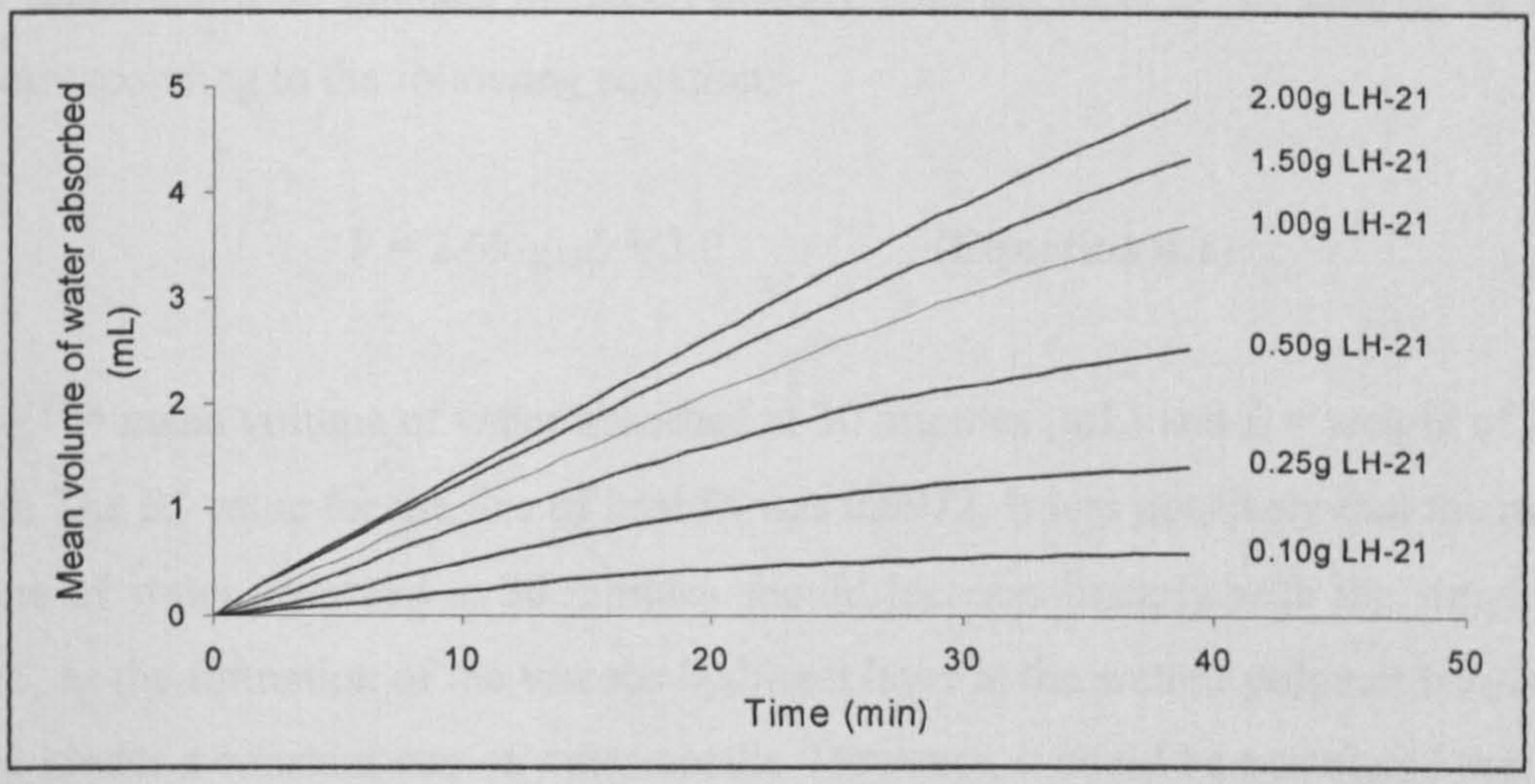

Figure 4.5: Effect of amount of LH-21 dispersed in 5mL corn oil on water uptake curves (n=3).

Despite the inhibitory effect of corn oil on the water uptake of LH-21, Figure 4.5 showed that increasing concentrations of LH-21 still resulted in increasing water uptake rates. Hence the water uptake capacity and consequent swelling power of LH-21 was not totally diminished by the addition of corn oil. In fact, control of both water uptake and swelling could be controlled by careful manipulation of LH-21 / corn oil concentrations.

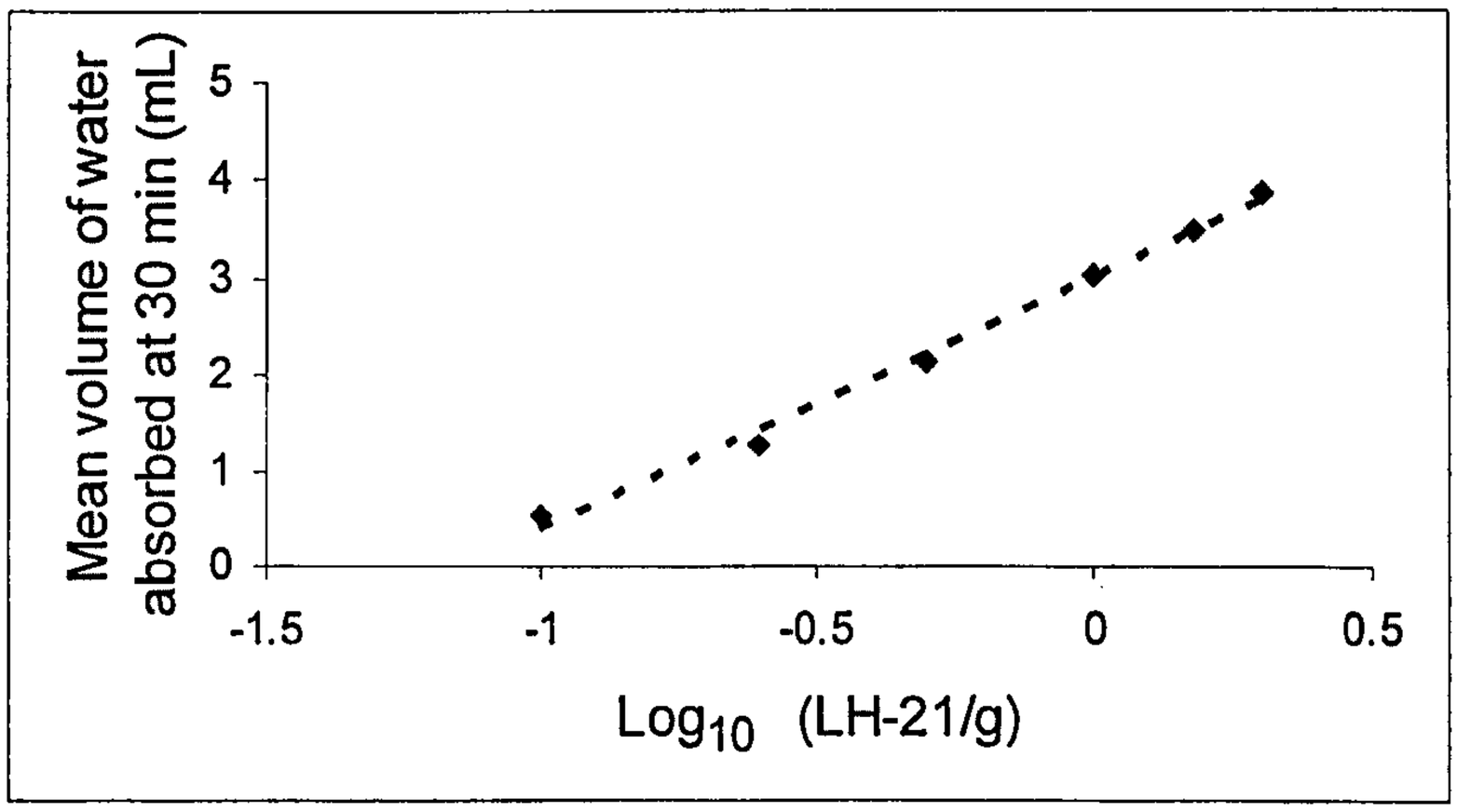

Figure 4.6: Log graph of amount of LH-21 versus mean volume of water absorbed at 30 min.

From linear regression analysis (Figure 4.6), it was found that the mean volume of water absorbed at 30 minutes increased linearly with the $\log_{10}$ of the amount of LH-21; corresponding to the following equation:

$$V = 2.6\log_{10}L + 3.0 \qquad \textbf{(Equation 4.1)}$$

where V = mean volume of water absorbed at 30 minutes (mL) and L = weight of LH-21 (g). The R^2 value for the line of best fit was 0.9972. It was not likely that the mean volume of water absorbed at 30 minutes should increase linearly with the weight of LH-21, as the formation of the viscous hydrogel layer at the water / polymer boundary would hinder a constant rate of water uptake. However, it could be postulated that the maximum volume of water absorbed by the polymer would be directly proportional to the concentration of LH-21, as observed with the dry polymer (Figure 3.12).

The detrimental effect the formation of the viscous hydrogel layer had on water uptake rates was again evidenced in Figure 4.7, which compares the initial rate of water uptake to the water absorbed per gram of LH-21 at 30 minutes.

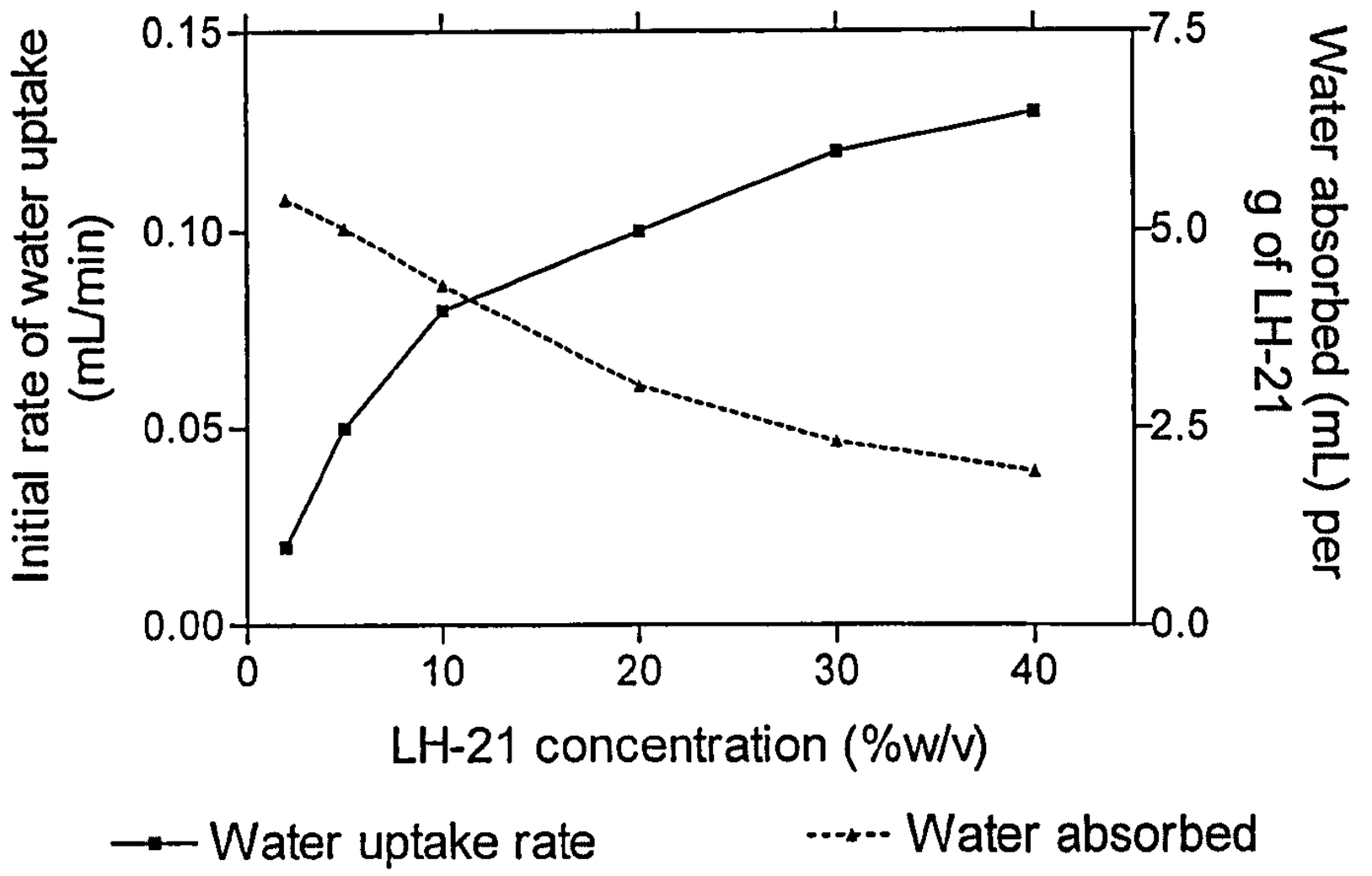

Figure 4.7: Influence of LH-21 concentration on water uptake rate* and water absorbed per g of LH-21 (n=3). * Measured over initial 20 minutes; ** At 30 minutes.**

Despite increasing rates of water uptake, indicating that the water sorption potential of the dispersion increased with higher concentrations of LH-21, the resultant volume of water absorbed per gram of LH-21 at 30 minutes tended to decrease. This could have been due to settling of the polymer at the base of the sample holder, giving rise to a high initial water uptake rate due to capillary effects. As the polymer hydrated, the growing hydrogel layer hindered further rapid water uptake so although the volume of water absorbed at 30 minutes increased as LH-21 concentration increased (Figure 4.3), the normalised ratio of volume of water absorbed per gram of LH-21 decreased (Figure 4.7).

4.4.1.3 Swelling force of LH-21 dispersed in corn oil

The force measurement apparatus described in Section 2.4.4 was used to quantify the force generated by dispersions of LH-21 in corn oil.

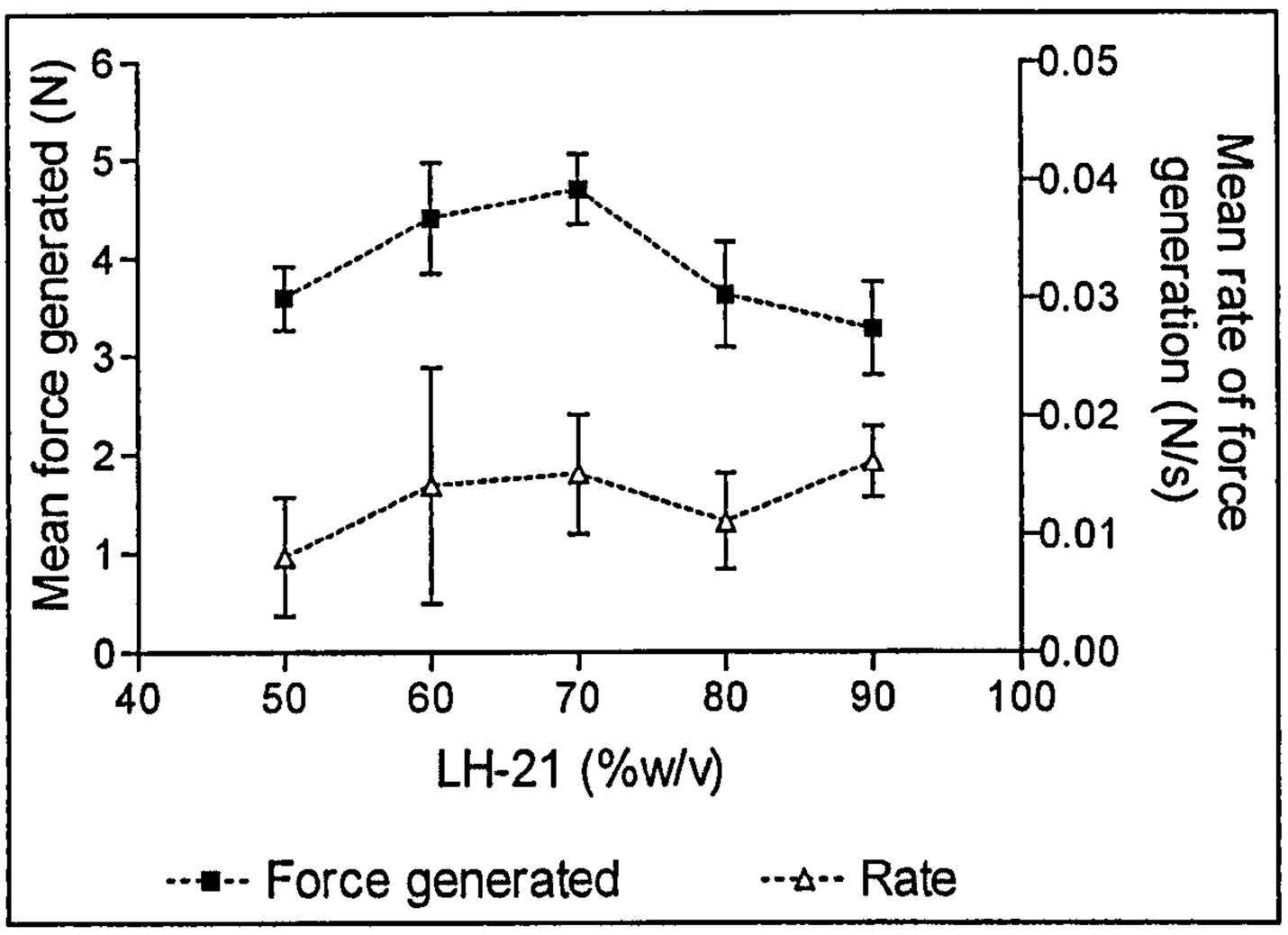

Figure 4.8: Mean force generated and mean rate of force generation of 50-90%(w/v) LH-21 in corn oil (n=3, ±S.D.).

Mixtures of LH-21 in corn oil with concentrations of polymer less than 50%(w/v) were more liquid-like in consistency, hence difficult to fill into the sample holder without leakage through the filter paper and wire mesh. Therefore, it was not possible to perform force generation studies on these samples. More granular mixtures were obtained with the higher concentrations of LH-21 and these could be filled into the sample holder.

There was not a clear trend as to the effect of LH-21 concentration on the mean force generated (Figure 4.8). The maximum force generated was observed with 70%(w/v) LH-21 and the lowest with 90%(w/v). Generally there was an increase in the mean rate of force generation as LH-21 concentration increased, indicating the greater water-absorbing capacity of larger amounts of the hydrophilic polymer.

However, these results may be artefacts of the apparatus design. It was impossible to fit the probe flush with the sample holder as effects of friction may impede the free movement of the probe. Hence the swelling of the oily mixture may have preferentially occurred through the slight gap that existed i.e. the path of least resistance. This may have resulted in the force generated not impacting on the probe

and was therefore not recorded by the Texture Analyser. Admittedly there are limitations to using this force measurement apparatus with samples that are not solid.

4.4.1.4 Imaging

The following images were obtained from light microscopy and captured on a 35mm film camera as detailed in Section 2.5.1.1.

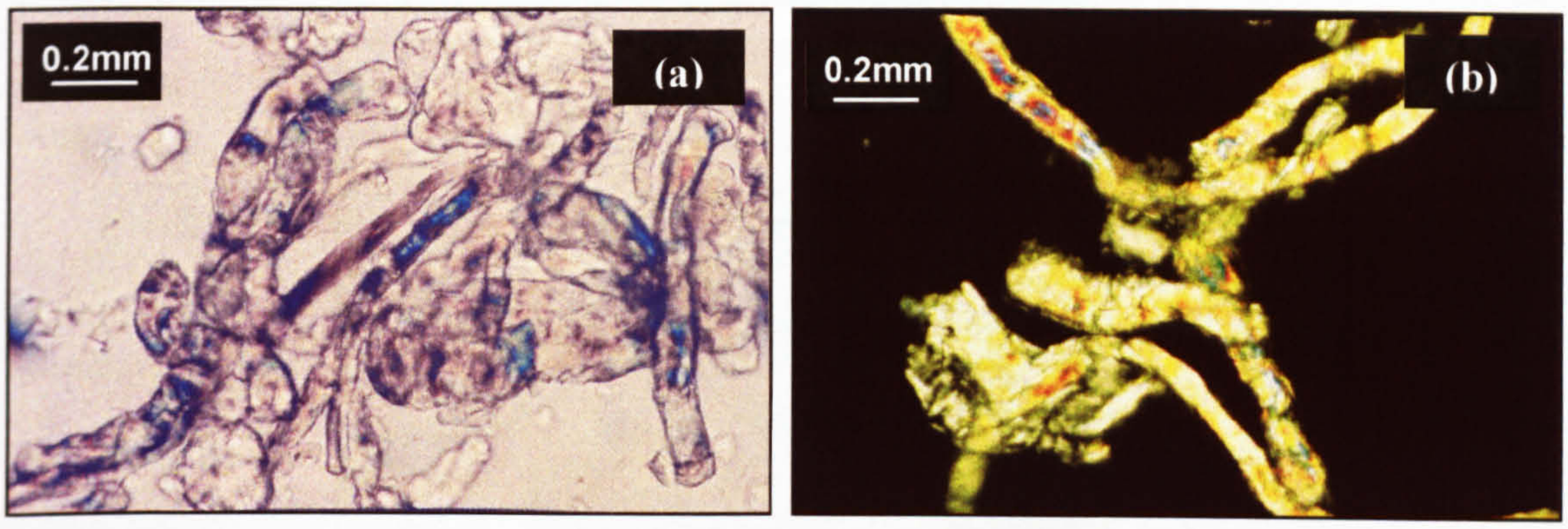

Figure 4.9: Dispersions of 5%(w/v) LH-21 in corn oil (X400), imaged under (a) unpolarised; and (b) polarised light.

These images of LH-21 dispersed in corn oil (Figure 4.9) showed the presence of the fibrous particles, but the more granule-like particles were not visible; rather they seemed to have already swollen and given rise to the mass-like hydrated particles seen in Figure 3.9, which was of hydrated LH-21. This indication that the water content of corn oil was sufficient to pre-swell LH-21 prior to hydration in an aqueous environment was investigated and discussed later in Section 4.4.1.5.

Regions of colour were visible on the fibrous particles, similar to the dry polymer, inferring that a certain degree of crystallinity was possessed by LH-21, even when dispersed in corn oil (Figure 4.9b).

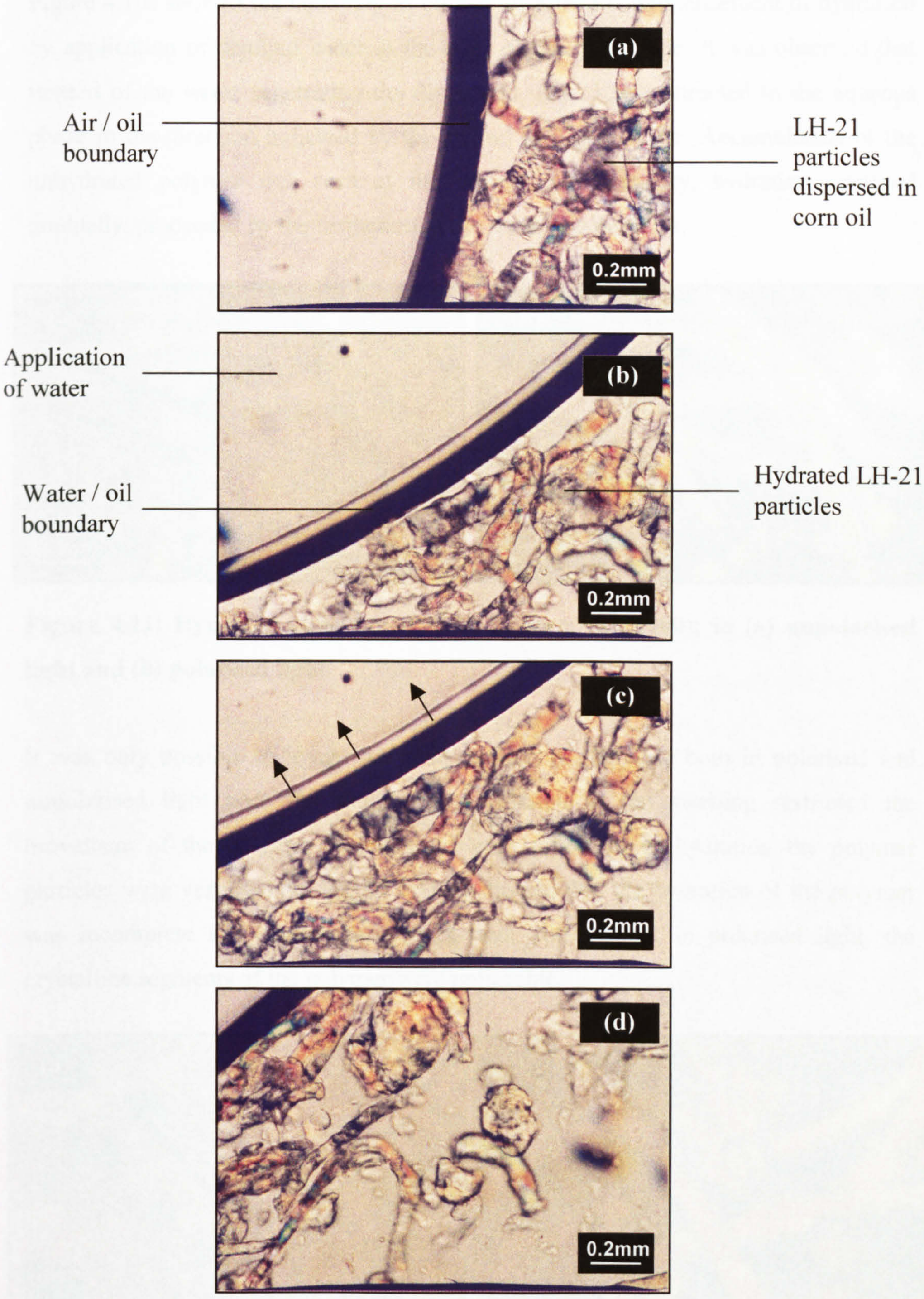

Figure 4.10: 5%(w/v) LH-21 dispersion in corn oil, (X400), imaged under unpolarised light. Chronological hydration from b-d. Time between images = 10s. Arrows in (c) show direction of oil/water boundary movement.

Figure 4.10a showed the boundary of oil and air prior to commencement of hydration by application of distilled water at the edge of the glass slide. It was observed that instead of the water penetrating the dispersion, LH-21 was attracted to the aqueous phase in the direction indicated by the arrows in Figure 4.10c. Accumulation of the unhydrated polymer was seen at the water / oil boundary, hydration occurred gradually, proceeded by the formation of the mass-like particles.

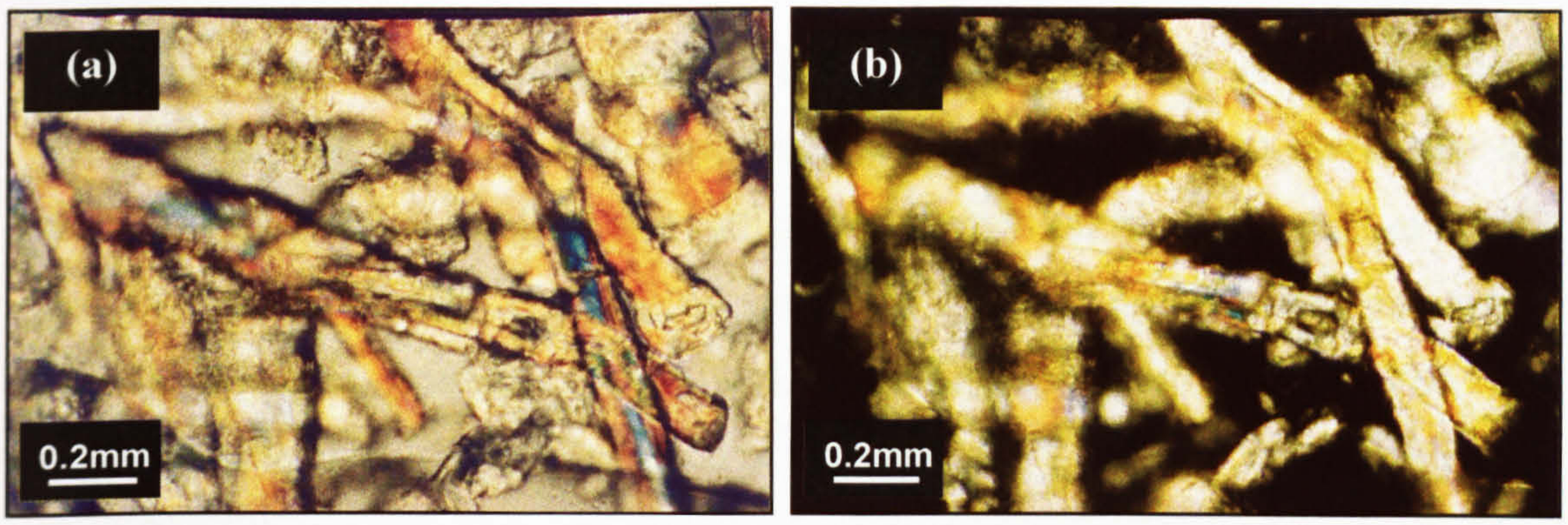

Figure 4.11: Hydrated 20%(w/v) LH-21 in corn oil (X400); in (a) unpolarised light and (b) polarised light.

It was only possible to image the same portion of the slide both in polarised and unpolarised light once the sample was hydrated as the swelling restricted the movement of the polymer fibres in the corn oil. Prior to hydration the polymer particles were very mobile. Figure 4.11(a) showed that the hydration of the polymer was incomplete and some intact fibres were still visible. In polarised light, the crystalline segments of the polymer were noticeable.

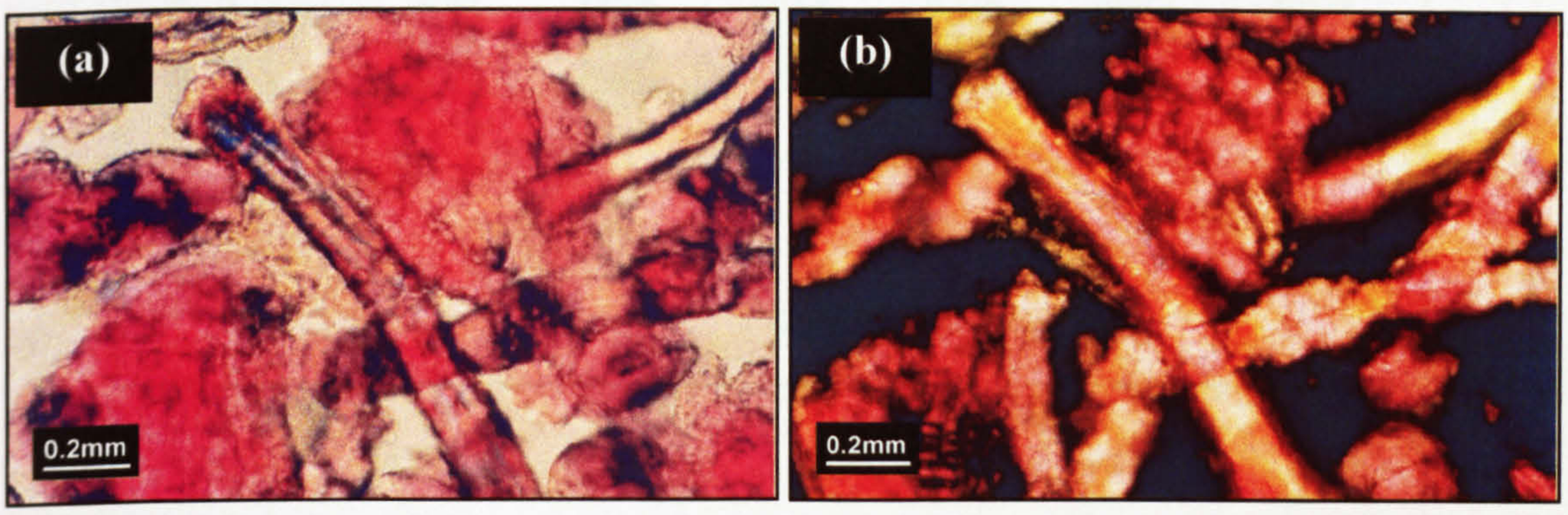

Figure 4.12: 20%(w/v) LH-21 in corn oil hydrated with aqueous red dye (X400); in (a) unpolarised light and (b) polarised light.

Addition of water-soluble dye, cochineal food colouring, to the water used for hydration, in Figure 4.12(a) and (b), revealed localisation of dye within the swollen particles. This indicated that it was uptake of water that caused swelling of LH-21, even when dispersed in corn oil.

4.4.1.5 Water content of corn oil

From the photomicrographs obtained by light microscopy, it was evident that there was pre-hydration of LH-21 upon dispersion in corn oil. In order to investigate the possibility that this pre-swelling was sufficient to depress the rate and extent of LH-21 swelling, determination of corn oil moisture content was carried out using thermogravimetric analysis (TGA) and dynamic vapour sorption (DVS), the methodologies of which were described in Sections 2.5.2.1 and 2.5.4 respectively.

Stock corn oil obtained direct from the supplier was compared to dehydrated corn oil and corn oil saturated with 10, 25, 50 and 80%(v/v) distilled water, annotated as A, B, C and D. All these samples were prepared using the methods in Section 2.5.2.1.

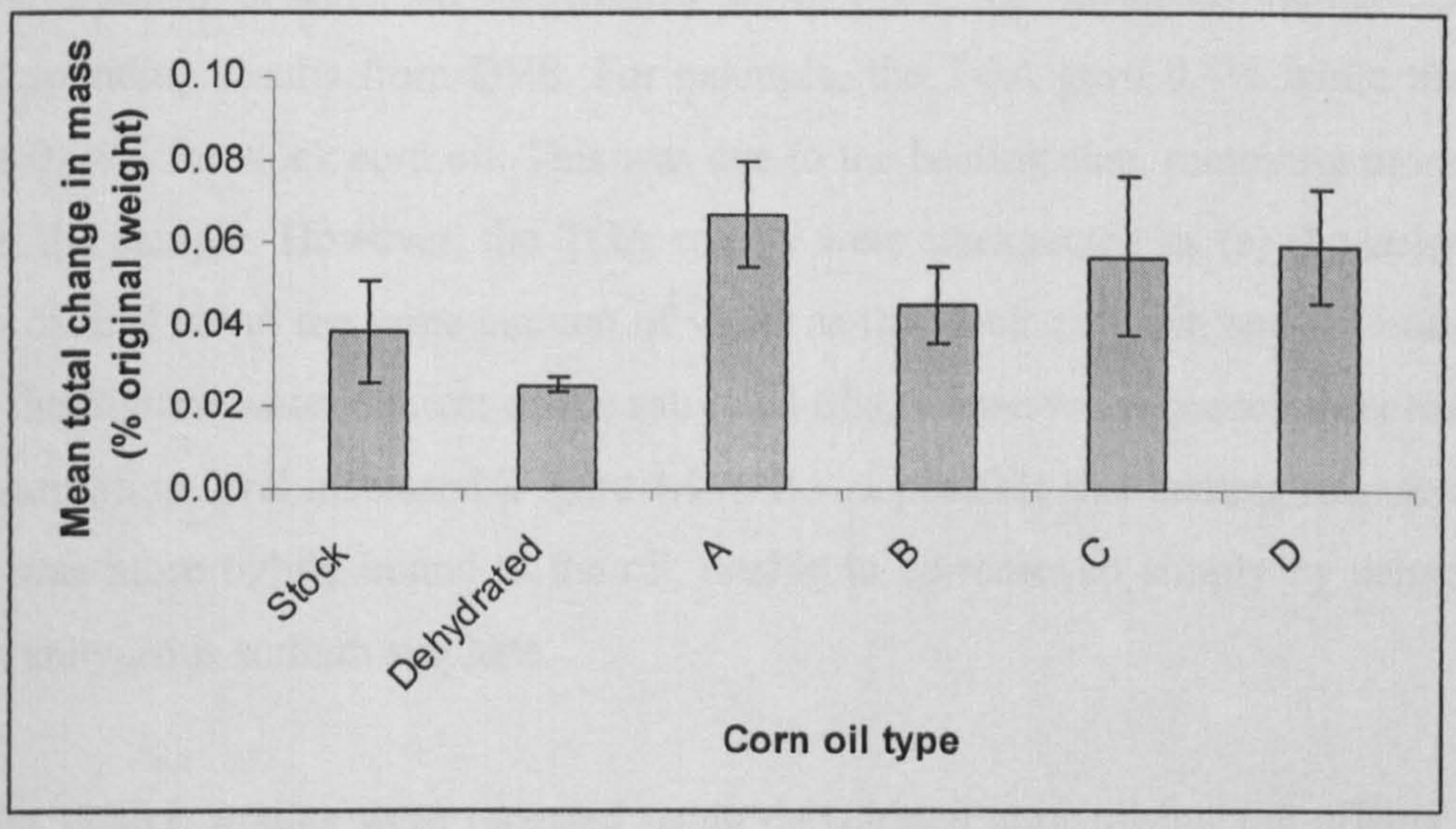

Figure 4.13: Moisture content of corn oils derived from DVS (n=3, ± S.D.)

The DVS program used was that of drying only, allowing the sample to lose water gradually as the relative humidity was fixed at 0%. It was assumed that dehydration

contributed to the entire weight loss of the sample. From Figure 4.13, it was deduced that the content of water in the dehydrated corn oil was less than that of the stock corn oil. The addition of water, at the minimum concentration of 10%(v/v), seemed to saturate the corn oil fully, as seen from the fact that corn oil A, B, C and D had similar water contents.

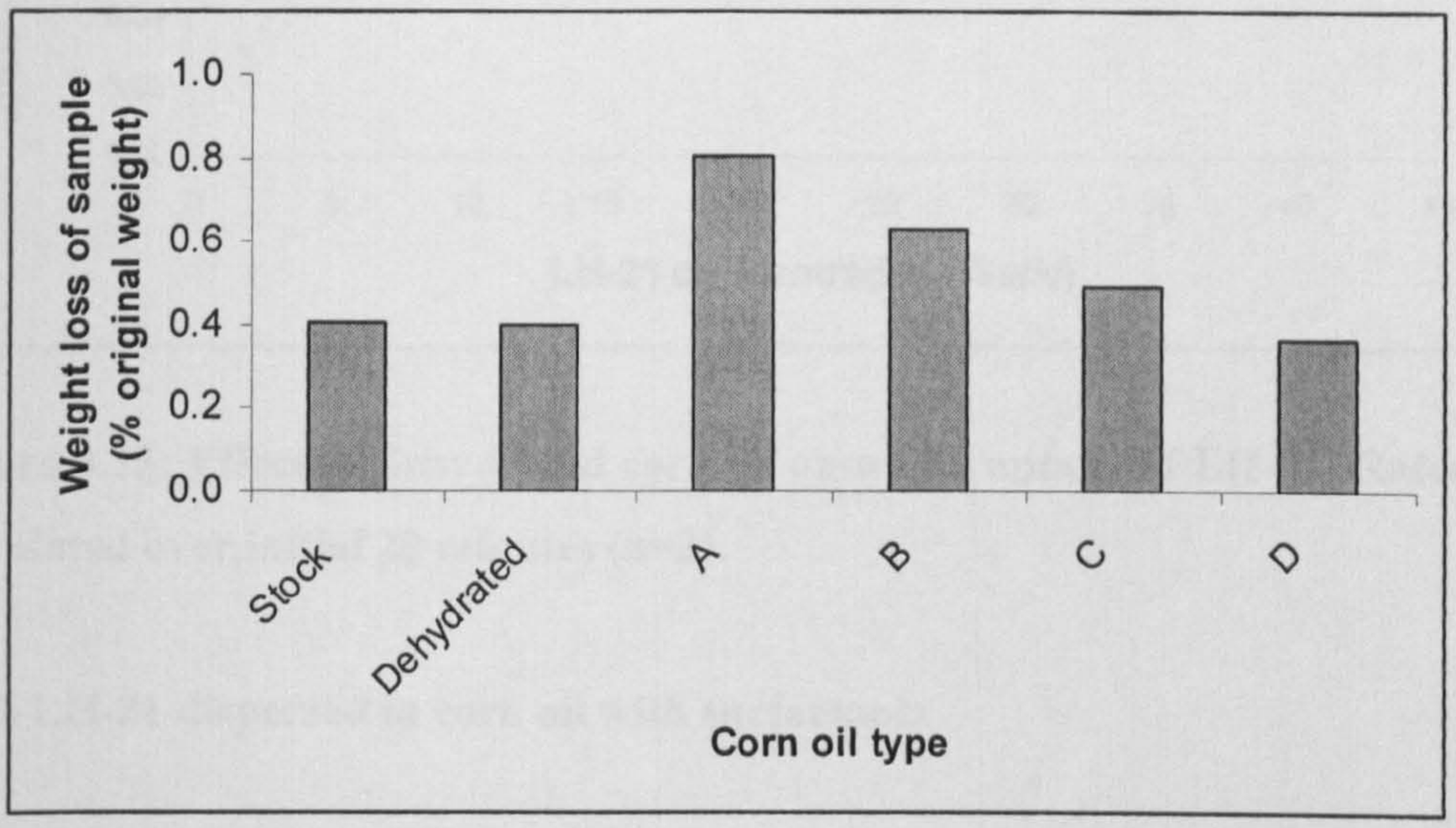

Figure 4.14: Moisture content of corn oils derived from TGA (1<n<3).

Water content of corn oil determined from TGA was generally higher than the corresponding results from DVS. For example, the TGA gave 0.4% while the DVS gave 0.04% for stock corn oil. This was due to the heating step, removing more water from the sample. However, the TGA results were unexpected as (a) the dehydrated corn oil had about the same amount of water as the stock corn oil; and (b) corn oil A had the highest water content of the saturated oils, whose water contents decreased as the saturation level increased (Figure 4.14). It was possible that heating released water that was more tightly bound to the oil, unable to be removed simply by dehydrating with anhydrous sodium sulphate.

Water uptake studies were repeated using dehydrated corn oil but the effects of the residual water content of corn oil were not significant, as shown in Figure 4.15. Although in general, the water uptake of LH-21 dispersed in dehydrated corn oil was slightly higher than that dispersed in stock corn oil, the magnitude of increase was minimal.

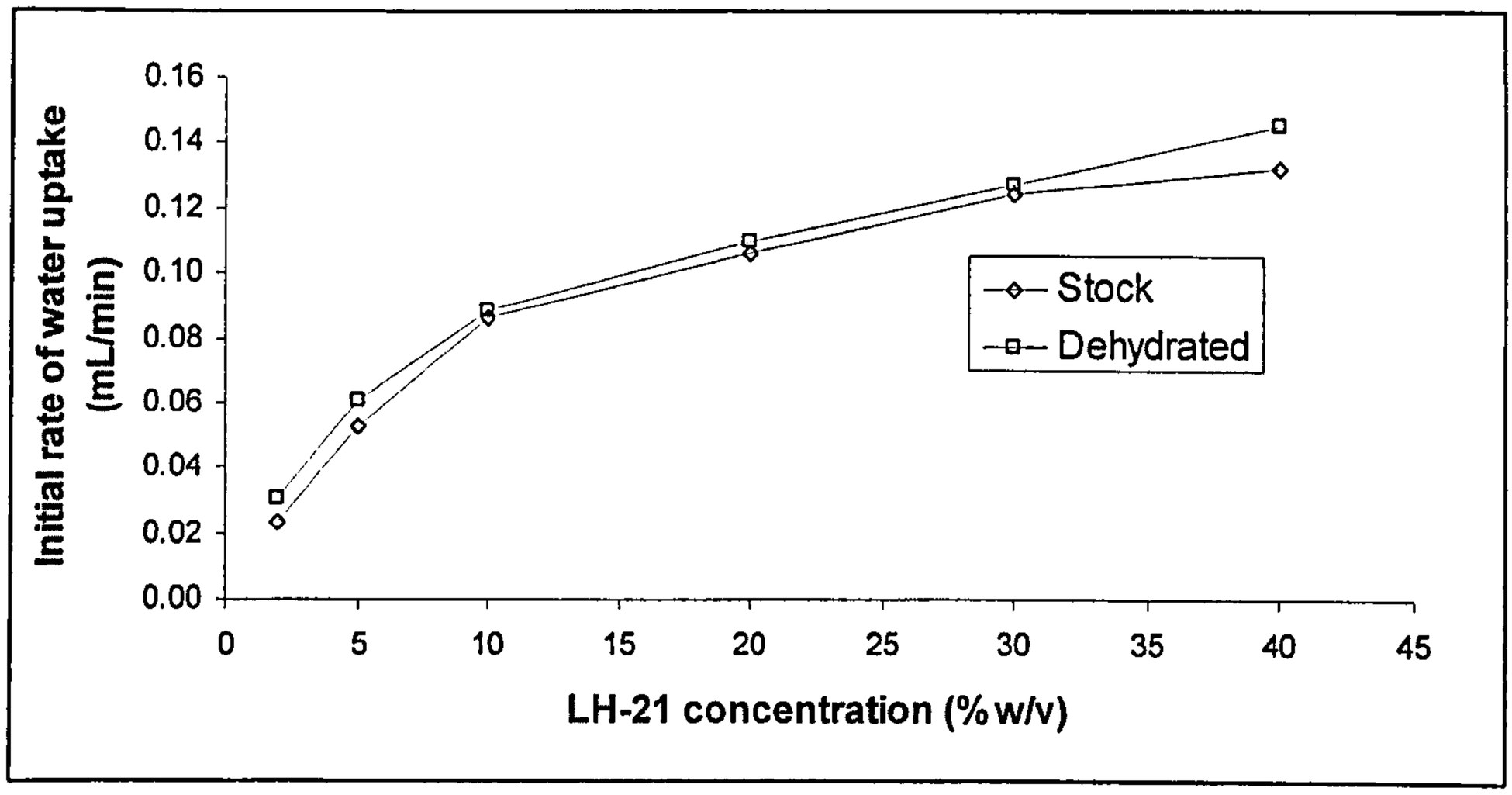

Figure 4.15: Effect of dehydrated corn oil on water uptake of LH-21. Rates were calculated over initial 20 minutes (n=3).

4.4.2 LH-21 dispersed in corn oil with surfactants

The basis of adding surfactants to the system was two-fold. Firstly, to improve the accessibility of water to the swellable polymer, thereby increasing the rate and extent of swelling and secondly, to investigate the possibility of creating a stable, self-emulsifying drug delivery system (SEDDS)-type formulation comprising of the corn oil and surfactant.

Two types of surfactant were chosen: anionic and non-ionic, which were sodium dodecyl sulphate (SDS) and Span 80 respectively. The effects of various concentrations of the surfactants were investigated on the water uptake of 0.5g LH-21 dispersed in 5mL corn oil.

4.4.2.1 Water uptake by LH-21 / corn oil dispersions with added surfactants

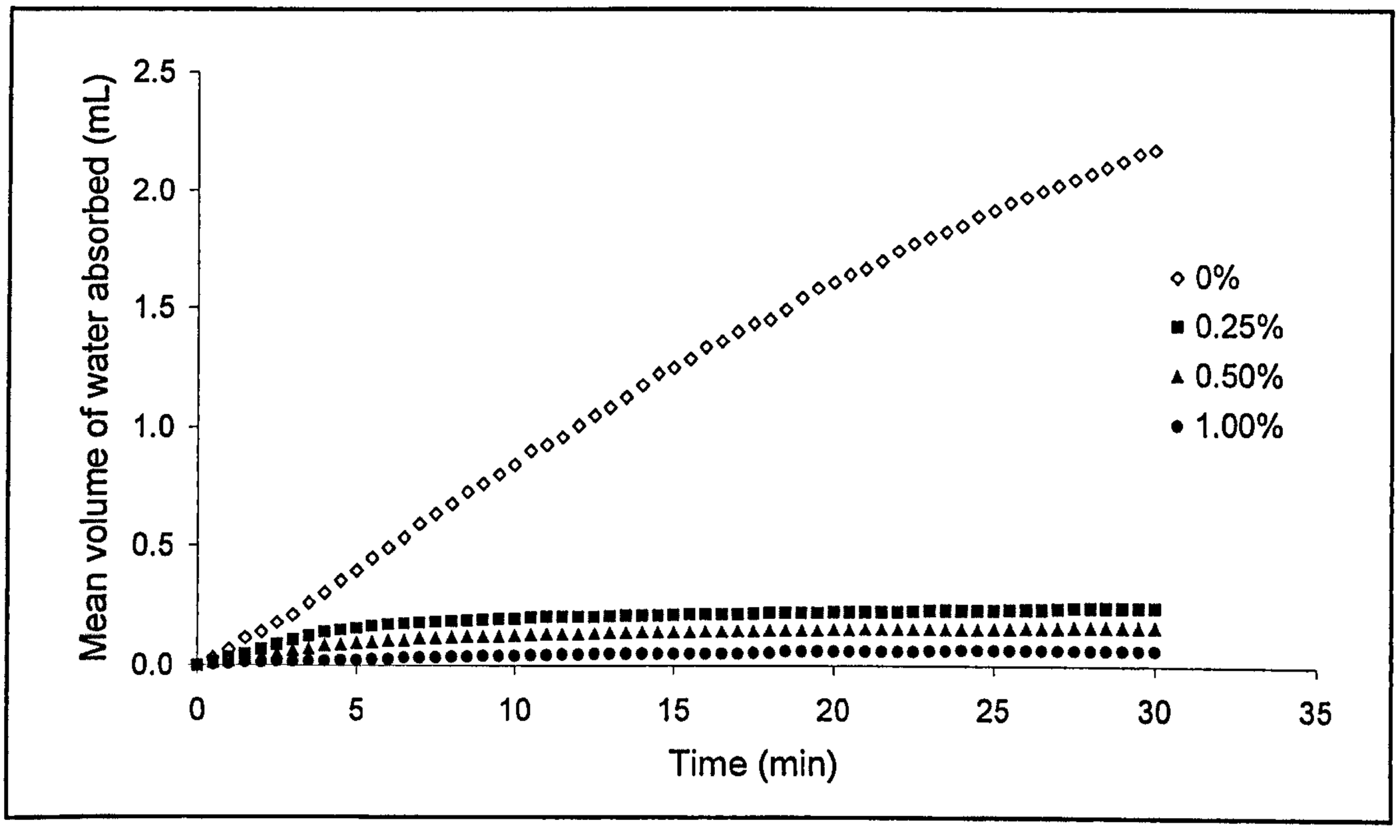

Figure 4.16: Effect of SDS on water uptake by LH-21 dispersed in corn oil (n=3).

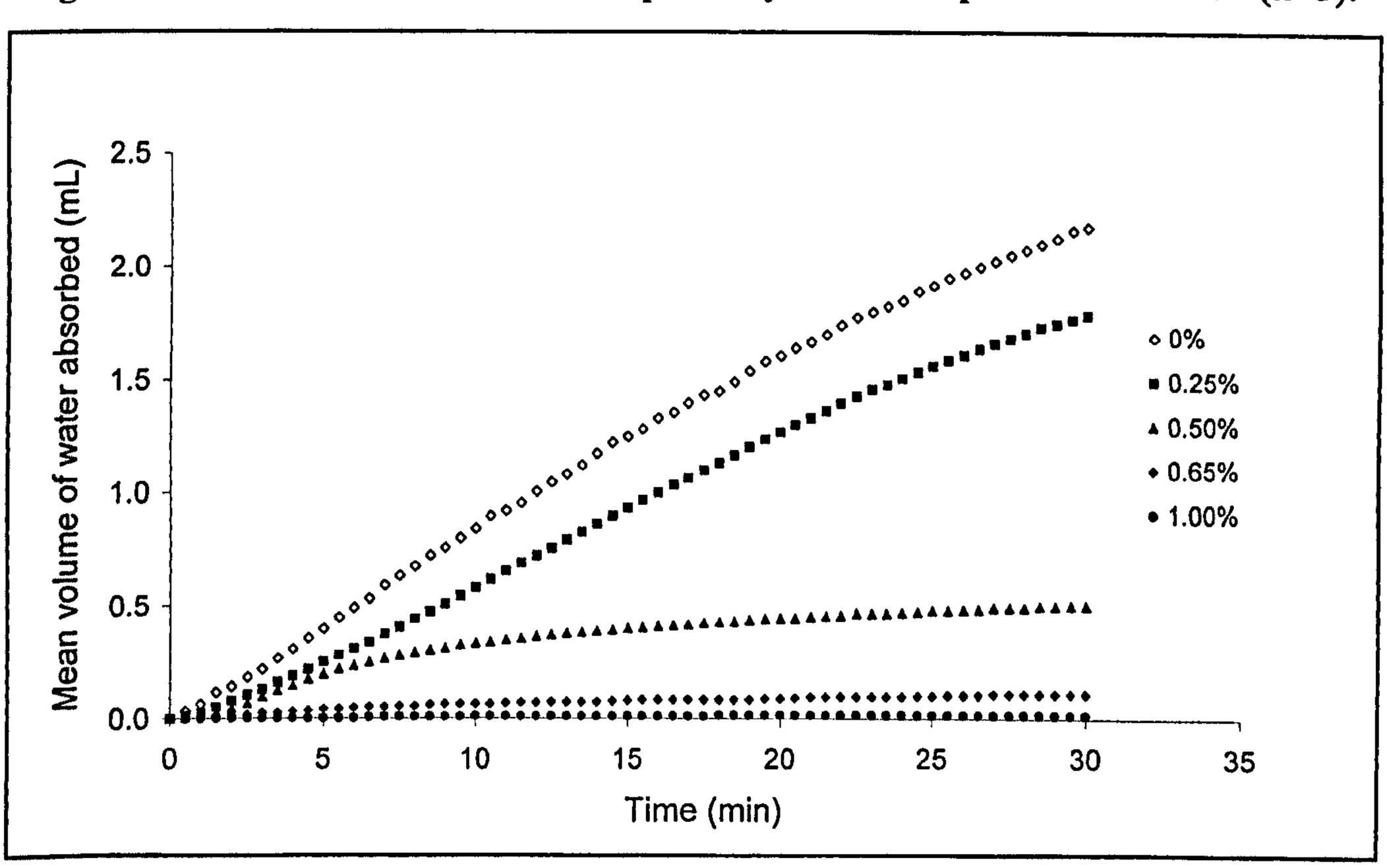

Figure 4.17: Effect of Span 80 on water uptake by LH-21 dispersed in corn oil (n=3).

Figures 4.16 and 4.17 displayed the unexpected depressive effect the surfactants had on the water uptake of LH-21. This effect was concentration-dependent, and more pronounced in the case of SDS. It was initially presumed that the surfactants would not only stabilise the formulation, but also improve penetration of water. These results showed that it could not perform the latter function when the surfactant was mixed with LH-21 and corn oil. Alternative water uptake studies with aqueous solutions of surfactant as a source of hydration could not be undertaken because the reduced surface tension meant that a clear vertical meniscus within the graduated pipette was not achievable.

Taking into consideration the hydrophilic nature of SDS in particular, its competing for water may have hindered the optimal swelling of LH-21. In addition to that, accumulation of the surfactant at the oil-water interface could have prevented access of water to LH-21.

4.4.3 LH-21 and paracetamol dispersed in corn oil

4.4.3.1 Imaging

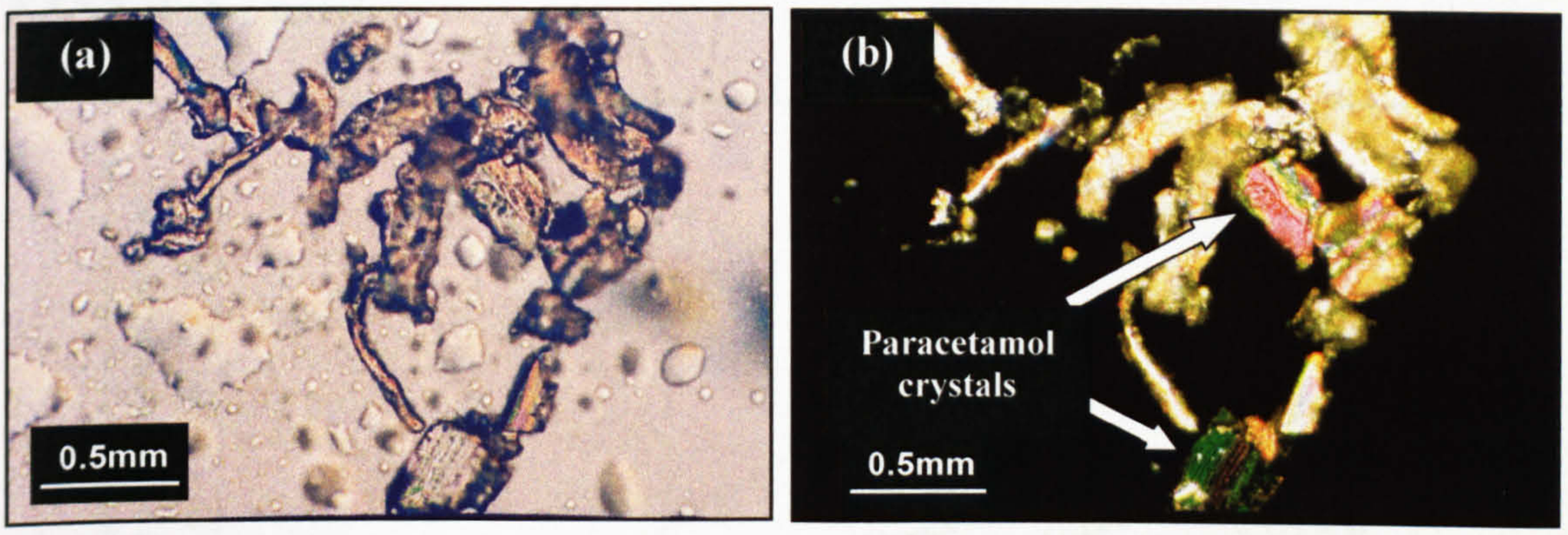

Figure 4.18: 25% corn oil: 70% LH-21: 5% paracetamol (w/w), X250, imaged under (a) unpolarised light and (b) polarised light.

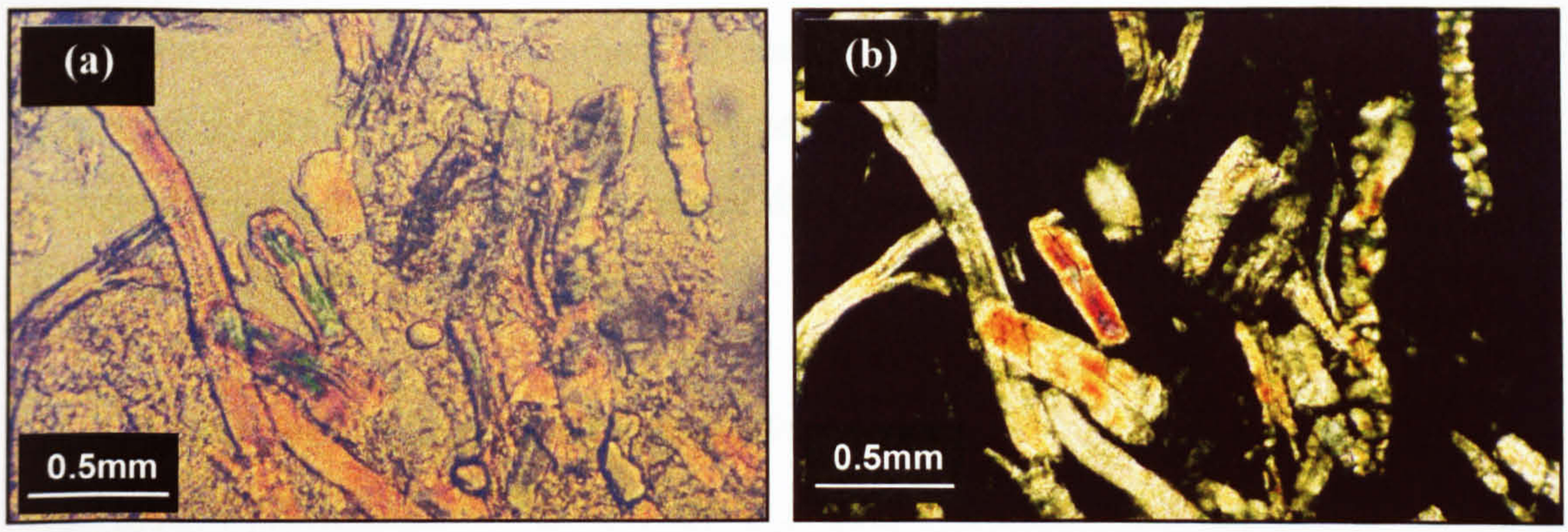

Figure 4.19: Hydrated 25% corn oil: 70% LH-21: 5% paracetamol (w/w), X250, imaged under (a) unpolarised light and (b) polarised light.

Figure 4.18(a) and (b) showed the presence of intact paracetamol crystals within the mixture of corn oil and LH-21 while post-hydration, the paracetamol crystals had totally dissolved (Figure 4.19a and b). This meant that neither corn oil nor LH-21 hindered the dissolution of the drug. Furthermore, with these formulations that contained high concentration of LH-21, the polymer that remained unhydrated was greater than that of the lower concentrations of LH-21.

4.4.3.2 Water uptake

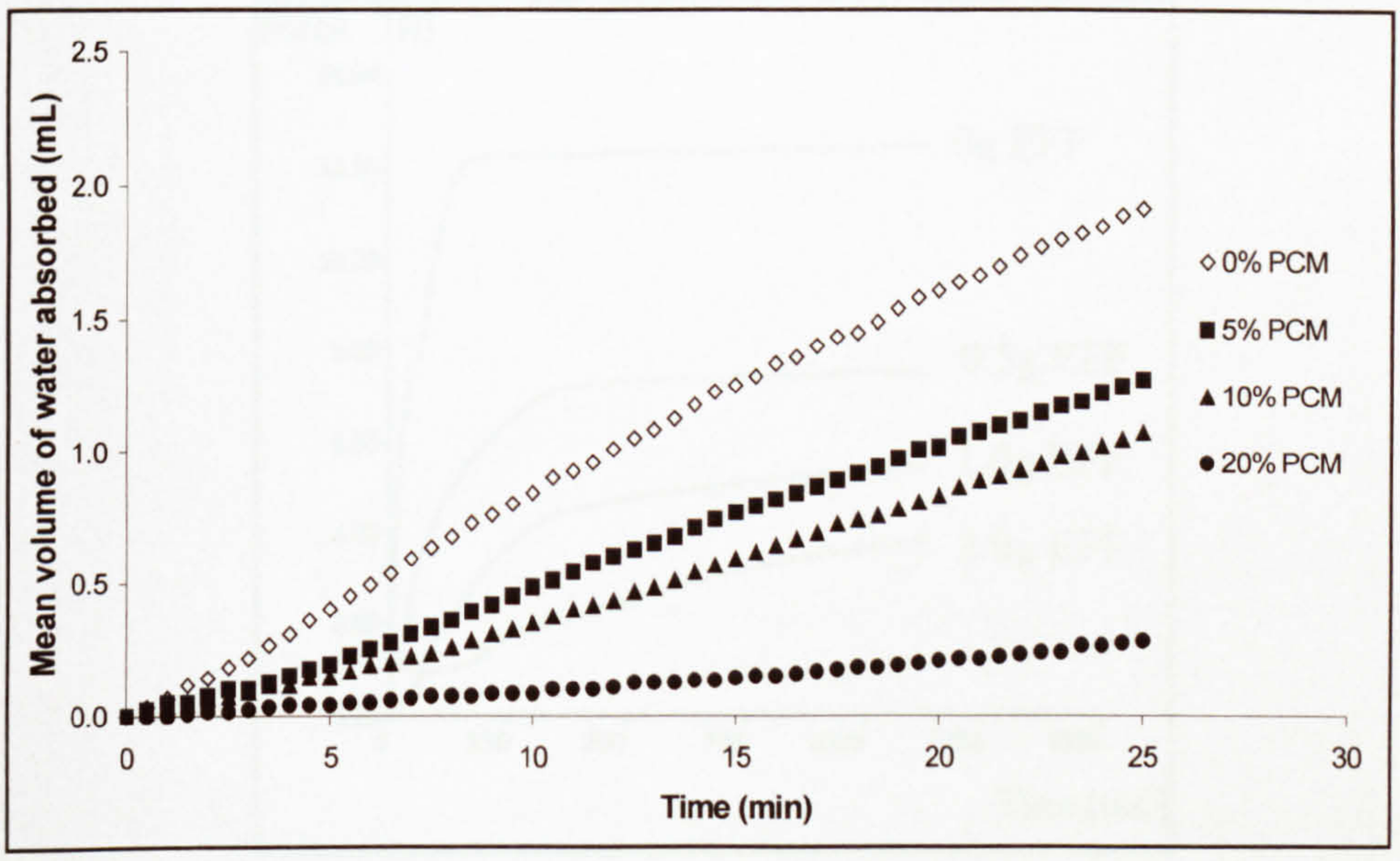

Figure 4.20: Effect of paracetamol on water uptake of 0.5g LH-21 dispersed in 5mL corn oil.

Yet another formulation component decreased both the rate and extent of swelling displayed by LH-21 in a concentration-dependent manner. The effect of paracetamol, shown in Figure 4.20, and other potential drug candidates had to be considered when formulating the final dosage form.

4.4.4 Mixture of LH-21 with effervescent material

An effervescent component was added to LH-21 in an effort to improve dislodgement of the swollen polymer from the cap of our dosage form (Variation 2). Comprising D-tartaric acid, sodium hydrogen carbonate and polyvinyl pyrrolidone, granulated with ethanol in a method described in Section 2.4.6, the resulting powder was dry blended with LH-21 and subjected to the force measurement test (Section 2.4.4).

4.4.4.1 Force generation

The studies were carried out to determine the effect of effervescent material on the swelling of LH-21. Circular discs of solution-cast EC films [3%(w/v) EC, 30%(w/w of EC) triacetin] were placed at the base of the sample holder as this was more reflective of the actual dosage form design.

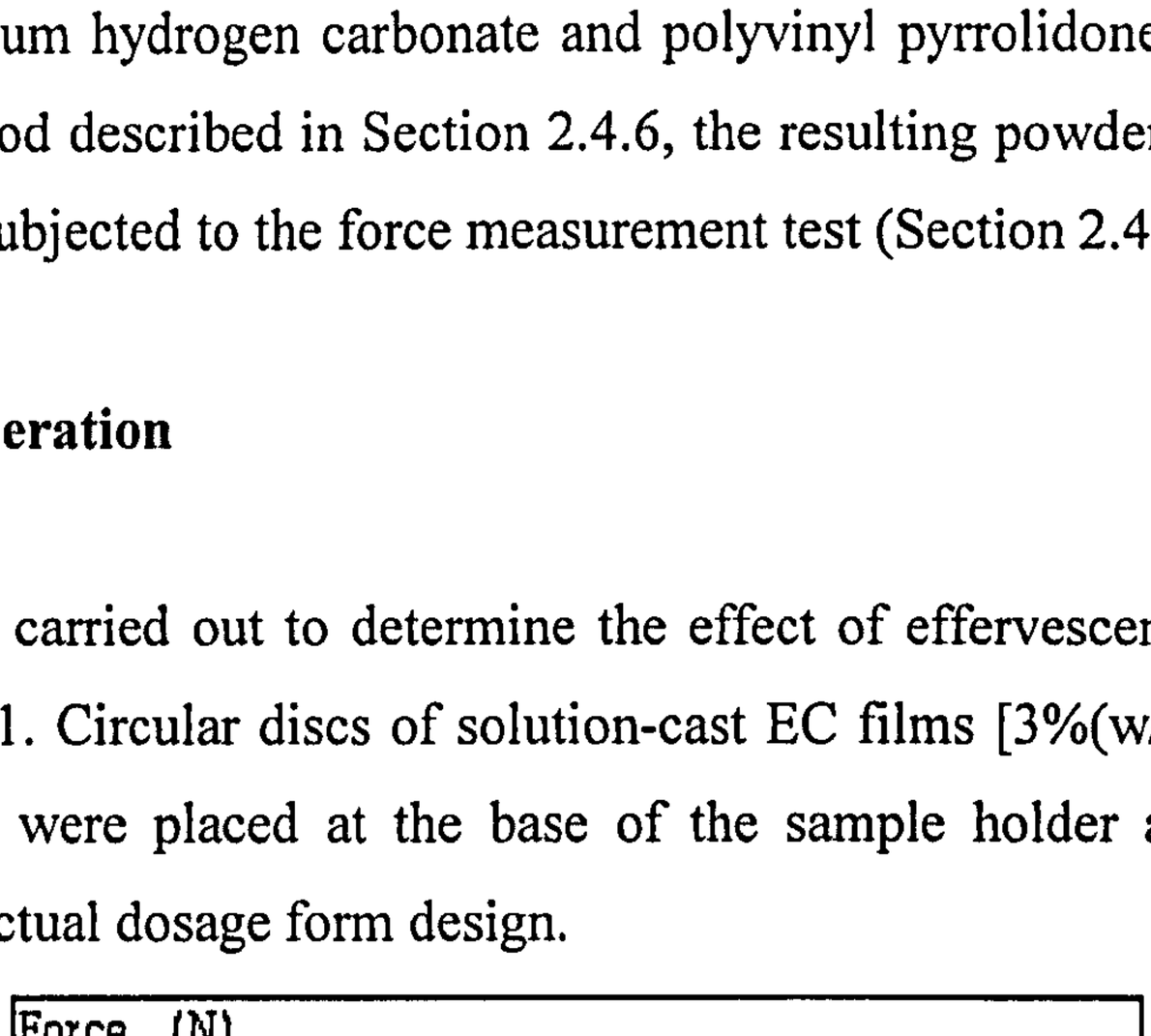

Figure 4.21: Sample force curves (n=1) derived from hydration and swelling of LH-21 with and without the addition of various amounts of effervescent material (abbreviated EFF in graph).

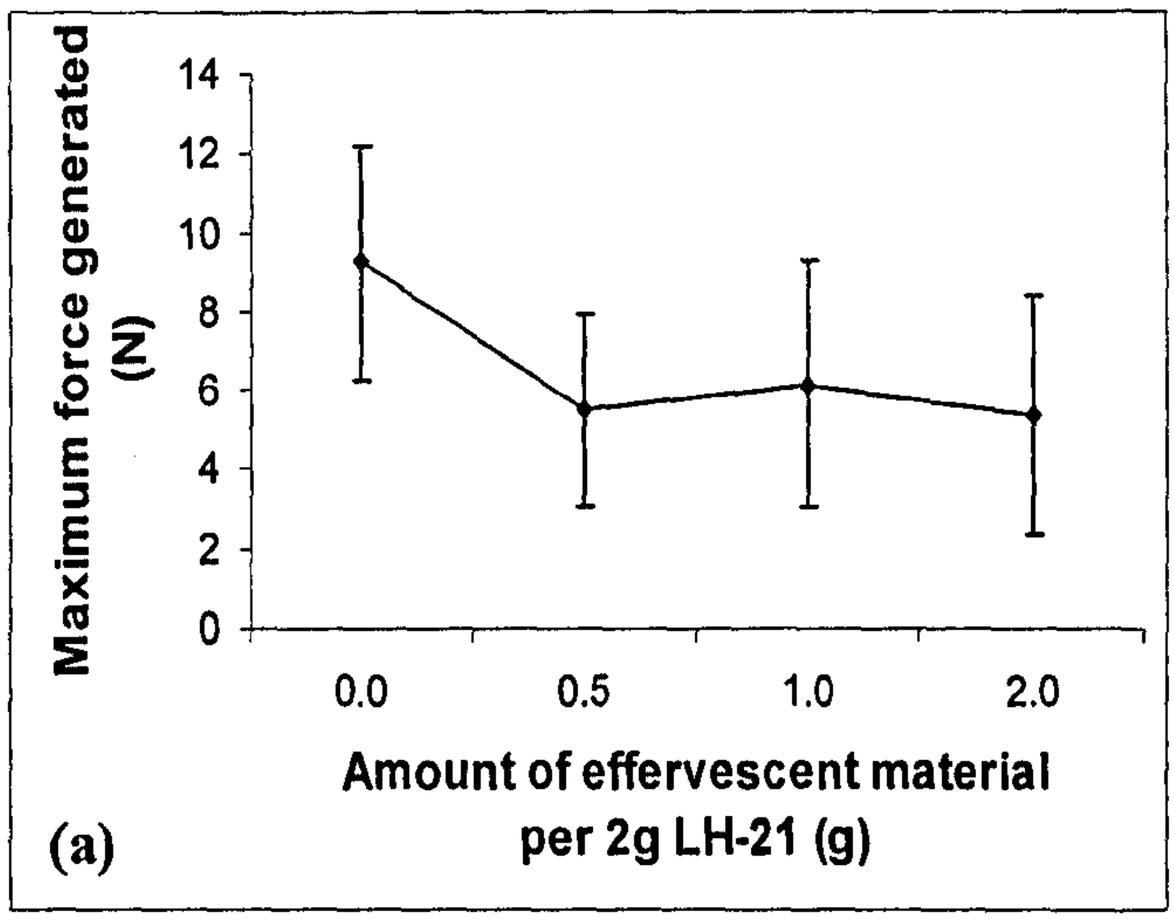

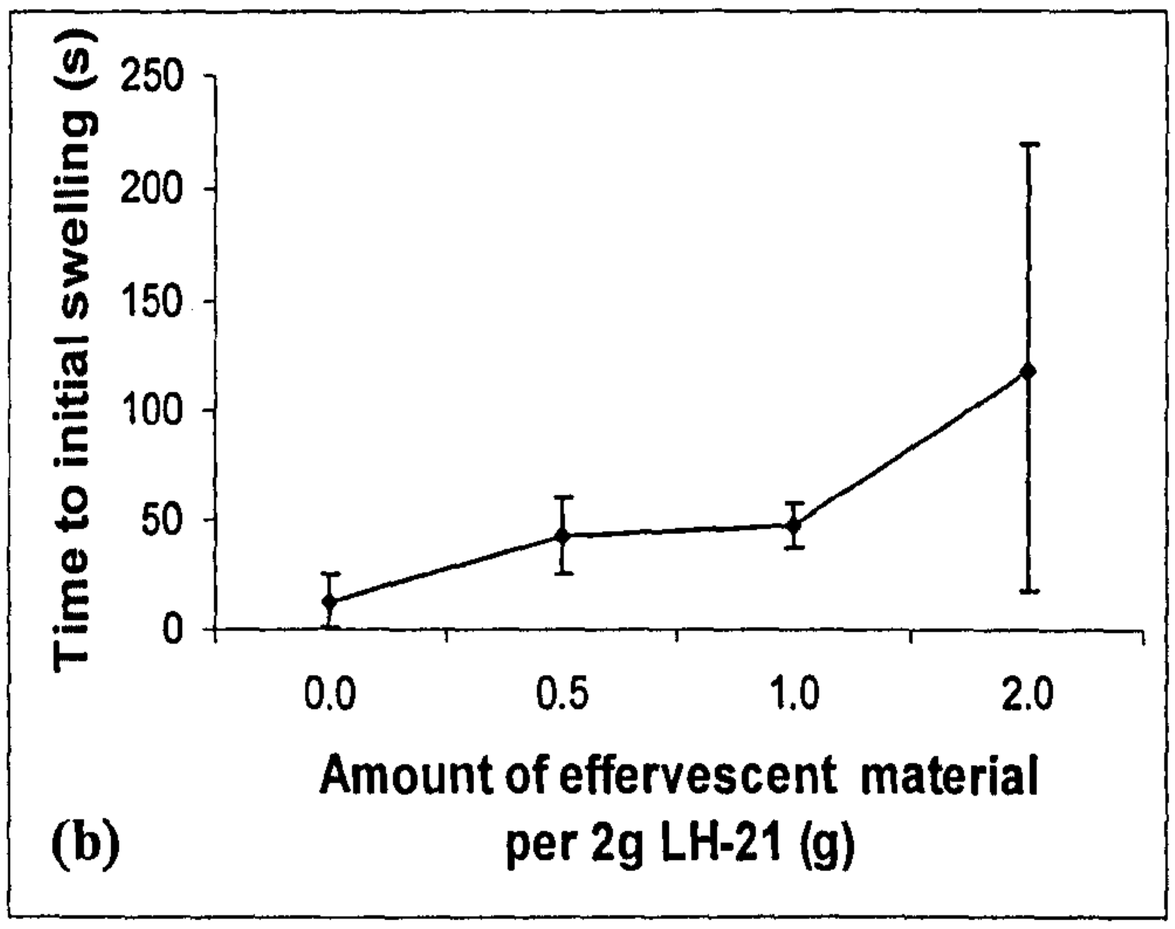

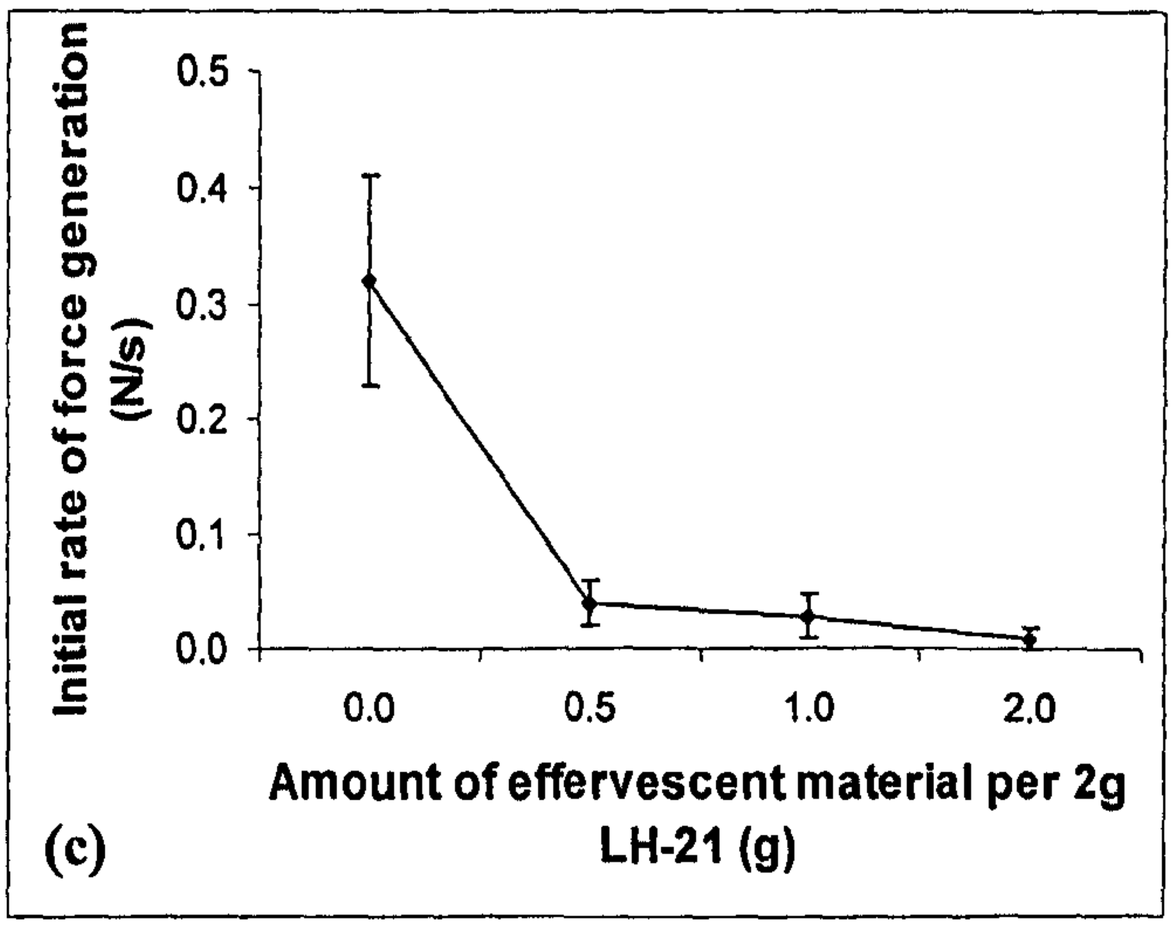

Figure 4.22: Effect of effervescent material on (a) mean maximum force generated, (b) time to initial swelling and (c) initial rate of force generation by 2g of LH-21. (n=12, ± S.D.)

One-way ANOVA (5% significance level) showed that increasing concentrations of effervescent material significantly decreased the mean maximum force generated (p=0.006) and the mean initial rate of force generated (p<0.0005) but increased the mean time to initiation of swelling (p<0.0005). These results did not necessarily mean that effervescent material was incompatible with LH-21 although they indicated that LH-21 swelling was compromised. However, it was also very likely that the contribution to force generation by gaseous expansion of the carbon dioxide produced would not have been detected by the Texture Analyser. Therefore, it was possible that upon incorporation into the dosage form, the dual sources of force generation may yet still be sufficient to rupture the brittle EC coat.

4.5 Conclusions

- All the formulation excipients added to LH-21 for possible incorporation in the dosage forms had negative effects on the polymer's swelling capacity. This was determined through simple model systems of water uptake and swelling force.

- Nevertheless these combinations might have yet been feasible for formulation due to the other properties that they conferred on the dosage form i.e.:
  a) corn oil offered improved solubilising power for hydrophobic drugs;
  b) paracetamol was a good model drug, with high water solubility for ease of detection with UV absorbance coupled to a dissolution apparatus; and
  c) effervescent material had the potential to dislodge the swollen LH-21 while adding to the forces for rupturing the EC coat of the capsule dosage form.

- It was important to determine whether the decrease in swelling was acceptable i.e. whether the force generated was still sufficient to rupture the EC coat.

- Only surfactant use was eliminated in the construction of the final dosage forms, discussed in Chapters 6 and 7, due to the overwhelming decrease in water uptake.

- Hence further approaches to designing the dosage form were contemplated with these findings in mind, appreciating the need for these excipients while minimising their inhibitory effect on LH-21 swelling. These are discussed in Chapters 6 and 7.

CHAPTER 5

CHARACTERISATION OF SOLUTION-CAST ETHYLCELLULOSE FILMS

5.1 Introduction

Ethylcellulose (EC), a water-insoluble polymer, has gained widespread use as an outer coating in various drug delivery devices. It possesses good film formability, excellent physicochemical stability and minimum toxicity (Narisawa *et al.*, 1993). EC exhibits thermoplastic behaviour and is strong and flexible in a variety of compositions (Nicholson and Merritt, 1985). Very popular as a matrix component and film former in controlled release systems, EC is arguably the most chemically stable of the cellulose derivatives, being resistant to alkali and salt while absorbing minimal amounts of water. It is available in a variety of grades which have specific utilisation in pharmaceutical formulations, which include controlled release coatings, micro-encapsulation, tablet coating, granulation and as a binder in direct compression.

5.1.1 Ethylcellulose coatings for controlled release

EC was utilised in a formulation to coat nonpareil beads containing rifampicin in an effort to produce a controlled release dosage form that would improve clinical efficacy of the drug and patient compliance. High, frequent dosing is required to maintain the high plasma concentrations necessary for tuberculosis treatment therapy. The EC film, applied with a pancoater, retarded the release of drug from the beads; the extent of retardation increasing as the thickness of the coat increased (Rao and Murthy, 2002).

Another example of EC being used as an outer coating to incorporate lag time into a drug delivery device is pressure-controlled colon delivery capsules (PCDCs) (Hu *et al.*, 2000). Caffeine powder, used as a model drug, was suspended in PEG 1000 suppository base at 50°C and subsequently hardened in 0 and 2 size capsular shapes.

Spray coating with 5%(w/v) ethanolic solution of EC produced the PCDCs detailed in Table 5.1.

Table 5.1: PCDC coating level and times to first detection of caffeine in saliva (Hu *et al.*, 2000).

Capsule size	Mean EC coat thickness (μm±S.D.)	Time to first detection of caffeine in saliva (h ±S.D.)
0	56 (1)	3.3 (0.3)
0	64 (1)	5.3 (0.3)
2	50 (1)	4.3 (0.5)
2	57 (1)	5.3 (0.3)

Table 5.1 clearly showed that increasing the level of EC coating impeded the release of drug from both sizes of PCDC. All the PCDCs displayed a colon arrival time of about 5h following oral administration as demonstrated by gastrointestinal magnetomarkergraphy. Hence from Table 5.1, the capsules with lower EC coating levels had released drug prior to arrival in the colon and were therefore inadequate for colon targeting. This implied that a minimum level of EC coating was required to avoid premature rupture of the PCDC and other colon targeting dosage forms.

EC is also used in one of the commercial preparations, Pentasa®, in which microgranules are coated with EC to ensure that no premature release of drug occurs prior to reaching the colon (Clemett and Markham, 2000). These microgranules release mesalazine in a diffusion-dependent manner.

As described above, EC can be applied via mainly two methods: aqueous-based or organic-based coating. Lin *et al.* (2001) departed from these more conventional means and attempted to directly compress micronised EC onto a tablet. The predominant consolidation mechanism for EC compacts following direct compression is plastic deformability (Lin and Lin, 1996). Fixing the weight of EC (140mg) and compaction pressure applied (300kg/cm^2 for 1 minute), decreasing the size of the EC particles prolonged the lag time of the device. For example, compression of EC powders with mean particle size of 4.0μm resulted in a lag time of almost 20 hours whereas drug

release occurred within an hour with EC powders of mean particle size 398μm. Lin and Lin (1996) determined that the major factor influencing water uptake and dissolution of the drug was porosity of the EC compact. This, in turn, was a consequence of the mean particle size of EC powder with smaller particles achieving lower porosities due to improved interparticular contact.

These are just a few of the controlled release systems designed with a coating of ethylcellulose. However, the main focus of this chapter is to investigate the physical properties of ethylcellulose films by evaluating free films. It is not uncommon to study free films rather than the actual coat applied onto the dosage form. Many workers including Hartman Kok *et al.* (2001) and Parikh *et al.* (1993) as well as those referred to in Table 5.2 employed this method, which is far simpler than examining membranes on coated pellets or tablets for example.

Generally there are two approaches to producing free films for testing: spray-coating and solution-casting. The former mimics the authentic sprayed membrane of a dosage form to a greater extent compared to the latter. However, solution-casting is the simplest means of obtaining free films. Sun *et al.* (1999) and Seoul & Mah (1997) have investigated the differences in spray-coated and solution-cast films of the same composition in terms of water vapour permeation, surface morphology and drug permeation. As a consequence of film-forming method, solution-cast films are denser and less porous than their spray-coated counterparts hence would not be expected to exhibit identical physical characteristics. Hence data obtained from characterisation of such films could reasonably only be assessed qualitatively unless in-depth correlation between free and *in situ* films was ascertained.

5.2 Aims and objectives

The function of EC coating on our dosage form was to impose a time-dependent barrier to drug release by rupturing only upon generation of sufficient internal pressure by expansion of swelling agent. Therefore the integrity of the EC coating in the dry and wet state was an important determinant of the lag time of our time-delayed capsules. Studies were undertaken to characterise solution-cast films of plasticised ethylcellulose films in order to extrapolate the results in predicting the performance of ethylcellulose, spray-coated onto the final dosage form. This method was chosen due to its ease of preparation and eliminating the need for specialised spraying equipment.

5.3 Methods

Various approaches of preparing free polymer films for characterisation have been described in the literature and some examples are detailed in Table 5.2 below.

Table 5.2 Methods of free film preparation.

Method	Reference
Solution-cast membranes • Plasticised Aquacoat® pseudolatex solution was poured onto rimmed glass plate • Dried for 2 hours in 60°C oven • Soaked in water for 5 minutes prior to removal • Surface water wiped off and vacuum-dried for 24h at room temperature	Sun *et al.*, 1999
Spray-coated membranes • Plasticised Aquacoat® pseudolatex solution was sprayed upwards onto horizontal stainless steel, Teflon-coated turn table and dried in jet of hot air	

Solution-cast membranes • Solution of EC in 90%(v/v) ethanol was cast on Teflon plate • Dried for 24 hours at room temperature	Bussemer *et al.*, 2003
Solution-cast films using a 'thin film applicator' • Pyrex glass tube containing 2%(w/w) EC / HPMC solution in methanol / methylene chloride kept in temperature-controlled oil bath • Cleaned microscope slide suspended over solution and solvent vapour for 20 minutes then lowered gradually into solution, remaining there for 20 minutes • Slide removed from solution at 1cm/min and suspended over solvent vapours to dry for 2 to 3 hours	Sakellariou and Rowe, 1995b
Spray-coated films • EC solution in dichloromethane and ethanol (60:40%v/v) sprayed onto rotating cylinder with substrates of either Teflon tape or tablets of model drug, remoxipride hydrochloride monohydrate	Arwidsson, 1991
Solution-cast films • EC dissolved in ethanol-water co-solvent system poured onto round polycarbonate plate, incubated for at least 24 hours Spray-dried films • EC dissolved in ethanol-water co-solvent system sprayed onto rotating cylinder	Hjärtstam and Hjertberg, 1999
Solution-cast films • Dispersions of Surelease®, Aquacoat® and Eudragit L 30 casted on levelled Teflon-coated glass plates and dried at 40°C (Eudragit L 30 D) and 55°C for Surelease® and Aquacoat®	Heng *et al.*, 2003

For our studies, the simple solution-cast method described in Section 2.4.3 was implemented to prepare films for testing, in order to determine the effects of the following parameters on the mechanical properties of the films:

- level of plasticisation
- type of plasticiser
- polymer concentration
- ageing
- incubation in 37°C water

Tensile testing i.e. stretching the films to the point of break (Section 2.4.5.1) was performed on plasticised EC films in order to quantify the following four tensile parameters:

Tensile stress at break of film, σ_b	Maximum tensile stress acting upon the film specimen at time of breaking. It gives insight into the mechanical strength of the film.
Tensile strain at break of film, ε_b	Maximum elongation of the film immediately prior to breaking. It is a measure of the overall extensibility of the material (Aulton, 1995).
Work done to break film, W_b	It is also known as work of failure and is equivalent to the area under the curve of a force-distance curve. Hogan (1995) stated that it is indicative of film toughness and more reflective of the film's ability to withstand mechanical stresses instead of tensile strength alone.
Elastic modulus of film, E_b	The slope of the stress-strain curve measured in the initial linear portion of the curve which obeys Hooke's Law. It is representative of the rigidity and stiffness of the film.

Puncture testing (Section 2.4.5.2) on the other hand, involved driving a stainless steel cylindrical probe through a taut, secured circular disc of film to determine the parameters listed as follows:

- Puncture strength, σ_p
- Strain at film puncture, ε_p
- Work done to puncture film, W_p
- Modulus, E_p

These puncture properties are indicative of similar mechanical characteristics of the film as their tensile counterparts.

Attempts were made to correlate these mechanical properties to certain physicochemical properties such as glass transition temperature, moisture content and moisture sorption capacity. Surface morphology of the films was also investigated.

All statistical analysis was performed using Minitab v.13 at the 5% significance level. The methods used are summarised in Table 5.3 below and referenced, where appropriate, to the detailed descriptions in Chapter 2.

Table 5.3: Summary of methods used in Chapter 5.

Section	Method	Methods section
5.4.1	**Preparation of solution-cast EC films**	
	Preparation of solution-cast ethylcellulose films	2.4.3
5.4.2	**Effect of plasticiser concentration and type**	
5.4.2.1	**Tensile properties**	
	Tensile properties	2.4.5.1
5.4.2.2	**Puncture properties**	
	Puncture properties	2.4.5.2
5.4.2.3	**Surface morphology**	
	Scanning electron microscopy	2.5.1.2
5.4.2.4	**Glass transition temperature**	
	Differential scanning calorimetry	2.5.2.2
5.4.2.5	**Moisture sorption**	
	Dynamic vapour sorption	2.5.4

5.4.3	**Effect of polymer concentration**	
5.4.3.1	**Tensile properties**	
	Tensile properties	2.4.5.1
5.4.3.2	**Puncture properties**	
	Puncture properties	2.4.5.2
5.4.3.3	**Surface morphology**	
	Scanning electron microscopy	2.5.1.2
5.4.4	**Effect of incubation in 37°C water**	
	Puncture properties	2.4.5.2
5.4.5	**Effect of film ageing**	
	Puncture properties	2.4.5.2

5.4 Results and discussion

5.4.1 Preparation of solution-cast EC films

The chosen method of solution-casting EC films on a Teflon plate and drying in a fume cupboard was adequate to produce films for testing. Although the usual composition of EC solution that was used for spray coating our time-delayed capsules was 3%(w/v) EC and only 5%(w/w of EC) plasticiser, it was not possible to produce a solution-cast film of this composition as it was too brittle for manual handling.

When casting 2%(w/v) EC solutions in 50:50%(v/v) acetone / isopropyl alcohol, films of sufficient integrity to be peeled off and cut into samples were only possible with a minimum plasticiser concentration of 10%(w/w of EC) and 20%(w/w of EC) for triacetin and dibutyl phthalate (DBP) respectively. 3%(w/v) EC films required at least 10-20%(w/w of EC) of either triacetin or DBP. Hence, films with these minimum plasticiser concentrations and higher were prepared and studied to obtain the overall effect of plasticisation on the films. The maximum concentrations for each plasticiser was 70%(w/w of EC) and 60%(w/w of EC) for triacetin and DBP respectively, as plasticisation to a higher extent produced films which were very sticky and difficult to handle.

Films with varying EC concentrations were also prepared, with either constant polymer:plasticiser weight ratio or constant plasticiser concentration. In general, as the content of polymer increased, the films gradually became thicker and less transparent.

5.4.2 Effect of plasticiser concentration and type

5.4.2.1 Tensile properties

The effects of triacetin, the more hydrophilic of the two plasticisers, and DBP, of a more hydrophobic nature, will be discussed concurrently. The concentration of EC was fixed at 2%(w/v) for this series of data.

Table 5.4: Mean film thickness of 2%(w/v) EC films of varying plasticiser concentration (10≤n≤12).

Concentration (%w/w of EC)	Mean thickness (mm) (S.D.)	
	Triacetin	DBP
10	0.04 (0.03)	*
12	0.05 (0.02)	*
14	0.05 (0.02)	*
16	0.05 (0.02)	*
18	0.05 (0.02)	*
20	0.05 (0.02)	0.04 (0.02)
30	0.05 (0.02)	0.05 (0.03)
40	0.05 (0.03)	0.05 (0.03)
50	0.05 (0.02)	0.05 (0.03)
60	0.06 (0.03)	0.06 (0.03)
70	0.06 (0.03)	*

***Denotes films which were not prepared.**

It was evident from Table 5.4 that the mean thicknesses of the films did not vary greatly among the plasticiser concentrations therefore treatment of data from tensile and puncture experiments did not include normalisation with respect to film thickness.

Manual inspection revealed that as the plasticiser concentration increased, the physical texture of the film changed from being brittle and very fragile to more malleable, stretchable and almost sticky.

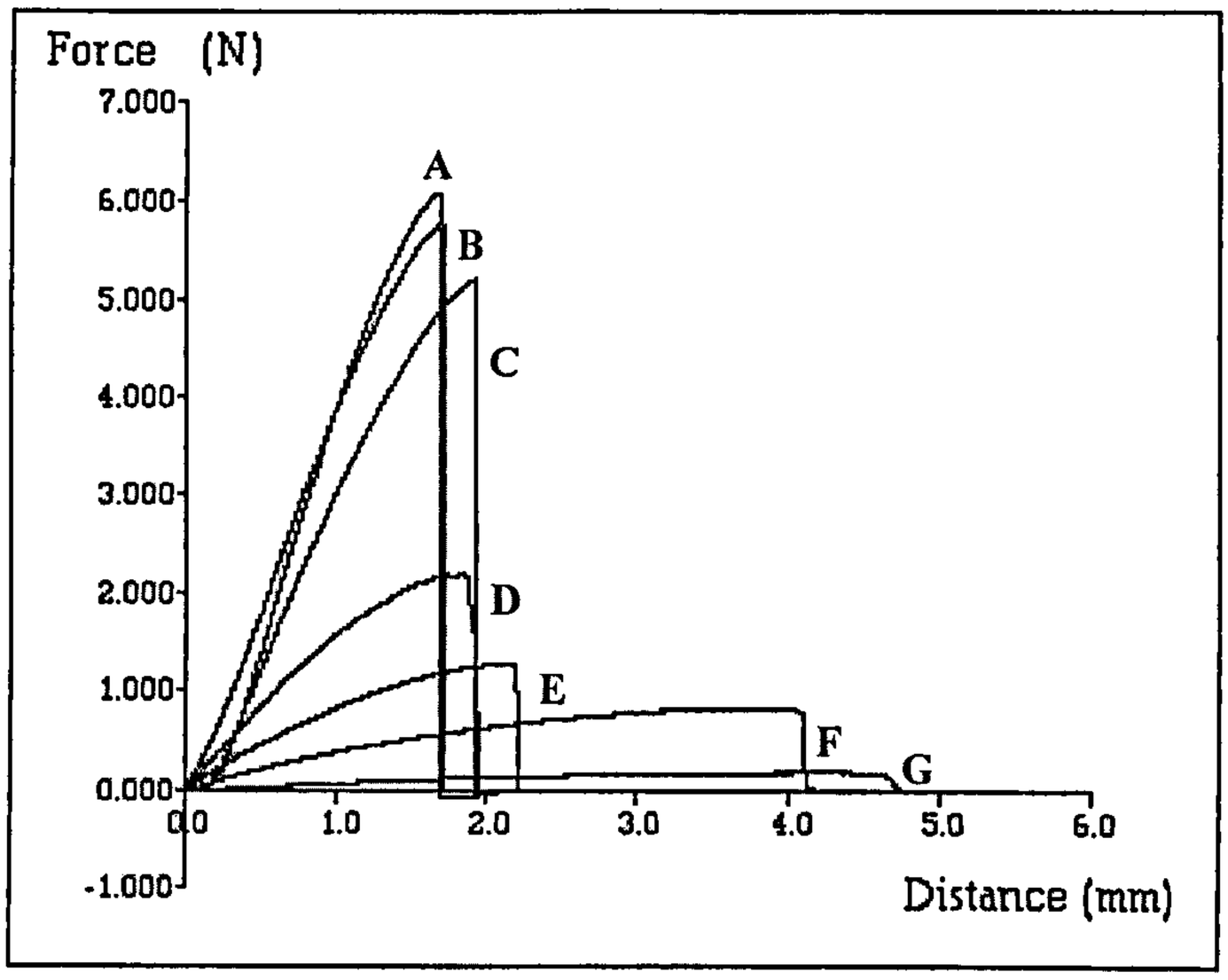

Figure 5.1: Sample force curves obtained by stretching triacetin-plasticised 2%(w/v) EC films to break point. A-G denotes the concentration of triacetin (%w/w of EC): A=10, B=20, C=30, D=40, E=50, F=60, G=70.

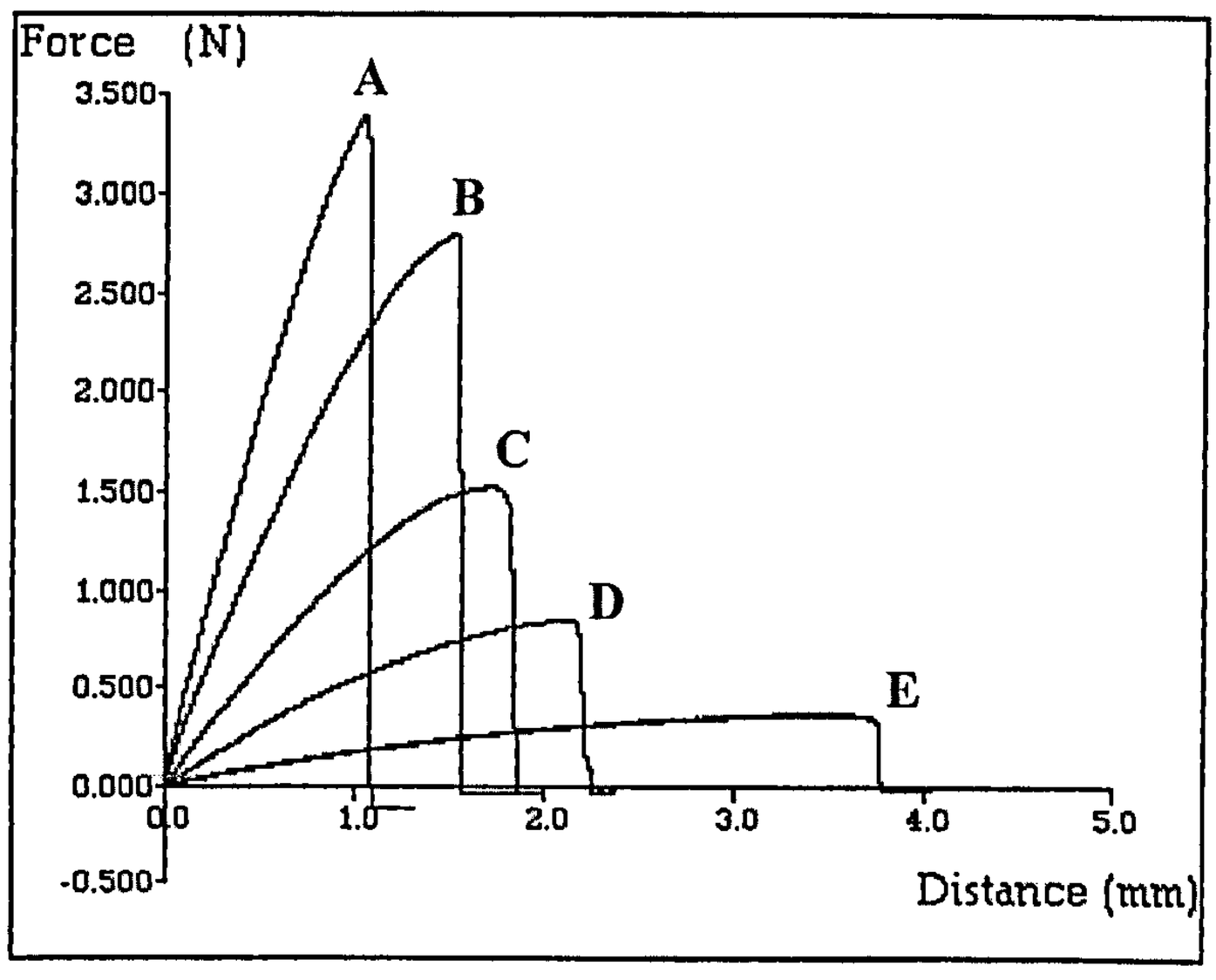

Figure 5.2: Sample force curves obtained by stretching DBP-plasticised 2%(w/v) EC films to break point. A-E denotes the concentration of triacetin (%w/w of EC): A=20, B=30, C=40, D=50, E=60.

The force curves depicted in Figures 5.1 and 5.2 showed that EC films plasticised with triacetin and DBP, regardless of plasticisation level, were generally stretched to break point and broke instantly. Hence the brittleness of the original EC polymer was maintained even to the highest concentration of plasticiser studied. This was

encouraging as the role of the EC film coat in the time-delayed capsules was to rupture immediately upon exceeding the stress limit.

By observing Figures 5.1 and 5.2, increasing plasticiser concentration tended to decrease the force required to break the film while increasing the length to which the film could be stretched without breaking. This was expected as plasticiser molecules act by becoming inserted between the polymer chains to reduce polymer-polymer interaction hence upon application of external forces, chain mobility is improved and dissipation of corresponding internal forces is possible. There is therefore minimisation of cracking and breaking (Rowe and Forse, 1980).

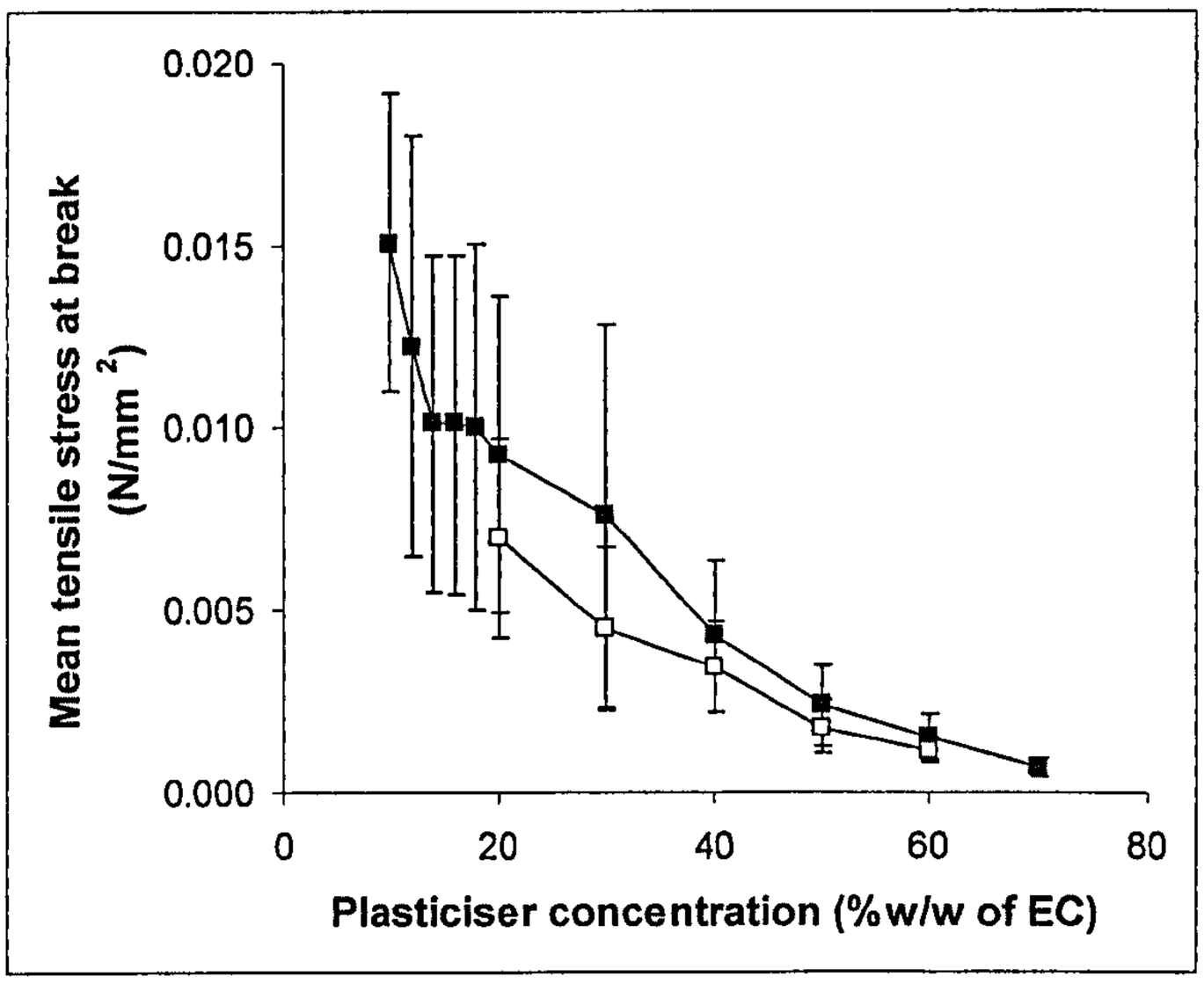

Figure 5.3: Effect of triacetin concentration (solid squares, ■) and DBP concentration (empty squares, □) on mean tensile stress at break of film, σ_b. ($10 \leq n \leq 12$, ± S.D.)

It was seen from Figure 5.3 that the effects of increasing plasticisation were more evident at the higher concentrations of triacetin. One-way ANOVA performed on the lower triacetin concentrations (10-20%w/w of EC) showed that the differences between the means were not statistically significant (p=0.699). Hence it was likely that small (2 – 10%w/w of EC) changes in triacetin concentration would not significantly affect the mean force required to rupture the EC films.

However when the increments in triacetin concentration proceeded in larger steps, the effect on mean σ_b became more evident. Again using one-way ANOVA, it was determined that increasing plasticiser concentration from 10 to 70%(w/w of EC) significantly reduced the mean tensile stress at break ($p<0.0005$). The same statistically significant effect was observed as DBP concentration increased from 20 to 60%(w/w of EC) where the p-value was less than 0.0005.

Taking into consideration the type of plasticiser, triacetin-plasticised films generally exhibited higher mean σ_b than those plasticised with DBP. Statistical treatment using the General Linear Model resulted in a significant p-value of 0.003 for the effect of differing plasticiser type on the overall mean σ_b.

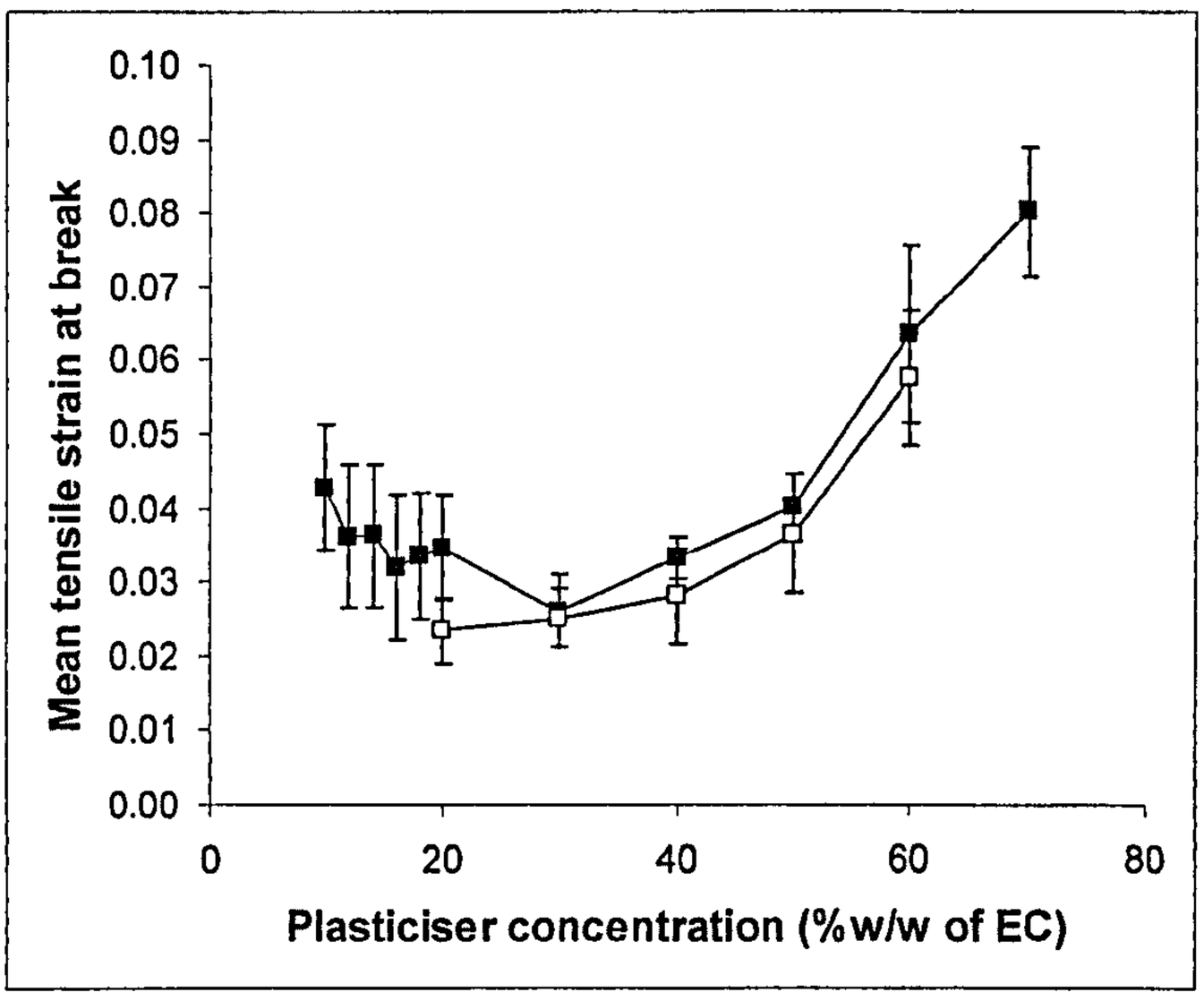

Figure 5.4: Effect of triacetin concentration (solid squares, ■) and DBP concentration (empty squares, □) on mean tensile strain at break of film, ε_b. ($10 \leq n \leq 12$, ± S.D.)

Increasing levels of triacetin generally increased the mean tensile strain at break, ε_b, as seen in Figure 5.4; the overall p-value was <0.0005. The statistical result was interpreted with care as this effect was only clearly shown when the triacetin concentration exceeded 60%(w/w of EC) hence overall extensibility of the films was only significantly increased when a concentration of plasticiser, not usually used in

practice, was incorporated into the film. At the lower concentrations, the mean ε_b was roughly the same as the concentrations increased from 10 to 50%(w/w of EC).

As for films plasticised with DBP, the same general effect was observed; increasing plasticiser concentration increased the maximum strain of the films significantly (p<0.0005). Again, by examining the overlap of the 95% confidence intervals, this effect was more pronounced only as the DBP concentration was 50%(w/w of EC) and over. The General Linear Model highlighted the fact that the mean ε_b for films containing triacetin was significantly higher than those plasticised with DBP (p<0.0005).

This effect was expected due to the action of plasticiser molecules which effectively insert themselves between individual polymer strands hence reducing inter-strand attractive forces (Hogan, 1995). Sliding of polymer chains would then be much more energetically amenable without incurring film breakage, therefore improving the pliability of the material, exemplified in the increased strain at break.

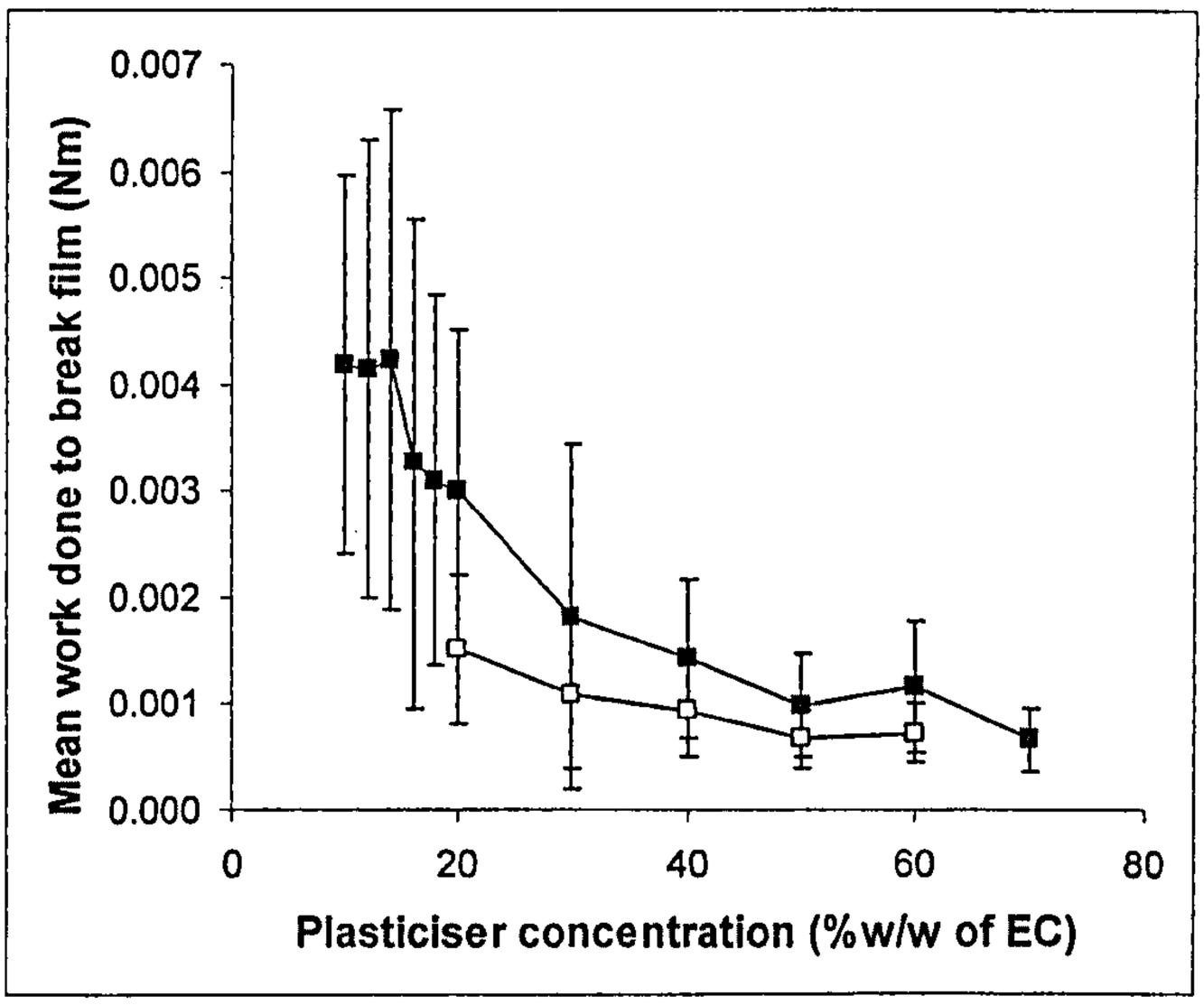

Figure 5.5: Effect of triacetin concentration (solid squares, ■) and DBP concentration (empty squares, □) on mean work done to break film, W_b. ($10 \leq n \leq 12$, ± S.D.)

Figure 5.5 showed the effect plasticisation with triacetin and DBP had on the mean work done to break film, $\mathbf{W_b}$, also known as the work of failure. Statistical treatment of the data with one-way ANOVA indicated that increasing the concentration of triacetin significantly decreased $\mathbf{W_b}$ ($p<0.0005$). Small increments of triacetin concentration i.e. from 10-20%(w/w of EC) in steps of 2%(w/w of EC) did not affect $\mathbf{W_b}$ significantly ($p=0.055$).

Film plasticised with DBP also exhibited decreasing requirements of mean work done to rupture film as plasticiser concentration increased ($p=0.001$) albeit at a generally lower magnitude than triacetin-plasticised films. This effect was statistically significant ($p<0.0005$) when tested with the General Linear Model.

The observations with mean work done tied in to the effects of plasticisation on mean tensile stress at break. Plasticisation in essence reduced the ability of the polymer films to withstand application of stress, therefore the energy required to break the film was reduced.

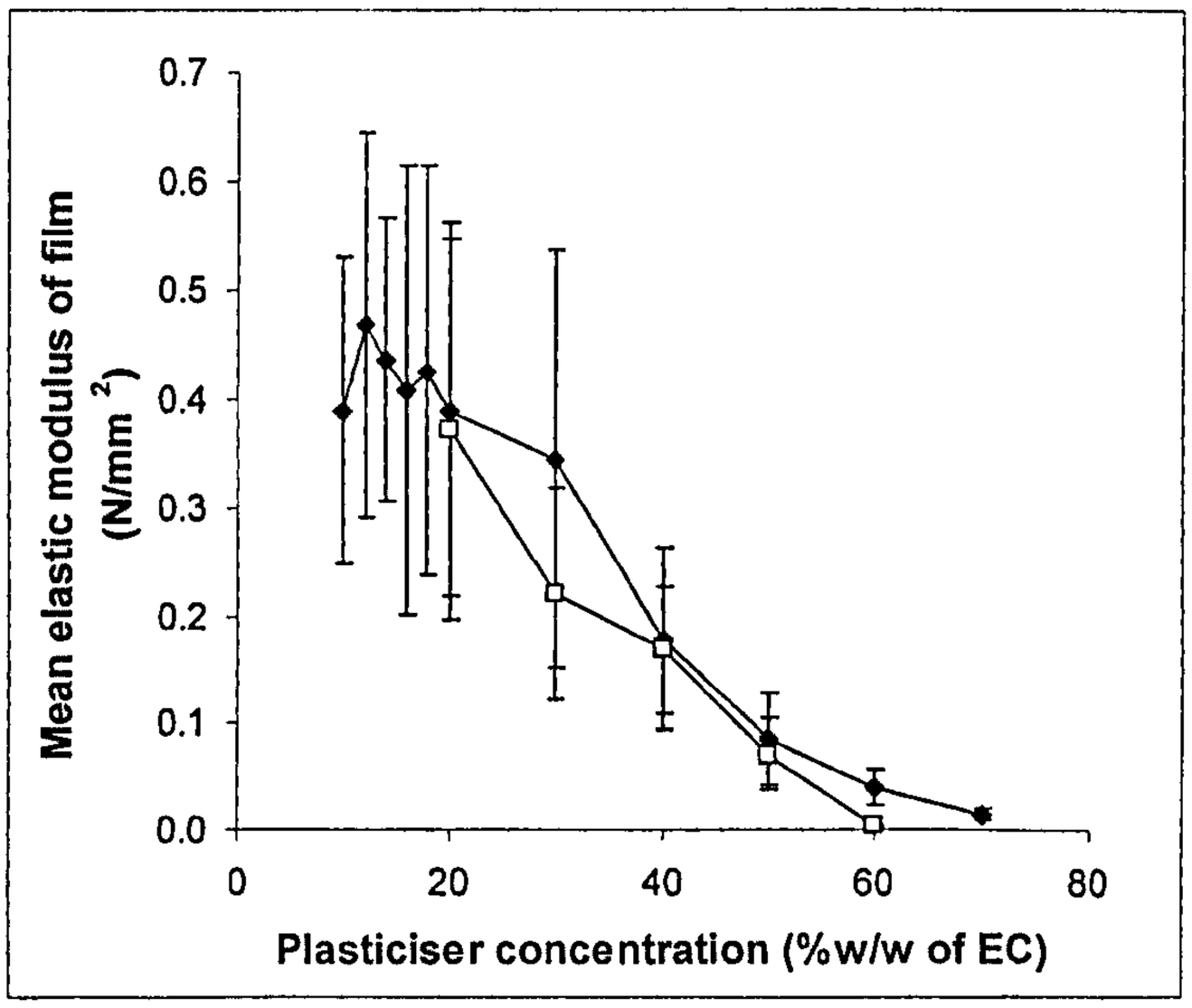

Figure 5.6: Effect of triacetin concentration (solid squares, ■) and DBP concentration (empty squares, □) on mean elastic modulus of film, E_b. ($10\leq n\leq 12$, ± S.D.)

Since elastic modulus at break of film, E_b, is representative of the overall rigidity of the film, Figure 5.6 indicated that with increasing triacetin content, the EC films

became gradually more flaccid. This effect was statistically significant as one-way ANOVA gave a *p*-value of <0.0005. Nevertheless it was observed again that this was another parameter that was unaffected by the increase in triacetin concentration from 10 to 20%(w/w of EC) as evidenced by a *p*-value of 0.924.

The effect of plasticisation of DBP on EC films was also to significantly decrease the mean elastic modulus (p<0.0005). 95% confidence intervals revealed that this effect was significant even as the concentration increased from 20 to 30%(w/w of EC). However, there was no significant difference between the values obtained with either plasticiser as the *p*-value from the General Linear Model was 0.097.

5.4.2.2 Puncture properties

The concentration of EC was increased to 3%(w/v) for these studies in order to more closely mimic the actual concentration applied onto the final dosage form. Table 5.5 listed the mean thicknesses of the EC films of varying plasticiser concentrations.

Table 5.5: Mean thicknesses of 3%(w/v) EC films plasticised by triacetin and DBP (n≥10).

Concentration (%w/w of EC)	Mean thickness (mm) (S.D.)	
	Triacetin	DBP
20	0.05 (0.03)	0.07 (0.01)
30	0.06 (0.03)	0.13 (0.01)
40	0.09 (0.03)	0.10 (0.03)
50	0.09 (0.02)	0.06 (0.02)
60	0.04 (0.01)	*

***Denotes data which were not obtained**

This set of films produced seemed to have larger differences in mean thicknesses as compared to the 2%(w/v) EC films, the thicknesses of which were shown in Table 5.4. Hence, analysis of data in this section factored in the normalisation of data with respect to thickness of film. This only applied to the calculations of tensile strain at rupture and work done to rupture film as the derivations of tensile stress at rupture and elastic modulus of film included a term for film thickness (refer to Table 2.6 in Section 2.4.5.2).

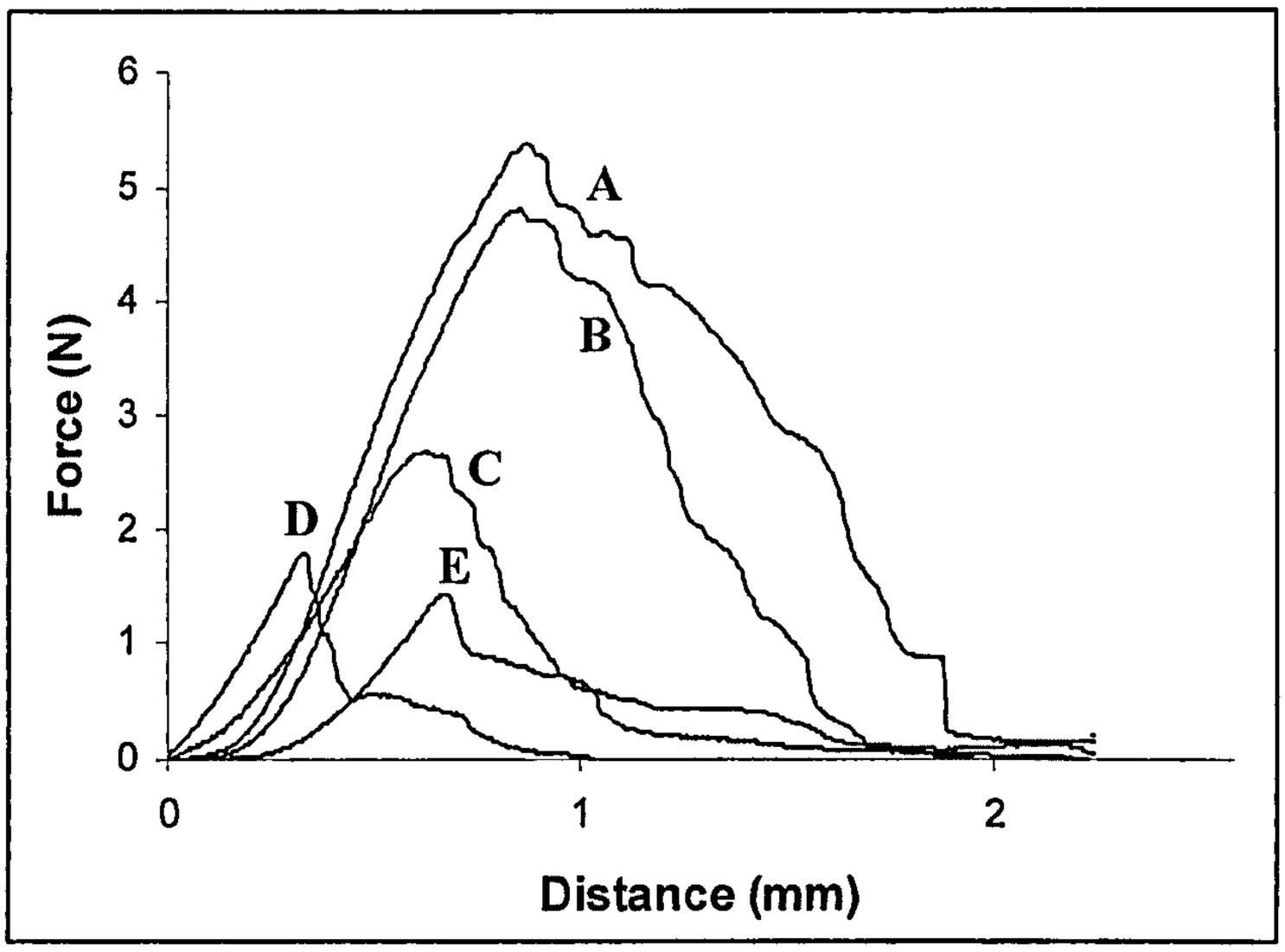

Figure 5.7: Sample force curves obtained by driving a stainless steel cylindrical probe through discs of triacetin-plasticised 3%(w/v) EC films to break point. Mean thickness of each selected film = 0.05mm. A-E denotes the concentration of triacetin (%w/w of EC): A=20, B=30, C=40, D=50, E=60.

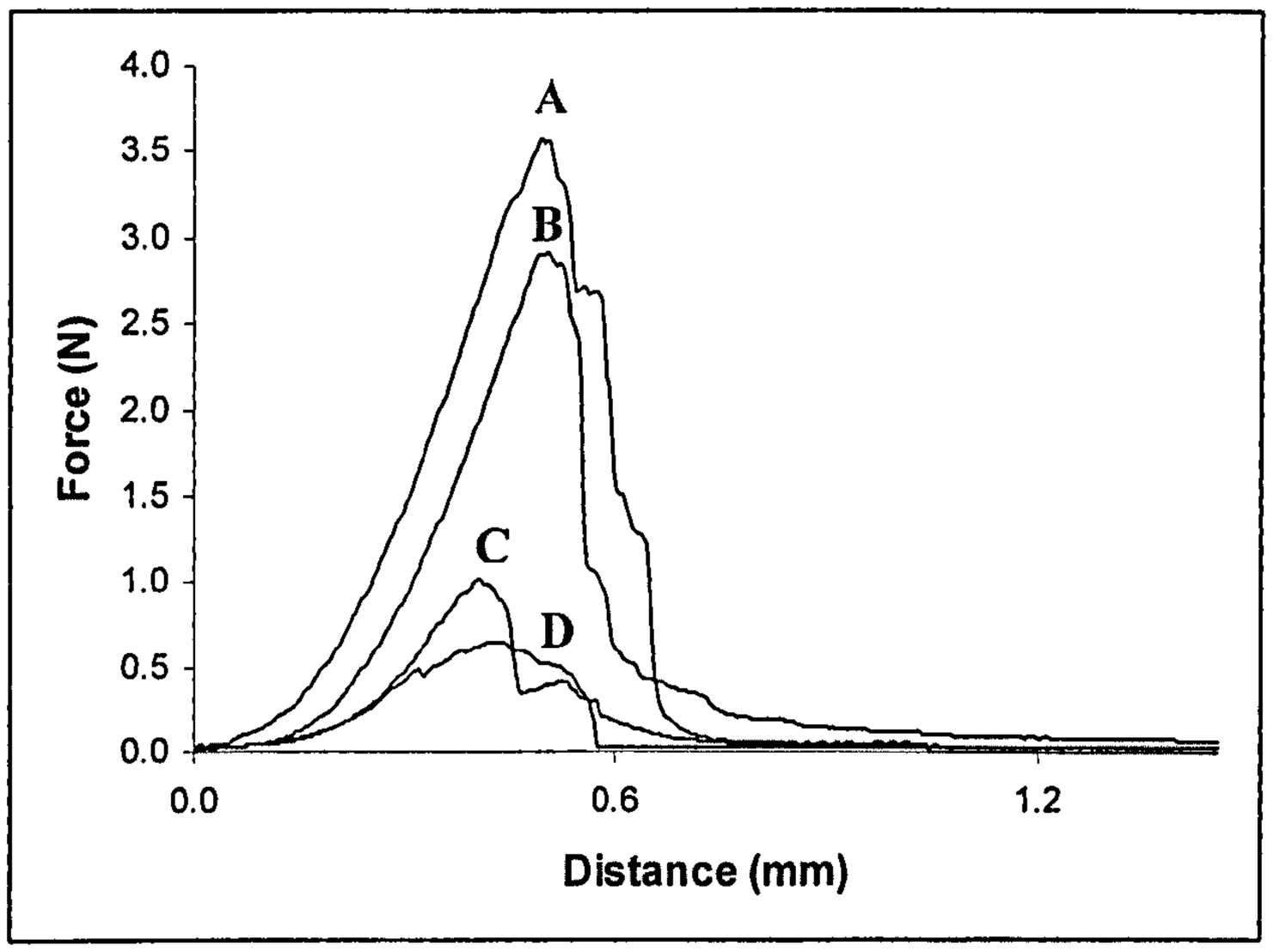

Figure 5.8: Sample force curves obtained by driving a stainless steel cylindrical probe through discs of DBP-plasticised 3%(w/v) EC films to break point. Mean thickness of each selected film = 0.05mm. A-D denotes the concentration of DBP (%w/w of EC): A=20, B=30, C=40, D=50.

Comparing the force curves from tensile testing and puncture testing (Figures 5.1, 5.2 and 5.7, 5.8 respectively), several differences and similarities were observed. While stretching the films elicited a sharp and obvious break, puncture testing detected the resistance offered by the yet rigid film after the first crack of the film was achieved. This would have been more representative of the actual phenomenon that occurs during rupture of the EC coating on the time-delayed capsules. The puncture test, like the tensile test, identified the region of linearity whereby the film exhibited Hookean properties.

In calculating the puncture properties of these EC films according to the equations detailed in Table 2.6 in Section 2.4.5.2, only the portion of the curve prior to initial rupture was considered as shown in Figure 5.9.

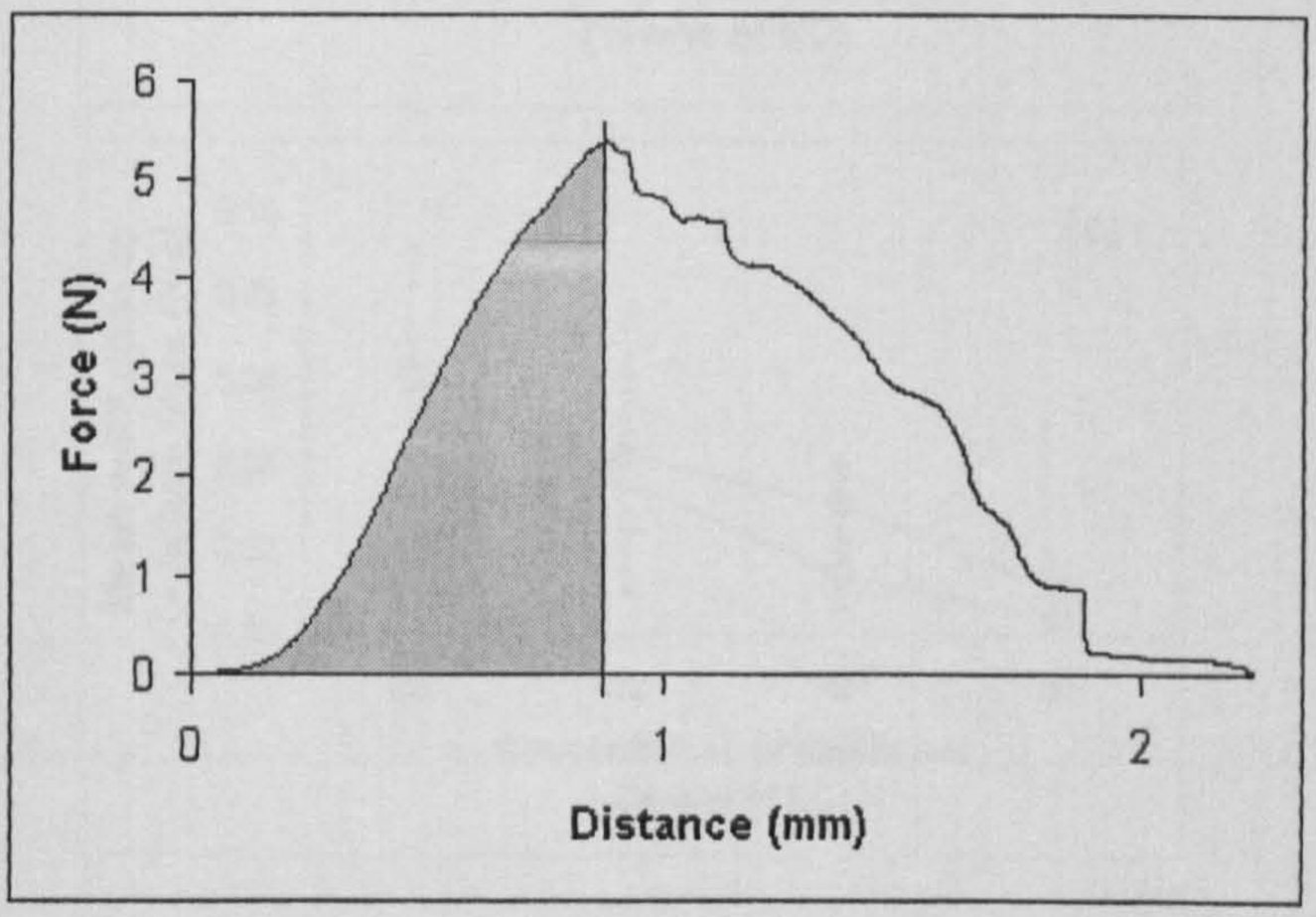

Figure 5.9: Sample force curve from puncture test of EC film. Shaded area indicates portion of curve considered for determination of puncture properties.

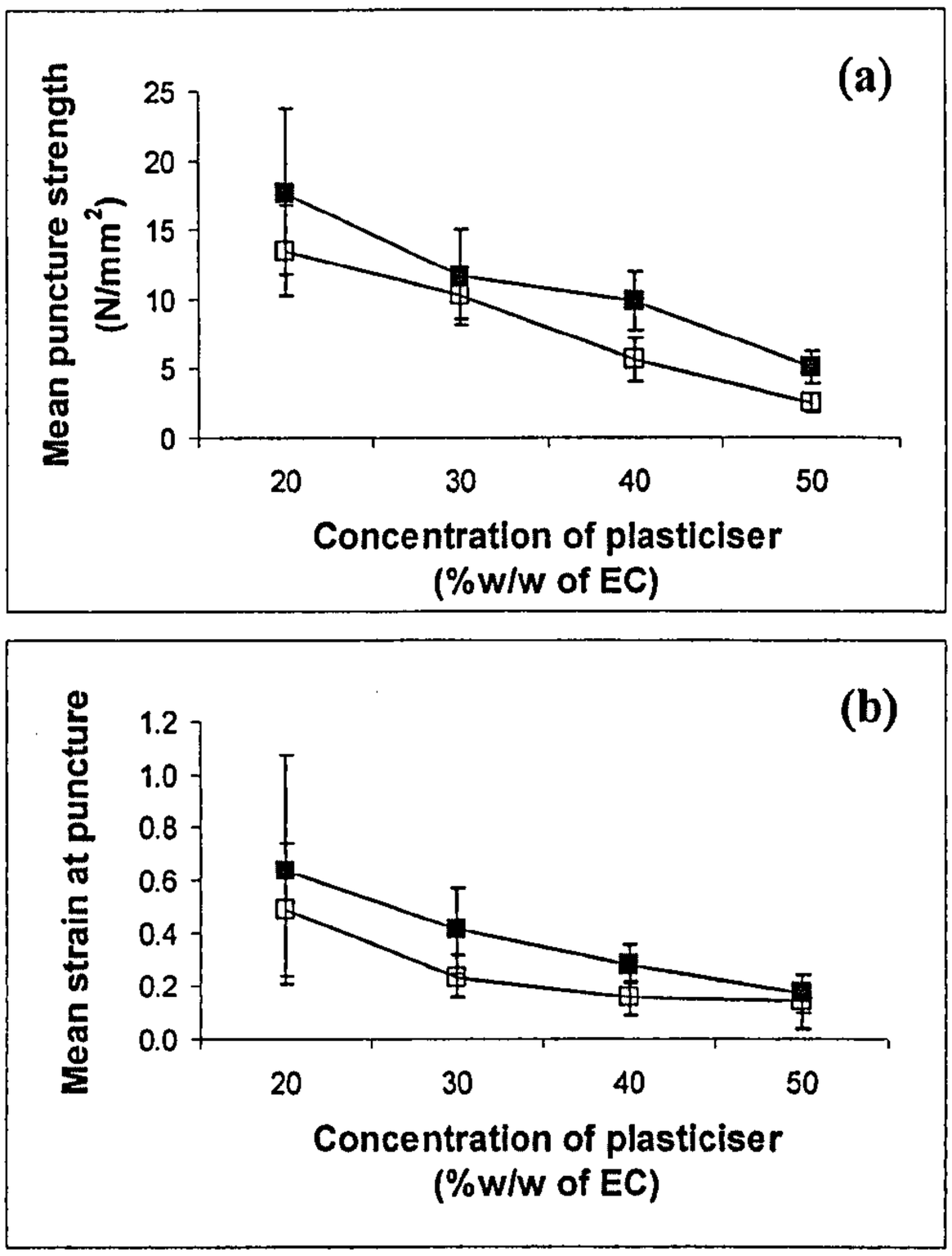

Figure 5.10: Effect of triacetin concentration (solid squares) and DBP concentration (empty squares) on (a) mean puncture strength of film, (b) mean strain at puncture of film, (c) mean work done to puncture film and (d) mean modulus of film. ($10 \leq n \leq 12$, ± S.D.)

In general, the effect of increasing plasticiser concentration was to decrease the magnitudes of all the puncture properties of the 3%(w/v) EC films. All effects were statistically significant with *p*-values <0.0005 with the exception of the mean modulus of film, $\mathbf{E_p}$, which was 0.002. The trends observed corresponded with the data obtained with tensile testing excluding the opposite effect seen with the mean strain at film puncture, $\boldsymbol{\varepsilon_p}$, data. This was not in accordance with the theoretically expected effect of increasing extensibility.

Data analysis of the puncture test, as described above, only considered the curve up to and including the point of initial rupture. It may have been possible that the trigger force for collection of data, 0.001N, was too low, and may have skewed the curve by detecting forces which were not related to probe impacting the film. Investigating the lower limits for trigger force is one of the proposed plans for future work (Chapter 8).

In comparing the two types of plasticiser, mean values were only significantly different for mean $\boldsymbol{\sigma_p}$ and mean $\boldsymbol{\varepsilon_p}$, $p<0.0005$ and $p=0.002$ respectively. The effect of type of plasticiser on mean $\mathbf{W_p}$ and mean $\mathbf{E_p}$ were not statistically significant, the *p*-values being 0.755 and 0.304, respectively. Hence, DBP exerted more of a plasticising effect in comparison to triacetin, decreasing the strength and increasing the elasticisity of the film to a greater extent. This effect was also observed with the tensile measurements described in Section 5.4.2.1.

Sakellariou and Rowe (1995a) proposed that the efficacy of a plasticiser was dependent upon its physicochemical structure: the closer the resemblance to the polymer to be plasticised, the more effective the plasticisation. For example, the hydroxyl groups possessed by glycerol and the polyethylene glycols made them suitable plasticisers for the cellulosic polymers. Heng *et al.* (2003) commented that it was the hydrophobicity of DBP that made it more compatible with the water-insoluble EC polymer. The results obtained from our tensile and puncture studies pointed to the fact that the plasticising power of DBP was greater than that of triacetin.

5.4.2.3 Surface morphology

Scanning electron microscopy was used to examine the surface of the cast films in an attempt to correlate the morphologies to the mechanical properties. The films were quite thermosensitive, and prolonged exposure to the electron beam tended to cause defects on the film. Therefore focusing was done as quickly and efficiently as possible, in order to preserve the original features of the film, without introducing artefacts.

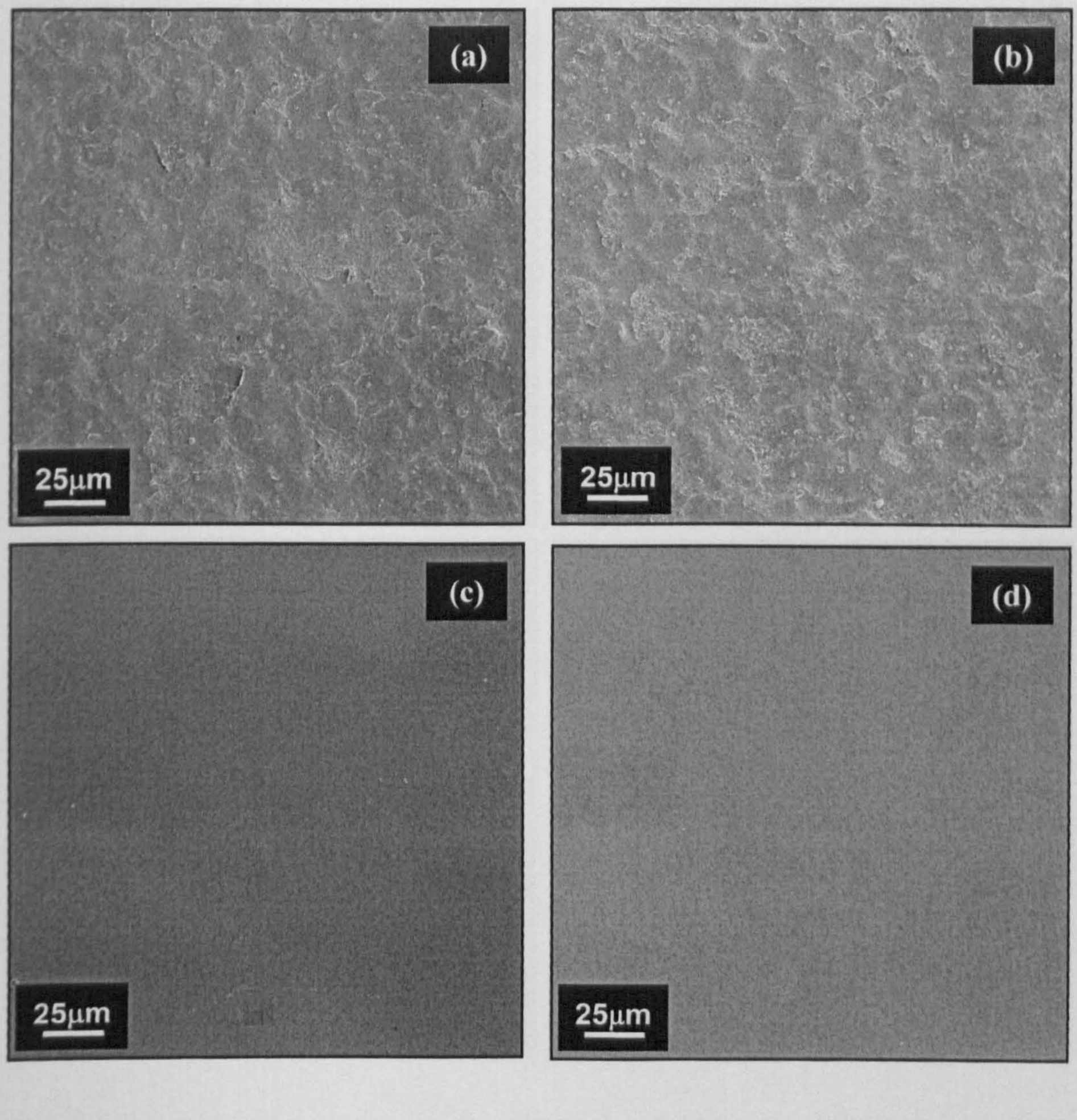

Figure 5.11: Electron micrographs (X500) of 3%(w/v) EC films with triacetin concentrations of (a) 10%(w/w of EC), (b) 20%(w/w of EC), (c) 30%(w/w of EC) and (d) 40%(w/w of EC).

The electron micrographs clearly showed how the surface texture of the films progressed from being quite rough and grainy to almost smooth as plasticisation levels increased. This implied that as number of plasticiser molecules which were introduced to the film increased, there was greater polymer-plasticiser interaction as opposed to interactions between polymer chains. Interlocking of polymer chains generally imparted a greater strength to the film as evidenced by the data from tensile and puncture testing while plasticisation enabled sliding of the polymer chains to a greater extent thereby reducing rigidity, but increasing ductility.

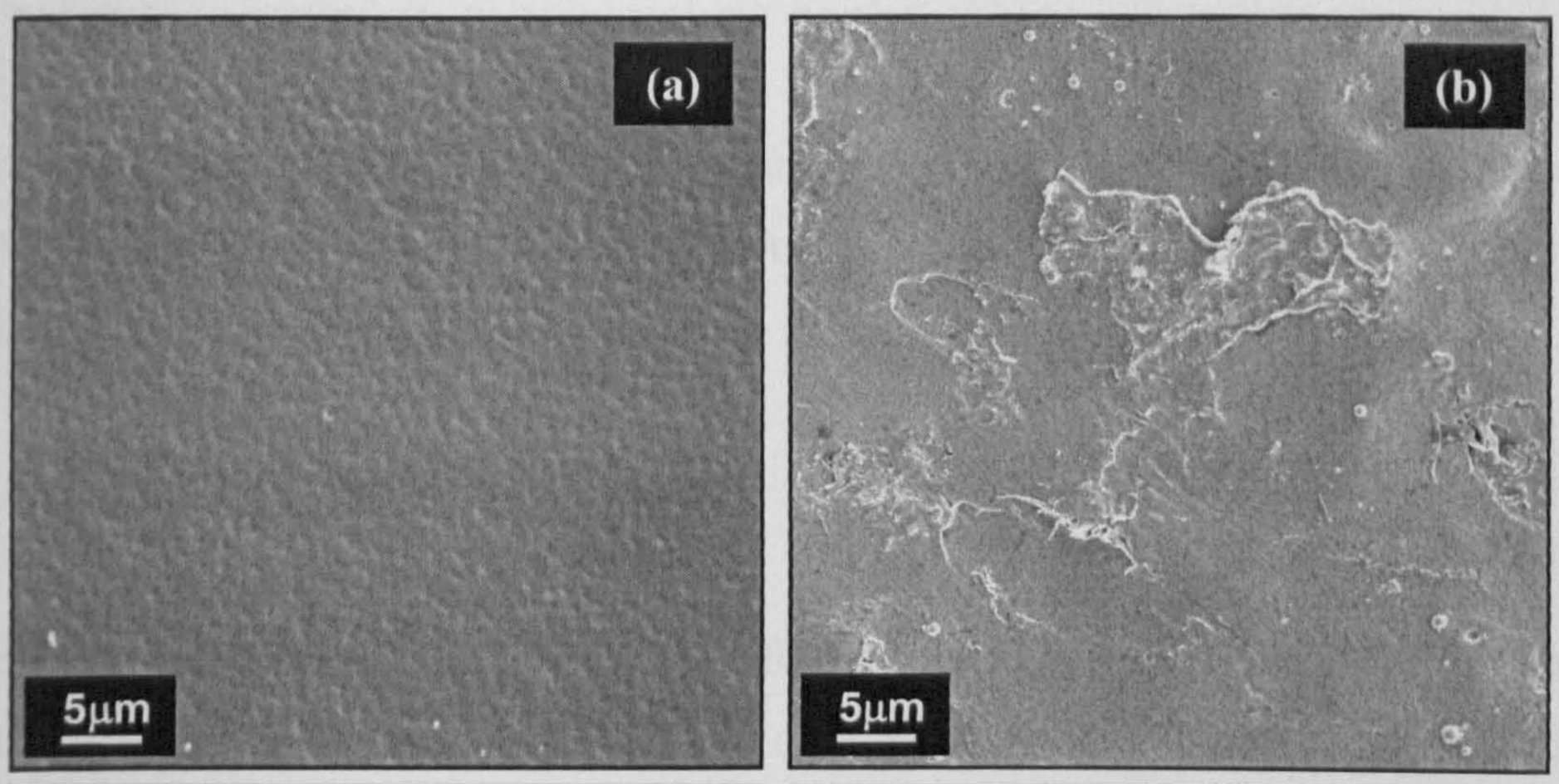

Figure 5.12: Electron micrographs (X2000) of 3%(w/v) EC films with DBP concentrations of (a) 20%(w/w of EC), (b) 30%(w/w of EC), (c) 40%(w/w of EC) and (d) 50%(w/w of EC).

The DBP-plasticised films were morphologically very different from their triacetin-containing counterparts. Increasing plasticisation levels were reflected in the film surface gradually changing from smooth (20%w/w of EC) to almost porous in nature (50%w/w of EC). Being quite hydrophobic, DBP molecules fitted well within the similarly hydrophobic EC polymer network at lower concentrations. Pores within the film became increasingly evident with excessive plasticisation, weakening the film and reducing its ability to tolerate applications of stress, as observed in the parameters quantified through tensile and puncture testing.

Although the surface structure of the films containing plasticisers of opposite chemical natures was highly dissimilar, the effect of plasticisation remained. Thresholds of stress were markedly reduced despite the capability of the film to dissipate the force applied by stretching to a greater extent.

5.4.2.4 Glass transition temperature

Differential scanning calorimetry was performed on the samples of 3%(w/v) EC films plasticised with different concentrations of triacetin and EC (Ethocel Standard 10) powder using the instrument and method described in Section 2.5.2.2. Two dynamic cycles of increasing the temperature from 25°C to 170°C separated by shock cooling were performed to remove any water that might obscure the glass transition temperature, T_g, and to confirm that the endotherm observed was indeed the T_g.

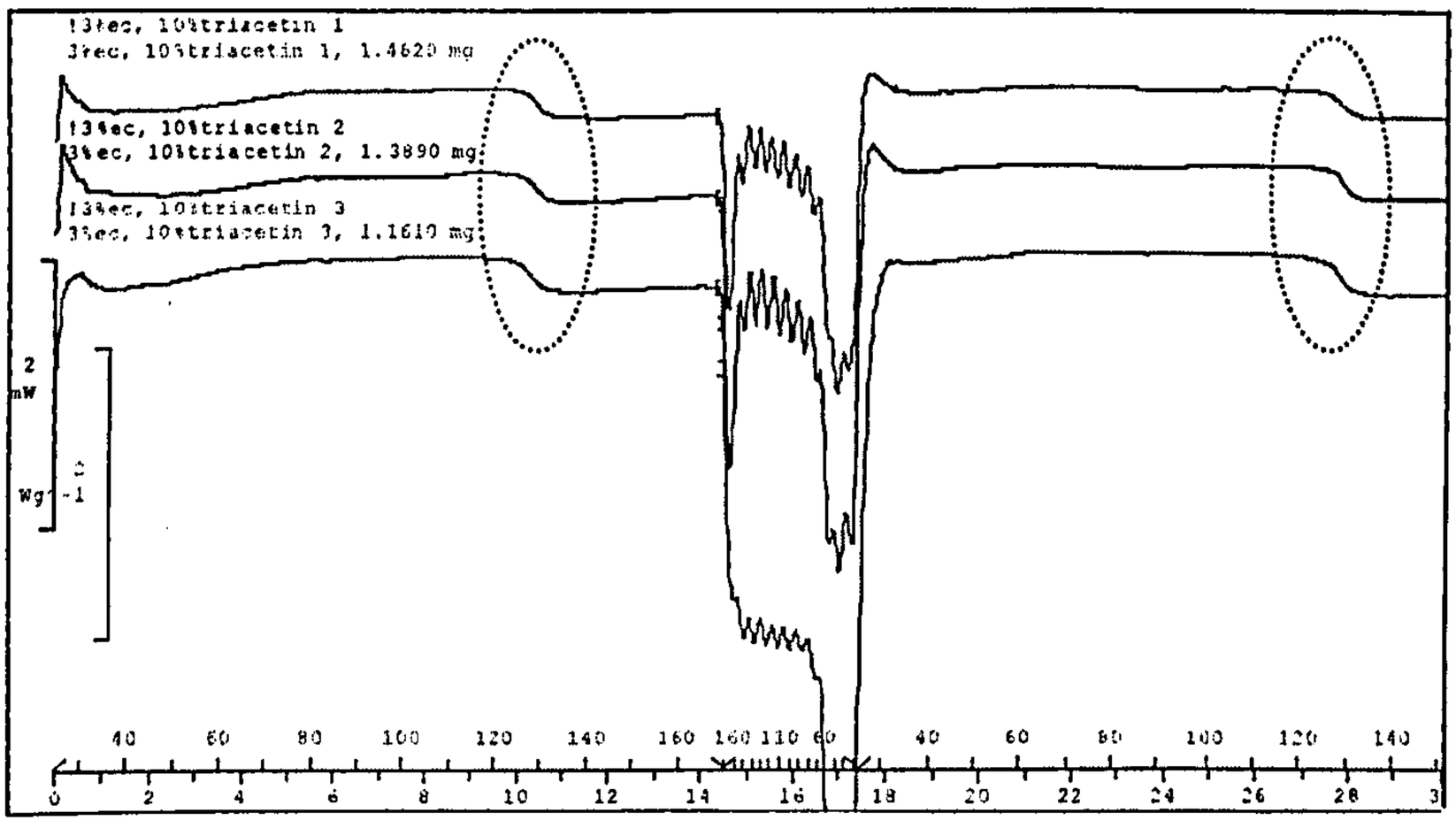

Figure 5.13: Triplicate DSC endotherms of 3%(w/v), 10%(w/w of EC) triacetin films. Circles denote endotherm of T_g.

The T_g was clearly observed in both the first and second cycles of the DSC program. An initial broad endotherm beginning at about 40°C was deemed to be due to the removal of residual moisture. The mean of the two endotherms were taken to be the overall T_g; this data was presented in Table 5.6.

Table 5.6: Mean onset temperatures of DSC cycles 1 and 2 (n=3).

Plasticiser (%w/w of EC)	Mean onset T (°C) (S.D.)	
	Triacetin	DBP
0	124.45 (1.07)	124.45 (1.07)
10	125.14 (0.55)	*
20	121.18 (2.73)	125.31 (1.18)
30	123.91 (0.52)	124.95 (1.69)
40	125.09 (0.50)	124.35 (1.28)
50	*	123.45 (0.44)

*** Denotes data not obtained.**

The data in Table 5.5 did not conclusively show the effect of increasing plasticisation on the films, whereby the T_g was expected to decrease with increasing triacetin concentration (Hogan, 1995). It was possible that the films did not have adequate contact with the bottom of the crucible, resulting in poor thermal contact and hence insufficient detection by the thermocouple. Further work suggested in Chapter 8 describes an alternative method for sample preparation.

It was also reported in the literature that DSC was not always the most suitable method for determining quantitative changes in T_g. Effects of plasticisation on the Tg of hydroxypropylmethylcellulose was unable to be established with DSC methodology (Entwistle and Rowe, 1979). Porter and Ridgway (1983) were unsuccessful in detecting any thermal differences in cellulose acetate phthalate and polyvinyl acetate phthalate films plasticised with varying concentrations of diethyl phthalate. They believed that the small heat changes arising were indistinguishable from the baseline drift due to lack of sensitivity of the instrument.

Therefore it was not possible to infer any relationship between T_g and tensile and puncture properties of the films from this set of data.

5.4.2.5 Moisture sorption

Dynamic vapour sorption, described in Section 2.4.5, was employed to determine the moisture sorption capacity of the EC films by subjecting squares of films weighing about 5mg to two identical cycles of ramping the relative humidity (R.H.) upwards and downwards in steps of 10% from 0 to 95%, the last step being only 5%.

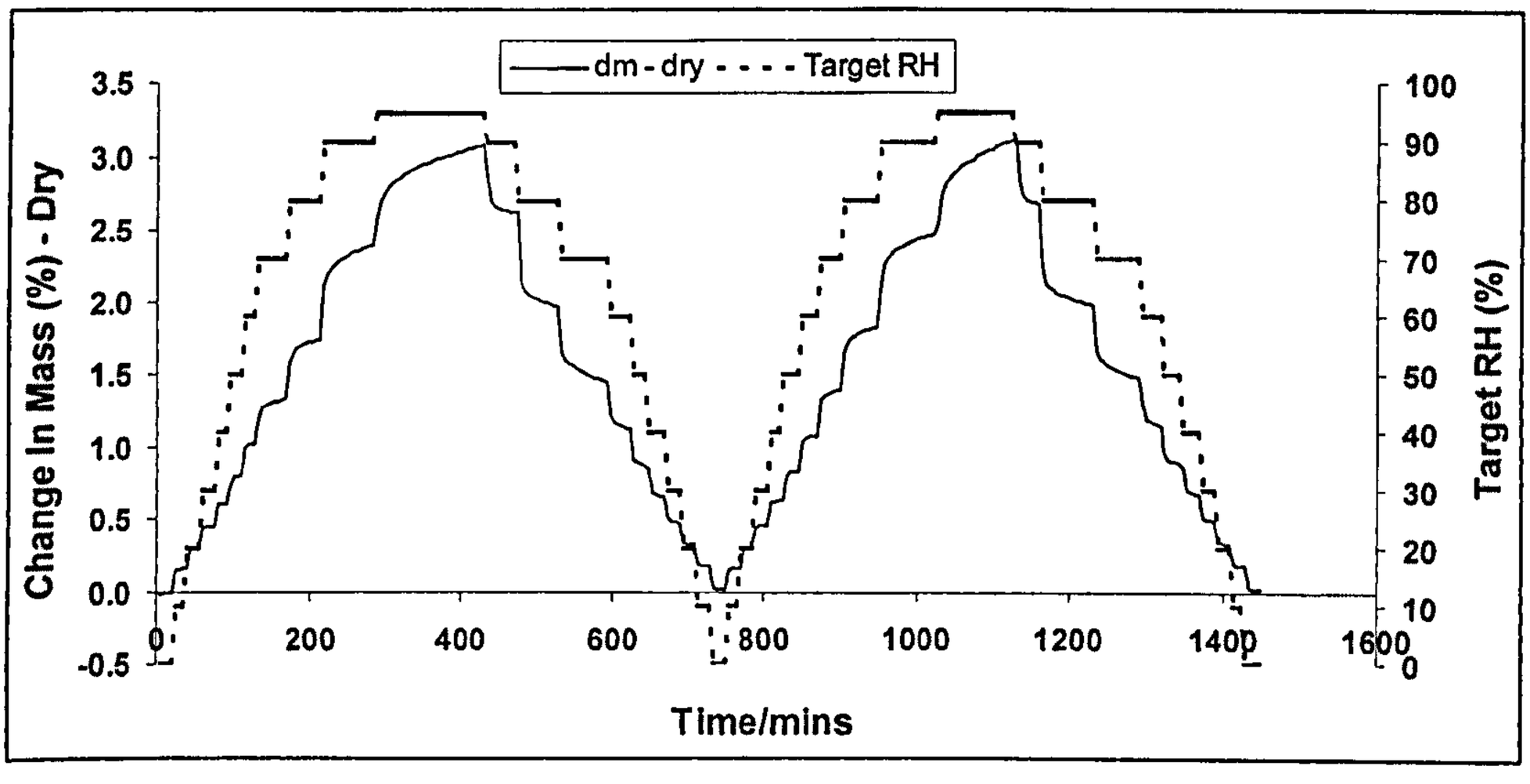

Figure 5.14: Sample moisture sorption curve of 3%(w/v) EC, 40%(w/w of EC) triacetin film.

Figure 5.14 showed that the two cycles resulted in similar-shaped curves, almost superimposable. This was confirmed in Figure 5.15(a) and (b), which depicted the mean maximum moisture uptake of the films over two cycles, inferring that the effect of water uptake on the films was reversible. The potential of water imparting additional plasticising properties has been well-documented (Bussemer *et al.*, 2003). Therefore this observation indicated that even if films were exposed to humid environments or even completely wetted, their inherent mechanical properties could be regained through adequate drying.

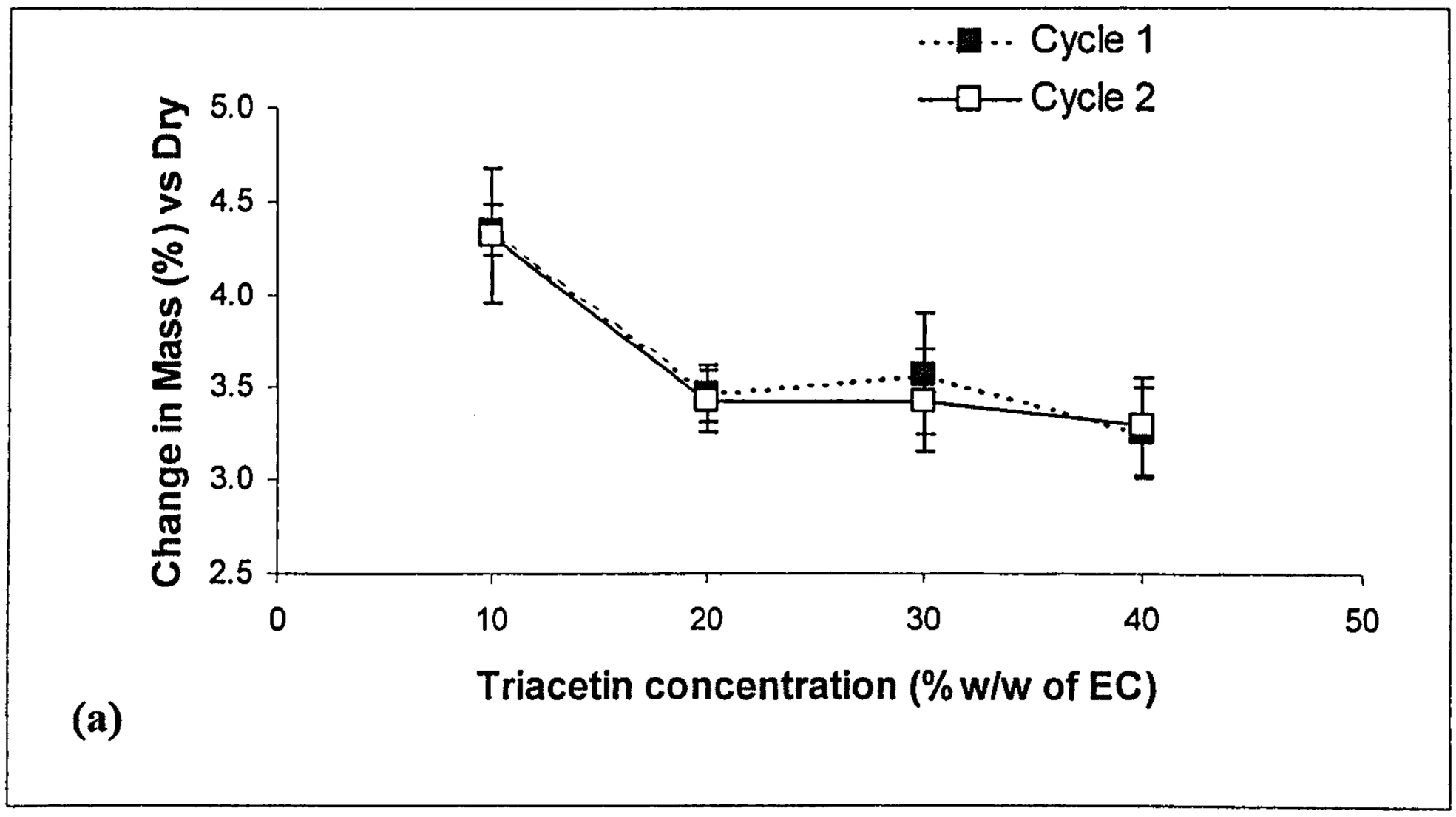

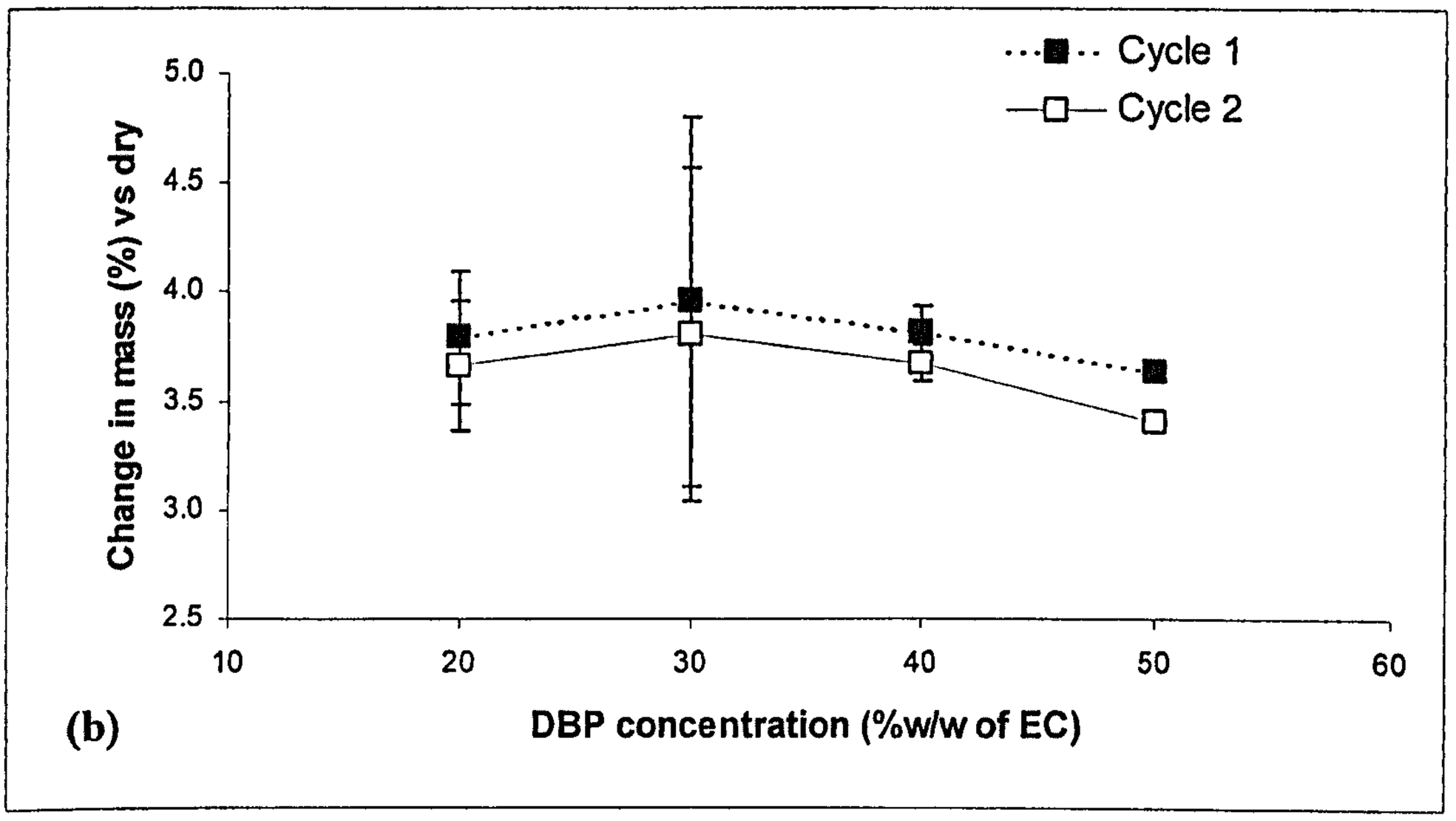

Figure 5.15: Effect of (a) triacetin and (b) DBP concentration on mean moisture sorption of 3%(w/v) EC films upon exposure to 95% R.H. (n=3, ±S.D.).

Figures 5.15(a) and (b) also highlighted the difference between the two types of plasticiser. While increasing triacetin levels decreased the mean maximum moisture sorption significantly (p<0.0005), the effect of DBP plasticisation was negligible. Due to its hydrophobic nature, DBP in any amount would probably not have affected moisture sorption to a great extent. However, it was surprising that the increasing hydrophilicity of the film from increasing triacetin concentration actually reduced moisture sorption, albeit modestly, when the opposite was expected.

5.4.3 Effect of polymer concentration

It was also important to evaluate the effect of EC content within the film to give an indication of how the amount of coating applied to the final dosage form would impact on the rupturability of the coat. This was done by maintaining either the polymer:plasticiser weight ratio (PPR) or plasticiser weight, separately. These studies were carried out using triacetin only. The compositions of films prepared according to the methods in Section 2.4.3 are described in Table 5.7 below. The total volume of solvent (50%v/v each of acetone and isopropyl alcohol) used was 150mL.

Table 5.7: Composition of EC films with varying polymer concentrations.

EC (%w/v)	A[a] Triacetin(%w/w of EC)	PPR	B[a] Triacetin (g)	PPR
2	20 (0.6)*	5:1	1.8	1.67:1
3	20 (0.9)*	5:1	1.8	2.5:1
4	20 (1.2)*	5:1	1.8	3.33:1
5	20 (1.5)*	5:1	1.8	4.17:1
6	20 (1.8)*	5:1	1.8	5:1

*** Values in parentheses denote amount of triacetin in g.**

[a] A and B refer to triacetin content being of constant plasticiser:polymer weight ratio or constant weight respectively.

5.4.3.1 Tensile properties

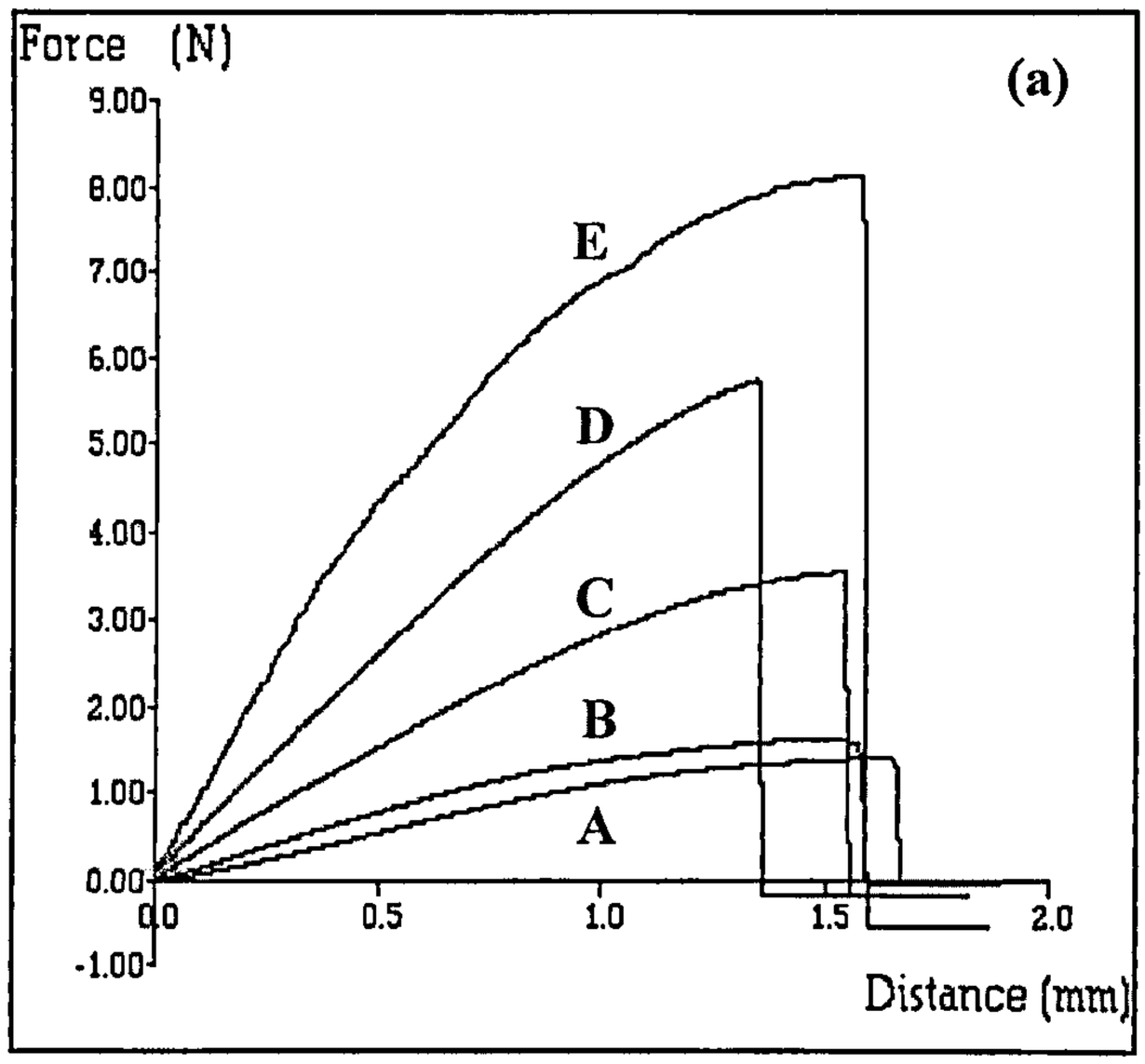

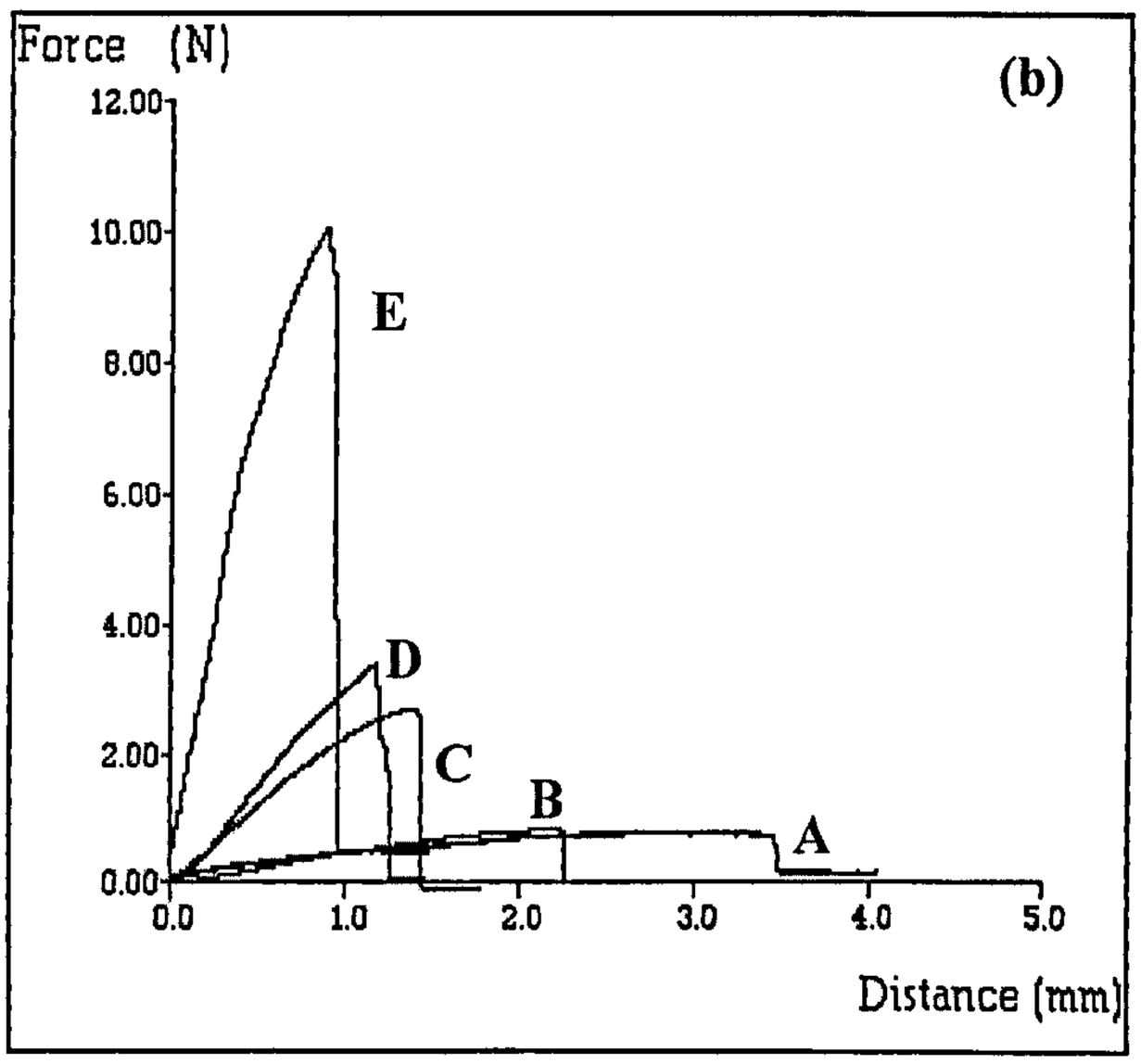

Figure 5.16: Sample force curves obtained by stretching EC films with (a) constant polymer:plasticiser weight ratio and (b) constant plasticiser weight to break point. A-G denotes the concentration of EC (%w/v): A=2, B=3, C=4, D=5, E=6. Range of film thicknesses (0.02 to 0.05mm).

Figures 5.16(a) and (b) highlighted the following effects of varying polymer and relative plasticiser concentrations:

(a) Increasing polymer concentration in both film types A and B resulted in greater force required to break the film.

(b) The resistance of film to break was not affected in film type A but decreased in film type B.

The mean thicknesses of the films prepared tended to increase as the polymer concentration increased as shown in Table 5.8.

Table 5.8: Mean thicknesses of films of type A and B (10≤n≤12).

EC (%w/v)	Mean thickness (mm) (S.D.)	
	A	B
2	0.06 (0.03)	0.05 (0.03)
3	0.08 (0.05)	0.07 (0.03)
4	0.08 (0.04)	0.09 (0.04)
5	0.10 (0.04)	0.10 (0.03)
6	0.12 (0.05)	0.12 (0.05)

The four tensile parameters, tensile strength at break, tensile strain at break, work done to break film and elastic modulus of film were determined through the tensile test described in Section 2.4.5.1. However, the raw data obtained was normalised with respect to mean thickness of film in order to eradicate the effect of that variable.

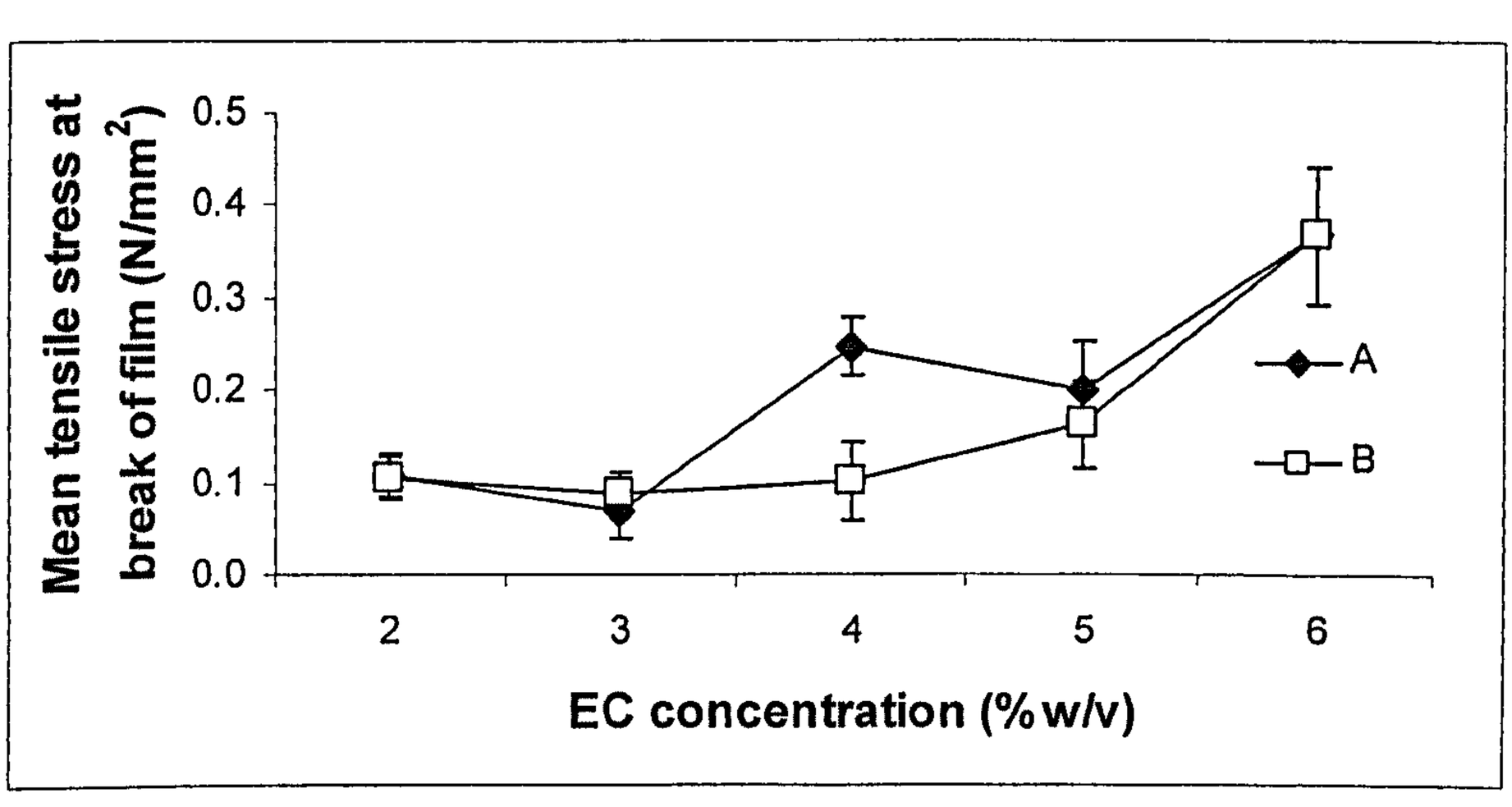

Figure 5.17: Effect of EC concentration on mean tensile stress at break of film. (10≤n≤12, ±S.D.) A=films with constant polymer:plasticiser weight ratio, B=films with constant plasticiser weight.

For both films type A and B, increasing EC concentration resulted in significantly increasing mean tensile stress at break of film (p<0.0005 for A and B). Therefore, the

introduction of larger quantities of EC polymer for inter- and intra-chain bonding exerted a positive effect on film tensile strength, irrespective of PPR.

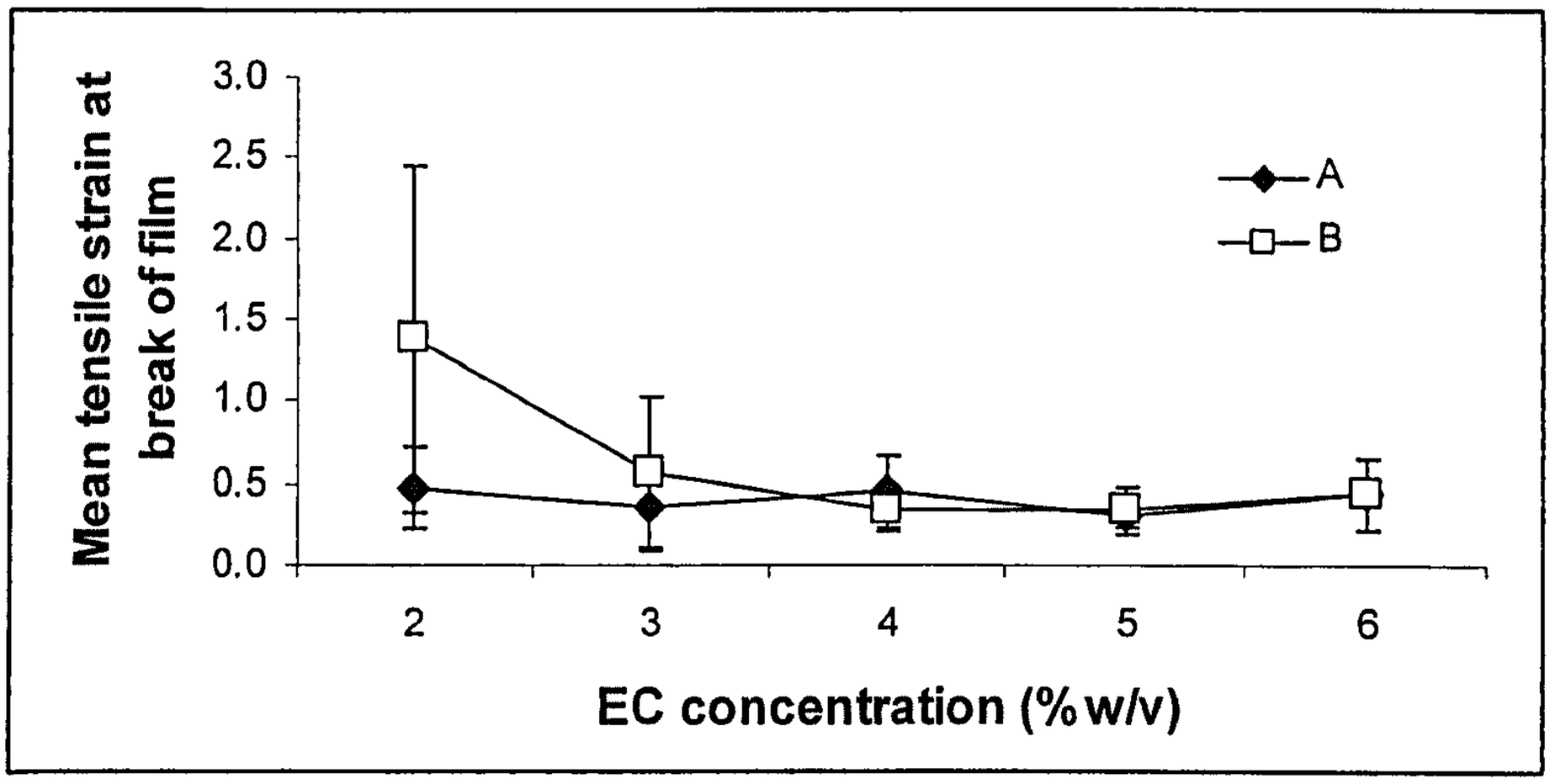

Figure 5.18: Effect of EC concentration on mean tensile strain at break of film ($10 \leq n \leq 12$, ±S.D.) A=films with constant polymer:plasticiser weight ratio, B=films with constant plasticiser weight.

It was evident from Figure 5.18 that maintaining a constant PPR resulted in no significant change in the mean tensile strain at break of film despite increasing the EC concentration (p=0.4). However as the PPR increased with simultaneous increments in EC concentration, the mean tensile strain at break of film significantly decreased (p<0.0005). Hence tensile strain seemed to be more influenced by plasticisation as compared to amount of polymer present.

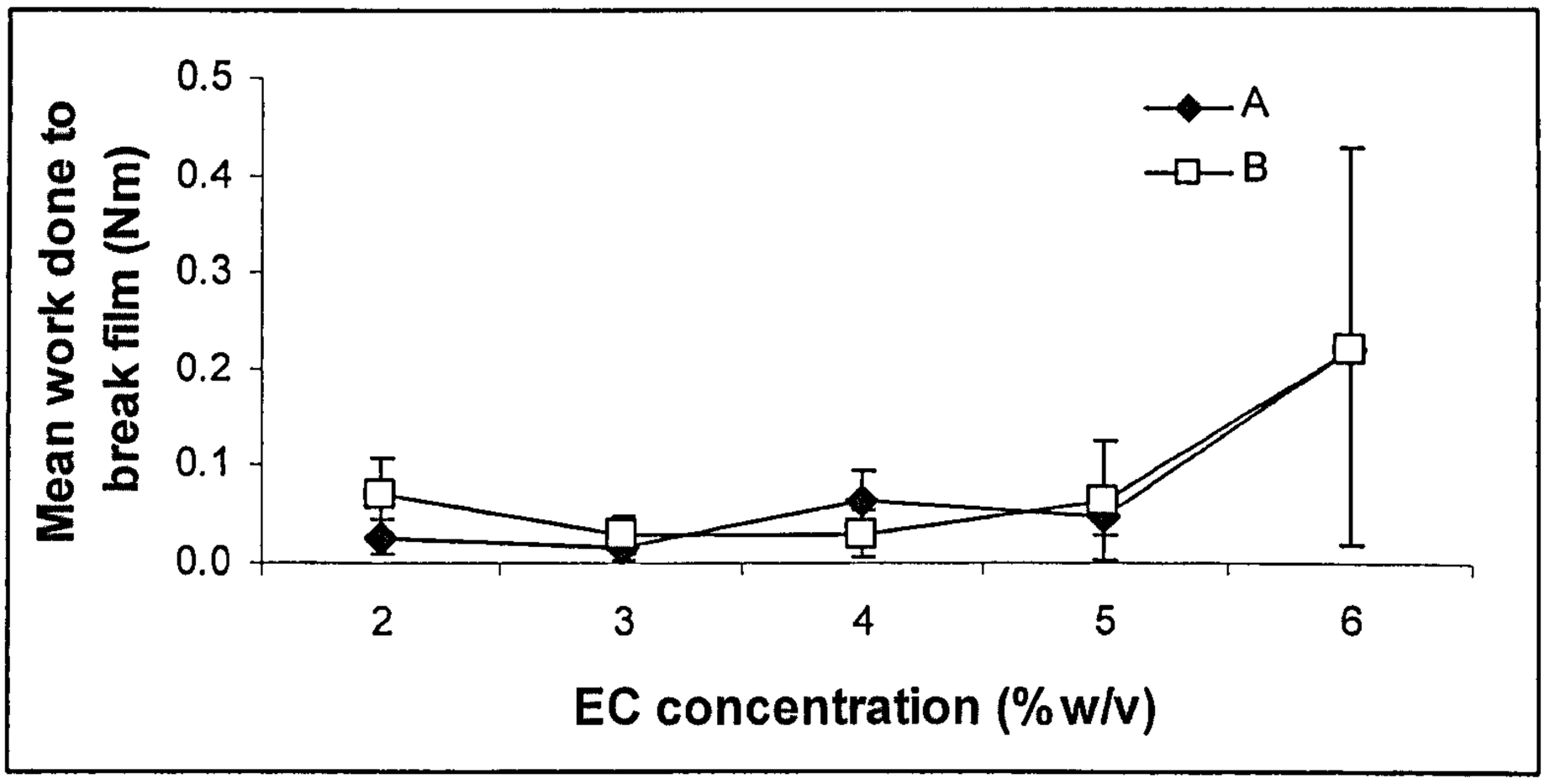

Figure 5.19: Effect of EC concentration on mean work done to break film. (10≤n≤12, ±S.D.) A=films with constant polymer:plasticiser weight ratio, B=films with constant plasticiser weight.

Figure 5.19 showed that both films type A and B produced similar concentration-effect curves in terms of mean work done to break film, which significantly increased upon increasing EC concentration (p<0.0005 for both film types).

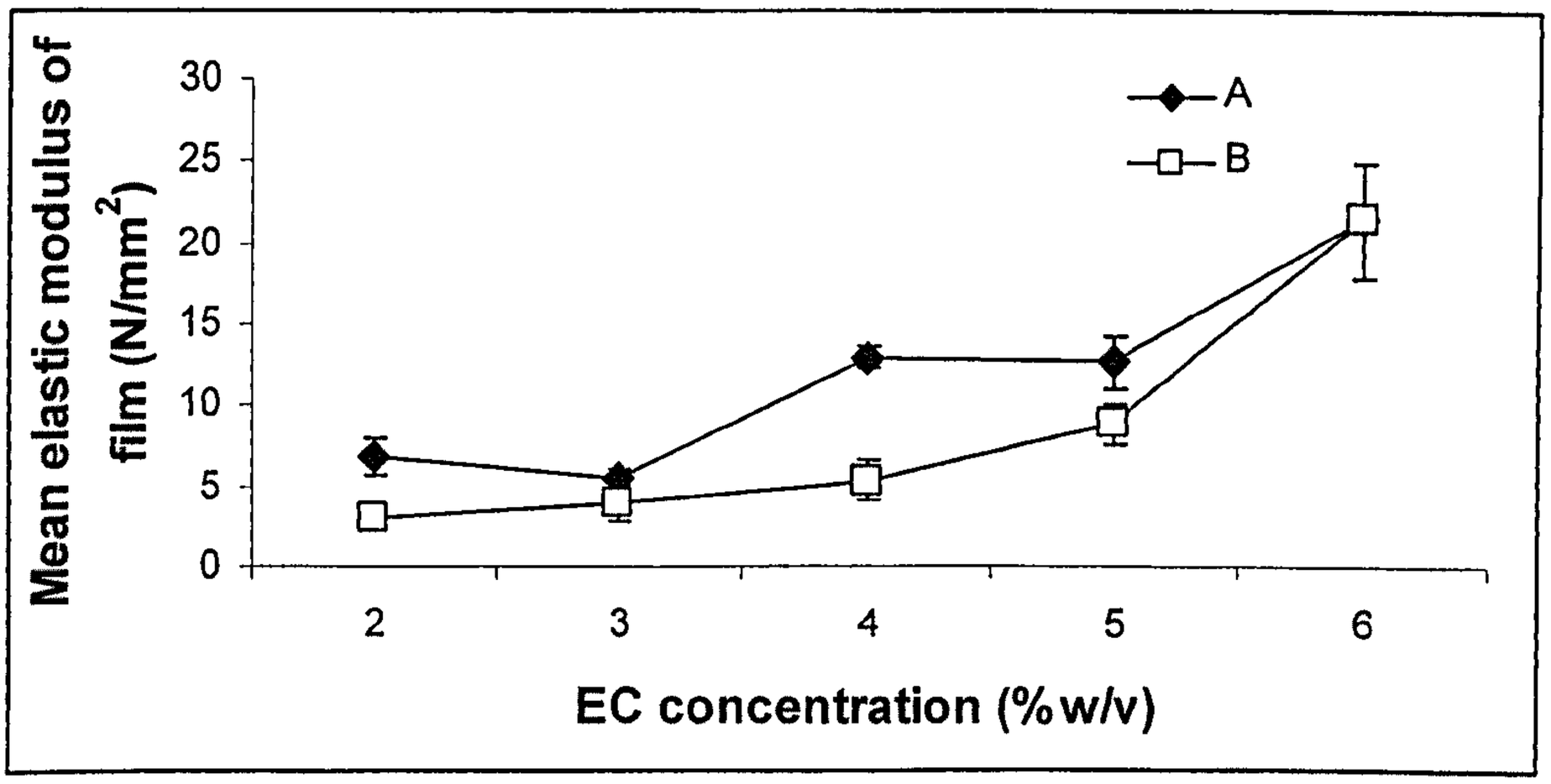

Figure 5.20: Effect of EC concentration on mean elastic modulus of film. (10≤n≤12, ±S.D.) A=films with constant polymer:plasticiser weight ratio, B=films with constant plasticiser weight.

Increasing EC concentration significantly increased the mean elastic modulus of film of both types A and B (p<0.0005).

In summary, of the four tensile parameters studied, only strain at break of film reflected the ductility and extensibility of the film while the other three were more indicative of strength and rigidity. It was evident from the data obtained that the more dominant determinant of strain was plasticisation while EC concentration impacted more on stress, work done and elastic modulus.

5.4.3.2 Puncture properties

The films with increasing PPR (type B) as detailed in Table 5.7 were also subjected to the puncture test (Section 2.4.5.2). Strain at puncture of film and work done to puncture film were normalised with respect to thickness of film, in a context similar to that in Section 5.4.2.2.

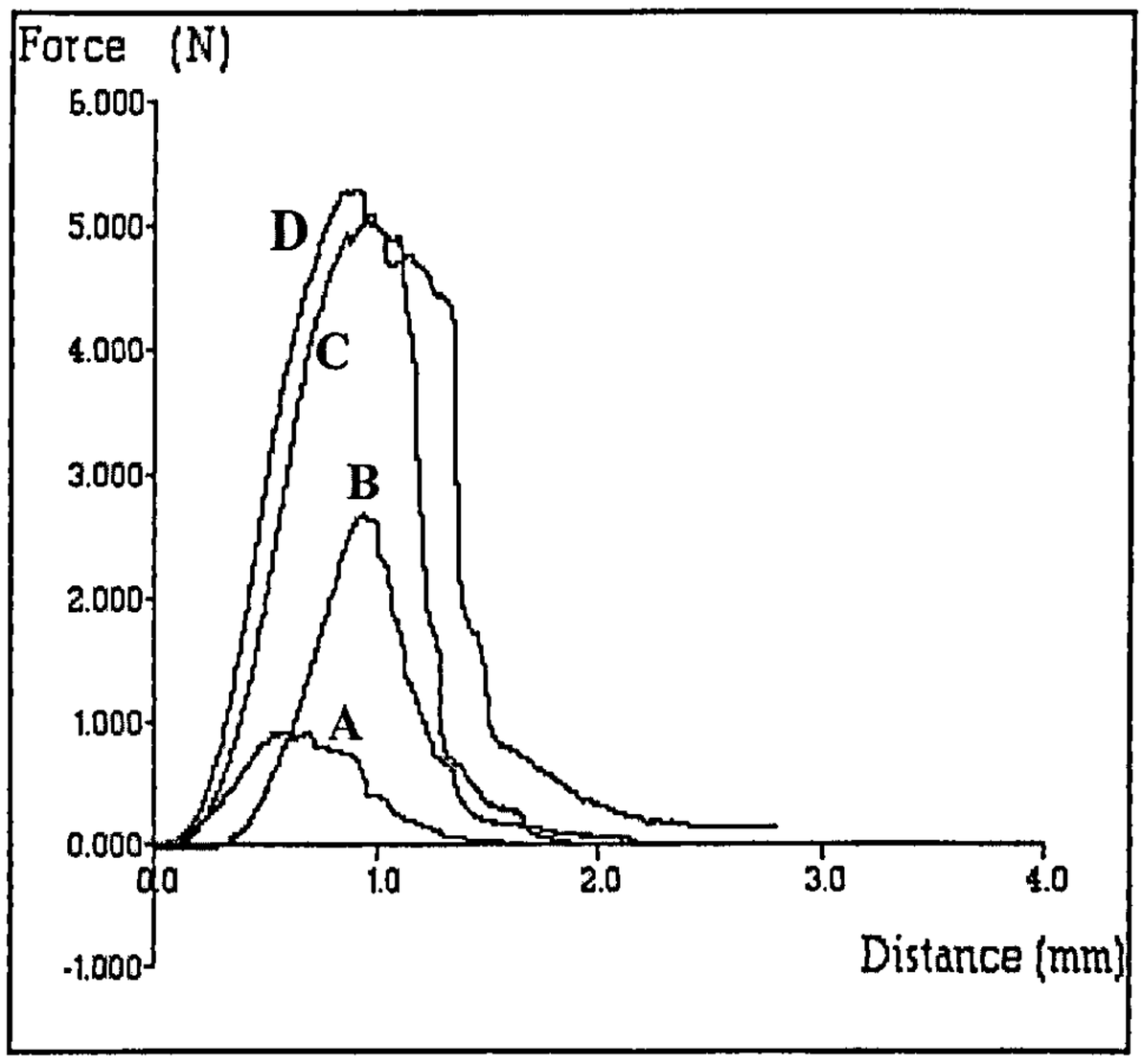

Figure 5.21: Sample force curves obtained by driving a stainless steel cylindrical probe through discs of EC films containing 1.8g triacetin to break point. Mean thickness of each selected film = 0.05mm. A-D denotes the concentration of EC (%w/v): A=2, B=3, C=4, D=5.

Table 5.9: Effect of EC concentration on puncture properties of solvent-cast films with constant plasticiser weight (n≥10).

EC (%w/v)	σ_p (N/mm^2 ±S.D.)	ε_p (S.D.)	W_p (Nm±S.D.)	E_p (N/mm^2 ±S.D.)
2	2.42 (0.48)	0.26 (0.09)	0.00534 (0.00150)	184.68 (49.40)
3	9.83 (2.07)	0.27 (0.07)	0.03037 (0.01222)	488.52 (182.26)
4	9.92 (3.36)	0.30 (0.13)	0.03482 (0.02354)	771.35 (153.56)
5	15.17 (5.31)	0.48 (0.18)	0.07231 (0.03707)	1007.08 (223.84)
p-value	<0.0005	<0.0005	<0.0005	<0.0005

As seen in Table 5.9, increasing the EC concentration while fixing the triacetin weight caused an increase in the four puncture parameters. The overall effects observed in this set of data were similar to the corresponding tensile properties in Section 5.4.3.1 with the exception of ε_p. Increases in σ_p, W_p and E_p could be attributed to the improved mechanical strength of the film afforded by stronger attractive forces between more EC polymer chains. Again (c.f. Section 5.4.2.2) the strain data were an anomaly, and the limitations described in that section probably apply in this case as well.

5.4.3.3 Surface morphology

SEMs (Section 2.5.1.2) revealed the surface characteristics of the EC films which gave insight to their tensile and puncture properties, as shown in Figure 5.22 on the next page. A low PPR (Figure 5.22a) displayed features of excessive plasticisation, with large pores and a rippled surface while a high PPR (Figure 5.22c) resulted in a film with areas of polymer aggregates. Of all the PPR values studied, a PPR of about 3:1 (Figure 5.22b) gave the smoothest film surface indicating a good balance of plasticiser and polymer.

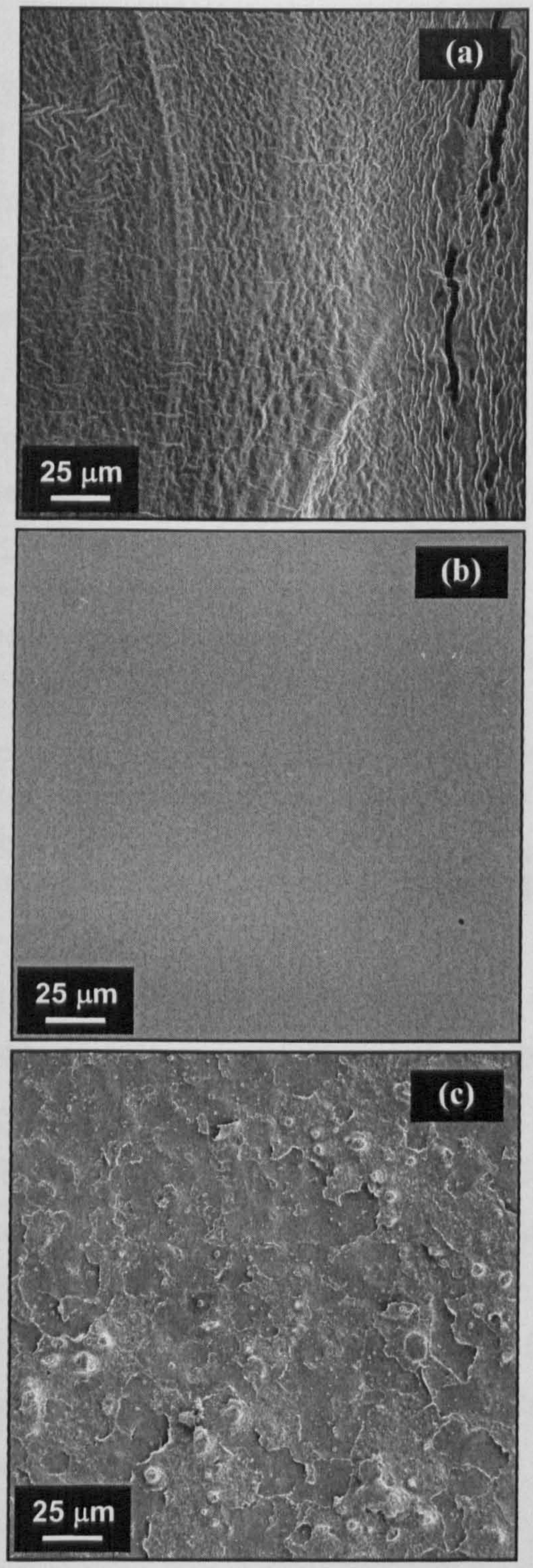

Increasing PPR

Figure 5.22: SEMs of solvent-cast EC films with 1.8g triacetin (X500). (a) 2%(w/v) EC; PPR=1.67:1, (b) 4%(w/v) EC; PPR=3.33:1, (c) 5%(w/v) EC; PPR=4.17:1.

5.4.4 Effect of incubation in 37°C water

Using the method described in Section 2.4.5.2, the effect of incubating the films in 37°C water was studied to postulate the stability of EC coat upon *in vivo* administration of the dosage form. In this series of experiments, only 3%(w/v), 20-50%(w/w of EC) triacetin films were tested. The films were cast from 50:50(v/v) acetone / isopropyl alcohol with a total volume of 150mL.

Table 5.10: Effects of incubation for 150min in 37°C water on puncture properties of EC films in terms of *p*-values derived from one-way ANOVA (n=12).

Puncture properties	Triacetin concentration (%w/w of EC)			
	20	30	40	50
Puncture strength	0.342	0.169	0.281	0.063
Strain at film puncture	0.183	0.469	0.008[a]	0.002[a]
Work done to puncture film	0.001[a]	0.335	0.617	0.035[a]
Elastic modulus of film	0.213	<0.0005[b]	0.576	<0.0005[b]

[a] denotes significant increase, [b] denotes significant decrease

Mean puncture strength was not affected by incubation in 37°C water. However, films with 40 and 50%(w/w of EC) triacetin exhibited significant increase in mean strain at film puncture, possibly due to the additional plasticising effect of water drawn into the film by the hydrophilic plasticiser. The effect on work done to puncture film was inconclusive as both the lowest and highest triacetin concentrations exhibited significant increases. A significant decrease in mean modulus of film was observed with both 30 and 50%(w/w of EC) triacetin films. Effects of incubation in 37°C water was most evident in films containing the highest concentration of plasticiser, indicating that over-plasticisation may cause changes to film properties which must be considered during construction of the dosage form.

5.4.5 Effect of film ageing

Films sealed in polyethylene bags, stored at room temperature in a dessicator for three months, were subjected to puncture testing. Two-sample t-tests were performed in Minitab v.13 to evaluate the effects of ageing on the films' puncture properties.

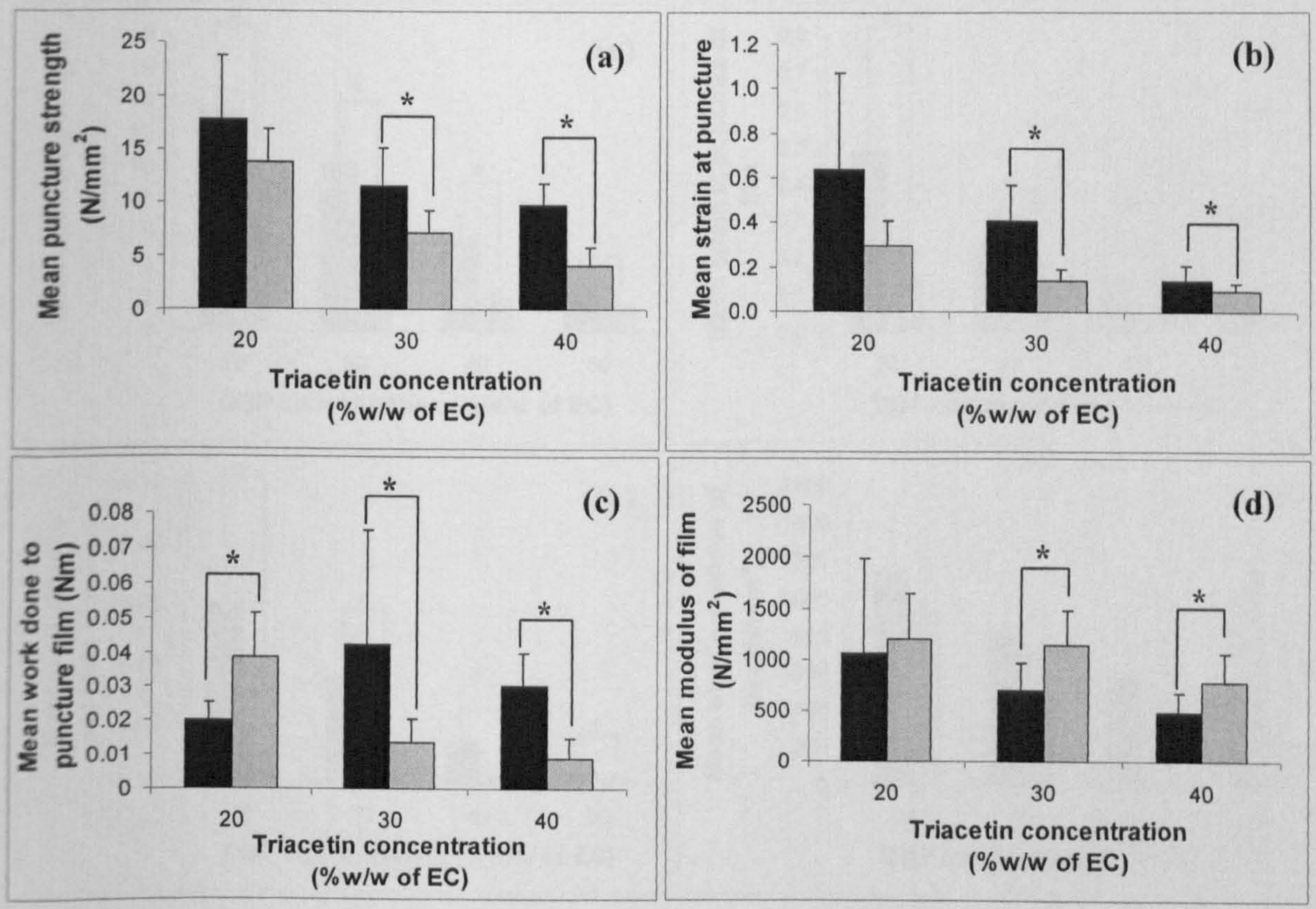

Figure 5.23: Effect of storage on (a) mean puncture strength, (b) mean strain at puncture, (c) mean work done to puncture film and (d) mean modulus of film (n=12 ± S.D.) ■ fresh; ■ aged 3 months 3%(w/v) films plasticised with triacetin. * denotes significant difference.

Ageing of films resulted in decreases in mean puncture strength, mean strain at puncture and mean work done to puncture film while mean modulus of film generally showed an increase (Figure 5.23). Significant effects were more evident with the higher concentrations of triacetin, implying that plasticisation impacts on the stability of EC films.

Decreases in all the puncture properties were observed in films plasticised with DBP (Figure 5.24). Similarly to the triacetin-plasticised films, DBP decreased the rigidity and extensibility of the films. They tended to age to a greater degree in comparison to those plasticised with triacetin based on the observation that significant effects were found at the lower concentrations of plasticiser (20%w/w of EC). Based on the fact that triacetin was more hydrophilic than triacetin, it was possible that water would be more attracted to the triacetin-plasticised films, reducing the extent of water loss.

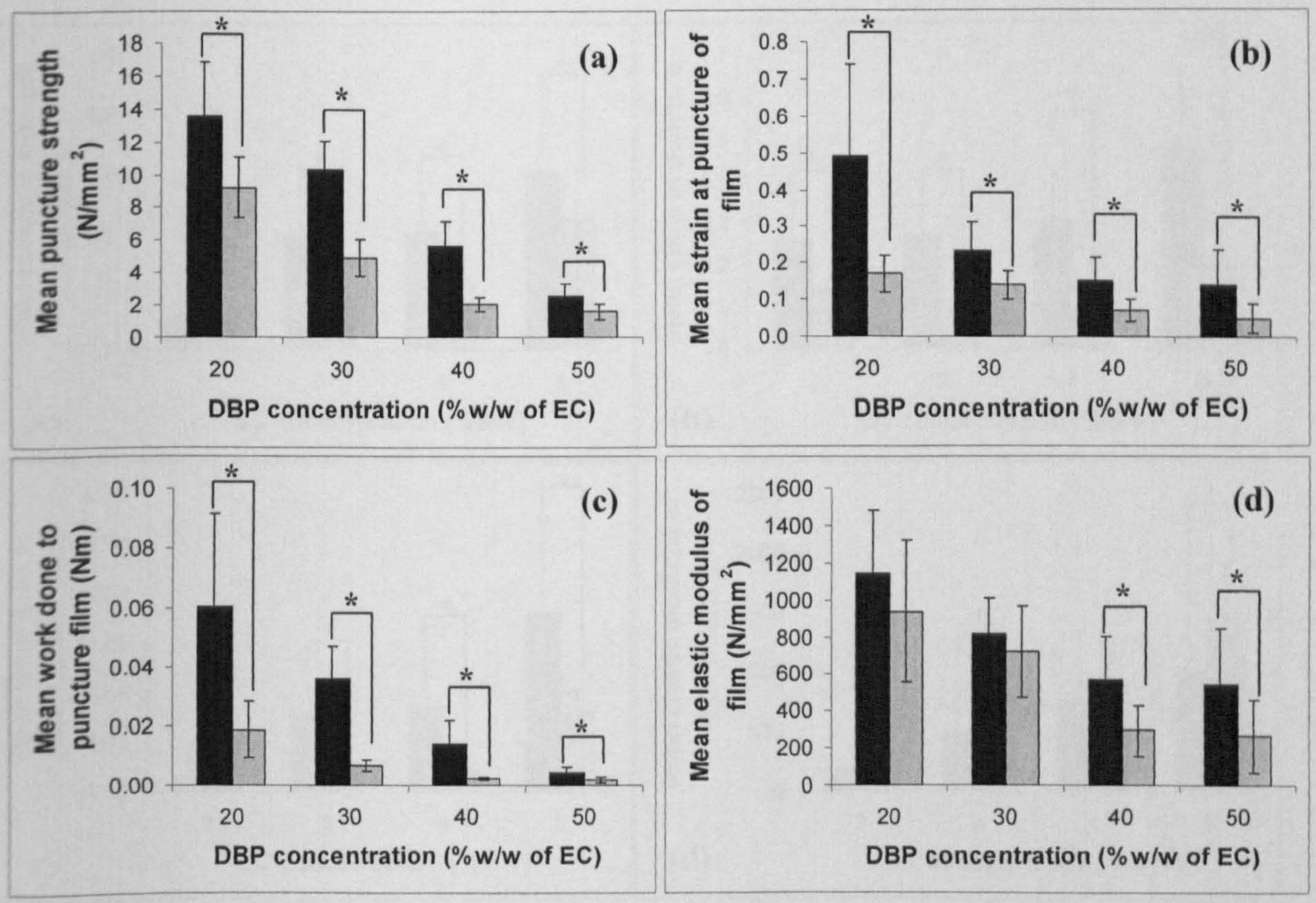

Figure 5.24: Effect of storage on (a) mean puncture strength, (b) mean strain at puncture, (c) mean work done to puncture film and (d) mean modulus of film (n=12 ± S.D.) ■ fresh; ■ aged 3 months 3%(w/v) films plasticised with DBP. * denotes significant difference.

The data presented in Figure 5.25 indicated that plasticisation was not the sole determinant of loss of mechanical integrity over time. The films of varying EC concentrations but constant plasticiser weight exhibited a reduced ability to withstand stress, rupturing at a lower force and poorer stretchability.

From Figures 5.23, 5.24 and 5.25, it was clear that these changes in properties over time will impact on the accuracy of the lag time incorporated by the EC coat, necessitating careful selection of packaging and storage requirements.

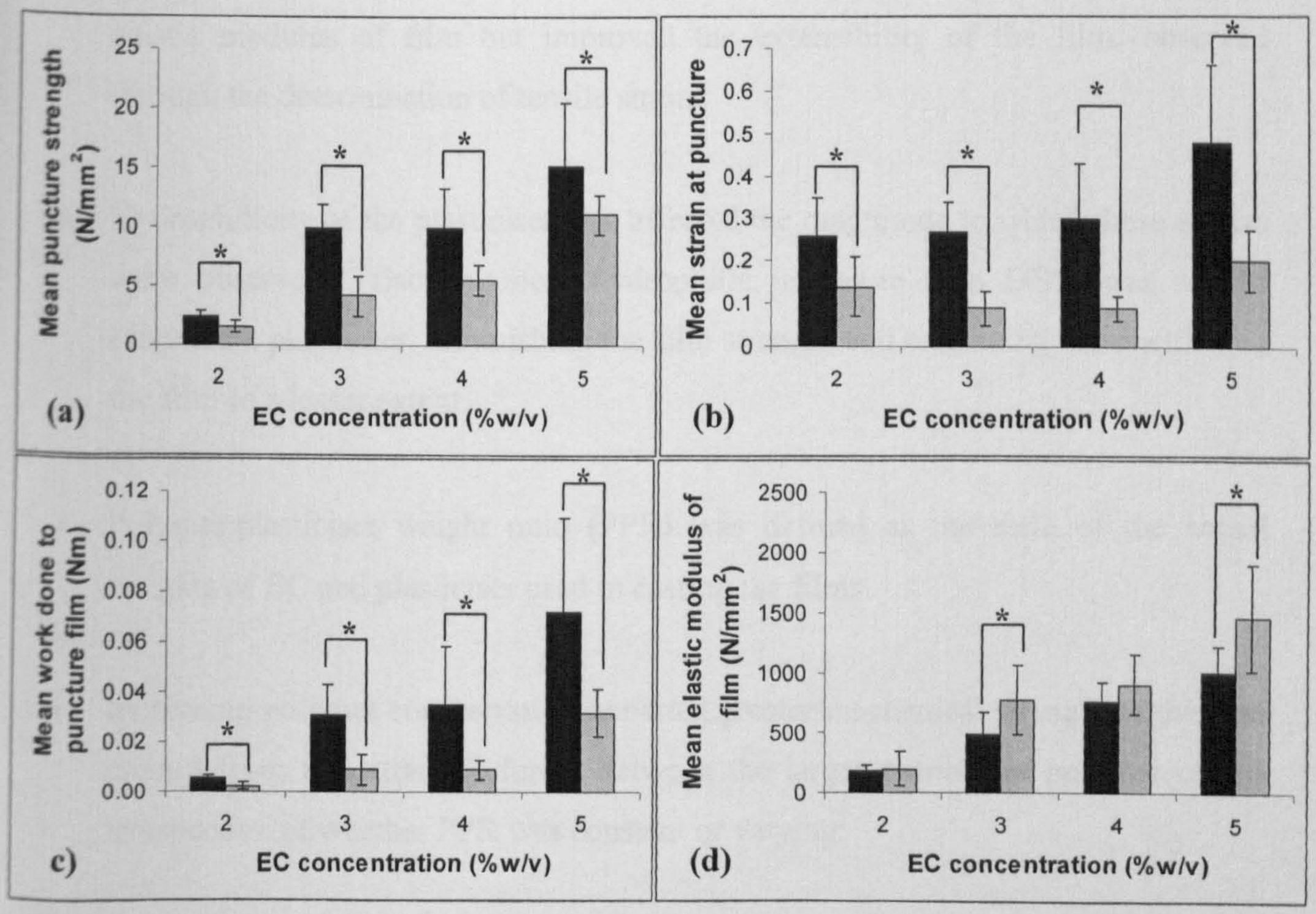

Figure 5.25: Effect of storage on (a) mean puncture strength, (b) mean strain at puncture, (c) mean work done to puncture film and (d) mean modulus of film (n=12 ± S.D.) ■ fresh; ■ aged 3months 1.8g triacetin-plasticised films. * denotes significant difference.

5.5 Conclusions

- Solvent-cast EC films proved to be a suitable model for predicting the effects of formulation variables such as plasticiser and polymer concentration as well as environmental effects e.g. water uptake and ageing.

- Mechanical properties of the films were determined through two methods, tensile testing which stretched the films to break point, and puncture testing which ruptured taut films using a stainless steel cylindrical probe, both using the Texture Analyser.

- Increasing plasticisation levels generally reduced the mechanical strength of the films, reflected in a decrease in tensile strength, work done to break film and

elastic modulus of film but improved the extensibility of the film, observed through the determination of tensile strain.

- Hydrophilicity of the plasticiser also affected the magnitude to which these effects were observed. Triacetin, more hydrophilic in nature than DBP, was not as effective a plasticiser, diminishing the film strength and enhancing the ductility of the film to a lesser extent.

- Polymer:plasticiser weight ratio (PPR) was defined as the ratio of the actual weights of EC and plasticiser used in casting the films.

- Increasing polymer concentration imparted greater mechanical strength to the film arising from the attractive forces between the larger number of polymer chains irrespective of whether PPR was constant or varying.

- It was evident that plasticisation was a more significant determinant of film ductility when films with constant PPR did not display any changes in strain when polymer concentration was altered. Tensile strain at break of film did decrease however when PPR increased.

- The puncture test was considered to mimic the actual conditions under which the EC coat of the dosage form would rupture. However, limitations were found from the strain data collated. Improvements on the experimental setup on the Texture Analyser will have to be made.

- Moisture sorption and desorption studies performed on the DVS showed that moisture uptake by the films was reversible; water was not permanently bound to the polymer or plasticiser molecules. Moisture uptake decreased as triacetin concentration increased, but was unaffected by DBP concentration.

- DSC of the EC films to determine the effects of plasticisation on glass transition temperature was unsuccessful, necessitating alternative experimental methods in preparation of the sample.

- Examination of the film surface through SEM revealed the effect of varying polymer and plasticiser concentration on the physical characteristics of the films. This allowed correlation to the tensile and puncture properties observed.

- Incubation in 37°C water did not affect the EC films except at extreme levels of plasticisation. This indicated that the EC films would retain their mechanical properties upon introduction to the gastrointestinal tract.

- Ageing of the films was performed at ambient temperature in a sealed, dry container. Puncture testing revealed that the films' resistance to applied stress generally decreased as well as their ability to withstand stretching. DBP-plasticised films became less rigid while their triacetin-plasticised counterparts increased in rigidity, shown in the elastic modulus measurements.

- These observations indicated that future packaging requirements for the final dosage form would have to be very strict in order to maintain the structural integrity of the EC coat as it was one of the most important determinants of lag time.

CHAPTER 6

FORMULATION, MANUFACTURE AND TESTING OF THE TIME-DELAYED OIL-FILLED CAPSULE

6.1 Introduction

As discussed in Section 1.3, time-controlled drug delivery enables the overcoming of various obstacles to optimisation of drug absorption. Colon targeting and pulsatile release coinciding with physiological events controlled by circadian rhythm are just two examples of drug delivery opportunities afforded by this field.

Fukui *et al.* (2000) devised enteric-coated, timed-release, press-coated (ETP) tablets which possessed both pH- and time-dependent characteristics. They acknowledged the difficulty of designing a dosage form which would be unaffected by gastric emptying time. Hence their tablet design, shown in Figure 6.1, incorporated an outer enteric coating to provide gastroresistance, while a layer of erodible material underneath that imparted the desired time lag prior to release of drug from the innermost core.

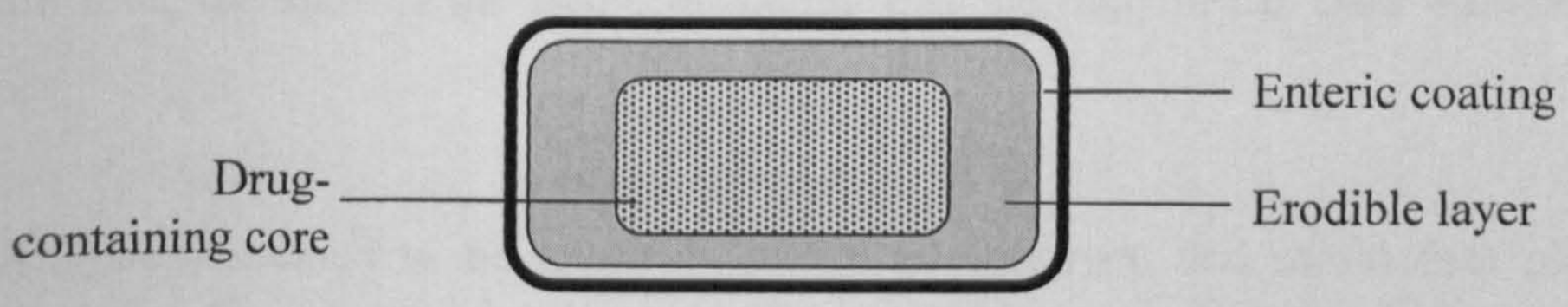

Figure 6.1: ETP tablet (Fukui *et al.*, 2000).

Upon ingestion, the enteric coating (hydroxypropylmethylcellulose acetate-succinate MF, AQOAT®-MF) offered protection against the acid environment of the stomach, preventing premature drug release. Entry into the higher pH conditions of the small intestine promoted the dissolution of the enteric coat, exposing the erodible layer of hydroxypropylcellulose (HPC) which was press-coated onto the core tablet. Once the

erosion front reached the core of drug (and other tabletting excipients) drug release was triggered.

In vitro testing in Japanese Pharmacopoeia (JP) 1st fluid (pH 1.2) revealed that the enteric coating provided acid-resistance even up to 16 hours using the paddle method at 100rpm. No drug release was observed, indicating that the tablets should withstand agitations and abrasions arising from gastrointestinal peristaltic action.

Release profiles from dissolution testing in JP 2nd fluid (pH 6.8) of tablets which had undergone pre-treatment in 1st fluid (as above), and of those which had not, were identical. A lag time of about 3 hours was observed in both cases. The authors claimed that lag time could be tailored by adjusting the weight and composition of the HPC layer.

In vivo testing was conducted in 3 fasted beagle dogs, water *ad libitum*, using tablets with an extra layer of phenylpropanolamine hydrochloride (PPA) between the HPC layer and the enteric coating. The drug incorporated in the core was diltiazem. Shown to be rapidly absorbed, this drug was incorporated as a marker of gastric emptying. Pharmacokinetic profiles from analysis of blood and plasma samples confirmed that the enteric coating provided adequate protection from the acid environment of the stomach; the first detection of PPA was at about 4 hours. Diltiazem was detected 7 hours after the start of the study, indicating that the built in lag time was about 3 hours.

This system seemed to be relatively simple to construct, and initial data pointed towards the achievement of reproducible release profiles. It was likely however, that the critical element in scale up manufacturing was the accuracy required in ensuring the placement of the drug core during press coating of the erodible layer.

The ETP tablet was very similar to the Chronotopic™ system first envisioned by Gazzaniga *et al*. (1994) that consisted of a drug loaded core coated by a hydrophilic swellable layer (Figure 6.2).

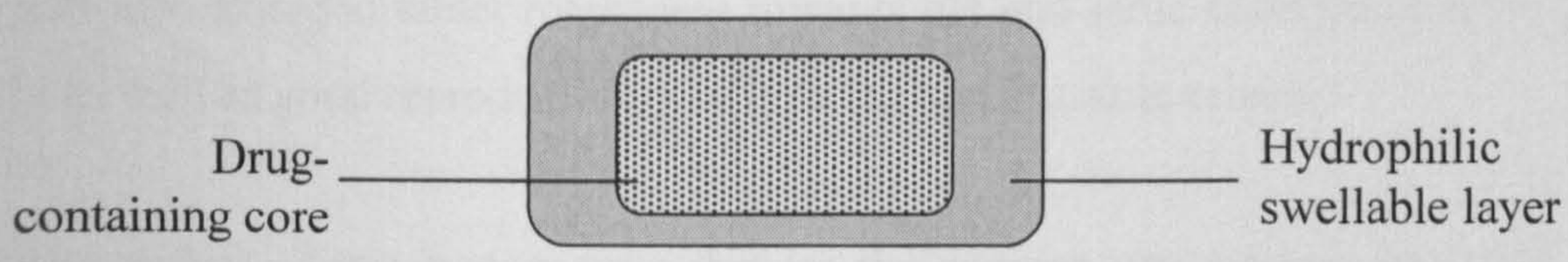

Figure 6.2: The basic Chronotopic™ system.

Upon immersion in an aqueous environment, the hydrophilic layer, HPMC, underwent transition from glassy to rubbery state, eliciting gradual erosion of the layer to finally expose the drug core allowing dissolution. Hence the desired profile of pulsatile release following a built-in lag time dependent on the physicochemical characteristics of the hydrophilic layer was obtained.

Sangalli *et al.* (2001) also capitalised on the relative independence of small intestinal transit time on the fasted or fed state and on the size and type of dosage form, applying an enteric coating to the Chronotopic™ system to prevent disintegration in the stomach. Therefore, the 'countdown' timer for the time-delayed component of the system was only started when the dosage form emptied from the stomach.

The group obtained good *in vivo-in vitro* correlation when the enteric-coated systems were tested on four human volunteers. Salivary antipyrine concentration was used as a marker for drug release. When compared to lag times derived from sequential dissolution in USP 24 simulated gastric fluid and simulated intestinal fluid, both without enzymes, the *in vivo* lag times matched very well. Furthermore, there was a linear correlation between HPMC layer thickness and lag time.

When considering scale up to manufacture, Sangalli *et al.* (2004) realised the importance of the spraying procedure being feasible in time, energy and costs spent on it. Three HPMC grades, Methocel® E5, E50 and K4M, of increasing viscosity, were studied, applied onto tablet cores containing paracetamol as marker.

The results obtained proved that the varying viscosities of the polymer were advantageous in one aspect but lacking in others. However, they determined that the polymer with the best balance of spray-coating time, retarding ability, size of the final dosage forms and ability to adjust the time lag incorporated was Methocel E50. This

polymer also afforded tablet robustness towards pH and ionic strength of dissolution media as well as good reproducibility of time lag and pulsatile release.

The plus points of this system were that (a) the concept was simple, requiring only two separate components which eases the progression to scale up and (b) manipulation of the physicochemical characteristics of the HPMC layer provided for adequate tailoring of the release profile for specific requirements.

Bussemer and Bodmeier (2003) attempted to formulate pulsatile release dosage forms based on soft gelatin capsules. Figure 6.3 depicted the basic structure of their design.

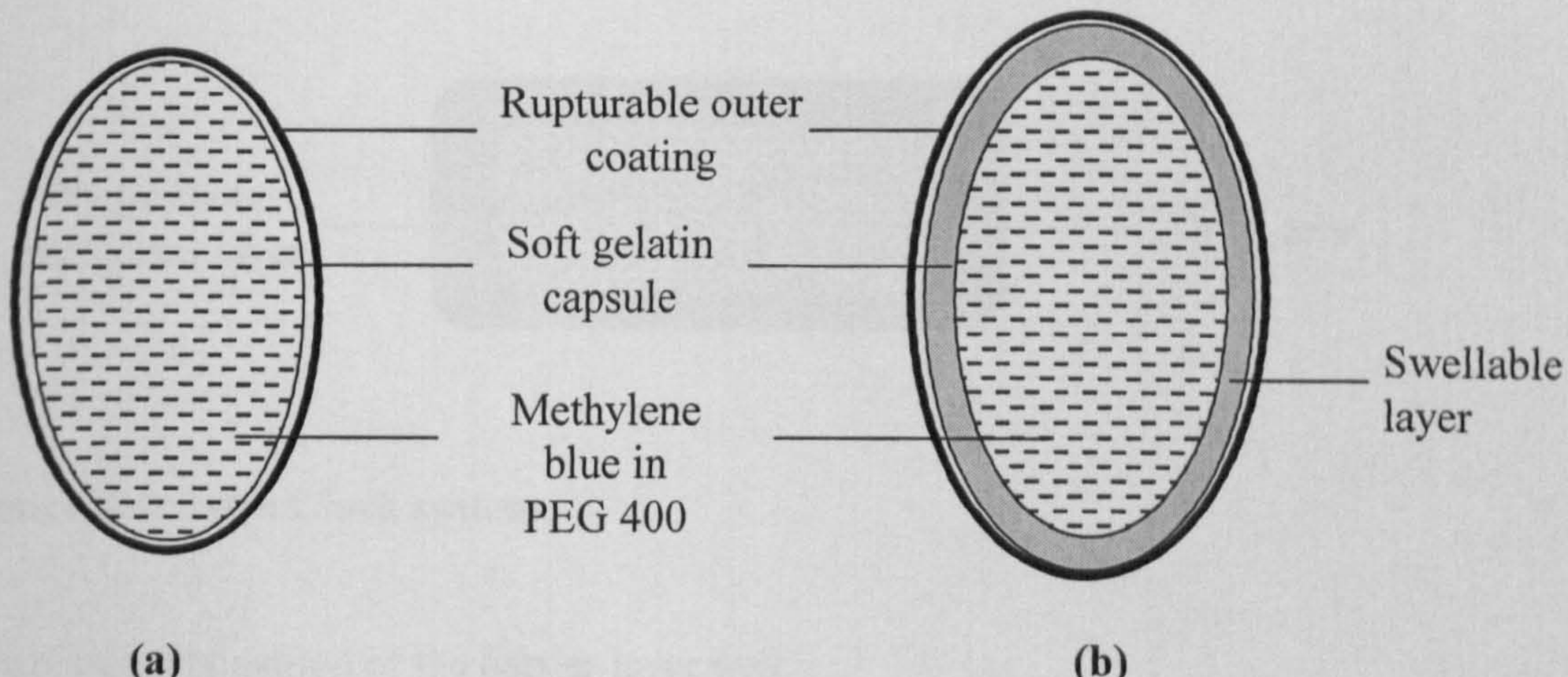

Figure 6.3: Coated soft gelatin capsule for pulsatile release: (a) without swellable layer, and (b) with swellable layer.

The workers believed that this system would be suited for pulsatile delivery of liquids after a pre-determined lag time built in by the water-insoluble but water-permeable outer coating. Ethylcellulose and cellulose acetate propionate were found to display desirable properties of ease of spray-coating and brittleness of the resultant coat which were lacking in the more flexible Eudragit RS. It was a prerequisite that the coating ruptures completely to allow drug release once its tolerance limit was exceeded, and not just expand and crack slightly on the surface, as was found with the Eudragit.

The second phase of formulation necessitated adaptation of the dosage form; incorporating a swelling layer to aid rupturing of the brittle coat. It was found that the

pressure generated by swelling of the gelatin capsule alone (Figure 6.3a) was insufficient. Ac-Di-Sol (croscarmellose sodium) was selected due to its superdisintegrant power, and was sprayed from an ethanolic solution with polyvinylpyrrolidone as binder.

This system proved promising from the initial *in vitro* dissolution profiles obtained, adjustment of lag time was enabled by changing coating thickness, and possibly thickness of the swelling layer, although not reported.

Pozzi *et al.* (1994) designed oral dosage forms, both tablets and capsules, based on the simple barrier method to incorporate time delay, as shown in Figure 6.4.

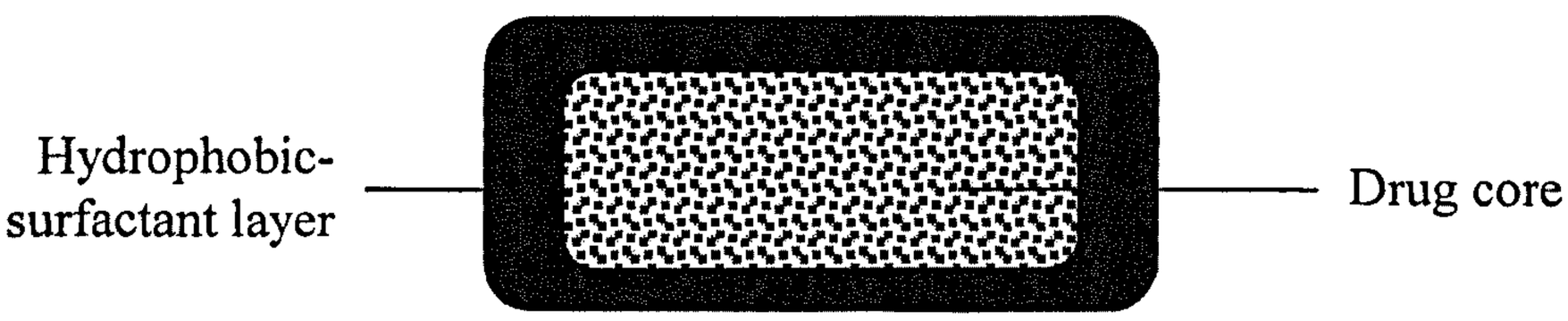

Figure 6.4: Time Clock system.

A typical composition of the barrier layer was:

(a) hydrophobic components: carnauba wax and white beeswax

(b) surfactant: polyoxyethylene sorbitan monooleate (Tween 80)

(c) hydrosoluble component for improved adhesion to core: HPMC (Methocel E15)

The hydrophobic-surfactant layer was sprayed onto the dosage form as an aqueous dispersion using conventional fluid bed coating equipment, hence removing the need for specialised spraying apparatus.

In an aqueous environment, the barrier layer would rehydrate and redisperse at a rate dependent on thickness and composition. Once the inner drug core, usually containing soluble components such as lactose and disintegrants e.g. corn starch was hydrated, it would disaggregate resulting in rapid and complete release of drug.

From *in vitro* and *in vivo* (pharmacoscintigraphic) studies, the performance of Time Clock tablets were shown to be independent of pH, gut peristalsis and the fed/fasted state. These initial studies were conducted on one tablet formulation but variations in hydrophobic barrier layer and drug core composition should allow for further manipulation of lag time and release properties.

This group also applied an enteric coating to the Time Clock system to achieve colonic targeting (Wilding *et al.*, 1994). Scintigraphic studies showed that the enteric-coated tablets did indeed start to disintegrate lower down the gastrointestinal tract as compared to the uncoated ones (Pozzi *et al.*, 1994). However, the actual disaggregation of the tablet was slower possibly due to the lack of motility in the large intestine compared to the upper regions of the gastrointestinal tract. Although only six subjects were used, the intra-subject variation in rate of tablet disintegration proved that timed-release formulations, with or without enteric coating, were still dependent on the quite unpredictable physiology of the gastrointestinal tract.

6.2 Aims and objectives

Utilising the information derived from the pre-formulation characterisation of the swelling agent, LH-21 and the ethylcellulose outer coating as well as literature sources, the manufacture of the novel time-delayed oil-filled capsule (Figure 6.5) was attempted.

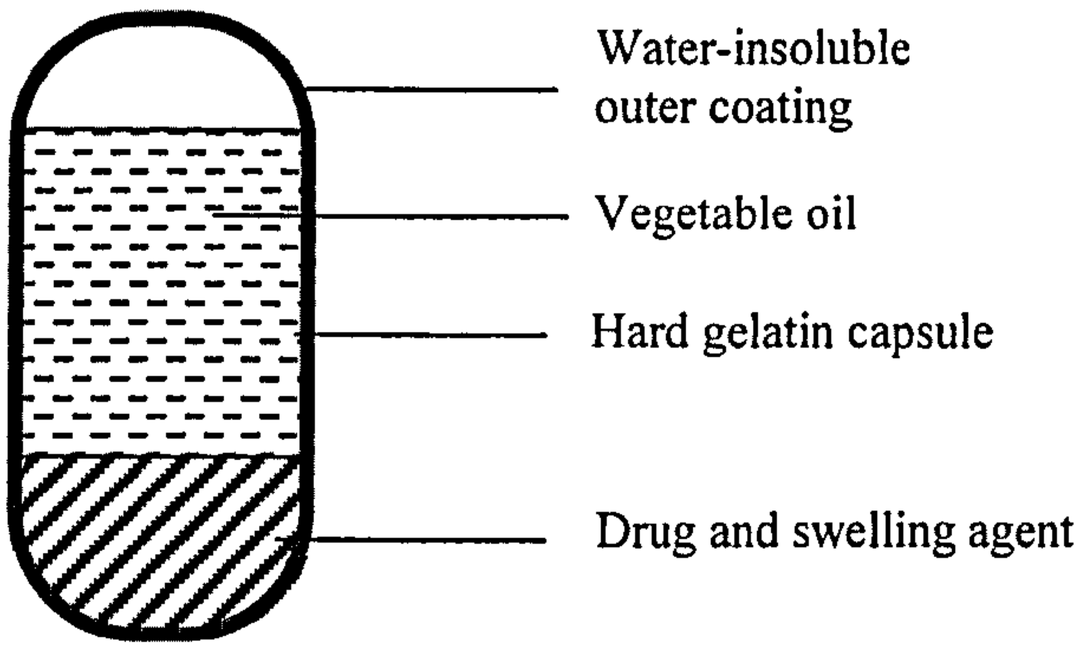

Figure 6.5: Proposed structure of novel dosage form.

Following assembly of the dosage form, dissolution testing was performed to determine the ability to generate reproducible pulsatile release profiles with a built in time lag. Variations in coating level and swelling agent content were also investigated in order to assess the feasibility of manipulating the release profile.

6.3 Methods

The methods used are summarised in Table 6.1 and referenced, where appropriate, to the detailed descriptions in Chapter 2.

Table 6.1: Summary of methods used in Chapter 6.

Section	Method	Methods section
6.4.1	**Manufacture of time-delayed oil-filled capsule**	
6.4.2	**Initial studies with griseofulvin as model drug**	
6.4.3	**Initial studies with paracetamol as model drug**	
6.4.4	**Paracetamol release from EC-coated capsule with higher LH-21: corn oil ratios**	
	Construction of Variation 1 capsule	2.6.1
	Gelatin banding with brush	2.6.3.1
	Adaptation of LEMS® technique	2.6.3.3
	Preparation of coating solution	2.6.4.1
	Spray coating with Aeromatic Strea fluidised bed coater	2.6.4.2
	Dissolution testing	2.6.6
6.4.5	**Gelatin banding capsule with bench-scale capsule banding machine**	
	Gelatin banding with bench-scale capsule banding machine	2.6.3.2
	Spray coating with Aeromatic Strea fluidised bed coater	2.6.4.2
	Capsule leak test	2.6.5
	Dissolution testing	2.6.6

6.4.6	**Dipcoating as an alternative coating method**	
	Adaptation of LEMS® technique	2.6.3.3
	Dipcoating	2.6.4.4
	Dissolution testing	2.6.6

6.4 Results and discussion

6.4.1 Manufacture of the time-delayed oil-filled capsule

Methods of manufacture initially attempted and problems encountered were as follows:

Table 6.2: Formulation methods and reasons for unsuitability.

Method	Problem
Filling the capsules under oil to prevent formation of air bubble which could lessen swelling impact of LH-21.	Exterior of capsule was coated with oil residue, hampering optimum coating.
Coating unsealed capsules in fluidised bed coater.	Leakage of capsule contents was overwhelming, impeding coating and resulting in writing off entire batch.
Sealing capsules with solution prepared from dissolving hard gelatin capsules in water to form a 15%(w/v) solution.	Insufficient sealing power, capsules still leaked in coater.

Hence the first capsules were produced by filling the suspension of model drug (griseofulvin) and LH-21 in soybean oil with a plastic syringe, capping and locking the capsules without sealing and coating in the fluidised bed coater. Instead of the 0.5%(w/w) weight gain anticipated from EC coating, a 1.5%(w/w) weight loss was calculated.

Various reasons for this anomaly were proposed:

- Leakage of capsule fill thereby causing weight loss from capsules
- Consequent oily surface prevented adherence of polymer solution rendering film formation impossible
- Water content of hard gelatin capsules (about 13%) was driven off due to heating of capsules in the coater

Nevertheless, the first capsules obtained were tested simply by placing them into a large glass beaker filled with warm distilled water, without agitation. Within 30 minutes, a droplet of oil had formed at the shoulder of the capsule, as shown in Figure 6.6.

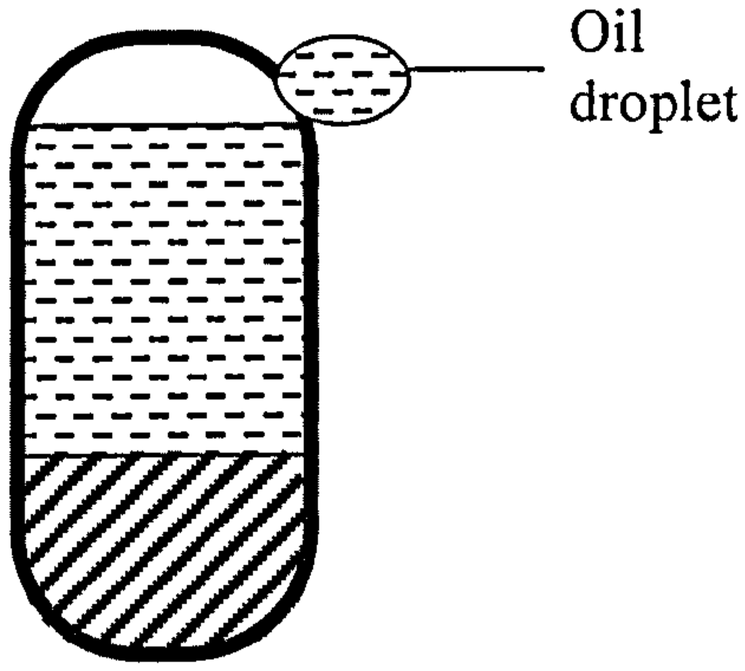

Figure 6.6: Release of oil droplet at shoulder of capsule.

However, at this early stage of product development, it could not be ascertained whether the release of oil was due to rupturing of the coat from swelling force generated by LH-21 or non-uniform coating of EC, resulting in an uncoated portion of the capsule allowing gelatin dissolution and escape of oil.

Trial and error led to the derivation of the method used for consequent manufacture of batches:

1. LH-21 and model drug (paracetamol or griseofulvin) were dry blended prior to trituration with corn oil.
2. Using a micropipette, the desired volume of suspension was filled into the body of the capsule from a stirred stock solution.
3. The capsules were sealed using one of the three methods described in Section 2.6.3 (molten gelatin banding with brush or bench-scale Qualiseal machine or adaptation of LEMS®).
4. Coating was performed in either a fluidised bed coater (Section 2.6.4.2); the different formulations being identified through different capsule colours, or by dipcoating, to minimise the possibility of leakage arising from the rough, tumbling motion of the coater.

6.4.2 Initial studies with griseofulvin as a model drug

This antifungal was chosen to be a model drug due to its hydrophobicity and possession of a chromophore, allowing ease of detection by UV absorbance. A 1mg/100mL solution in distilled water was prepared and from this stock, serial dilutions were made and analysed using a stand-alone UV spectrophotometer. Peak absorbances were observed at 295, 238 and 211 nm, the first wavelength giving the maximum absorbance value for the stock solution, therefore it was selected for dissolution testing (Section 2.6.6).

Testing of blank capsules i.e. without griseofulvin, showed negligible absorbances at 295nm, ensuring that any detected absorbance would be due to release of drug alone.

6.4.2.1 Effect of LH-21 concentration

In this set of studies, the amount of drug per capsule was fixed at 2mg contained within a 0.4mL suspension of drug and LH-21 in soybean oil. The capsules (and dummy capsules to give a total bed load of about 300g) were coated batch by batch, according to LH-21 concentration, in the fluidised bed coater to achieve a nominal mean weight gain of 0.5%.

Table 6.3: Weight gain by griseofulvin capsules (and dummy capsules) post-coating.

LH-21(%w/v)	Weight gain (%w/w)
0	-0.30
10	-0.58
20	0.52
30	0.12

These variations in coating efficiency could be attributed to the reasons proposed in Section 6.4.1. Nevertheless, visual inspection showed no obvious deformities hence these capsules underwent automated dissolution testing.

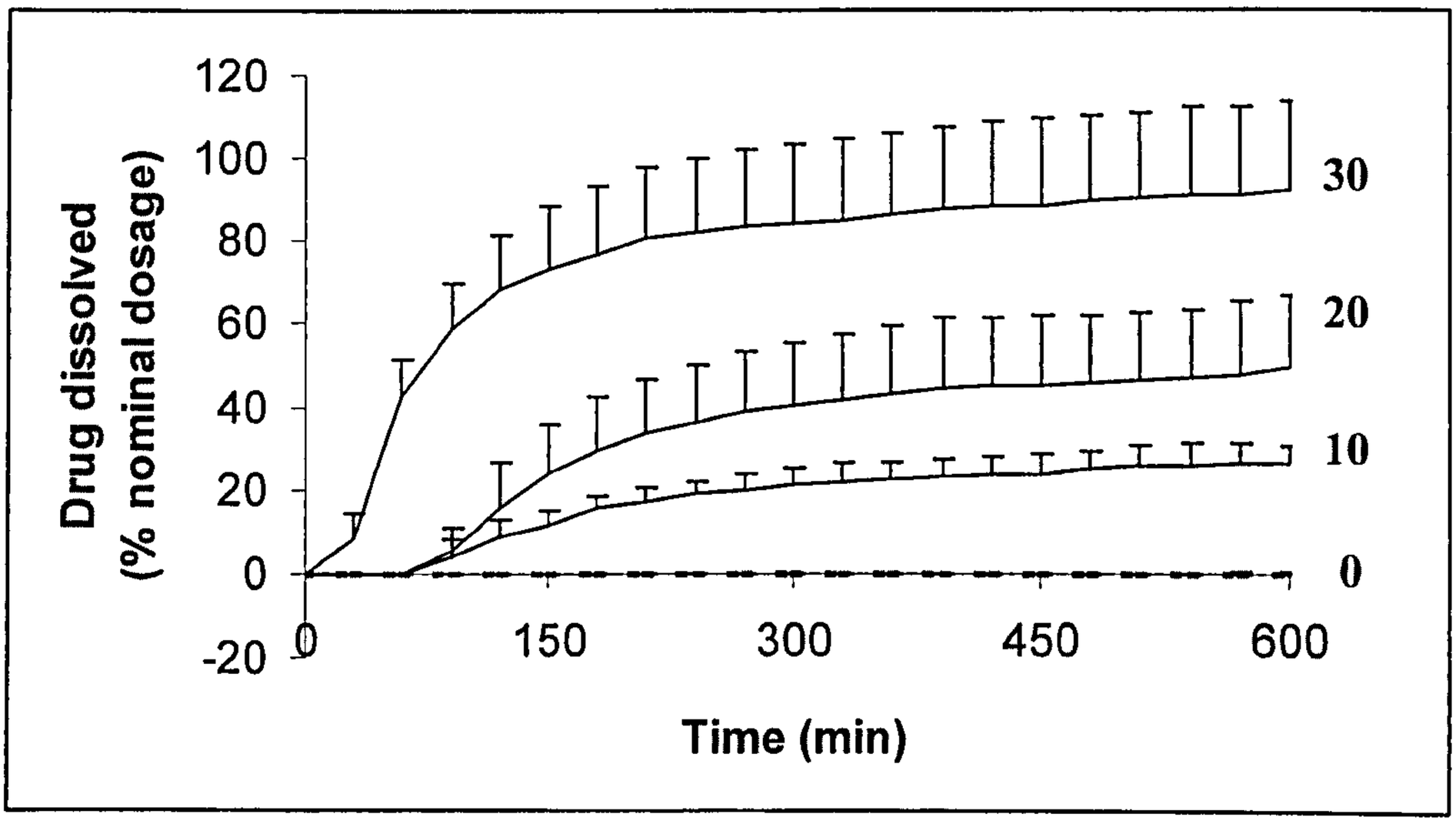

Figure 6.7: Effect of LH-21 concentration on release of griseofulvin from oil-filled capsules with nominally 0.5%(w/w) EC coating (3<n<6, ± S.D.) Numbers 0 to 30 denoted concentration of LH-21 per capsule.

A control set of capsules was prepared without any LH-21. These displayed minimal release of drug throughout the 10-hour dissolution. As the LH-21 concentration increased, the overall amount of drug released also increased, indicating that the swelling agent was aiding expulsion of drug from the capsule cylinder. Furthermore, the lag time decreased with increasing LH-21 concentration, possibly due to the greater swelling force generated inducing rupture of the EC coat at a faster rate.

These preliminary studies were promising and strengthened the credibility of the concept. However, griseofulvin was not a suitable model drug as its solubility in water was very limited. A better dissolution medium would contain bile salts such as sodium cholate and sodium taurocholate (De Smidt *et al.*, 1991). These surfactants were proposed as cholic acid is one of the major bile acids in the small intestine which have been shown to increase the solubility and hence, absorption, of the drug via micellar solubilisation. Preparation of dissolution media with added surfactants was not feasible with the number of studies planned to investigate the various parameters, hence a more water-soluble drug, paracetamol was introduced, in order to retain distilled water as a simple dissolution medium. Soybean oil was also replaced with corn oil, which was available in abundance in our laboratory. It was not expected to impact greatly on the mechanism of drug release.

6.4.3 Initial studies with paracetamol as a model drug

Calibration of the UV spectrophotometer connected to the automated dissolution apparatus was performed according to the method in Section 2.5.3.2. The wavelength at which peak absorbance was obtained was 249nm.

The capsules in this series were filled by weight, as volumetric dosing was not accurate due to the high viscosity of the suspension. Corn oil density was estimated to be 0.88±0.06g/mL, by weighing 20mL corn oil samples (n=5). Table 6.4 detailed the formulations prepared, with each capsule containing 20mg paracetamol and 0.35mL (0.31g) corn oil. Each LH-21 concentration was assigned a specific colour code for capsule body and cap in order to aid identification once all were placed in the fluidised bed coater.

Table 6.4: Capsule fill weights. Capsules were filled to ± 1mg of target weight.

LH-21 (%w/v)	LH-21 (mg)	Total weight of capsule fill (mg)
5	17.5	346
10	35.0	363
20	70.0	398
30	105.0	433
40	140.0	468
50	175.0	503

In addition to investigating the effect of LH-21 concentration, the coating thickness was also varied; 0.5, 1.0 and 2.0%(w/w) in terms of weight gain of capsules post-coating as described previously in Section 6.4.2.1. Fresh capsules were coated on each occasion; the volume of coating solution calculated to nominally provide sufficient polymer for the coating level desired. Figure 6.8 showed the actual weight gains from the coating cycles performed.

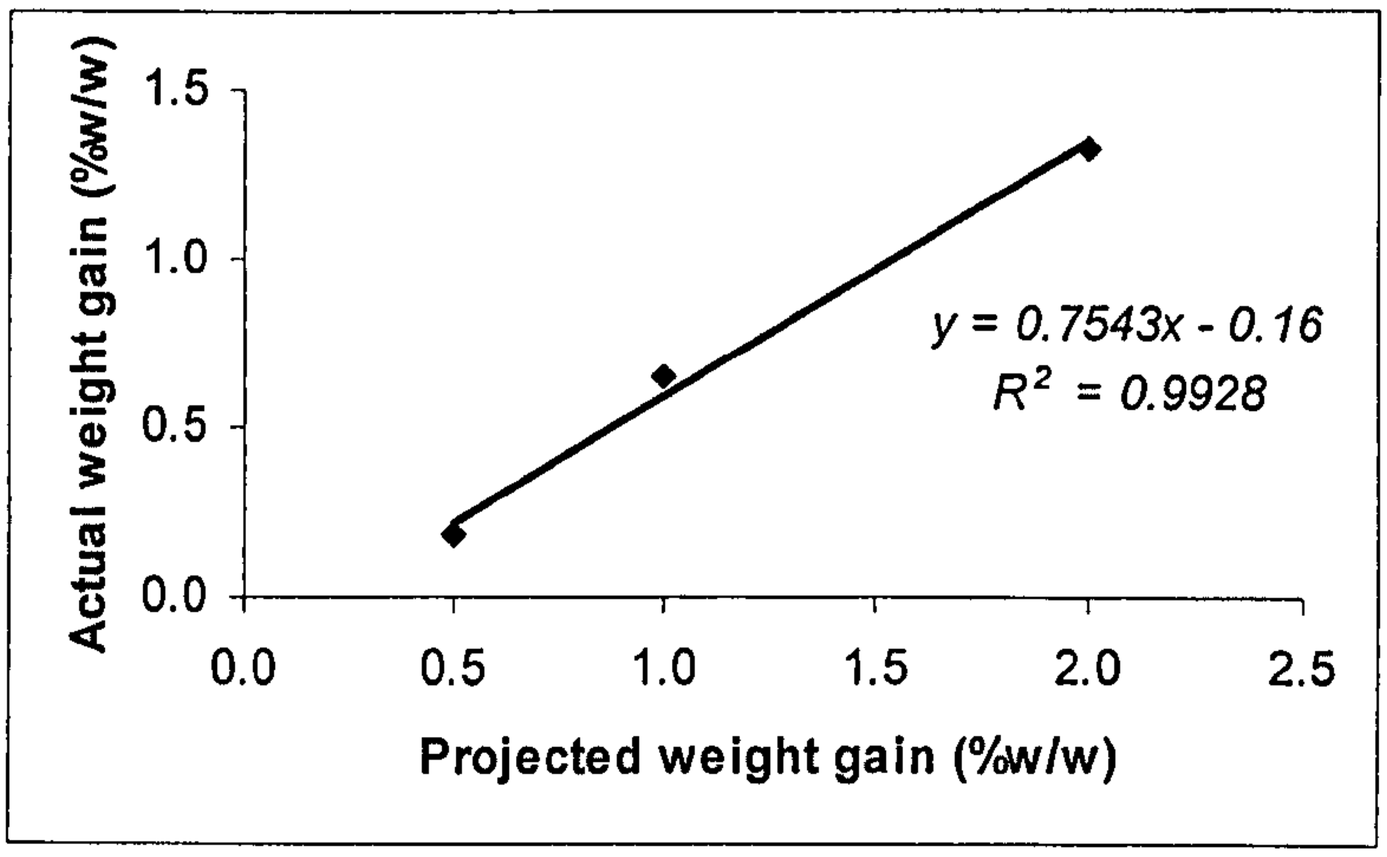

Figure 6.8: Linear relationship between projected and actual weight gains from capsule coating (n=1).

From Figure 6.8, the equation of the line of best fit indicated that the coating efficiency of the Aeromatic Strea-1 fluidised bed coater was about 75%, determined from the slope of the curve. This could be attributed to:

(a) coating polymer deposited on the walls of the chamber; and

(b) poor adhesion of the coating polymer to the capsules due to oily surfaces.

Furthermore, the y-intercept, -0.16, could partially be a consequence of residual water of hard gelatin capsules being driven off by heating cycle, correlating well with the content of water in these capsules nominally being between 13-16% (Capsugel, 1987).

Nevertheless, for ease of comparison, the nominal weight gains will be used in the following discussion of the results obtained from these coated capsules. Sections 6.4.3.1 and 6.4.3.2 discuss the effects of LH-21 concentration and EC coating on capsules based on 0.35mL corn oil volume.

6.4.3.1 Effect of LH-21 concentration

It was anticipated that LH-21 would function as an excellent swelling agent which would firstly swell in contact with water, generating forces sufficient to rupture the outer EC coat. Secondly, it would aid in the expulsion of the capsule contents.

The data presented here focused on the 2%(w/w) EC coat series, although dissolution on 0.5 and 1.0(w/w) EC coat series were also performed. The general trends were similar across the three levels of EC coating.

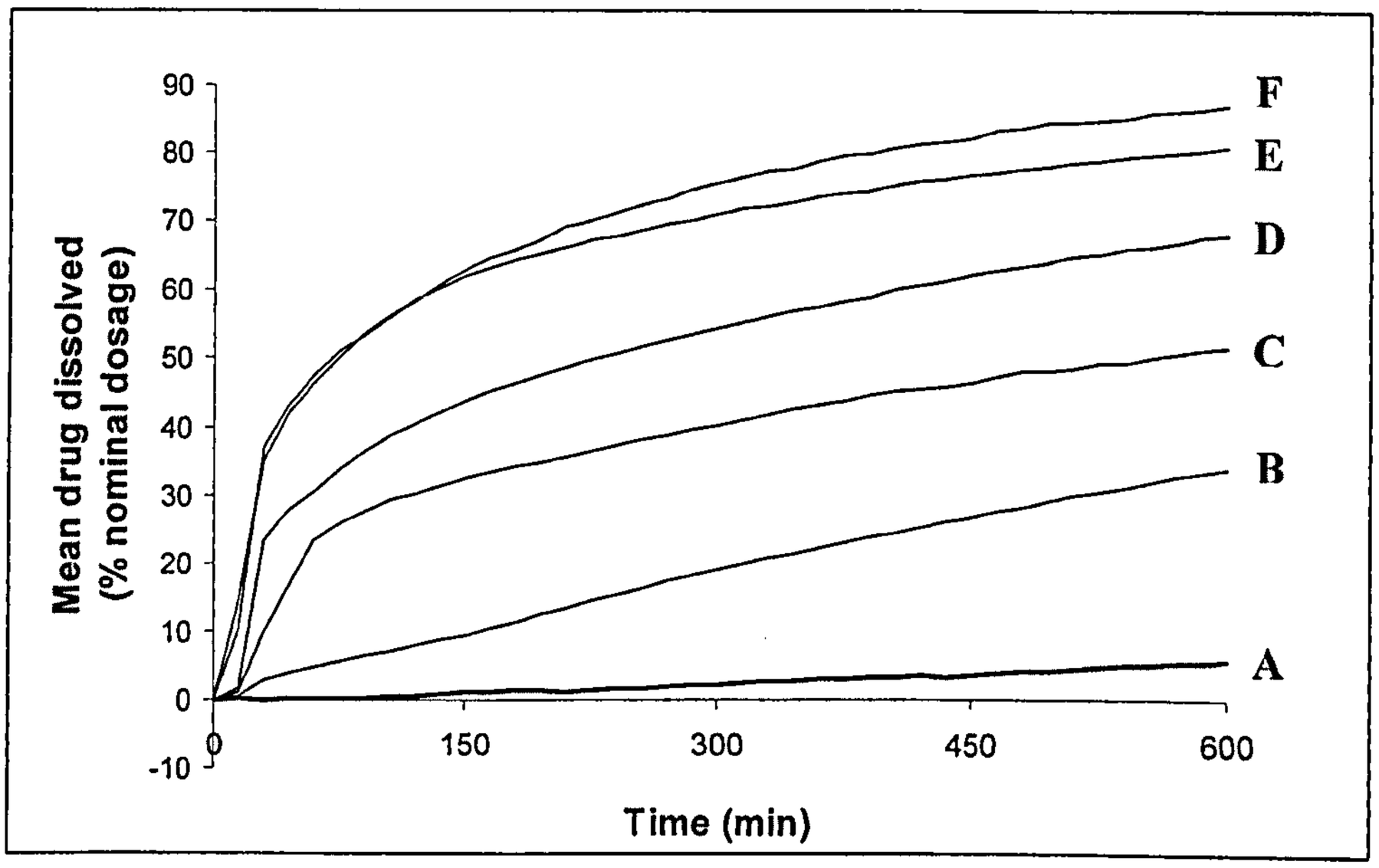

Figure 6.9: Effect of LH-21 concentration on paracetamol release profiles from 2%(w/w) EC-coated capsules (n=6). A-F denote LH-21 concentration (%w/v) whereby A=5, B=10, C=20, D=30, E=40, F=50.

Figure 6.9 confirmed the role of LH-21 as postulated above. As the amount of LH-21 per capsule increased, the following effects were observed:

(a) lag time to initial rupture of capsule and drug release was shortened;

(b) drug release profile changed from sustained release (A and B) to burst release (C, D, E and F); and

(c) total drug released over 10 hour dissolution increased.

Following on from point (b) above, although the burst release effect was more evident as the LH-21 concentration increased, the actual lag time built in by the EC coating was not as pronounced as was expected. 20 and 30%(w/v) LH-21 formulations displayed a mean lag time of about 20 minutes while those containing 40 and 50%(w/v) LH-21 initiated drug release almost immediately. Further studies were conducted to evaluate whether this was due to inadequate thickness of the EC layer or other factors. The results will be discussed in later sections of this chapter.

All concentrations of LH-21 studied were able to rupture the EC coating; the only difference was the rate at which this was effected. This therefore was a variable that could be utilised to manipulate the length of lag time. The only concern was that the release of drug post-rupture was not the desired pulsatile release but that of sustained release, observed with 5 and 10%(w/v) LH-21. Being quite hydrophilic, paracetamol was expected to easily diffuse out of the dosage form interior and dissolve in the medium (water). This was probably hindered by its coating with corn oil. In the capsules with higher concentrations of LH-21 (20-50%w/v) the greater swelling capacity afforded improved expulsion of the drug to the dissolution medium, overcoming the barrier layer of oil. This was confirmed in pictures of the capsules taken after 10-hour dissolution (Figure 6.10).

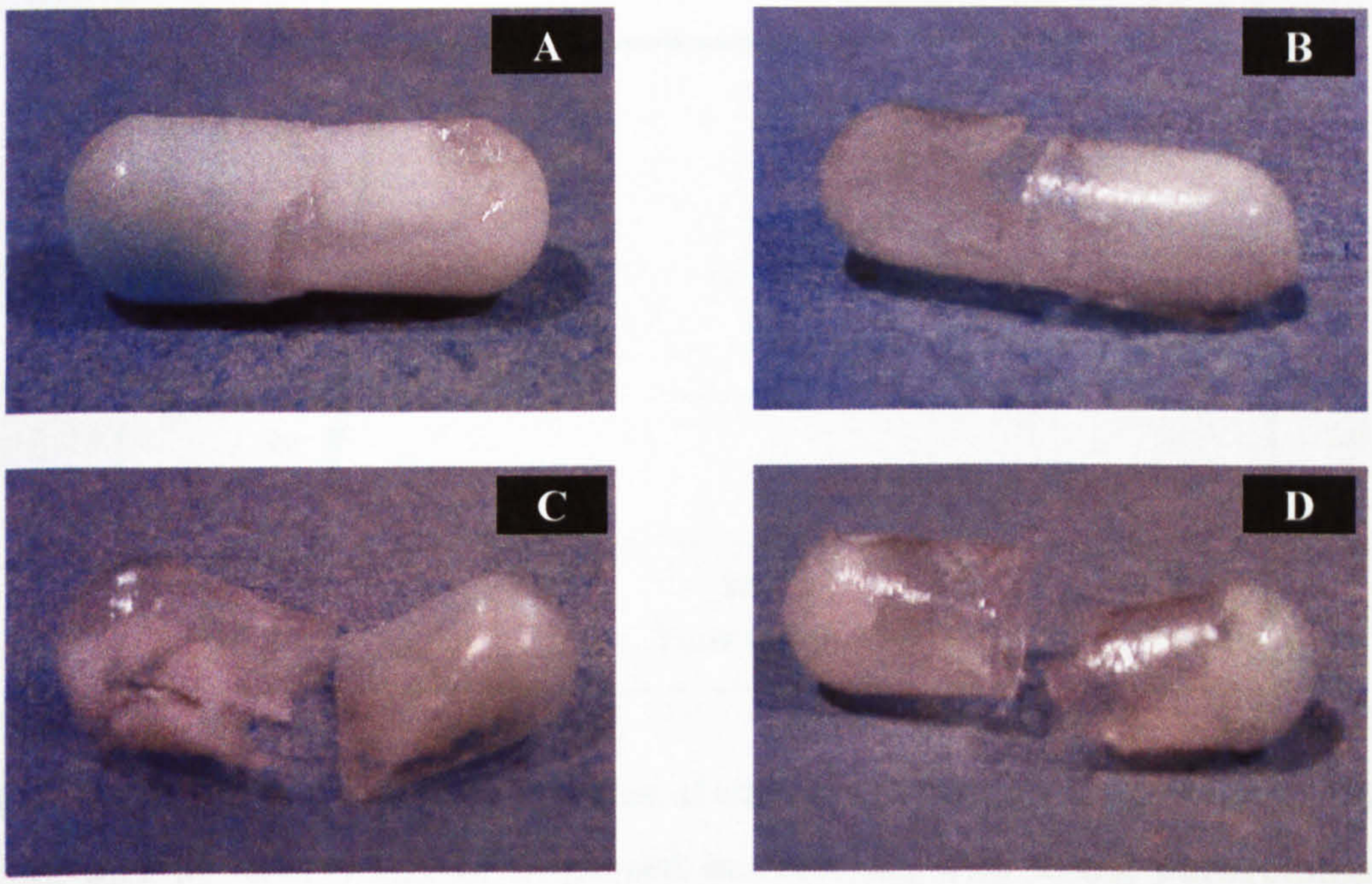

Figure 6.10: Appearance of 2%(w/w) EC-coated capsules post-10 hour dissolution. A-D denote LH-21 concentration (%w/v) where A=5, B=20, C=30 and D=40.

From Figure 6.10, the similarity observed was that all the capsules, except for the 5%(w/v) formulation, cracked in the middle section, at the joint between the capsule body and cap. This could be postulated to be the weakest point of the capsule, which was effected by the banding of an aqueous gelatin solution. Although it prevented

leakage of the oily capsule contents, once immersed in water the extra residual water content structurally weakened that junction.

Capsules of the 30 and 40%(w/v) LH-21 formulations had roughly the same amount of fill remaining. This indicated that the swelling of LH-21 functioned in a concentration-dependent manner to bring about the initial rupturing of the EC coat and to expel the capsule contents.

6.4.3.2 Effect of EC coating level

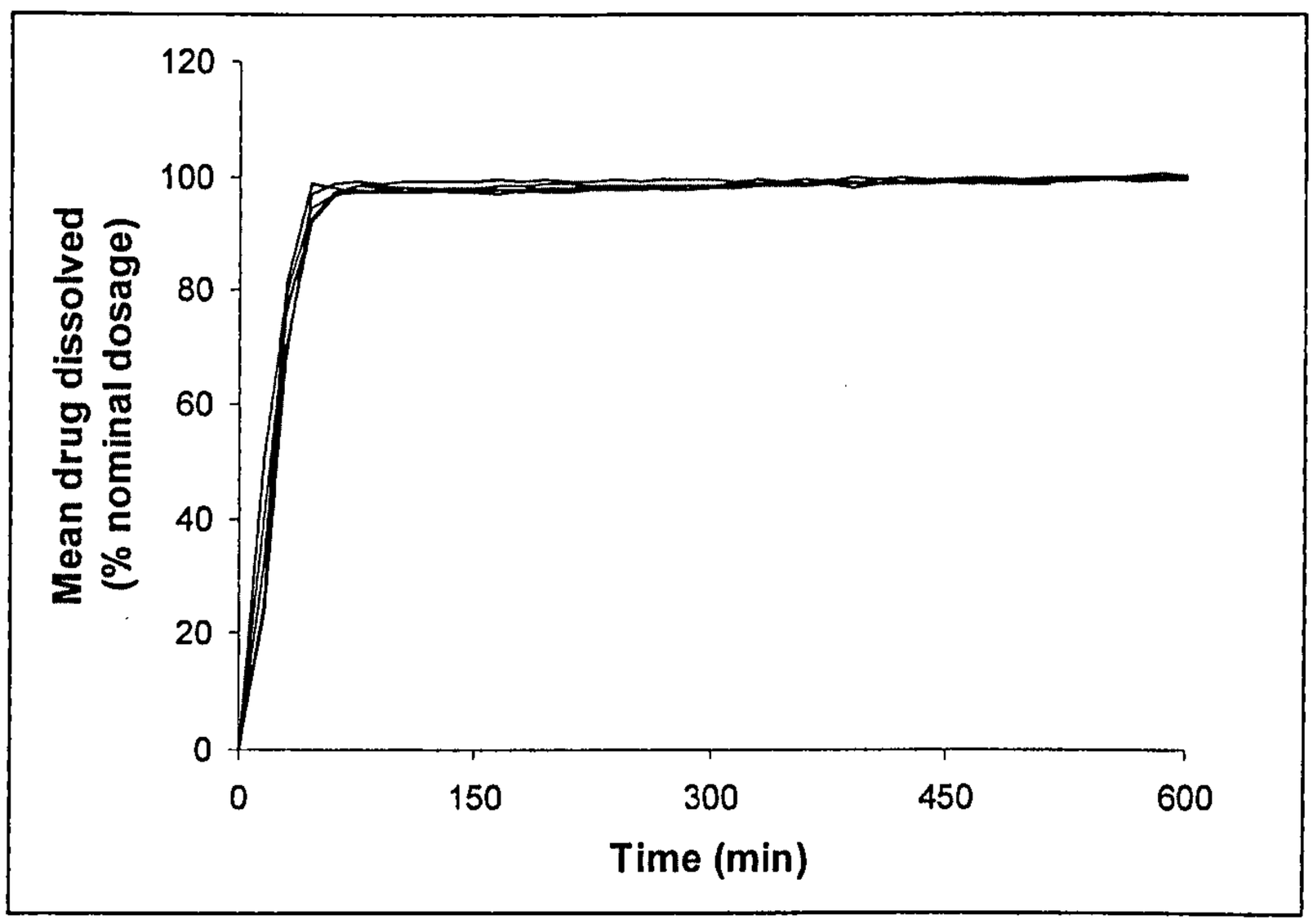

Figure 6.11: Mean dissolution profiles of uncoated capsules containing 5, 10, 20, 30, 40 and 50%(w/v) LH-21 dispersed in corn oil, with 20mg paracetamol as marker drug (n=6).

The control experiment, the results of which were shown in Figure 6.11, showed that the dissolution profiles were independent of LH-21 concentration and corn oil content when there was no EC coating on the capsules. Drug was released immediately after dissolution of the hard gelatin capsule. The hydro-soluble drug was freely available for dispersion and consequent dissolution in the sink conditions of the dissolution vessel. Any barrier effect imposed by the hydrophobic corn oil would have been negligible due to the vast difference in volume between the corn oil and overall dissolution medium.

These results also proved that filling by weight from a suspension of LH-21 and drug in corn oil allowed for accurate dosing.

Taking 40%(w/v) LH-21 as an example, Figure 6.12 showed the effects of increasing levels of EC coating on the mean dissolution profiles.

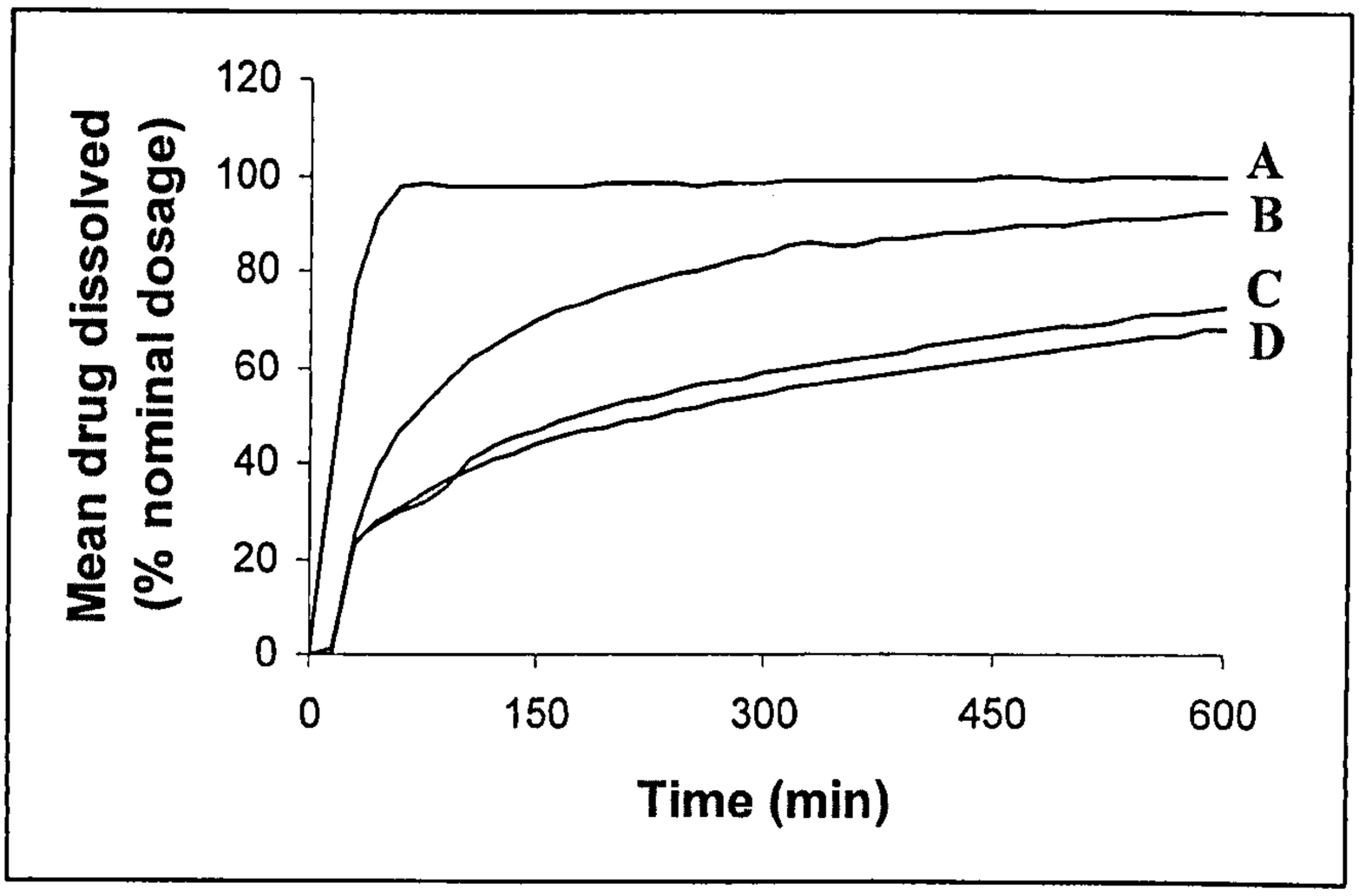

Figure 6.12: Effect of EC coating level of mean dissolution profiles of capsules containing 40%(w/v) LH-21 (n=6). A-D denote nominal EC coating level (%w/w) where A=0, B=0.5, C=1.0 and D=2.0.

The presence of an EC coat introduced a modest lag time to the dissolution profiles shown in Figure 6.12. With increasing levels of EC coating, the magnitude of the initial burst release decreased although the dissolution profiles of 1.0 and 2.0%(w/w) EC coated capsules were almost identical. Additionally, the subsequent release of drug proceeded in a more sustained manner. The total drug released over a 10-hour dissolution cycle also decreased.

Hence the EC coat not only functioned to incorporate timed-release characteristics, it also provided a barrier to drug release as it was a water-insoluble shell containing the drug, mixed into a slurry with the LH-21 and corn oil. The initial burst release was most likely due to drug that was on the outer regions of the slurry, closest to the point of EC coat rupture. Drug that remained was dependent on the influx of water into the EC shell for dissolution and diffusion. The rate of water ingress was then a net result of the impediment posed by hydrophobic corn oil and the attraction of water-soluble

LH-21. On the other hand, since the swollen LH-21 may not actually be expelled from the capsule, there is the possibility that it physically hindered drug release. This was highlighted in Figures 6.10A and B whereby swollen LH-21 was still present post-dissolution.

The data obtained were also analysed in terms of lag time and time to 50% drug release ($T_{50\%}$), shown in Figure 6.13. The graphs show that both LH-21 concentration and EC coating level affect these two parameters.

From Figure 6.13a, the nominal coating of 0.5%(w/w) only increased the mean lag times slightly compared to the uncoated capsules. (Lag time of zero was allocated to formulations which showed drug release at the first reading taken after zero minutes, which was 15 minutes). LH-21 concentration did not seem to affect the mean lag time either. For both 1.0 and 2.0%(w/w) EC coating, there was greater lag time with 5, 10 and 20%(w/v) LH-21 capsules. For LH-21 concentrations above that, the mean lag times were very similar.

This led to the understanding that at lower concentrations of LH-21, EC coating level affected the lag time more than LH-21 concentration. Conversely, at higher LH-21 concentrations, lag time seemed to be independent of coating level. Therefore there was a threshold LH-21 concentration beyond which the swelling power generated would be able to adequately rupture the EC coat, irrespective of its thickness. Similarly for the EC coating level, if higher levels were applied, there would very likely be a limit at which cracking would be impossible despite any amount of LH-21 swelling.

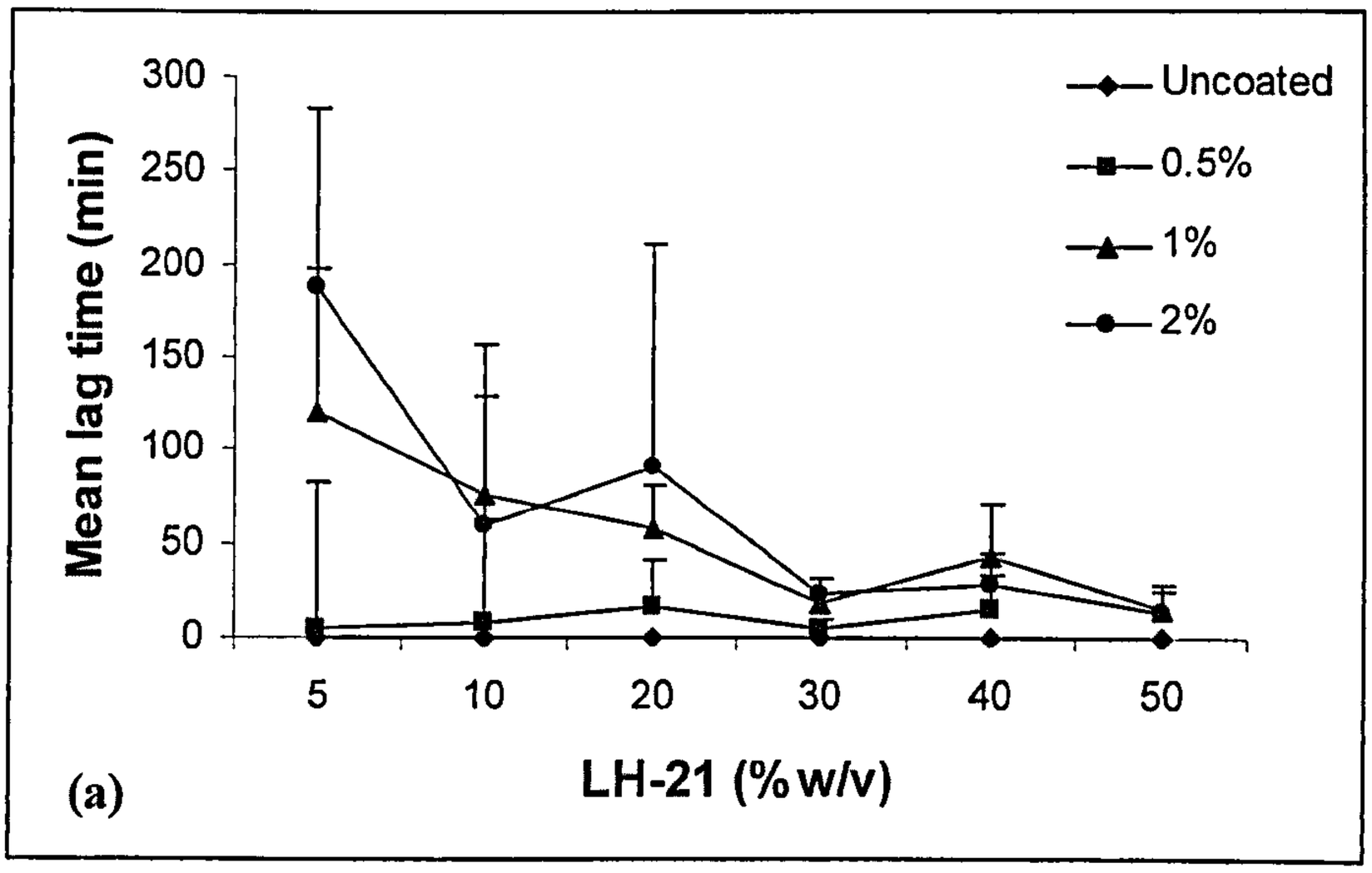

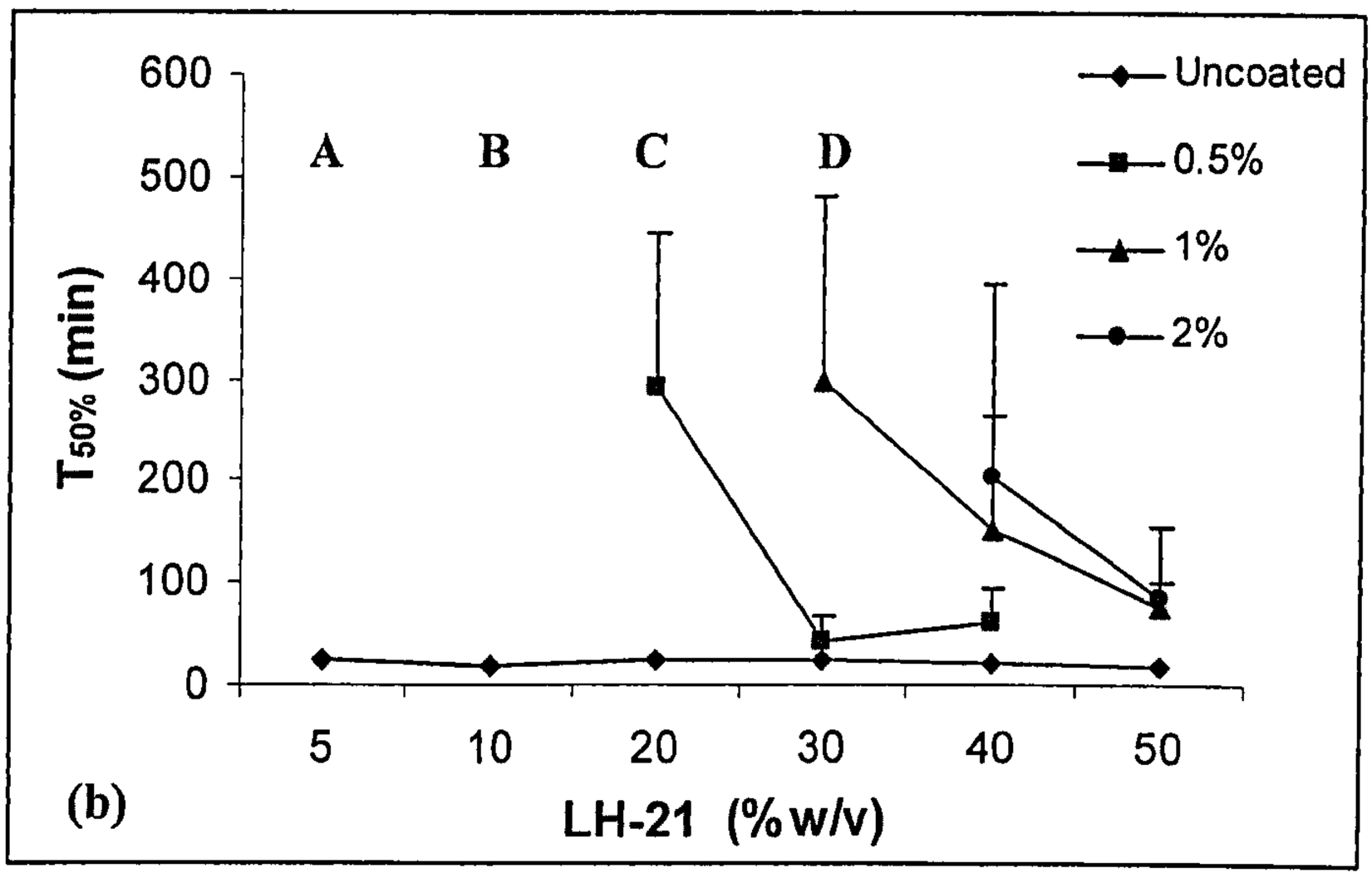

Figure 6.13: Effect of EC coating level and LH-21 concentration on (a) mean lag time and (b) mean $T_{50\%}$ (n=6, +S.D.). In (b) A-D denote formulations with EC coats which did not reach 50% drug release within 10 hours, where A= B= 0.5, 1.0 and 2.0%, C= 1.0 and 2.0%, D= 2.0%. Data points missing from 50%(w/v) LH-21 with 0.5% EC coat as lower LH-21 concentrations exhibited rapid release with almost no lag time therefore dissolution deemed unnecessary.

Mean $T_{50\%}$ (Figure 6.13b) reflected the overall rate of drug release from the capsule, while mean lag time was only an indicator of when drug release was first detected. In A and B (Figure 6.13b), the rate of drug release after capsule cracking was so delayed that 50% drug release was not achieved within 10 hours for 5 and 10%(w/v) LH-21 formulations with any level of coating. It followed that for 20 and 30%(w/v) LH-21

formulations, $T_{50\%}$ gradually fell within 10 hours as the EC coating level also decreased. 40 and 50%(w/v) LH-21 concentrations displayed all $T_{50\%}$ within 10 hours (except the missing data point, which would also likely be within the 10-hour range).

This could be due to one or all of the following factors:

(a) EC coating decreased the ease of access of water to the interior of the capsule for dissolution and diffusion of paracetamol.
(b) Lower concentrations of LH-21 were only sufficient to crack the EC coat, no further swelling for expulsion of paracetamol was possible.
(c) Swollen, insoluble LH-21 formed a type of matrix within which the paracetamol was embedded and water access was limited.

Hence, there would need to be a balance struck between the level of EC coating and LH-21 concentration in order to incorporate a satisfactory time delay while providing enough expulsion capacity for drug release.

6.4.3.3 Effect of paddle speed

This set of experiments was performed to evaluate the effect of paddle speed on dissolution and hence predict the robustness of the dosage form to changes in gastrointestinal motility. Only 2%(w/w) EC-coated capsules with 10%(w/v) LH-21 in corn oil (refer to Table 6.4) and 20mg paracetamol were tested at 25, 50 and 100 rpm paddle speeds.

It was evident from Figure 6.14 that there was no obvious difference between the drug release profiles at paddle speeds 25 and 50 rpm. However, 100rpm did change the type of profile from sustained release to that of a burst release to near 100%. This was reflected in the condition of the capsules post-dissolution which had completely disintegrated. It was likely that the excessive agitation might reduce the diffusional barrier created by swollen LH-21 by physically removing it from the capsule. These results indicated that the dosage form and its timed-release characteristics might not withstand excessive gastrointestinal motility hence efforts must be made to improve its robustness.

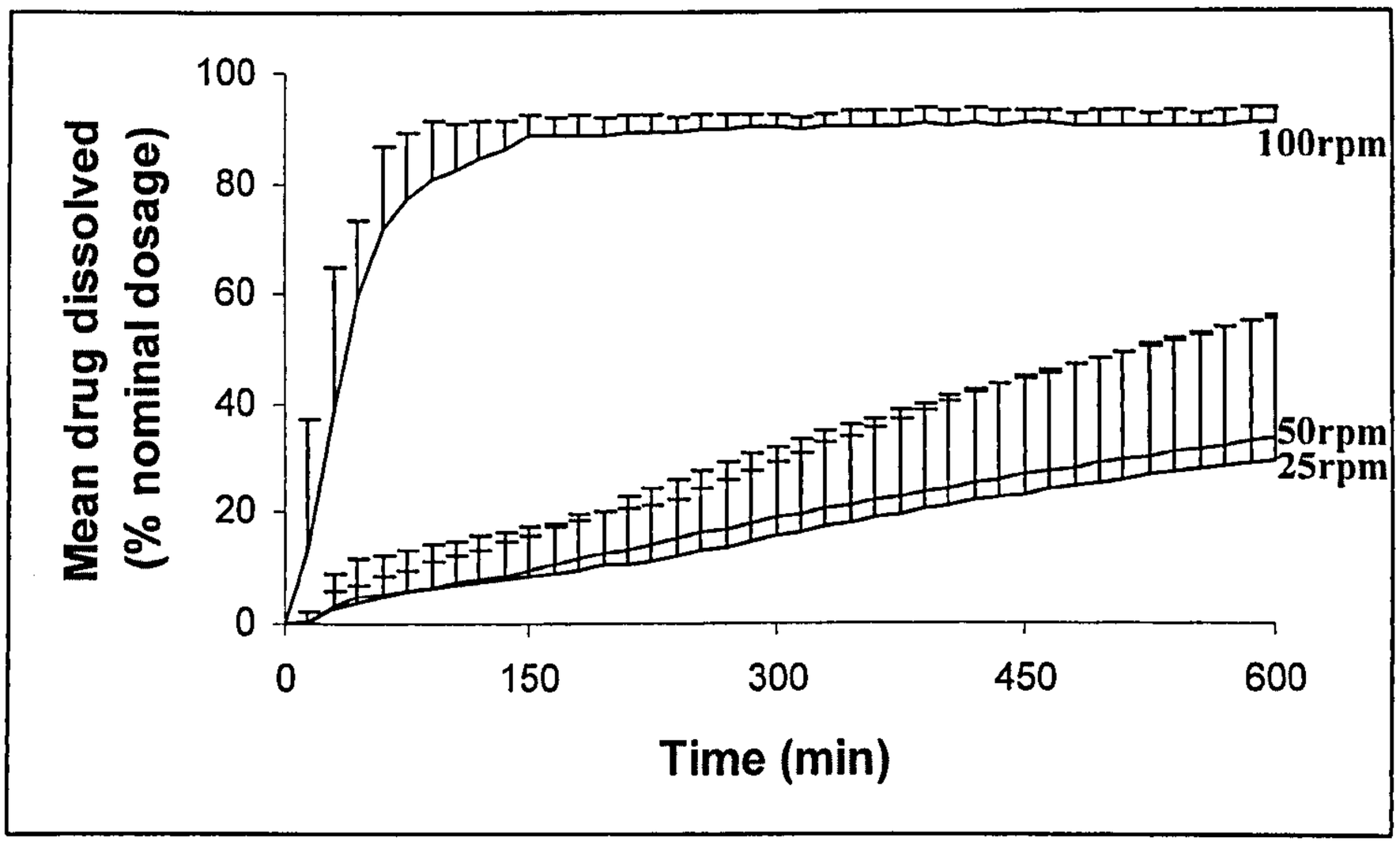

Figure 6.14: Effect of paddle speed on drug release from 2%(w/w) EC-coated capsules with 10%(w/v) LH-21 in corn oil (n=6, +S.D.).

6.4.4 Paracetamol release from EC-coated capsules with higher LH-21:corn oil weight ratios

It was believed that the LH-21 concentrations studied to date were not sufficient to impart the swelling capacity required for complete burst release. The following section discusses the studies carried out with the following formulations filled into Size 1 hard gelatin capsules using the method described in Section 2.6.1. Each capsule also contained 20mg paracetamol as marker drug.

Table 6.5: Capsule fills with higher LH-21:corn oil weight ratios. Capsules were filled to within ±1mg of target weight.

LH-21:corn oil weight ratio (%w/w)	LH-21 (mg)	Corn oil (mg)	Total capsule fill weight (mg)
50:45	200	180	400
55:40	220	160	400
60:35	240	140	400
65:30	260	120	400
70:25	280	100	400

50 capsules were prepared of each formulation and sealed with the adapted LEMS® method (Section 2.6.3.3). All the capsules, and dummies added to produce a bed load of about 300g, were coated with EC solution (Section 2.6.4.1) in an Aeromatic Strea-

1 fluidised bed coater (Section 2.6.4.2). This series of capsules were successively coated for a 1% weight gain each time for 4 cycles i.e. producing capsules with nominally 1, 2, 3 and 4%(w/w) EC coat. The effect of any capsule leakage that occurred was minimised by carefully inspecting the capsules post-coating and wiping each capsule with a clean tissue to blot off any oil coating the surface. However, the actual weight gain calculated was not close to that which was predicted as shown in Table 6.6.

Table 6.6: Coating efficiency of the fluidised bed coater.

Coating cycle	Predicted weight gain (%w/w)	Actual weight gain (%w/w)
1	1	0.082
2	1	0.412
3	1	0.505
4	1	0.559

It followed on that the coated capsules prepared cumulatively possessed 0.1, 0.5, 1.0 and 1.6%(w/w) coating levels, which will be used in further discussion.

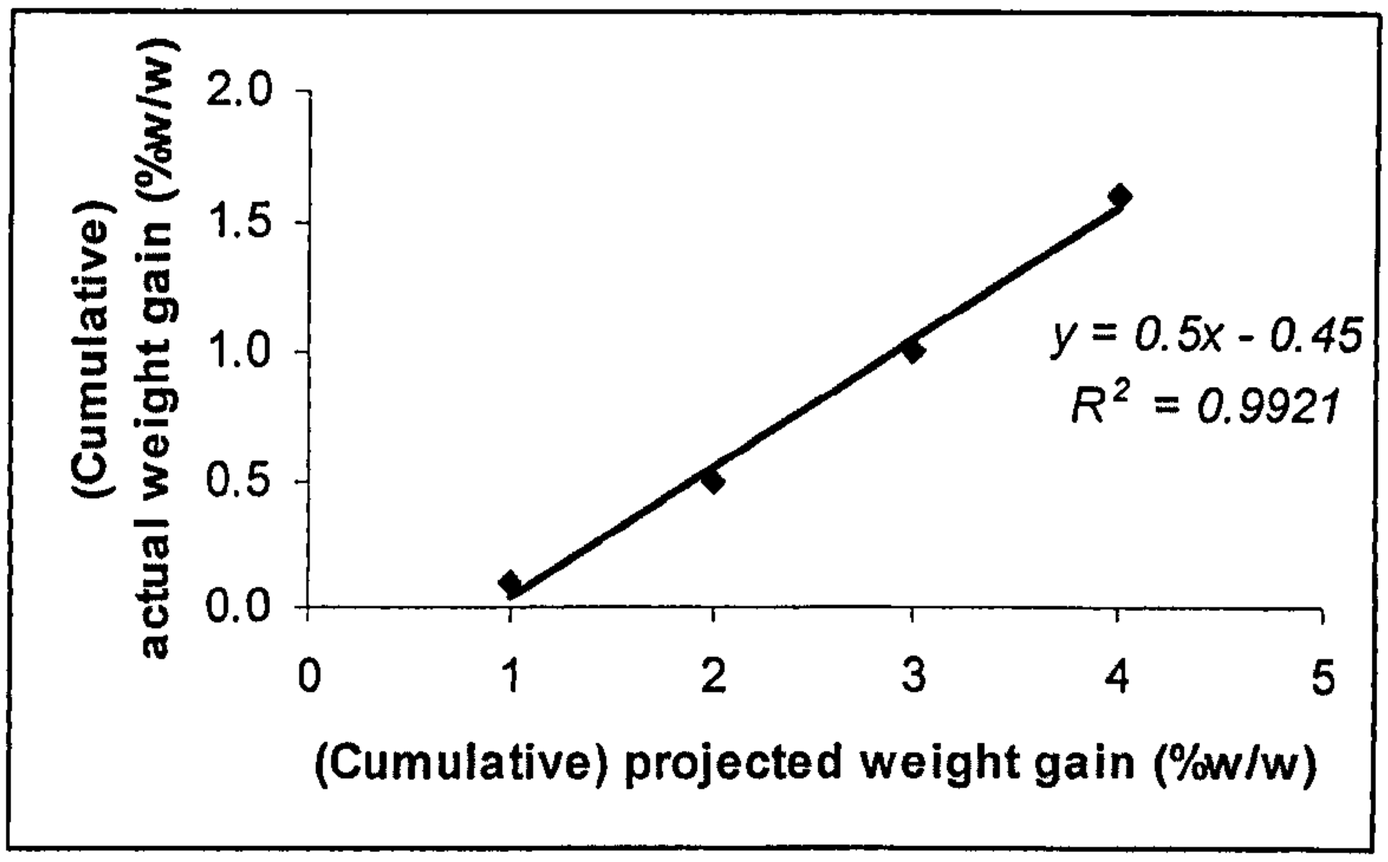

Figure 6.15: Cumulative coating efficiency of the Aeromatic Strea-1.

Compared with Figure 6.8, this set of coating cycles was only 50% efficient and the y-intercept was -0.45. With this large deviation, it was likely that the capsules were coated with greater levels of film than predicted through weight gain. The reasons proposed in Section 6.4.3 should have still held true, but the larger value of the y-intercept indicated that it could not have all been due to residual water content of the

hard gelatin capsules. Some capsules might have leaked resulting in loss of contents during the first cycle. This leakage of oily contents would consequently form an oily layer over the capsule surface, deterring optimum application of EC. The linear relationship between projected and actual weight gain that proceeds was an indicator that the more fragile capsules were eliminated during the first cycle and the more robust ones were able to endure the rough, tumbling motion of the coater.

6.4.4.1 Effect of LH-21 concentration and EC coating

The capsule fill weights were fixed at 400mg, in order to minimise the effect of fill volume on the dissolution profiles. However, this led to the inability to fix the weight of corn oil hence the effect of LH-21 concentration could not be accurately seen as the effect of changing corn oil weight could not be eliminated.

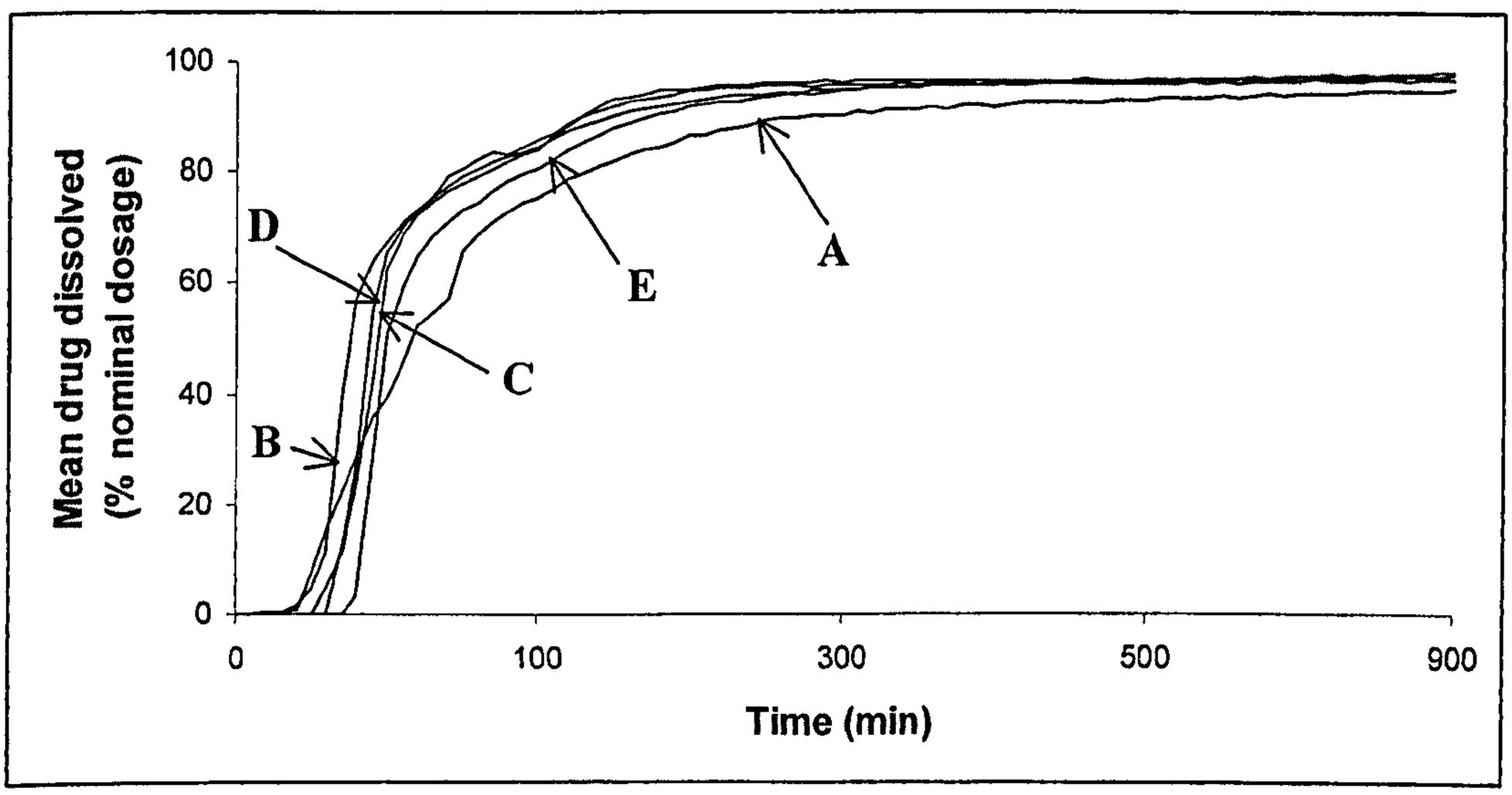

Figure 6.16: Mean dissolution profiles of capsules with 0.1%(w/w) EC coating (n=6). A-E denote the LH-21 concentration where A=50, B=55, C=60, D=65, E=70.

At this low level of EC coating, the effects of LH-21 concentration were not evident and no trend could be observed. However, it was noted that the desired pulsatile release post lag time was obtained with all LH-21 concentrations. Again, the lag times obtained were very modest (20 to 40 minutes) and not greatly influenced by EC concentrations.

Table 6.7: Mean lag times afforded by varying LH-21 and EC coating levels (n=6).

LH-21 (%w/w)	Mean lag time (min) (S.D.)				
	Uncoated	0.1%EC	0.5%EC	1.0%EC	1.6%EC
50	13 (4)	40 (18)	79 (20)	149 (117)	37 (22)
55	18 (2)	33 (5)	22 (7)	14 (12)	31 (12)
60	10 (2)	41 (7)	21 (9)	51 (37)	43 (40)
65	17 (5)	41 (5)	51 (14)	28 (13)	69 (45)
70	5 (1)	47 (5)	132 (90)	*	96 (42)

*** Missing data point due to malfunction of dissolution apparatus. Repeat experiment could not be performed due to lack of samples.**

The results in Table 6.7 would suggest that LH-21 concentration, or rather, LH-21:corn oil ratio, did not cause any specific trend with respect to lag times. With the uncoated capsules, it was not expected to, as seen with the results of the previous formulations in Section 6.4.3.2. No trend was observed with the 0.1% EC coating either. For 0.5% EC, the minimum lag time was displayed by 60:35%(w/w) LH-21:corn oil while for 1.0% EC, the lag times fluctuated as the LH-21 concentration increased. The 1.6% EC series showed that increasing LH-21 concentration and decreasing corn oil concentration tended to increase the mean lag time.

As for the effect of EC coating level, there was a general trend that increasing the EC coat increased the mean lag time as well (p=0.05), despite some fluctuations and large standard deviations.

Table 6.8: Mean $T_{50\%}$ afforded by varying LH-21 and EC coating levels (n=6).

LH-21 (%w/w)	Mean $T_{50\%}$ (S.D.) (min)				
	Uncoated	0.1%EC	0.5%EC	1.0%EC	1.6%EC
50	17 (2)	49 (17)	105 (21)	268 (283)	72 (38)
55	22 (2)	37 (6)	45 (33)	22 (10)	95 (44)
60	13 (1)	44 (6)	34 (11)	90 (56)	52 (46)
65	22 (5)	44 (5)	62 (17)	40 (30)	94 (45)
70	7 (1)	51 (6)	141 (89)	*	122 (49)

*** Missing data point due to malfunction of dissolution apparatus. Repeat experiment could not be performed due to lack of samples.**

Similar effects as seen with mean lag time were observed for mean $T_{50\%}$ when analysing the data vertically in Table 6.8. The large standard deviations in both data

sets implied that these capsules were unable to generate reproducible dissolution profiles.

It was possible that this method of successively coating the capsules was unsuitable as the larger variations in dissolution profiles were more apparent with the higher coating levels. Perhaps some capsules were not sufficiently robust to withstand multiple coating cycles.

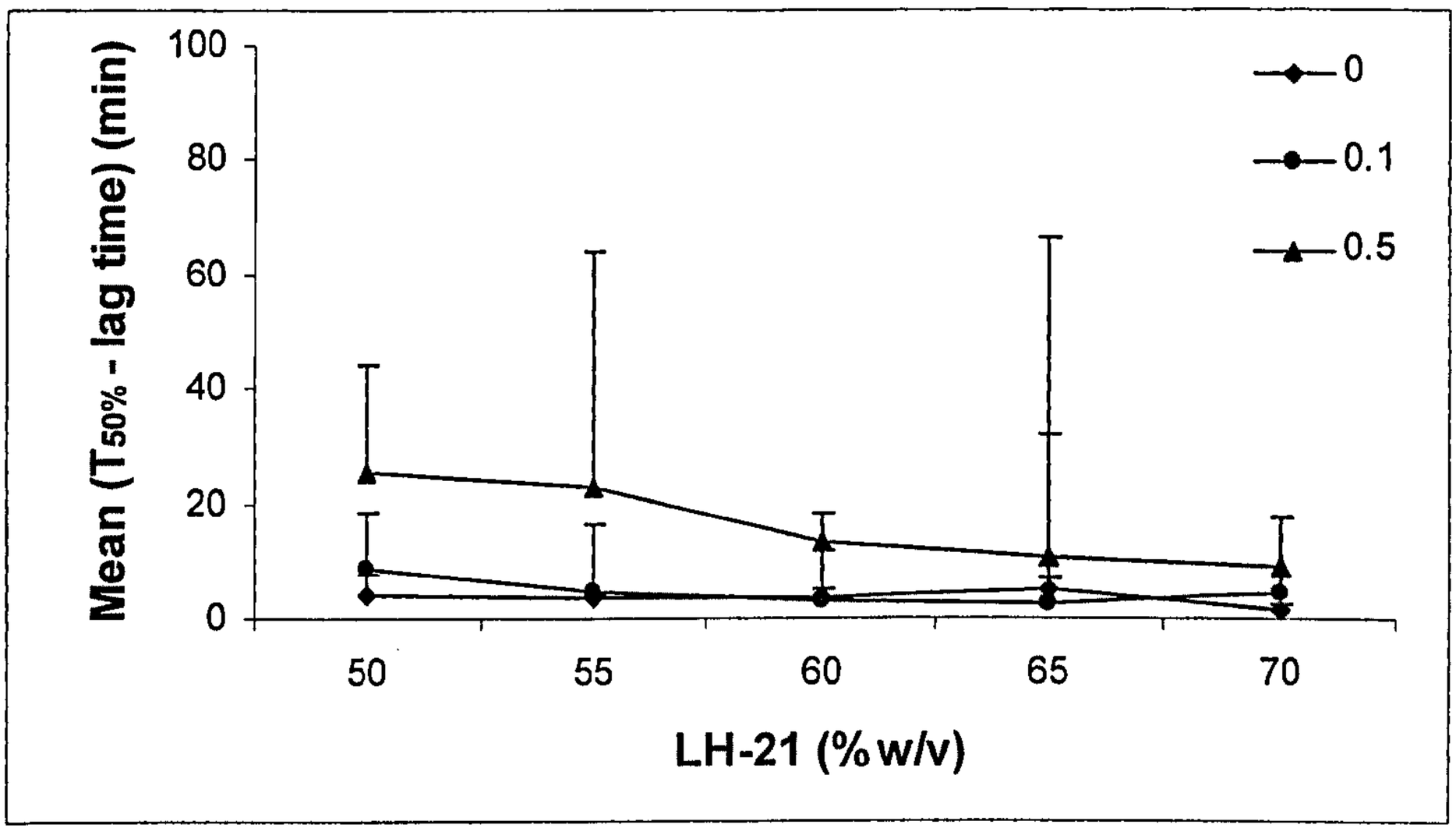

Figure 6.17: Effect of LH-21 concentration on mean ($T_{50\%}$-lag time) (n=6, +S.D.).

The mean ($T_{50\%}$-lag time) reflected the rate of the pulsatile release, independently of the lag time. The lower the value, the quicker the drug within the capsule was expelled. With uncoated and 0.1% EC-coated capsules (Figure 6.17), there was almost no effect of LH-21 concentration on the mean ($T_{50\%}$-lag time), implying that the EC coat was sufficiently brittle and/or the LH-21 concentration was adequate for complete rupturing of the capsule.

However, increasing the EC coating level did increase the mean ($T_{50\%}$-lag time) indicating that the EC shell posed a barrier to unhindered pulsatile drug release. With 0.5%, there was a decrease in mean ($T_{50\%}$-lag time) as the LH-21 concentration increased. Here was another indication that LH-21 not only functioned to rupture the outer coating but also to aid expulsion of the capsule fill. It seemed that swollen LH-

21 impeded drug release from capsules with lower LH-21 concentrations (Section 6.4.3.1). The results here indicated that higher LH-21 concentrations were required to fully exploit the expulsion power of the swelling agent.

6.4.5 Gelatin banding capsules with bench-scale capsule banding machine

The lack of reproducibility in the previous series of capsules was worrying and pointed to non-uniformity in the manual construction process and/or the poor cohesiveness of capsule sealing. In order to improve the latter, gelatin banding with a Qualiseal bench-scale capsule banding machine, courtesy of Encap Drug Delivery, Livingston, UK, was implemented (Section 2.6.3.2). Table 6.9 detailed the formulations which were gelatin banded in this manner. All capsules contained 20mg paracetamol, 5% of total capsule weight.

Table 6.9: Formulations prepared for gelatin banding by Qualiseal banding machine. Capsules were filled to within ±1mg of target weight.

LH-21:corn oil weight ratio	400mg fill	
	LH-21	Corn oil
(%w/w)	(mg)	(mg)
15:80	60	320
25:70	100	280
35:60	140	240
45:50	180	200
55:40	220	160
65:30	260	120

The capsule leak test described in Section 2.6.5 was performed on all the banded capsules as well as unbanded capsules of the same formulation composition, as control. None of the unbanded capsules showed any signs of leaking but two of the banded capsules did. These were discarded but the remaining capsules which passed the test were coated in the Aeromatic Strea-1 fluidised bed coater as described in Section 2.6.4.2.

The capsules were coated using the successive coating method for a nominal 1% weight gain per cycle as used in Section 6.4.4 for a total of three cycles.

Table 6.10: Coating efficiency of Aeromatic Strea-1.

Coating cycle	Actual weight gain (%w/w)
1	-0.05
2	0.5
3	0.5

Again, as seen in Table 6.10, initial weight loss was observed but the subsequent coating cycles were consistently producing weight gains of 0.5%. In the following discussion, EC coating levels will be referred to as coats 1, 2 and 3 with reference to the coating cycles in Table 6.10.

6.4.5.1 Effect of LH-21:corn oil weight ratio

Figure 6.18 showed that all formulation compositions exhibited lag times but the release profile post-capsule rupture varied according to the LH-21:corn oil ratio. Formulation A (according to Figure 6.18) released paracetamol in a dissolution-diffusion dependent manner, barely achieving any drug release within 15 hours. With Formulation B, the release followed zero order release kinetics, increasing the plausibility of the assumption that the swollen, insoluble LH-21 could act as a matrix, entrapping the drug. Formulations C, D and E gave similar profiles of pulsed release following a time delay. However, the initial burst release did not reach 100% drug release but merely to about 50%, then a gradual release of drug proceeded. Furthermore, not all six capsules per formulation released drug during the entire dissolution cycle.

The area of concern here was the variability in time delay afforded by the capsules.

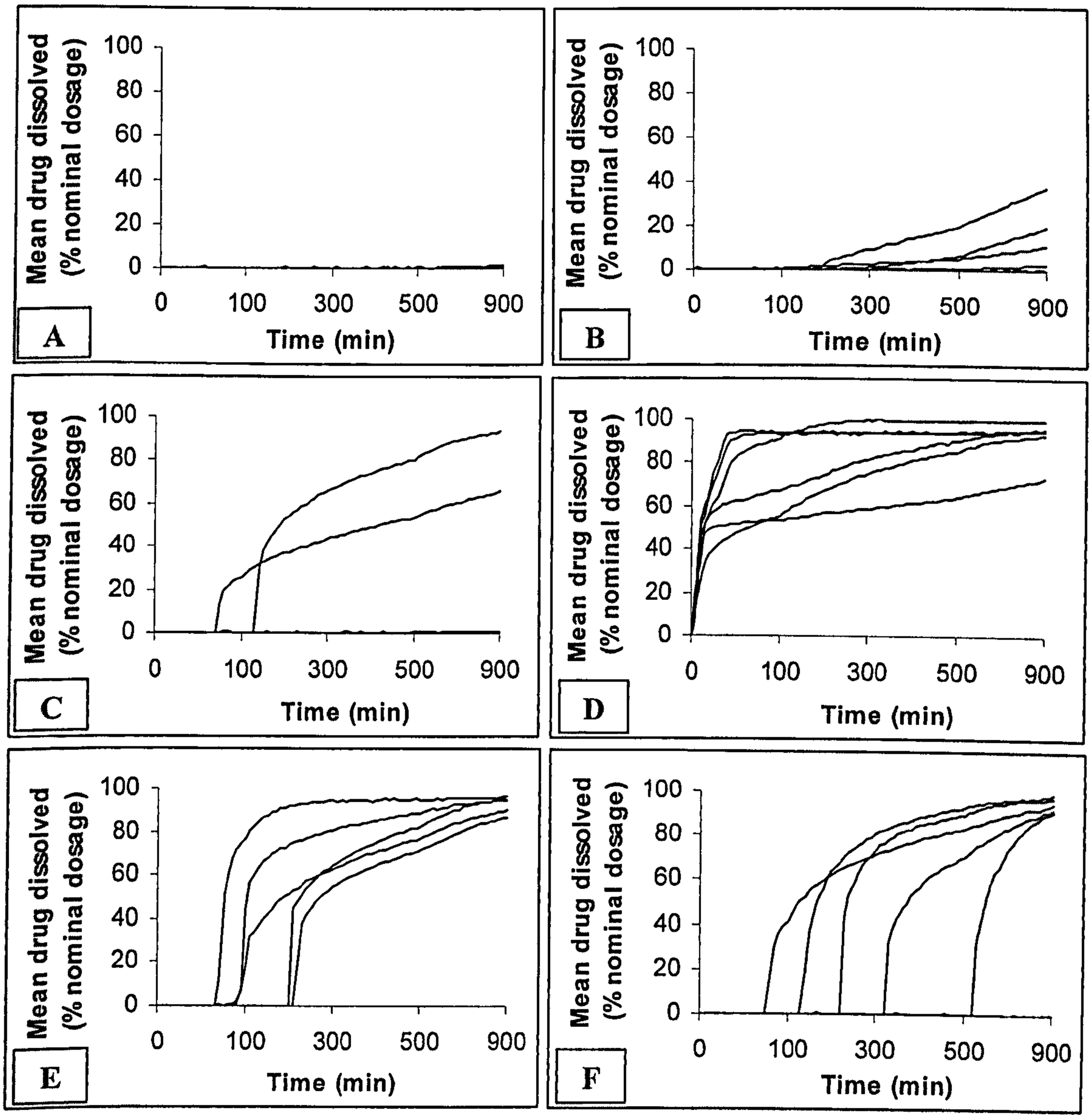

Figure 6.18: Effect of LH-21:corn oil ratio on mean dissolution profiles of coat 2 EC-coated, banded capsules (n=6). A-F denote LH-21: corn oil weight ratios (%w/w) where A=15:80, B=25:70, C=45:50, D=55:40, E=65:30, F=75:20.

Analysing these data in terms of mean lag time and mean $T_{50\%}$ (Figure 6.19), the effect of insufficient LH-21 for expulsion of drug became more evident. The data from uncoated capsules confirmed that the variations in $T_{50\%}$ were not completely due to the presence of an EC coat, but more likely an effect of lack of LH-21 since the lag times across the LH-21 concentrations were similar. This discernment of greater, albeit modest, differences in lag time and $T_{50\%}$ even in uncoated capsules might not be entirely contradictory to the results in Section 6.4.3.2. It was likely to be a consequence of being able to take absorbance readings at 2 minute intervals with an

alternative dissolution apparatus (Caleva) while the initial Copley dissolution apparatus had a minimum interval of 5 minutes.

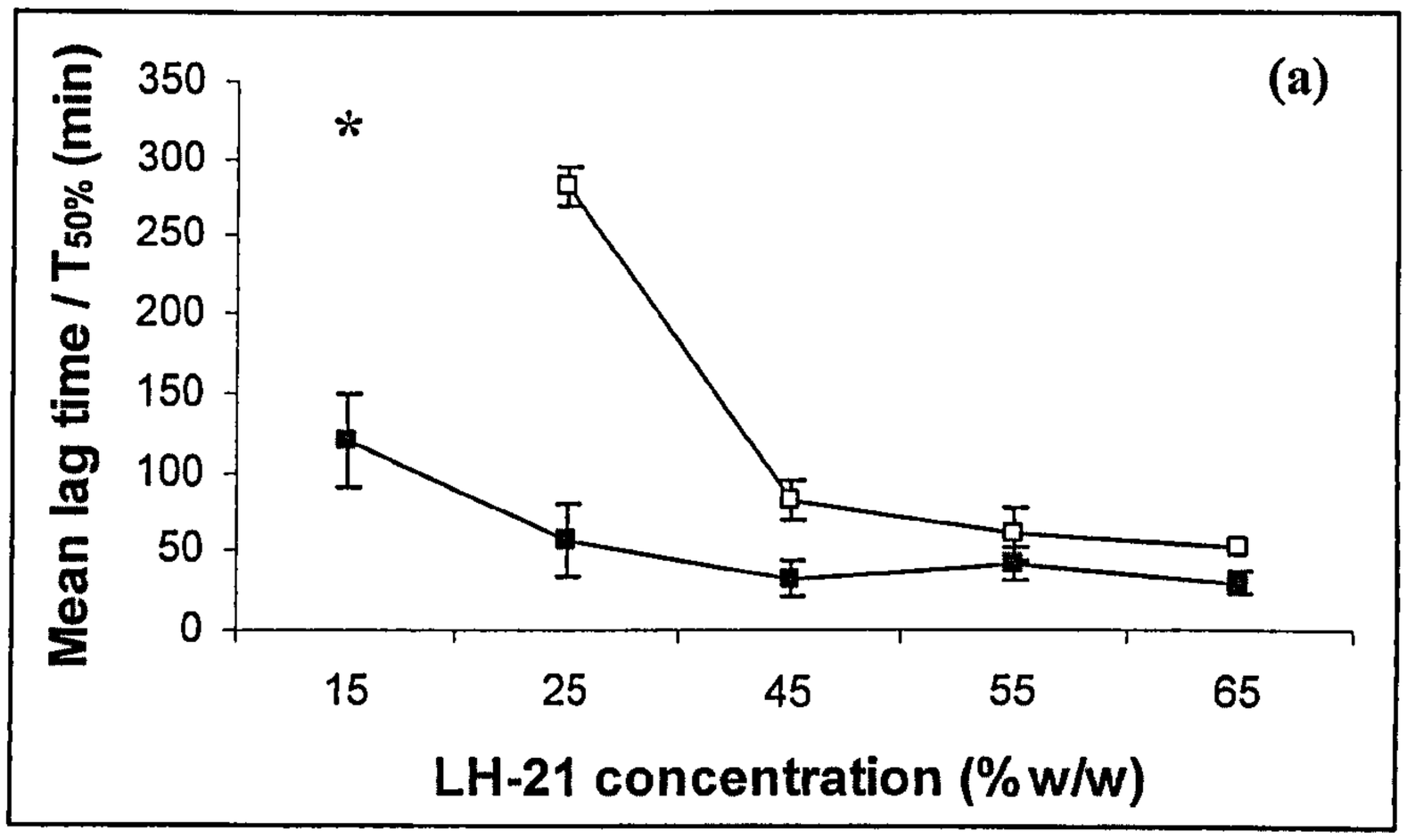

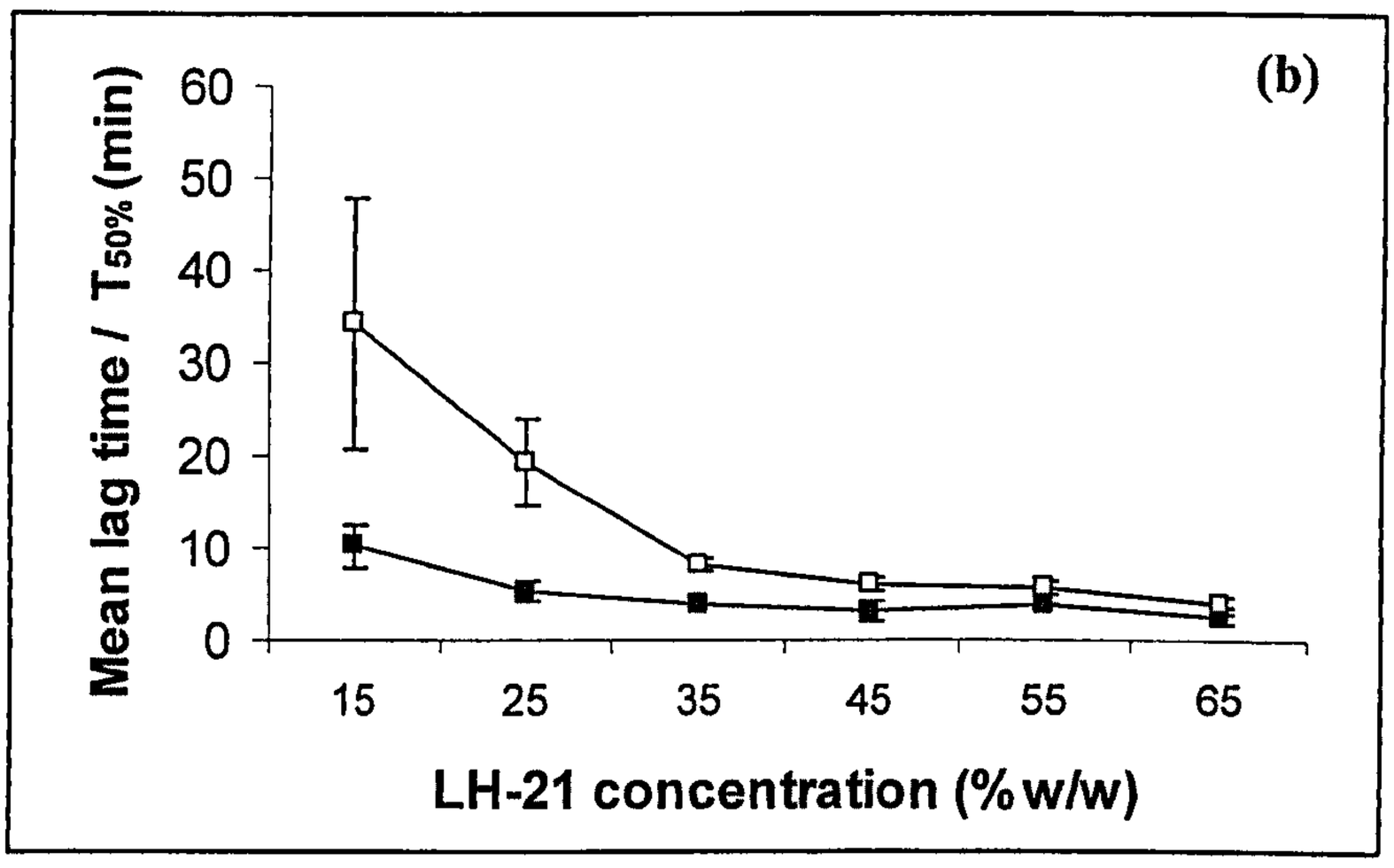

Figure 6.19: Effect of LH-21:corn oil ratio on mean lag time and mean $T_{50\%}$ for (a) coat 2 EC-coated and (b) uncoated, banded capsules (n=6, ±S.D.). Solid squares, ■=lag time, empty squares, □=$T_{50\%}$. *$T_{50\%}$ not achieved within 15-hour dissolution.

It was also encouraging to note that the standard deviations were quite narrow, implying that the reproducibility of the capsules' performances had improved due to the banding process.

6.4.5.2 Effect of EC coating level

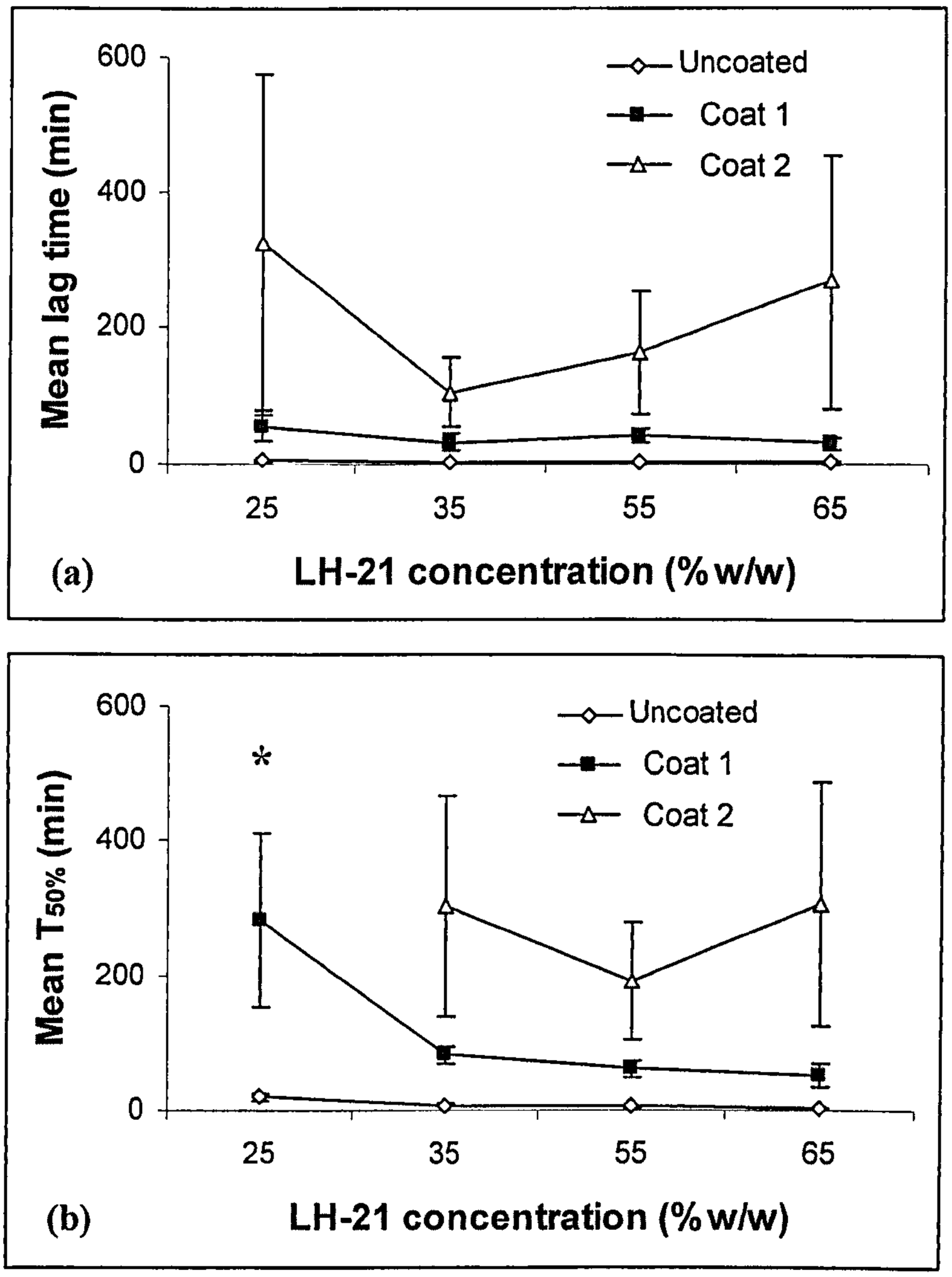

Figure 6.20: Effect of EC coating level on (a) mean lag time and (b) mean $T_{50\%}$ of banded capsules (n=6, ±S.D.). *$T_{50\%}$ not achieved within 15-hour dissolution.

Increasing the level of EC coating increased the mean lag time and mean $T_{50\%}$ (p<0.0005 for both parameters) in a concentration-dependent manner. However, the large standard deviations resulting from nominally 2% EC-coated capsules implied that ability of the capsule formulation to accurately produce the desired release profile required was limited.

6.4.6 Dipcoating as an alternative coating method

Despite the achievement of the desired profile of pulsatile release preceded by a lag time, the performance of the time-delayed oil-filled capsule was far from optimised as there were large variations in the onset of the burst release. It was likely that the hand-made capsules were insufficiently robust to withstand the comminuting forces arising from the spray coating process, leading to leakage of capsule contents and substandard coating.

Hence an alternative method, which would subject the capsules to minimal stress, was employed. Dipcoating, described in Section 2.6.4.4, also allowed for smaller batches of test samples to be prepared. The capsules were made with the procedure in Section 2.6.1 and sealed with the adapted LEMS® method (Section 2.6.3.3) with the fill contents described in Table 6.11. Paracetamol content per capsule was fixed at 20mg, 5% of total capsule fill weight.

Table 6.11: Capsule fills for dipcoating. Capsules were filled to within ±1mg of target weight.

LH-21:corn oil weight ratio (%w/w)	400mg fill	
	LH-21 (mg)	Corn oil (mg)
50:45	200	180
60:35	240	140
70:25	280	100

6.4.6.1 Dipcoating efficiency

Dipcoating efficiency was evaluated in terms of mean weight gain after each coating cycle. Each series of capsule fills, in sets of 6, were dipcoated 5, 7 and 10 times resulting in overall mean EC coating levels of 2.1±0.5, 2.9±0.3 and 4.0±0.6%(w/w) respectively. It was assumed that the dipcoating process produced even, uniform coating on all occasions and the results obtained were comparable over the series. Figure 6.21 depicted a sample weight gain curve obtained by dipcoating which was representative of the entire series of capsules coated. The near linear increase in weight was indicative of the uniformity of application of polymer film to the capsule surface.

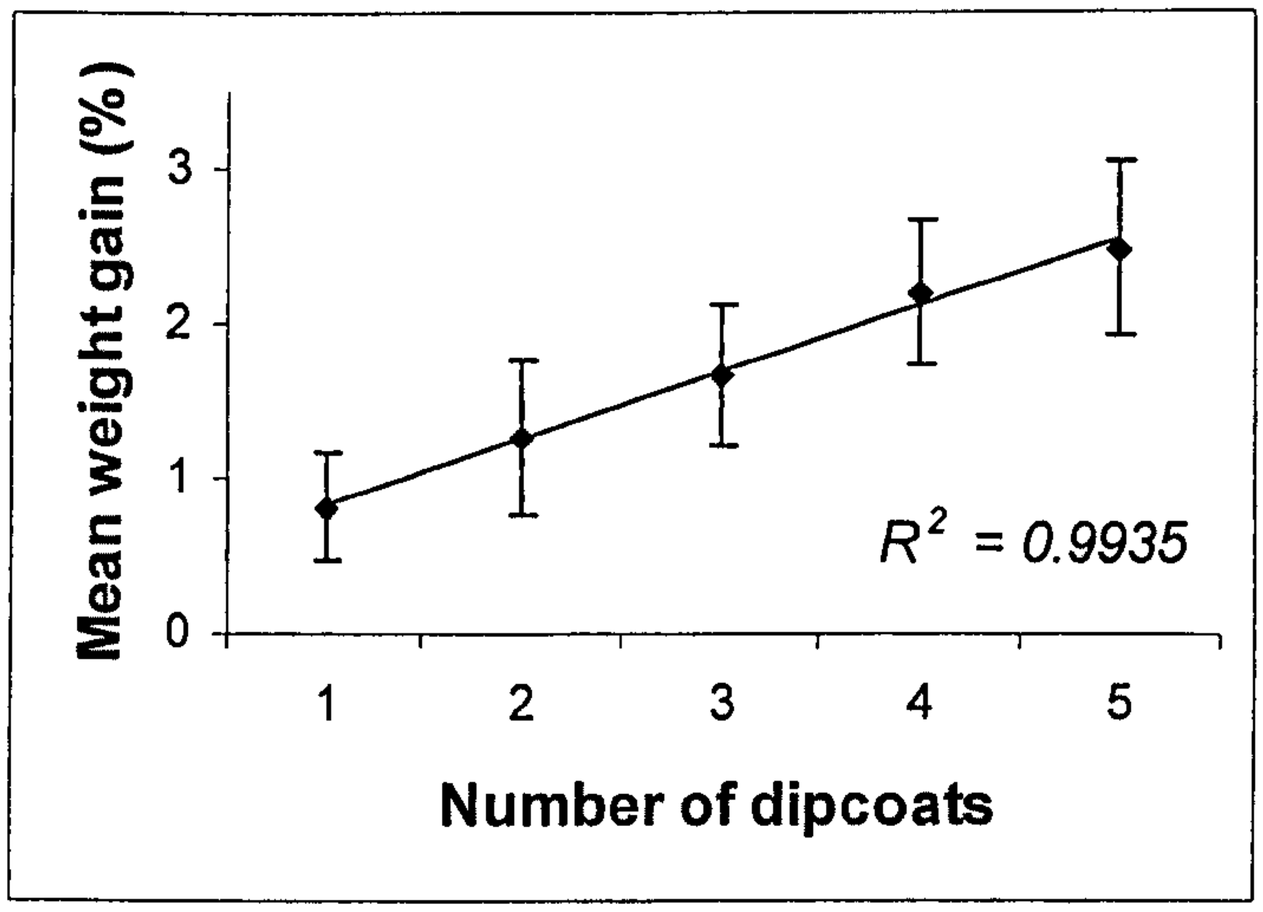

Figure 6.21: Mean weight gain from dipcoating capsules containing 70%(w/w) LH-21, 25%(w/w) corn oil and 5%(w/w) paracetamol 5 times in a 3%(w/v) EC, 5%(w/w of EC) triacetin solution (n=6, ±S.D.).

6.4.6.2 Effect of EC coating level and LH-21 concentration

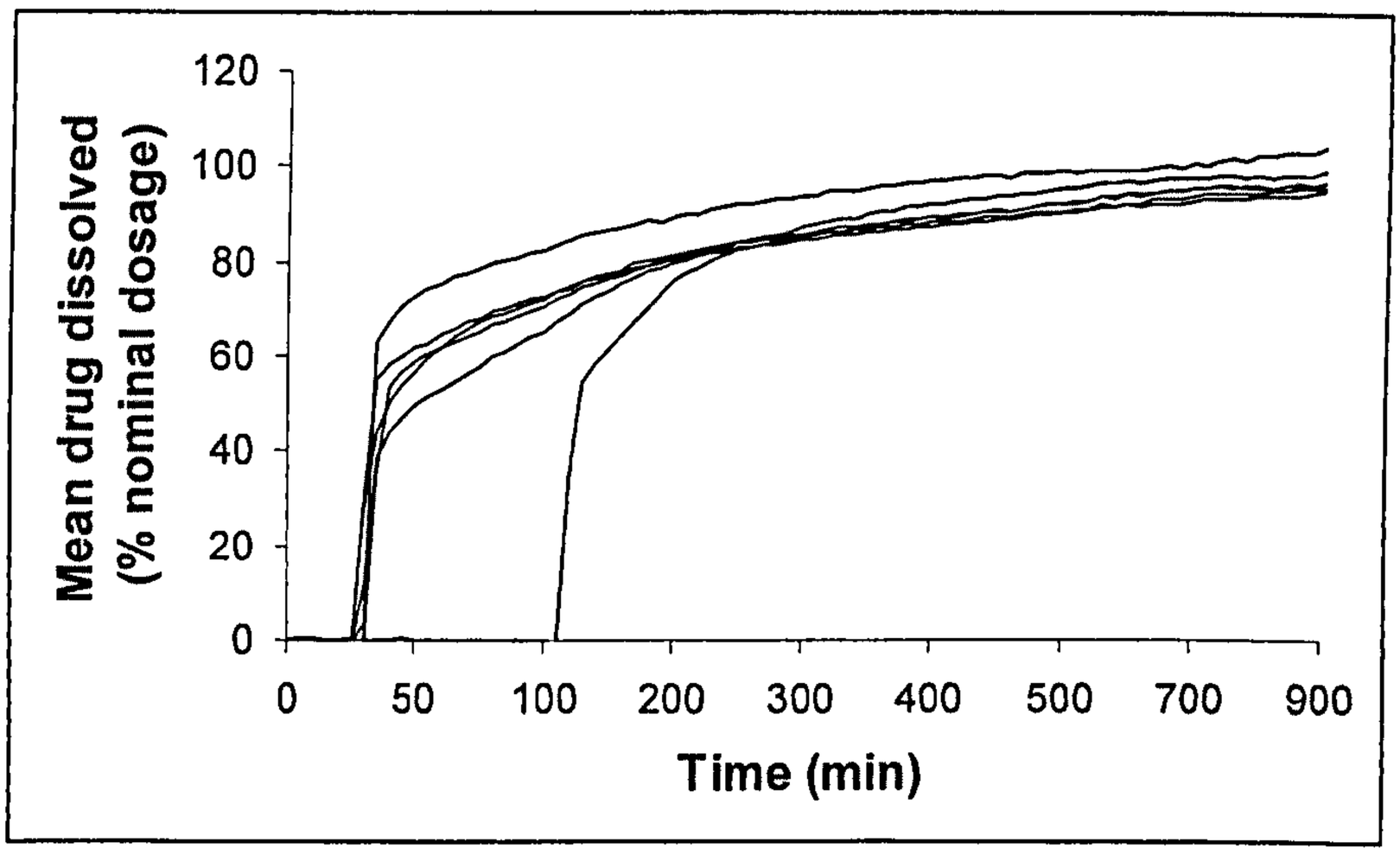

Figure 6.22: Dissolution curves of six capsules containing 70%(w/w) LH-21, 25%(w/w) corn oil and 5%(w/w) paracetamol dipcoated 5 times in 3%(w/v) EC, 5%(w/w of EC) triacetin solution.

In general, the dissolution profile exhibited a burst release to between 70 and 90%, followed by a gradual release of the remaining drug, not unlike the spray-coated capsules (Figure 6.22).

Over all the capsule fill formulations studied (Figure 6.23), increasing the coating level did significantly increase both the mean lag times and mean T_{50} (p<0.0005, one-

way ANOVA). Similar treatment of data showed that LH-21: corn oil ratio did not significantly affect lag time (p=0.717) or $T_{50\%}$ (p=0.258). The threshold amount of LH-21 required to rupture the coat might be lower than the minimum used in this study.

Although the dipcoating process did allow for reasonably uniform weight gain, it was still unable to minimise variation in the release profiles within the same batch of capsules. Poor EC coating was not the only cause of lack of reproducibility. The capsule fill was contributing as well, possibly due to non-uniformity of its position within the capsule. The air pocket that existed probably absorbed some of the swelling force and varied LH-21's impact on rupturing the EC coat. Furthermore, despite great care exercised in capsule preparation, capsule fill leakage could not be completely eliminated.

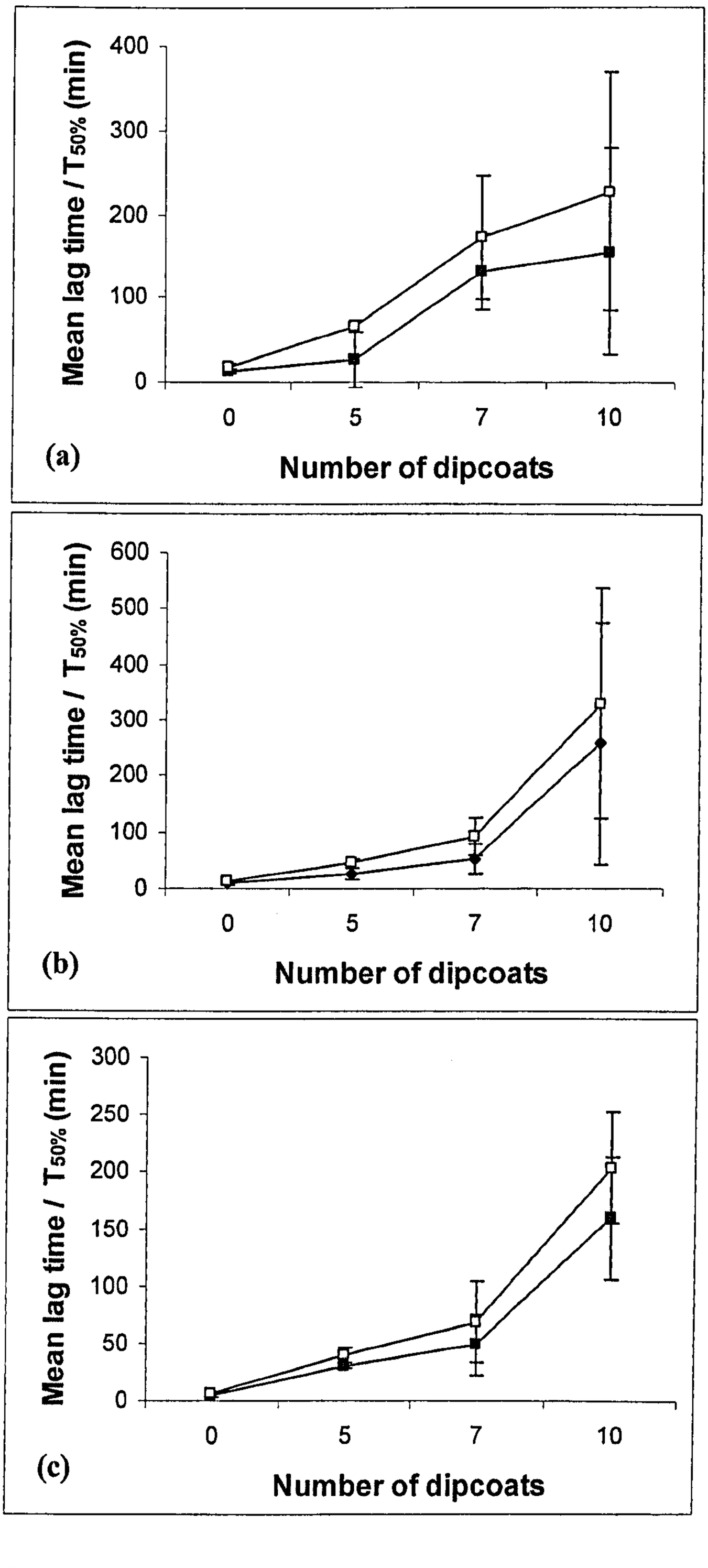

Figure 6.23: Effect of dipcoating level on mean lag time (solid squares, ■) and mean $T_{50\%}$ (empty squares, □) of (a) 50%(w/w) LH-21, 45%(w/w) corn oil, 5%(w/w) paracetamol, (b) 60%(w/w) LH-21, 35%(w/w) corn oil, 5%(w/w) paracetamol and (c) 70%(w/w) LH-21, 25%(w/w) corn oil, 5%(w/w) paracetamol capsules.

6.5 Conclusions

- Taking the cue from the various time-delayed formulations that had been reported and the characterisation studies in Chapter 3, 4 and 5, a series of experiments in formulating a novel time-delayed oil-filled capsule was implemented.

- The basic composition of the time-delayed oil-filled capsule was that of a dispersion of LH-21 and drug in vegetable oil within an EC-coated hard gelatin capsule. The premise was that the water-insoluble, but water permeable outer coat would allow water ingress whilst maintaining the rigid shell of the dosage form. Swelling of LH-21 would occur upon contact with water and generate forces sufficient to rupture the brittle coating, thereby initiating drug release.

- The desired release profile was that of a burst release preceded by a time delay, which has tremendous prospects in the fields of chronotherapy and colonic drug delivery.

- With the aim of delivering hydrophobic drugs in a vegetable oil-based dispersion, griseofulvin was selected as a model drug. Initial studies proved that varying LH-21 concentration and EC coating level did change the release profile accordingly.

- However the poor water-solubility of griseofulvin, necessitating dissolution in bile salt-containing mediums, hindered the study of varying many formulation parameters. Hence the focus was shifted to designing the actual release mechanism and the more water-soluble paracetamol was employed as a model drug.

- Increasing the LH-21 concentration in a fixed volume of corn oil changed the consistency of the capsule fill from that of a liquid dispersion to that of a thick paste. Capsules filled with the higher LH-21 concentrations managed to produce

the burst release of a significant amount of drug while lower LH-21 concentrations tended to release drug with near zero-order kinetics.

- From the onset of experiments, the main challenge was to successfully seal the capsules to prevent any leakage of fill which would not only result in non-uniform capsule contents but also prove detrimental to the coating process. The bursting of just one capsule during the spray coating process could coat a large proportion of the other capsules with an oily film, preventing optimum polymer film coating.

- Sealing with an adapted LEMS® process as well as gelatin banding with either a brush or bench-scale banding machine improved the situation but did not fully eliminate the problem of leakage.

- Dipcoating was employed to coat the capsules via a gentler method, with the aim of reducing the effect tumbling in the spray coater had on the mechanical integrity of the capsules.

- Decreases in the variability among the dissolution profiles were observed, but again, not completely eradicated. This implied that the capsule fill itself was causing poor correlation among the same batch of capsules. Mixing LH-21 and corn oil might not have been a suitable approach to creating a swellable, rupturable system. The variations in swelling force depression could not be tightly controlled.

- In the next chapter, a change in capsule fill configuration is described, with hope for improvement in release profiles.

CHAPTER 7

FORMULATION, MANUFACTURE AND TESTING OF THE COMPARTMENTALISED CAPSULE

7.1 Introduction

An alternative configuration was proposed for our time-controlled delivery device, retaining the individual components of swelling agent and hydrophobic phase contained within a hard gelatin capsule with a rupturable outer coating. This approach was based on the hypothesis that the expansion of the swelling agent and hence the rupturing of the capsule coat would be better controlled if the swelling component and the hydrophobic phase were separated. It was seen in the previous studies that mixing of the swelling agent and hydrophobic phase resulted in diminished capacity for swelling. However, it was possible that this effect was not adequately controlled resulting in severe inability to obtain reproducible drug release profiles.

7.2 Aims and objectives

The first step in this series of experiments was to evaluate the suitability of various excipients to form a barrier between the two main components, and following that, to determine the best method of constructing the dosage form. Upon achieving an appropriate configuration, the effects of varying excipients in the swelling component, barrier layer and drug carrier phase were studied.

7.3 Methods

The methods used are summarised in Table 7.1 and referenced, where appropriate, to the detailed descriptions in Chapter 2.

Table 7.1: Summary of methods used in Chapter 7.

Section	Method	Methods section
7.4.1	**Choice of barrier between swelling agent and hydrophobic phase**	
	Construction of Variation 2 capsule	2.6.2
	Dipcoating	2.6.4.4
	Dissolution testing	2.6.6
7.4.2	**Effect of tablet composition**	
	Tablet erosion studies	2.4.6
	Construction of Variation 2 capsule	2.6.2
	Dipcoating	2.6.4.4
	Dissolution testing	2.6.6
7.4.3	**Effect of swelling compartment composition**	
	Construction of Variation 2 capsule	2.6.2
	Dipcoating	2.6.4.4
	Dissolution testing	2.6.6
7.4.4	**Comparison between HPMC capsules and hard gelatin capsules**	
	Construction of Variation 2 capsule	2.6.2
	Dipcoating	2.6.4.4
	Dissolution testing	2.6.6
7.4.5	**EC film coating with minicoater**	
	Spray coating with minicoater/drier	2.6.4.3

7.4 Results and discussion

7.4.1 Choice of barrier between swelling agent and hydrophobic phase

7.4.1.1 Molten gelatin

Gelatin was selected as the first excipient to be studied as it should bind strongly to the inner wall of the capsule, ensuring a tight seal. Moreover, it is water-soluble and dissolves easily at body temperature. The first attempt at creating a barrier with gelatin used the following method:

1. Capsule body was filled with 150mg LH-21.
2. 25%(w/v) gelatin solution (Gelatin Type B, approximately 225 bloom) was prepared by dissolving 1.25g gelatin in 5mL distilled water, heated to 60°C.
3. 100µL of the warm solution was added on top of the compacted powder.
4. The capsule was positioned upright to allow the gelatin to cool and dry until it solidified.
5. 100µL of a 20%(w/v) suspension of paracetamol in corn oil was added to the capsule.
6. The capsule was capped then banded with gelatin by brushing the gelatin solution prepared in (2) and dipcoated five times (Section 2.6.4.4) with coating solution consisting of 3%(w/v) ethylcellulose (EC), 5%(w/w of EC) triacetin, 50:50%(v/v) acetone: isopropyl alcohol (IPA).

The gelatin solution did form a plug that separated the two components but caused shrinking of the capsule body at the juncture where it was situated. This phenomenon was still observed in the pictures of the capsules post-dissolution (Figure 7.1). Nevertheless, six of these capsules underwent dissolution but only one produced the desired burst release after lag time, implying that the manufacturing process had to be improved.

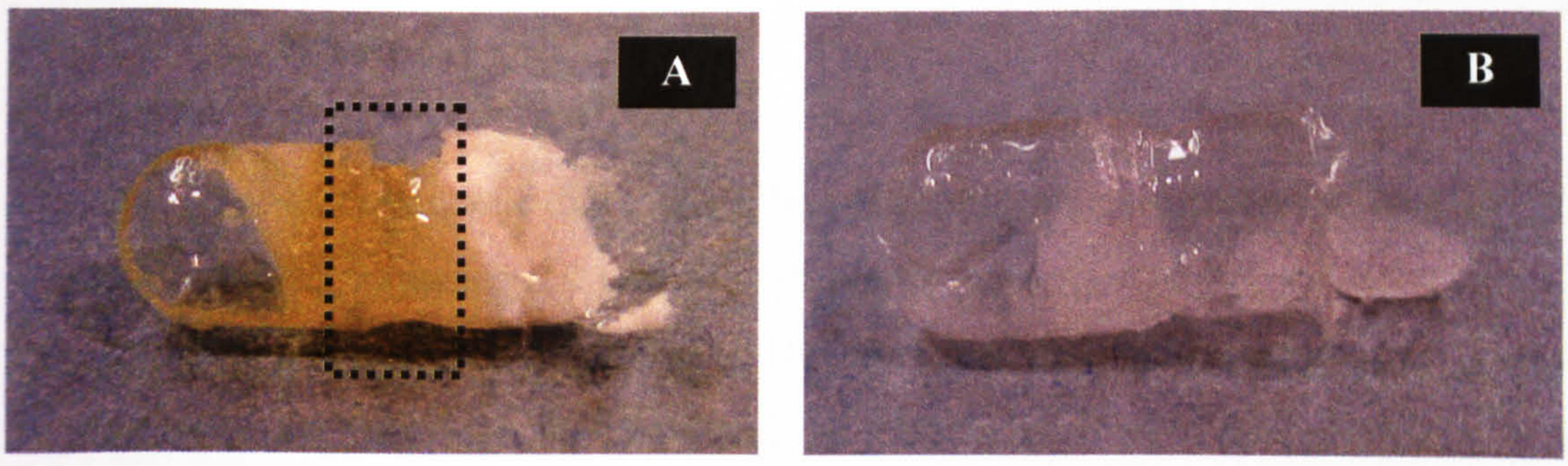

Figure 7.1: Compartmentalised capsules with gelatin plugs post-dissolution. Descriptions of A and B in text. Dotted lines demarcate region of shrinking.

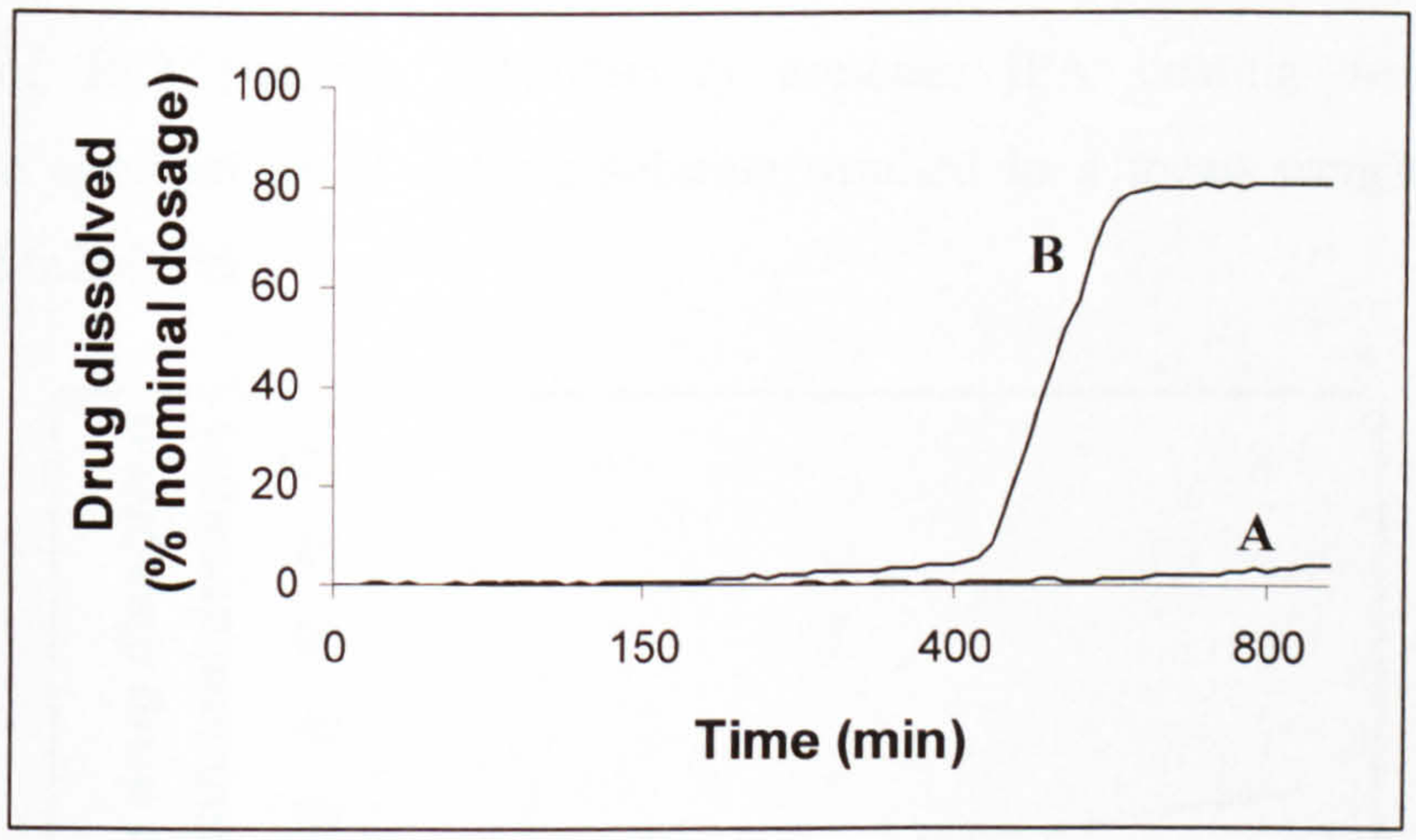

Figure 7.2: Dissolution profiles of capsules A and B. Description of A and B in text.

Figures 7.1 and 7.2 exemplified the large disparities between the performances of two capsules, nominally from the same batch, manufactured under similar conditions. It was clear from capsule A in Figure 7.1 that the gelatin plug was still intact, and the LH-21 had yet to be completely expelled from the cap of the capsule. The drug/oil phase was also still contained in the lower part of the capsule resulting in the dissolution profile shown in Figure 7.2.

All that remained of capsule B however, was the EC shell (Figure 7.1). A lag time of about 400 minutes was observed prior to a pulsed release of the drug (Figure 7.2). This showed that the capsule configuration was able to produce timed-release profiles and hence the next step was to ensure reproducibility of the profiles.

7.4.1.2 Waxy materials

The shrinkage of the capsule due to the effect of gelatin plug adhesion and contraction was addressed by replacing the gelatin with Apifil (a mixture of polyethylene glycol, PEG-8 and beeswax) in the molten state. However, the waxy plug tended to shrink on cooling hence the seal between the oil and LH-21 was not impervious, allowing oil to seep into LH-21. The oil also seemed to mix with the wax and no oil layer could be discerned. Gelatin banding with 25%(w/v) gelatin solution (Section 2.6.3.1) and dipcoating (Section 2.6.4.4) was performed on these capsules with 3%(w/v) EC, 5%(w/w of EC) triacetin, 50:50%(v/v) acetone: IPA coating solution. Five consecutive applications of coating solution resulted in a mean weight gain by 6 capsules of 6.7±0.3%.

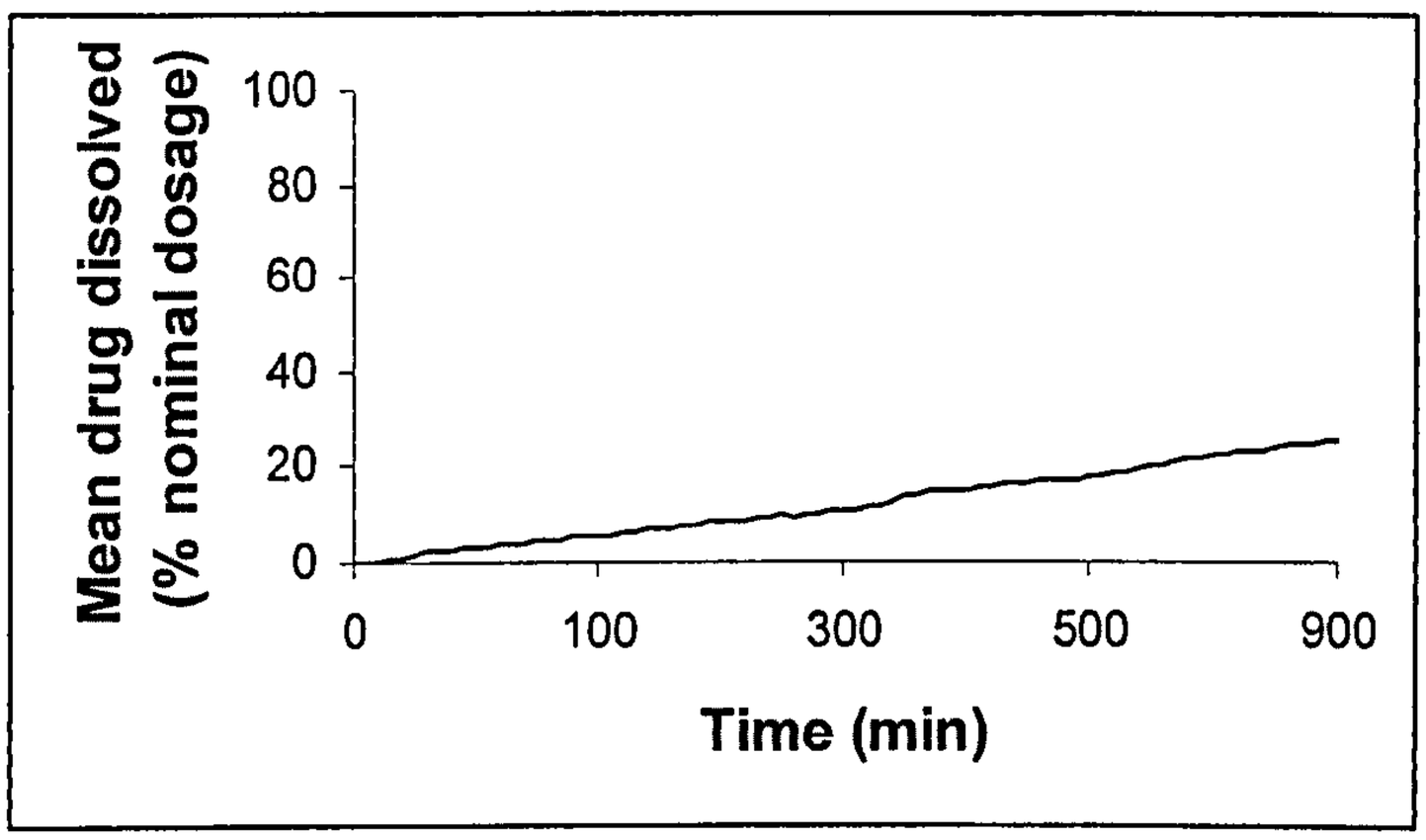

Figure 7.3: Mean dissolution profile of compartmentalised capsules containing 100mg LH-21, 100µL Apifil plug and 20mg paracetamol dispersed in 100µL corn oil (n=6).

There was a mean lag time of about 20 minutes observed with this formulation, followed by gradual near zero-order release of drug. It was possible that Apifil exerted a detrimental effect on the swelling capacity of LH-21 and/or the 6% EC coat was too thick thereby retarding water penetration and consequently insufficient swelling force was generated for rupturing of the EC coat.

7.4.1.3 Gelatin tablets

Waxy plugs were hence deemed unsuitable for this formulation necessitating a return to gelatin. Convex gelatin tablets (8mm diameter) were made by direct compression using a Manesty SP single punch tablet machine and inserted at the neck of the capsule, creating the barrier between oil and swelling phases. The initial dissolution results with this configuration were promising and hence capsules prepared in this manner (Section 2.6.2) were used in further studies.

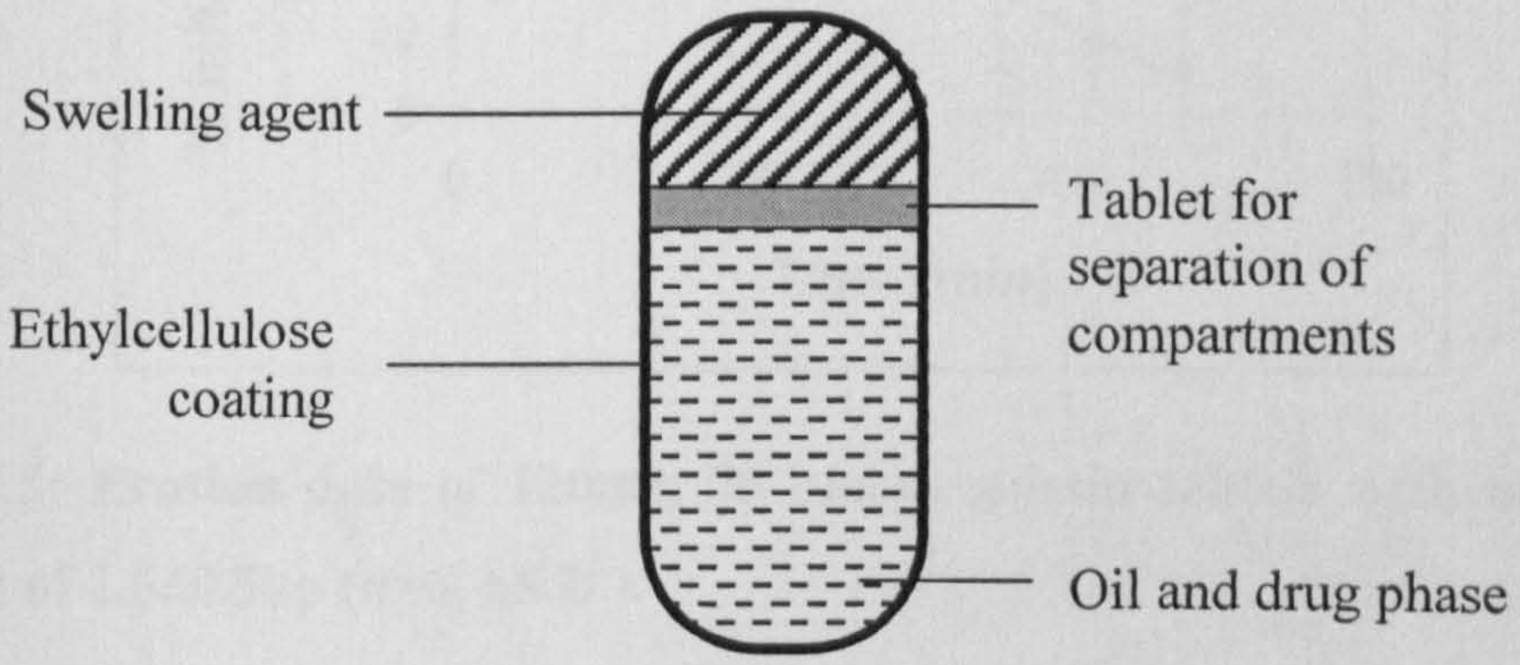

Figure 7.4: Final configuration of compartmentalised capsule.

Figure 7.4 highlighted the various components within the compartmentalised capsule as well as the potential for varying excipients to produce desired pharmaceutical profiles. The following sections detail the experiments conducted to investigate the effects of changing the constituents of the compartments on the dissolution profile.

7.4.2 Effect of tablet composition

Preformulation testing in terms of a tablet erosion study as well as dissolution testing of the final capsule formulation were conducted.

7.4.2.1 Tablet erosion study

The experimental protocol as described in Section 2.4.6 was carried out to determine, independently of the potential effects of wetting by corn oil, the rate at which the tablet would erode, exposing the drug and oil phase for dissolution. Addition of effervescent material (D-tartaric acid and sodium hydrogen carbonate with polyvinyl

pyrrolidone as binder, wet granulated with ethanol) was expected to not only increase the tablet erosion rate but also to aid expulsion of the swollen LH-21 from the capsule cap. From here on, 'effervescent material' refers to the mixture described above.

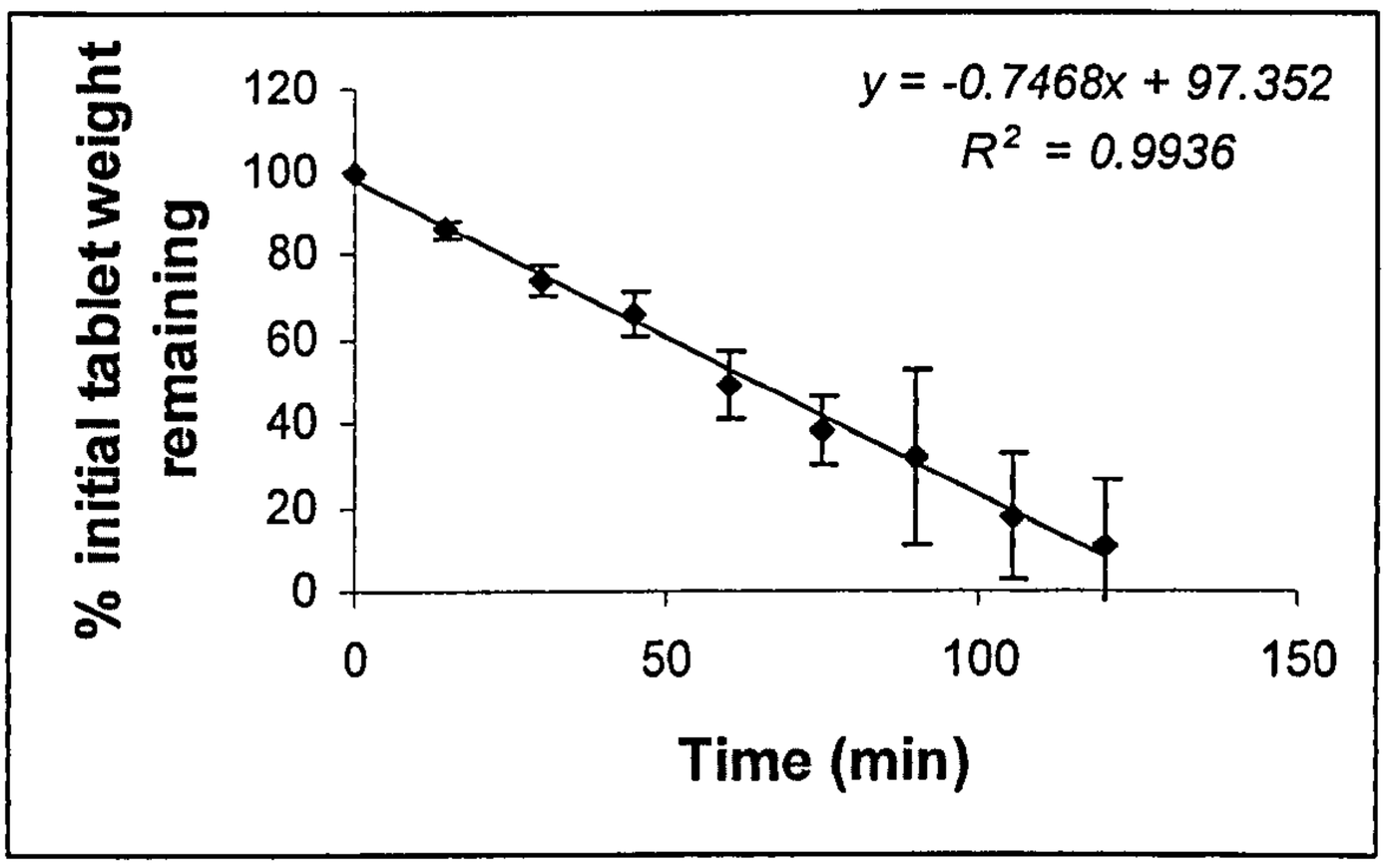

Figure 7.5: Erosion data of 120mg, 75 bloom gelatin tablets with mean tablet hardness of 2.6±0.5kp (n=6, ±S.D.).

From Figure 7.5, it was observed that tablet erosion proceeded in a near linear fashion, $R^2 = 0.994$, with a mean erosion rate of 0.9mg/min, calculated from the gradient of the curve, based on a 120mg tablet. These results were in agreement with the drug release profiles of the Case 4 Geomatrix tablet of Conte *et al.* (1993) in which only one face of a matrix tablet was uncoated while the rest of the tablet was coated with an impervious polymer (Figure 7.6a). This concept was similar to our system, whereby in this tablet erosion study, only one face of the gelatin-based tablet was exposed to the dissolution medium and the other face and the sides of the tablet was fitted into the plastic Beem® capsule (Figure 7.6b).

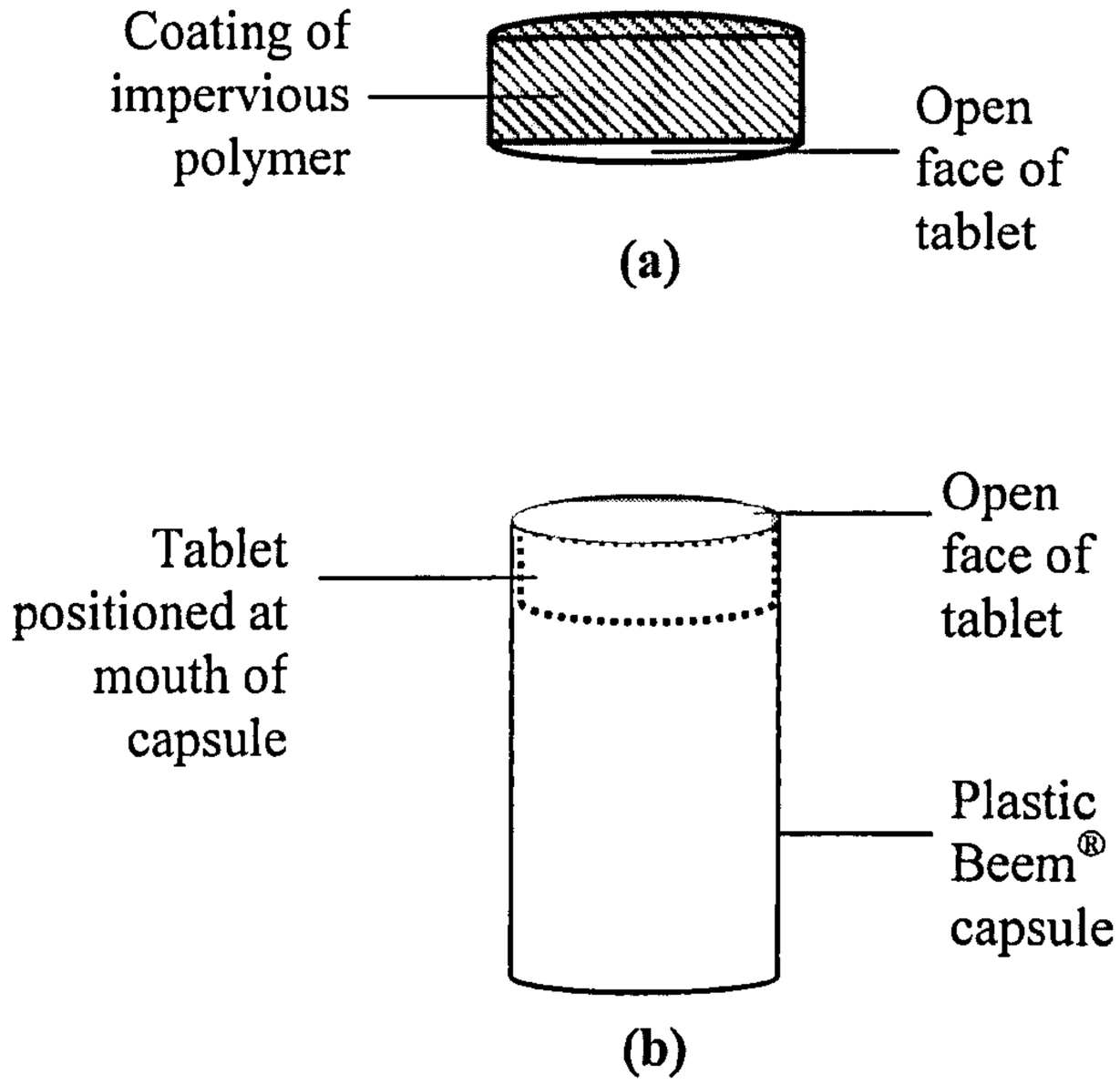

Figure 7.6: (a) Case 4 Geomatrix tablet of Conte *et al.* (1993), (b) capsule-tablet assembly for tablet erosion study.

Tablets of about 2kp hardness were prepared by direct compression of pre-weighed powder mixes. Addition of 12mg, 24mg, 36mg, 48mg and 60mg effervescent material separately to the 120mg of gelatin prior to direct compression resulted in increasing initial tablet erosion rates in a concentration-dependent manner ($p<0.0005$, one-way ANOVA). Tukey's pairwise comparisons showed that 10% effervescent material did not significantly increase the tablet erosion rate whereas effervescent material content of greater than 20% did significantly increase the tablet erosion rate. It also caused faster elimination of the tablet from the capsule assembly altogether (Table 7.2 and Figure 7.7). These studies showed that incorporation of effervescent material in a controlled fashion allowed for manipulation of the disintegration rate of the tablet.

Table 7.2: Mean tablet erosion rates of 75 bloom gelatin tablets containing effervescent material (n=6).

Effervescent material (% weight of gelatin)	Mean tablet erosion rate* (mg/min)
10	1.0
20	2.3
30	5.7
40	6.6
50	16.9

*** Determined from initial linear portion of graph.**

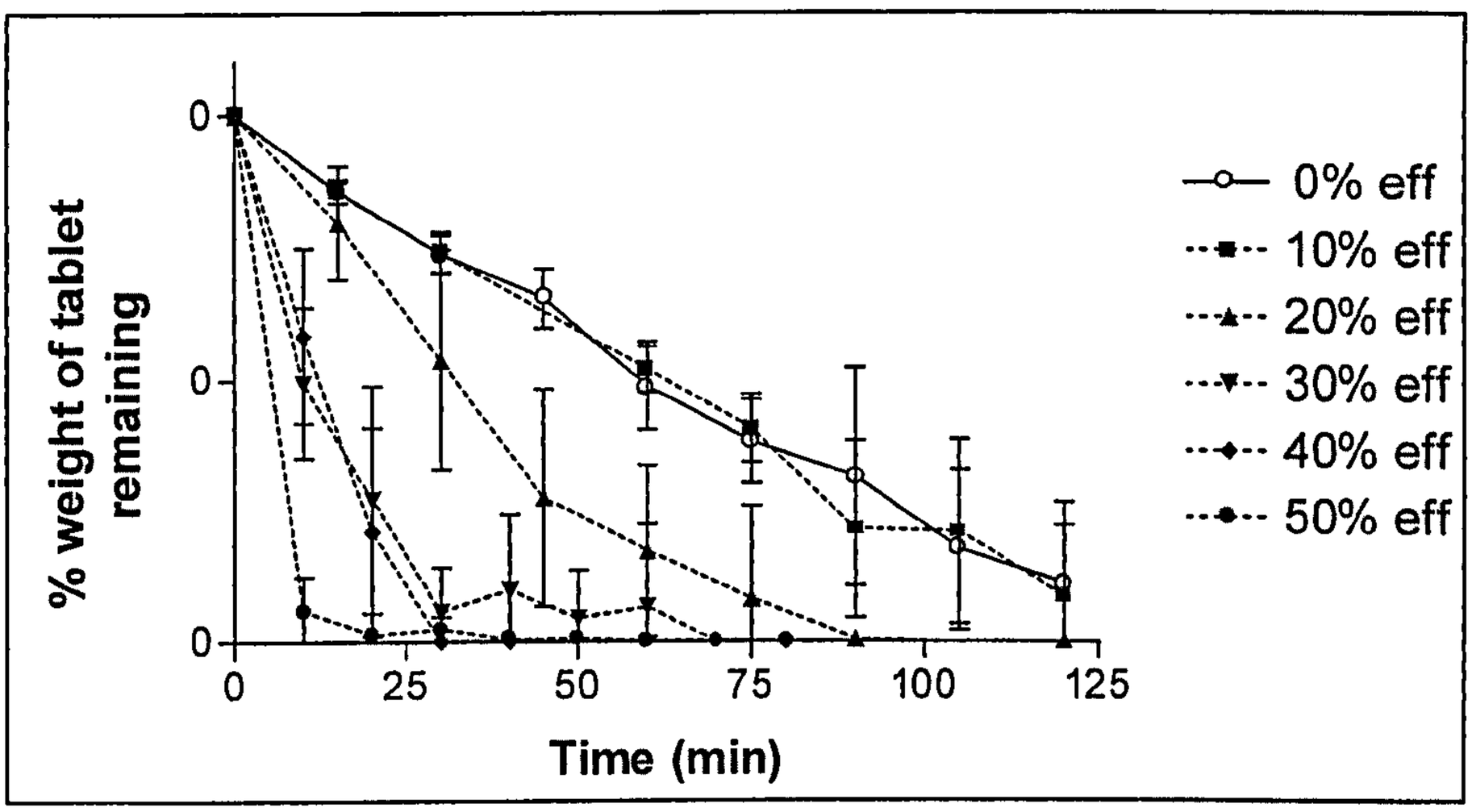

Figure 7.7: Mean erosion profiles of gelatin tablets with varying amounts of added effervescent material (eff, in graph) (n=6, ±S.D.).

The effect of tablet hardness on erosion rates was then investigated, concentrating on tablet hardness within the nominal ranges of 2-2.9, 3-3.9, 4-4.9, 5-5.9 and 6-6.9kp. Tablet hardness was determined by testing with a Schleuniger tablet hardness tester. The destructive test was implemented on 9 randomly selected samples from the batch of 120mg, 75 bloom gelatin tablets. The mean hardness from each range of tablets were as follows: 2.6±0.5, 3.3±0.3, 4.9±0.6, 5.7±0.4 and 6.6±0.4kp.

Figure 7.8 showed that varying tablet hardness did not seem to affect the mean tablet erosion rates and this was confirmed by one-way ANOVA which gave a *p*-value of 0.854. Hence the ranges of tablet hardness studied were believed to not have a significant effect on the tablet erosion rates thereby allowing for greater flexibility

during manufacture of the actual compartmentalised capsule without compromising its performance.

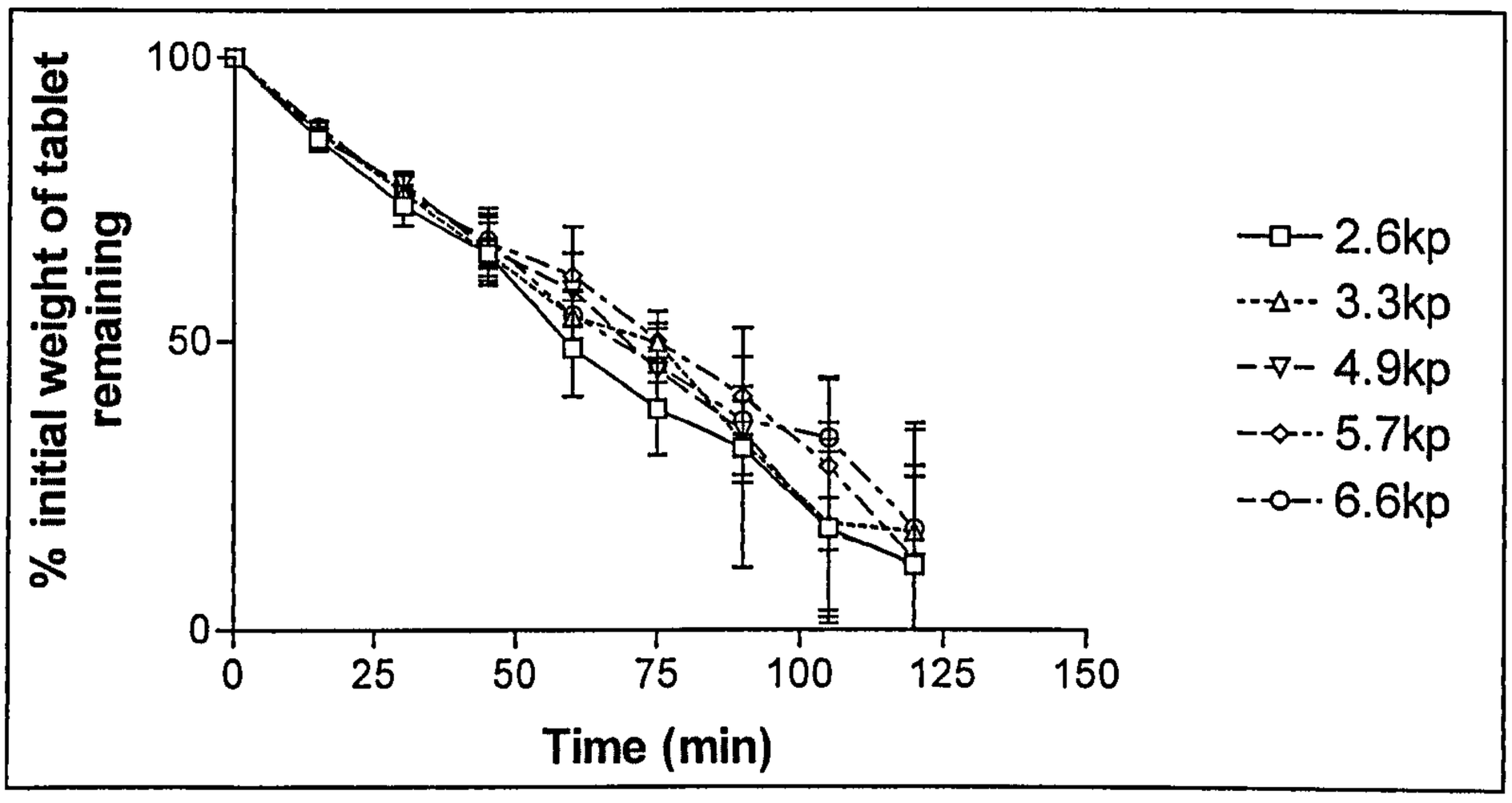

Figure 7.8: Effect of tablet hardness on mean erosion rates of 120mg 75 bloom gelatin tablets (n=6, ±S.D.).

7.4.2.2 *In vitro* dissolution studies

These initial dissolution studies were carried out with gelatin type B, approximately 225 bloom, instead of the 75 bloom gelatin used in the tablet erosion study above as this was the only gelatin available at the time. All hard gelatin capsules studied in this section contained 60mg LH-21 as swelling agent and 15mg paracetamol in 0.75mL corn oil as the hydrophobic phase. Sealing of the capsules was by adaptation of the LEMS® technique (Section 2.6.3.3) and dipcoating (Section 2.6.4.4) was performed 5 times using the basic coating solution (Section 2.6.4.1). Automated dissolution testing (Section 2.6.6) was used to determine the release profile of paracetamol from these capsules. The physical mixtures of the tablet formulations studied were detailed in Table 7.3 below; the total weight of each tablet was 150mg and mean hardness was 3kp.

Table 7.3: Tablet composition and final EC coating level for compartmentalised capsules.

	Tablet composition	EC coating level (%w/w) (±S.D.)
A	100% gelatin	2.2 (0.2)
B	90% gelatin, 10% sodium hydrogen carbonate	1.3 (0.3)
C	90% gelatin, 10% sodium chloride	1.1 (0.3)
D	80% gelatin, 10% D-tartaric acid, 10% sodium hydrogen carbonate	2.0 (1.0)
E	80% gelatin, 10% sodium chloride, 10% sodium hydrogen carbonate	1.9 (0.6)
F	50% gelatin, 50% Fast-Flo lactose	1.7 (0.6)

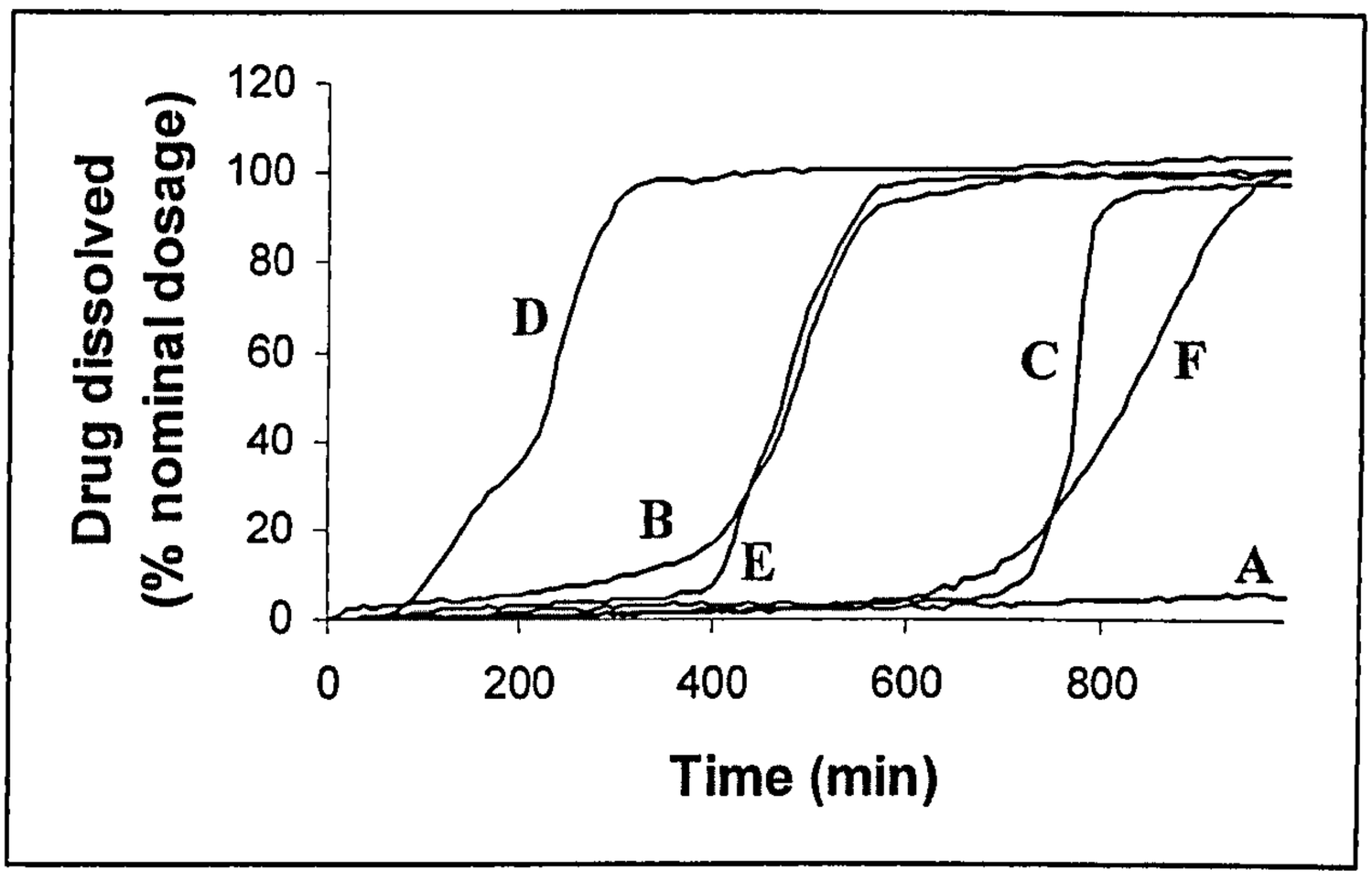

Figure 7.9: Sample dissolution curves of compartmentalised capsules with varying tablet compositions. A-F denote tablet composition as in Table 7.3.

Figure 7.9 displayed sample dissolution curves, rather than mean dissolution curves, as the variations between the 6 capsules tested were quite large. Capsules containing the pure gelatin tablet (A) did not release the entire drug load within 16.5 hours, shown in Figure 7.10. Figure 7.11A confirmed that although the swelling agent LH-21 had ruptured the EC coat, drug release was prevented by incomplete dissolution of the gelatin tablet. This could be due to the amount of gelatin used to form the tablet (150mg) being excessive and dissolution was not possible within the timeframe. Furthermore, the bloom of the gelatin, 225, also imparted a depressive effect on the tablet's ability to dissolve quickly.

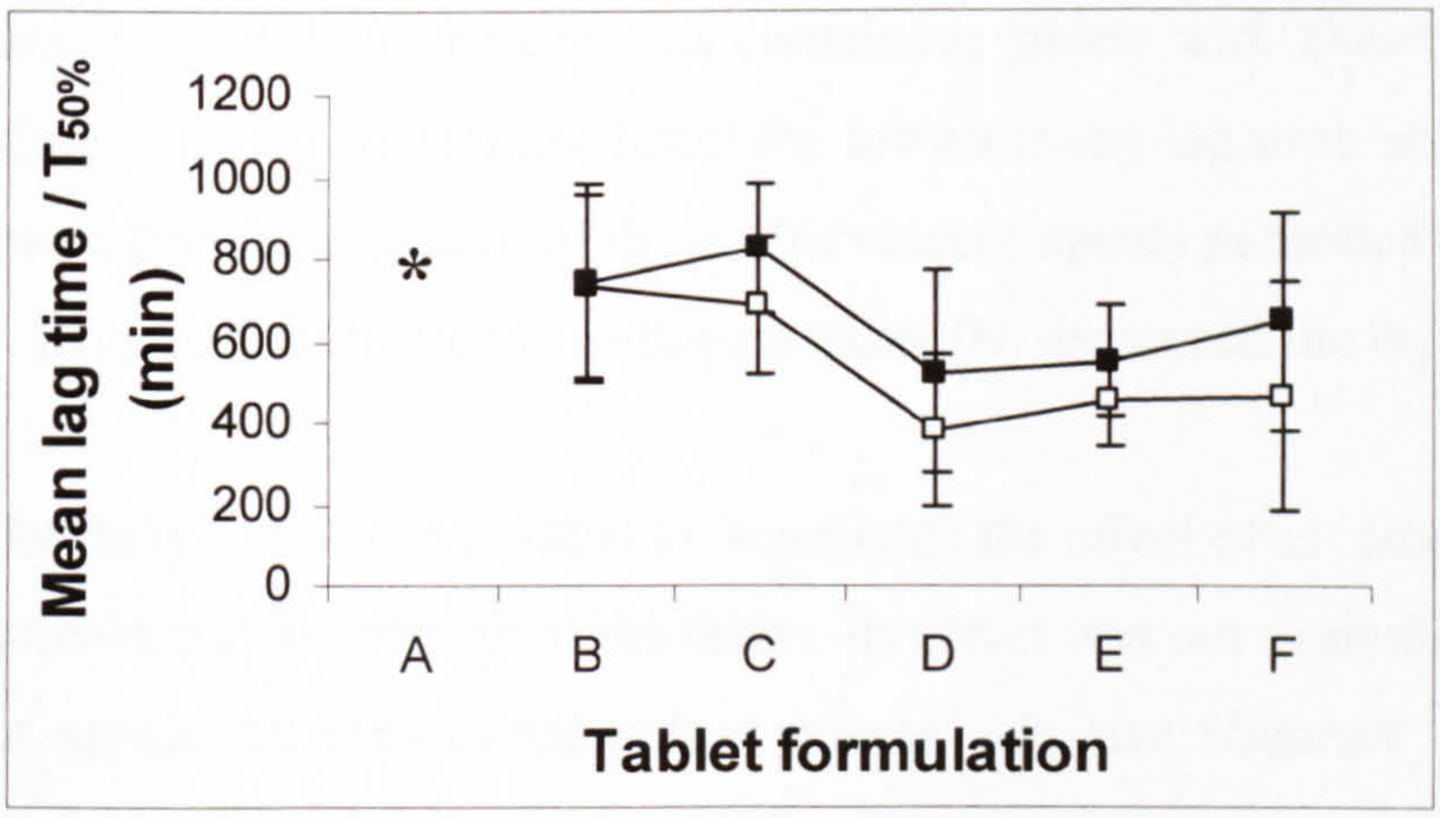

Figure 7.10: Mean lag times (empty squares, □) and mean $T_{50\%}$ (solid squares, ■) of compartmentalised capsules with varying tablet formulations, A-F as in Table 7.3 (n=6, ±S.D.). *Denotes lag time and $T_{50\%}$ not achieved within 16.5 hours.

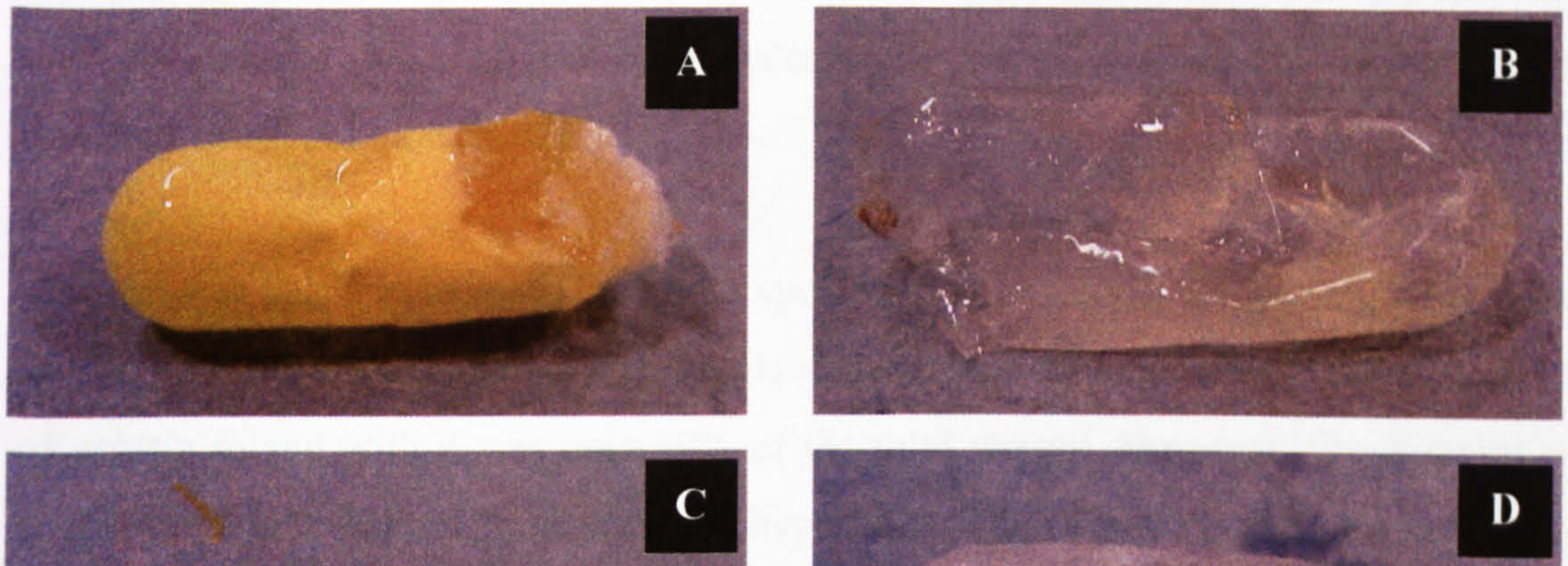

Figure 7.11: Photographs of compartmentalised capsules with varying tablet formulations post-dissolution. A-F was as according to descriptions in Table 7.3.

From Figures 7.9 and 7.10, the capsules containing tablets with D-tartaric acid and sodium hydrogen carbonate (D) displayed the lowest mean lag time and mean $T_{50\%}$. This confirmed that the inclusion of these effervescent agents permitted manipulation of lag time. Even sodium hydrogen carbonate alone (B) decreased the lag time.

Sodium chloride (C) was incorporated to investigate the effect of an osmotic agent on the disintegration and dissolution of the tablet. Its effect was not as pronounced as the effervescent agents but the desired pulsed release was also obtained, albeit with a more prolonged lag time. Mixing sodium chloride and sodium hydrogen carbonate (E) did not decrease the lag time any further than with sodium hydrogen carbonate alone (B).

The photographs of capsules B, C, D and E post-dissolution (Figure 7.11) confirmed that the capsule contents had been successfully expelled from the dosage form, leaving behind only the EC shell.

Tablets with Fast-Flo lactose (F), were expected to dramatically decrease the lag time, not only because the excipient was highly water-soluble but also because the amount of gelatin mixed with it was only 50% of the total weight. However, the dissolution profiles obtained did not agree with this hypothesis. The condition of the capsule post-dissolution (Figure 7.11F) also verified that dissolution of the capsule was incomplete.

Following this initial set of studies, the effect of changing the bloom strength of gelatin and the weight of the gelatin tablet were investigated. Figure 7.12 showed the dissolution profiles of selected capsules where firstly, 225b gelatin was replaced with 75b gelatin (profile 2) and then, the weight of the 75b gelatin tablet was reduced to 120mg (profile 3). Profile 1 corresponded to the drug release of paracetamol from a compartmentalised capsule with 150mg, 225b gelatin tablet.

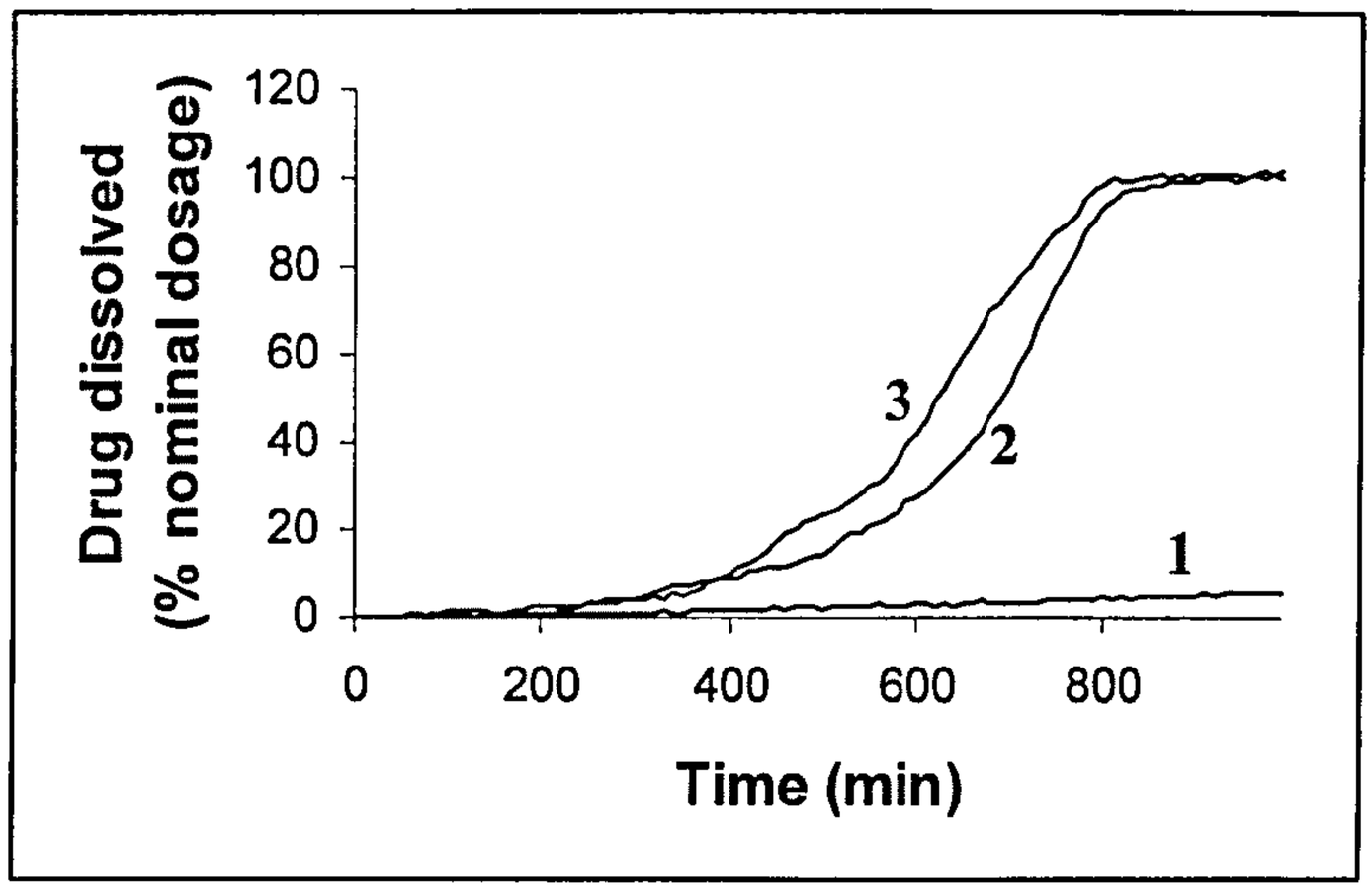

Figure 7.12: Sample dissolution profiles of compartmentalised capsules with (1) 150mg, 225b gelatin tablet, (2) 150mg, 75b gelatin tablet and (3) 120mg, 75b gelatin tablet.

Lowering the bloom strength of the gelatin used produced a dissolution profile that incorporated lag time and pulsed release. Reducing the amount of gelatin used to form the plug shifted the profile to the left, albeit only slightly. Hence it was observed that bloom strength was a strong determinant of the rate of tablet disintegration.

7.4.3 Effect of swelling compartment composition

7.4.3.1 Capsule rupture studies with methylene blue as marker

Initial studies to determine the contribution to lag time offered by the expansion rate of the swelling agent leading to rupture of the EC coat involved using a water-soluble marker within the swelling compartment that would be detected by UV spectrometry. The bodies of size 00 Conisnap® hard gelatin capsules were filled with 750mg Emcompress® and 120mg, 75 bloom gelatin tablets were fitted snugly into the neck of the capsules. The capsule caps were filled with 51mg LH-21 and 9mg methylene blue, fitted onto the prepared capsule bodies and locked in place. Banding was performed by brushing a single layer of 25%(w/v) 75 bloom gelatin solution onto the cap/body junction. The capsules, dried in a dessicator for 24 hours, were coated in the Aeromatic Strea-1 fluidised bed coater at the usual settings (Section 2.6.4.2) with the generic coating solution (Section 2.6.4.1). Two coating cycles resulted in coating

levels of 0.5%(w/w) and 1.0%(w/w) as determined from pre- and post-coating weights of the capsules. Automated dissolution was carried out according to the method outlined in Section 2.6.6, the absorbance measured at 668nm.

For capsules with 0.5%(w/w) coating, only one capsule ruptured at about 115 minutes giving a burst release of methylene blue while the remaining five capsules did not release any marker within the 3-hour dissolution run. As for the 1.0%(w/w) coated capsules, no methylene blue was detected throughout a 10-hour dissolution run.

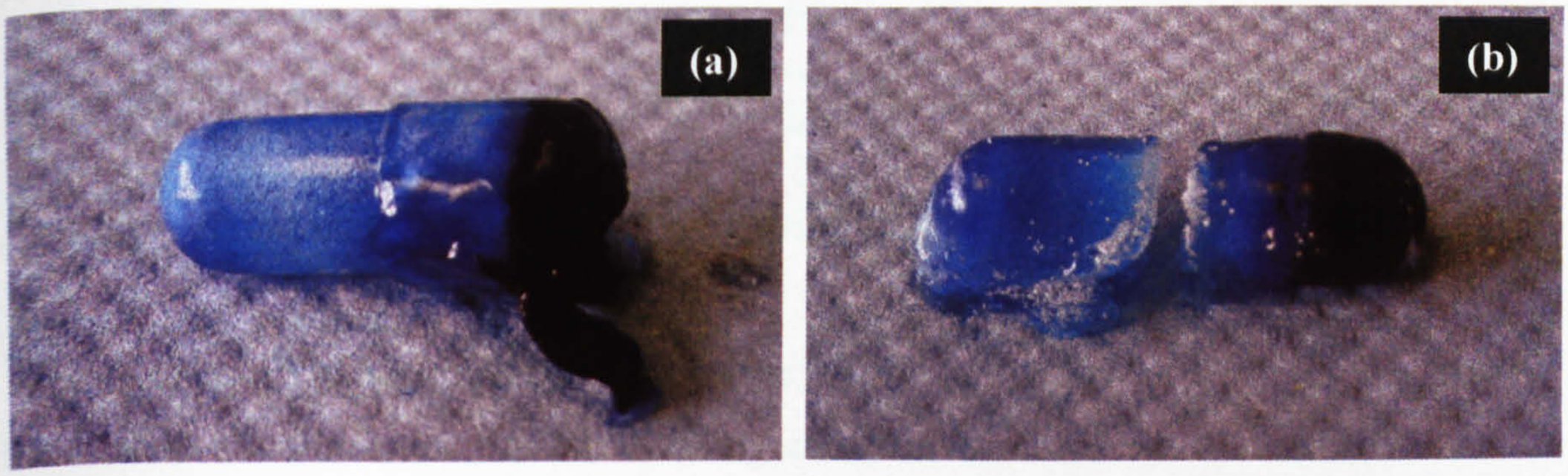

Figure 7.13: Photographs of compartmentalised capsules with methylene blue as marker in swelling compartment which (a) ruptured at cap and (b) did not rupture at the cap, but at the middle section within 3-hour dissolution.

Figure 7.13(a) highlighted the rupturing of the EC coat due to swelling of LH-21 giving rise to detection of methylene blue release by the UV spectrometer. Other capsules, which did not release any methylene blue, were of the final structure shown in Figure 7.13(b), ruptured in the middle, most likely the region of greatest weakness arising from the banding with aqueous gelatin. Previous studies in Section 7.4.2.2 indicated that 60mg LH-21 was able to rupture the coating; it was highly unlikely that a reduction of 9mg would exert such a detrimental effect on the swelling capacity. Instead, it was postulated that methylene blue suppressed the swelling of LH-21, in a manner yet undetermined. Hence an alternative marker was proposed for this study: paracetamol.

Section 4.4.3 described the concentration-dependent depressive effect that paracetamol had on water uptake of LH-21 but the absolute weights of LH-21 used in this study were much less than the 500mg used in the water uptake studies hence additional experiments were performed as detailed below.

7.4.3.2 Capsule rupture studies with paracetamol as marker

The swelling compartment formulations studied were as follows:

Table 7.4: Swelling compartment formulations with 20mg paracetamol as marker of capsule rupture.

Formulation	LH-21 (%w/w)	Emcompress® (%w/w)	Effervescent material* (%w/w)
A	100	0	0
B	80	20	0
C	60	40	0
D	40	60	0
E	60	0	40

***Effervescent material prepared as described in Section 2.4.6.**

Emcompress® (dibasic calcium phosphate) was incorporated as an inert filler to maintain the fill volume of the swelling compartment. The total fill weight in the swelling compartment was fixed at 60mg. The capsules also contained 120mg 75 bloom gelatin tablets and 750mg Emcompress® in the capsule body. They were sealed by gelatin banding with 25%(w/v) 75 bloom gelatin solution and spray coated for a nominal weight gain of 1.5%(w/w).

Table 7.5: Lag time to rupture of EC coat.

Formulation*	Number of ruptured capsules**	Lag times per capsule (min)
A	2	40, 130
B	1	70
C	3	10, 20, 40
D	0	-
E	3	40, 40, 290

***As per Table 7.4. ** Out of six replicates.**

Each dissolution cycle was performed on six capsules of the same formulation and lasted for six hours. Table 7.5 showed the great variability within the same batch of capsules. Hence the search for a suitable marker and filler was ended here since it was becoming increasingly difficult to locate one that would not interact with LH-21, compromising its swellability.

7.4.3.3 Prediction of lag time through swelling force and puncture test experiments

As it was not possible to directly measure the lag time due to swelling agent expansion prior to EC shell rupture, the results obtained from independent swelling force studies (Section 3.4.4) and EC film puncture testing (Section 5.4.2.2) were combined to predict the ability of swelling agent to rupture the EC coating.

The surface area of the capsule cap upon which the swelling agent acts was estimated to be 100mm^2. This was done by cutting the portion of the cap exposed to swelling agent into quarters and estimating the area using graph paper. Mean puncture strength (N/mm^2) was then converted to the mean force required to rupture the film coat at the capsule cap (N). It was determined from linear regression of the results of the swelling force studies that

$$F = kL \qquad \textbf{(Equation 3.2,} \text{ Section 3.4.4)}$$

whereby F = maximum force generated by LH-21(N), and L = weight of LH-21(g). k is a constant of the value 4.4. R^2 value for linear regression = 0.974; n=3.

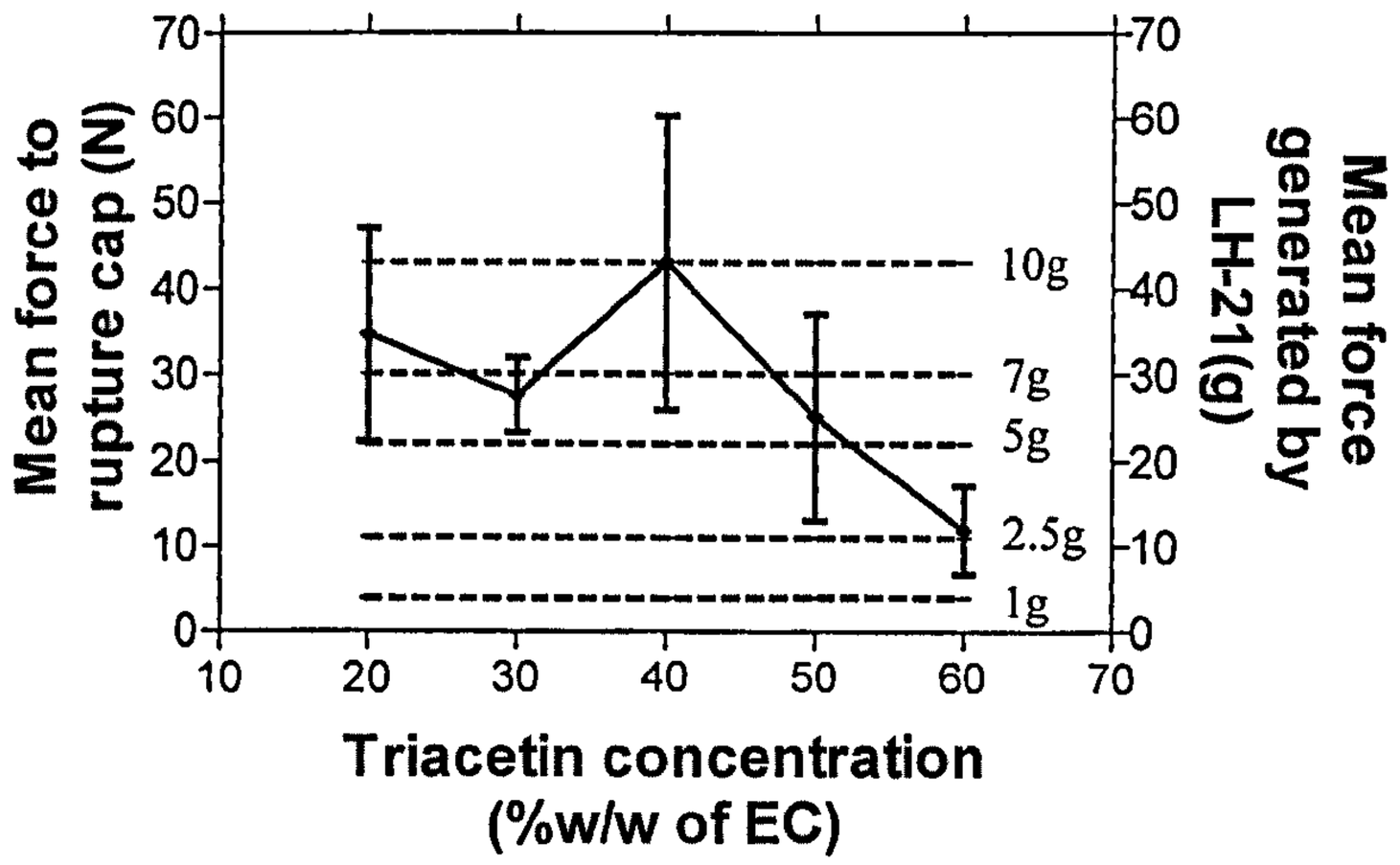

Figure 7.14: Theoretical requirements of LH-21 to rupture 3%(w/v) EC films.

The horizontal lines depicted on Figure 7.14 were derived from Equation 3.2 and represented the mean force generated by the varying amounts of LH-21. This correlation resulted in highly excessive amounts of LH-21 theoretically required to rupture the EC shell which were not required, as shown in preliminary data. It must be noted that these studies may not accurately reflect the actual *in vivo* performance of the capsule, as temperature control was not implemented. Furthermore, the lag time afforded by the resistance to rupture of the capsule coat is also affected by other factors, such as shear stress caused by peristaltic movement of the gastrointestinal tract. In practice the EC coat was sprayed onto the capsule and the tensile properties of this coat would have been different from that of solution-cast films. This, and the limits of space available for expansion of LH-21 within the cap of the capsule, should reduce the amount of LH-21 required for capsule rupture.

7.4.3.4 *In vitro* dissolution studies

In investigating the effect of changing the swelling compartment composition, the other components of the compartmentalised capsule were fixed as follows: 150mg 225 bloom gelatin tablet with mean hardness of 3kp, 15mg paracetamol dispersed in 0.75mL corn oil in a Size 00 Conisnap® hard gelatin capsule, sealed with the adapted LEMS® method and dipcoated 5 times with coating solution (3%(w/v) EC, 5%(w/w of EC) triacetin, 50:50%(v/v) acetone: IPA).

Table 7.6: Composition of swelling compartment (total weight fixed at 60mg) and final EC coating level.

Formulation	Swelling compartment	EC coating level (%w/w) (±S.D.)
A	100% LH-21	2.0 (0.5)
B	90% LH-21, 10% sodium hydrogen carbonate	1.0 (0.2)
C	80% LH-21, 10% sodium hydrogen carbonate, 10% D-tartaric acid	1.2 (0.2)
D	80% LH-21, 10% sodium hydrogen carbonate, 10% sodium chloride	2.4 (0.2)
E	70% LH-21, 10% sodium chloride, 10% sodium hydrogen carbonate, 10% D-tartaric acid	2.1 (0.7)

These capsules were subjected to automated dissolution testing (Section 2.6.6). Only the batch of formulation B ruptured and achieved $T_{50\%}$ within the 16.5 hour

dissolution for all six capsules (Figure 7.15) with the dissolution profiles of individual capsules showing variability in drug release.

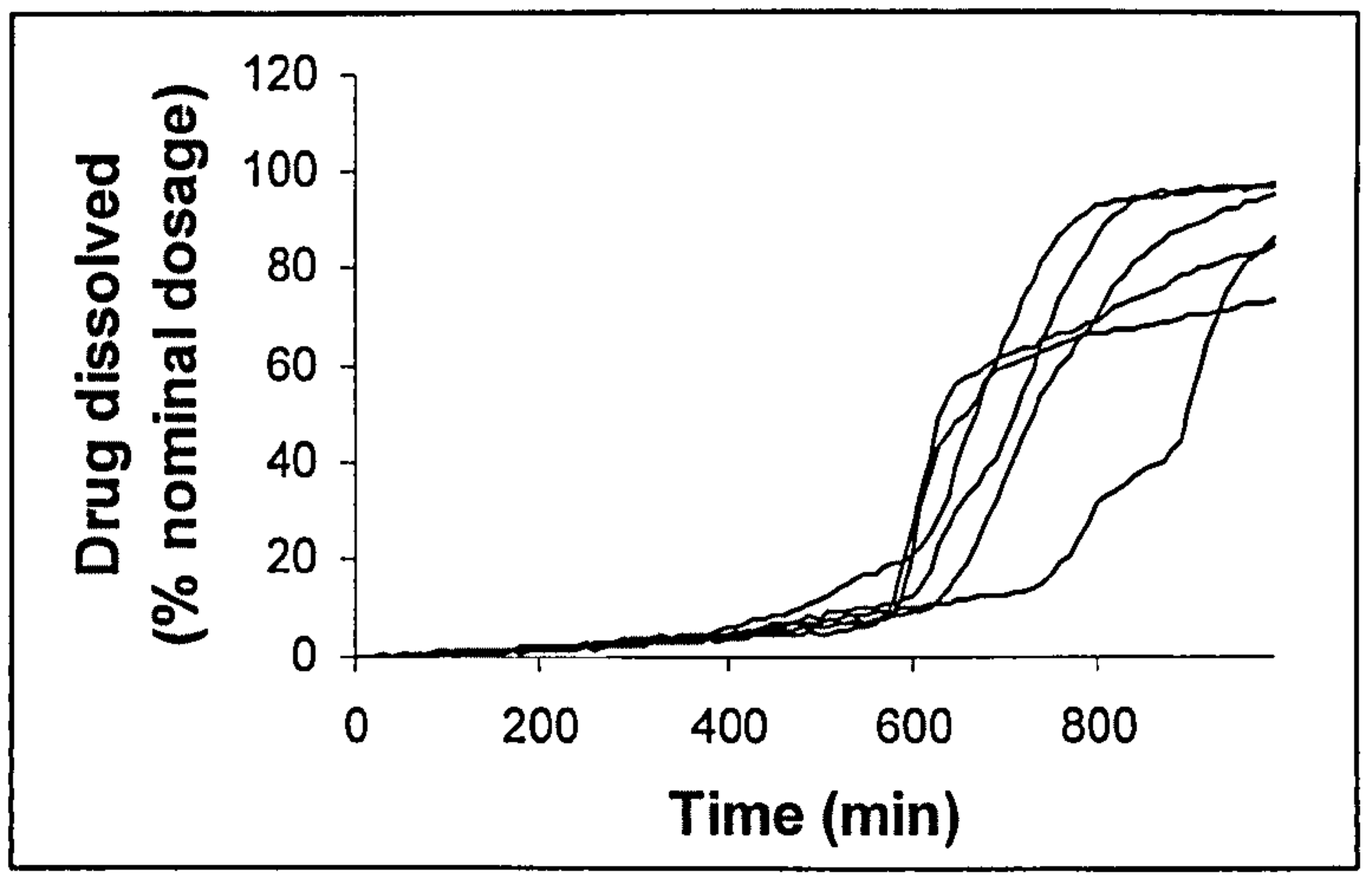

Figure 7.15: Dissolution profiles of 6 capsules of formulation B.

No release of drug was detected from formulation A, three capsules ruptured for formulation C and two each for formulations D and E. The variations among dissolution profiles of the same batch of capsules were very great, indicating that there were problems within the manufacturing process that were yet to be addressed and corrected.

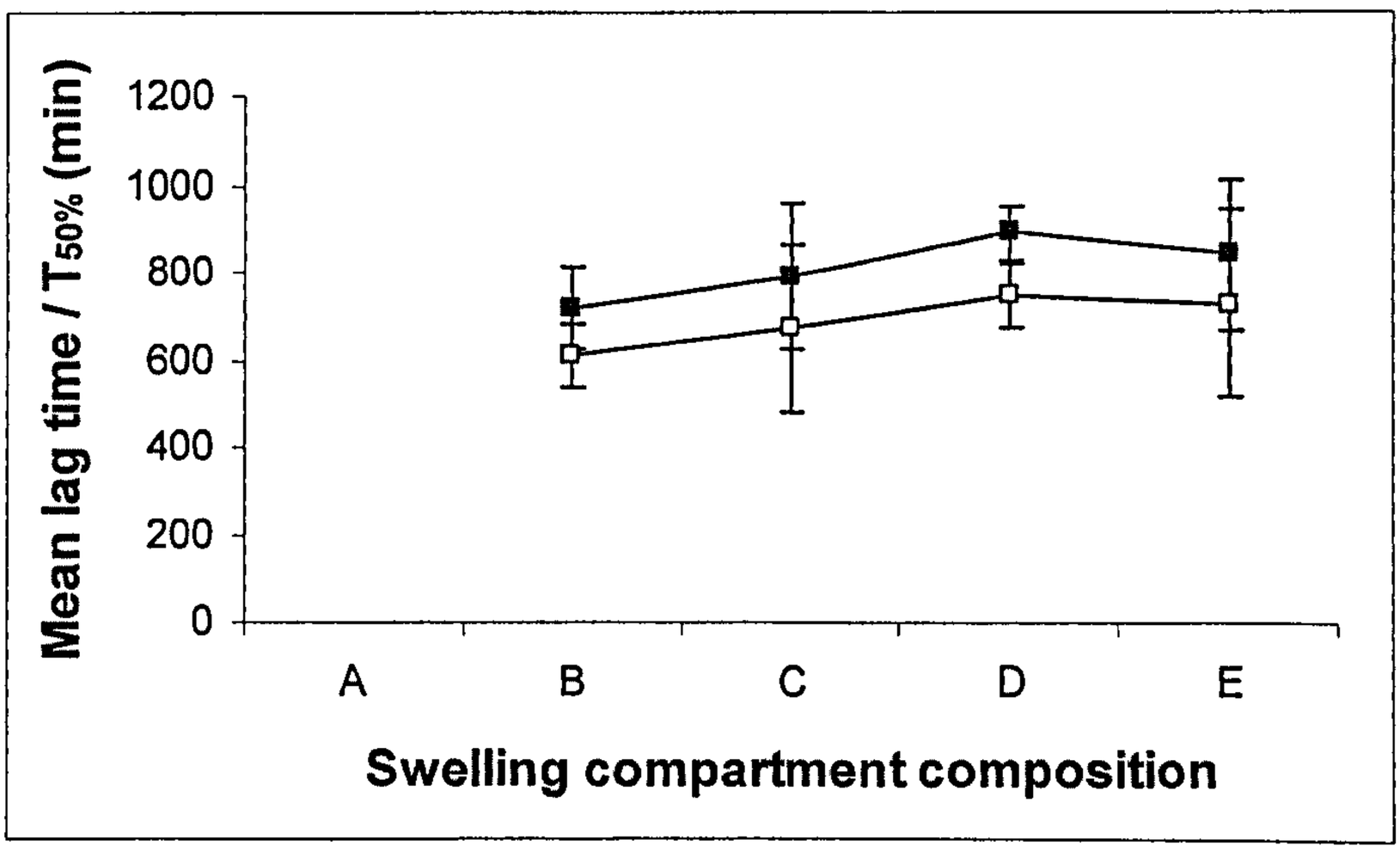

Figure 7.16: Effect of swelling compartment composition on mean lag time (empty squares, □) and mean $T_{50\%}$ (solid squares, ■). (n=6, ±S.D.)

Mean lag times and $T_{50\%}$ did not vary greatly among the swelling compartment formulations studied, hence the effects of changing the compositions could not be conclusively determined.

7.4.4 Comparison between HPMC capsules and hard gelatin capsules

Hydroxypropylmethylcellulose (HPMC) capsules (e.g. Vcaps® of Capsugel) were advocated as a vegan/vegetarian alternative to hard gelatin capsules which are derived from animal sources. Although not part of the initial objectives, it was possible to compare the performances of both these types of capsules which were claimed to be performance-equivalent.

The same formulations as detailed in Table 7.6 were filled into Size 00 HPMC capsules, with the other variables (tablet composition, hydrophobic phase fill and coating level) also remaining fixed as per the set of studies in Section 7.4.3.4. Final coating levels (%w/w) (±S.D.) from successive dipcoating five times were as follows for each formulation: A=2.2 (0.2), B=1.8 (0.3), C=1.7 (0.4), D=2.2 (0.5) and E=1.9 (0.9). These capsules then underwent automated dissolution (n=6).

Again, variability among the dissolution profiles from capsules of the same batch was observed but most capsules did release drug within 16.5 hours, compared to those filled into hard gelatin capsules (Section 7.4.3.4).

A constant, the rupture factor (*RF*), was introduced here, to compare the performances of the HPMC and hard gelatin capsules. This value was derived from the product of the number of capsules that achieved 50% drug release within 16.5 hours and the mean coating level (%w/w) of the capsule batch. Inclusion of the latter variable enabled the effect of the coating level to be considered while comparing across the data series. The higher the *RF* value, the more likely the capsule was to release drug within the 16.5 hour dissolution period. *RF* values for both types of capsule with varying swelling compartment formulations were shown in Figure 7.17.

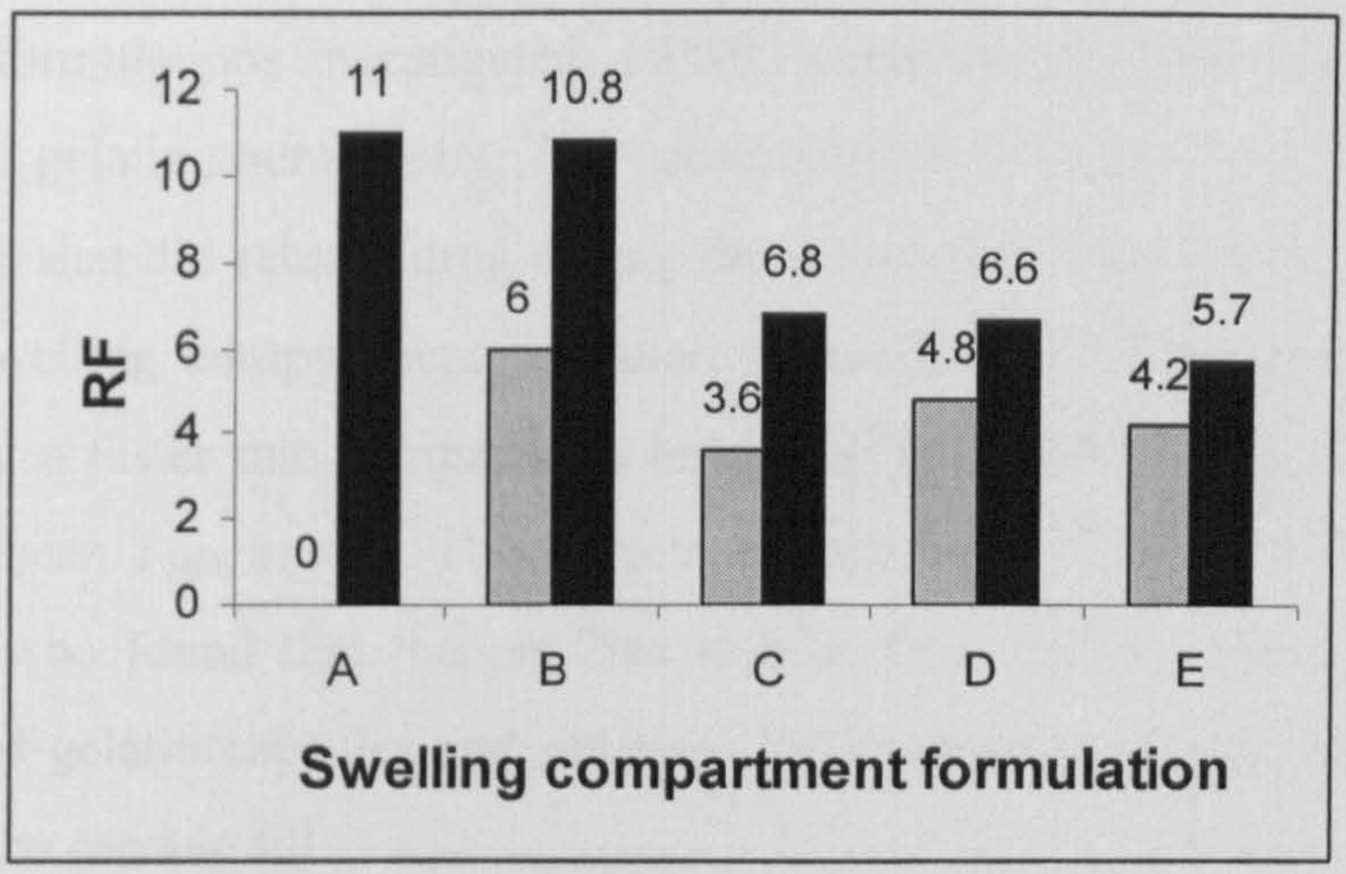

Figure 7.17: *RF* values for hard gelatin (shaded columns) and HPMC (black columns) capsules containing different swelling compartment formulations as per Table 7.6.

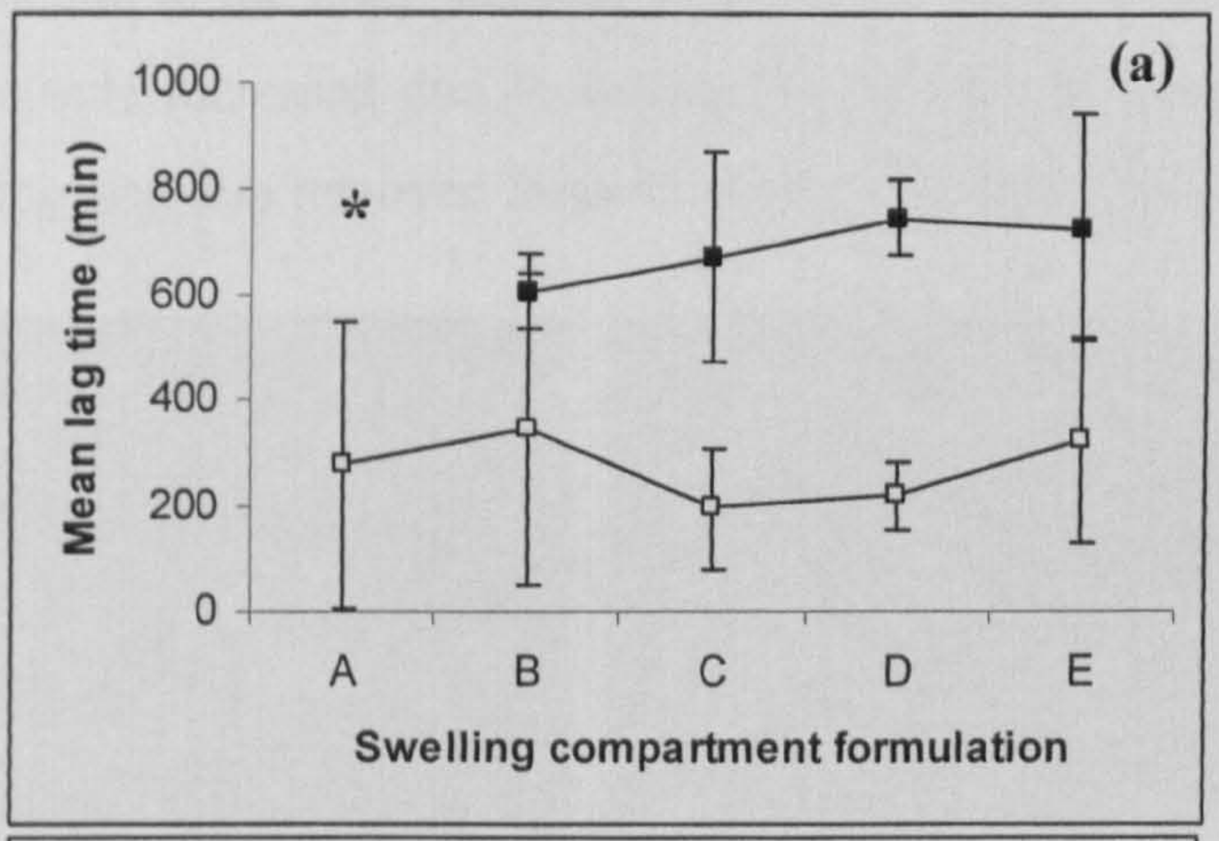

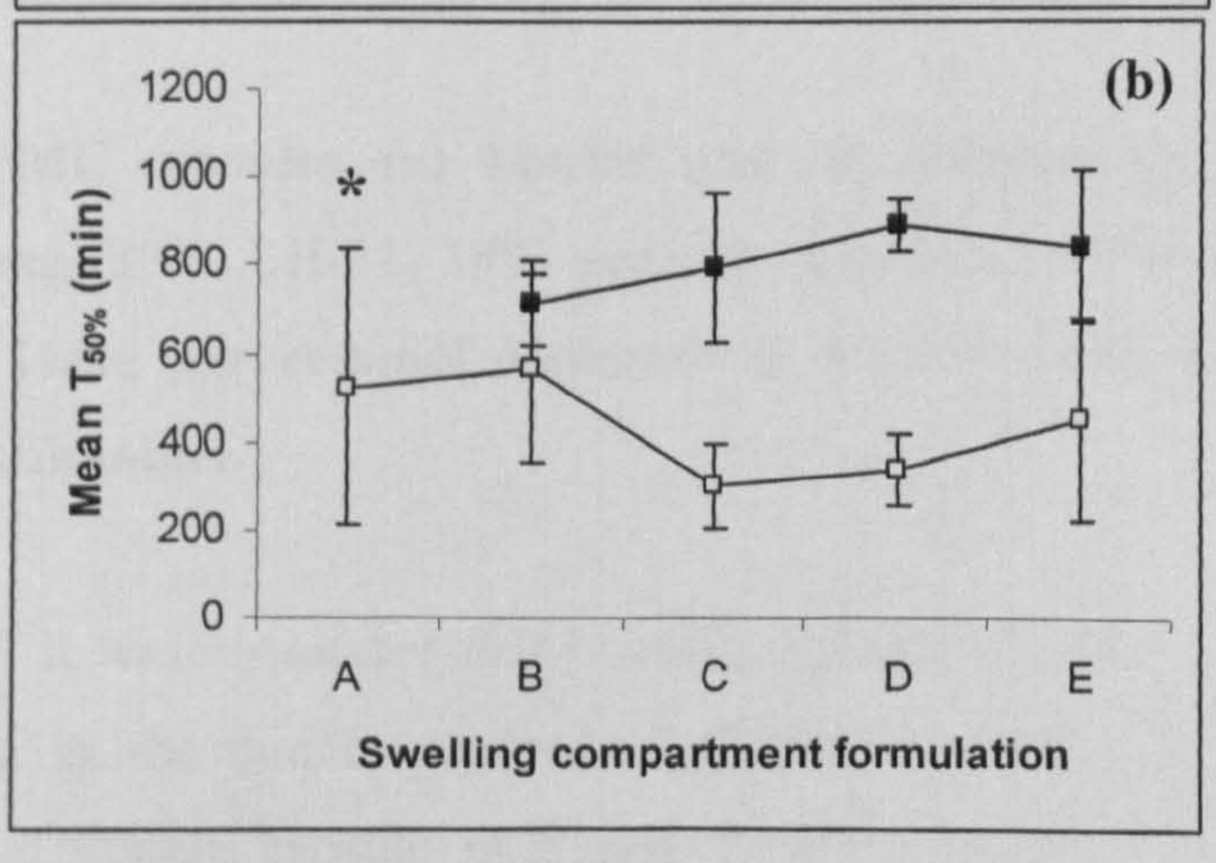

Figure 7.18: Effect of HPMC (empty squares, □) and hard gelatin capsules (solid squares, ■) on (a) mean lag time and (b) mean $T_{50\%}$ of compartmentalised capsules with varying swelling agent compositions. * Denotes none of the six capsules ruptured in 16.5 hours.

Over all the formulations investigated, HPMC capsules exhibited higher *Rf* values than their hard gelatin counterparts. The values plotted in Figure 7.18 were restricted to the capsules that did release drug during the dissolution time frame of 16.5 hours. Among the swelling compartment formulations studied, HPMC capsules tended to release drug at a faster rate compared to hard gelatin capsules, exemplified in mean lag time and mean $T_{50\%}$ values. This correlated well to the findings of Podczeck and Jones (2002) who found that theophylline release from HPMC capsules was faster than from hard gelatin capsules and gelatin / PEG capsules irrespective of the other excipients in the capsule fill.

Inspection of the HPMC capsules post-dissolution (sample capsule in Figure 7.19a) revealed that cracking of the EC shell consistently occurred in the middle of the capsule, at the junction of the body and cap. In order to eliminate the possibility that fragility of the capsule increased due to wetting of the capsule during the banding process, the banding step was removed from the manufacturing process.

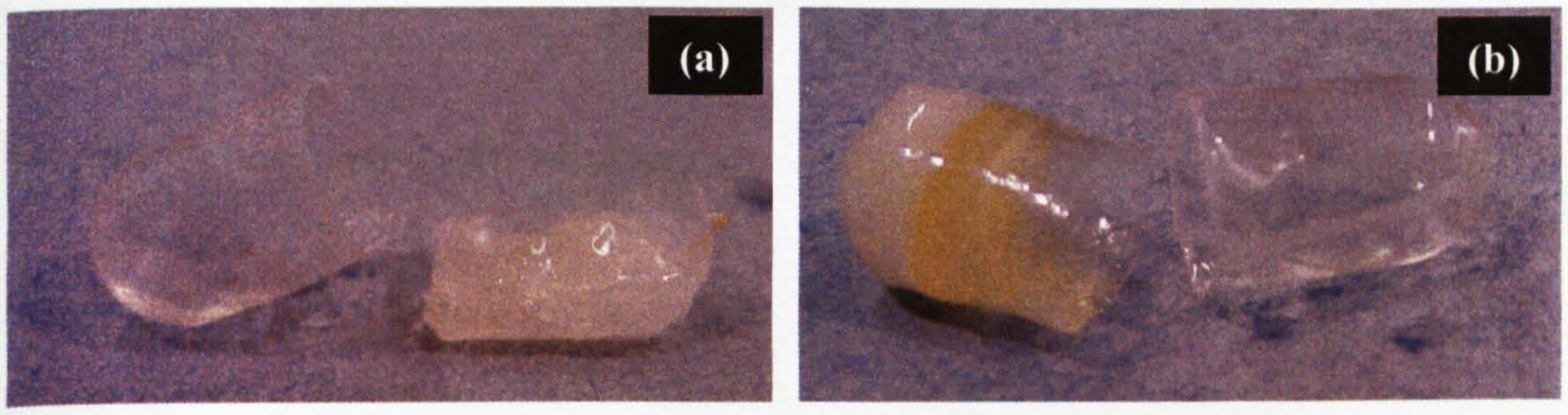

Figure 7.19: HPMC capsules, (a) banded and (b) unbanded, post-dissolution. Capsule fill: 60mg (80% LH-21, 10% sodium chloride, 10% sodium hydrogen carbonate) and 15mg paracetamol dispersed in 0.75mL corn oil, separated by 150mg 225b gelatin tablet.

From Figure 7.19 it was concluded that banding was not the main cause of HPMC capsules cracking in the middle section as opposed to rupturing in the swelling compartment. The sample capsule in Figure 7.19(b) also showed that premature capsule rupture in the middle caused release of oil/drug phase without prior rupturing of the EC shell by swelling agent and dissolution of the tablet. This meant that the postulated release mechanism was not adhered to and was not uniform throughout the batch of capsules prepared.

Preferential cracking at the mid-section of the EC shell could be explained by the findings of Chiwele *et al.* (2000). They showed that HPMC capsule dissolution *in vitro* occurred uniformly across the entire shell, as opposed to hard gelatin capsules which initially disintegrate at the weak points of the shell i.e. the shoulder of the round ends, followed by disintegration of the whole body. This would pose a problem to the equivalency of the compartmentalised capsule when formulated in a HPMC capsule as opposed to a hard gelatin capsule. These results also highlighted the possibility that rupture at the swelling compartment could be promoted by the fact that the capsule shoulder was structurally weaker than the rest of the capsule.

Although studies by Honkanen *et al.* (2002) and Cole *et al.* (2004) have suggested that HPMC and hard gelatin capsules offered similar bioavailability when tested *in vivo*, the formulations studied were for immediate release with no incorporation of any aspect of controlled release. Especially for rupturable dosage forms, seen in the studies here on compartmentalised capsules, there may very likely be variations in performance if HPMC and hard gelatin capsules were to be used interchangeably.

7.4.5 EC film coating with minicoater

The Minicoater / Drier (Caleva Process Solutions, Dorset, U.K.) proved to be a valuable tool for coating small quantities of capsules. Its method of operation was described in Section 2.6.4.3. Prior to coating with this equipment, the optimum coating parameters were determined through trial and error on dummy capsules of the same weight as the compartmentalised capsules.

It was found that coating parameters were dependent upon the type of coating solution to be delivered, and the opportunity was taken to experiment with pseudolatexes as an alternative to organic solutions. The coating conditions deemed to produce optimum coating were detailed in Table 7.7.

Table 7.7: Optimal coating parameters for organic and aqueous-based coating using minicoater.

Operational parameter	Organic coating*	Aqueous coating**
Inlet airflow (m/s)	7	7
Temperature (°C)	40	60
Vibrational amplitude (mm peak-peak)	3	3
Vibrational frequency (Hz)	17	17
Solution flowrate (mL/h)	50	30
Nozzle height (mm)	140	140
Atomising air pressure (bar)	0.4	0.4
Drying time (min)	5	5
Type of tubing	Platinum cured silicone	Plastic

*** 3%(w/v) EC, 5%(w/w of EC) triacetin, 50:50(%v/v) acetone:IPA**

**** Surelease composition: EC 20cP (25%w/w), ammonium hydrochloride (28%), medium chain triglycerides, oleic acid, purified water. Diluted by mixing 40%(w/w) distilled water and 60%(w/w) Surelease.**

From Table 7.7, the only parameters that were dependent on the type of coating were the temperature and the solution flowrate. The solvent composition of the organic coating solution, 50:50%(v/v) acetone and IPA, had a lower boiling point that that of water hence the lower temperature at which the minicoater was operated. These chosen temperatures allowed for a suitable evaporation rate of solvent which would provide adequate deposition of polymer molecules while preventing overwetting of the dosage forms.

The temperatures that were chosen in this study correlated well with the temperatures chosen by other workers in their investigations with both organic and aqueous coatings. Wesseling and Bodmeier (1999) used 45-50°C for spraying of Aquacoat® and 35°C for ethanolic solution of EC. It must be noted that they used a fluidised bed coater, which is in essence a closed system. The slightly higher temperatures that were required with the minicoater were likely to be a consequence of generated heat being easily lost to the surroundings.

The difference in solution flow rates was also due to the chemical properties of the coating solutions. The lower the boiling point, the easier it was to form a film. In

order to prevent this occurring at the nozzle aperture, the solution flowrate was upped to ensure smooth flow of the coating solution, reducing the risk of nozzle clogging.

Changing the tubing was essential when using different types of coating solution. The rigidity of the plastic tubing decreased substantially upon continuous pumping of the organic solution. Platinum cured silicone tubing was more suited to the organic solution, maintaining its structural integrity over many coating cycles.

7.4.5.1 Calibration of minicoater with Surelease

Initial testing with the minicoater was performed using Surelease as platinum cured tubing for coating with organic solutions was not yet available. Water-soluble colouring was added to the Surelease suspension [60:40(%w/w) Surelease: distilled water] in order to visually appreciate the level of coating applied.

A drop of cochineal food colouring and approximately 5mg of methylene blue powder were added to separate batches of Surelease suspension. Six dummy capsules filled with corn oil banded with 25%(w/v) 225b gelatin solution were coated according to the parameters detailed in Table 7.7 for aqueous coating. The spray period was fixed at 15 minutes and four consecutive runs were carried out.

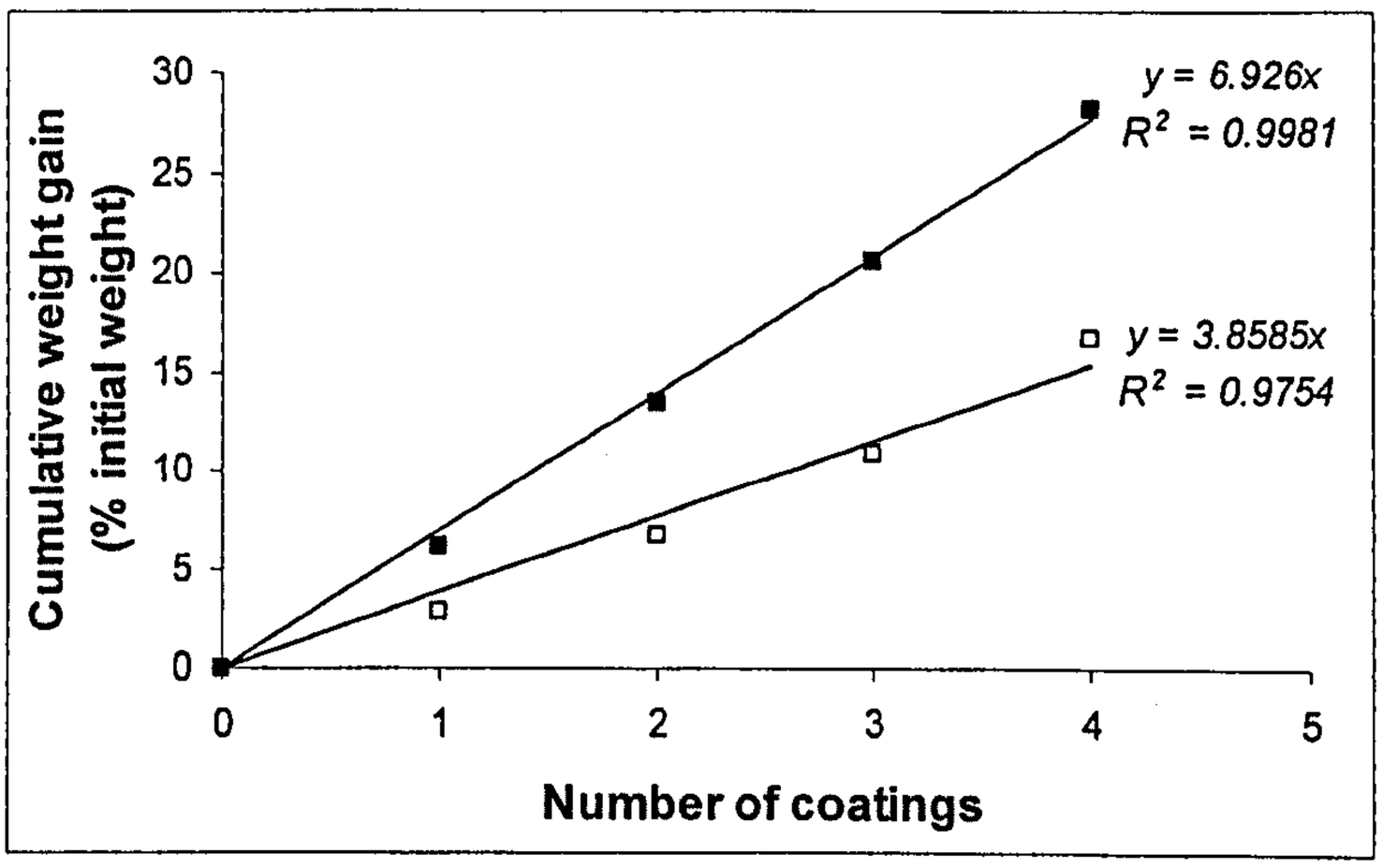

Figure 7.20: Coating level obtained by application of Surelease containing methylene blue (solid squares, ■) or cochineal food colouring (empty squares, □).

Figure 7.20 gave rise to the following observations:

(a) Capsule weight gain due to application of film coating increased linearly with consecutive spraying cycles.

(b) Methylene blue-coloured Surelease tended to increase the weight gain to a greater extent, almost 1.8 times, compared to the coating solution containing cochineal.

(c) Uniform capsule coating was achievable with the minicoater using aqueous-based coating solutions.

(d) Higher levels of coating was possible with the minicoater by consecutive applications of coating solution, rather than spraying all the solution required in one cycle. This approach would minimise the possibility of nozzle clogging from operating the machine for long periods of time.

Visual inspection of the final coated dosage forms also showed that this coating method was suitable for oil-filled capsules as there was no leakage of oil at all. This was possible due to good sealing afforded by the gelatin banding and the reduction in attrition forces among the small number of capsules within the coating chamber.

7.4.5.2 Calibration of minicoater with organic coating solution

Due to the differing chemical nature of the organic and aqueous coating solutions, it was necessary to also determine how changing the type of coating solution would impact the coating efficiency.

A coating solution containing 3%(w/v) of EC sprayed onto capsules for 10 minutes at 50mL/h should theoretically provide 0.25g of solids content. Since the mean weight of six compartmentalised capsules pre-coating was 5.56±0.03g, this would translate into 4.5% weight gain. In practice, the mean weight gain was only 0.08±0.02%(w/w), translating into an efficacy of only 1.7%. As the spray period increased to 15 minutes, the efficiency improved to 4.8% i.e. a mean weight gain of 0.32±0.03%(w/w). This was still less than optimal.

Comparing this efficiency rate to that obtained by spray coating in the fluidised bed coater which ranged from 50% (Section 6.4.4) to 75% (Section 6.4.3), the minicoater

was far inferior. Since the minicoater was operating in top spray mode, while the fluidised bed coater was set up for bottom spray, this was in agreement with Mehta *et al.* (1986). They concluded in their study of enteric-coated systems that application of film coating by top spraying retarded drug release to a lesser extent than when bottom spraying was implemented. This inequality in coating efficiency was attributed to the premature drying of coating droplets prior to impacting the substrate surface, effectively reducing the coating material and hence resulting in sub-optimal coating.

Assessment of the film morphology was performed using scanning electron microscopy (Figure 7.21).

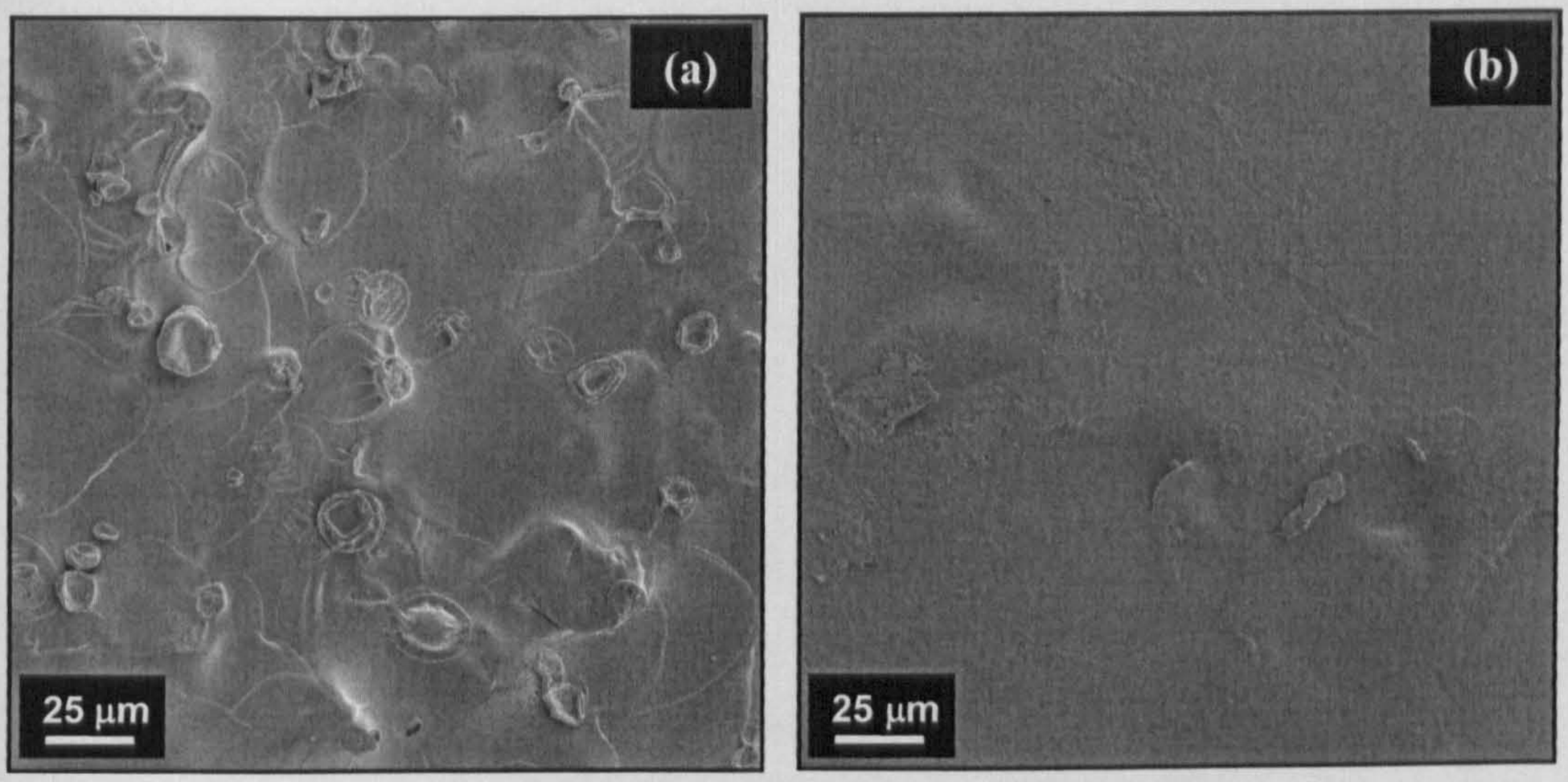

Figure 7.21: Electron micrographs (X500) of films spray coated onto empty hard gelatin capsules using (a) minicoater, spray period 15 minutes, 0.3% weight gain and (b) fluidised bed coater, 0.5% weight gain.

The electron micrographs in Figure 7.21 clearly showed the difference in the surface morphology of the films spray coated using the minicoater and fluidised bed coater. Minicoater-sprayed films were generally rougher than those obtained by fluidised bed coating. Although our methods here compared the two types of equipment, it was essentially the mode of operation that was the fundamental difference. The electron micrographs of Bertelson *et al.* (1994) who studied the film coats obtained by top and bottom spraying in fluidised bed equipment, were very similar to the images obtained here. A coating solution containing ethylcellulose, paraffin, Aerosil 200 (colloidal silica) and IPA as the organic solvent was sprayed onto potassium chloride crystals.

Quantification of the coating material deposited on the crystals as well as the film coat thickness implied that bottom spraying did indeed apply a significantly greater amount of coating onto the crystals. Films from top spraying were also more porous than those from bottom spraying. This, in addition to the thinner layer of coating applied by top spraying, resulted in increased rate of drug release from crystals coated by top spraying (Bertelson *et al.*, 1994).

The implications of these findings in our study here was that scale up from the small batches sprayed with the minicoater to larger batches prepared in the fluidised bed coater may result in differences in capsule performance.

7.5 Conclusions

- Poor reproducibility of the time-delayed capsule described in Chapter 6 necessitated a configuration change in the design of a novel time-controlled release device.

- Separating the swelling and hydrophobic components was the approach decided upon in order to localise the swelling and concentrate the force to rupture the brittle outer coating to one section of the capsule.

- After eliminating waxes and molten gelatin as possible compartment dividers, a tablet formed by directly compressing gelatin powder was found to be suitable.

- A simple tablet erosion study showed that incorporation of effervescent excipients could improve the rate of tablet dissolution in a concentration-dependent manner. Tablet hardness however did not significantly affect the tablet dissolution rate.

- Attempts to independently quantify the lag time afforded by the expansion rate of the swelling agent for consequent rupture of the EC shell proved futile as the various markers and fillers tested depressed the swelling rate of LH-21.

- The correlation of results from swelling force studies with puncture testing of EC films were not sufficiently accurate to predict the amount of LH-21 required to rupture the EC shell of the capsule. Other variables such as gastrointestinal motility, temperature and the variability between sprayed and solution-cast films have to be considered.

- *In vitro* dissolution studies on the assembled compartmentalised capsules were performed, changing the composition of the swelling agent and tablet separately while maintaining the content of other components of the system.

- Certain capsule formulations did generate reproducible dissolution profiles within the same batch but the intra-batch variability found with other formulations was of great concern.

- Dissolution performance was also affected by the type of capsule used, be it hard gelatin or HPMC. In general, HPMC capsules tended to crack in the mid-section, predisposing the capsule to empty its drug/oil phase without the lag time imposed by prior rupturing of the EC shell and dissolution of tablet.

- Improvements to reproducibility were hoped with the use of a new piece of equipment, the minicoater, in the belief that reduced tumbling and attrition forces affecting the capsules would hinder leakage and enhance coating uniformity.

- However, as time was limited, a comprehensive study on minicoater-coated capsules was not possible, although initial attempts to eliminate capsule fill leakage proved very promising.

CHAPTER 8

SUMMARY OF CONCLUSIONS AND FUTURE WORK

8.1 General discussion

The focus of this work was to produce a capsule formulation that was capable of delivering hydrophobic drugs solubilised in oil in a time-dependent manner. GRAS excipients such as ethylcellulose (EC) and low-substituted hydroxypropylcellulose (grade LH-21) were utilised in order to achieve this purpose. The proposed capsule formulation was reliant on the swelling power of LH-21 rupturing the brittle outer coating of EC upon aqueous immersion. A lag time would therefore be incorporated, generally dependent on

a) the rate of water ingress,
b) the rate of LH-21 swelling, and
c) the tolerance limit of the EC coat to the internal pressure generated by LH-21 swelling.

Adopting a rational approach to developing this system, pre-formulation studies on the suitability of both LH-21 and EC, essential components of the system, were carried out.

While LH-21 has been successfully incorporated into delivery systems as a disintegrant and a sustained release matrix, dependent on its particle size, our aim here was to exploit its excellent swelling capacity. Hence simple devices for measuring water uptake of LH-21 and the consequent swelling force generated were designed and used. It was indeed capable of rapid water uptake rates and swelling to its maximum extent in a matter of seconds. Microscopically, the substituted cellulose retained the fibrous features of the original cellulose while possessing additional smaller, granular particles as well. It also displayed an intermediate degree of crystallinity, between that of entirely crystalline microcrystalline cellulose and entirely amorphous hydroxypropylcellulose.

On its own, LH-21 could definitely be classed as a superdisintegrant due to its well-documented swelling power. However, when combined with other excipients, the general consensus was that its swellability diminished, the extent of which was dependent on the excipient. Both soybean and corn oil changed the swelling force profile of LH-21 from that of rapidly achieving its maximum, to that of a more sustained, controlled swelling. Manipulation of the swelling rate by carefully titrating the LH-21 with vegetable oils was possibly useful in that a longer lag time could be built into the final dosage form. However, addition of drugs such as paracetamol also resulted in a negative effect on the LH-21 swelling rate and power. Therefore, each drug proposed for the dosage form should undergo preliminary studies with the simple water uptake and swelling force devices. Even surfactants, anionic and non-ionic, proved detrimental to the swelling of LH-21 when the opposite was expected.

Characterisation of EC avoided the examination of *in situ* film coats on the actual capsules as removing them for study would be very difficult. Instead, solution-cast free films were prepared and subjected to various tensile and puncture tests in order to quantify the effects of polymer and plasticiser concentrations. Increasing plasticisation generally weakened the films resulting in breakage at lower applied forces. The ductility was increased as reflected in greater ability to stretch prior to breaking. Increments in polymer concentration conferred improved strength to the films. The puncture test was deemed to be more reflective of the phenomenon occurring in the constructed dosage form, whereby the internal force generated by LH-21 swelling would push outwards onto the EC coat. Combining the data from the swelling force studies of LH-21 and the puncture properties of the EC coat, it was then theoretically possible to postulate the quantities of either component required to impart a specified lag time. However, it must be emphasised that testing on solution-cast films do not exactly reflect the film coat sprayed on to the final dosage form due to the differences in the means of film coalescence. Solution-cast films tend to be more molecularly cohesive and hence stronger than their sprayed counterparts. Additionally, the LH-21 swelling force acts radially upon the EC coat of the capsule while theoretical calculations assumed that force was impacting on a single plane only.

With the data compiled from the initial characterisation studies, construction of the two configurations of the oil-filled capsule was attempted. The first configuration mixed both the LH-21 and corn oil together (time-delayed oil-filled capsule) while in the second, the two components were separated by a gelatin-based tablet (compartmentalised capsule).

Both kinds of capsules experienced problems with leakage of the oily fill. This proved unfavourable to achieving optimal EC coating of the capsules in the spray coater. Rupturing of even one capsule would envelope the entire batch in an oily film preventing adhesion of EC. Gelatin banding eventually alleviated the problem. Three means of coating were employed: spray coating in a fluidised bed coater, dipcoating and spray coating in a minicoater. All capsule formulations were tested using an *in vitro* dissolution method, the USP Apparatus II. Variables studied included:

Time-delayed oil-filled capsule	**Compartmentalised capsule**
LH-21 concentration with fixed oil volume	Hydroxypropylmethylcellulose and hard gelatin capsules
LH-21: corn oil weight ratio	Swelling compartment composition
EC coating level	Barrier tablet composition
Paddle speed	

8.2 Final conclusions

Overall, this work has been successful in terms of characterising LH-21 and solution-cast EC films, on which future development of controlled release systems could be based. Various excipient combinations were studied and the results were useful in identifying those that had potential for further study. Admittedly the initial aim of designing a drug delivery system suitable for reproducible time-controlled delivery of hydrophobic drugs has yet to be fully accomplished. Flaws in the manufacturing process need to be addressed in order to firstly eliminate capsule fill leakage completely. It then follows that the mechanism of action should be critically examined in order to determine the rate-limiting factors for drug release and how these can be regulated to achieve the desired drug release profile.

8.3 Suggested future work

During the course of this work, there arose certain findings that as yet have been unexplained in this thesis. This section contains proposals for means of obtaining the answers to these questions as well as future work that will further develop this novel drug delivery system.

8.3.1 Follow-up experiments

Interaction of LH-21 with water. More thorough characterisation of the latent moisture content and sorption capacity of LH-21 would be useful to fully understand its interaction with water. Dynamic vapour sorption (DVS), differential scanning calorimetry (DSC) and thermogravimetric analysis (TGA) should be undertaken on LH-21 samples which are a) fresh and b) subjected to environments of specific temperatures and relative humidity. This would give insight into the effects of ageing upon storage as well. Magnetic resonance imaging (MRI) can be used investigate the mechanism of water diffusion in an actively swelling system as seen in the work of Melia *et al.* (1998), Sutch *et al.* (2003) and Snaar *et al.* (1998).

Interaction of LH-21 with surfactants. The reason behind the effect of surfactants on LH-21 swellability could be determined through contact angle measurements as well as surface tension measurements using either a Langmuir balance or a Wilhelmy plate as described by Buckton (1995). These interfacial phenomena could also give insight to the interaction of LH-21 with other excipients.

Strain observations with puncture test. The Texture Analyser program should be developed further by varying the parameters set such as the lower limit for detection of force and rate of probe travel.

Glass transition temperature of plasticised EC films. Samples for DSC could be prepared as follows: solutions of EC and plasticiser of specified concentrations weighed into the DSC sample pans and evaporated under controlled conditions to form the film *in situ*. This approach ensures optimum contact between sample and pan.

8.3.2 Developmental ideas

Sprayed EC films. Design of a system for spraying free films would prove valuable in investigating the effects of polymer and plasticiser levels on EC films. This would firstly permit closer correlation to films sprayed onto actual dosage forms. Comparisons between the two methods of obtaining free films would also be possible.

Incorporation of hydrophobic drug. Griseofulvin was abandoned as a hydrophobic marker drug due to difficulties in preparing dissolution media. Research into suitable media and dissolution apparatus would allow better understanding of the partitioning of drug from the oil and its consequent absorption. It is hoped that accurate *in vivo in vitro* correlation (IVIVC) would be achieved.

Incorporation of self-emulsifying drug delivery systems (SEDDS). Discussed in the Chapter 1, development of this type of system was not possible with the time constraints during the course of this research.

Elimination of capsule fill leakage. Gelatin banding proved to be a good barrier to leakage. However, the paintbrush method could be substituted with a more uniform method such as the banding machine.

Optimisation of EC coat application. Spray coating was perhaps the most suitable method of polymer application. Further studies using the minicoater should prove fruitful.

Confirmation of mechanism of action. Thus far the drug release mechanisms for both configurations of capsules have merely been postulations based on examples found in the literature and the characterisation studies of LH-21 and EC. The mechanism of action must be defined and components which may cause the delivery device to fail must be identified and corrected.

REFERENCES

Alvarez-Lorenzo, C., Gomez-Amoza, J.L., Martinez-Pacheco, R., Souto, C., Concheiro, A. (2000a) Evaluation of low-substituted hydroxypropylcelluloses (L-HPCs) as filler-binders for direct compression. *Int. J. Pharm.* **197** (1-2): 107-116.

Alvarez-Lorenzo, C., Gomez-Amoza, J.L., Martinez-Pacheco, R., Souto, C., Concheiro, A. (2000b) Interactions between hydroxypropylcelluloses and vapour/liquid water. *Eur. J. Pharm. Biopharm.* **50**: 307-318.

American Society for Testing and Materials (1988) Standard test method for tensile properties of plastics. In Annual Book of ASTM Standards, American Society for Testing and Materials. Philadelphia PA, USA. pp 156-167.

Arwidsson, H. (1991) Properties of ethyl cellulose films for extended release. I. Influence of process factors when using organic solutions. *Acta Pharm. Nord.* **3** (1): 25-30.

Aulton, M. E. (1995) Mechanical properties of film coats. In: Pharmaceutical Coating Technology. Cole, G., Hogan, J., Aulton, M. (eds.) Taylor & Francis, London. pp 305-317.

Bertelson, P., Christensen, F.N., Holm, P., Jorgensen, K. (1994) Comparison of organic solvent-based ethylcellulose coatings on KCl crystals applied by top and bottom spraying in fluidised-bed equipment. *Int. J. Pharm.* **111**: 117-125.

Bi, Y.X., Sunada, H., Yonezawa, Y., Danjo, K., Otsuka, A., Iida, K. (1996) Preparation and evaluation of a compressed tablet rapidly disintegrating in the oral cavity. *Chem. Pharm. Bull.* **44** (11): 2121-2127.

Blanco, M.D., Trigo, R.M., Garcia, O., Teijon, J.M. (1997) Controlled release of cytarabine from poly(2-hydroxyethylmethacrylate-co-N-vinyl-2-pyrrolidone) hydrogels. *J. Biomater. Sci. Polym. Ed.* **8** (9): 709-719.

Brazel, C.S., Peppas, N.A. (1999) Mechanisms of solute and drug transport in relaxing, swellable, hydrophilic glassy polymers. *Polymer*. **40**: 3383-3398.

Buckton, G. (1995) Surface tension and liquid/liquid interfaces. In Interfacial phenomena in drug delivery and targeting. Harwood Academic Publishers. Switzerland. pp 1-26.

Bussemer, T., Dashevsky, A., Bodmeier, R. (2003) A pulsatile drug delivery system based on rupturable coated hard gelatin capsules. *J. Contr. Rel.* **93**: 331-339.

Bussemer, T., Bodmeier, R. (2003) Formulation parameters affecting the performance of coated gelatin capsules with pulsatile release profiles. *Int. J. Pharm.* **267**: 59-68.

Campbell, R.J., Sackett, G.L. (1999) Film coating. In Pharmaceutical unit operations: coating. Avis, K.E., Shukla, A.J., Chang, R.-K. (eds). IHS Health Group, Colorado. pp 55-176.

Capsugel, (1987) All about the hard gelatin capsule. Pontypool, Gwent, UK.

Cardinal, J.R. (1984) Matrix systems. In Medical applications for controlled release. Langer, R.S., Wise, D.L. (eds). CRC Press, Boca Raton. pp 42-65.

Charman, S.A., Charman, W.N., Rogge, M.C., Wilson, T.D., Dutko, F.J., Pouton, C.W. (1992) Self-emulsifying drug delivery systems – formulation and biopharmaceutic evaluation of an investigational lipophilic compound. *Pharm. Res.* **9** (1): 87-93.

Chiwele, I., Jones, B.E., Podczeck, F. (2000) The shell dissolution of various empty hard capsules. *Chem. Pharm. Bull.* **48**: 951-956.

Clemett, D., Markham, A. (2000) Prolonged-release mesalazine – a review of its therapeutic potential in ulcerative colitis and Crohn's disease. *Drugs.* **59** (4): 929-956.

Cole, E.T., Scott, R.A., Cade, D., Connor, A.L., Wilding, I.R. (2004) *In vitro* and *in vivo* pharmacoscintigraphic evaluation of ibuprofen hypromellose and gelatin capsules. *Pharm. Res.* **21** (5): 793-798.

Conte, U., Maggi, L., Colombo, P, La Manna, A. (1993) Multi-layered hydrophilic matrices as constant release devices (Geomatrix™ Systems). *J. Contr. Rel.* **26**: 39-47.

De Smidt, J.H., Offringa, J.C.A., Crommelin, D.A. (1991) Dissolution rate of griseofulvin in bile salt solutions. *J. Pharm. Sci.* **80** (4): 399-401.

Doelker, E. (1993) Cellulose derivatives. *Adv. Polym. Sci.* **106**: 199-265.

Entwistle, C.A., Rowe, R.C. (1979) Plasticisation of cellulose ethers used in the film coating of tablets. *J. Pharm. Pharmacol.* **31** (5): 269-272.

Fassihi, R.A., Ritschel, W.A. (1993) Multiple-layer, direct compression, controlled-release system: *in vitro* and *in vivo* evaluation. *J. Pharm. Sci.* **82** (7): 750-754.

Fujimori, J., Machida, Y., Tanaka, S., Nagai, T. (1995) Effect of magnetically controlled gastric residence of sustained release tablets in bioavailability of acetaminophen. *Int. J. Pharm.* **119**: 47-55.

Fukui, E., Miyamura, N., Uemura, K., Kobayashi, M. (2000) Preparation of enteric coated timed-release press-coated tablets and evaluation of their function by in vitro and in vivo tests for colon targeting. *Int. J. Pharm.* **204**: 7-15

Gazzaniga, A., Sangalli, M.E., Giordano, F. (1994) Oral Chronotopic™ drug delivery systems: achievement of time and/or site specificity. *Eur. J. Pharm. Biopharm.* **40** (4): 246-250.

Gupta, P., Vermani, K., Garg, S. (2002) Hydrogels: from controlled release to pH-responsive drug delivery. *Drug Discov. Today.* **7** (10): 569-579.

Halbaut, L., Barbe, C., del Pozo, A. (1996) An investigation into physical and chemical properties of semi-solid self-emulsifying systems for hard gelatin capsules. *Int. J. Pharm.* **130** (2): 203-212.

Hartman Kok, P.J.A., Vonk, P., Hoekzema, M.A., Kossen, N.W.F. (2001) Development of particulate pulse-release formulations and their mathematical description. *Powder Tech.* **119**: 33-44.

Hastings, M.H. (1997) The vertabrate clock: localisation, correction and entrainment. In Physiology and pharmacology of biological systems. Redfer, P.H., Lemmer, B. (eds). Springer-Verlag, Berlin. pp 1-21.

Heller, J. (1984) Bioerodible systems. In Medical applications for controlled release. Langer, R.S., Wise, D.L. (eds). CRC Press, Boca Raton. pp 69-102.

Heng, P.W.S., Chan, L.W., Ong, K.T. (2003) Influence of storage conditions and type of plasticisers on ethylcellulose and acrylate films formed from aqueous dispersions. *J. Pharm. Pharmaceut. Sci.* **6** (3): 334-344.

Hirayama, F., Uekama, K. (1999) Cyclodextrin-based controlled drug release systems. *Adv. Drug. Deliv. Rev.* **36** (1): 125-141.

Hjärtstam, J., Hjertberg, T. (1999) Studies of the water permeability and mechanical properties of a film made of an ethyl cellulose – ethanol – water ternary mixture. *J. Appl. Polym. Sci.* **74**: 2056-2062.

Ho, H.-O., Hsieh, C.-M., Sheu, M.-T. (2002) Characteristics of codried products of microcrystalline cellulose with saccharides and low-substituted hydroxypropylcellulose. *Powder Tech.* **127**: 45-55.

Hogan, J.E. (1995) Film-coating materials and their properties. In Pharmaceutical Coating Technology. Cole, G., Hogan, J., Aulton, M. (eds.) Taylor & Francis, London. pp 7-35.

Honkanen, O., Pia, L., Janne, M., Sari, E., Raimo, T., Martti, M. (2002) Bioavailability and *in vitro* oesophageal sticking tendency of hydroxypropyl methylcellulose capsule formulations and corresponding gelatine capsule formulations. *Eur. J. Pharm. Sci.* **15**: 479-488.

Hostetler, V.B. (1986) Capsules. Part One. Hard capsules. In The theory and practice of industrial pharmacy. Lachman, L, Liebermann, H.A., Konig, J.L. (eds) 3rd edition. Lea & Febiger, Philadelphia. pp 374-397.

Hu, Z.P., Mawatari, S., Shimokawa, T., Kimura, G., Yoshikawa, Y., Shibata, N., Takada, K. (2000) Colon delivery efficiencies of intestinal pressure-controlled colon delivery capsules prepared by a coating machine in human subjects. *J. Pharm. Pharmacol.* **52** (10): 1187-1193.

Huang, X., Brazel, C.S. (2001). On the importance and mechanisms of burst release in matrix-controlled drug delivery systems. *J. Contr. Rel.* **73**: 121-136.

Jones, B.E., Seager, H., Aulton, M.E., Morton, F.S.S. (1996) Capsules. In Pharmaceutics: the science of dosage form design. Aulton, M.E. (ed) Churchill Livingstone, Edinburgh. pp 322-340.

Kawashima, Y., Takeuchi, H., Hino, T., Niwa, T., Lin, T.-L., Sekigawa, F., Kawahara, K. (1993a) Low-substituted hydroxypropylcellulose as a sustained-drug release matrix base or distintegrant depending on its particle size and loading in formulations. *Pharm. Res.* **10** (3): 351-355.

Kawashima, Y., Takeuchi, H., Hino, T., Niwa, T., Lin, T.-L., Sekigawa, F., Ohya, M. (1993b) Preparation of prolonged-release matrix tablet of acetaminophen with pulverized low-substituted hydroxypropylcellulose via wet granulation. *Int. J. Pharm.* **99**: 229-238.

Kawashima, Y., Takeuchi, H., Hino, T., Niwa, T., Lin, T.-L., Sekigawa, F. (1993c) Preparation of a sustained-release matrix tablet of acetaminophen with pulverized

low-substituted hydroxypropylcellulose via dry granulation. *Chem. Pharm. Bull.* **41** (10): 1827-1831.

Khan, M.A., Sastry, S.V., Vaithiyalingam, S.R., Agarwal, V., Nazzal, S., Reddy, I.K. (2000) Captopril gastrointestinal therapeutic system coated with cellulose acetate pseudolatex: evaluation of main effects of several formulation variables. *Int. J. Pharm.* **193**: 147-156.

Kleinbudde, P. (1994a) Shrinking and swelling properties of pellets containing microcrystalline cellulose and low substituted hydroxypropylcellulose: I. Shrinking properties. *Int. J. Pharm.* **109**: 209-219.

Kleinbudde, P. (1994b) Shrinking and swelling properties of pellets containing microcrystalline cellulose and low substituted hydroxypropylcellulose: II. Swelling properties. *Int. J. Pharm.* **109**: 221-227.

Kojima, M., Ando, S., Kataoka, K., Hirota, T., Aoyagi, K., Nakagami, H. (1998) Magnetic resonance imaging (MRI) study of swelling and water mobility in micronised low-substituted hydroxypropylcellulose matrix tablets. *Chem. Pharm. Bull.* **46** (2): 324-328.

Landin, M., Martinez-Pacheco, R., Gomez-Amoza, J.L., Souto, C., Concheiro, A., Rowe, R.C. (1993) Effect of batch variation and source of pulp on the properties of microcrystalline cellulose. *Int. J. Pharm.* **91** (2-3): 133-141.

Langer, R. (1980) Polymeric drug delivery systems for controlled drug release. *Chem. Eng. Commun.* **6**: 1-48.

Lee, V.H.-L., Robinson, J.R. (1978) Methods to achieve sustained drug delivery. The physical approach: oral and parenteral dosage forms. In Sustained and controlled release drug delivery systems. Robinson, J.R. (ed) Marcel Dekker, Inc. New York. pp 123-210.

Lemmer, B. (1996) The clinical relevance of chronopharmacology in therapeutics. *Pharmacol. Res.* **33**: 107-115.

Licaps® brochure. www.capsugel.com/pdf/brochure_licaps.pdf

Lin, S.Y., Lin, K.H. (1996) Water uptake and drug release behaviour of drug-loaded compacts prepared from different grades of ethylcellulose. *Eur. J. Pharm. Biopharm.* **43**: 193-208.

Lin, S.Y., Lin, K.H., Li, M.J. (2001) Micronised ethylcellulose for designing a directly-compressed time-controlled disintegrating tablet. *J. Contr. Rel.* **70** (3): 321-328.

Mascher, H., Kikuta, C., Schiel, H. (2001) Pharmacokinetics of menthol and carvone after administration of an enteric coated formulation containing peppermint oil and caraway oil. *Arzneimittel-Forsch.* **51** (6): 465-469.

Mehta, A.M., Valazza, M.J., Abele, S.E. (1986) Evaluation of fluid-bed processing for enteric coating systems. *Pharm. Technol.* **10**: 46-56.

Mehta, A.M. (1997) Processing and equipment considerations for aqueous coatings. In Aqueous polymeric coatings for pharmaceutical dosage forms. 2nd edition, revised and expanded. McGinity, J.W. (ed.) Marcel Dekker Inc., New York. pp 287-326.

Melia, C.D., Rajabi-Siahboomi, A.R., Bowtell, R.W. (1998) Magnetic resonance imaging of controlled release pharmaceutical dosage forms. *Pharm. Sci. Technol. Today* **1** (1): 32-39.

Mettler (1986) Technical Literature; Mettler TA 3000 Thermal Analysis System ME-724074.

Miyazaki, K., Sakai, T., Ishida, N. (2001) Circadian rhythm biochemistry: from protein degradation to sleep mating. *Biochem. Biophys. Res. Commun.* **286** (1): 1-5.

Narisawa, S., Yoshino, H., Hirakawa, Y., Noda, K. (1993) Porosity-controlled ethylcellulose film coating. 1. Formation of porous ethylcellulose film in the coating process and factors affecting film density. *Chem. Pharm. Bull.* **41** (2): 329-334.

Nelson, M.L., O'Connor, R.T. (1964) Relation of certain infrared bands to cellulose crystallinity and crystal lattice type. Part II. A new infrared ratio for estimation of crystallinity in celluloses I and II. *J. Appl. Polym. Sci.* **8**: 1325-1341.

Neslihan Gursy, R., Benita, S. (2004) Self-emulsifying drug delivery systems (SEDDS) for improved oral delivery of lipophilic drugs. *Biomed. Pharmacother.* **58**: 173-182.

Nevell, T.P., Zeronian, S.H. (1985) Cellulose chemistry fundamentals. In Cellulose chemistry and its applications. Nevell, T.P., Zeronian, S.H. (eds) Ellis Horwood Ltd., West Sussex. pp 15-29.

Nicholson, M.D., Merritt, F.M. (1985) Cellulose ethers. In Cellulose chemistry and its applications. Nevell, T.P., Zeronian, S.H. (eds) Ellis Horwood Ltd., West Sussex. pp 363-383.

Obara, S., Maruyama, N., Nishiyama, Y., Kokubo, H. (1999) Dry coating: an innovative enteric coating method using a cellulose derivative. *Eur. J. Pharm. Biopharm.* **47**: 51-59.

Oo, C., Snell, P., Barrett, J., Dorr, A., Liu, B., Wilding, I. (2003) Pharmacokinetics and delivery of the anti-influenza drug oseltamivir to the small intestine and colon using site-specific delivery capsules. *Int. J. Pharm.* **257**: 297-299.

Panomsuk, S.P., Hatanaka, T., Aiba, T., Katayama, K., Koizumi, T. (1996) A study of the hydrophilic cellulose matrix. Effect of indomethacin and a water-soluble additive on swelling properties. *Int. J. Pharm.* **126** (1-2): 147-153.

Parikh, N.H., Porter, S.C., Rohera, B.D. (1993) Tensile properties of free films cast from aqueous ethylcellulose dispersions. *Pharm. Res.* **10**: 810-815.

Perrin, D.E., English, J.P. (1997) Polyglycolide and polylactide. In Handbook of biodegradable polymers. Domb, A.J., Kost, J., Wiseman, D.M. (eds). Harwood Academic Publishers, Amsterdam. pp 3-28.

Peppas, N.A. (1984) Mathematical models for controlled release kinetics. In Medical applications for controlled release. Langer, R.S., Wise, D.L. (eds). CRC Press, Boca Raton. pp 170-186.

Peppas, N.A., Bures, P., Leobandung, W., Ichikawa, H. (2000) Hydrogels in pharmaceutical formulations. *Eur. J. Pharm. Biopharm.* **50**: 27-46.

Podczeck, F. Jones, B.E. (2002) The *in vitro* dissolution of theophylline from different types of hard shell capsules. *Drug Dev. Ind. Pharm.* **28** (9): 1163-1169.

Porter, S.C., Ridgway, K. (1983) An evaluation of the properties of enteric coating polymers – measurement of glass-transition temperature. *J. Pharm. Pharmacol.* **35** (6): 341-344.

Pouton, C.W. (1997) Formulation of self-emulsifying drug delivery systems. *Adv. Drug Deliv. Rev.* **25**: 47-58.

Pouton, C.W. (2000) Lipid formulations for oral administration of drugs: non-emulsifying, self-emulsifying and 'self-microemulsifying' drug delivery systems. *Eur. J. Pharm. Sci.* **11** (Suppl. 2): S93-S98.

Pozzi, F., Furlani, P., Gazzaniga, A., Davis, S.S., Wilding, I.R. (1994) The TIME CLOCK system: a new oral dosage form for fast and complete release of drug after a predetermined lag time. *J. Contr. Rel.* **31**: 99-108.

Qiu, Y., Park, K. (2001) Environment-sensitive hydrogels for drug delivery. *Adv. Drug Deliv. Rev.* **53**: 321-339.

Quintanar-Guerrero, D., Allemann, E., Fessi, H., Doelker, E. (1999) Pseudolatex preparation using a novel emulsion-diffusion process involving direct displacement of partially water-miscible solvents by distillation. *Int. J. Pharm.* **188** (2): 155-164.

Rao, S.B., Murthy, K.V.R. (2002) Studies on rifampicin release from ethylcellulose coated nonpareil beads. *Int. J. Pharm.* **231** (1): 97-106.

Reinberg, A.E. (1992) Concepts in chronopharmacology. *Annu. Rev. Pharmacol. Toxicol.* **32**: 51-66.

Ridgway, K. (ed) (1987) Hard capsules: development and technology. The Pharmaceutical Press, London.

Rowe, R.C. and Forse, S.F. (1980) The effect of film thickness on the incidence of the defect bridging of intagliations on film coated tablets. *J. Pharm. Pharmacol.* **32**: 647-648.

Sakellariou, P., Rowe, R.C. (1995a) Interactions in cellulose derivative films for oral drug delivery. *Prog. Polym. Sci.* **20** (5): 889-942.

Sakellariou, P., Rowe, R.C. (1995b) The morphology of blends of ethylcellulose with hydroxypropyl methylcellulose as used in film coating. *Int. J. Pharm.* **125**: 289-296.

Sangalli, M.E., Maroni, A., Zema, L., Busetti, C., Giordano, F., Gazzaniga, A. (2001) In vitro and in vivo evaluation of an oral system for time and/or site-specific drug delivery. *J. Contr. Rel.* **73**: 103-110.

Sangalli, M.E., Maroni, A., Foppoli, A., Zema, L., Giordano, F., Gazzaniga, A. (2004) Different HPMC viscosity grades as coating agents for an oral and/or site-controlled delivery system: a study on process parameters and in vitro performances. *Eur. J. Pharm. Biopharm.* **22**: 469-476.

Schultz, P., Kleinbudde, P. (1997) A new multiparticulate delayed release system. Part I: Dissolution properties and release mechanism. *J. Contr. Rel.* **47**: 181-189.

Seoul, C., Mah, S.I. (1997) Drawing of sprayed poly(vinyl alcohol) films. *Polymer.* **38** (22): 5551-5555.

Shin-Etsu (1992) L-HPC. *In* Shin-Etsu Technical Information. No. L-1. pp 1-35.

Siepmann, J., Peppas, N.A. (2001) Modeling of drug release from delivery systems based on hydroxypropylmethylcellulose (HPMC). *Adv. Drug Deliv. Rev.* **48**: 139-151.

Shirai, Y., Sogo, K., Fujioka, H., Nakamura, Y. (1994) Role of low-substituted hydroxypropylcellulose in dissolution and bioavailability of novel fine granule system for masking bitter taste. *Biol. Pharm. Bull.* **17** (3): 427-431.

Smith, B. (1999) Infrared spectral interpretation: a systematic approach. CRC Press. Boca Raton, Florida : 177-194.

Smolensky, M.H., D'Alonzo, G.E. (1997) Progress in the chronotherapy of nocturnal asthma. In Medical applications for controlled release. Langer, R.S., Wise, D.L. (eds) CRC Press, Boca Raton. pp 2-5-241.

Snaar, J.E.M., Bowtell, R.W., Melia, C.D., Morgan, S., Narasimhan, B., Peppas, N.A. (1998) Self-diffusion and molecular mobility in PVA-based dissolution-controlled systems for drug delivery. *Magn. Reson. Imaging* **16** (5-6): 691-694.

Sun, Y.M., Huang, W.F., Chang, C.C. (1999) Spray-coated and solution-cast ethylcellulose pseudolatex membranes. *J. Membr. Sci.* **157** (2): 159-170.

Sutch, J.C.D., Ross, A.C., Kockenberger, W., Bowtell, R.W., MacRae, R.J., Stevens, H.N.E., Melia, C.D. (2003) Investigating the coating-dependent release mechanism of a pulsatile capsule using NMR microscopy. *J. Contr. Rel.* **92** (3): 341- 347.

Takeuchi, H., Handa, T., Kawashima, Y. (1987) Enhancement of the dissolution rate of a poorly water-soluble drug (tolbutamide) by a spray-drying solvent deposition method and disintegrants. *J. Pharm. Pharmacol.* **39** (10): 769-773.

Takeuchi, H., Sasaki, H., Niwa, T., Hino, T., Kawashima, Y., Uesugi, K., Kayano, M., Miyake, Y. (1991) Preparation of powdered redispersible vitamin E acetate emulsion by spray-drying technique. *Chem. Pharm. Bull.* **39** (6): 1528-1531.

Theeuwes, F. (1975) Elementary osmotic pump. *J. Pharm. Sci.* **64** (12): 1987-1991.

Thombre, A.G., Cardinal, J.R. (1990) Biopolymers for controlled drug delivery. In Encyclopaedia of pharmaceutical technology. Vol. 2. Swarbrick, J., Boylan, J.C. (eds) Marcel Dekker Inc., New York. pp 61-68.

Ueda, Y., Hata, T., Yamaguchi, H., Ueda, S., Kotani, M. (1989) US Patent 4871549.

Ueda, S., Hata, T., Asakura, S., Yamaguchi, H., Kotani, M., Ueda, Y. (1994a) Development of a novel drug release system, Time-Controlled Release System (TES). I. Concept and design. *J. Drug. Target.* **2** (1): 35-44.

Ueda, S., Yamaguchi, H., Kotani, M., Kimura, S., Tokanuga, Y., Kagayama, A., Hata, T. (1994b) Development of a novel drug release system, Time-Controlled Release

System (TES). II. Design of multiparticulate TES and *in vitro* drug release properties. *Chem. Pharm. Bull.* **42** (2): 359-363.

Ueda, S., Ibuki, R., Kimura, S., Murata, S., Takahashi, T., Tokunaga, Y., Hata, T. (1994c). Development of a novel drug release system, Time-Controlled Release System (TES). III. Relation between lag time and membrane thickness. *Chem. Pharm. Bull.* **42** (2): 364-367.

Vanderhoff, J.W. (1993) Recent advances in the preparation of latexes. *Chem. Eng. Sci.* **48** (2): 203-217.

Vergnaud, J.-M. (1993) The diffusion equations and basic considerations. In Controlled drug release of oral dosage forms. Ellis Horwood Ltd., West Sussex. pp 1-20.

Wan, L.S.C., Heng, P.W.S., Wong, L.F. (1991) The effect of hydroxypropylmethylcellulose on water penetration into a matrix system. *Int. J. Pharm.* **73**: 111-116.

Wesseling, M., Bodmeier, R. (1999) Drug release from beads coated with an aqueous colloidal ethylcellulose dispersion, Aquacoat®, or an organic ethylcellulose solution. *Eur. J. Pharm. Biopharm.* **47**: 33-38.

Wijmans, J.G., Baker, R.W. (1995) The solution-diffusion model: a review. *J. Membr. Sci.* **107**: 1-21.

Wilding, I.R., Davis, S.S., Pozzi, F., Furlani, P., Gazzaniga, A. (1994) Enteric coated timed release systems for colonic targeting. *Int. J. Pharm.* **111**: 99-102.

Williams, D.H., Fleming, I. (1989) Infrared spectra. In Spectroscopic methods in organic chemistry. 4th edition revised. McGraw-Hill Book Company (UK) Ltd. pp 29-62.

Yang, S.T., Van Savage, G., Weiss, J., Ghebresellassie, I. (1992) The effect of spray mode and chamber geometry of fluid-bed coating equipment and other parameters on an aqueous-based ethylcellulose coating. *Int. J. Pharm.* **86** (2-3): 247-257.

Yuk, S.H., Cho, S.H., Lee, H.B. (1995) pH-sensitive drug delivery system using o/w emulsion. *J. Contr. Rel.* **37** (1-2): 69-74.